NATIONAL COOPERATIVE
HIGHWAY RESEARCH PROGRAM REPORT 338

ASPHALT-AGGREGATE MIXTURE ANALYSIS SYSTEM

AAMAS

TRANSPORTATION RESEARCH BOARD
NATIONAL RESEARCH COUNCIL

NATIONAL COOPERATIVE HIGHWAY RESEARCH PROGRAM
REPORT 338

ASPHALT-AGGREGATE MIXTURE ANALYSIS SYSTEM
AAMAS

H. L. VON QUINTUS, J. A. SCHEROCMAN, C. S. HUGHES and T. W. KENNEDY
Brent Rauhut Engineering Inc.
Austin, Texas

RESEARCH SPONSORED BY THE AMERICAN ASSOCIATION OF STATE HIGHWAY AND TRANSPORTATION OFFICIALS IN COOPERATION WITH THE FEDERAL HIGHWAY ADMINISTRATION

AREAS OF INTEREST

Pavement Design and Performance
Bituminous Materials and Mixes
(Highway Transportation and Air Transportation)

TRANSPORTATION RESEARCH BOARD
NATIONAL RESEARCH COUNCIL
WASHINGTON, D. C.

MARCH 1991

NATIONAL COOPERATIVE HIGHWAY RESEARCH PROGRAM

Systematic, well-designed research provides the most effective approach to the solution of many problems facing highway administrators and engineers. Often, highway problems are of local interest and can best be studied by highway departments individually or in cooperation with their state universities and others. However, the accelerating growth of highway transportation develops increasingly complex problems of wide interest to highway authorities. These problems are best studied through a coordinated program of cooperative research.

In recognition of these needs, the highway administrators of the American Association of State Highway and Transportation Officials initiated in 1962 an objective national highway research program employing modern scientific techniques. This program is supported on a continuing basis by funds from participating member states of the Association and it receives the full cooperation and support of the Federal Highway Administration, United States Department of Transportation.

The Transportation Research Board of the National Research Council was requested by the Association to administer the research program because of the Board's recognized objectivity and understanding of modern research practices. The Board is uniquely suited for this purpose as: it maintains an extensive committee structure from which authorities on any highway transportation subject may be drawn; it possesses avenues of communications and cooperation with federal, state and local governmental agencies, universities, and industry; its relationship to the National Research Council is an insurance of objectivity; it maintains a full-time research correlation staff of specialists in highway transportation matters to bring the findings of research directly to those who are in a position to use them.

The program is developed on the basis of research needs identified by chief administrators of the highway and transportation departments and by committees of AASHTO. Each year, specific areas of research needs to be included in the program are proposed to the National Research Council and the Board by the American Association of State Highway and Transportation Officials. Research projects to fulfill these needs are defined by the Board, and qualified research agencies are selected from those that have submitted proposals. Administration and surveillance of research contracts are the responsibilities of the National Research Council and the Transportation Research Board.

The needs for highway research are many, and the National Cooperative Highway Research Program can make significant contributions to the solution of highway transportation problems of mutual concern to many responsible groups. The program, however, is intended to complement rather than to substitute for or duplicate other highway research programs.

NCHRP REPORT 338

Project 9-6(1) FY '85 and FY '90

ISSN 0077-5614

ISBN 0-309-04861-3

L. C. Catalog Card No. 90-65151

Price $20.00

NOTICE

Special Notice

Published reports of the

NATIONAL COOPERATIVE HIGHWAY RESEARCH PROGRAM

are available from:

Transportation Research Board
National Research Council
2101 Constitution Avenue, N.W.
Washington, D.C. 20418

Printed in the United States of America

FOREWORD

By Staff
Transportation Research Board

This report represents a significant step toward improved design of asphaltic concrete paving mixtures. It will be of special interest to pavement engineers and laboratory technicians working with asphalt. Concepts presented in this report are new. The asphalt-aggregate mixture analysis system (AAMAS), proposed herein, provides an initial link between mix design and pavement performance. For many years, asphalt technologists have used the Marshall and Hveem mix design methods, and the resulting asphalt mixtures, when placed and properly compacted, provided pavements that often performed well. However, neither one of those mix design methods has been correlated with pavement performance. This report presents the findings of research to correlate mix-design methods with pavement performance and contains a complete asphalt-aggregate mixture analysis system and asphalt mixture design procedure; it also lays the groundwork on which other research can build.

Improved mix-design methods for asphaltic concrete should optimize the selection, proportioning, and processing of asphalt binders and aggregate materials to produce pavements uniformly resistant to all forms of distress such as fatigue cracking, thermal cracking, permanent deformation, moisture damage, and age hardening. The initial phase of research on NCHRP Project 9-6 involved an investigation of the feasibility of an asphalt-aggregate mixture analysis system and the selection of a plan for its development. Three concurrent Phase I contracts were conducted by ARE, Inc.; Brent Rauhut Engineering, Inc.; and the University of Maryland. Each concluded that AAMAS development was feasible and desirable and recommended a plan. Brent Rauhut Engineering, Inc., was selected to develop a mixture analysis and design system capable of encompassing conventional ashphalt binders, modified asphalts, mixture modifiers, and the range of aggregate materials used in the United States. Open-graded friction courses and drainage layers were not included in the study. The system that was developed is also capable of evaluating mixtures under conditions analogous to those found in service, including a wide range of climate, traffic, and age factors. The recommended system for laboratory evaluation of asphaltic concrete mixtures calls for specimens that, as nearly as possible, duplicate the characteristics of mixtures in the field. Five laboratory tests are recommended: the diametral resilient modulus test, the indirect tensile strength test, the gyratory shear strength test, and the indirect tensile and uniaxial unconfined compression creep tests. These tests measure properties required by most models used for structural design of asphalt pavement sections. The mixture-design procedure presented herein was developed in the final phase of the research. NCHRP Project 9-6(1) is linked to the broader ranging Strategic Highway Research Program (SHRP) studies, and it constitutes an interim step in the evolution of AAMAS procedure development that is being continued by SHRP.

Part I of the final report is a Procedural Manual, prepared in specification language specifically for the pavement engineer and laboratory technician; it takes the reader step-by-step through the entire analysis and mix design procedure. Part II documents the research that produced the analysis system and the mixture design procedure. The Appendixes to this final report are not published herein, but copies may be obtained on loan or purchased at a cost of $25.00, from the National Cooperative Highway Rsearch Program, Transportation Research Board, 2101 Constitution Ave., N.W., Washington, D.C. 20418.

Contents

Part I
Procedural Manual for Mixture Design and AAMAS

INTRODUCTION 1

Section 1 Guidelines for Selection of Mixture Components 6

1.1 Scope 6
1.2 Materials 6
1.3 Grading Considerations 7
1.4 Voids 7
1.5 VMA and VFA Considerations 7
1.6 Asphalt Content and Denseness 9

Section 2 Guidelines for Mixture Design 10

2.1 Scope 10
2.2 Summary of Procedure 10
2.3 Significance and Use 10
2.4 Applicable Documents 10
2.5 Apparatus 11
2.6 Preparation of Mixtures 12
2.7 Resistance to Fracture 12
2.8 Resistance to Shear Displacements 14
2.9 Resistance to Uniaxial Deformations 16
2.10 Interpretation of Data 17

Section 3 Guidelines for Mixture Analyses 22

3.1 Scope 22
3.2 Summary of Procedure 22
3.3 Significance and Use 22
3.4 Applicable Documents 22
3.5 Apparatus 23
3.6 Preparation of Laboratory Test Specimens 24
3.7 Grouping of Test Specimens 25
3.8 Preconditioning of Test Specimens 25
3.9 Testing Procedure 29
3.10 Calculations 30
3.11 Report 30
Addendum A Test Methods for Indirect Tensile Strength of Bituminous Mixtures 30
Addendum B Test Methods for Creep Modulus Testing of Bituminous Mixtures 35

Section 4 Guidelines for Mixture Performance Evaluation 41

4.1 Scope 41
4.2 Asphalt Pavement/Mixture Evaluation Methodology 41
4.3 Guidelines for Establishing Laboratory Test Conditions 42
4.4 AASHTO Structural Layer Coefficient 42
4.5 Rutting 43
4.6 Fatigue Cracking 46
4.7 Thermal Cracking 51
4.8 Moisture Damage 53
4.9 Disintegration 53

Section 5 AAMAS—Mixture Design Example Problem 54

5.1 Assumptions for Example Problem 54
5.2 Mixture Performance Evaluation 55
5.3 Mixture Design 58

Part II

Research Report for Evaluation and Design of Asphaltic Concrete Mixtures

SUMMARY 65

Chapter 1 Introduction 66

1.1 Background 66
1.2 Research Problem Statement 67
1.3 Project Objective 67
1.4 Research Approach 67

Chapter 2 Findings 68

2.1 Factors Considered in AAMAS 69
2.2 Mixtures Selected for Study 74
2.3 Mixture Compaction and Air Voids 86
2.4 Mixture Testing and Evaluation 94
2.5 Mixture Conditioning 112
2.6 Supplemental Analyses and Study Areas 124

Chapter 3 Interpretation, Appraisal, Application 135

3.1 Selection of Mixture Components 135
3.2 Laboratory Simulation of Field Compaction 141
3.3 Specimen Preparation 149
3.4 Relationship between Mixture and Structural Design 156
3.5 Mixture Performance Evaluation 161

Chapter 4 Conclusions and Recommendations 177

4.1 Conclusions 177
4.2 Implementation 179
4.3 Recommendations for Continued Research 179

Appendix A through Appendix R Unpublished Material 180

REFERENCES 180

NOTATIONS AND SYMBOLS 184

ACKNOWLEDGMENTS

The research effort reported herein was performed under NCHRP Project 9-6(1) by Brent Rauhut Engineering Inc. Brent Rauhut Engineering was the prime contractor for this study and the University of Idaho, University of Florida, and Texas Transportation Institute participated as subcontractors.

Mr. Harold L. Von Quintus, President, Brent Rauhut Engineering, was the Principal Investigator, and Mr. James Scherocman, the Co-Principal Investigator. The other authors of this report are Mr. Chuck Hughes and Dr. Thomas W. Kennedy, who were both technical advisors on NCHRP Project 9-6(1).

The authors of this report acknowledge the valuable assistance and information provided by four consultants: Dr. Dallas Little, Professor of Civil Engineering at the Texas A&M University; Dr. Byron Ruth, Professor of Civil Engineering at the University of Florida; Dr. Robert Lottman, Professor of Civil Engineering at the University of Idaho; and Dr. James Burati, Professor of Civil Engineering at Clemson University. The assistance and technical direction provided by these professional engineers is gratefully acknowledged.

The authors also acknowledge the cooperation and efforts of the following State Highway Agencies and contractors, who participated in constructing the field test sections of AAMAS and provided additional mixtures for laboratory evaluation using AAMAS. Those State Highway Agencies and contractors involved in Project 9-6(1) are: Dennis Donnelly, Colorado Department of Highways (Flatiron Construction); Frederick Copple, Michigan Department of Transportation (Saginaw Paving); Nick Turnham, Texas State Department of Highways and Public Transportation (Young Brothers); Chuck Hughes, Virginia Transportation Research Council (Project 1: Tri-County Asphalt, Project 2: Rea Construction Co.); Robert Warburton, Wyoming State Highway Department (McMurray Brothers); Dr. Ed Dukatz, (Vulcan Materials Cabarrus Quarry); Bob Page, California Department of Transportation (Baldwin Contracting); Ronald Collins, Georgia Department of Transportation; James Murphy, New York Department of Transportation (Prima Asphalt); and John Pope, Wisconsin Department of Transportation).

Part I—Procedural Manual For Mixture Design and AAMAS

INTRODUCTION

Part I of this report presents the procedures for an Asphalt-Aggregate Mixture Analysis System (AAMAS) developed under NCHRP Research Project 9-6(1). The procedures included in the manual are intended to be used for the design and evaluation of dense-graded hot-mix asphaltic concrete mixtures, based on performance-related criteria for high-volume roadways. This manual is the first of two documents, and constitutes the Procedural Manual for mixture design and AAMAS. Part 2 provides discussion on all tasks and findings conducted under Project 9-6(1).

Background

The two methods commonly used in the United States for the design of dense-graded hot-mix asphaltic concrete are "Marshall" and "Hveem". Both methods are empirical procedures that were developed many years ago and have generally served well under traffic. The current philosophies behind the design of asphaltic concrete mixtures using the Hveem and Marshall approaches are reasonable, and the basic principles of providing proper air voids, adequate stability, and accounting for aggregate absorption are adequate. Premature distress in many flexible pavements, however, suggests that these empirical mixture design procedures do not consider all pertinent mixture properties for some distresses, especially for those mixtures that are subjected to greater vehicle loads and higher tire pressures than those in use when the methods were developed.

Typically, the structural design of asphaltic concrete pavements is based on assumed material properties (layer stiffness coefficient, resilient modulus, fatigue, and permanent deformation constants). After the structural design has been completed, materials are submitted and a mixture design is completed. The question then becomes: Does the as-placed mixture meet the assumptions initially used for the structural design? Unfortunately, the engineering properties used in structural design are not those dealt with or measured in these empirical mixture design procedures. Certainly, asphaltic concrete mixture design and analyses need to be related to those factors that affect asphalt pavement performance. Mixture design and structural design also need to be tied together and based on the same criteria and parameters for compatibility.

The highway community, specifically AASHTO, recognized this need for improved procedures and analysis systems for the design of asphaltic concrete mixtures that are resistant to heavy truck loads, the use of higher tire pressures, and the wide extremes of climate encountered in the United States. In response to this need, research was initiated, under NCHRP Project 9-6(1), to develop an Asphalt-Aggregate Mixture Analysis System (AAMAS) for the laboratory evaluation of asphaltic concrete mixtures based on performance-related criteria. Part I of this report, the *Procedural Manual for Mixture Design and AAMAS,* presents the AAMAS procedures.

AAMAS Methodology

Any mixture design must, as a minimum, provide for acceptable voids in the mixture and an acceptable level of stability. Thus, one design approach is to build on the presently accepted methods of mixture design which account for air voids and stability similar to the Hveem and Marshall procedures. A more rational approach for mixture design would be to use those engineering properties that are related to pavement distress. Section 2 of this manual recommends such a mixture design procedure based on performance-related criteria. The mixture design can be completed in accordance with either the user agency's current practice or Section 2 of Part I.

Once an initial mixture design has been developed, efficient and effective mixture preparation and characterization procedures can be used to determine the engineering properties of the materials and mixtures. Results of tests that measure engineering properties can then be judged by appropriate failure criteria for each test mode simulated. Figure 1 shows a conceptual flow chart of the different steps that are required in the AAMAS.

To design mixtures based on performance-related criteria it is necessary to use a test that measures those engineering properties and the characteristics of an asphaltic concrete mixture that are related to a distress or performance measure. The distresses selected for incorporation into AAMAS include rutting, fatigue cracking, low temperature cracking, and moisture damage. Secondary consideration is given to disintegration, such as raveling and loss of skid resistance.

For AAMAS to be useful to the highway construction industry and applicable over a range of mixtures, tests used to measure these properties must be reliable, reproducible, sensitive to mixture variables, efficient, and simple. The test procedures and equipment must also be capable of testing oversize samples when larger aggregates (greater than 1 in. in diameter) are used in the mixture.

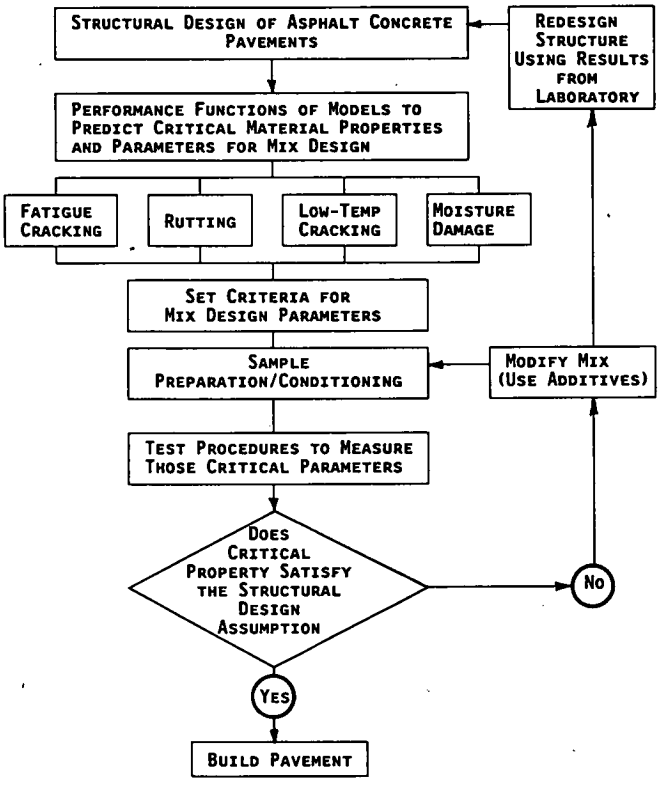

Figure 1. Conceptual flow chart illustrating the different steps in AAMAS.

Five tests were selected as tools for mixture evaluation in AAMAS, because they measure those properties required by most structural models. These are the diametral resilient modulus test, indirect tensile strength test, gyratory shear strength test, and the indirect tensile and uniaxial unconfined compression creep tests. Most of these properties and tests are becoming standardized and are being used on more of a routine basis by some state agencies. On the other hand, the mathematical models that are needed to predict mixture behavior and performance from these properties are numerous and vary considerably.

The one standardized procedure used in the United States is the "AASHTO Guide for the Design of Pavement Structures." Although the AASHTO design procedure was recently updated and improved (1986), it still uses empirical relationships. Layer thicknesses are determined by using structural layer coefficients that do not consider the different types of distress separately. AAMAS, however, must consider the different types of distress individually.

NCHRP Project 1-26 recommended mechanistic-empirical analysis and design procedures for reliable relationships between traffic loading, environmental and material conditions, and pavement distress for use with the AASHTO procedures. These recommendations are under development. Thus, the models selected for use in the NCHRP 1-26 project were accepted and incorporated into the AAMAS.

Scope of Manual

This manual (Part I) is divided into five sections including suggested guidelines for (1) selection of mixture components, (2) mixture design (3) mixture analyses, (4) mixture performance evaluations, and (5) mixture design example. The first section provides criteria and values recommended for selecting the mixture components, and Section 2 presents the procedures used to design dense-graded asphaltic concrete mixtures. Figure 2 shows the mixture design procedure in flow chart form. Section 3, the mixture analyses section, includes procedures for preparing, conditioning, and testing specimens for measuring properties required for structural design and evaluation. Section 4, the mixture performance evaluation, discusses mechanistic-empirical models used to evaluate asphaltic concrete pavements. Section 5 is an example problem for mixture design and evaluation using AAMAS.

Figure 3 shows the current AAMAS procedure in flow chart form, identifying the four sections, and Table 1 summarizes the approximate time required for the laboratory compaction, conditioning, and testing of asphaltic concrete mixtures. As shown, a large number of specimens are compacted to the air void content established from the construction specifications, because this represents the more critical condition for fracture type distresses and moisture damage. Currently, AAMAS is limited to hot-mixed asphaltic concrete, which includes binders, aggregates, and modifiers used in construction, and provides an evaluation for the four major forms of distress (both load and environmental).

Future Improvement of AAMAS

Although the initial use of AAMAS is to check specific mixtures for resistance to various forms of distress, the ultimate use, when fully developed and after correlations with field performance, will be to optimize the structural and mixture design process to produce the desired pavement performance at least cost. NCHRP Project 9-6(1) is the first step in the evolutionary process to design asphaltic concrete mixtures based on performance-related criteria, and to tie mixture design to structural design. The

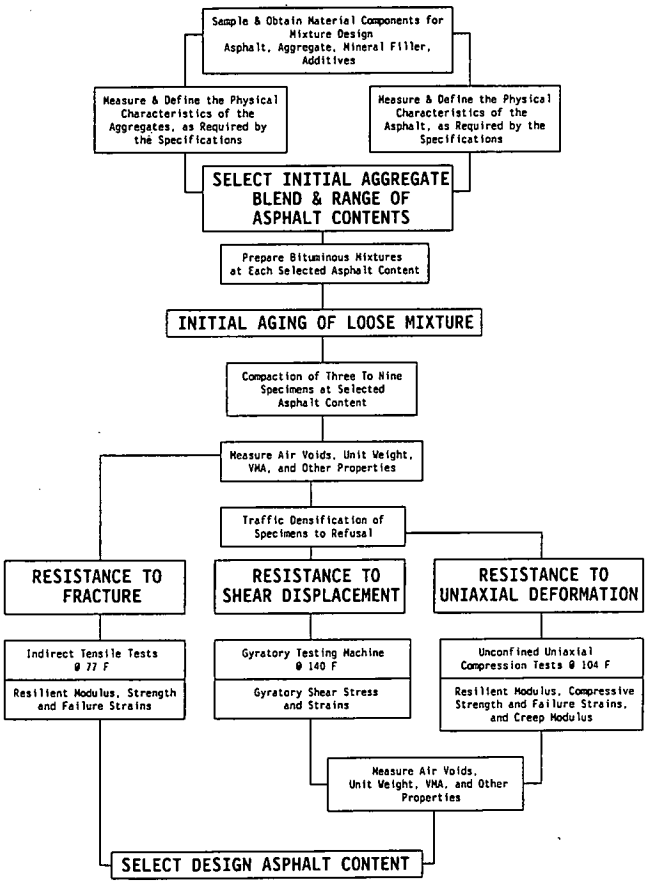

Figure 2. Flow chart for the design of dense-graded asphaltic concrete mixtures.

next step of the evolutionary process is being initiated through a coordinated national asphalt research program that includes different sponsors and studies, each accomplishing important goals for the final product. These ongoing studies and funding agencies are listed, as follows:

Study Number	Study Title	Study Sponsor
1-26	Calibrated Mechanistic Structural Analysis Procedures for Pavements	NCHRP
10-26A	Performance-Related Specification for Hot-Mix Asphalt Concrete	NCHRP
DTFH61-89-C-00015	Development of Performance-Related Specifications for Asphaltic Concrete—Part II	FHWA
A001	Asphalt Experimental Design, Coordination, and Control of Mixture	SHRP
A002A	Binder Characterization and Evaluation	SHRP
A003A	Performance-Related Testing and Measuring of Asphalt-Aggregate Interactions and Mixtures	SHRP
A003B	Fundamental Properties of Asphalt-Aggregate Interaction Including Adhesion and Absorption	SHRP
A004	Asphalt Modification Practices and Modification	SHRP
A005	Performance Models and Validation of Test Results	SHRP
A006	Performance-Based Specifications for an Asphalt-Aggregate Mixture Analysis System	SHRP

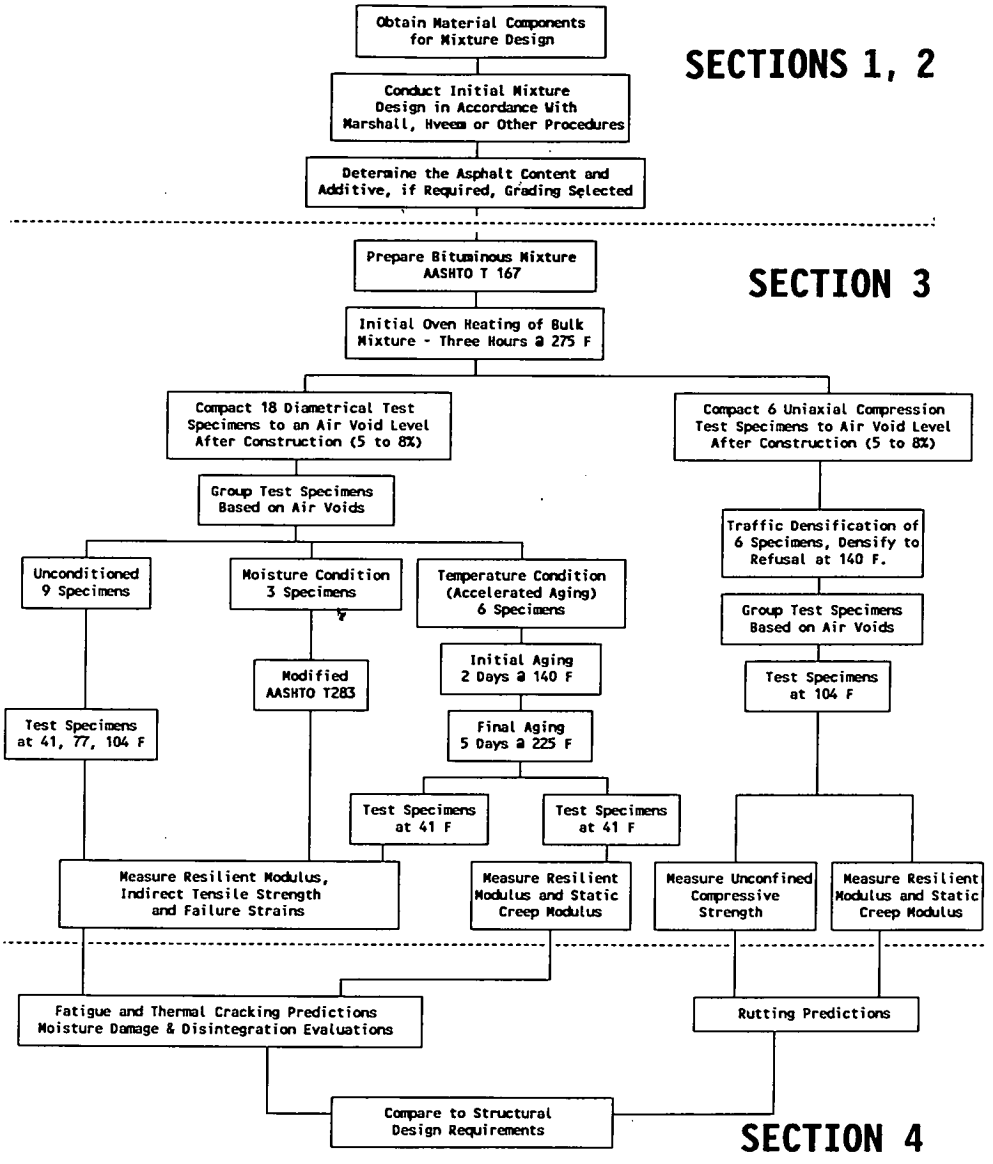

Figure 3. Flow chart for the AAMAS procedure.

The SHRP A006 project is to combine all findings within each study to develop specifications for the selection of type and gradation of aggregate, type and amount of asphalt cement, and type and amount of additive, if required, and to provide guidelines for AAMAS adoption. In addition, the SHRP Long-Term Pavement Performance (LTPP) studies should provide the much-needed field performance data along with the asphaltic concrete fundamental engineering properties to optimize the structural and mixture design process. The overall goal of all of these research projects is to maximize the performance of asphaltic concrete pavements and reduce life-cycle costs.

Table 1. Summary of the approximate time required for the laboratory compaction, conditioning, and testing of asphaltic concrete mixtures using AAMAS.

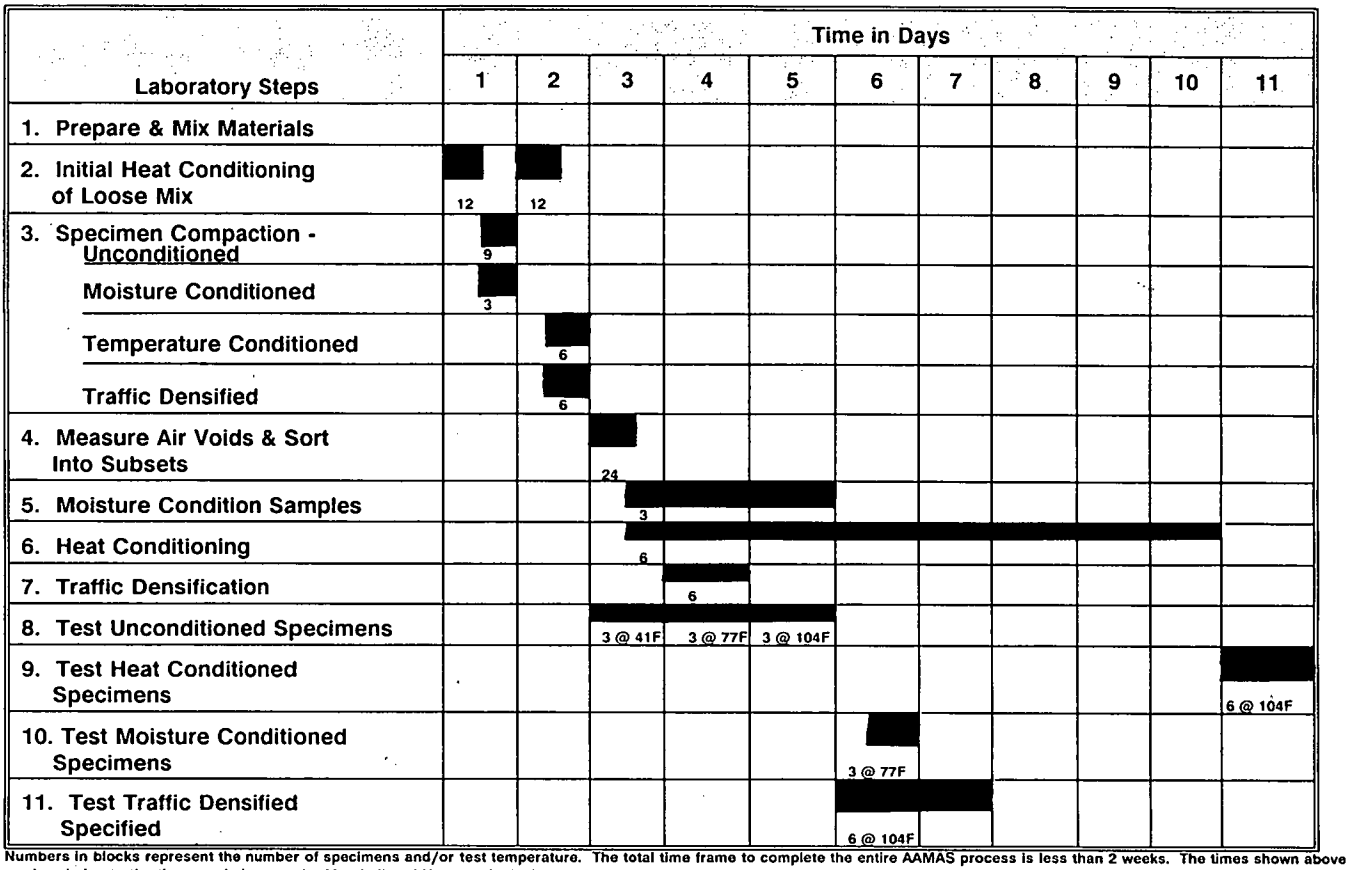

Numbers in blocks represent the number of specimens and/or test temperature. The total time frame to complete the entire AAMAS process is less than 2 weeks. The times shown above are in relation to the time needed to run the Marshall and Hveem mix design methods.

SECTION 1
GUIDELINES FOR SELECTION OF MIXTURE COMPONENTS

1.1 SCOPE

The overall design process for asphaltic concrete mixtures is a compromise between several mixture characteristics. Traditionally, mixture characteristics used for design have included stability, durability, unit weight and air voids. More recently, fundamental engineering properties have been considered in the mixture design process. Some of these properties are indirect tensile strength, resilient modulus, creep modulus, and indirect tensile strain at failure. All of these properties are dependent, to some degree, on asphalt content.

These fundamental engineering properties are also dependent on the material factors and traditional mixture characteristics used in mixture design. For example, resilient modulus has been found to be dependent on air voids, asphalt viscosity, asphalt content, and minus 200 material, to name four parameters. Thus, in selecting the design asphalt content for a dense-graded mixture, gradation, minus 200 material, air voids, voids in mineral aggregate (VMA), and voids filled with asphalt (VFA) are factors to be considered in determining the job mix formula target and, as such, limit the number of possible alternatives for preparing trial mixtures. As stated previously, the mixture design can be completed in accordance with the user agency's current practice, or in accordance with Section 2 of the Procedural Manual. Sections 3 and 4 of the manual are used to evaluate an asphaltic concrete mixture design using performance-related criteria.

1.2 MATERIALS

In many cases, the types of materials used become a choice restricted by economical considerations (i.e., the use of locally

available aggregates). AAMAS is not intended to restrict the use of local materials that could be marginal, but the intent is to evaluate their use in terms of pavement performance based on project specific conditions. However, the recommended procedures and practices outlined in the FHWA Technical Advisory T 5040.27, dated March 10, 1988, should be used as initial guidelines for producing asphaltic concrete mixtures for high-type facilities. Limiting values for some of the physical properties of the aggregate and asphalt that are suggested for use in T 5040.27 are given, in the following, for ready reference:

- Aggregates should be nonplastic. The minus No. 4 sieve material should have a minimum sand equivalent value of 45 in accordance with AASHTO Test Method T 176.
- The amount of clay lumps and friable particles should be less than 1 percent.
- The Los Angeles Abrasion Value should be 45 percent, or less, when measured in accordance with AASHTO T 96.
- The amount of plus No. 4 sieve material with two fractured faces should be at least 60 percent.
- The amount of natural sand should be limited to 20 percent for high-volume pavements and 25 percent for low-volume pavements.
- The ratio of dust (minus No. 200 sieve material) to asphalt cement by mass should be between 0.6 and 1.2.
- The low-temperature ductility test on the asphalt should be in accordance with Table 2 of AASHTO M 226.

1.3 GRADING CONSIDERATIONS

The guidelines for blending aggregates should be consistent with the FHWA 0.45 power gradation chart (Figure 4), using different combinations of coarse and fine aggregates, except that the fine fraction is adjusted to maintain adequate VMA and film thickness.

For dense-graded mixtures, gradations should be selected that are reasonably close to the FHWA 0.45 power gradation curves, but not so close that the VMA is so low as to allow an insufficient asphalt content (thin film thicknesses) to maintain adequate air voids. Theoretically, a gradation that follows the 0.45 power gradation curve will result in the maximum aggregate density that has few or no air voids (i.e., all spaces are filled with solids). The addition of asphalt to this maximum density gradation only serves to separate the aggregates particles, which reduces the shear strength of the mix and increases the potential for lateral flow.

Some state agencies have set limits on the "primary control" sieves to reduce the potential for lateral flow (i.e., plastic condition). The upper limiting values suggested by the WASHTO Committee from field observations of pavement distress are included in AAMAS for selecting an initial aggregate blend. These are:

Primary Control Sieve Size, No.	Maximum Percent Passing, %
4	55
10	37
40	16
200	3 to 7

For mixtures that support high tire pressures (greater than 100 psi) or heavy traffic loads, the amount of minus 200 material, as well as the quality of the aggregate, is very important. Typically, the amount of minus 200 material is limited to a value between 3 to 7 percent by weight for high tire pressures. Large amounts of minus 200 material can result in a low asphalt content leading to higher stability but lower durability. Small amounts of minus 200 material can result in the mixture requiring a higher asphalt content resulting in lower stabilities but higher durability. When tire pressures exceed 200 psi, it is suggested that 100 percent crushed materials be used, based on airfield performance data (*1*).

1.4 AIR VOIDS

Any mixture design procedure must, as a minimum, provide for acceptable voids in the mixture and an acceptable level of stability. The asphalt content selected is based on a target air voids content following a compaction procedure intended to simulate field compaction followed by additional densification caused by traffic. This is called final compaction, and the air void content associated with final compaction is called final voids content. These values are, of course, dependent on tire pressure, wheel load magnitudes and number of applications, and environmental conditions. For AAMAS, the percentage of the total volume that are air voids, V_a, is calculated using the following equation:

$$V_a = \left(1 - \frac{G_{mb}}{G_{mg}}\right) \times 100 \qquad (1\text{-}1)$$

where G_{mb} is bulk specific gravity of the compacted mixture, as measured by AASHTO T 166 or T 275, whichever applies; and G_{mg} is maximum specific gravity of the paving mixture, measured in accordance with AASHTO T 209.

A final or design air void range of 3 to 5 percent has been found to be acceptable in most environments. Program "ASPHALT," developed by Jimenez (*2*), can be used initially to estimate the relationship between asphalt content, asphalt film thickness, and air voids for different aggregate blends prior to preparing specimens for mixture design. This program calculates the asphalt film thickness as a function of asphalt content and gradation. The results can be used to look at numerous combinations of materials in order to select candidate job mix formulas (JMFs) prior to running any laboratory mixture design tests. Program ASPHALT was calibrated based on specimens compacted in the laboratory using kneading compaction.

If program ASPHALT is unavailable to the user, local experience must dictate the gradation to be initially selected. Without the use of program ASPHALT or experience, optimization becomes more of a trial and error process or a relative optimization of a few variables.

1.5 VMA AND VFA CONSIDERATIONS

Both VMA and VFA have been considered as mixture design parameter specifications. The Asphalt Institute and many state highway agencies have adopted minimum VMA requirements for mixture design. The Corps of Engineers and Federal Aviation Administration have adopted limits on final air voids of 3 to 5 percent and a VFA requirement of 75 to 85 percent to ensure

HOT-MIX ASPHALT DESIGN

DATE : _____ TECHNICIAN : _____ LAB. NO. _____

PROJECT : _____ FILE NO. _____

GRADATION CHART

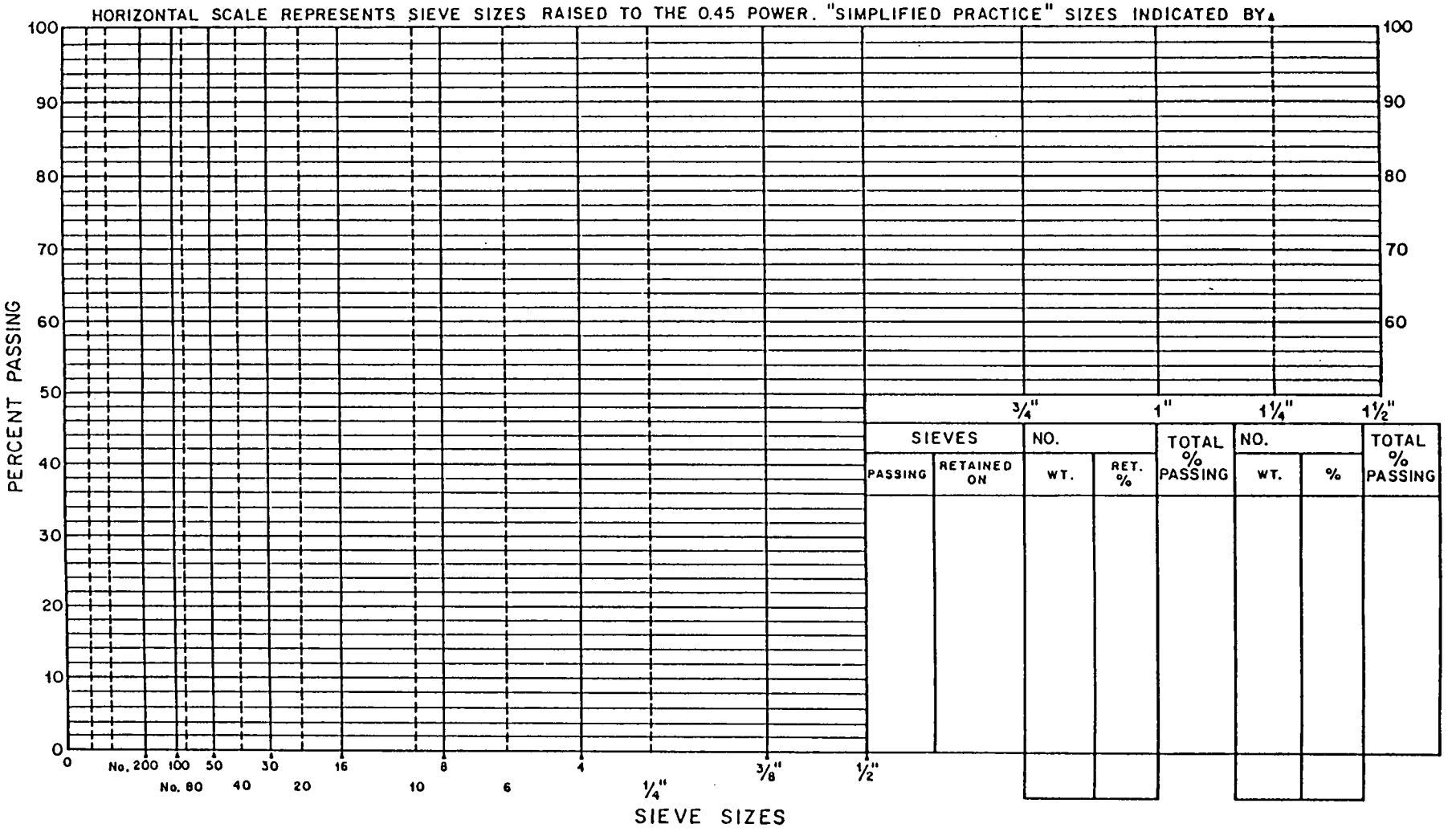

Figure 4. FHWA 0.45 power gradation chart.

the mixture's durability. For purposes of selecting a JMF and a design asphalt content, the following guidelines are suggested for VMA and VFA (unless local experience suggests a tighter control):

Property	Maximum Aggregate Size, In.	Suggested Minimum Value	Suggested Maximum Value
VMA	1½	12*	20
	1	13*	20
	¾	14*	21
	½	15*	21
VFA	---	75	85

*Taken directly from the Asphalt Institute's MS-2 Manual.

Both VMA and VFA are volume percentages, and are calculated using the following two equations:

$$VMA = 100 - \frac{G_{mb}P_s}{G_{sb}} \quad (1\text{-}2)$$

$$VFA = \frac{VMA - V_a}{VMA} \quad (1\text{-}3)$$

where P_s is aggregate percent by total weight of mixture, %; and G_{sb} is bulk specific gravity of the combined aggregate blend.

The aggregates used in the laboratory during mixture design are in a dry condition, and during production are assumed to be dry when mixed with the asphalt cement. Thus, it is necessary that the bulk specific gravity of the combined aggregate blend, G_{sb}, be determined and used during mixture design. As defined in AASHTO T 85, "The bulk specific gravity is the ratio of the weight in air of a unit volume of aggregate (including the permeable and impermeable voids in the particles, but not including the voids between particles) at a stated temperature to the weight in air of an equal volume of gas-free distilled water at a stated temperature." Using this definition, VMA calculated with Eq. 1-2 excludes the voids in the aggregate that are both impermeable and permeable to asphalt.

1.6 ASPHALT CONTENT AND DENSENESS

The behavior of most mixtures is dependent on the fluids content and denseness of that mixture. The denseness of a mixture is usually described by three fundamental terms or properties. These are air voids, porosity, and degree of saturation, all of which are volume quantities that cannot be weighed.

The porosity of a material or mixture is defined as the percentage of total volume that are voids. This is the same terminology used for VMA of asphaltic concrete mixtures. The degree of saturation of a mixture is defined as the percentage of total voids that are filled with fluid, which is the same terminology as VFA. Air voids were discussed in subsection 1.4, and are a percentage of the total volume. Thus, a paving mixture must first be analyzed on a volume basis, even though a weight basis is needed and used for practical reasons, such as plant and field control. In addition, a volume basis also normalizes the differences between mixes caused simply by different aggregate specific gravities.

The total volume of an asphaltic concrete sample is considered to be 100 percent bulk volume, and the proportion of each material component can be designated in terms of its 100 percent bulk volume. The bulk volume of each material can be converted into a weight for plant and field control by multiplying its bulk volume by the materials specific gravity and by 62.4 pcf, the unit weight of water. The percentage of total bulk volume that is asphalt, V_b, is calculated using Eq. 1-4:

$$V_b = P_a\left[\frac{G_{mb}}{G_a}\right] \quad (1\text{-}4)$$

where P_a is percent of asphalt by total weight of mixture, %; and G_a is specific gravity of the asphalt cement.

The bulk specific gravity of the aggregate blend is used because the aggregates are in a dry condition prior to mixing. After mixing, however, some of the asphalt cement is absorbed into the permeable voids of the aggregate, which are included in the aggregate bulk specific gravity measurement, G_{sb}. This amount of absorbed asphalt must be accounted for and considered in the laboratory during mixture design. In other words, the amount of asphalt cement binder must be adjusted or increased to account for that portion that is absorbed into the permeable voids of the aggregate.

The effective asphalt content by total volume, V_{be}, becomes an important variable regarding the fundamental engineering and compaction properties of the mixture. The effective asphalt content by total volume is simply the total asphalt content minus the asphalt content absorbed by the aggregate. This value is calculated using:

$$V_{be} = G_{mb}\left[\frac{100}{G_{mg}} - \frac{P_s}{G_{sb}}\right] \quad (1\text{-}5)$$

Unfortunately, absorption is a time-dependent variable, so the effective asphalt content is also time dependent. Thus, the time interval between initial mixing and initial compaction (both in the laboratory and on the roadway) becomes important, especially for highly absorptive aggregates. A time delay between mixing and compaction allows some of this absorption to occur, and is considered in both the mixture design (Section 2) and the AAMAS (Section 3) procedures. This time delay was based on physical properties of the asphalt to minimize some of the differences between the laboratory and plant and field conditions.

The percentage of total volume of absorbed asphalt, V_{ba}, can be calculated in accordance with Eq. 1-6:

$$V_{ba} = P_{ba}P_s\left(\frac{G_{mb}}{G_a}\right) \quad (1\text{-}6)$$

where P_{ba} is percent absorbed asphalt by weight of aggregate, %:

$$P_{ba} = G_a\left(\frac{G_{se} - G_{sb}}{G_{sb}G_{se}}\right) \times 100 \quad (1\text{-}7)$$

and G_{se} is effective specific gravity of the combined aggregate blend:

$$G_{se} = \frac{100 - P_a}{\frac{100}{G_{mg}} - \frac{P_a}{G_a}} \quad (1\text{-}8)$$

The effective specific gravity of the aggregate, G_{se}, is defined as the ratio of the weight in air of a unit volume of a permeable material (including only those voids impermeable to asphalt) at a stated temperature to the weight in air of equal density of an equal volume of gas-free distilled water at a stated temperature.

The aggregate unit weight is plotted as a function of the effective asphalt content by volume (Eq. 1-5) to select the value that will result in the maximum aggregate density for a specified compactive effort.

SECTION 2
GUIDELINES FOR MIXTURE DESIGN

2.1 SCOPE

2.1.1. The AAMAS procedures for mixture design cover the measurement of the resistance to fracture, to uniaxial deformation, and to shear displacements of cylindrical specimens of bituminous paving mixtures. The procedures are intended for use with dense-graded mixtures containing asphalt cement, and exclude open-graded friction courses and drainage layers. AAMAS accommodates those mixture variables normally used in the construction of asphalt paving mixtures, such as binders, aggregates and fillers, and provides the data required for the design of mixtures to resist selected asphalt pavement distresses associated with both wheel loads and the environment.

2.1.2. The results from the conditioning and testing of laboratory-prepared specimens at different asphalt contents are used to select the design asphalt content and allowable tolerance for project specific conditions.

2.2 SUMMARY OF PROCEDURE

2.2.1. Nine test specimens at selected asphalt contents are tested. Three specimens per asphalt content are tested at 77°F (25°C) using diametral loadings (indirect tensile testing techniques) to define the fracture characteristics of the specimens. A second set of three specimens at each asphalt content are compacted and tested using the Corps of Engineers Gyratory Testing Machine (GTM). The GTM device is used to estimate the change in shear characteristics under repeated loads at 140°F (60°C). Using the results of the indirect tensile and gyratory shear tests as a guide, a final set of three specimens at selected asphalt contents are tested at 104°F (40°C) using uniaxial compression loads to define the deformation and creep characteristics of the mixture.

2.2.2. The design asphalt content and range of allowable values are determined from these test results using performance-related criteria. Density, air voids, VMA, and VFA are also considered in selecting the design asphalt content.

2.2.3. A full-scale design for mix optimization includes nine specimens at each asphalt content (three for indirect tensile testing, three for uniaxial compression testing, and three for gyratory shear testing). If five asphalt contents are used, a total of 45 test specimens is required. However, a full-scale design is only required when the user agency has little or no previous experience with these tests. A more realistic and practical approach is to use the indirect tensile strength and resilient modulus tests (performed on the same specimen) to select an initial design value and an allowable range of asphalt contents based on fracture (subsection 2.7). The fracture criteria will generally establish the most upper limit of asphalt contents. At this initial design value, three specimens are tested using the GTM in accordance with subsection 2.8. If these results do not exceed the minimum design requirements, additional specimens are prepared and tested at lower asphalt contents to redefine the design value and an allowable range of asphalt contents that satisfy the fracture and shear resistance criterion. At this revised design value, three specimens are tested using uniaxial compression testing techniques, in accordance with subsection 2.9, to ensure that the revised design value will satisfy the deformation or creep criteria. In other words, the GTM (subsection 2.8) and uniaxial compression (subsection 2.9) specimens are used as "checks and balances" for the paving mixture designs based initially on fracture. Using this approach and assuming five initial asphalt contents, the number of test specimens required for mixture design can vary from 21 (15 for indirect tensile testing, 3 for gyratory testing, and 3 for uniaxial compression testing) to 45.

2.3 SIGNIFICANCE AND USE

2.3.1. The results of the deformation and strength tests can be used for specifications and mixture design purposes. These procedures are also intended to provide fundamental engineering properties of the mixture that are required for evaluating asphaltic concrete pavements. In other words, these test procedures provide values that can be used to characterize asphaltic concrete mixtures for use in pavement thickness design and in structural analysis of layered pavement systems, under a variety of stress states and temperature conditions.

2.3.2. The indirect tensile test method also provides the information required for determining the structural layer coefficient of asphaltic concrete surface and base course mixtures for use with the 1986 AASHTO "Guide for Design of Pavement Structures."

2.4 APPLICABLE DOCUMENTS

2.4.1 AASHTO Standards.

T 166 Bulk Specific Gravity of Compacted Bituminous Mixtures
T 167 Compressive Strength of Bituminous Mixtures
T 209 Maximum Specific Gravity of Bituminous Paving Mixtures
T 245 Resistance to Plastic, Flow of Bituminous Mixtures Using Marshall Apparatus
T 246 Resistance to Deformation and Cohesion of Bituminous Mixture by Means of Hveem Apparatus
T 269 Percent Air Void in Compacted Dense and Open Bituminous Paving Mixtures
T 275 Bulk Specific Gravity of Compacted Bituminous Mixtures Using Paraffin-Coated Specimens

2.4.2. ASTM Standards.

D 3387 Compaction and Shear Properties of Bituminous Mixtures by Means of the U.S. Corps of Engineers Gyratory Testing Machine (GTM)
D 3497 Dynamic Modulus of Asphalt Mixtures
D 4013 Preparation of Test Specimens of Bituminous Mixtures by Means of Gyratory Shear Compactor
D 4123 Indirect Tension Test for Resilient Modulus of Bituminous Mixtures

2.5 APPARATUS

2.5.1. Equipment for preparing and compacting specimens is required from one of the following methods: ASTM D 3387 (Method A) or D 4013 (Method B). However, ASTM D 3387 is required for the test method specified in subsection 2.8. The use of an oil-filled roller is specified in ASTM D 3387, but the air-roller is the preferred device. Both rollers are interchangeable in the GTM, but the gyratory shear stresses (subsection 2.8) and initial air voids will be different. The use of the oil-filled roller will result in higher gyratory shear stresses than for the air roller. The use of both rollers is permitted until pavement performance data are collected that may dictate the use of one over the other. Table 2 gives the compactive efforts recommended for each type of roller for initially compacting the test specimens. If an air or oil-filled roller from ASTM D 3387 is unavailable, the mixture design is based only on the test results from subsections 2.7 and 2.9.

2.5.2. A forced air draft oven is required that is capable of maintaining a temperature up to 325 ± 5.4°F (163 ± 3°C).

2.5.3. Aluminum pans are required that have a surface area of 100 to 180 in.^{2} (0.06 to 0.1 m^2) in the bottom and a depth of approximately 1 in. (2.54 cm).

2.5.4 Axial Loading Machine from ASTM D 4123.

Note 2.1: Any loading machine capable of providing a repetitive sinusoidal or square type compression load of fixed cycle in duration can be used. Typically, a cam and switch and timer control of solenoid valves operating a pneumatic air piston, or a closed-loop electrohydraulic system is used. Pneumatic systems are the simplest, while closed-loop electrohydraulic systems allow more versatility (variable wave forms, higher loads, and higher frequency response). Generally, a haversine wave form is characteristic of closed-looped electrohydraulic equipment, while rectangular wave forms are used with pneumatically operated loading equipment. Both wave forms can be used for resilient tests. A loading frequency of 1 cycle per second has been found to be satisfactory for most applications. With a pneumatic loading system, a square wave form with a load duration of 0.1 second and a rest period of 0.9 seconds is recommended.

Table 2. Compactive efforts recommended for the oil-filled and air-rollers to initially compact test specimens using the Corps of Engineers GTM device.

VARIABLE	TYPE OF ROLLER	
	AIR ROLLER	OIL-FILLED ROLLER
Initial Angle of Gyration, Degrees	3	2
Vertical Pressure, psi (kPa)	90 (620)	120 (827)
Number of Revolutions	15	12

2.5.5 Specimen Axial Deformation Measurement Devices from ASTM D 4123.

Note 2.2: The resilient modulus, creep modulus, and indirect tensile strength tests require deformation transducers with a sufficient range to cover the cumulative deformation during the test and also a high resolution for the smallest resilient strains to be measured. The linear variable differential transducer (LVDT) is generally considered to be the most suitable deformation transducer for the test.

Note 2.3: LVDT Clamps are used to hold the LVDTs in place during indirect tensile testing. There are different sample holding devices that can be used in the test program. One such device is described in ASTM D 4123, and another in Federal Highway Administration Report No. FHWA/RD-88/118 (3,4). Either of these devices can be used provided that the specimen has smooth surfaces, and is centered under the axial load (i.e., no load eccentricity). For uniaxial compression loadings LVDT clamps are not required if a friction reducing material is placed between the specimen and top and bottom platens. Thin Teflon tape can be used as a friction reducing material.

2.5.6 Specimen Axial Load Measurement Device from ASTM D 4123.

Note 2.4: The axial load measuring device is an electronic load cell. The load may be measured by placing the load cell between the specimen cap and the loading piston. The total load capacity of the load transducer (load cell) should be of the proper order of magnitude with respect to the maximum total loads to be applied to the test specimen. Generally, its capacity should be no greater than five times the total maximum load applied to the test specimen to ensure that the necessary measurement accuracy is achieved. The axial load-measuring device shall be capable of measuring the axial load to an accuracy within 1 percent of the applied axial load.

2.5.7 Recording Device from ASTM D 4123.

Note 2.5: Specimen behavior is evaluated from continuous time records of applied load and specimen deformation. Commonly, these parameters are recorded on a multichannel strip-chart recorder. Analog to digital data acquisition systems may be used provided that data can be converted later into a convenient form for data analysis and interpretation. Fast recording system response is essential if accurate specimen performance is to be monitored.

Note 2.6: For analog strip-chart recording equipment, the load and deformation recorder trace must be of sufficient amplitude and time resolution to enable accurate data reduction. Resolution of each variable should be better than 2 percent of the maximum value being measured. To take advantage of recorder accuracy and for subsequent data analysis 2 to 4 cycles per inch of recording paper is acceptable. The clarity of the trace with respect to the background should provide sufficient contrast and minimum trace width, so that the minimum resolution of 2 percent of the maximum value of the recorded parameter is maintained, and the trace should be included in the reports.

Note 2.7: For uniaxial compression testing, the number of recording channels can be reduced by wiring the leads from the LVDTs so that only the average or total signal from a pair is recorded. For indirect tensile loadings, the signal from each LVDT shall be recorded separately.

This permits observation of individual LVDT readings, rather than an average or total signal, to determine if significant differences are being recorded between the two LVDTs. If the differences between LVDTs is large, the specimen shall be repositioned.

2.5.8. Calibration of Equipment. If multichannel strip recorders are used, calibration of the measurement transducers through the recording system is essential. In this case, the calibration shall be recorded periodically (at least once a week when in use) to provide a permanent record. If the LVDTs are wired pairs, such that the total deformation is measured, they must be calibrated together, not separately.

2.5.9. The use of a loading jack and ring dynameter from AASHTO T 245, or a mechanical or hydraulic testing machine from AASHTO T 167, is required to provide a range of accurately controllable rates (within 5 percent) of vertical deformation including 0.05 and 2 in. per min (1.27 and 50.8 mm per min).

2.5.10. Temperature and Control System. The temperature control system shall be capable of control over a temperature range from 77 to 104°F (25 to 40°C) and within ± 1.8°F (1°C) of the specified temperature within the range. The system can be a room, chamber and/or cabinet that shall be large enough to hold at least three specimens for a period of 12 hours prior to testing. If the testing machine is located in a room without the specified temperature control system, a controlled temperature cabinet shall be used during the entire test.

2.5.11. Other required equipment for specific types of tests are listed separately under subsections 2.7, 2.8, and 2.9.

2.6 PREPARATION OF MIXTURES

2.6.1. Prepare the asphaltic concrete mixture in accordance with AASHTO T 167, with the exception that sufficient mixture should be prepared to compact at least three specimens per test at any one time. The amount of mixture required is dependent on the specimen size, which is provided in subsections 2.7, 2.8, and 2.9. The mixing temperature should be selected in accordance with AASHTO T 246 (see Note 2.8).

Note 2.8: Mixture mixing and compaction temperatures will generally be somewhere in the range of 250 to 325°F (121 to 149°C). Some agencies use AASHTO T 245 to determine the mixing and compaction temperatures, whereas others use AASHTO T 246. Selection of the mixing and compaction temperatures should be consistent with plant operations and mixture production. More importantly, once the mixing temperature is selected it should be controlled so that the viscosity of the bitumen will not vary more than ± 50 centistokes during the mixing/compaction process.

2.6.2 Initial Heat Conditioning.

2.6.2.1. After initial mixing, the mixture shall be placed in an aluminum pan having a surface area of 100 to 180 in.^{2} (0.06 to 0.1 m^2) at the bottom and a depth of approximately 1 in. (2.54 cm). The mixture shall then be placed in a forced draft oven set at 275°F (135°C) for 1.5 hours (± 5 min) of heating. The pan shall be placed on spacers to allow air circulation under the pan, if the shelves are not perforated.

2.6.2.2. After 1.5 hours of heating at 275°F (135°C), the pan shall be removed from the oven and the mixture remixed in the pan with a hand-mixing tool. After remixing, the pan is replaced in the oven for an additional 1.5 hours (± 5 min) of heating.

Note 2.9: The purpose of this heating time is to simulate plant hardening (as defined by the penetration and viscosity values) and allow some of the asphalt absorption to occur prior to compaction. This heating time should be expected to vary for different asphalt concrete mixtures and plants (drum mix versus batch plants). The 3 hour time interval specified above is an approximate time that should be verified in the laboratory for the specific asphalt and plant being used. For those cases when the asphalt plant is unavailable and there is no historical data, the Thin-Film Oven Test (AASHTO T 179) can be used to estimate the asphalt properties (penetration and viscosity) after mix production.

2.6.3. After initial heat conditioning, a representative sample of the mixture shall be taken and allowed to cool. The maximum theoretical specific gravity of this sample shall be measured in accordance with AASHTO T 209.

2.6.4. Compaction of the laboratory test specimens is discussed in subsections 2.7, 2.8, and 2.9 for specific types of tests. A set of at least three specimens is compacted at selected asphalt contents for each type of test. For resistance to fracture (subsection 2.7) and shear displacements (subsection 2.8), a set of specimens at each asphalt content shall be compacted and tested. For resistance to uniaxial deformations, a set of specimens only need to be compacted and tested at those allowable asphalt contents established by the resistance to fracture and shear displacement. Compaction of these sets of test specimens for indirect tensile and gyratory shear testing can commence immediately after initial heat conditioning. Compaction of the uniaxial specimens should be delayed until the results from the indirect tensile and gyratory shear tests are known and can be used to select those asphalt contents to be considered for resistance to uniaxial deformations.

Note 2.10: The gyratory-shear molding press is recommended for use in compacting all test specimens for mixture design. However, many agencies may not have access to the compaction devices specified in ASTM D 3387 nor D 4013. If a gyratory-shear molding press is unavailable, test specimens can be compacted using kneading compaction (AASHTO T 247), so that the agency can become familiar with the test procedures and engineering properties recommended for consideration in mixture design. It should be understood, however, that the type of device used for compacting the test specimens can have an effect on some of the engineering and compaction properties. The Marshall Hammer (AASHTO T 245) is not recommended for use in compacting test specimens for determining the engineering properties of asphalt concrete mixtures.

2.7 RESISTANCE TO FRACTURE

2.7.1 Apparatus. Diametral loading strips are specified from ASTM D 4123.

2.7.2 Compaction of Test Specimens.

2.7.2.1. The specimens to be tested shall have a diameter of 4 in. (10 cm) for mixtures that contain aggregates with a maximum aggregate size of 1.0 in. (2.5 cm) or less, or a minimum diameter of 6 in. (15 cm) for mixtures that contain maximum size aggregates up to 1.5 in. (3.8 cm) in diameter.

2.7.2.2. The height of all diametral specimens to be tested shall be at least one-half the diameter of the specimen. If possible, the height should approximate the compacted lift thickness on the roadway, unless the previous statement is violated.

2.7.2.3. A minimum of three specimens per asphalt content shall be compacted. The mixture shall be compacted using the procedure as in accordance with ASTM D 3387 (Method A) or ASTM D 4013 (Method B), with the following exceptions.

2.7.2.3.1. The mixture compaction temperature should be in accordance with AASHTO T 246 (see Note 2.8).

2.7.2.3.2. Method A, ASTM D 3387. Set the initial angle of gyration and the vertical pressure in accordance with Table 2 for the type of roller being used. The total number of revolutions used to initially compact the specimen is given also in Table 2.

2.7.2.3.3. Method B, ASTM D 4013. The pregyration stress shall be 60 psi (414 kPa), the number of gyrations used shall be 12 (or four sets of three gyrations each), and no end point stress shall be used during initial compaction.

2.7.2.4. After compaction, the specimens shall be cooled to room temperature and then extracted from the molds. All test specimens shall be marked and numbered to identify the mixture and percent asphalt used.

2.7.2.5. Two diametral axes shall be marked on each test specimen. The two axes shall be perpendicular to one another.

2.7.3 Testing Procedure.

2.7.3.1. Measure the bulk specific gravity of each test specimen in accordance with AASHTO T 166 or T 275, whichever applies.

2.7.3.2. Place the test specimens in a controlled temperature cabinet and bring them to the test temperature of 77 ± 1.8°F (25 ± 1°C). Unless the temperature is monitored and the actual temperature known, the specimen should remain in the cabinet at the specified test temperature for at least 12 hours prior to testing.

Note 2.11: The specimen must be dry prior to resilient modulus and indirect tensile strength testing. Moisture retained in the permeable voids will have an effect on the test results.

2.7.3.3. Place the test specimen in the loading apparatus, position as stated in Test Method ASTM D 4123, adjust and balance the electronic measuring system, as necessary.

2.7.3.4. Precondition the specimen by applying a repeated haversine (or other suitable wave form) to the specimen without impact, using a loading frequency of 1 cps (0.1-sec load duration and 0.9-sec rest period) for a minimum period sufficient to obtain uniform deformation readout (less than 2 percent deviation). In most cases, a preconditioning time of 25 to 45 sec is sufficient (25 to 45 loading cycles). The fixed load applied to the specimen is that which will result in a horizontal deformation greater than 0.0001 in. (0.00254 mm). Normally, the load established by this criterion will induce a tensile stress in the range of 5 to 20 percent of the indirect tensile strength.

2.7.3.5. After preconditioning, measure the total and instantaneous resilient deformations for the next three loading cycles along each of the two axes marked from paragraph 2.7.2.5. A loading frequency of 1 cps (0.1-sec load duration and 0.9-sec rest period) shall be used. The total resilient modulus is the parameter used for mixture design. The instantaneous resilient modulus is used for information purposes only.

2.7.3.5.1. The total resilient horizontal deformation shall be measured in accordance with ASTM D 4123.

2.7.3.5.2. The instantaneous resilient horizontal deformation shall be measured at the time defined as twice the time interval from load application (or horizontal movement) to peak horizontal movement (see Figure 5).

2.7.3.6. After the resilient modulus test is completed, apply a compressive load at a controlled deformation rate of 2 in. (5 cm) per min along the axis with the larger resilient deformations. If the specimen must be rotated to the first axis tested, a sufficient number of loading cycles are to be applied to ensure that the loading strips are properly seated. In most cases, 10 to 25 additional loading cycles are adequate. However, at the higher asphalt contents, indentation of the loading strips into the test specimen is possible. This condition is undesirable. If these indentations are observed, the tensile and compressive stresses will vary; therefore, the fewest number of loading cycles should be used as possible.

2.7.3.7. Measure both the vertical and horizontal deformations during the entire loading time, or until the load sustained by the specimen begins to decrease. It is recommended that the test be stopped prior to fracturing the specimen, so that damage to the horizontal deformation measuring equipment does not occur (Figure 6).

2.7.4. Calculations.

2.7.4.1. For each specimen tested, calculate the total resilient modulus, E_{RT}, for the last 3 cycles after the preconditioning part of the procedure (paragraph 2.7.3.5), and plot the results on Figure 7. The instantaneous resilient modulus can be calculated for information purposes, if needed.

$$E_{Rt} = \frac{P}{hH_R}(A_3 + A_4\nu_R) \qquad (2\text{-}1)$$

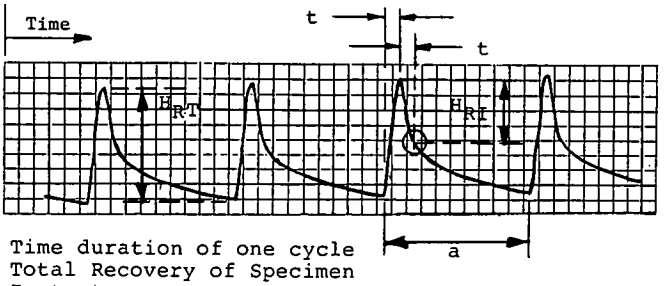

a = Time duration of one cycle
H_{RT} = Total Recovery of Specimen
H_{RI} = Instantaneous Recovery of Specimen
t = Time duration from initial specimen response from load application to the peak of deformation

Figure 5. Typical deformation (horizontal or vertical) versus time relationship for repeated-load indirect tensile test using a haversine wave form.

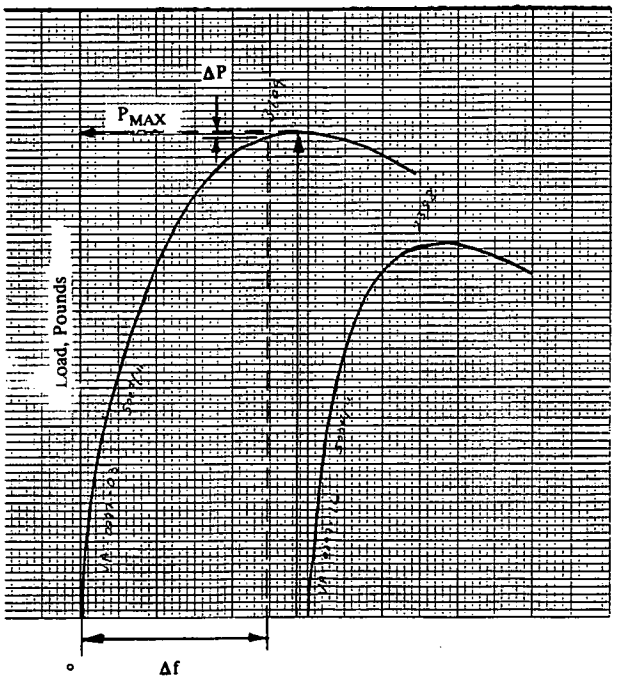

Horizontal Deformation, inches

P = Maximum load sustained by the specimen.
Δf = Total horizontal deformation at failure or yielding.
ΔP = Change in load at which yield or failure is assumed; Less than a 1% increase in the total load.

Figure 6. Typical load versus horizontal deformation relationship for the indirect tensile strength test.

where P is applied load or repeated load, lb; H_R is total or instantaneous resilient deformation, whichever applies, measured along the horizontal axis, in.; h is height of specimen, in.; ν_R is resilient Poisson's ratio (assumed to be 0.35 for a test temperature of 77°F); A_3 equals 0.2692 for 4-in. (10 cm) diameter specimens, and 0.2714 for 6-in. (15 cm) specimens; and A_4 equals 0.9974 for 4-in. (10 cm) diameter specimens, and 0.9988 for 6-in. (15 cm) specimens.

2.7.4.2. For each specimen tested, calculate the indirect tensile strength, S_t, and plot the results on Figure 7. The indirect tensile strength is used for field control.

$$S_t = \frac{P_f \cdot A_0}{h} \tag{2-2}$$

where P_f is total load sustained by the specimen, lb; and A_0 equals 0.156 for 4-in. (10 cm) diameter specimens, and 0.105 for 6-in. (15 cm) specimens.

2.7.4.3. For each specimen tested, calculate the tensile strain at yield or failure ϵ_f, and plot the results on Figure 7.

$$\epsilon_h = \Delta_h \left[\frac{A_5 + \nu_R A_6}{A_1 + \nu_R A_2} \right] \tag{2-3}$$

where Δ_h is total horizontal deformation at failure or where yielding occurs, in. (see Figure 6); A_5 equals 0.03896 for 4-in. diameter specimens, and 0.01752 for 6-in. specimens; A_6 equals 0.1185 for 4-in. diameter specimens, and 0.05289 for 6-in. specimens; A_1 equals 0.0673 for 4-in. diameter specimens, and 0.0452 for 6-in. specimens; and A_2 equals 0.2494 for 4-in. diameter specimens, and 0.1665 for 6-in. specimens.

2.7.4.4. For each specimen, calculate the air voids in accordance with AASHTO T 269. These air voids represent the initial condition of the compacted mixture.

2.8 RESISTANCE TO SHEAR DISPLACEMENTS

2.8.1 Apparatus. A gyratory testing machine (GTM) and spacer blocks are specified in accordance with ASTM D 3387 (Method A). The use of an oil-filled roller is specified in ASTM D 3387, but use of the air-filled roller is preferred, if available. If a GTM device is unavailable, this section cannot be performed.

2.8.2 Compaction of Test Specimens.

2.8.2.1. After initial heat conditioning, compact at least three specimens at each asphalt content in accordance with ASTM D 3387 (Method A). The initial compaction shall be performed at an angle of gyration and a vertical pressure in accordance with Table 2 for the type of roller being used. The total number of revolutions used to initially compact the specimen is also given in Table 2.

2.8.2.2. After initial compaction, the specimens shall be cooled to 140°F ± 5.4°F (60°C ± 3°C) and left in the molds.

2.8.3 Testing Procedure.

2.8.3.1. Additional compactive effort is applied to the specimens to measure the decrease in air voids and the refusal air void content of the mixture under simulated loading conditions (see Note 2.12). For traffic densification, the angle of gyration is 2 degrees with a vertical pressure of 120 psi (827 kPa) and the specimen is densified using the procedure described in ASTM D 3387. The gyratory shear test shall be conducted along with the compaction test to determine and evaluate any reduction in the shear strength with number of gyrations.

Note 2.12: The compactive effort used to simulate traffic is dependent on many variables, some of which include number of axle loadings, axle weight, tire inflation pressure and type of tire. It is generally accepted that AASHTO T 247 has been a reasonable estimation of air voids after traffic, based on historical studies. However, as tire types change and inflation pressures increase, these compaction procedures may be inadequate. Unfortunately, little data exist to determine the effects of increased tire pressures and wheel loads on air voids and material properties. The following procedures are provided as guidelines, but they may need to be revised after sufficient data are collected to simulate, in the laboratory, variations of tire types and inflation pressures.

2.8.3.2. Densify the specimens to the refusal air void level; defined as the air void content at which there is no reduction in air void of the specimen with additional gyrations. Traffic simulation tests are performed up to 300 gyrations with the GTM (see Note 2.13). Initial sample height readings shall be obtained prior to densification and concurrently with roller pressure readings at 25, 50, 75, 100, 150, 200, 250, and 300 gyrations (see Note 2.14).

Note 2.13: ASTM D 3387 uses the oil-filled roller for the gyratory shear stress test. However, an air-roller can also be used and is believed to be more representative of mixture behavior under traffic. In either case, the test is performed on each specimen to evaluate the change in shear stress with number of revolutions. The design asphalt content selected to resist shear displacements appears to be independent of type of roller used.

HOT MIX ASPHALT CONCRETE DESIGN
GRAPHIC ANALYSES

MIXTURE DESIGN IDENTIFICATION NO:_____ DATE:_____

MIXTURE DESIGNATION:_____ PROJECT:_____

COMPACTION METHOD & DEVICE:_____

INDIRECT TENSILE STRENGTH, PSI

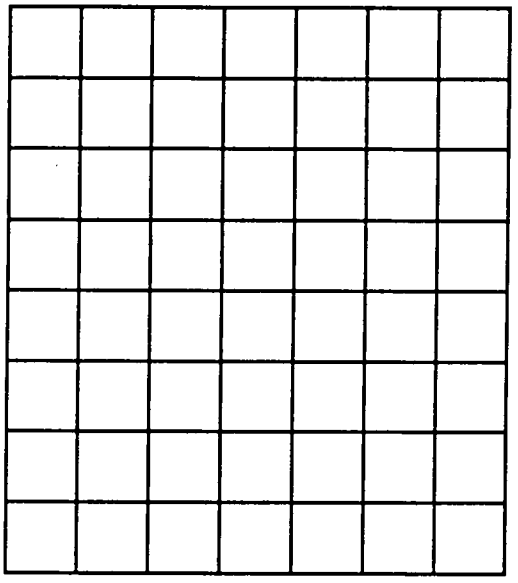

ASPHALT CONTENT BY VOLUME, %

UNCONFINED COMPRESSIVE STRENGTH, PSI

RESILIENT MODULUS, KSI

INDIRECT TENSILE

UNCONFINED COMPRESSION

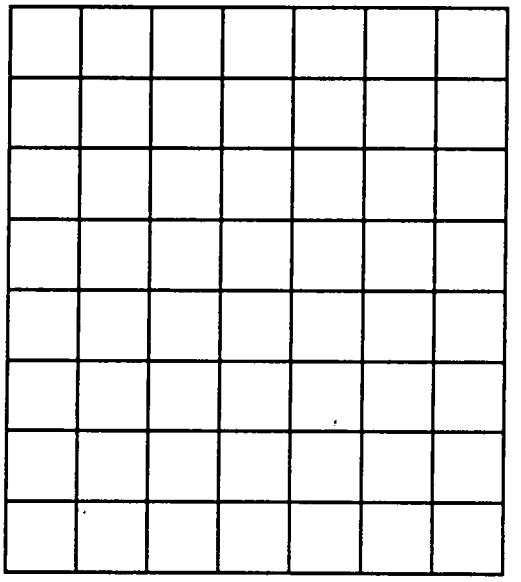

ASPHALT CONTENT BY VOLUME, %

STRAIN AT FAILURE, MILS, INCH

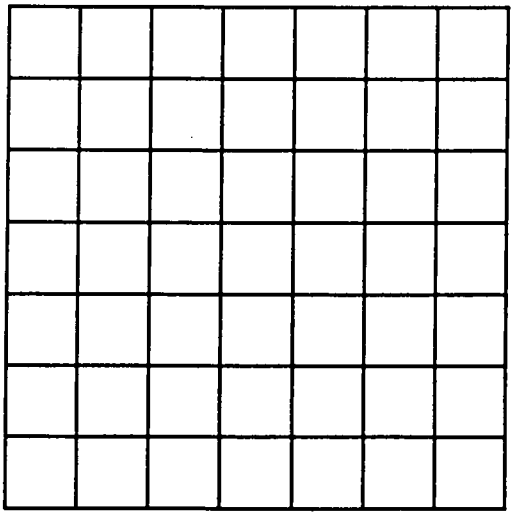

ASPHALT CONTENT BY VOLUME, %

CREEP MODULUS, KSI

GYRATORY SHEAR STRESS, PSI
(REVOLUTIONS=_____)

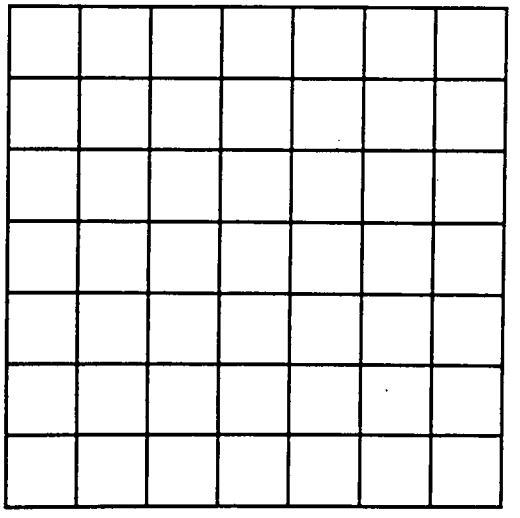

ASPHALT CONTENT BY VOLUME, %

Figure 7. AAMAS graphical presentation of mix design data for the engineering properties.

But, use of the oil-filled roller will result in higher gyratory shear stresses than those for the air roller.

Note 2.14: In some cases, mixture resistance may reduce excessively prior to 300 gyrations. An excessive reduction in air roller pressure and increase in angle of gyration may warrant stopping the test.

2.8.3.3. After densification, the bulk specific gravity of each specimen is measured in accordance with AASHTO T 166 or T 275, whichever applies.

2.8.4 Calculations.

2.8.4.1. Calculate the gyratory shear stress and other required values in accordance with ASTM D 3387. Plot the gyratory shear stress at the final number of revolutions versus asphalt content on Figure 7.

2.8.4.2. Calculate the air voids of each specimen in accordance with AASHTO T 269. These air voids represent the final condition of the compacted mixture.

2.9 RESISTANCE TO UNIAXIAL DEFORMATIONS

2.9.1 Apparatus. A gyratory shear molding press and gyratory mold are specified in accordance with ASTM D 4013 (Method B). The GTM, ASTM D 3387 (Method A), can also be used to compact specimens for uniaxial testing. However, mold sizes required are different from those specified in ASTM D 3387. Specimen size for uniaxial testing is described in paragraph 2.9.2.1.

2.9.2 Compaction of Test Specimens.

2.9.2.1. The uniaxial compression specimens to be tested shall have a height of at least 4 in. (10 cm) and a minimum diameter of 4 in. (10 cm) for mixes that contain aggregates with a maximum aggregate size of 1.0 in. (2.5 cm) or less, and a height of at least 6 in. (15 cm) and a minimum diameter of 6 in. (15 cm) for mixes that contain maximum size aggregates up to 1.5 in. (3.8 cm) in diameter.

2.9.2.2 Method A. ASTM D 3387 specifies the use of specimen heights different from those specified above. If molds are available to meet the specimen size requirements specified in paragraph 2.9.2.1, ASTM D 3387 can be used in accordance with the same traffic densification procedure described in paragraphs 2.8.2 and 2.8.3.

2.9.2.3 Method B—ASTM D 4013. If a GTM device is unavailable, the mixture shall be initially compacted using the procedure as in accordance with ASTM D 4013, with the following exceptions.

2.9.2.3.1. The mixture compaction temperature shall be in accordance with AASHTO T 246 (Note 2.8).

2.9.2.3.2. The pregyration stress shall be 90 psi (620 kPa).

2.9.2.3.3. Compactive effort is applied to these specimens to the refusal air void level. For most mixtures, 45 revolutions (or 15 sets of three revolutions each) of the gyratory molding press (ASTM D 4013) is sufficient to determine the final air void content (see Note 2.12).

2.9.2.3.4. After final compaction, the samples shall be cooled to 77 ± 5.4°F (25 ± 3°C) and removed from the molds.

2.9.3 Testing Procedure.

2.9.3.1. Measure the bulk specific gravity of each test specimen in accordance with AASHTO T 166 or T 275, whichever applies.

2.9.3.2. Place the test specimen in a controlled temperature cabinet and bring it to the specified test temperature of 104 ± 1.8°F (40 ± 1°C). Unless the temperature is monitored and the actual temperature known, the specimen shall remain in the cabinet at the specified test temperature for at least 12 hours prior to testing.

Note 2.15: If the bulk specific gravity of the test specimens is measured in accordance with AASHTO T 166, the specimens must be allowed to dry prior to testing and preconditioning. Moisture or water trapped in the permeable voids can have an effect on the test results. Retaining the specimens in the temperature cabinet for 12 hours should be sufficient to reduce the effects of moisture to an acceptable level on the resilient modulus.

2.9.3.3 Resilient Modulus Testing.

2.9.3.3.1. Place the test specimen in the loading apparatus, position as stated in ASTM D 3497, adjust, and balance the electronic measuring system as necessary.

Note 2.16: End effects and lateral restraint between the top and bottom platens and the specimen can have a significant effect on the measured vertical deformation for uniaxial compression testing. For specimens less than six inches (15 cm) in height and where the entire specimen is used to measure the deformation, a material with low frictional resistance must be used between the specimen and top and bottom platens. Materials that can be used include silicon grease, graphite, and Teflon tape. Without use of this type of material, shear stresses between the specimen and top and bottom platens can cause the specimen to bulge and underestimate the amount of vertical displacement.

2.9.3.3.2. Precondition the specimen by applying a repeated haversine (or other) wave form to the specimen, without impact, using a loading frequency of 1 cps (0.1-sec load duration and 0.9-sec rest period) for a minimum period sufficient to obtain uniform deformation readout (less than 2 percent deviation).

Note 2.17: In most cases, a preconditioning time of 25 to 45 seconds is sufficient (25 to 45 loading cycles).

2.9.3.3.3. At the end of the preconditioning step, measure the uniaxial (vertical) total and instantaneous resilient (or recoverable) deformations. The instantaneous resilient modulus is used for deformation purposes only.

2.9.3.4 Unconfined Compressive Creep.

2.9.3.4.1. After the resilient modulus test has been completed, rezero (or rebalance) the electronic measuring system and apply a static load of fixed magnitude (± 2 percent) to the specimen. The fixed load applied should result in a compressive stress of 10 to 20 percent of the unconfined compressive strength.

2.9.3.4.2. Monitor the vertical deformation during the entire loading time. The load shall be applied for a period of 60 min, ± 15 sec. The vertical deformation measured at 60 min is the only value required for mixture design. The vertical deformations are monitored during the loading time because of their applicability to the mixture analysis system (Section 3).

2.9.3.4.3. After the fixed load has been applied over a period of 60 min, the load is released and the rebound (resilient) deformation can be monitored and recorded for an additional 60 min of no load. The rebound or recovery measurements are not used for mixture design, but are recorded because of their applicability to the mixture analysis system (Section 3).

2.9.3.5 Unconfined Compressive Strength.

2.9.3.5.1. After creep testing of the traffic-densified specimens has been completed, measure the unconfined triaxial compressive strength of each specimen at a temperature of 104°F (40°C) in accordance with AASHTO T 167, with the exception that a compressive (vertical) strain rate of 0.15 in./min per in. (3.81

mm/min per mm) height of specimen shall be used. The unconfined compressive strengths are used for field control.

2.9.4 Calculations.

2.9.4.1. Calculate the total resilient modulus, E_R, for the last three cycles of the preconditioning part of the procedure, and plot the results on Figure 7. The instantaneous resilient modulus can be calculated for information purposes, if needed. The total and instantaneous vertical resilient deformations are as those defined for the indirect tensile test in Figure 5.

$$E_R = \frac{P \cdot \ell}{A_s V_R} \tag{2-4}$$

where A_s is cross-sectional area of the uniaxial specimen, in.^{2}; ℓ is gauge length, in.; P is repeated load applied to the specimen, lb; and V_R is total or instantaneous resilient vertical deformations, whichever applies, in.

2.9.4.2. Calculate the unconfined compressive strength in accordance with AASHTO T 167, and plot the results on Figure 7.

2.9.4.3. Calculate the creep modulus, E_c, at 3,600-sec loading time.

$$E_c = \frac{P_s \ell}{A_f \Delta_c} \tag{2-5}$$

where A_f is cross-sectional area of the uniaxial specimen measured at the end of the test, in.^{2}; P_s is static load applied to the specimen, lb; and Δ_c is total uniaxial creep deformation measured at 3,600-sec loading time. (This creep deformation excludes any permanent deformation that occurred during specimen preconditioning, inches.)

2.9.4.4. Calculate the air voids of each specimen in accordance with AASHTO T 269, and plot the results on Figure 8. These air voids represent the final condition of the compacted mixture.

2.10 INTERPRETATION OF DATA

2.10.1. The determination of the design asphalt content is based upon the compaction and engineering properties of the mixture as tested under subsections 2.7, 2.8, and 2.9. Air voids, aggregate unit weight, VMA, and VFA are calculated and the results are plotted on Figure 8. The engineering properties are summarized on Figure 7. Figure 9 is used to select the design asphalt content by volume and range of allowable values that will result in a mixture which meets all of the established design criteria.

2.10.2 Compaction Properties.

2.10.2.1. Those asphalt contents that result in 95 percent of the maximum aggregate bulk unit weight (paragraph 2.7.3.1) of the mixture for the specified compactive effort are determined and entered in Figure 9.

2.10.2.2. Using the criteria given in Section 1, those asphalt contents that will result in an adequate level of final air voids, VMA, and VFA are listed in Figure 9. Average final air voids, VMA, and VFA (Figure 9) are determined from the measurements and calculations made in accordance with paragraphs 2.8.4.2. and 2.9.4.4.

2.10.3 Structural Design Property—Layer Coefficient.

2.10.3.1. In accordance with the AASHTO 1986 "Guide for the Design of Pavement Structures," the minimum total resilient modulus shall be defined by the relationship between the structural layer coefficient and total resilient modulus. This relationship is included as Figure 10 for ready reference. The average total resilient modulus for each asphalt content is determined from measurements and calculations made in accordance with paragraphs 2.7.3.5 and 2.7.4.1. Those asphalt contents that result in the minimum total resilient modulus which meets or exceeds the layer coefficient assumed for structural design are entered in Figure 9.

2.10.4 Engineering Properties.

2.10.4.1. Fatigue Cracking Criteria. Figure 11 is used to plot the relationship between indirect tensile total resilient modulus and indirect tensile strain at failure (paragraph 2.7.3) for each asphalt content used in design. Those asphalt contents that fall above the minimum design relationship are assumed to meet the minimum fatigue cracking criteria, and are incorporated on Figure 9.

2.10.4.2 Minimum Shear Stress Criteria. Those asphalt contents that result in a shear stress value that exceeds the minimum value of 54 after 300 revolutions with the air roller, without becoming plastic, are plotted on Figure 9. Plastic is defined as the condition when the shear strain (or angle) begins to increase and the shear stress decreases significantly. This minimum value of 54 is also used with the oil-filled roller.

2.10.4.3 Uniaxial Deformation Criteria. Those asphalt contents that result in a creep modulus at 3,600 sec that exceeds the minimum value, listed below, are selected for use in design and entered on Figure 9.

Pavement/Material Description	Minimum Creep Modulus, ksi
1. Asphalt concrete over a rigid base.	10
2. Surface layer of a full-depth asphalt concrete pavement.	8
3. Surface layer of a thin flexible pavement or the lower layers of full depth sections.	4

2.10.5 Selection of Design Asphalt Content. Those asphalt contents that meet all engineering design criteria and air voids, as established on Figure 9, can be used for design of the mixture. Using Figure 9, both the design and allowable range of asphalt contents are determined.

2.10.5.1. The allowable range of asphalt contents is defined as those values that are within the minimum and maximum limits as established by the structural design value (paragraph 2.10.3), shear stress criteria, fatigue criteria, and creep. If this allowable range is too narrow for normal construction and material variability, the mixture should be redesigned. A narrow allowable range of asphalt contents is referred to as a sensitive mixture.

2.10.5.2. The design asphalt content is selected as the median value within the allowable range that satisfies all compaction and engineering properties and air void criteria and results in the highest mix density.

HOT MIX ASPHALT CONCRETE DESIGN
GRAPHIC ANALYSES

MIXTURE DESIGN IDENTIFICATION NO:_____ DATE:_____

MIXTURE DESIGNATION:_____ PROJECT:_____

COMPACTION METHOD & DEVICE:_____

AIR VOIDS, %

INITIAL REFUSAL

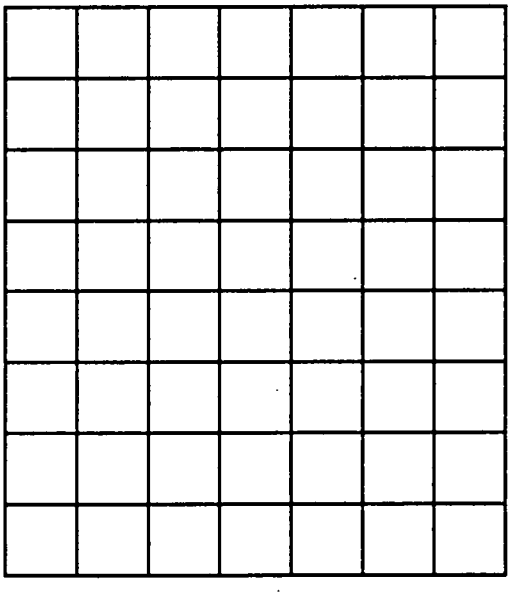

ASPHALT CONTENT BY VOLUME, %

VOIDS FILLED WITH ASPHALT, %
(AT REFUSAL)

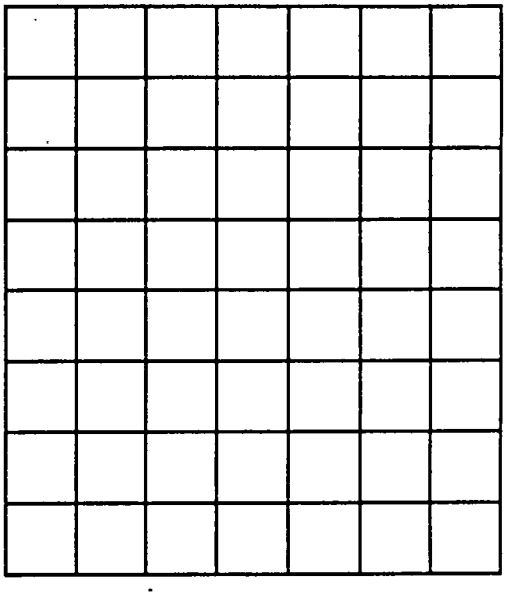

ASPHALT CONTENT BY VOLUME, %

MIX UNIT WEIGHT, PCF
INITIAL

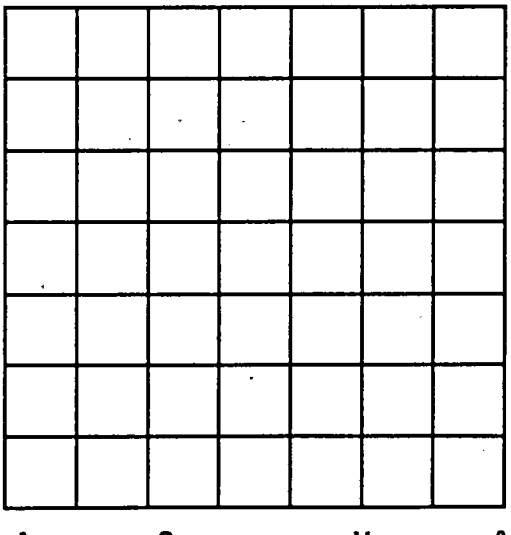

ASPHALT CONTENT BY VOLUME, %

VOIDS IN MINERAL AGGREGATE, %
(AT REFUSAL)

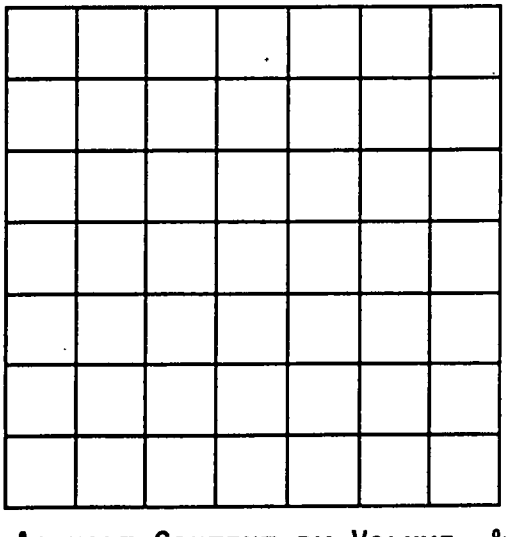

ASPHALT CONTENT BY VOLUME, %

Figure 8. AAMAS Graphical presentation of mix design data for the compaction properties.

SUMMARY OF MIXTURE DESIGN TESTS FOR SELECTING A DESIGN ASPHALT CONTENT AND AN ALLOWABLE TOLERANCE

	ASPHALT CONTENT BY TOTAL VOLUME, %						
ENGINEERING PROPERTIES							
Total Resilient Modulus (Layer Coefficients)							
Tensile Strain at Failure and Total Resilient Modulus							
Gyratory Shear Stress and Shear Index							
Creep Modulus							
COMPACTION PROPERTIES							
Aggregate Unit Weight							
Final Air Voids, %							
VMA (Porosity), %							
VFA (Degree of Saturation), %							
Allowable Range of the Design Asphalt Content							
	ASPHALT CONTENT BY TOTAL WEIGHT, %						

Figure 9. Worksheet for summarizing the test results and selecting allowable asphalt contents.

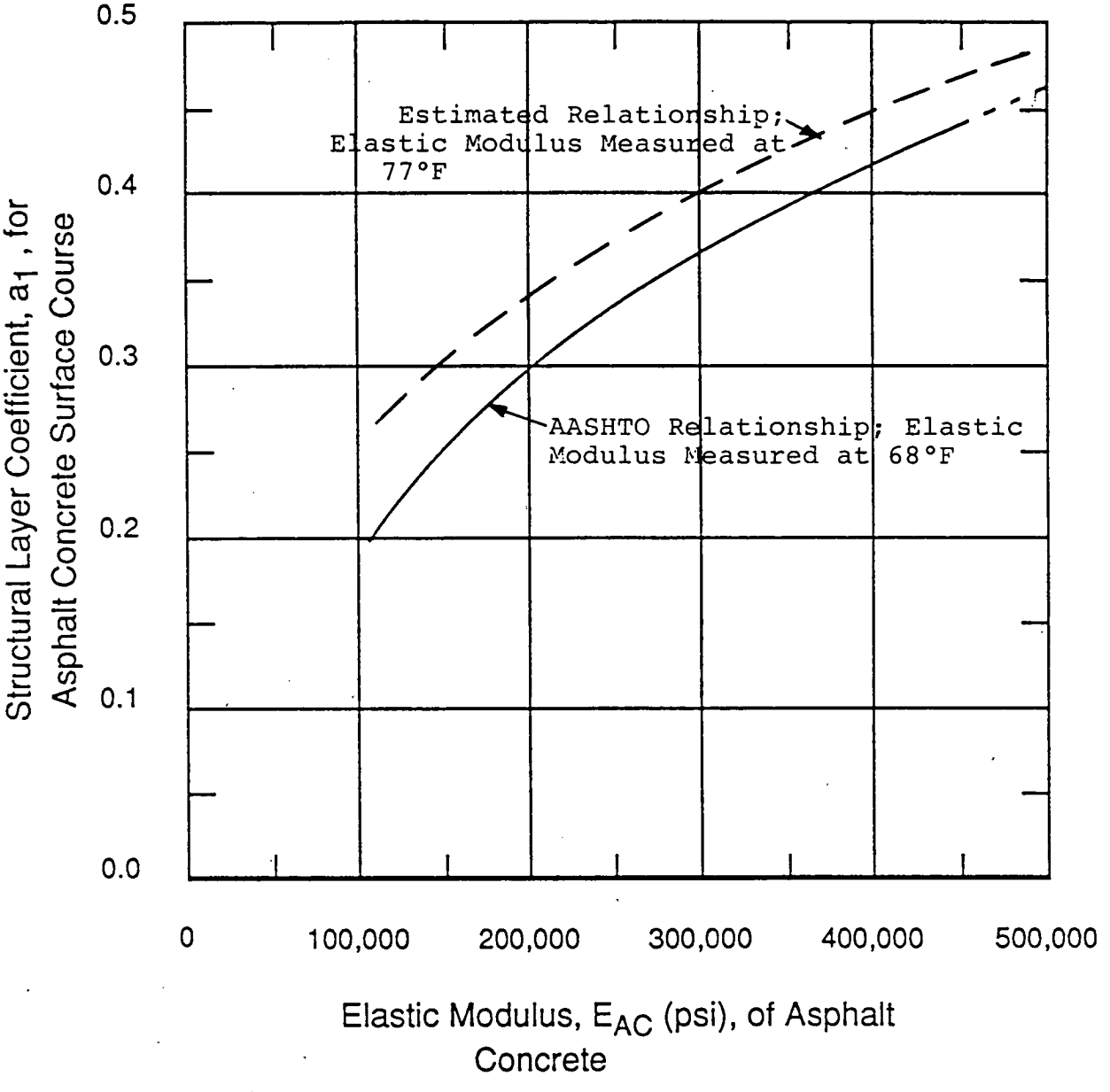

Figure 10. Chart for estimating structural layer coefficient of dense-graded asphaltic concrete based on the elastic (resilient) modulus.

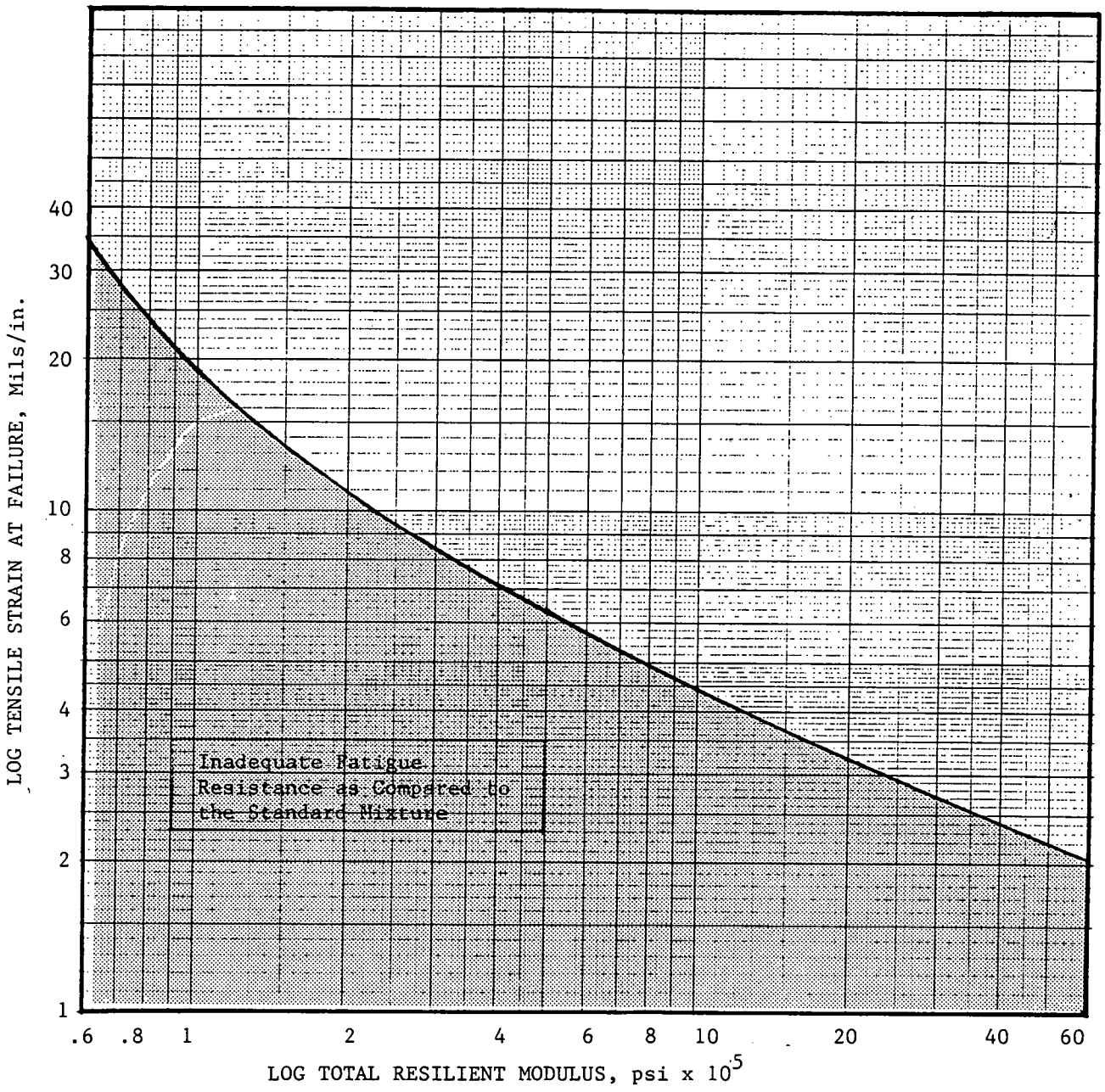

Figure 11. Minimum tensile failure strains required for the mix as a function of resilient modulus.

SECTION 3
GUIDELINES FOR MIXTURE ANALYSES

3.1 SCOPE

3.1.1. The AAMAS analysis procedures cover the preparation and conditioning of specimens and measurement of engineering properties for the laboratory evaluation of asphaltic concrete mixtures, primarily for high-volume roadways. The laboratory analysis method is limited to hot-mix asphaltic concrete, and excludes open-graded friction courses and drainage layers. The method accommodates those mixture variables normally used in the construction of asphalt paving mixtures, such as binders, aggregates, and fillers, and provides the data required for an analysis of selected asphalt pavement distresses associated with both wheel loads and the environment.

3.1.2. The values of the engineering properties measured in the procedure (resilient moduli, indirect tensile strength, creep modulus, and so on) can be used in linear-elastic and nonlinear-elastic-layered system theories to calculate the response of asphalt pavement structures subjected to wheel loadings. The values stated in inch-pound units are to be regarded as the standard. All values given in parentheses are for information only.

3.1.3. The results from the conditioning and testing of laboratory-prepared specimens can be used to compare the behavior and expected performance of different asphaltic concrete mixtures, such that the optimum mixture design can be selected for project-specific conditions.

3.2 SUMMARY OF PROCEDURE

3.2.1. Twenty-four test specimens for each set of mixture conditions (aggregate gradation, asphalt content and type, and/or mixtures with or without additives or antistripping agents) are tested. Eighteen are tested using diametral loadings (indirect tensile testing techniques) and six using uniaxial compression loads, as shown earlier by Figure 3.

3.2.2. The indirect tensile specimens (loads applied along the diametral axis) are divided into sets of three, based on air voids of each specimen. Three sets of three specimens are tested without conditioning, two sets are tested after environmental aging, and one set is tested after moisture conditioning.

3.2.3. The uniaxial compression specimens are divided into two sets of three specimens, based on air voids of each specimen. Both sets are tested after laboratory simulation of traffic densification. One set is tested to measure the creep modulus as a function of time, and the other set is used for measuring the compressive total resilient modulus and unconfined triaxial compressive strength.

3.2.4. Five tests are used as tools for mixture evaluation and testing. These tests are: (1) the indirect tensile resilient modulus test, (2) the indirect tensile strength test, (3) the gyratory shear strength test, and (4) the indirect tensile and (5) uniaxial unconfined compressive creep tests. The test program described herein requires a combination of these laboratory tests and conditioning procedures to evaluate the behavior and predict the performance characteristics of asphaltic concrete mixtures.

3.3 SIGNIFICANCE AND USE

3.3.1. The laboratory analysis of asphaltic concrete mixtures is intended to provide the fundamental engineering properties that are used in the structural design and evaluation of asphaltic concrete pavements. In other words, these test procedures provide values that can be used to characterize asphaltic concrete mixtures for use in pavement thickness design and in structural analyses of layered pavement systems, under a variety of stress states and temperature conditions.

3.3.2. These test methods also provide the information and properties required for establishing structural layer coefficients of asphaltic concrete surface and base course mixtures for use with the AASHTO "Guide for Design of Pavement Structures."

3.4 APPLICABLE DOCUMENTS

3.4.1 AASHTO Standards.

T 49 Penetration of Bituminous Materials
T 166 Bulk Specific Gravity of Compacted Bituminous Mixtures
T 167 Compressive Strength of Bituminous Mixtures
T 179 Effect of Heat and Air on Asphalt Materials (Thin-Film Oven Test)
T 202 Viscosity of Asphalts by Vacuum Capillary Viscometer
T 209 Maximum Specific Gravity of Bituminous Paving Mixtures
T 245 Resistance to Plastic Flow of Bituminous Mixtures Using Marshall Apparatus
T 246 Resistance to Deformation and Cohesion of Bituminous Mixtures by Means of Hveem Apparatus
T 269 Percent Air Voids in Compacted Dense and Open Bituminous Paving Mixtures
T 283 Resistance of Compacted Bituminous Mixtures to Moisture Induced Damage.

3.4.2 ASTM Standards.

D 3387 Compaction and Shear Properties of Bituminous Mixtures by Means of the U.S. Corps of Engineers Gyratory Testing Machine (GTM)
D 3497 Dynamic Modulus of Asphalt Mixtures
D 3549 Thickness or Height of Compacted Bituminous Paving Mixture Specimens
D 4013 Preparation of Test Specimens of Bituminous Mixtures by Means of Gyratory Shear Compactor
D 4123 Indirect Tension Test for Resilient Modulus of Bituminous Mixtures

3.5 APPARATUS

3.5.1. Equipment for preparing and compacting specimens is required from one of the following methods: ASTM D 3387 (Method A) or D 4013 (Method B).

3.5.2. A forced air draft oven is required that is capable of maintaining a temperature up to 325 ± 1.8°F (163 ± 1°C).

3.5.3. The use of a loading jack and ring dynameter from AASHTO T 245, or a mechanical or hydraulic testing machine from AASHTO T 167, is required to provide a range of accurately controllable rates (within 5 percent) of vertical deformation including 0.05 and 2 in. per min (1.27 and 50.8 mm per min).

3.5.4. Diametral loading strips are specified from ASTM D 4123.

3.5.5. An axial loading machine is specified from ASTM D 4123.

Note 3.1: Any loading machine capable of providing a repetitive sinusoidal or square type compression load of fixed cycle and duration can be used. Typically, a cam and switch or timer control of solenoid valves operating a pneumatic air piston, or a closed-loop electrohydraulic system is used. Pneumatic systems are the simplest, while closed-loop electrohydraulic systems allow more versatility (variable wave forms, higher loads, and higher frequency response). Generally, a haversine wave form is characteristic of closed-looped electrohydraulic equipment, while rectangular wave forms are used with pneumatically operated loading equipment. Both wave forms can be used for the resilient modulus test. A loading frequency of 1 cycle per second has been found to be satisfactory for most applications. With a pneumatic loading system, a square wave form with a load duration of 0.1 second and a rest period of 0.9 seconds is recommended.

3.5.6 Specimen Axial Deformation Measurement Devices from ASTM D 4123.

Note 3.2: The resilient modulus, creep modulus and indirect tensile strength tests require deformation transducers with a sufficient range to cover the cumulative deformation during the test and also a high resolution for the smallest resilient strains to be measured. The linear variable differential transducer (LVDT) is generally considered to be the most suitable deformation transducer for the test. Table 3 provides the required accuracy of the axial deformation measurement device.

Note 3.3: LVDT Clamps are used to hold the LVDTs in place during indirect tensile testing. There are different sample holding devices that can be used in the test program. One such device is described in ASTM D 4123, and another in Federal Highway Administration Report No. FHWA/RD-88/118 (3,4). Either of these devices can be used provided that the specimen has smooth surfaces, and is centered under the axial load (i.e., no load eccentricity). For uniaxial compression loading, LVDT clamps are not required if a friction reducing material is placed between the specimen and top and bottom platens. Thin teflon tape can be used as a friction reducing material.

3.5.7 Specimen Axial Load Measurement Device from ASTM D 4123.

Note 3.4: The axial load measuring device is an electronic load cell. The load may be measured by placing the load cell between the specimen cap and the loading piston. The total load capacity of the load transducer (load cell) should be of the proper order of magnitude with respect to the maximum total loads to be applied to the test specimen. Generally, its capacity should be no greater than five times the total maximum load applied to the test specimen to ensure that the necessary measurement accuracy is achieved. The minimum performance characteristics of the load cell are presented in Table 3. The axial load-measuring device shall be capable of measuring the axial load to an accuracy within 1 percent of the applied axial load.

Table 3. Data acquisition—minimum response characteristics for resilient modulus tests.

Analog Recorders Recording Speeds: 0.5 to 50 cm/sec (0.2 to 20 in./sec) System Accuracy (include linearity and hysteresis): 0.5%[1] Frequency Response: 100 Hz		
Measurement Transducers	Load Cell	Displacement Transducer (LVDT)[2]
Minimum Sensitivity, mv/v	2	0.2 mv/0.25 mm/v (AC LVDT) (5 mv/0.025 mm/v) (DC LVDT)
Nonlinearity, % Full Scale	+0.25	+0.25
Hysteresis, % Full Scale	+0.25	+0.0
Repeatability, % Full Scale	+0.10	+0.01
Thermal Effects on Zero Shift or Sensitivity, % of Full Scale/F(c)	+0.005 (+0.025)	--
Maximum Deflection at Full Rated Value in Inches (mm)	0.005 (0.125)	

1 System frequency response, sensitivity, and linearity are functions of the electronic system interfacing, the performance of the signal conditioning system used, and other factors. It is therefore a necessity to check and calibrate the above parameters as a total system and not on a component basis.

2 LVDT's unlike strain gauges, cannot be supplied with meaningful calibration data. System sensitivity is a function of excitation frequency, cable loading, amplifier phase characteristics, and other factors. It is necessary to calibrate each LVDT-cable-instrument system after installation, using a known input standard.

3.5.8 Recording Device from ASTM D 4123.

Note 3.5: Specimen behavior is evaluated from continuous time records of applied load and specimen deformation. Commonly, these parameters are recorded on a multichannel strip-chart recorder. Analog to digital data acquisition systems may be used provided that data can be converted later into a convenient form for data analysis and interpretation. Fast recording system response is essential if accurate specimen performance is to be monitored. It is recommended that the response characteristics in Table 3 be satisfied.

Note 3.6: For analog strip-chart recording equipment, the load and deformation recorder trace must be of sufficient amplitude and time resolution to enable accurate data reduction. Resolution of each variable should be better than 2 percent of the maximum value being measured. To take advantage of recorder accuracy and for subsequent data analysis 2 to 4 cycles per inch of recording paper is acceptable. The clarity of the trace with respect to the background should provide sufficient contrast and minimum trace width, so that the minimum resolution of 2 percent of the maximum value of the recorded parameter is maintained, and the trace should be included in the reports.

Note 3.7: For uniaxial compression testing, the number of recording channels can be reduced by wiring the leads from the LVDTs so that only the average or total signal from a pair is recorded. For indirect tensile loadings, the signal from each LVDT shall be recorded separately. This permits observation of individual LVDT readings, rather than an average or total signal, to determine if significant differences are being recorded between the two LVDTs. If the differences between LVDTs is large, the specimen shall be repositioned.

3.5.9 Calibration of Equipment. If multichannel strip-chart recorders are used, calibration of the measurement transducers through the recording system is essential. In this case, the calibration shall be recorded periodically (at least once a week when in use) to provide a permanent record. If the LVDTs are wired pairs, such that the total deformation is measured, they must be calibrated together, not separately.

3.5.10. A vacuum container, preferably Type D, and vacuum pump or water aspirator are required from AASHTO T 209, including manometer or vacuum gauge.

3.5.11. Balance and water bath are specified in accordance with AASHTO T 166.

3.5.12. Water bath should be capable of maintaining a temperature of 140 ± 1.8°F (60 ± 1°C)

3.5.13. Freezer should be maintained at 0 ± 5.4°F (−18 ± 3°C).

3.5.14. A supply of plastic film for wrapping and heavy-duty leak proof plastic bags for enclosing saturated and unconditioned specimens and masking tape are required.

3.5.15. Aluminum pans should have a surface area of 100 to 180 in.^{2} (0.06 to 0.1 m^2) in the bottom and a depth of approximately 1 inch (2.54 cm).

3.5.16 Temperature and Control System. The temperature control system shall be capable of control over a temperature range from 0 to 104°F (−18 to 40°C) and within ± 1.8°F (1°C) of the specified temperature within the range. The system can be a room chamber and/or cabinet that shall be large enough to hold at least three specimens for a period of 12 hours prior to testing. If the testing machine is located in a room without the specified temperature control system, a controlled temperature cabinet shall be used during the entire test.

3.6 PREPARATION OF LABORATORY TEST SPECIMENS

3.6.1. Prepare the asphaltic concrete mixture in accordance with AASHTO T 167, with the exception that sufficient mixture should be prepared to compact at least three specimens per test at any one time. The mixing temperature should be selected in accordance with AASHTO T 246 (see Note 3.8).

Note 3.8: Mixture mixing and compaction temperatures will generally be somewhere in the range of 250 to 325°F (121 to 149°C). Some agencies use AASHTO T 245 to determine the mixing and compaction temperatures, whereas others use AASHTO T 246. Selection of the mixing temperature should be consistent with plant operations and mixture production. More importantly, once the mixing temperature is selected it should be controlled so that the viscosity of the bitumen will not vary more than ± 50 Cst during the mixing/compaction process.

3.6.2 Initial Heat Conditioning.

3.6.2.1. After initial mixing, the mixture shall be placed in an aluminum pan having a surface area of 100 to 180 in.^{2} (0.06 to 0.1 m^2) at the bottom and a depth of approximately 1 in. (2.54 cm). The mixture shall then be placed in a forced draft oven set at 275°F (135°C) for 1.5 hours (± 5 min) of heating. The pan shall be placed on spacers to allow air circulation under the pan, if the shelves are not perforated.

3.6.2.2. After 1.5 hours of heating at 275°F (135°C) the pans shall be removed from the oven and the mixture remixed in the pan with a hand-mixing tool. After remixing, the pan is replaced in the oven for an additional 1.5 hours (± 5 min) of heating.

Note 3.9: The temperature of the oven will affect the results or heating time interval. A temperature of 275°F (135°C) was selected for use, because the mixture temperature after production normally varies from 250 to 325°F (121 to 149°C). If plants are operated at significantly different temperatures, this temperature may need to be revised. The purpose of this heating time interval is to simulate plant hardening (as defined by the penetration and viscosity values of the asphalt after production) and allow some of the asphalt absorption to occur prior to compaction. The 3 hour time specified above is an approximate time. It should be expected that different asphalts produced by different type plants will have different aging effects as determined in the laboratory. Thus, this heating time interval should be verified in the laboratory for the specific asphalt plant and asphalt being used. For the cases when the asphalt plant is unavailable and/or there is no historical hardening data, the Thin-Film Oven Test (AASHTO T 179) can be used to estimate the asphalt properties after mix production. Different amounts of the asphalt concrete mixture should be placed in a pan and placed in an oven at a temperature 275°F (135°C) for varying periods of time. The asphalt shall then be extracted and the penetration (AASHTO T 49) and viscosity (AASHTO T 202) measured on the recovered asphalt. The time of heating that more closely simulates the penetration and viscosity values measured from materials recovered from the plant (or estimated with AASHTO T 179) shall be used to simulate plant aging for the initial heat conditioning.

3.6.2.3. After initial heating, a representative sample of the aged mixture shall be taken and allowed to cool. On this sample, measure the maximum specific gravity of the asphaltic concrete mixture in accordance with AASHTO T 209.

3.6.3 Specimen Size.

3.6.3.1. The specimens to be tested shall have a diameter of 4 in. (10 cm) for mixtures that contain aggregates with a maximum aggregate size of 1.0 in. (2.5 cm) or less, or a minimum diameter of 6 in. (15 cm) for mixtures that contain maximum size aggregates up to 1.5 in. (3.8 cm) in diameter.

Note 3.10: The size of test specimens has an influence on the results from the various tests to measure the engineering properties of the mixture. The sample diameter to maximum aggregate size diameter ratio was determined by testing oversized cores. If at all possible, the specimen diameter to maximum aggregate size diameter should have a ratio greater than 4.

3.6.3.2. The height of all diametral specimens to be tested shall be at least one-half the diameter of the specimen. If possible, the height should approximate the compacted lift thickness placed on the roadway, unless the previous statement is violated.

3.6.3.3. The height of the uniaxial compression specimens to be tested shall be at least equal to the diameter of the specimen, when a friction-reducing material is used (see Note 3.3). If LVDTs are used and a friction reducing material is not used, the height of the specimen should be twice the specimen's diameter.

3.6.4 Specimen Compaction.

3.6.4.1. After initial heat conditioning, the mixture shall be compacted to the air void level expected in the field immediately after compaction. This level of air voids can be obtained by adjusting the number of gyrations, angle of gyration and/or gyration pressure in ASTM D 3387 (Method A), and the gyration and/or end pressures or sets (3 gyrations equals a set) of gyrations in ASTM D 4013 (Method B). The exact procedure must be determined experimentally for each mixture before compacting the specimens for each set. Use of the Corps of Engineers GTM air-filled roller is the preferred device, but the GTM oil-filled roller can also be used. ASTM D 4013 and the GTM fixed roller mode of ASTM D 3387 can only be used for compaction testing.

Note 3.11: The type of compaction device used to compact the specimens will have an influence on the test results, especially creep modulus values. ASTM D 3387 and D 4013 are the preferred techniques, because specimens compacted with the gyratory compactor (ASTM D 4013) to air voids measured on field cores were found to be most similar, in terms of fundamental engineering properties, to cores recovered from the roadway shortly after construction. AASHTO T 247 produced specimens that were reasonably similar to those engineering properties measured on field cores. AASHTO T 245 (Marshall Hammer) is not recommended

for preparing specimens for resilient and creep modulus testing, because large differences were found between laboratory compacted specimens and field cores.

Note 3.12: Normally test specimens for asphaltic concrete mixture design and testing are compacted using a standard compactive effort. However, a specific compactive effort may not reproduce the air voids measured on field cores. Specimens should be compacted to the air voids anticipated shortly after construction, or to the air voids used to control compaction during construction of the asphalt concrete lifts. Compactive effort curves may be needed to determine the proper compactive efforts to simulate the air voids after construction and at refusal. If needed, these curves can be prepared by compacting triplicate samples at each selected compactive effort. At least three compactive efforts should be used. The compactive effort curves are formulated by plotting air voids (measured in accordance with AASHTO T 269) versus compactive effort. The compactive effort that yields the after-constructed air void content is the value used to compact the test specimens. Compactive efforts for compacting the diametral and uniaxial compression specimens will be different because of the height difference.

3.6.4.2 Method A—ASTM D 3387. The initial compaction of both the diametral and the uniaxial compression specimens shall be performed at an angle of gyration of 3 degrees in accordance with ASTM D 3387. If an angle of gyration of 3 degrees yields test specimens significantly below the after-constructed air voids, this angle can be reduced to 2 degrees.

3.6.4.3 Method B—ASTM D 4013. When using ASTM D 4013, the angle of gyration is fixed. The initial compaction of the diametral specimens shall be performed at a pregyration stress of 60 psi (414 kPa), while adjusting the number of gyrations. If 60 psi (414 kPa) yield test specimens significantly below or above the after-constructed air voids, this pregyration stress can be varied from 25 to 90 psi (172 to 620 kPa). For compacting the uniaxial compression specimens refer to paragraph 3.8.3.3.

3.6.4.4. After compaction, the diametral specimens shall be cooled to room temperature and then extracted from the molds. The uniaxial compression specimens, if compacted by Method A (ASTM D 3387), are to be left in the molds and used in the traffic densification procedure (refer to paragraph 3.8.3).

3.6.5. After extraction from the molds, all diametral test specimens shall be marked and numbered. Two diametral axes shall be marked on each test specimen. The two axes shall be perpendicular to each other.

3.7 GROUPING OF TEST SPECIMENS

3.7.1. Determine the thickness of each specimen in accordance with ASTM D 3549.

3.7.2. Measure the bulk specific gravity in accordance with AASHTO T 166 or T 275, whichever applies.

3.7.3. Calculate the air voids for each test specimen in accordance with AASHTO T 269.

3.7.4. Sort the diametral specimens into six subsets of three specimens each so that the average air voids of the different subsets are approximately equal.

Note 3.13: This is a trial and error process to select specimen subsets to minimize the effect of air void difference between the different subsets. The technique used depends on the overall variation of air voids between all specimens. One technique used is to select one specimen on the high side of the mean, a second specimen low of the mean, and the third specimen as close to the overall mean air void as possible. Another technique is to select one specimen on the high side and two slightly on the low side of the mean air voids, while another subset would include one specimen of the low side and two slightly on the high side of the overall mean.

3.7.5. Label three subsets as unconditioned and identify one subset for each test temperature, 41, 77, and 104°F (5,25, and 40°C). Place these specimens in plastic bags, seal, and store at room temperature. Label two subsets as environmental aging specimens and one subset for moisture conditioning. Record the air voids of each specimen in Figure 12.

3.8 PRECONDITIONING OF TEST SPECIMENS

3.8.1 Moisture Conditioning.

3.8.1.1. Three diametral specimens, or one subset, shall be used in the moisture damage evaluation. These specimens shall be moisture conditioned as noted in the following paragraphs.

3.8.1.2. Place the three specimens on individual porous spacers in a vacuum container. Fill the container with distilled water at room temperature so that the specimens have at least 1 in. (2.5 cm) of water above their surface. Apply a vacuum of 26 in. of mercury for 15 min (± 2 min). Remove the vacuum and leave the three specimens submerged in water for an additional 30 min.

3.8.1.3. Measure the bulk specific gravity of each specimen in accordance with AASHTO T 166. Compare the saturated surface-dry weight after moisture conditioning with the saturated surface dry weight determined in paragraph 3.7.2. Immediately return the specimens to the water-filled vacuum container. Calculate the volume of absorbed water.

3.8.1.4. Determine the degree of saturation by comparing volume of absorbed water with volume of air voids from paragraph 3.7.3. If the volume of water is greater than 55 percent of the volume of air, proceed to paragraph 3.8.1.5. If the volume of water is less than 55 percent, repeat the procedure beginning with paragraph 3.8.1.2. If 55 percent saturation is not reached by the third attempt, proceed to paragraph 3.8.1.5.

3.8.1.5. Cover the vacuum-saturated specimens tightly with a plastic film (Saran wrap or equivalent). Place each wrapped specimen in a plastic bag containing 0.3 oz (10 ml) of water and seal the bag.

3.8.1.6. Place the plastic bag containing the specimen in a freezer set at 0 ± 5.4°F (−18 ± 3°C) for 16 hours.

3.8.1.7. After 16 hours, place the specimens into a 140 ± 1.8°F (60 ± 1°C) water bath for 24 hours.

3.8.1.8. After 24 hours in the 140°F (60°C) water bath, remove the specimens and place them in a water bath already at 77 ± 1.8°F (25 ± 1°C) for 2 hours. It may be necessary to add ice to the water bath to prevent the water temperature from rising above 77°F (25°C). Test the specimens as described in paragraph 3.9.3.

3.8.2 Accelerated Aging (Temperature Conditioning).

3.8.2.1. Two subsets of three diametral specimens shall be placed in the forced draft oven set at a temperature of 140°F (60°C). These specimens shall be heated for approximately 48 hours (2 days) ± 30 min.

3.8.2.2. After initial aging, the temperature of the forced draft oven shall be elevated to 225°F (107°C) for an additional 120 hours (± 0.5 hours) or 5 days of aging. After aging, the six specimens (two subsets) shall be removed from the oven and placed in a temperature cabinet set at 41°F (5°C) and stored for at least 12 hours prior to testing, as described in paragraph 3.9.4.

AAMAS DATA SHEET
SUMMARY OF TEST RUSULTS

1. IDENTIFICATION

Project No. _____

Highway _____ County _____

Mixture I.D._____ Asphalt Content _____%

Compaction Device _____ Max. Specific Gravity _____

2. UNCONDITIONED SPECIMEN DATA

Temperature, F									
Sample No.									
Bulk Specific Gravity									
Percent Air Voids, %									
Total Resilient Deformations, in., H_{RT}: Axis A									
Axis B									
Total Resilient Modulus, ksi, E_{RT}: Axis A									
Axis B									
Indirect Tensile Strength, psi, S_t									
Tensile Strain at Failure, mils/in, ε_t									

Figure 12. AAMAS worksheet and summary of results.

3.8.3 Traffic Densification.

3.8.3.1. Six uniaxial compression specimens are used in the traffic densification study.

3.8.3.2 Method A—ASTM D 3387. Six specimens are initially compacted as discussed in paragraph 3.6.4. Additional compactive effort is applied to these specimens to measure the decrease in air voids and the ultimate or final air void content of the mixture under simulated loading conditions.

Note 3.14: The compactive effort used to simulate traffic is dependent on many variables, some of which include number of axle loadings, axle weight, tire inflation pressure and type of tire. It is generally accepted that AASHTO T 247 has been a reasonable estimation of air voids after traffic, based on historical studies. However, as tire types change and inflation pressures increase, these compaction procedures may be inadequate. Unfortunately, little data exist to determine the effects of increased tire pressures and wheel loads on air voids and material properties. The following procedures are provided as guidelines, but they may need to

3. MOISTURE CONDITIONED SPECIMEN DATA, AFTER CONDITIONING

Temperature, F						
Sample No.						
Bulk Specific Gravity						
Percent Air Voids, %						
Degree Saturation, %						
Total Resilient Modulus, ksi, E_{RTm}: Axis A						
Axis B						
Indirect Tensile Strength, psi, S_{tm}						
Tensile Strain at Failure, mils/in., ε_{tm}						

4. ENVIRONMENTAL AGED/HARDENED SPECIMEN DATA

Temperature, F									
Sample No.									
Bulk Specific Gravity									
Percent Air Voids, %									
Total Resilient Modulus, ksi, E_{RTA}: Axis A									
Axis B									
Indirect Tensile Strength, psi, S_{tA}									
Tensile Strain at Failure, mils/in., ε_{tA}									
IDT Creep Modulus Testing: Slope of Creep Curve, b_t									
Intercept of Creep Curve, a_t									
Creep Modulus at 3,600 seconds, ksi, C_t									

Figure 12. Continued

5. TRAFFIC Ddensified SPECIMEN DATA

Temperature, F									
Sample No.									
Prior to Densification: Bulk Specific Gravity									
Percent Air Voids, %									
After Densification: Bulk Specific Gravity									
Percent Air Voids, %									
Total Resilient Modulus, ksi, E_{CT}									
Unconfined Compressive Strength, psi, S_{qu}									
Compressive Strain at Failure, mils/in., ε_{qu}									
Compressive Creep Modulus Testing: Slope of Creep Curve, b									
Intercept of Creep Curve, a									
Creep Modulus, ksi, $C_c(t)$ 10 sec									
100 sec									
1,000 sec									
3,600 sec									

Figure 12. Continued

be revised after sufficient data are collected to simulate, in the laboratory, variations of tire types and inflation pressures.

3.8.3.2.1. Using ASTM D 3387 as the compaction device, the gyratory shear test shall be conducted along with the compaction test to determine and evaluate any reduction in shear strength with number of gyrations.

3.8.3.2.2. After initial compaction, allow the specimens to cool in the mold to 140°F (60°C).

3.8.3.2.3. Reinsert the mold in the GTM using an angle of gyration of 2 degrees and a vertical pressure of 120 psi (827 kPa) for the oil-filled roller. Both the air roller and oil-filled rollers are interchangeable in the GTM, but the gyratory shear stresses will be different. The use of the oil-filled roller will result in higher gyratory shear stresses than for the air roller.

3.8.3.2.4. Densify the uniaxial compression specimens to refusal. This refusal air void content can be estimated from the compactive effort curves, as explained in Note 3.12.

Note 3.15: The variables selected for use in the traffic densification of mixtures from other studies have varied. The variables most commonly used are: The GTM is set at a 2 degree angle, 100 psi (7.03 kg/cm^2) ram pressure, and 13 psi (0.91 kg/cm^2) air-roller pressure. These values may need to be revised after additional data are collected and evaluated under the SHRP A-006 Project.

3.8.3.2.5. When the oil-filled or air rollers are used, traffic simulation tests are performed up to 300 gyrations with the GTM. Initial sample height readings shall be obtained prior to densification and concurrently with roller pressure readings at 25, 50, 75, 100, 150, 200, 250, and 300 gyrations. Gyratory shear stresses shall be computed for each pressure reading in accordance with ASTM D 3387, and graphically presented in a plot of gyratory shear versus number of gyrations.

Note 3.16: In some cases, mixture resistance may reduce excessively prior to 300 gyrations. An excessive reduction in roller pressure and increase in angle of gyration may warrant stopping the test.

3.8.3.3 Method B—ASTM D 4013. IF ASTM D 4013 is used as the compaction device, a compactive effort is initially applied to these test specimens to the refusal air void content. For most mixtures, 45 revolutions of the gyratory molding press (pregyration stress of 90 psi (620 kPa)) is sufficient to determine the final air void content. Unlike Method A, when using ASTM D 4013, the uniaxial compression samples are not initially compacted to an after-constructed air void content.

3.8.3.4. After densification, the traffic-densified specimens shall be grouped based on air voids in accordance with subsection 3.7. The six specimens are placed in plastic bags and stored for uniaxial compression testing, as described in paragraph 3.9.5.

3.9 TESTING PROCEDURE

3.9.1. Place all test specimens in a controlled temperature cabinet or water bath, as previously identified, to the specified test temperature. Unless the temperature is monitored, the specimens shall remain in the cabinet at the specified test temperature for at least 12 hours prior to testing.

Note 3.17: If thermistors are used in "dummy" specimens, then the testing program can begin shortly after the specimen temperature reaches the test temperature.

3.9.2 Unconditioned Diametral Specimens.

3.9.2.1. Three sets of three specimens each shall be tested at different temperatures. One set at 41°F (5°C), one at 77°F (25°C), and one at 104°F (40°C).

3.9.2.2. Place the test specimen in the loading apparatus, position as stated in ASTM D 4123, adjust and balance the electronic measuring system as necessary.

3.9.2.3. Precondition the specimen by applying a repeated haversine (or other suitable wave form) to the specimen without impact using a loading frequency of 1 cps (0.1-sec load duration and 0.9-sec rest period) for a minimum period sufficient to obtain uniform deformation readout (less than 2 percent deviation). A preconditioning time of 25 to 45 sec (25 to 45 loading cycles) is sufficient in most cases.

3.9.2.4. The fixed load to be used in the diametral repeated load resilient modulus test for each test temperature can be selected by using elastic layer theory to calculate the tensile stress and strain at the bottom of the asphaltic concrete layer (refer to subsection 4.3 of Section 4 for additional discussion on selecting laboratory stress states). For those conditions where the asphaltic concrete layers are in compression (for example, an asphaltic concrete overlay placed over a portland cement concrete pavement), the fixed load applied to the specimen should be of a sufficient magnitude to result in a horizontal deformation greater than 0.0001 in. (0.00254 mm). In most cases, the load established by these criteria will induce a tensile stress in the specimen in the range of 5 to 20 percent of the indirect tensile strength.

Note 3.18: To use elastic layer theory requires that a stiffness or modulus of elasticity be assumed for each layer in the pavement structure, including the asphalt concrete. Thus, after testing the first specimen of each subset, the assumed value should be compared to the measured value for reasonableness. If these values are significantly different, the stress state in the laboratory should be altered to be consistent with the theoretical value. If elastic layer theory is unavailable, extra specimens can be compacted and the strength measured to establish the stress levels to be used for testing the unconditioned specimens at each test temperature, based on a percentage of the indirect tensile strength, given above.

3.9.2.5. After preconditioning, measure the total resilient deformation in accordance with ASTM D 4123, along one of the two axes marked from paragraph 3.6.5 at the specified test temperature of each subset. A loading frequency of 1 cps (0.1-sec load duration and 0.9-sec rest period) shall be used. The total resilient modulus is calculated in accordance with Addendum A. The total resilient deformation and modulus values shall be recorded on the AAMAS worksheet (Figure 12).

3.9.2.6. Rotate the specimen to the second axis and repeat paragraphs 3.9.2.2 through 3.9.2.5.

Note 3.19: At high asphalt contents and/or temperature, indentation of the loading strips into the test specimen is possible. This condition is undesirable. If these indentations can be observed, the tensile and compressive stresses will vary, so the fewest number of loading cycles should be used as possible.

3.9.2.7. After resilient modulus testing of the unconditioned specimens, measure the indirect tensile strength at the same specified temperature of each subset in accordance with Addendum A. A loading rate of 2 in. (50.8 mm) per min shall be used. The indirect tensile strength and failure strain shall be measured along the axis which was found to have the larger resilient deformations. These values shall be recorded on the AAMAS worksheet (Figure 12). If the specimen must be rotated to the first axis tested, a sufficient number of loading cycles are to be applied to ensure that the loading strips are properly seated. (See Note 3.19).

3.9.3 Moisture Conditioned Specimens.

3.9.3.1. Using the same indirect tensile stress as used for the unconditioned specimens, measure the total resilient deformation at 77°F (25°C) and calculate the total resilient modulus in accordance with paragraphs 3.9.2.2 through 3.9.2.6 along each of the two axes marked from paragraph 3.6.5. A loading frequency of 2 cps (0.1-sec load duration and 0.9-sec rest period) shall be used. The total resilient modulus shall be reported on the AAMAS worksheet (Figure 12).

3.9.3.2. After resilient modulus testing of the moisture conditioned subset is complete, measure the indirect tensile strength at 77°F (25°C) in accordance with Addendum A, along the axis that was found to have the larger resilient deformation. If the specimen must be rotated to the first axis tested, a sufficient number of loading cycles are to be applied to ensure that the loading strips are properly seated (see Note 3.19). A loading rate of 2 in. (50.8 mm) per min shall be used to measure the indirect tensile strength.

3.9.4 Temperature Conditioned Specimens.

3.9.4.1. For the first subset of temperature-conditioned specimens, measure the total resilient modulus in accordance with paragraphs 3.9.2.2 through 3.9.2.6, along each of the two axes marked, at a test temperature of 41°F (5°C). The indirect tensile stress selected for a test temperature of 41°F (5°C) from paragraph 3.9.2.4 shall be applied at a loading frequency of 1 cps (0.1-sec load duration and 0.9-sec rest period). The total resilient deformation and modulus values shall be reported on Figure 12.

3.9.4.2. After resilient modulus testing of the temperature-conditioned specimens, measure the indirect tensile strength at 41°F (5°C) in accordance with Addendum A, along the axis that

was found to have the larger resilient deformation. A loading rate of 0.05 in. (1.27 mm) per min shall be used.

3.9.4.3. For the second subset of temperature-conditioned specimens, measure the indirect tensile creep modulus at a test temperature of 41°F (5°C) in accordance with Addendum B. The indirect tensile stress that was used to measure the resilient modulus of the temperature conditioned specimens (the first subset) shall also be used for tensile creep testing.

3.9.5 Traffic Densified Specimens.

3.9.5.1. For the first subset of the traffic-densified specimens, measure the total uniaxial compressive resilient modulus at a test temperature of 104°F (40°C).

3.9.5.1.1. Place the test specimen in the loading apparatus, position as stated in ASTM D 3497, adjust and balance the electronic measuring system, as necessary.

3.9.5.1.2. Precondition the specimen by applying a repeated haversine wave form (or other suitable wave form) to the specimen without impact using a loading frequency of 1 cps (0.1-sec load duration and 0.9-sec rest period) for a minimum period sufficient to obtain uniform deformation readout (less than 2 percent deviation).

3.9.5.1.3. The compressive stress applied to the specimen can be selected by using elastic layer theory to calculate the compressive stresses in the pavement structure, as explained in subsection 4.3 of Section 4. If elastic layered theory is unavailable, the expected tire inflation pressures can be assumed to be the compressive stress and used in the test program.

3.9.5.1.4. At the end of the preconditioning step, measure the uniaxial (vertical) total resilient deformations, and calculate the total compressive resilient modulus for the last 1 cycle of the preconditioning part of the procedure, in accordance with paragraph 2.9.4.1 of Section 2.

3.9.5.1.5. After resilient modulus testing of the traffic densified specimens, measure the unconfined triaxial compressive strength of each specimen at a temperature of 104°F (40°C) in accordance with AASHTO T 167, with the exception that a compressive (vertical) loading rate of 0.15 in./min per in. (3.81 mm/min per mm) height shall be used.

3.9.5.2. For the second subset of traffic-densified specimens, measure the axial compressive creep modulus in accordance with Addendum B at a temperature of 104°F (40°C). The same compressive stress used to measure the resilient modulus of the traffic-densified specimens shall be used for unconfined compressive creep testing.

3.10 CALCULATIONS

3.10.1. All calculations shall be performed in accordance with the identified AASHTO and ASTM test standards or in accordance with Section 3, Addendum A and Addendum B.

3.11 REPORT

3.11.1. The report shall include the information provided in Figure 12 for each asphalt content and mixture selected for evaluation.

ADDENDUM A—TEST METHODS FOR INDIRECT TENSILE STRENGTH OF BITUMINOUS MIXTURES

A.1 SCOPE

A.1.1. This method covers the determination of the indirect tensile strength of compacted, dense-graded hot-mixed, hot-laid bituminous mixtures. The indirect tensile strength test is used to characterize bituminous mixtures in tension for thermal and fatigue cracking analyses.

A.1.2. This method is applicable to dense-graded hot-mixed, hot-laid asphaltic concrete mixtures, as defined by ASTM D 3515 (Bituminous Paving Mixtures, Hot-Mix, Hot-Laid), and may be used on cores recovered from roadways or specimens compacted in the laboratory.

A.1.3. The values of indirect tensile strength and failure strains determined with this method can be used to estimate the low temperature and fatigue cracking potential of bituminous materials subjected to thermal and wheel loadings. These values can also be used to determine the optimum asphalt content for bituminous mixture designs. The values stated in inch-pound units are to be regarded as a standard. All values given in parentheses are for information only.

A.2 APPLICABLE DOCUMENTS

A.2.1 AASHTO Documents.

T 209 Maximum Specific Gravity of Bituminous Paving Mixtures
T 166 Test Method for Bulk Specific Gravity of Compacted Bituminous Mixtures
T 245 Test Method for Resistance to Plastic Flow of Bituminous Mixture Using the Marshall Apparatus
T 247 Method for Preparation of Test Specimens of Bituminous Mixture by Means of California Kneading Compactor
T 269 Percent Air Voids in Compacted Dense and Open Bituminous Paving Mixtures

A.2.2. ASTM Documents.

D 3202 Preparation of Bituminous Mixture Beam Specimens by Means of the California Kneading Compactor
D 3387 Test for Compaction and Shear Properties of Bitumi-

nous Mixtures by Means of the U.S. Corps of Engineers Gyratory Testing Machine (GTM)
D 3496 Method for Preparation of Bituminous Mixture Specimens for Dynamic Modulus Testing
D 3515 Specifications for Hot-Mixed, Hot-Laid Bituminous Paving Mixtures
D 4013 Preparation of Test Specimens of Bituminous Mixtures by Means of Gyratory Shear Compactor

A.3 SUMMARY OF METHOD

A.3.1. An asphaltic concrete sample is loaded in compression along the diametral axis at a fixed deformation rate, until failure. Failure is defined as the point or deformation when the load no longer increases. This maximum load sustained by the specimen is used to calculate the indirect tensile strength.

A.4 SIGNIFICANCE AND USE

A.4.1. The values of indirect tensile strength and failure strain can be used to evaluate the relative quality of bituminous materials, as well as to generate input for pavement design and evaluation models and mixture designs. The test can be used to study the effects of temperature, moisture, aging, and loading rates on these materials.

A.4.2. When used in conjunction with other physical properties, the indirect tensile strength and failure strain may contribute to the overall mixture characterization and are factors for determining its suitability for use as a highway paving material under given traffic loading and environmental conditions.

A.4.3. Reheated, recompacted mixtures may be used in this method, but the resulting indirect tensile strength and failure strains will be different from newly prepared mixtures because of changes in binder viscosity, an important factor of tensile strain as measured under the specific loading conditions and temperature.

A.5 APPARATUS

A.5.1. Equipment for preparing and compacting specimens is specified from one of the following methods: AASHTO T247, ASTM D 3387 or D 4013.

A.5.2. Axial loading machine required is any loading machine or press capable of providing a compressive load at a controlled vertical deformation rate (within 5 percent) from 0.05 to 2 in. (1.27 to 50.8 mm) per min.

A.5.3. Diametral loading strips are specified in accordance with ASTM D 4123.

A.5.4. Specimen axial deformation measurement and recording device is from ASTM D 4123.

A.5.5. Specimen axial load measurement device is required from ASTM D 4123.

A.5.6. Temperature control system is required from ASTM D 4123.

A.6 PREPARATION OF TEST SPECIMENS

A.6.1. Laboratory molded specimens are prepared in accordance with acceptable procedures, such as AASHTO T 247 or ASTM D 3387 and D 4013. Other procedures include cores cut from laboratory-prepared beams (for example, ASTM D 3202).

Note A.1: Normally test specimens are compacted using a standard compactive effort. However, a specific compactive effort may not reproduce the air voids measured on field cores. If the specimens are to be compacted to a target air void content, the compactive effort will need to be varied. For AASHTO T 247 (kneading compactor) the number of tamps, foot pressure and/or leveling load can be altered; for ASTM D 3387, the number of gyrations, angle of gyration and/or gyration pressure can be altered; and for ASTM D 4013 the gyration and/or end pressures or sets (3) of gyrations can be altered.

A.6.2. Core specimens shall have smooth and parallel surfaces and conform to the height and diameter requirements specified for specimens under paragraph A.6.3.

A.6.3. Indirect tension specimens to be tested shall have a height (or thickness) of at least 2 in. (5cm) and a minimum diameter of 4 in. (10 cm) for mixtures that contain aggregates with a maximum aggregate size of 1.0 in. (2.5 cm) or less, and a height of at least 3 in. (7.6 cm) and a minimum diameter of 6 in. (15 cm) for mixtures that contain maximum size aggregates up to 1.5 in. (3.8 cm) in diameter. The specimen height-to-diameter ratio shall be greater than 0.50 (see Note A.2).

Note A.2: The size of test specimens has an influence on the results from the indirect tensile test. The sample diameter to maximum aggregate size diameter ratio was studied by testing oversized cores. If at all possible, the sample diameter to maximum aggregate size diameter shall have a ratio greater than 4. Regarding the height-to-diameter ratio, four-inch diameter cores will not always be able to meet the minimum ratio of 0.50. When it is impossible to meet this criterion, it can be relaxed, but the variation in test results will increase requiring additional samples to be tested. For indirect tensile strength testing, the absolute minimum height of 4-inch (10 cm) diameter cores is 1.5 inches (3.8 cm) and 2.5 inches (6.3 cm) for 6-inch (15 cm) diameter cores.

A.6.4. Two diametral axes shall be marked on each test specimen, and the two axes shall be perpendicular to one another.

A.7 PROCEDURE

A.7.1. Measure the bulk specific gravity of each test specimen in accordance with AASHTO T 166 or T 275, whichever applies.

A.7.2. Place the test specimens in a controlled temperature cabinet and bring them to the specified test temperature. Unless the temperature is monitored and the actual temperature known, the specimen should remain in the cabinet at the specified test temperature for at least 12 hours prior to testing.

Note A.3: If the bulk specific gravity of the test specimens is measured in accordance with AASHTO T 166, the specimens must be allowed to dry prior to testing. Moisture or water trapped in the permeable voids can have an effect on the test results. Retaining these specimens in the temperature cabinet for 12 hours should be sufficient to allow the moisture to evaporate from the permeable voids.

A.7.3. Place the test specimen in the loading apparatus, position as stated in Test Method ASTM D 4123, adjust and balance the electronic measuring system as necessary.

A.7.4. Precondition the specimen by applying a repeated haversine (or other suitable wave form) to the specimen along each diametral axis marked in paragraph A.6.4, without impact, using a loading frequency of 1 cps for a minimum period sufficient to obtain uniform deformation readout (less than 2 percent deviation). Apply the preconditioning procedure described in ASTM

D 4123. In most cases, a preconditioning time of 25 to 45 sec is sufficient (25 to 45 loading cycles). The fixed load to be used for conditioning is that which will induce a tensile stress in the specimen of 5 to 20 percent of the indirect tensile strength, and result in a horizontal deformation greater than 0.0001 in. (0.00254 mm). This requires that at least one specimen be tested without conditioning to get an estimate of the indirect tensile strength of the mix.

A.7.5. At the end of the preconditioning step, measure the horizontal recoverable deformation along the two diametral axes in accordance with Section 2, paragraph 2.7.4 (Figure 5) to calculate the resilient modulus. The two axes shall be perpendicular to one another. Both the instantaneous and total resilient modulus shall be calculated and reported.

A.7.6. After the specimens have been preconditioned, apply a compressive load at a controlled deformation rate along the axis of the lower resilient modulus. A deformation rate of 2 in. (5 cm) per min is typically used for test temperatures of 77°F (25°C) and greater, whereas loading rates of 0.05 and 0.065 in. (1.27 and 1.65 mm) per min are typically used for the lower test temperatures (less than 50°F (10°C).

A.7.7. Monitor both the vertical and horizontal deformations during the entire loading time, or until the load sustained by the specimen begins to decrease. It is recommended that the test be stopped prior to fracturing the bituminous sample, so that damage to the horizontal deformation measuring equipment does not occur.

A.8 CALCULATIONS

A.8.1. Calculate the total and instantaneous resilient modulus for the last 3 cycles of the preconditioning part of the procedure, in accordance with Eq. 7 given in Table 4. The instantaneous and total resilient deformations are as defined by Section 2 (Mixture Design), paragraph 2.7.3.5.1 and 2.7.3.5.2 (Figure 5).

Table 4. Equations for calculating tensile properties (5).

STATIC PROPERTIES

(1)	Tensile strength S_t, psi	$= \frac{P_{fail}}{h} \cdot A_0$
(2)	Poisson's ratio ν	$= \frac{DR \cdot A_1 + B_1}{DR \cdot A_2 + B_2}$
(3)	Modulus of elasticity E, psi	$= \frac{S_h}{h} (A_3 - \nu \cdot A_4)$
(4)	Tensile strain ε_t, microunits	$= \Delta_h \left[\frac{A_5 - \nu \cdot A_6}{A_1 - \nu \cdot A_2} \right]$
(5)	Compressive strain ε_c, microunits	$= \Delta_v \left[\frac{B_3 - \nu \cdot B_4}{B_1 - \nu \cdot B_2} \right]$

REPEATED-LOAD PROPERTIES

(6)	Instantaneous Resilient Poisson's ratio ν_{RI}	$\frac{\frac{V_{RI}}{H_{RI}} A_1 + B_1}{\frac{V_{RI}}{H_{RI}} A_2 + B_2}$
(7)	Instantaneous Resilient Modulus of Elasticity E_{RI}, psi	$= \frac{P}{H_{RI} h} (A_3 - \nu_{RI} \cdot A_4)$
(8)	For Total Resilient Modulus, simply use the total resilient horizontal and vertical deformations, instead of the instantaneous deformations.	

P_{Fail} = total load at failure (maximum load P_{max} or load at first inflection point), pounds

P = applied load or repeated load, pounds

h = height of specimen, inches

DR = deformation ratio $\frac{Y_T}{X_T}$ (the slope of line of best fit* between vertical deformation Y_T and the corresponding horizontal deformation X_T up to failure load)

Δ_h = total horizontal deformation, inches

Δ_v = total vertical deformation, inches

S_H = horizontal tangent modulus $\frac{P}{X_T}$ (the slope of the line of best fit* between load P and horizontal deformation X_T for loads up to failure load)

H_{RI}, V_{RI} = instantaneous resilient horizontal and vertical deformations, respectively

A_0, A_1, A_2, A_3, A_4, A_5, A_6, B_1, B_2, B_3, B_4, = constants (SEE TABLE 5)

* It is recommended that the line of best fit be determined by the method of least squares.

A.8.2. For each specimen tested, calculate the indirect tensile strength in accordance with Eq. 1 in Table 4, using the constants given in Table 5.

A.8.3. For each specimen tested, calculate the tensile strain at failure in accordance with Eq. 4 in Table 4. The horizontal deformation used to calculate the tensile strain at failure (or yielding) is defined in Section 2, paragraph 2.7.4.3 (Figure 6).

A.8.4. Table 4 provides a listing of other equations that can be used to calculate other properties from the indirect tensile test.

A.9 REPORTS

A.9.1. The report shall include the following information, as a minimum. Figure 13 can be used as a guide in reporting these test data.

A.9.1.1. The bulk specific gravity of each specimen tested.

A.9.1.2. The maximum specific gravity of asphaltic concrete material.

A.9.1.3. The height and diameter of all specimens tested.

A.9.1.4. The test temperature and loading or deformation rates used during the test.

A.9.1.5. The total and instantaneous resilient modulus measured during the preconditioning section of the test specimen.

A.9.1.6. The vertical and horizontal tensile strains at maximum load, as a minimum.

A.9.1.7. A continuous load deformation plot of each specimen shall be included with the report.

Table 5. Constants for use in equations for indirect tensile properties (5).

Diameter inches	A_0	A_1	A_2	A_3	A_4	A_5	A_6	B_1	B_2	B_3	B_4
4.0	.156	.0673	-.2494	.2692	-.9974	.03896	-.1185	-.8954	-.0156	-.1185	.03896
4.1	.152	.0657	-.2433	.2694	-.9975	.03712	-.1129	-.8810	-.0149	-.1129	.03712
4.2	.149	.0642	-.2375	.2696	-.9976	.03541	-.1076	-.8671	-.0142	-.1076	.03541
4.3	.145	.0627	-.2320	.2698	-.9977	.03381	-.1027	-.8537	-.0136	-.1027	.03381
4.4	.142	.0613	-.2268	.2699	-.9978	.03232	-.09808	-.8407	-.0130	-.9809	.03232
4.5	.139	.0600	-.2218	.2701	-.9979	.03092	-.09379	-.8282	-.0124	-.9380	.03092
4.6	.136	.0587	-.2170	.2702	-.9980	.02961	-.08978	-.8161	-.0118	-.8979	.02961
4.7	.133	.0575	-.2124	.2703	-.9981	.02838	-.08602	-.8043	-.0114	-.8603	.02839
4.8	.131	.0563	-.2080	.2704	-.9982	.02723	-.08249	-.7930	-.0109	-.8250	.02723
4.9	.128	.0552	-.2037	.2706	-.9983	.02615	-.07917	-.7820	-.0105	-.7918	.02615
5.0	.126	.0541	-.1997	.2707	-.9983	.02512	-.07605	-.7714	-.0100	-.7606	.02513
5.1	.123	.0531	-.1958	.2708	-.9984	.02416	-.07311	-.7610	-.0966	-.7312	.02416
5.2	.121	.0521	-.1920	.2709	-.9985	.02325	-.07034	-.7510	-.0929	-.7034	.02325
5.3	.119	.0511	-.1884	.2709	-.9985	.02239	-.06772	-.7413	-.0895	-.6772	.02240
5.4	.116	.0502	-.1849	.2710	-.9986	.02158	-.06524	-.7319	-.0862	-.6525	.02158
5.5	.114	.0493	-.1816	.2711	-.9986	.02081	-.06290	-.7227	-.0832	-.6291	.02081
5.6	.112	.0484	-.1783	.2712	-.9987	.02008	-.06068	-.7138	-.0803	-.6069	.02008
5.7	.110	.0476	-.1752	.2713	-.9987	.01939	-.05858	-.7051	-.0775	-.5858	.01939
5.8	.109	.0468	-.1722	.2713	-.9988	.01874	-.05658	-.6967	-.0749	-.5659	.01874
5.9	.107	.0460	-.1693	.2714	-.9988	.01811	-.05469	-.6884	-.0724	-.5469	.01811
6.0	.105	.0452	-.1665	.2714	-.9988	.01752	-.05289	-.6804	-.0700	-.5289	.01752

Strip width a = 0.5 in.

INDIRECT TENSILE STRENGTH TEST

PROJECT NO. _____
HIGHWAY _____ COUNTY _____
MIXTURE I.D. _____

RICE SPECIFIC GRAVITY _____
TEST TEMPERATURE _____ F
LOADING RATE _____ IN./MIN

Core/Specimen I.D.					
Date Cored/Compacted					
Bulk Specific Gravity					
Air Voids, %					
Diameter, in., D_s	1				
	2				
	3				
	Avg.				
Height, in., h	1				
	2				
	3				
	Avg.				
Total Resilient Modulus, ksi, E_{RT}					
	Axis 1				
	Axis 2				
	Avg.				
Total Maximum Vertical Load (At Failure), lbs., P_t					
Vertical Deformation At Maximum Vertical Load, in., V_{RT}					
Horizontal Deformation At Maximum Vertical Load, in., H_{RT}					
Indirect Tensile Strain At Failure, in./in., ε_t					
Indirect Tensile Strength, psi, S_t					

REMARKS _____

TESTED BY _____ DATE TESTED _____

Figure 13. Indirect tensile strength data sheet.

ADDENDUM B—TEST METHODS FOR CREEP MODULUS TESTING OF BITUMINOUS MIXTURES

B.1 SCOPE

B.1.1. This method covers the determination of creep modulus at different loading times using diametral and uniaxial compression loadings for compacted dense-graded, hot-mixed, hot-laid bituminous mixtures. Uniaxial compression testing is used to characterize asphaltic concrete mixtures in compression for rutting evaluation, and indirect tensile testing is used to characterize the same mixture in tension for thermal and fatigue cracking analyses.

B.1.2. This method is applicable to dense-graded hot-mixed, hot-laid asphaltic concrete mixtures, as defined by ASTM D 3515 (Bituminous Paving Mixtures, Hot-Mix, Hot-Laid), and may be used on cores recovered from roadways or specimens compacted in the laboratory.

B.1.3. The values of creep modulus determined with this method can be used in linear-elastic and nonlinear-elastic layered system theories to predict the stiffness of asphaltic concrete materials or to calculate the expected rut depth or low temperature cracking potential of asphaltic concrete layers subjected to thermal and wheel loadings.

Note B.1: Lateral confinement for uniaxial compression testing is a very important factor in measuring the creep properties of asphaltic concrete materials. However, most pavement performance models have been developed and, more importantly, calibrated on the basis of unconfined test results. Therefore, this test method covers samples tested without confinement, which represents the more critical condition from a mixture design point of view. It is also difficult to simulate in the laboratory the vertical distribution of confining pressures that occur in the asphaltic concrete layer on the roadway.

B.1.4. The test method is divided into two parts, one for uniaxial compression testing and the second for indirect tensile testing.

B.2 APPLICABLE DOCUMENTS

B.2.1 AASHTO Documents.

T 166 Test Method for Bulk Specific Gravity of Compacted Bituminous Mixtures
T 167 Compressive Strength of Bituminous Mixtures
T 209 Maximum Specific Gravity of Bituminous Paving Mixtures
T 245 Test Method for Resistance to Plastic Flow of Bituminous Mixture Using the Marshall Apparatus
T 247 Method for Preparation of Test Specimens of Bituminous Mixture by Means of California Kneading Compactor
T 269 Percent Air Voids in Compacted Dense and Open Bituminous Paving Mixtures

B.2.2 ASTM Documents.

D 3202 Preparation of Bituminous Mixture Beam Specimens by Means of the California Kneading Compactor
D 3387 Test for Compaction and Shear Properties of Bituminous Mixtures by Means of the U.S. Corps of Engineers Gyratory Testing Machine (GTM)
D 3497 Dynamic Modulus of Asphalt Mixtures
D 3515 Specifications for Hot-Mixed, Hot-Laid Bituminous Paving Mixtures
D 4013 Preparation of Test Specimens of Bituminous Mixtures by Means of Gyratory Shear Compactor

B.3 SUMMARY OF METHOD

B.3.1 Uniaxial Compression. A static load of fixed magnitude is applied along the cylindrical axis of a preconditioned or densified cylindrical asphaltic concrete specimen for a fixed duration of time. The total uniaxial (compressive) deformation of the specimen is measured and used to calculate a compressive creep modulus at a particular duration of time. After the load is released, the resilient (recoverable) deformation is measured over a fixed duration of time and used to calculate the compression recovery efficiency from a static load.

B.3.2 Indirect Tension. A static load of fixed magnitude is applied along the diametral axis of a preconditioned specimen for a fixed duration of time. The total horizontal deformation of the specimen is measured and used to calculate an indirect tensile creep modulus at a particular duration of time. After the load is released, the resilient (recoverable) horizontal deformation is measured over a fixed duration of time and used to calculate the indirect tensile recovery efficiency from a static load.

B.4 SIGNIFICANCE AND USE

B.4.1. The values of creep modulus can be used to evaluate the relative quality of materials, as well as to generate input for pavement design and evaluation models. The test can be used to study effects of temperature, load magnitude, binder content, and creep loading time. For uniaxial cylindrical compression specimens, the test can be performed with or without a confining pressure. For purposes of this standard, all creep modulus testing is to be conducted without lateral confinement (See Note B.1).

B.4.2. When used in conjunction with other mixture physical properties, the creep modulus may contribute to the overall mixture characterization and is one factor for determining its suitability for use as a highway paving material under given traffic and environmental conditions.

B.4.3. Reheated, recompacted mixtures may be used in this method, but the resulting creep modulus values will be higher than for newly prepared mixtures because of changes in binder viscosity, an important factor of creep strains as measured under these specific loading conditions and temperatures.

B.5 APPARATUS

B.5.1 Axial Loading Machine. Any loading machine capable of

providing a load of fixed cycle and duration can be used. Typically, a cam and switch or timer control of solenoid valves operating a pneumatic air piston, or a closed-looped electrohydraulic system is used. Pneumatic systems are the least complex, while closed-looped electrohydraulic systems allow more versatility (variable wave forms, higher loads, and higher frequency response). Variable wave forms and different frequencies are used in preconditioning the test specimens.

B.5.2 Temperature and Control System. The temperature control system shall be capable of control over a temperature range from 0 to 104°F (−18 to 40°C) and within ± 1.8°F (1°C) of the specified temperature within the range. The system can be a room, chamber and/or cabinet that shall be large enough to hold at least three specimens for a period of 12 hours prior to testing. If the testing machine is located in a room without the specified temperature control systems, a controlled temperature cabinet shall be used during the entire test.

B.5.3 Specimen Deformation Measurement Devices. The creep modulus test requires deformation transducers with high resolution and a small range during the preconditioning part of the test and less resolution but a larger range during the test. The linear variable differential transducer (LVDT) is considered to be the most suitable deformation transducer for the test. The LVDT must have a range of at least 20 percent of the gage length, but should not exceed 60 percent of the gage length.

B.5.4 Specimen Load Measurement Device. The load measuring device is to be an electronic load cell. The load is to be measured by placing the load cell between the specimen cap and the loading position. The total load capacity of the load transducer (load cell) should be of the proper order of magnitude with respect to the maximum total load to be applied to the test specimen. Generally, its capacity should be no greater than 5 times the total maximum load applied to the test specimen to ensure that the necessary measurement accuracy is achieved. The load-measuring device shall be capable of measuring the load to an accuracy of ± 1 percent of the applied load.

B.5.5 Recording Device. Specimen behavior in the creep modulus test is evaluated from time records of applied load and specimen deformation. Commonly, these parameters are recorded on a multichannel strip-chart recorder. Analog to digital data acquisition systems may be used provided that the data can be converted later into a convenient form for data analysis and interpretation. For analog strip-chart recording equipment, the deformation recorder trace must be of sufficient magnitude and time resolution to enable accurate data reduction. Resolution of each variable should be better than 2 percent of the maximum value being measured. The clarity of the trace with respect to the background should provide sufficient contrast and a minimum resolution of 2 percent of the maximum value of the recorded parameter that is maintained, so that the trace may be included in reports.

B.5.6 Oven. The oven for the preparation of hot mixtures shall be capable of being set to maintain any desired temperature from room temperature to 325°F (163°C).

B.6 PREPARATION OF TEST SPECIMENS

B.6.1 Laboratory Molded Specimens. Prepare the laboratory-molded specimens in accordance with acceptable procedures, such as AASHTO T 247 or ASTM D 3387 and D 4013. Other procedures include cores cut from laboratory-prepared beams (for example, ASTM D 3202).

Note B.2: The type of compaction device will influence the test results or creep modulus values. ASTM D 3387 and D 4013 are preferred techniques but AASHTO T 247 produces specimens that are reasonable. AASHTO T 245 (Marshall Hammer) is not recommended for preparing specimens for creep modulus testing.

Note B.3: Normally test specimens are compacted using a standard compactive effort. However, a specific compactive effort may not reproduce the air voids measured on field cores. If specimens are to be compacted to a target air void content, the compactive effort will need to be varied. For AASHTO T 247 (kneading compactor) the number of tamps, foot pressure and/or leveling load can be altered; for ASTM D 3387 (Corps of Engineers Gyratory Testing Machine), the number of gyrations, angle of gyration and/or gyration pressure can be altered; and for ASTM D 4013 the gyration and/or end pressures or sets (3) of gyrations can be altered. The actual compactive effort to be used should be determined experimentally.

B.6.2 Core Specimens. Cores shall have relatively smooth and parallel surfaces and conform to the height and diameter requirements specified for specimens under paragraph B.6.3.

B.6.3 Specimen Size.

B.6.3.1. Uniaxial compression specimens to be tested shall have a height of at least 4 in. (10 cm) and a minimum diameter of 4 in. (10 cm) for mixes that contain aggregates with a maximum aggregate size of 1.0 in. (2.5 cm) or less, and a height of at least 6 in. (15 cm) and a minimum diameter of 6 in. (15 cm) for mixes that contain maximum size aggregates up to 1.5 in. (3.8 cm) in diameter. The specimen height-to-diameter ratio shall always exceed 1.0.

Note B.4: End effects and lateral restraint between the top and bottom platens and the specimen can have a significant effect on the measured vertical deformation for uniaxial compression testing. For specimens less than 6 inches (15 cm) in height and where the entire specimen is used to measure the deformation, a friction reducing material must be used between the specimen and top and bottom platens. Materials that can be used include silicon grease, graphite, and Teflon tape. Without use of this friction reducing material, shear stresses between the specimen and top and bottom platens can cause the specimen to bulge and underestimate the amount of vertical displacement.

B.6.3.2. Indirect tensile specimens to be tested shall have a height (or thickness) of at least 2 in. (5 cm) and a minimum diameter of 4 in. (10 cm) for mixtures that contain aggregate with a maximum aggregate size of 1.0 in. (2.5 cm) or less, and a height of at least 3 in. (7.6 cm) and a minimum diameter of 6 in. (15 cm) for mixtures that contain maximum size aggregates up to 1.5 in. (3.8 cm) in diameter. The specimen height-to-diameter ratio shall exceed 0.50 (see Note B.5).

Note B.5: The size of test specimens has an influence on results from the tensile creep modulus test. If at all possible, the sample diameter to maximum aggregate size diameter should have a ratio greater than 4. Regarding the height-to-diameter ratio, four-inch diameter cores will not always be able to meet the minimum ratio of 0.50. When it is impossible to meet this criterion, it can be relaxed, but the variation in test results will increase requiring additional samples to be tested. For indirect tensile creep testing, the absolute minimum height of 4-inch (10 cm) diameter cores is 1.5 inches (3.8 cm) and 2.5 inches (6.3 cm) for 6-inch (15 cm) diameter cores.

B.7 PROCEDURE

B.7.1. Measure the bulk specific gravity of each test specimen in accordance with AASHTO T 166 or T 275, whichever applies.

B.7.2. Place the test specimen in a controlled temperature cabinet and bring it to the specified test temperature. Unless the temperature is monitored and the actual temperature known, the specimen shall remain in the cabinet at the specified test temperature for at least 12 hours prior to testing.

Note B.6: If the bulk specific gravity of the test specimens is measured in accordance with AASHTO T 166, the specimens must be allowed to dry prior to testing and preconditioning. Moisture or water trapped in the permeable voids can have an effect on the test results. Retaining the specimens in the temperature cabinet for 12 hours should be sufficient to allow the moisture to evaporate from the permeable voids.

B.7.3 Uniaxial Compression Specimens.

B.7.3.1. Place the test specimen in the loading apparatus, position as stated in ASTM D 3497, adjust, and balance the electronic measuring system as necessary.

B.7.3.2. The fixed load to be used for uniaxial compression creep modulus testing is that which will induce a compressive stress of 5 to 25 percent of the unconfined compressive strength, as measured by AASHTO T 167, and result in a vertical deformation greater than 0.0001 in. (0.00254 mm).

B.7.3.3. Precondition the specimen by applying a repeated haversine (or other wave form) to the specimen without impact using a loading frequency of 1 cps (0.1-sec load duration and 0.9-sec rest period) for a minimum period sufficient to obtain uniform deformation readout (less than 2 percent deviation). Apply the preconditioning procedures described in ASTM Method D 3497.

Note B.7: In most cases, a preconditioning time of 25 to 45 seconds is sufficient (25 to 45 loading cycles).

B.7.3.4. At the end of the preconditioning step, measure the vertical uniaxial recoverable deformations to calculate the total or instantaneous resilient modulus in accordance with Section 2, paragraph 2.9.4 of Part I.

B.7.3.5. After the samples have been preconditioned, rezero or rebalance the electronic measuring system and apply a static load of fixed magnitude (± 2 percent) to the specimen.

B.7.3.6. Monitor the vertical deformation during the entire loading time. The load shall be applied for a period of 60 min, ± 15 sec.

B.7.3.7. After the fixed load has been applied over a period of 60 min, the load shall be released and the rebound or resilient deformation monitored and recorded for an additional 60 min of no load. After 60 min, ±15 sec, the amount of permanent vertical deformation shall be measured and recorded from the strip chart recorder or the continuous deformation trace.

B.7.4 Indirect Tensile Specimens.

B.7.4.1. Place the test specimen in the loading apparatus, position as stated in Test Method ASTM D 4123, adjust, and balance the electronic measuring system as necessary.

B.7.4.2. The fixed load to be used for indirect tensile creep modulus testing is that which will induce a tensile stress in the specimen of 5 to 20 percent of the indirect tensile strength, and result in a horizontal deformation greater than 0.0001 in. (0.00254 mm).

B.7.4.3. Precondition the specimen by applying a repeated haversine (or other suitable wave form) to the specimen without impact using a loading frequency of 1 cps (0.1-sec load duration and 0.9-sec rest period) for a minimum period sufficient to obtain uniform deformation readout (less than 2 percent deviation). Apply the preconditioning procedure described in ASTM D 4123 (see Note B.7).

B.7.4.4. At the end of the perconditioning step, measure the horizontal recoverable deformation to calculate the total or instantaneous resilient modulus in accordance with Section 2, paragraph 2.7.4 of Part I (Figure 5).

B.7.4.5. The recommended load range to be used for indirect tensile or creep modulus testing is that to induce 5 to 20 percent of the indirect tensile strength.

B.7.4.6. After the test specimens have been preconditioned, rezero or rebalance the electronic measuring system and apply a static load of fixed magnitude (± 2 percent) to the specimen.

B.7.4.7. Monitor both of the vertical and horizontal deformations during the entire loading time. The load shall be applied for a period of 60 min ± 15 sec.

B.7.4.8. After the fixed load has been applied over a period of 60 min, the load shall be released and the rebound or resilient deformation (both in the vertical and horizontal directions) recorded and monitored for an additional 60 min of no load. After 60 min, ± 15 sec, the amount of permanent deformations (horizontal and vertical) shall be measured and recorded from the strip-chart recorder or the continuous deformation trace.

B.7.5. After testing has been completed, the specimens shall be broken down and the maximum specific gravity measured in accordance with AASHTO T 209.

B.8 CALCULATIONS

B.8.1. Calculate the resilient modulus of elasticity for the preconditioning part of the procedure, as stated in paragraphs B.7.3.3 or B.7.4.3, whichever applies.

B.8.2. For each specimen tested, calculate the creep modulus at times of 1, 10, 100, 1,000 and 3,600 sec, as a minimum. Additional times may be required to define the deformation-time curve for mixture evaluation.

B.8.2.1. Uniaxial compression sample calculations are as follows:

$$E_{cq}(t) = \sigma_c / \epsilon_c(t) \qquad \text{(B-1)}$$

where

$E_{cq}(t)$ = creep modulus at time t, psi;
σ_c = compressive stress applied to the specimen, psi;
$\epsilon_c(t)$ = uniaxial strain at time t, in./in.;

$$\epsilon_c(t) = \Delta_v(t)/\ell \qquad \text{(B-2)}$$

ℓ = gage length which is the distance between the LVDTs, or the average height of the specimen being tested, if clamps are not used on the specimen, in.;
$\Delta_v(t)$ = uniaxial deformation at time t, in.

B.8.2.2. Indirect tensile sample calculations for 4-in. diameter specimens (see Note B.8 for other size specimens) include:

$$E_{ct4}(t) = \sigma_{t4} / \epsilon_{t4}(t) \qquad \text{(B-3)}$$

where:

σ_{t4} = tensile stress along the diametral axis of a 4-in. diameter specimen, psi;

$$\sigma_{t4} = \frac{P}{h}(0.156) \qquad \text{(B-4)}$$

$\epsilon_{t4}(t)$ = tensile creep strain for specimens with a 4-in. diameter, in./in.;

$$\epsilon_{t4} = \Delta_H(t)\left[\frac{0.03896 + (\nu)\,0.1185}{0.0673 + (\nu)\,0.2494}\right] \quad \text{(B-5)}$$

$\Delta_H(t)$ = the horizontal deformation in inches at time t, in.;
ν = Poisson's ratio; and
P = load applied to the specimen, lb.

Note B.8: For other size specimens, refer to Addendum A (Tables 4 and 5) to obtain the coefficients for specimens with different diameters.

B.8.2.3. Calculate the recovery efficiency, X, of the test specimen.

$$X = \frac{\Delta_r(3,600)}{\Delta_{v(H)}(3,600)} \quad \text{(B-6)}$$

where:

$\Delta_r(3,600)$ = the recoverable vertical deformation for uniaxial compression tests or horizontal deformation for indirect tensile tests at the end of the test (i.e., after 3,600 sec of no load); and
$\Delta_{v(H)}$ = the vertical deformation for uniaxial compression tests or horizontal deformation for indirect tensile tests just prior to removing the load from the specimen (load time = 3,600 sec).

B.9 REPORT

B.9.1. The report shall include the following information as a minimum. Figures 14 and 15 can be used as a guide in reporting these test data.

B.9.1.1. The bulk specific gravity of each specimen tested.

B.9.1.2. The maximum specific gravity of the asphaltic concrete mixture.

B.9.1.3. The height and diameter of all test specimens.

B.9.1.4. The test temperature and load levels used during the test.

B.9.1.5. The resilient modulus measured at the end of the preconditioning part of the test procedure.

B.9.1.6. The creep modulus values for the times specified, as a minimum.

B.9.1.7. The permanent strain measured at the end of the test, after no-load rebound, and the recovery efficiency of the mixture.

NOTES

CREEP MODULUS TEST
(UNIAXIAL COMPRESSION LOADING)

IDENTIFICATION:

PROJECT NO. _____

HIGHWAY _____ COUNTY _____

MIXTURE I.D. _____

CORE I.D. _____ STATION _____ DATE CORED _____

COMPACTED SPECIMEN _____ DATE _____

REMARKS _____

SAMPLE DATA

RICE SPECIFIC GRAVITY _____

BULK SPECIFIC GRAVITY _____ AIR VOIDS _____%

AVERAGE DIAMETER (IN.) 1) _____ 2) _____ 3) _____ AVG. _____

AVERAGE HEIGHT (IN.) 1) _____ 2) _____ 3) _____ AVG. _____

TEST CONDITIONS

TOTAL LOAD _____LBS. APPLIED STRESS _____PSI TEMPERATURE _____°F

PRECONDITIONING

NO. OF CYCLES _____ TOTAL RESILIENT MODULUS _____KSI

Loading Time (sec.)	Vertical Deformation (in.)	Compressive Creep Strain (in./in.)	Compressive Creep Modulus (psi)	Load Release Time (sec.)	Vertical Deformation (in.)
0				0	
1				1	
3				3	
10				10	
30				30	
100				100	
300				300	
1,000				1,000	
3,600				3,600	

TESTED BY _____ DATE TESTED _____

Figure 14. Uniaxial compression creep modulus data sheet.

CREEP MODULUS TEST
(INDIRECT TENSILE LOADING)

IDENTIFICATION:

PROJECT NO. _____
HIGHWAY _____ COUNTY _____
MIXTURE I.D. _____

CORE I.D. _____ STATION _____ DATE CORED _____

COMPACTED SPECIMEN _____ DATE _____

REMARKS _____

SAMPLE DATA

RICE SPECIFIC GRAVITY _____
BULK SPECIFIC GRAVITY _____ AIR VOIDS _____%
AVERAGE DIAMETER (IN.) 1) _____ 2) _____ 3) _____ AVG. _____
AVERAGE HEIGHT (IN.) 1) _____ 2) _____ 3) _____ AVG. _____

TEST CONDITIONS

TOTAL LOAD _____LBS TEMPERATURE _____°F
APPLIED TENSILE STRESS _____PSI COMPRESSIVE STRESS _____PSI

PRECONDITIONING

NO. OF CYCLES _____ TOTAL RESILIENT MODULUS _____KSI

Loading Time (sec.)	Vertical Deformation (in.)	Horizontal Deformation (in.)	Tensile Creep Strain (in./in.)	Tensile Creep Modulus (psi)	Load Release Time (sec.)	Vertical Deformation (in.)	Horizontal Deformation
0					0		
1					1		
3					3		
10					10		
30					30		
100					100		
300					300		
1,000					1,000		
3,600					3,600		

TESTED BY _____ DATE TESTED _____

Figure 15. Indirect tensile creep modulus data sheet.

SECTION 4
GUIDELINES FOR MIXTURE PERFORMANCE EVALUATION

4.1 SCOPE

The guidelines presented in this section of the manual provide a recommended practice for evaluating asphaltic concrete mixtures based on performance-related criteria. The concept of basing a mixture design procedure directly on performance predictions of asphalt pavements is logical and appropriate, and a requirement in order to optimize mixture and structural designs. Mathematical models, however, are required to support this methodology, and all available models are limited in use to some degree. Thus, the types of models suggested for use in NCHRP Project 1-26 (*12*) were simply accepted and used for mixture evaluation.

4.2 ASPHALT PAVEMENT/MIXTURE EVALUATION METHODOLOGY

There are mechanistic models available that can be used to calculate stresses, strains and deflections within the pavement structure. The weak links of the methodology are the empirical or regression models relating pavement response parameters to pavement distress. These regression models, which are needed to support the methodology, either do not exist or they are limited (especially for asphaltic concrete overlays). Some of these performance models are under development, but are unavailable for incorporation in AAMAS at this time. Thus, only a recommended practice for asphaltic concrete mixture evaluation is given.

A number of good methods of evaluating and designing pavements have evolved through the years, each with merit. All require that the physical and strength characteristics of the subgrade soil and other pavement layers be estimated, the loading frequency be determined, and a thickness of improved materials necessary to distribute the loads to the subgrade be established. Some of the mechanistic/empirical models that have been developed from previous studies are briefly discussed in Part II of this report. Most use similar engineering properties, such as Poisson's ratio, modulus of elasticity, tensile strength, and fatigue constants. The key requirement of the AAMAS is that it control the material and engineering properties that are considered significant input parameters for the structural design and performance of asphalt pavements.

4.2.1 Design and Evaluation Models. Two common methods used for the structural design and evaluation of asphaltic concrete pavements are AASHTO (*6*) and the Asphalt Institute's Program "DAMA" (*7*). AASHTO uses the serviceability index to define pavement failure. In the AASHTO procedure, the decrease in serviceability is related to an increase in roughness (and cracking, patching, and rutting to a lesser degree). The Asphalt Institute's Program "DAMA" is a mechanistic-empirical procedure, which uses fatigue cracking and rutting (permanent deformation) to define failure. The fatigue criterion is based on minimizing tensile strains at the bottom of the asphaltic concrete layer, whereas the rutting criterion is based on limiting vertical compressive strains at the top of subgrade. Both strains are computed with elastic layer theory.

In most models, with the exception of Shell (*8*), rutting is considered to occur in the subgrade and has been related to the vertical compressive strain at the top of the subgrade. This assumption implies that the structural layers above the subgrade will be constructed such that only negligible rutting will occur within them. Of course, this is an inaccurate assumption for those cases where the asphaltic concrete mixtures have inadequate shear strength and are susceptible to one-dimensional densification or lateral flow. For the AAMAS, the assumption of negligible rutting is inappropriate and cannot be made.

4.2.2 Asphalt Pavement Performance Measures. Most of the original structural design work sponsored as part of FHWA and NCHRP projects (*10, 11*) recognized three distresses. These were: (1) thermal or low temperature cracking, (2) fatigue cracking, and (3) rutting or permanent deformation. Other distress types can be equally important, but have historically received much less study. These include stripping or moisture damage, reduced skid resistance, raveling and bleeding. Although all distresses could be considered, the following four distresses, resulting from load or environmental conditions, are believed to be the most important with respect to reductions in serviceability and in asphalt pavement performance: fatigue cracking, thermal cracking, permanent deformation, and moisture damage.

Asphalt hardening or aging is also important to long-term pavement performance. However, this is not a distress, but a factor having an important impact on the distresses given previously. This phenomenon must therefore be evaluated. Secondary consideration is given to surface deterioration in the form of raveling or disintegration and loss of skid resistance.

4.2.3 Mixture Evaluation. For the AASHTO procedure, the final product from a mixture evaluation procedure is simply a resilient modulus value at 68°F. Although AAMAS and the AASHTO Design Guide (*6, 7*) should be compatible, a resilient modulus measured at 68°F by itself is no more accurate than the empirical mixture design values, such as a stability number. Different material properties and a range of test conditions are needed to evaluate the distresses noted above.

Application of the models suggested for use in NCHRP Project 1-26 (*12*) permits a design–performance comparison of different pavement structures supporting different traffic levels over varying subsurface and climatic conditions. Although these models consider a wide range of variables and are reasonably detailed, the distress or damage predictions may only be claimed to be as good as the state of the art allows and *only when traffic estimates, loads, and tire pressures are reasonably accurate.* In other words, the damage and distress predictions offer valuable information for purposes of comparisons, but they are approximate, as are most engineering analyses involving soils and bituminous mixtures.

The AAMAS procedure consists of a series of steps using results from the test program, discussed in Section 3, as well as interactions with various models predicting the four types of

distresses noted earlier. The final product of the AAMAS provides the structural and material combinations needed to meet the design requirements or assumptions used by the pavement design engineer.

4.3 GUIDELINES FOR ESTABLISHING LABORATORY TEST CONDITIONS

One of the important parameters in evaluating asphaltic concrete mixtures in the laboratory is to use realistic stress states for measuring the pertinent engineering properties. Typically, most of the properties are measured in the steady state or low stress range. In most cases, this is adequate if only relative comparisons of different asphaltic concrete materials are made. For mixture evaluations, relative comparisons can be inadequate. Thus, one question to be answered is: Are the stress states used in the laboratory close to those that actually occur on the roadway under traffic and environmental loads? Stress state depends on tire pressure, tire type, axle load, temperature, layer thicknesses, pavement type, and so on.

As an example, use of the AASHTO Design Guide requires that the resilient modulus of asphaltic concrete be measured at 68°F in accordance with ASTM D 4123 to determine the layer coefficient for thickness determination. In other words, the same resilient modulus, or layer coefficient, would be selected for a given material regardless of the environment. However, a mixture placed in southern New Mexico will perform significantly different from the same mixture placed in northern Maine, even though both mixtures could have the same resilient modulus at 68°F. Thus, temperature and other environmental factors must be considered in establishing realistic test conditions for evaluating asphaltic concrete mixtures.

Three test temperatures have been specified in the laboratory analyses section for testing asphaltic concrete mixtures. These temperatures are 41, 77 and 104°F, which are consistent with most AASHTO and ASTM procedures. For extreme climates, however, other temperatures will need to be used, or additional ones added to the test program to cover the expected temperature range for the site-specific conditions.

To estimate the roadway conditions to be simulated in the laboratory, elastic layer theory or other response models can be used to calculate the stresses and strains in an asphaltic concrete layer under different loading and environmental conditions. Of course, all assumptions used with elastic layer theory apply to these recommendations, and the normal and principal stresses calculated on an element in an asphaltic concrete layer will not be the same as those, for example, in an indirect tensile specimen. Thus, it is recommended that the octahedral shear stress theory (distortion energy theory) be used to calculate those horizontal and vertical stresses in an indirect tensile specimen to result in an equivalent maximum octahedral shear stress calculated in the asphaltic concrete layer. The octahedral shear stress is given by:

$$\tau_{oct} = 1/3\ ((\sigma_1 - \sigma_2)^2 + (\sigma_2 - \sigma_3)^2 + (\sigma_3 - \sigma_1)^2)^{0.5} \qquad (4\text{-}1)$$

where σ^1, σ^2, and σ^3 are the first, second, and third principal stresses.

The octahedral shear stress at failure represents the critical shearing stress at yielding. For a precise analysis of stress, elastic layer theory or finite element analysis can be used to calculate the normal and principal stresses that exist in an element within the asphaltic concrete layer for determining the appropriate laboratory loading conditions. This allows factors such as contact pressures, tire types and total loads to be considered in the laboratory during mixture design to ensure that the mix can sustain the imposed stresses. The stresses predicted using the octahedral shear stress theory are used in the resilient modulus and static creep tests.

Guidelines are included in the subsections that follow and in Section 3 for selecting representative values of the compressive and tensile stresses (or loads) to be used in the test program. The important point to emphasize for AAMAS is that a similar or equivalent stress state must be used in the laboratory to characterize asphaltic concrete mixtures and measure those properties required to predict how they will perform under traffic and the environment.

4.4 AASHTO STRUCTURAL LAYER COEFFICIENT

As stated earlier, the structural layer coefficient for dense-graded asphaltic concrete is estimated from the resilient modulus measured at 68°F in accordance with ASTM D 4123. However, the response and performance of asphaltic concrete materials are dependent on the environmental conditions, as well as tire and axle configurations. One technique that can be used to evaluate the environmental effects on the structural design is to consider seasonal fatigue damage. In other words, use seasonal resilient moduli to calculate seasonal fatigue damage and sum the seasonal damage to determine an annual damage. From the annual damage, an equivalent asphaltic concrete resilient modulus can be calculated by the following equation.

$$E_{RE} = \sum \frac{E_{Rt}(i) \times FF(i)}{\sum FF} \qquad (4\text{-}2)$$

where E_{RE} is the equivalent resilient modulus based on a fatigue damage approach; E_{R_t} is the total resilient modulus as measured by ASTM D 4123 at the average pavement temperature for season i; and FF is the fatigue factors obtained from Figure 16.

Equation 4-2 includes only the damage associated with fatigue cracking and ignores any damage caused by permanent deformation and disintegration. This is a necessary assumption because of the limited tie between resilient modulus and fatigue cracking and layer coefficients. It does, however, allow seasonal and environmental effects to be used in estimating the AASHTO structural layer coefficient. Figure 17 is a chart for plotting the test results of total resilient modulus (unconditioned) versus temperature, as compared to the range of values that are appropriate for higher volume roadways.

The following is a step-by-step procedure that can be used to ensure that the asphaltic concrete mixture meets or exceeds the layer coefficient assumed during structural design.

- Obtain the seasonal average pavement temperature for each season.
- Determine the total resilient modulus at each seasonal temperature.
- Obtain the fatigue factor for each seasonal resilient modulus from Figure 16.
- Calculate the equivalent resilient modulus using Eq. 4-2.

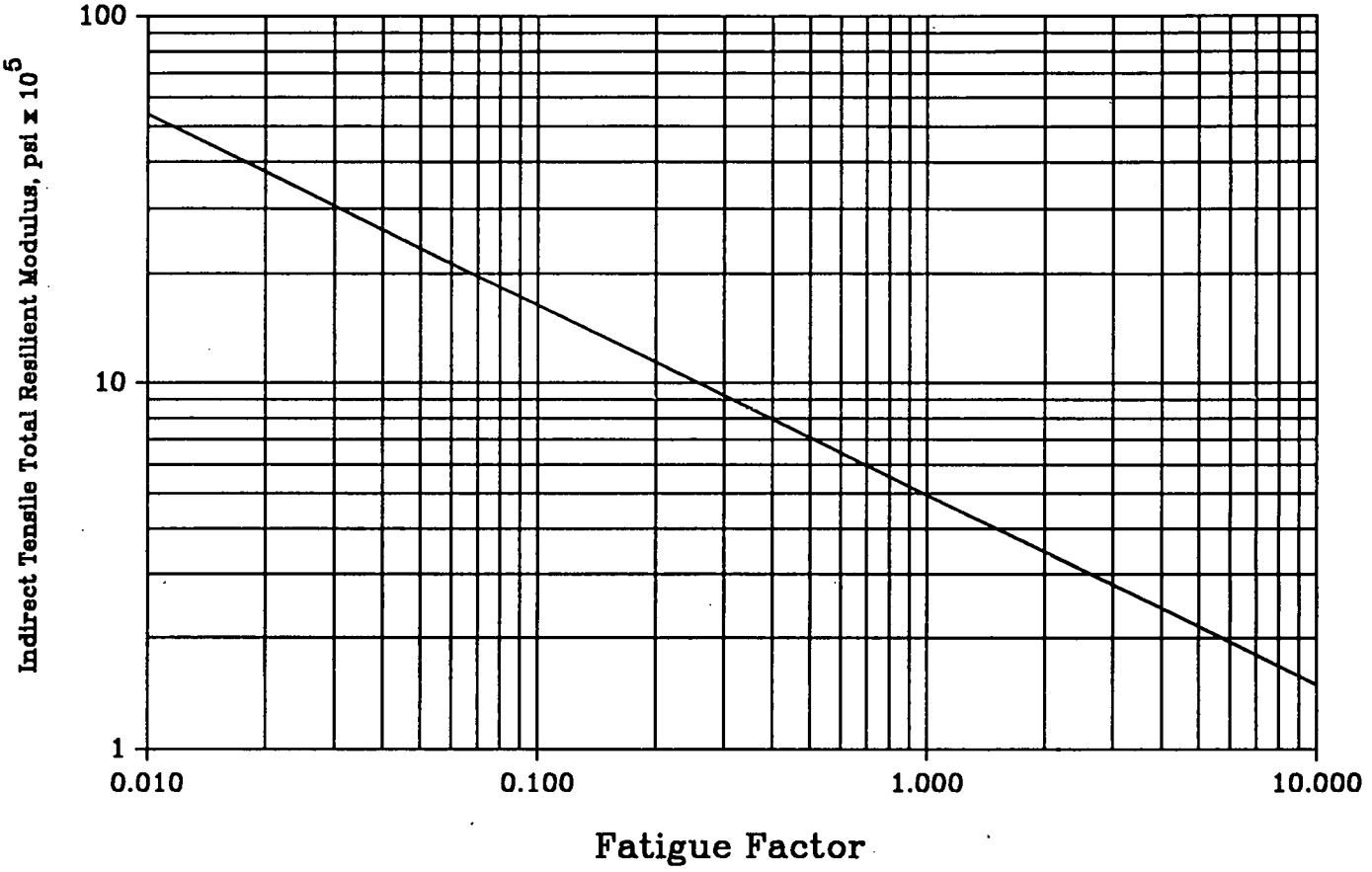

Figure 16. Estimation of the fatigue factor to determine an equivalent annual resilient modulus (10).

This equivalent resilient modulus should equal or exceed the modulus value used to estimate the AASHTO structural layer coefficient used for design (Figure 18 (*6*). The General Pavement Sections (GPS) projects of the SHRP Long-Term Pavement Performance (LTPP) program are to provide the necessary pavement performance data to find the resilient modulus-AASHTO layer coefficient relationship to be adequate, with or without modification, or inappropriate.

4.5 RUTTING

Resurfacing and rehabilitation have become major items in asphaltic concrete mixture use. This usually means paving adjacent to traffic and opening the fresh mix to traffic, as soon as possible. Under these conditions, the earliest distress that must be designed against is rutting or shoving. It should not be expected, however, that a mix design procedure alone can overcome all cases of construction expediency. Some restraint in this operation is necessary to prevent early rutting, even with the most stable mixtures.

4.5.1 Types of Rutting. Two types of rutting are considered. These are (1) one dimensional densification and (2) the lateral movement or plastic flow of asphalt. The more severe premature rutting failures and distortion of asphaltic concrete materials are related to lateral flow and loss of shear strength of the mix, rather than densification. However, there is no mechanistic-empirical model that adequately considers the lateral flow problem. In the laboratory, there are devices that have been used (such as the rolling wheels over beam specimens) to evaluate lateral flow, but with varying degrees of success.

Rutting caused by traffic densification of high air void mixtures is usually not considered during initial mixture design, because it is assumed that good engineering and construction practices will be followed and proper compaction will be achieved on the roadway. Current mixture design procedures do address rutting and instability caused by overfilling the total voids with asphalt.

Rutting from one-dimensional densification can be estimated using the traffic densification procedure (see Section 3). This reduction in layer thickness of the asphaltic concrete is based on testing cylindrical compression samples. More directly, however, the reduction in air voids (one-dimensional densification) can be estimated using the Corps of Engineers GTM or Texas Gyratory Shear device by simply increasing the compactive effort (number of gyrations) to mixture refusal. Densification with these devices is restricted to the vertical direction. Limiting the air voids at mixture refusal limits the amount of additional densification caused by traffic, assuming that the mixture is properly com-

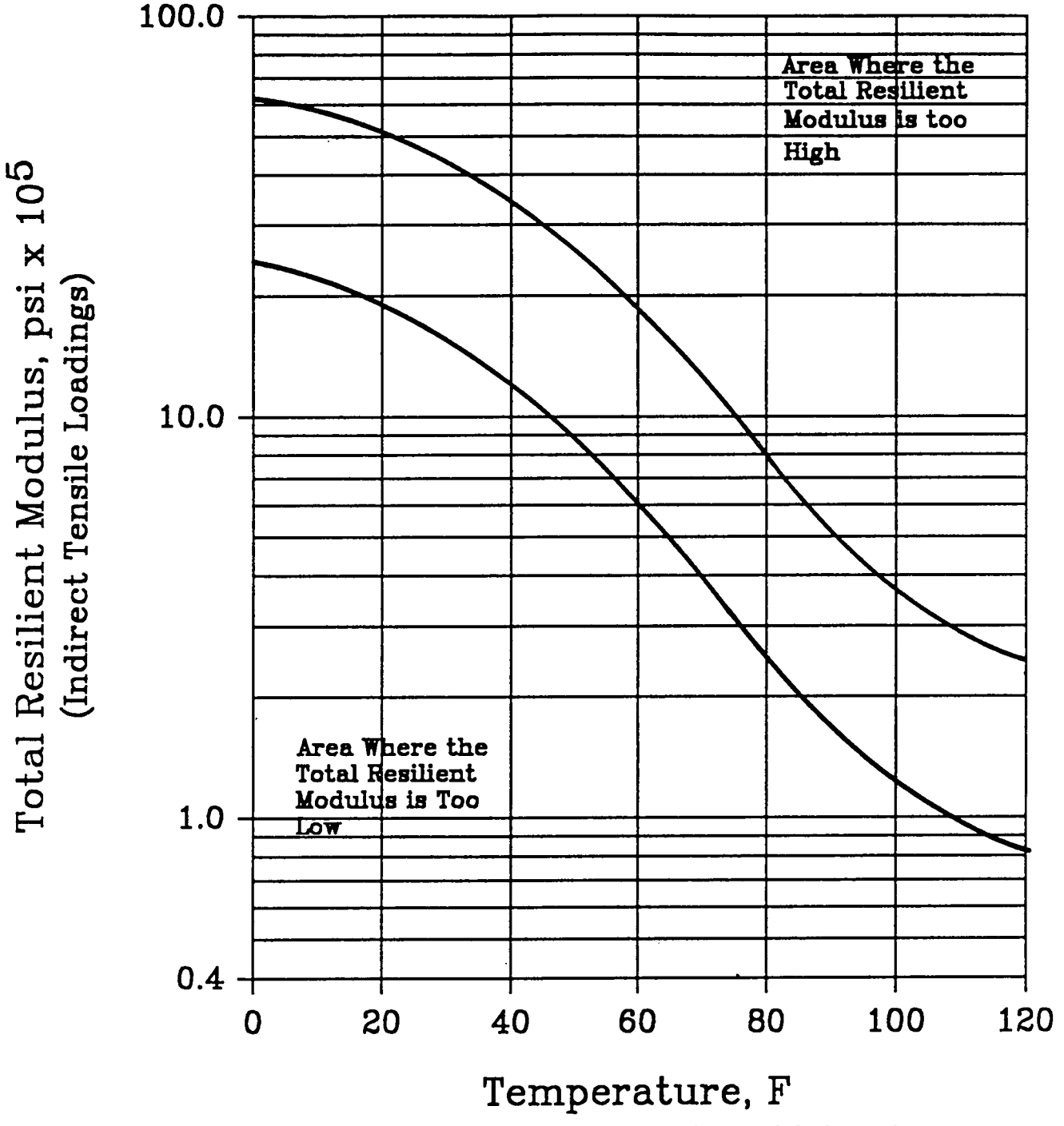

Figure 17. Chart for total resilient modulus versus temperature using indirect tensile loading conditions.

pacted on the roadway. The air voids at mixture refusal should be greater than 3 percent when compacted with the gyratory devices.

The air void content at which no reduction in air voids occurs with additional compactive effort was defined as the ultimate or refusal air void content for the JMF. If the asphaltic concrete layers are compacted in the field to a proper air void range (typically 5 to 7 percent) and the mix is designed such that the ultimate air void content is greater than 3 percent, one-dimensional densification of the mixture should not be a problem. From a rutting point of view, AAMAS assumes that the mixture will be adequately compacted on the roadway.

However, mixtures have been placed with air void contents in excess of 10 percent. At these high air voids, one dimensional

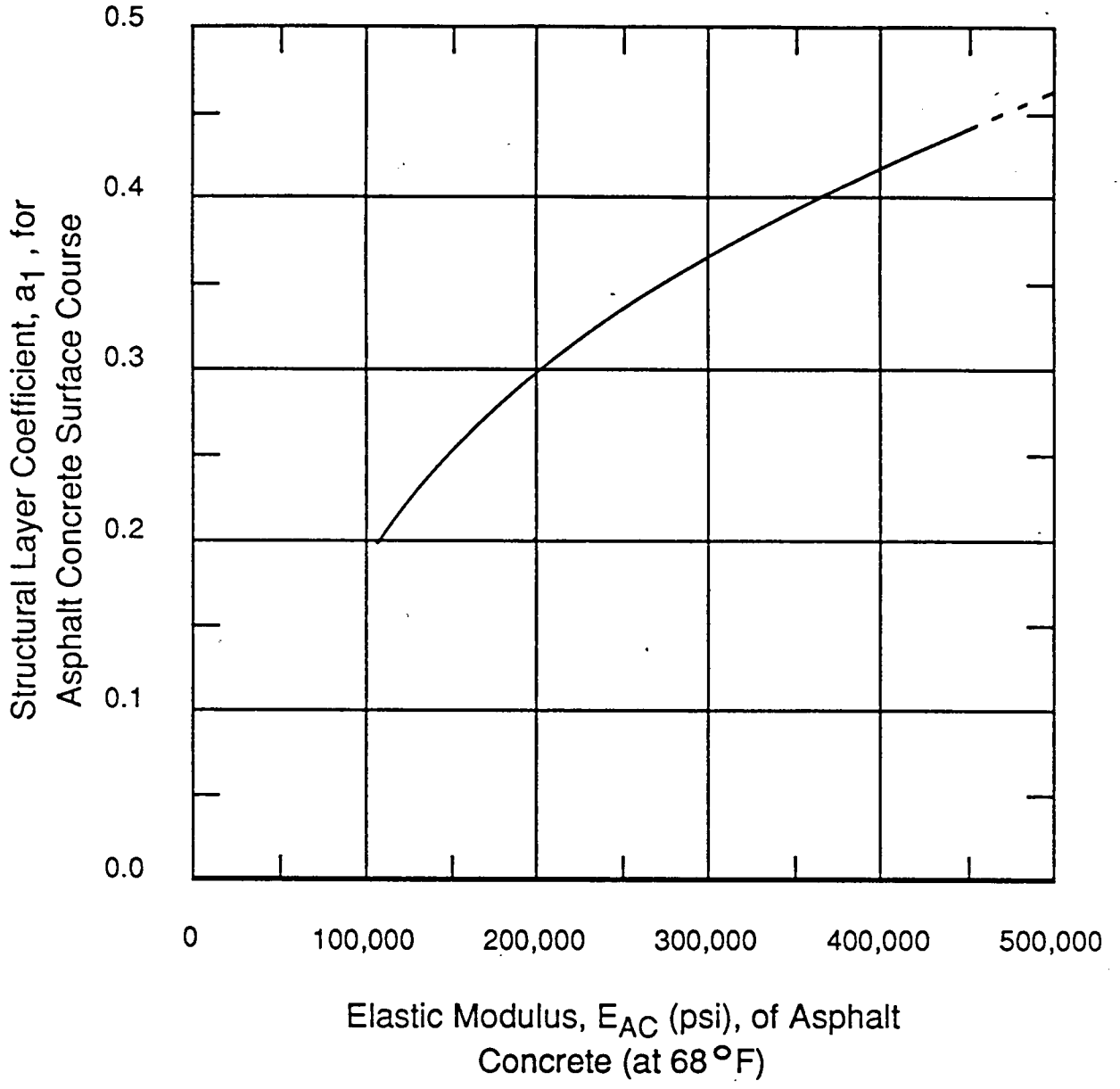

Figure 18. Chart for estimating structural layer coefficient of dense-graded asphaltic concrete based on the elastic (resilient) modulus (7).

densification can be a problem. If high air void mixtures are to be evaluated from a rutting standpoint, the initial compaction of test specimens prior to the traffic densification procedure of Section 3 must be experimentally varied to result in a higher air void content designated by the user. The same type of tests would then be employed as for the traffic densification procedure to measure those properties at the higher air void contents.

The Corps of Engineers GTM (using the air or oil-filled roller) is the only compaction device that will directly evaluate one-dimensional densification and the reduction in shear strength of the mixture with number of revolutions, to simulate thousands or millions of traffic applications. Goetz (*13*) and Ruth at the University of Florida have both found it to be a good tool for measuring changes in compaction and shear strain properties due to traffic densification of asphaltic concrete materials. Both have suggested its use in mixture design and evaluation, and it is recommended for use in AAMAS to estimate the potential for lateral movement of materials (reduction in shear strength) under traffic loads. However, the test results from the GTM are not required by the mechanistic-empirical models suggested for use by NCHRP Project 1-26. Thus, a limiting shear stress value of 54 is suggested for use for high volume roadways. Mixtures with lower shear stress values (50 to 54) can be used, as long as the shear stress is not decreasing with number of revolutions. The use of other tests is required to provide those parameters for the model suggested for use by NCHRP Project 1-26 (*12*).

4.5.2 Rutting Models. Using the stiffnesses of the asphaltic concrete mixture, the level of permanent deformation or rutting

in the wheel path can be predicted by rutting rate equations. One of these equations (reviewed by Thompson (*12*) in NCHRP Project 1-26) is shown below:

$$RR = AN^{m} \tag{4-3}$$

where RR is the rutting rate (or the change in sample height) per load application; N is the number of repeated load applications, and A,m are constants developed from field calibrated laboratory testing data.

The integral of Eq. 4-3 over the total number of traffic applications is the expected rut depth. Another approach to modeling rut depths (in terms of permanent strain) yields the following equation that is more applicable to an asphaltic concrete mixture design procedure.

$$\log \epsilon_p = \log A + m \log N \tag{4-4}$$

where ϵ_p is the accumulated permanent strain in the asphaltic concrete layer, and A,m are constants developed from laboratory test data using repetitive loading techniques, and correlated to field performance data.

The constants A and m can be estimated from static creep tests for the same loading conditions by use of the following relationships, which are correlated to a loading frequency of 1 cps.

$$A = a(t_\ell)^{m_c} - \epsilon_{rt} \tag{4-5}$$

and

$$m = \frac{\log a + 3.5563\, m_c + \log(\ell - X) - \log[a\,(0.1)^{m_c} - \epsilon_{rt}]}{4.5563} \tag{4-6}$$

where m_c is the slope of the static creep-time curve in the steady state region; a is the intercept of the creep-time curve on the axial creep strain axis at time equal to 1 sec; t_ℓ is loading time, sec; ϵ_{rt} is total resilient or recovered strain from the repeated load test; and X is percent recoverable creep or the recovery efficiency from static loads.

Using this approach, the asphaltic concrete layer can be subdivided into discrete lifts and the accumulated permanent strain calculated for each of the lifts. The accumulated permanent strain is then summed for the entire asphaltic concrete layer to determine the expected change in total layer thickness:

$$\Delta h = \sum_{i=i}^{N_n} \epsilon_{pi} h_i \tag{4-7}$$

where h_i is the thickness of lift i, and N_n is the number of discrete lifts.

Subdividing the asphaltic concrete layer into separate lifts permits the stress state on an asphaltic concrete element to be varied with layer depth. The limiting value of the accumulated permanent strain is defined so that strain hardening and other distortions do not occur in the asphaltic concrete material. This value is estimated by the following equation:

$$\epsilon_p < 0.5\, \epsilon_{qu} - \epsilon_{rt} \tag{4-8}$$

where ϵ_{qu} is the asphaltic concrete axial compressive strain measured at maximum load during an unconfined triaxial compression test; and ϵ_{rt} is the total strain (recovered) that is used to calculate the compressive resilient modulus for a loading frequency of 1 cps (0.1-sec load duration and 0.9-sec rest period).

The compressive stress applied to the specimens during the resilient modulus and creep tests should be consistent with the calculated stress state in the pavement structure. Figures 19 through 22 show graphical solutions of the range of data that can be generated for different pavements, climates and loading conditions, as initially developed by Mahboub and Little (*14*). The figures can be used as "rough" guidelines for mixture evaluation on high-volume roadways.

4.6 FATIGUE CRACKING

A longer term distress mode considered by most design and evaluation procedures is fatigue cracking. Fatigue failures are accelerated by high air voids, which in addition to creating a weaker mixture, also increases the oxidation rate of the asphalt film. The development of fatigue cracks is related to the tensile strain at the bottom of the asphaltic concrete layer. Most models use either a two or a three parameter form of fatigue curve that relates the number of load applications to some defined failure condition to an initial tensile strain. A typical relationship used for evaluating the fatigue resistance of asphaltic concrete mixtures is:

$$N = K_1\, (\epsilon_t)^{-n} \tag{4-9}$$

where N is number of allowable wheel load applications to failure, ϵ_t is the tensile strain at the bottom of the asphaltic concrete layer, and K_1, n are the fatigue regression constants developed from correlations between field and laboratory test data.

The fatigue constants K_1 and n have been related to different material properties, such as resilient modulus and indirect tensile strength. Use of the resilient modulus is the more common. One set of relationships to calculate these constants from the resilient modulus (*9*) is shown, as follows:

$$K_1 = K_{1R}\, (E_R/E_{Rr})^{-4} \tag{4-10}$$

$$n = 1.75 - 0.252 \log K_1 \tag{4-11}$$

in which: E_R is the resilient modulus of the asphaltic concrete at a selected temperature, psi; E_{R_r} is the reference modulus (from the AASHO Road Test, E_{R_r} = 500,000 psi); and K_{1R} is the reference coefficient for $E_R = E_{R_r}$ (from AASHO Road Test data, $K_{1R} = 7.87 \times 10^{-7}$).

By using ASTM D 4123, as recommended by the AASHTO Design Guide (*6*), either a total or an instantaneous resilient modulus can be calculated. The one to be used for fatigue cracking evaluation depends on how the stiffness measurements were made during development of the selected fatigue curve. For example, the resilient modulus values considered in the above fatigue equations were originally taken from NCHRP Project 1-10B (*10*) and the curves were modified based on the total resilient modulus and other field data. Thus, the total resilient modulus calculated from total recoverable deformations should be used for compatibility with the above fatigue relationship and AASHTO layer coefficients (see subsection 4.4). The total resilient modulus obtained at each temperature should be greater

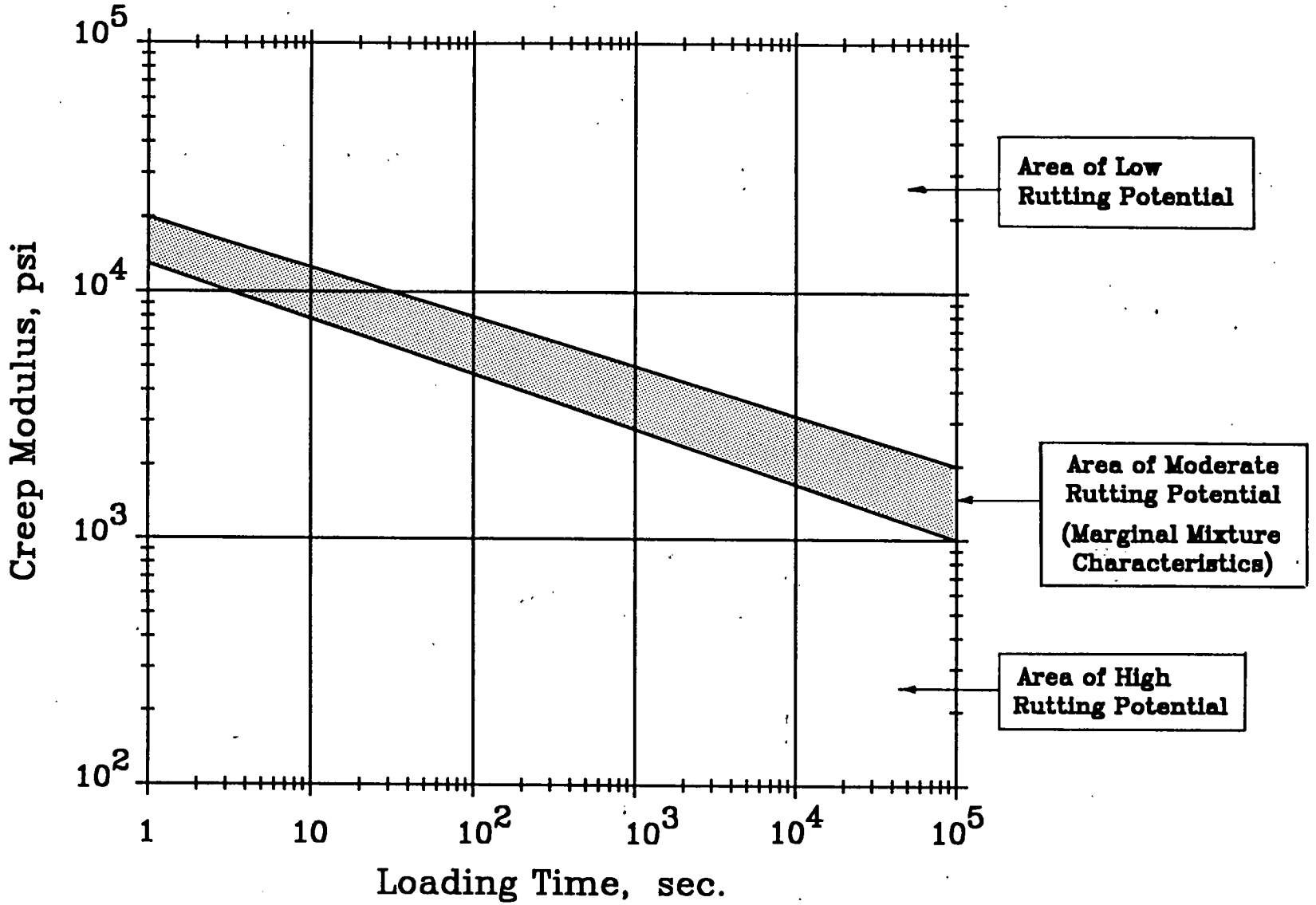

Figure 19. Asphaltic concrete mixture rutting potential for the lower layers of full-depth asphalt pavements.

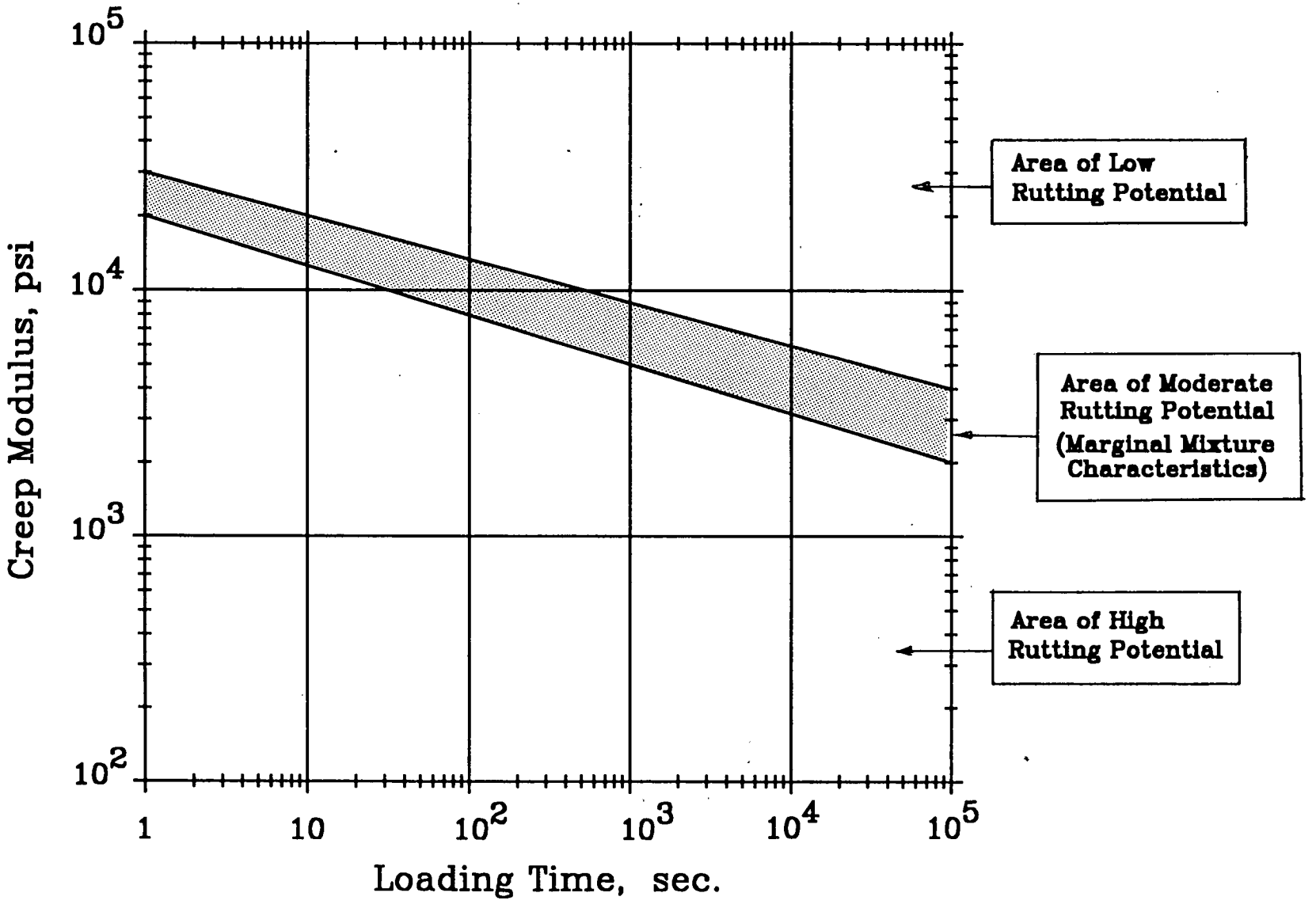

Figure 20. Asphaltic concrete mixture rutting potential for intermediate layers in thick or full-depth asphalt pavements.

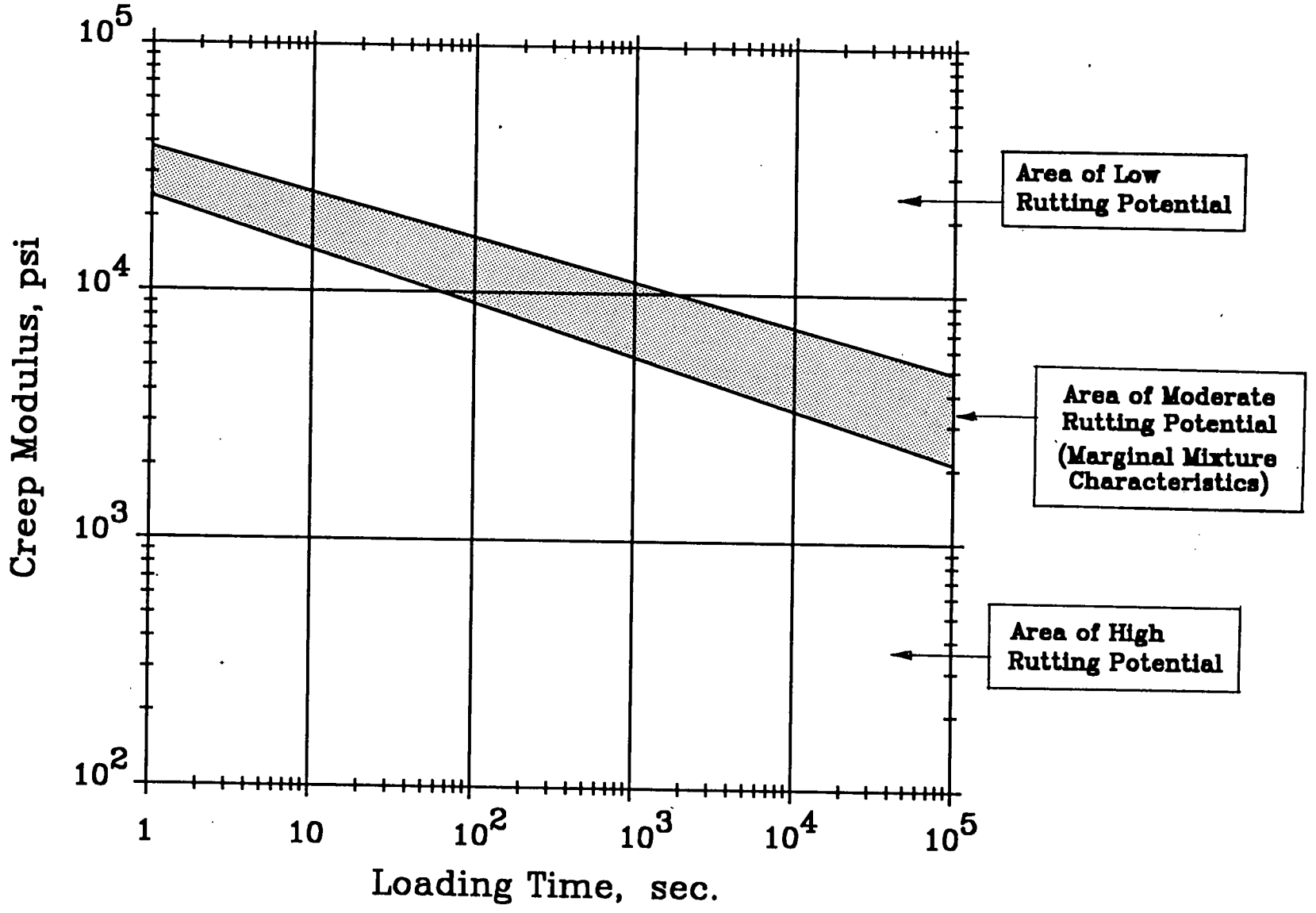

Figure 21. Asphaltic concrete mixture rutting potential for surface layers of asphaltic concrete pavements.

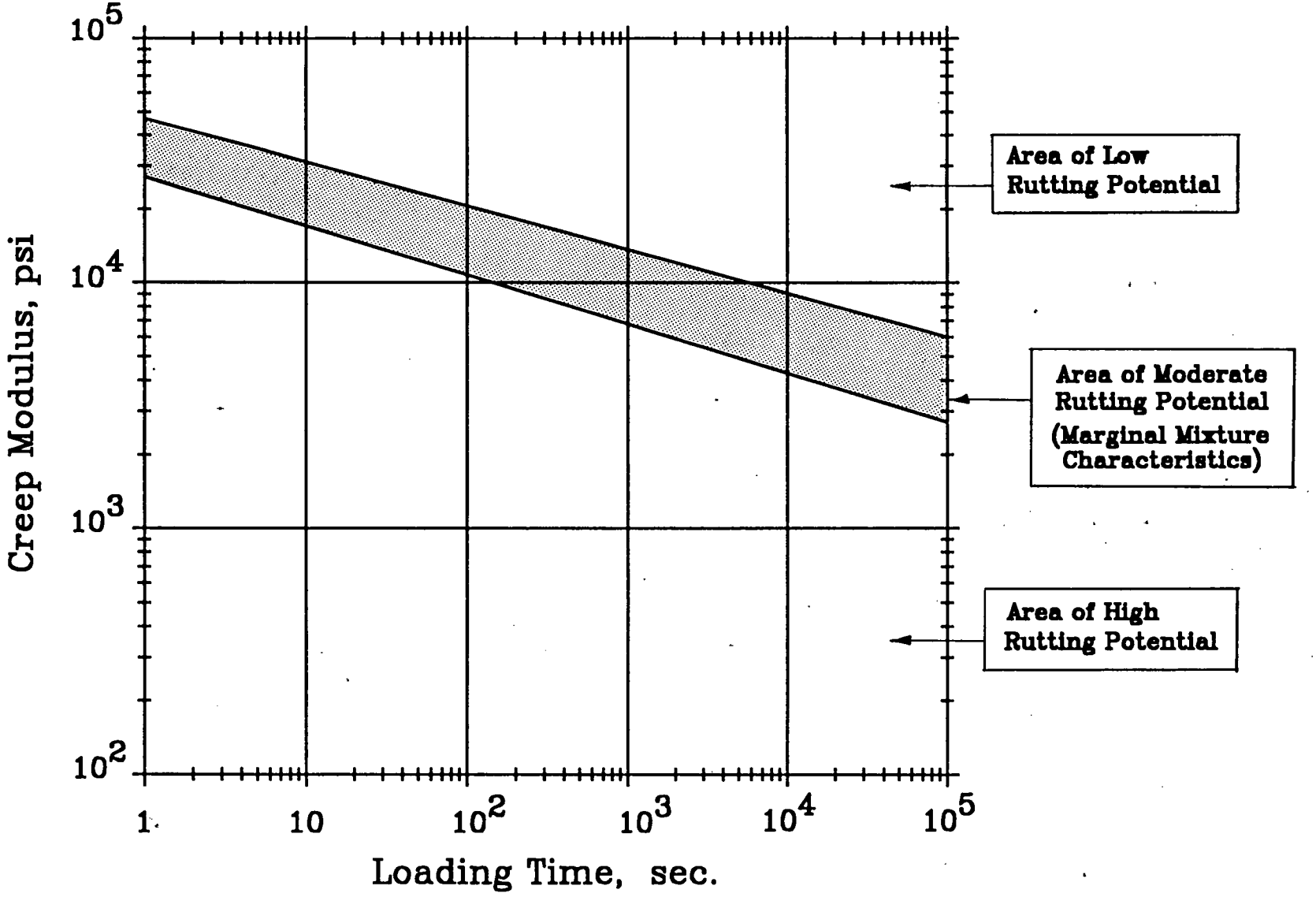

Figure 22. Asphaltic concrete mixture rutting potential for layers placed over rigid pavements or rigid base materials.

than the values assumed for structural design. If these values are less than the assumed design values, especially at 77 and 104°F, the mixture will need to be revised or the pavement redesigned using the actual measured values.

The same reasoning applies to the selection of a structural response model for calculation of tensile strains at the bottom of the asphaltic concrete layer. If tensile strains were calculated with elastic layer theory to develop the fatigue curves, elastic layer theory must also be used to calculate the same strains for a fatigue cracking analysis of a pavement structure to ensure compatibility. In other words, finite element analysis should not be used to calculate tensile strains for use with fatigue curves that were developed using elastic layer theory or some other model.

There are two methods that can be used for evaluating asphaltic concrete mixtures for fatigue cracking. The first is to ensure that the mixture meets or exceeds the fatigue resistance of a "standard" material (which is assumed in structural design), and the second is to ensure that the mixture has the required fatigue resistance for the specific environment and pavement cross section. This second method requires that the fatigue properties of the mixture be measured from laboratory fatigue tests or estimated from other mixture properties.

For purposes of AAMAS, the standard mixture will be the dense-graded asphaltic concrete placed at the AASHTO Road Test. The fatigue curves from NCHRP 1-10B (*10*) were developed from these data, which have been used in other research and design studies (*9, 11*). Figure 23 shows two relationships between the total resilient modulus and indirect tensile strain at failure for the standard mixture. The difference is that NCHRP 1-10B (*10*) assumed a constant slope of the fatigue curves, whereas, the FHWA study (*9*) varied the slope of the fatigue curves.

If the total resilient modulus and indirect tensile strains at failure for a particular mixture plot above the standard mixture (FHWA fatigue curve is recommended), it is assumed that the mixture has better fatigue resistance than the standard mixture. Again, this assumes that the layer thickness design was based on the "standard" mixture. If the standard mixture was not used for the layer thickness design, the following equations can be used to calculate the fatigue coefficients of Eq. 4-9 to ensure that the asphaltic concrete layer has the necessary fatigue resistance for the specific structure, traffic loads, and environment:

$$\epsilon_f(i) < \epsilon_h(i)$$

$\epsilon_h(T_i)$ = indirect tensile strain at failure (unconditioned) measured at temperature T_i

$\epsilon_f(T_i)$ = accumulated permanent tensile strain (fatigue) for temperature T_i

$$N = \mathrm{K}_1 (\epsilon_t)^{-\mathrm{n}}$$

$$\mathrm{n} = 1.75 - 0.252 \log \mathrm{K}_1$$

$$\mathrm{K}_1 = C_r [E_R / E_{Rr}]^{K_r} \qquad (4\text{-}12)$$

$$\log C_r = \frac{1.35 \log \epsilon_t (T_i)}{1 + 0.252 \log \epsilon_t (T_i)} + K_r \log \left[\frac{E_R (T_i)}{E_{Rr}(68)}\right] \qquad (4\text{-}13)$$

Estimating the fatigue curves using the above procedure requires that equations for different test temperatures be solved simultaneously, and a pavement response model (elastic layer theory) be used to calculate tensile strains in the asphaltic concrete layer for different seasonal temperatures for a specific pavement structure. This is time consuming and requires numerous computations. Thus, it is recommended that the test results be compared to the "standard" mixture in Figure 23 for evaluating the fatigue resistance of mixtures.

4.7 THERMAL CRACKING

Thermal cracking is considered a nontraffic-associated fracture distress that is common, but not confined, to the northern United States. This type of cracking presents a serious problem during mixture design because it is difficult to evaluate and predict. The reason for this difficulty is related to the aging characteristics and viscoelastic properties of the asphalt. Low-temperature cracking results when the tensile stresses, caused by temperature drops, exceed the mixture's fracture strength. The rate at which thermal cracks occur is dependent on the asphalt rheology properties, mixture properties, and environmental factors.

Many detailed studies have focused on thermal cracking, and some have resulted in the development of detailed prediction models. Their success in predicting actual performance observations, however, has been limited. Most of these models make use of the mixture strength-temperature and mixture stiffness-temperature relationships to predict the critical temperature at which low-temperature cracking is expected to occur. Program TC, which was considered a candidate in NCHRP Project 1-26, is one of these programs.

To evaluate thermal cracking, certain critical mixture properties, as well as project-specific environmental conditions, must be measured. These mixture properties include indirect tensile strength, low-temperature creep modulus, failure strains and the thermal coefficient of contraction. The thermal coefficient of contraction is usually not measured, but assumed for the thermal tensile stress calculations. A value typically used for dense-graded asphaltic concrete mixes is 1.25×10^{-5} in./in./°F. The other three properties, however, are measured over the range of low temperatures to which the pavement is subjected.

The mixture's strength is measured using the indirect tensile strength test on aged/hardened specimens (environmental aging simulation) at a loading rate of 0.050 in. per min. Although thermal loads are applied at a much slower rate, values of 0.05 and 0.065 in. per min were used in developing the prediction models. With these values, Program TC can be used to calculate the occurrence of thermal cracks with time. Program TC estimates the creep modulus used in low-temperature cracking evaluations at a minimum loading time of 3,600 sec (1 hour) from regression equations for material properties of the asphalt.

In summary, the change in tensile stress, $\Delta\sigma\ (T_i)$, caused by a drop in temperature of the asphaltic concrete surface layer can be calculated with the following equation:

$$\Delta\sigma\ (T_i) = \alpha_A\ (\Delta T_i)\ \Delta E_{ct} \qquad (4\text{-}14)$$

where α_A is the thermal coefficient of contraction of the asphaltic concrete (typical values range from 1.0×10^{-5} to 1.8×10^{-5} in./in./°F; ΔT_i is the change or drop in temperature, °F; and ΔE_{ct} is the change in mixture stiffness (creep modulus) caused by a drop in temperature of ΔT_i, psi.

The tensile strength and stiffness of the mixture can be mea-

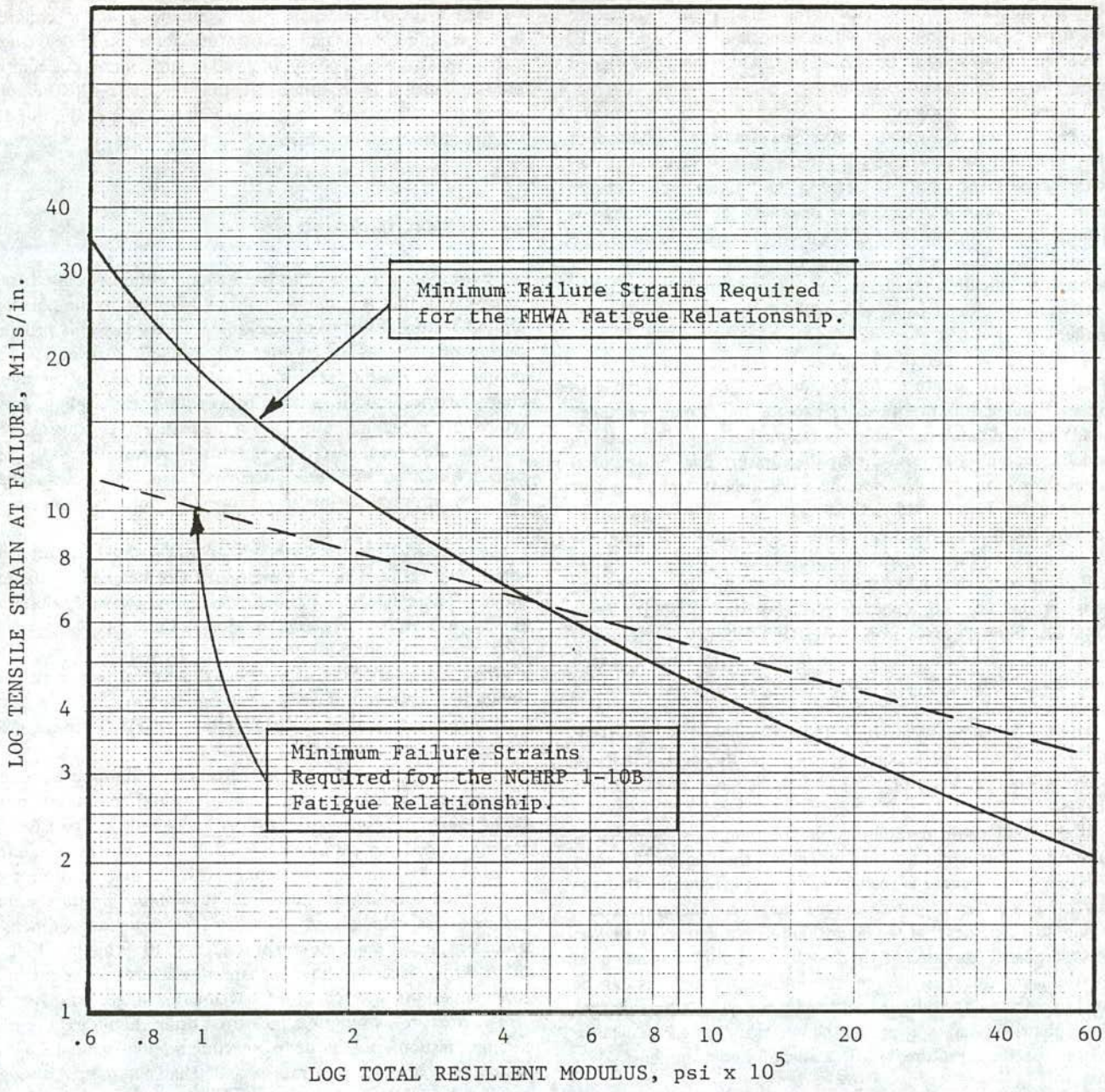

Figure 23. Relationship between indirect tensile strains and resilient modulus using two different fatigue relationships.

sured at various temperatures using slow loading rates and extended loading times, respectively. For most mixtures within a reasonable temperature range, there is a relationship between stiffness and strength that can be represented by:

$$\log E_{ct}(T_i) = \log E_o + n_t \log S_t(T_i) \qquad (4\text{-}15)$$

where $S_t(T_i)$ is the indirect tensile strength measured at temperature T_i, psi; E_o is a regression constant developed from the laboratory test data; n_t is the slope of the relationship between indirect tensile strength and total resilient modulus of the mixture measured at temperatures of 41, 77, and 104°F (unconditioned); and $E_{ct}(T_i)$ is the indirect tensile creep modulus measured at temperature T_i.

The stiffness and strength of the asphaltic concrete mixture vary with both temperature and loading time, as the temperature

decreases. The tensile strain is constant at a particular temperature change, but the tensile stress decreases because of stress relaxation during a constant strain test. The decrease in the thermal stress due to stress relaxation can be approximated by:

$$\sigma_t(T_i) = \alpha_A(\Delta T)\, E_o(T_i)\, (t_r)^{-n_c} \qquad (4\text{-}16)$$

where n_c is the slope of the indirect tensile creep curve at temperature T_i; $E_o(T_i)$ is the intercept of the indirect tensile creep curve at temperature T_i, psi; t_r is the relaxation time, and is assumed to be 3,600 sec for most examples; and ΔT is the critical temperature change at which cracking is expected to occur, °F.

Obviously, measuring all of these properties over a range of temperatures, including values less than 0°F, is time consuming and unpractical from a mixture design/evaluation point of view. Thus, the foregoing relationships were combined and it was assumed that the slopes, at these lower temperatures, are independent of temperatures. The critical temperature change at which cracking occurs can be estimated by the following equation.

$$\Delta T = \left[\frac{E_{ct}(T_i)}{E_o}\right]^{1/n_t} \frac{t_r^{n_c}}{\alpha_A\, E_o(T_i)} \qquad (4\text{-}17)$$

4.8 MOISTURE DAMAGE

Moisture damage is a serious problem, particularly on high traffic roadways. It is caused by a loss of adhesion or bond between the asphalt and aggregate in the presence of moisture. Currently, the moisture damage evaluation (tensile strength and resilient moduli ratios, TSR and MRR) of AAMAS is simply used as a means of accepting or rejecting a mixture. However, programs ACOMDAS 2 and 3 can be used to evaluate the effect of moisture on fatigue cracking and rutting potential of the asphaltic concrete mixture, respectively. These programs can be obtained from the University of Idaho. Both of the above ratios should exceed a value of 0.80 for dense-graded asphaltic concrete. If values less than 0.80 are measured, an asphalt additive or antistripping agent may be required or the aggregate blend may need modification. If these values are less than 0.70, an antistripping agent will be required for the aggregate blend.

It should be pointed out that additional work with the use of tensile strains in the moisture damage area was conducted as part of NCHRP Project 9-6(1). For example, the adhesion properties are believed to be more directly related to failure strains than stiffness. For example, using ASTM D 4123, the resilient moduli is calculated using recoverable strains; no provision is provided for measuring either the total or the nonrecoverable strain. However, if the nonrecoverable or plastic strain after moisture conditioning increases more than the recoverable strain does and, if the total strain remains constant, then the resilient moduli will increase after moisture conditioning. A total strain ratio would be capable of evaluating these effects, whereas the MRR ratio can not. Until more data can be accumulated, the tensile strain ratio should be greater than 0.80.

4.9 DISINTEGRATION

Disintegration is primarily related to environmental and material factors, but the severity of the distress is dependent on the magnitude and number of wheel load applications. Raveling and reduced skid resistance are the two disintegration distresses considered in AAMAS. Increasing the asphalt content in the mix will increase film thickness and decrease asphalt aging, reducing the severity of raveling. Conversely, this increase in asphalt content will also reduce air voids, which can increase the possibility of flushing (or bleeding) and reduce skid resistance. Thus, both upper and lower bounds on asphalt content exist and must be considered in mixture design to reduce disintegration distresses.

Raveling is directly related to the adhesion between the asphalt and aggregate. The factors that have an effect on the adhesion property include a combination of asphalt consistency and film thickness, aggregate cleanliness, shape and texture, air void content of the mix, and absorption. Reduced skid resistance in the form of flushing is also related to a combination of these same factors (asphalt consistency and amount, air voids, and aggregate shape and texture).

Disintegration distresses are important but are considered secondary, because there are no mechanistic-empirical models that can be used to relate performance to mixture design values. The LTPP program of SHRP is collecting performance and materials data to develop such models. In the interim, subjective parameters and values must be used for mixture evaluation. Three of these parameters are tensile strain at failure, tensile strength ratio (moisture damage), and air voids.

Tensile strain at failure is a measure of the bond or adhesion between the aggregate and asphalt. Obviously the greater the bond, the less probability for raveling. A low tensile strength ratio is a measure of moisture damage or loss of bond between the asphalt and aggregate caused by water. Thus, if a surface mixture is susceptible to moisture damage, it is similarly susceptible to raveling. Reducing the air voids will generally reduce moisture damage and asphalt aging. Conversely, for asphaltic concrete mixes to be resistant to reduced skid resistance and flushing at the surface, the mix must contain adequate air voids after traffic densification.

The following summarizes the criteria that can be used as guidelines, in the interim, to evaluate the acceptability of surface mixtures as related to disintegration: (1) air voids at refusal > 3 percent; (2) indirect tensile strength ratio, TSR > 0.80; (3) bonding loss < 50; and (4) tensile strain at failure > 10 mils/in. at 77°F and greater than 2.0 mils/in. at 41°F after accelerated aging.

$$\text{Bonding Loss} = [1 - \epsilon_{ht}/\epsilon_{ho}] \times 100 \qquad (4\text{-}18)$$

where ϵ_{ht} is the indirect tensile strain at failure measured on specimens that have been temperature conditioned (accelerated aging); and ϵ_{ho} is the indirect tensile strain at failure measured on unconditioned specimens.

Retained bond is simply a value that represents the decrease in tensile strain at failure as a result of age/hardening and/or moisture damage.

SECTION 5

AAMAS—MIXTURE DESIGN EXAMPLE PROBLEM

The following subsections describe an example problem illustrating the use of Sections 2 and 4 of Part I. Section 3 covers the laboratory testing procedures for mixture analyses; therefore, only the results from these tests are used in the example problem.

The first part of the example problem (subsection 5.2) includes an evaluation of a dense-graded asphaltic concrete mixture using the test procedures (Section 3) and analysis methods described in Section 4 of the manual. The second part of the example problem (subsection 5.3) includes a redesign of the mixture using performance-related criteria. To facilitate the use of the example problem, the appropriate charts and worksheets have been included to demonstrate the procedures.

5.1 ASSUMPTIONS FOR EXAMPLE PROBLEM

A dense-graded asphaltic concrete mixture has been proposed for use on an interstate highway in central Texas. For simplicity, only the cumulative number of 18 kip equivalent single axle loads (ESALs) will be considered in the example, which is five million 18-kip ESALs over a 20-year design life. It is anticipated that the tire pressures of those trucks that will use this facility on a routine basis will be operated in the range of 120 to 140 psi. The pavement structure designed for this facility is as follows:

Material	Layer Thickness, (Inches)	Assumed Layer Coefficient
Surface mix—HMAC	1½	0.44
Base course mix—HMAC	6	0.40
Crushed stone flexible base	12	0.14
Lime stabilized subgrade	8	—

The structural number for this proposed pavement is 4.74.

A mixture design for the asphaltic concrete base course material was completed in accordance with Marshall procedures. The

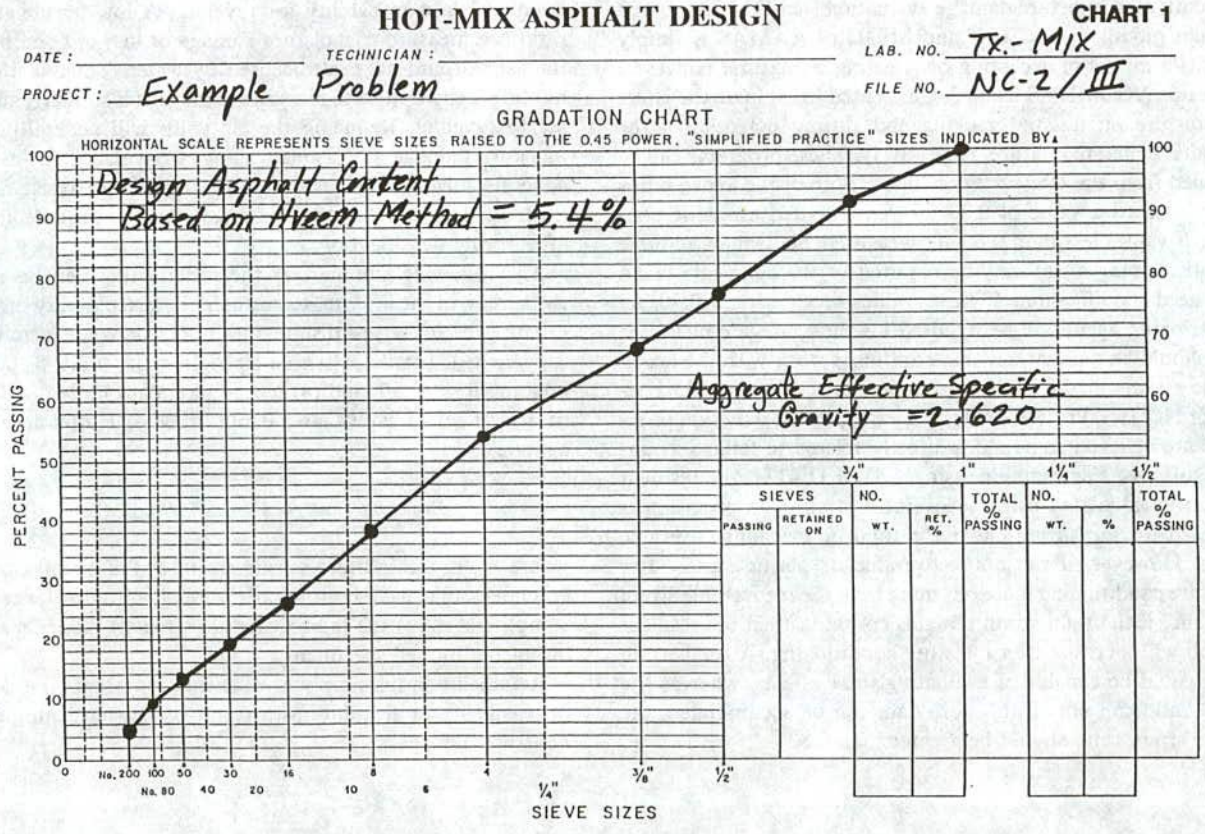

FHWA 0.45 Power Gradation Chart

results of this design (aggregate gradation and design asphalt content (5.4 percent), based on total mix weight) is shown on the FHWA 0.45 Power Gradation Chart (see Chart 1). Other material properties for both the asphalt and aggregate blend have been included on the mixture gradation chart.

The problem is to determine whether this mixture, as designed, has sufficient strength and durability to meet or exceed the initial design requirements without experiencing premature or accelerated pavement distress.

5.2 MIXTURE PERFORMANCE EVALUATION

An asphaltic concrete mixture for the dense-graded asphaltic concrete base material was prepared and mixed in the laboratory in accordance with Section 3 of the manual. Details of the mixture preparation and compaction will not be discussed in detail for the example problem.

Program ASPHALT was initially used to theoretically determine a design asphalt content at a 3.0 percent air void content. This theoretical target value was 4.5 percent, significantly less than the laboratory target value. This is the first indication that the proposed mix may be insufficient.

The following discusses how the test results from Section 3 are used in Section 4 for the mixture evaluation based on performance-related criteria. The presentation of the test data used in this example is included in the charts that follow this section.

1. Confirm AASHTO Layer Coefficient (Section 4, Subsection 4.4)

1.a—The indirect tensile strength and total resilient modulus are measured on the unconditioned diametral specimens in accordance with subsection 3.9.2 of Section 3. The tensile stress used at each temperature (41, 77, and 104°F) is that required only to obtain an accurate deformation reading (20, 10, and 5 psi were used for each test temperature, respectively). The total resilient modulus is plotted as a function of test temperature (see Chart 2).

1.b—The modulus of elasticity at 68°F is interpolated from the laboratory test data. For this example, the AASHTO modulus of elasticity is 350,000 psi (Chart 2), which correlates to an AASHTO coefficient of 0.39 (Chart 3). This value is slightly less than the value assumed in structural design (0.40; refer to subsection 5.1).

1.c—For simplicity, the average seasonal pavement temperatures assumed for this example are 41, 70, and 104°F for winter, fall and spring, and summer, respectively. From the repeated load indirect tensile test (Chart 2) the total resilient moduli are estimated for each season. For this example, these values are 1,250 ksi for winter, 290 ksi for the spring and fall, and 84 ksi for the summer months (Chart 2). The fatigue factors are then determined for each season using these total resilient moduli, and are 0.17 for winter, 3.0 for the spring and fall, and 34.0 for the summer (see Chart 4). Equation 4-2 in Section 4 is used to calculate the equivalent total resilient modulus based on a fatigue damage approach. The resulting equivalent total resilient modulus is 120 ksi for the assumed conditions, as shown below:

$$\frac{1250\text{ ksi }(0.17) + 290\text{ ksi }(3.0) + 290\text{ ksi }(3.0) + 84\text{ ksi }(34.0)}{0.17 + 3.0 + 3.0 + 34.0} = 120\text{ ksi}$$

The layer coefficient that correlates to this modulus value (120

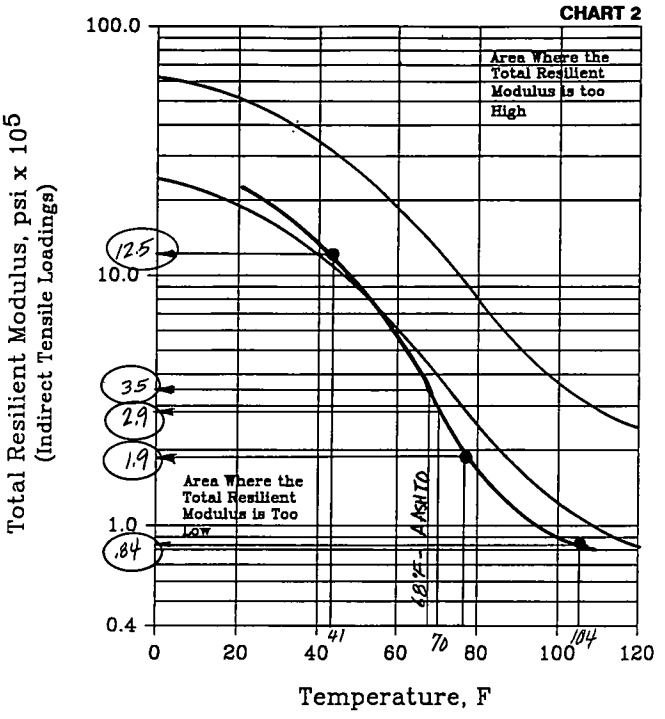

Chart for Total Resilient Modulus Vs. Temperature Using Indirect Tensile Loading Conditions.

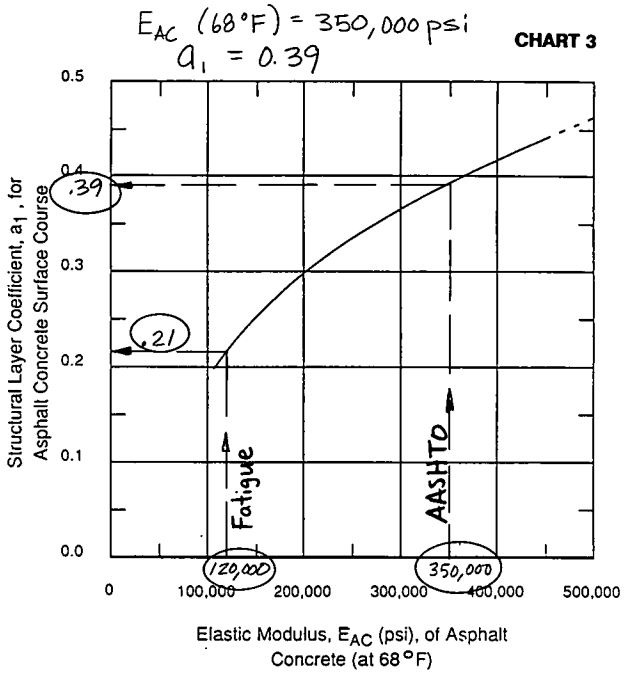

Chart for Estimating Structural Layer Coefficient of Dense-Graded Asphalt Concrete Based on the Elastic (Resilient) Modulus (7).

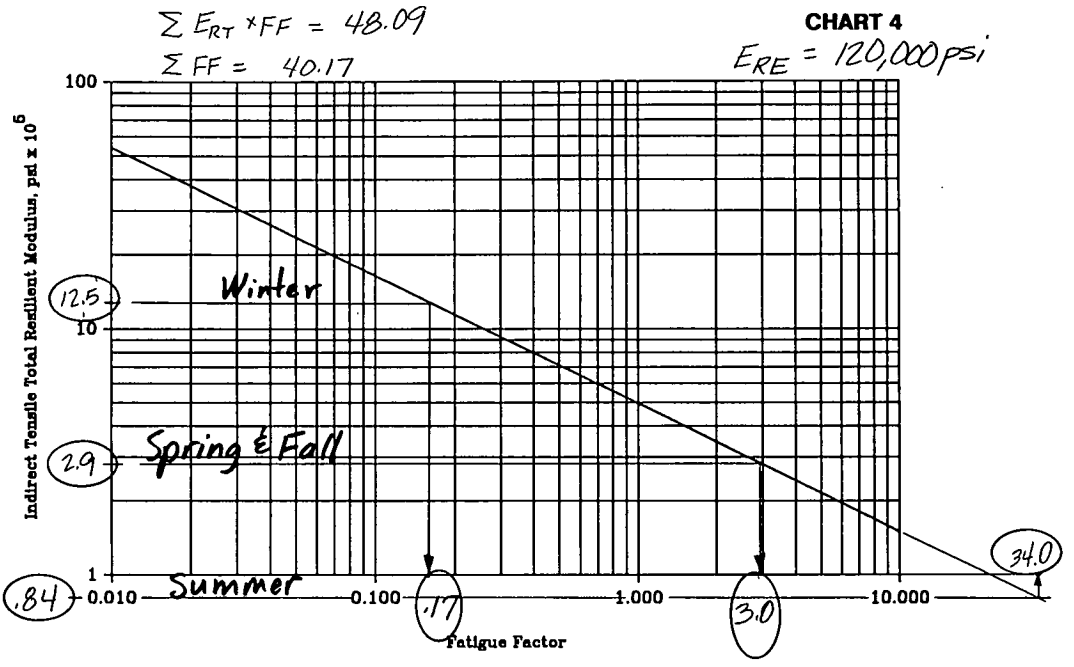

Estimation of the Fatigue Factor to Determine Equivalent Annual Modulus (10)

ksi) is 0.21 (Chart 3), which is significantly less than the value assumed for the structural design.

2. Check Resistance to Fatigue Cracking

2.a—For this example, the test results will only be compared to the "standard" mixture curve (Figure 23 in Section 4). The indirect tensile strains at failure and total resilient moduli are measured on the same specimen in accordance with subsection 4.9.2 of Section 4. Values are measured at 41, 77, and 104°F.

2.b—The test results from each specimen are plotted on Figure 23 of Section 4 and compared to the "standard" mix (see Chart 5). In summary, the proposed mixture for the base course has slightly deficient fatigue resistance when compared to the standard mix. Thus, fatigue cracking should be expected, prior to 20 years.

3. Check for Resistance to Rutting

3.a—Using the indirect tensile instantaneous resilient modulus measured at 104°F (150 ksi), elastic layer theory is used to calculate the stresses and strains at different intervals in the asphaltic concrete base course layer. An average tire pressure of 130 psi was used in the computations. The compressive stresses for this example vary from 115 psi at the top of the layer to 20 psi at the bottom of the layer—a significant variation. With this large variation it would be better to subdivide the layer into intervals and characterize the mixture's response at the critical condition (i.e., near the surface) or vary the compressive stresses in the test program, which requires additional specimens. For this example, a compressive stress of 65 psi (the point at which the horizontal stresses are approximately 0) was used, for simplicity, to represent the entire layer.

3.b—The repeated load uniaxial compression resilient modulus and the compressive creep modulus are measured on the traffic densified specimens at a test temperature of 104°F in accordance with subsection 3.9.5 of Section 3. The compressive stress used in the creep test is the value listed above (65 psi).

3.c—These test results or creep moduli at different loading times can be plotted on the chart illustrating the rutting potential for asphaltic concrete pavements (see Chart 6). These results indicate that the proposed asphaltic concrete base mixture is highly susceptible to permanent deformation or rutting. The Corps of Engineers Gyratory Testing Machine (GTM) was also used to densify and test the proposed mixture. The gyratory shear value after initial densification was 80 psi; however, the mixture became plastic after approximately 100 revolutions. Thus, the GTM also indicated that the mixture would be highly susceptible to permanent deformation and lateral flow. These results are not graphically presented because they are part of the test procedure in Section 3, paragraph 3.8.3.2.

3.d—Results of the creep test were also used to calculate the amount of rutting in accordance with the equation recommended by NCHRP Project 1-26. First, the creep strain is plotted as a function of loading time (see Chart 7). From these test results, the slope of the creep curve, n, and the intercept of the creep curve, a, are calculated from the test results. For this example, the slope of the creep curve was measured at 0.212 and the intercept was 6.2 mils/in. (Chart 7).

After 1 hour of no load on the test specimen, a permanent strain of 5.04 mils/in. was measured at the end of the test. Thus, the recovery efficiency, X, of this mixture was 20 percent ($1 - (5.04/6.33) = 0.20$).

CHART 5

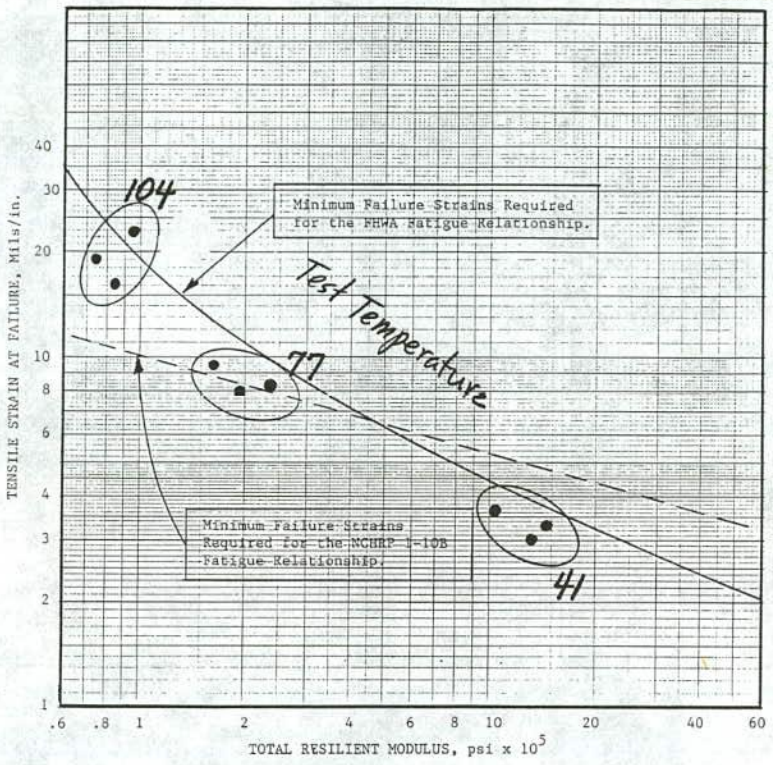

Relationship Between Tensile Strains at Failure and the Total Resilient Modulus Using Two Different Fatigue Equations.

CHART 6

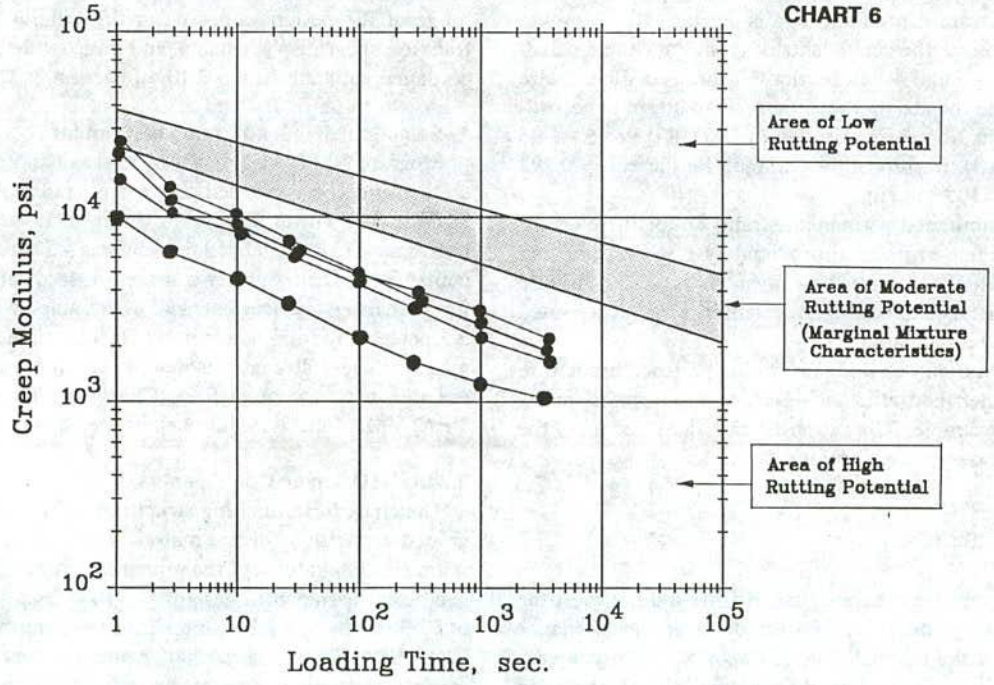

Asphalt Concrete Mixture Rutting Potential for Surface Layers of Asphalt Concrete Pavements.

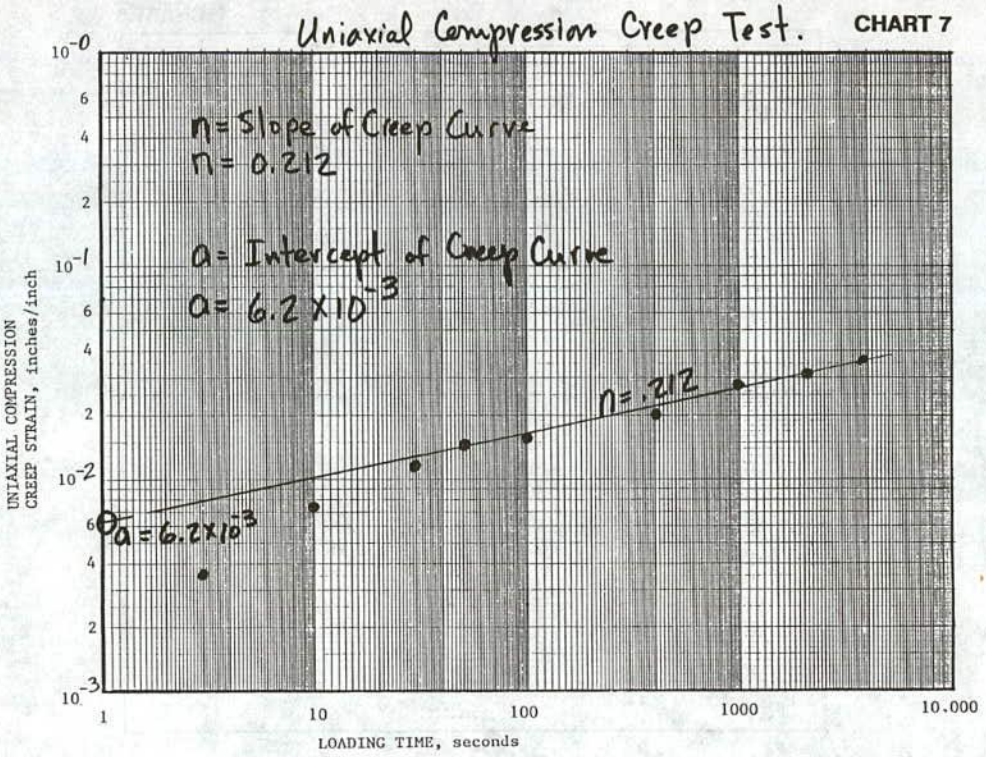

CHART FOR PLOTTING THE CREEP TEST RESULTS: CREEP STRAIN AS A FUNCTION OF LOADING TIME.

The total resilient deformation measured during the repeated load uniaxial compression test (preconditioning period prior to the creep test) was measured at 2.5 mils per in.

Using these values, the coefficients of A and m can be calculated using Eqs. 4-5 and 4-6 in Section 4. These coefficients are used to determine the accumulated permanent strain in accordance with the equation recommended by NCHRP Project 1-26 (Eq. 4-4, Section 4). Results of the computations are m = 0.293 and A = 3.7×10^{-3} in./in.

Thus, the accumulated permanent strain, ϵ_p, for these coefficients was 0.226 in. per in. or approximately 1.36 in. of rutting for the entire asphaltic concrete base layer. As such, the mixture has deficient resistance to rutting, or premature and accelerated rutting should be anticipated.

In summary, the mix as designed will experience premature deterioration under the traffic and environmental conditions assumed for this example. The proposed mix does not meet the initial structural design assumptions.

5.3 MIXTURE DESIGN

Because the asphaltic concrete base mixture did not meet the initial design assumption, this mix was redesigned in accordance with Section 2 of the manual. The redesign of the mix is very briefly discussed in this section. Results of the mixture design tests are graphically presented in the hot-mix asphaltic concrete design analyses chart. These results have been plotted as a function of asphalt content by volume. Section 2 of this manual was used to determine a design asphalt content and an allowable range of the design values using the criteria for resistance to fracture, shear displacements, and uniaxial deformations, in accordance with subsection 2.10, of Section 2.

1. Selection of "Seed" Asphalt Content

Program ASPHALT was used to select an initial asphalt concrete using the combined aggregate gradation shown on the FHWA 0.45 Power Gradation Chart. The "seed" asphalt content at an air void level of 3 percent was 4.5 percent. Five asphalt contents (two below and two above this seed value) were selected for preparing test specimens. These values were 3.5, 4.0, 5.0, 5.5 percent by total mix weight. Results of the indirect tensile, gyratory shear strength, and uniaxial compression creep tests are shown on the worksheet (Chart 8). The refusal air voids, VFA, VMA, and mix unit weight are shown on Chart 9.

2. AASHTO Layer Coefficient

The chart for estimating structural layer coefficient of dense-graded asphaltic concrete materials is used to define the minimum elastic modulus of the asphaltic concrete mix for the layer coefficient assumed in design. For this case, an assumed value of 0.40 results in a minimum elastic modulus at 77°F of 300 ksi (see Chart 10). Those asphalt content values by volume that exceed the minimum value range from 6.9 to 9.7 percent (see Chart 8). This allowable range of values is entered on the worksheet for the summary of mixture design tests (see Chart 12).

HOT MIX ASPHALT CONCRETE DESIGN
GRAPHIC ANALYSES

CHART 8

MIXTURE DESIGN IDENTIFICATION NO: Example DATE: _____
MIXTURE DESIGNATION: _____ PROJECT: _____
COMPACTION METHOD & DEVICE: _____

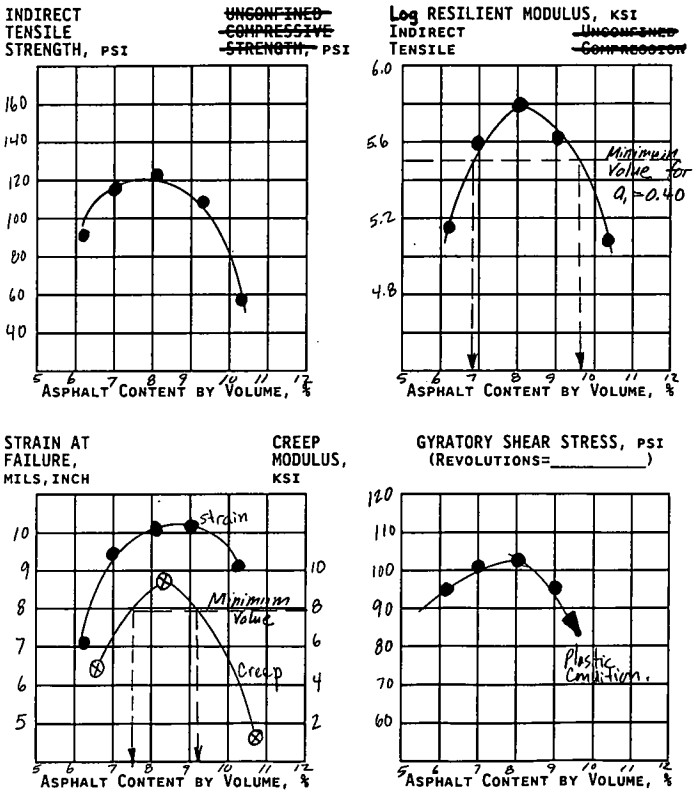

HOT MIX ASPHALT CONCRETE DESIGN
GRAPHIC ANALYSES

CHART 9

MIXTURE DESIGN IDENTIFICATION NO: Example DATE: _____
MIXTURE DESIGNATION: _____ PROJECT: _____
COMPACTION METHOD & DEVICE: _____

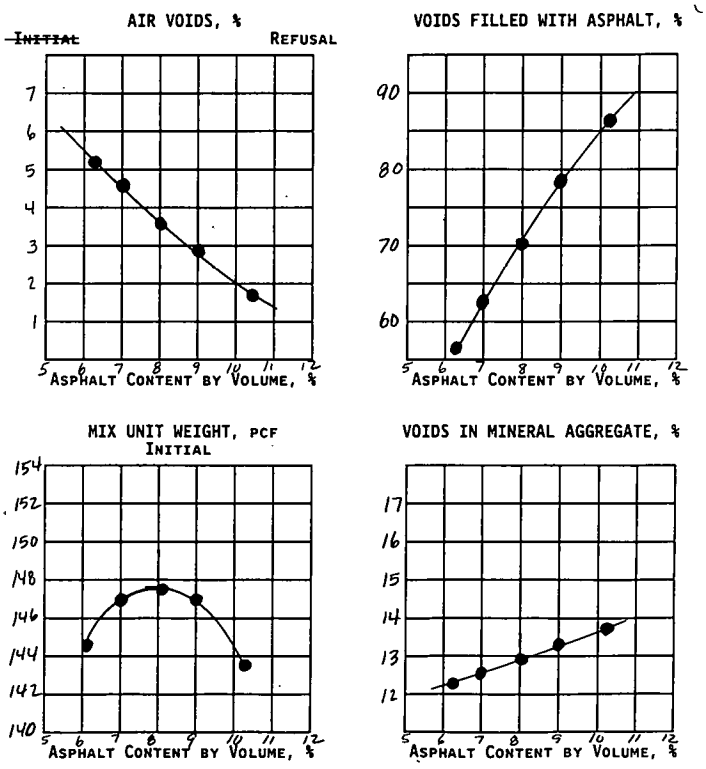

3. Fracture

The tensile strains at failure and total resilient moduli measured on each diametral specimen at the different asphalt contents are plotted on the chart to define the asphalt contents that exceed the standard mixture (see Chart 11). This allowable range for fracture was 6.9 to 9.6 percent and is also included on the worksheet for mixture design tests (Chart 12).

4. Shear

The gyratory shear test was used to define those asphalt contents at which the mix becomes plastic (significant loss in shear strength) and those that exceed the absolute minimum value of 50. The mix became plastic at asphalt contents greater than 9.0 percent by volume. At the lower values included in the test program, the mixture had sufficient shear strength. These results are not graphically presented because they are part of the test procedure in Section 2.

5. Displacement

For this example, a minimum creep modulus of 8 ksi was used (refer to Section 2, paragraph 2.10.4.3). Those asphalt contents by volume that result in creep moduli greater than 8 ksi are 7.6 percent to 9.1 percent (see Chart 8), which are entered on the worksheet for the mixture design tests (Chart 12). Similarly, those allowable values which satisfy the design criteria for air

CHART 10

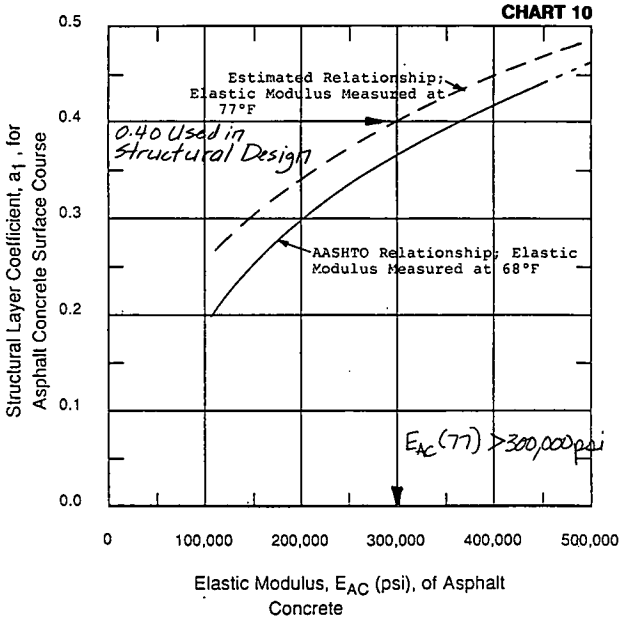

Chart for Estimating Structural Layer Coefficient of Dense-Graded Asphalt Concrete Based on the Elastic (Resilient) Modulus.

CHART 11

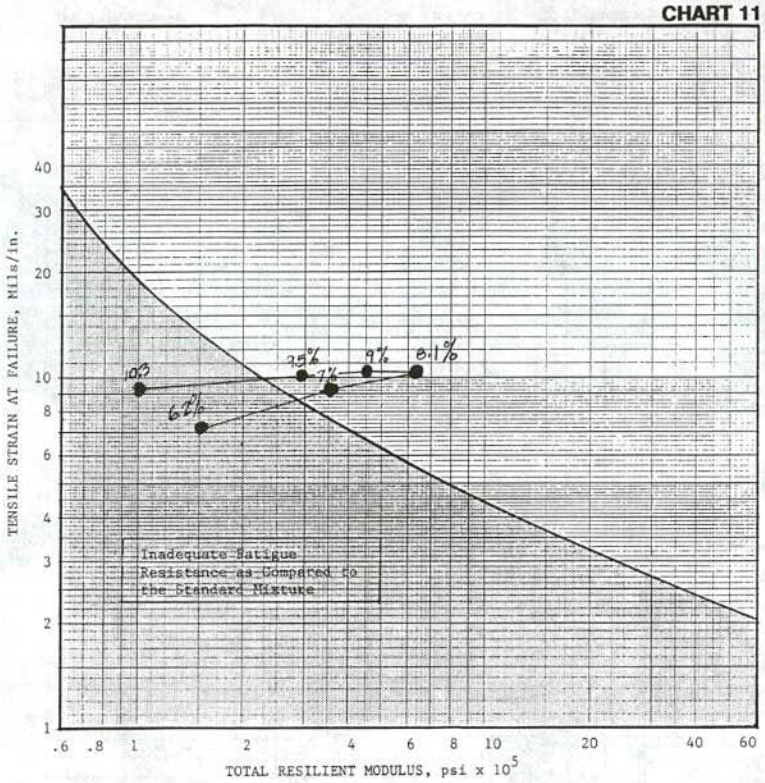

Minimum Tensile Strains at Failure Required for a Mixture as a Function of Total Resilient Modulus as Measured by Indirect Tensile Testing Techniques.

SUMMARY OF MIXTURE DESIGN TESTS FOR SELECTING A DESIGN ASPHALT CONTENT AND AN ALLOWABLE TOLERANCE

CHART 12

Example Problem

Effective Asphalt Content by Total Volume, V_{be}, %

ENGINEERING PROPERTIES	6	7	8	9	10	11
Total Resilient Modulus/ Layer Coefficients		Allowable Values				
Tensile Strain at Failure and Total Resilient Modulus						
Gyratory Shear Stress and Shear Index						
Creep Modulus						
COMPACTION PROPERTIES				Allowable values for Engineering Properties		
Aggregate/Mix Unit Weight			← Maximum Unit Weight			
Final Air Voids, %						
VMA (Porosity), %						
VFA (Degree of Saturation), %						
Allowable Range of the Design Asphalt Content	Allowable Range 7.5 – 8.8 % by Volume			Design Asphalt Content by Volume = 8.1 %		

Worksheet for Summarizing the Test Results and Selecting Allowable Asphalt Contents.

voids, VMA, and VFA are also entered on the Worksheet (Chart 9). For this specific case, the VMA is relatively low for all asphalt contents.

Using results summarized on the worksheet for mixture design tests the design asphalt content by volume is 8.1 percent to satisfy all engineering properties and results in the maximum unit weight of the mixture (see Chart 12). The allowable range of asphalt contents that will satisfy all of the engineering properties and most of the compaction properties (with the exception of VMA) is 7.5 to 8.8 percent by volume. Thus, a design asphalt content of 8.1 percent by volume (approximately 4.6 percent by total mix weight) was selected.

Section 4 of the manual was used to reevaluate the job mix formula, but with the new design asphalt content to demonstrate the change in material properties at these different asphalt contents. These results are reported in the same manner as for the first part of the example problem, but are included at the end of this section. The following summarizes those values previously noted in the first part:

- The elastic moduli of the asphaltic concrete at 68°F is 900 ksi (see Chart 13), which will greatly exceed the assumed layer coefficient of 0.40 (see Chart 14).
- The equivalent annual modulus for the revised asphaltic concrete mix is 373 ksi (calculated from Chart 15), and corresponds to a layer coefficient of 0.41 (Chart 14), exceeding the assumed value.
- The indirect tensile strain at failure and repeated load resilient modulus tests exceed the minimum requirements of the standard mixture (see Chart 16). Thus, the mix equals or exceeds the design requirements for fatigue cracking.
- The creep moduli values measured are in the upper portion of the area for moderate rutting potential (see Chart 17). The equations presented in Section 4 of this manual were used to calculate an expected rut depth. Results of the creep testing were (see Chart 18): the slope of the creep curve, $m_c = 0.218$; the intercept, $a = 1.6$ mils/in.; the recovery efficiency, $X = 0.38$; and the total resilient deformation, $\epsilon_{rt} = 0.335$ mils/in. Using the equations in Section 4, the coefficients for the permanent deformation equation are m = 0.213 and A = 1.27 mils/in.

Using these coefficients, the permanent strain, $\epsilon_p = 0.0253$ in./in., for only the summer months. This results in an approximate rut depth of 0.15 in. Thus, the revised mixture satisfies all conditions assumed during the structural design.

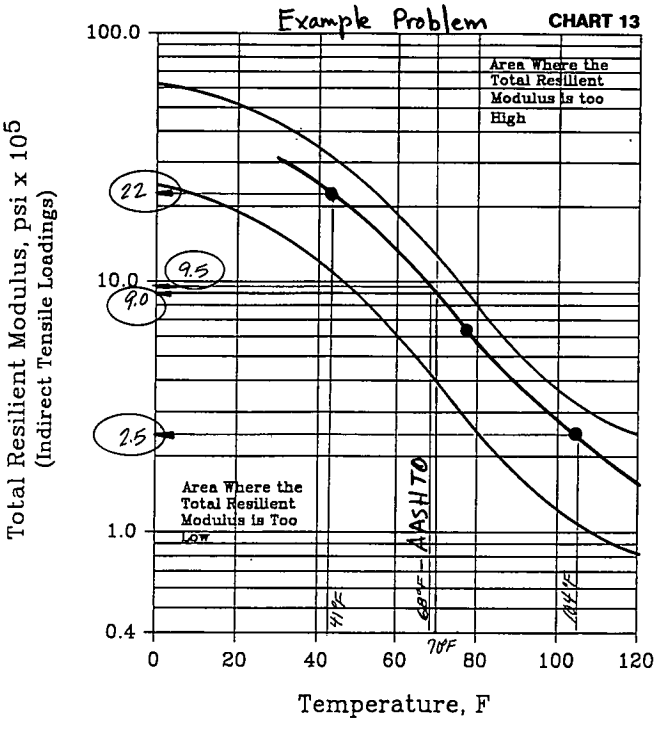

Chart for Total Resilient Modulus Vs. Temperature Using Indirect Tensile Loading Conditions.

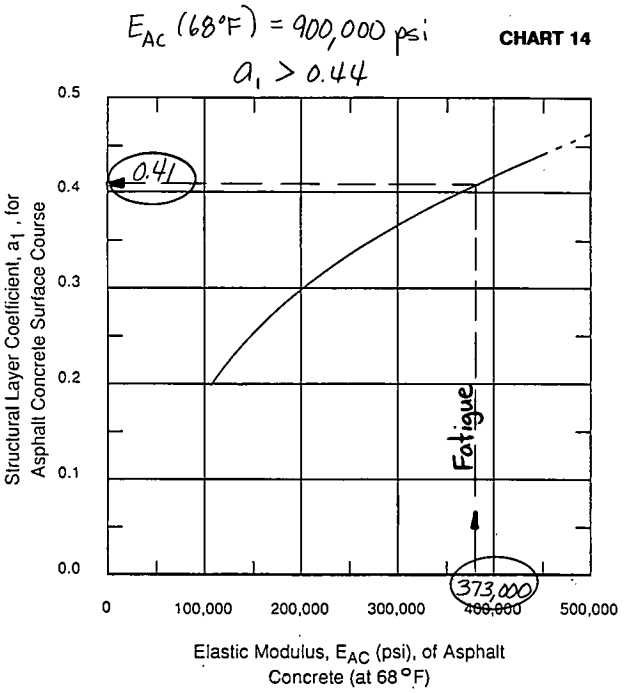

Chart for Estimating Structural Layer Coefficient of Dense-Graded Asphalt Concrete Based on the Elastic (Resilient) Modulus (7).

CHART 15

$\Sigma E_{RT} \times FF = 15.632$ $E_{RE} = 373{,}000$ psi
$\Sigma FF = 4.191$

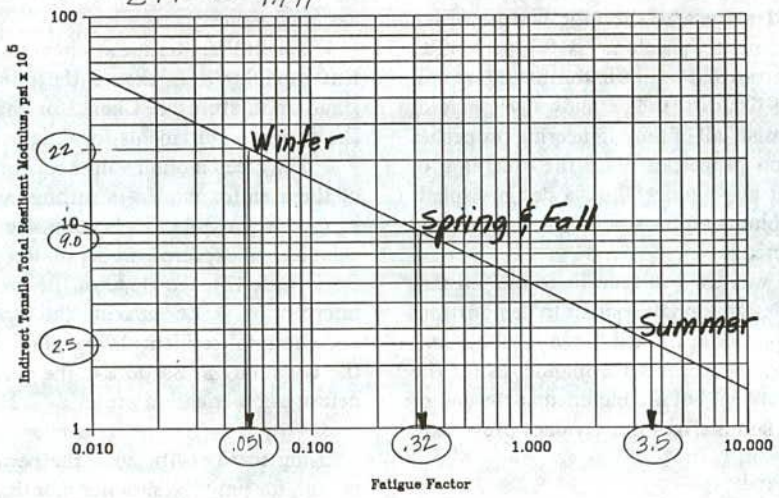

Estimation of the Fatigue Factor to Determine Equivalent Annual Modulus (10)

CHART 16

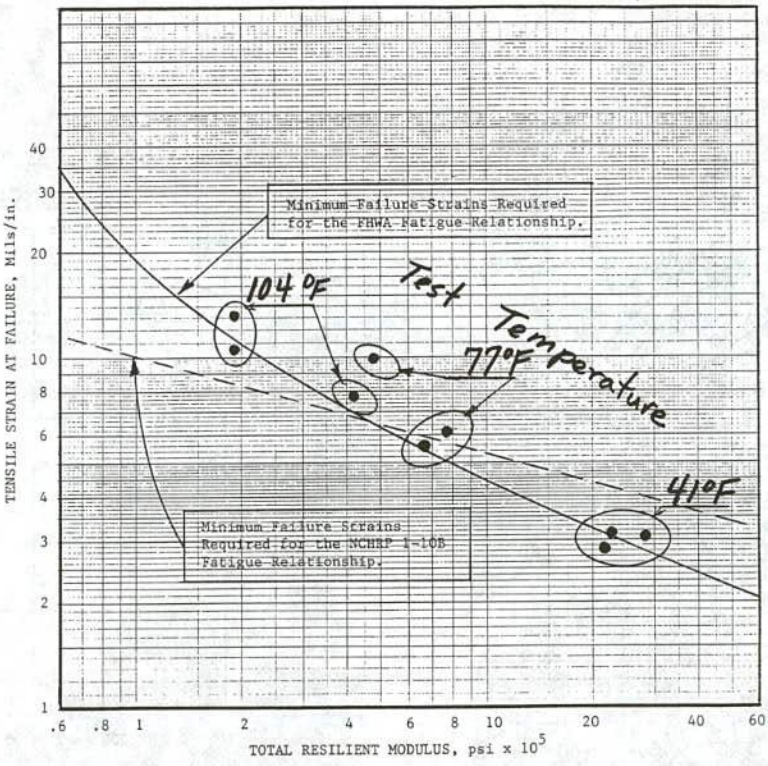

Relationship Between Tensile Strains at Failure and the Total Resilient Modulus Using Two Different Fatigue Equations.

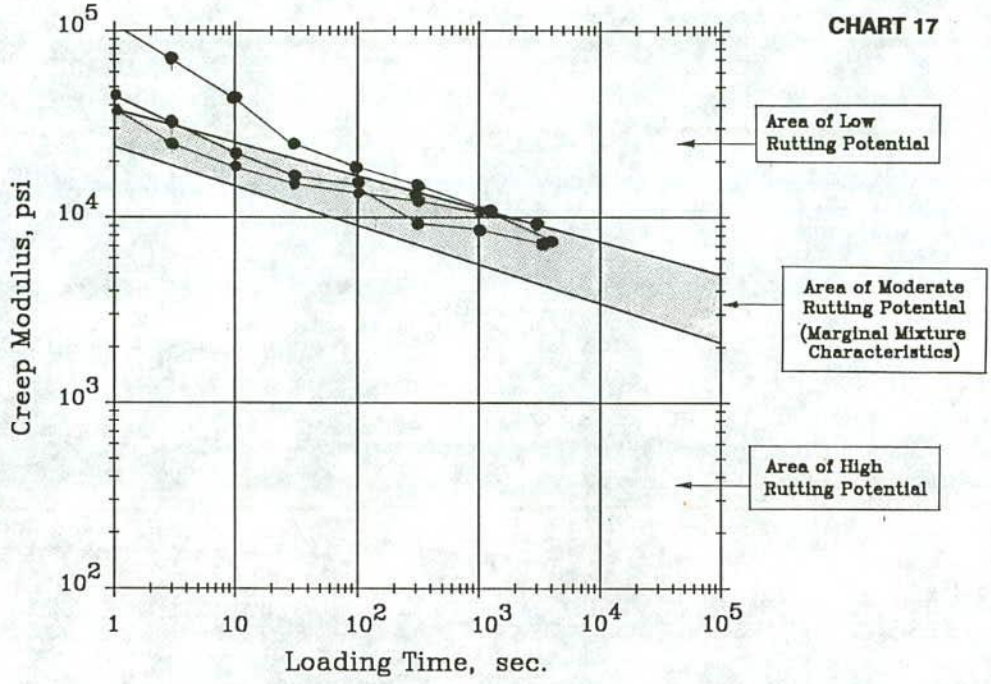

Asphalt Concrete Mixture Rutting Potential for Surface Layers of Asphalt Concrete Pavements.

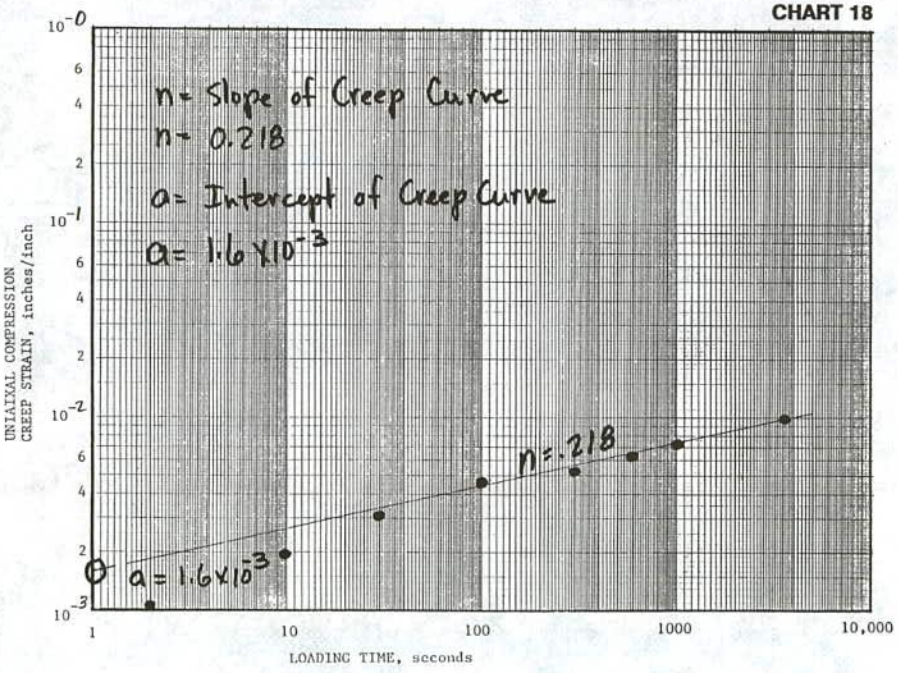

CHART FOR PLOTTING THE CREEP TEST RESULTS: CREEP STRAIN AS A FUNCTION OF LOADING TIME.

Part II—Research Report For Evaluation and Design of Asphaltic Concrete Mixtures

SUMMARY

This report presents the results of a study to develop an Asphalt-Aggregate Mixture Analysis System (AAMAS) for the evaluation of paving mixtures based on performance-related criteria. The final report is divided into two parts. Part I is the Procedural Manual for mixture design and AAMAS, and Part II provides discussion on all tasks conducted under Project 9-6(1).

Part I of this report is divided into five sections. Section 1, Selection of Mixture Components, presents the guidelines and criteria recommended for selecting the mixture components; Section 2 is the mixture design procedure; Section 3, Mixture Analyses, discusses the test procedures that are required for AAMAS; and Section 4, Mixture Performance Evaluation, discusses the mechanistic-empirical procedures used to predict mixture behavior under traffic and environmental loads. Section 5 presents an example problem illustrating the use of Sections 2, 3, and 4 of Part I, together with the applicable worksheets.

The design of dense-graded asphaltic concrete mixtures can be completed in accordance with either the user agency's current practice or in accordance with Part II of this manual. Sections 3 and 4 (Part I) are used to evaluate the proposed job mix formula target based on performance-related criteria, primarily for high-volume roadways.

Specific steps required by Sections 2 and 3 of the manual include compaction, conditioning, and testing of laboratory mixtures to simulate the characteristics of mixtures placed on the roadway. Laboratory conditioning of materials includes simulation of the plant production process and simulation of the long-term effects of traffic and the environment. This includes densification caused by traffic and accelerated aging and moisture damage. Test procedures used to measure critical properties of the mixture include the indirect tensile, gyratory shear, and the uniaxial compression tests.

Guidelines are given in Section 4 of the manual for executing the AAMAS concept and evaluating the expected performance of dense-graded asphaltic concrete mixtures. These guidelines and evaluation criteria were based on those models suggested for use by NCHRP Project 1-26. It should be noted that the AAMAS procedure presented in Part I (Section 3) is a procedure for evaluation of a selected mixture and not a mixture design procedure by itself. Section 2 of Part I is the mixture design procedure.

Part II discusses the development of the different factors that were included in AAMAS. Specific items addressed in this Part include compaction of laboratory mixtures to simulate the characteristics of mixtures placed in the field, preparation and mixing of materials in the laboratory to simulate the asphaltic concrete plant production process, simulation of the long-term effects of traffic and the environment (this includes accelerated aging and densification of the mixes caused by traffic), and the conditioning of laboratory samples to simulate the effects of moisture-induced damage and hardening of the asphalt.

The AAMAS methodology as it currently exists is applicable to hot-mixed asphaltic concrete, and includes mixture variables such as binders, aggregates, and fillers used in the construction of asphaltic concrete pavements. AAMAS currently excludes such materials or layers as open-graded friction courses and drainage layers.

This report documents the first step of the evolutionary improvement of AAMAS and mixture design based on performance-related criteria. The next step of the evolutionary process is being initiated through the Strategic Highway Research Program (SHRP) asphalt research program and FHWA. In all probability, there will be some modification to the current AAMAS after the 5-year, multi-million dollar SHRP research study has been completed and finalized through the SHRP Project A-006. All users of the AAMAS methodology are encouraged to obtain periodic updates on the SHRP asphalt research program. The expected year of completion for the SHRP program is 1993.

CHAPTER 1
INTRODUCTION

1.1. BACKGROUND

Asphaltic concrete mixture and structural designs for pavements were initially "trial and error" processes, with the design criteria depending greatly on the experience of the materials engineer. With time, empirical mixture and structural design methods evolved and were standardized, but were considered independent functions. As such, the structural design of asphaltic concrete pavements was, and still is, based on assumed material properties (layer stiffness coefficient, resilient modulus, fatigue and permanent deformation constants). Only after the structural design has been finalized, are materials submitted and a mixture design completed. The question then becomes: Does the as-placed material meet the assumptions initially used for the structural design? Certainly, asphaltic concrete mixture design and analyses need to be related to those factors that affect pavement performance. Thus, mixture design and structural design need to be tied together and based on the same criteria and parameters.

1.1.1 Empirical Mixture Designs

The two methods most commonly used in the United States for design of dense-graded hot-mix asphaltic concrete are Marshall and Hveem. Both methods are empirical procedures that were developed many years ago. Although the mixtures designed by these two processes have generally served well under traffic, the conditions for which the Marshall and Hveem methods were determined have changed dramatically over time. For example, today's asphaltic concrete mixtures contain asphalts that are produced from different crudes and by a variety of different processes, involve the use of a variety of additives, can be produced using drum mixers rather than only batch or continuous plants, are placed with new paving and compaction equipment, and, more importantly, are subjected to larger loads and higher tire pressures.

Premature distress in many flexible pavements suggest that these empirical mixture design procedures are inadequate, or at least do not measure mixture properties that are pertinent for some distresses. In addition, it is apparent that mixture design, pavement design, and pavement performance need to be considered simultaneously and should not be independent functions.

1.1.2 Performance-Related Mixture Designs

The accelerating development of mechanistic models capable of predicting responses to wheel loading (i.e., in the forms of deflections, strains, and stresses) and the development of "distress models" to predict the occurrence of fatigue cracking, rutting, thermal cracking, and loss of serviceability from these responses, has offered opportunities for at least evaluating those "engineering properties" that are desirable to minimize distress or loss of serviceability. Numerous such studies have been conducted in the past. One study, by Rauhut et al. (*15*) for the FHWA, applied selected mathematical models to identify those material properties that could extend the maintenance-free life of premium pavements. Engineering properties as defined by Rauhut, et al., for that project are: "Those properties that may be used with a constitutive equation to predict the physical behavior of a material in a particular environment." Unfortunately, engineering properties are not those that are usually dealt with in mixture design, and correlations between stability, flow, or other mix design values and fundamental engineering properties have not been well defined.

Performance-related specifications, however, are starting to be implemented as evidenced by Welborn's work for FHWA (*16*), the State of Virginia's work (*17*), the more recent NCHRP (*18*) and FHWA (*19*) studies, and the SHRP asphalt research project A-006 entitled "Performance Based Specifications for Asphalt-Aggregate Mixtures." All of this work is aimed at tying performance into specifications. As Hughes (*17*) discusses, "mix design is the single control variable influencing almost every distress mode." The lack of a rational mix design procedure that considers the factors that are *directly* related to construction and the development of distresses hampers the further development of performance-related specifications. Thus, there exists a need,

as recognized by AASHTO, to bring structural performance of pavements into the optimization of mixture design. This is schematically illustrated in Figure 24.

1.2 RESEARCH PROBLEM STATEMENT

The highway community, specifically AASHTO, recognizes the need for improved procedures and analysis systems for the design of asphaltic concrete pavement mixtures that will be resistant to heavy truck loads, the use of higher tire pressures, and the wide extremes of climate. Such systems should optimize the selection, proportioning, and processing of asphalt binders and aggregate materials to produce pavements resistant to all forms of distress.

The Strategic Highway Research Program (SHRP) plans to develop improved asphalt and/or new binders, tests and specifications for these binders, and performance-related specifications for asphaltic concrete paving materials. Improved procedures and analysis systems could be used for evaluation of the improved or new binders and for the design of the paving mixtures for test sections of SHRP to obtain the necessary pavement performance information to develop performance-related specifications.

Research is needed to develop and refine an asphalt-aggregate mixture analysis system (AAMAS) for design of optimum paving mixtures based on performance-related criteria. These criteria would encompass a wide variety of failure modes, e.g., fatigue cracking, thermal cracking, permanent deformation, moisture damage, and age hardening. In the future, the AAMAS should be capable of accommodating conventional asphalt binders, modified asphalts, mixture modifiers, and the range of aggregate materials used in the United States. It should also be capable of evaluating the mixtures under conditions analogous to those found in service, including a wide range of climate, traffic, and age factors.

1.3 PROJECT OBJECTIVE

The objective of this research is to develop an asphalt-aggregate mixture analysis system (AAMAS) for the laboratory evaluation of asphaltic concrete mixtures. The system shall be based on specimens that as nearly as possible duplicate the characteristics of the mixtures in the field. Its application shall be limited to hot-mixed asphaltic concrete, excluding open-graded friction courses and drainage layers; shall accommodate mixture variables, such as modified binders, aggregates, and fillers, used in the construction of asphaltic concrete pavements; and shall provide for resistance to all forms of distress associated with both load and environment. The evaluation system shall include such elements as the preparation of test specimens, conditioning of the specimens, testing the specimens, and criteria for mixture selection.

1.4 RESEARCH APPROACH

The focus for the development of AAMAS was to develop new laboratory mixture design procedures or modify existing procedures based on pavement performance, rather than on empirical numbers, such as Marshall or Hveem stability. One of

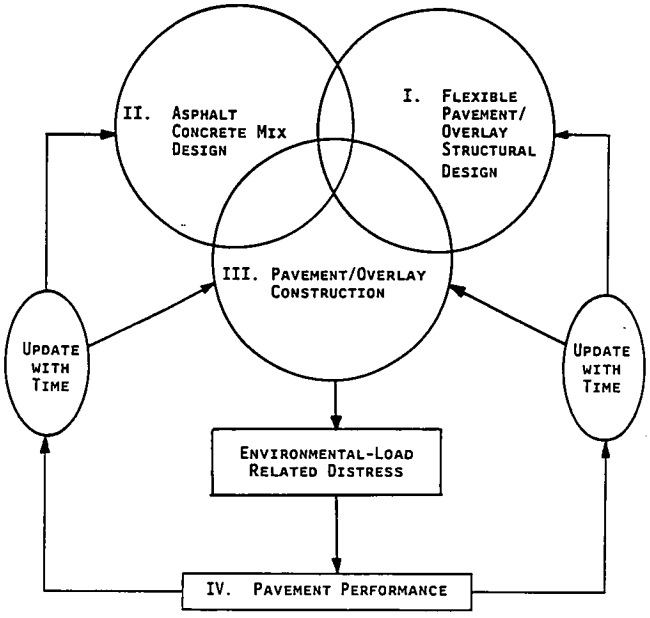

Figure 24. The AAMAS concept or triangle.

the critical factors in the development of the concept for an AAMAS is that the system must be able to evaluate in the laboratory material placed and compacted under field conditions and account for the effects of time (environment) and traffic.

Four areas were considered in the design of an asphalt-aggregate mixture analysis system. These were sample preparation, sample conditioning, testing procedure(s), and mixture selection criteria or optimization. The preparation, conditioning, and testing of samples and selection criteria must also take into account effects from the environment and traffic. A generalized flow chart for the conceptual design procedure for asphaltic concrete is provided in Figure 1 of Part I (reproduced here for easy reference). The following is a listing of those tasks included in the work plan.

Task 1—Define detailed work plan and guidelines for blending aggregates and selection of an initial asphalt content.

Task 2—Select and obtain materials from actual construction projects across the United States. This includes samples from each component of the mixture, bulk mix sampled after mix production, and cores recovered from the roadway.

Task 3—Conduct initial mixture designs using both Marshall and Hveem procedures and compare these results to what was actually being produced and placed.

Task 4—Define laboratory specimen preparation/conditioning methods that provide a reasonably close representation, in terms of fundamental engineering properties, of the mixture placed on the roadway. This includes compaction techniques, initial age hardening for plant production, densification due to traffic, environmental aging and moisture conditioning.

Task 5—Prepare and condition specimens in the laboratory for testing.

Task 6—Laboratory test to measure and evaluate the fundamental engineering properties of those mixtures. Evaluate each

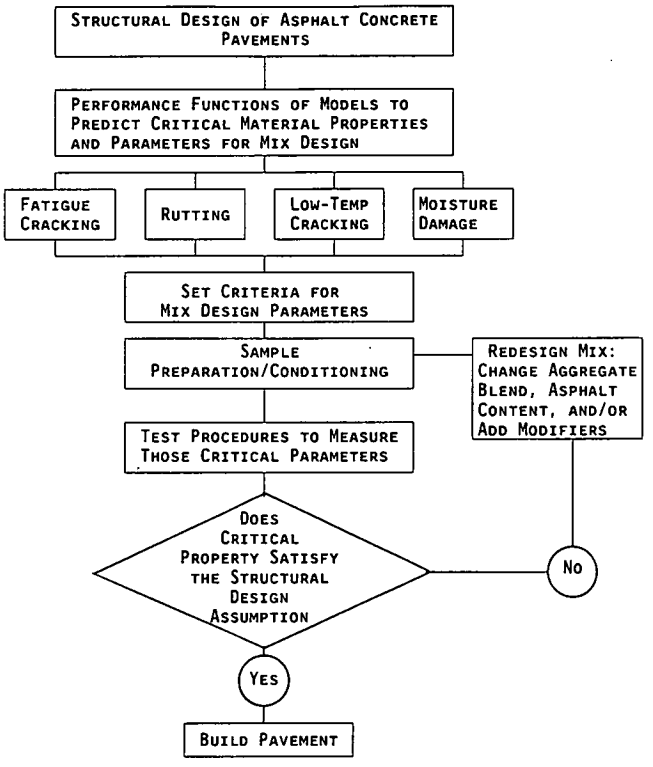

Figure 1. Conceptual flow chart illustrating the different steps in AAMAS.

of the mixtures for resistance to rutting, fatigue cracking, low-temperature cracking, and stripping.

Task 7—Develop initial guidelines and criteria for optimization of mixture and structural design, and coordinate with other NCHRP and SHRP projects that are related to AAMAS.

Task 8—Prepare a report that documents all findings and conclusions.

Task 9—Provide oral briefings to the NCHRP panel.

This report provides the results of NCHRP Project 9-6(1). It presents and documents all work conducted and results obtained, analysis and interpretation of those results, and recommendations for further study. In particular, the AAMAS emphasizes the importance of sample preparation (in terms of sample size, void content, and particle orientation), sample conditioning (which includes age hardening, moisture conditioning, and traffic densification), and testing methods and configurations to determine the engineering properties for evaluating the mixture's performance.

As shown in Figure 24, there should be an interaction between the structural design of asphaltic concrete pavements and mixture design. Although the initial use of AAMAS is to check specific mixtures for resistance to various forms of distress, the ultimate use, when fully developed and after correlations with field performance of pavements, will be to optimize the structural and mixture design process to produce the desired pavement performance at least cost.

Figure 1 (from Part I) shows the conceptual flow chart of the different steps that are included in AAMAS. As stated earlier, the final intent of AAMAS is to produce and implement a design and analysis system for selection of the type and gradation of aggregate, type and amount of asphalt cement, and type and amount of additive, if required. Initially, AAMAS is limited to hot-mix asphaltic concrete (including binders, aggregates and modifiers used in construction) and provides an evaluation for all major forms of distress (both load and environmental).

CHAPTER 2
FINDINGS

A concept for the design of an AAMAS was developed and presented in the Phase I report (*20*). This conceptual design identified the importance of sample preparation and conditioning, and of testing methods for evaluating mixture performance. Although some conventional procedures and tests may be used in AAMAS, most procedures and tests will require modifications for most effective use. Thus, the focus of the Phase II work effort for the development of AAMAS was to modify existing laboratory mixture design procedures and those tests that measure the same engineering properties used in structural design and pavement performance predictions.

Chapter 2 is subdivided into six sections because of its length. These are: 2.1, factors considered important in AAMAS; 2.2, discussion of the field test sections; 2.3, mixture compaction and air voids; 2.4, mixture testing; 2.5, mixture conditioning; and 2.6, supplemental study areas. The first section on factors considered important in AAMAS does not include findings from this study but discusses those numerous factors, assumptions, and critical parameters used in developing the initial AAMAS. This section was included as an introduction to Chapter 2 because it reviews "real life" conditions that place large demands on both current and future mixture analysis systems. The second section reviews the field projects and materials used as data to develop the AAMAS principles. The third section overviews mixture compaction and air voids on both field and laboratory compacted specimens. The fourth section presents the test results in terms

of fundamental engineering properties of the mixtures used in the study. The fifth section presents test data on mixture conditioning for time, temperature and traffic, and the final or sixth section discusses additional study areas that are important to the overall development of AAMAS.

2.1 FACTORS CONSIDERED IN AAMAS

For a mixture analysis system to simulate and, hence, predict the behavior of the mixture in the field, it must consider the production and construction processes, as well as the behavior of the mixture under traffic and the environment. Ideally, AAMAS should be able to predict in-place properties of the asphaltic concrete in the laboratory during the mix-design stage. These material properties must be related to the critical parameters affecting the occurrence of pavement distress. In addition to simulating, within reason, the production and construction processes, a rational mixture design must predict performance as soon as construction ceases, as well as after the mixture has undergone many millions of load repetitions. This requires some type of accelerated conditioning depending on the environment and load repetitions.

There are six important components that must be included in AAMAS. These are: (1) selection of mixture components, (2) preparation of test specimens, (3) conditioning of test specimens, (4) testing configurations and conditions, (5) performance predictions and evaluations, and (6) criteria for mixture selection.

This section reviews real world conditions that complicate a universal mix analysis system.

2.1.1 Traditional Mix Design Procedures

By far the two most popular mix design procedures are the Marshall and Hveem, with the former much more widely used over the latter. The Marshall stability value is generally considered to be a measure of the mixture's strength, but not a measure of resistance to shear stress. The flow index value, however, is believed to represent a measure of resistance to creep or plastic flow. The Hveem stability value is generally considered to be a measure of its tensile strength. However, the Hveem cohesiometer value is a measure or indication of the tensile strength.

Both procedures have been extremely useful in designing good mix designs over the past 40 years, although they are based on empirical relationships. Present mixture design requirements are much more severe than those Marshall and Hveem addressed in their procedure developments. Most correlations between these empirical values and engineering properties required in mathematical models are too restrictive and limited. However, it is only reasonable to expect that some of the concepts they proposed and that have 40 years experience behind them can serve as a starting point in AAMAS.

It has been found that neither the impact compaction of the Marshall method nor the kneading compaction used in the Hveem method simulate construction compaction. While this is true, comparisons performed on samples compacted to comparable air voids by the Marshall hammer and by the California kneading compactor and tested by the Marshall procedure gave comparable stability and flow values (*21*). This indicates that the void relationships that have grown out of the Marshall procedure may be useful in the AAMAS concept. If AAMAS can use a similar void analysis system to Marshall (or Hveem), the transition to, and eventual implementation of, AAMAS will be easier. However, it is well recognized that test methods which measure properties required to predict the distress mechanisms, discussed below, must be used that are more rationally based than the Marshall stability and flow tests and the Hveem stabilimeter and cohesiometer tests.

2.1.2 Structural Design/Pavement Performance Models

There are many models currently available that can be used to evaluate and structurally design asphaltic concrete pavements. Most of these use similar engineering properties, such as Poisson's ratio, resilient modulus, tensile strength, and fatigue constants. The key requirement of AAMAS is that it use or produce material and engineering properties that are considered significant or correlated to the input parameters for the structural designs of pavements.

Certainly, the direct measurement of a critical material property is always more accurate and is the preferred technique, rather than measuring some other material factor or property and predicting the required property using correlation or regression equations. Boundary conditions and other limitations then play important roles in the application of the regression model for mixture evaluation. In some cases, however, use of prediction equations and measuring dependent variables are necessary because of the time requirement, variability, and inaccuracies of some test procedures. For example, measuring the fatigue coefficients K_1 and K_2 at different asphalt contents considered in a mixture design would be time consuming, expensive and is an impractical approach, even though the coefficients are basic parameters required for predicting flexible pavement performance. In these cases, measurement of the dependent variables in the regression equation, such as resilient modulus for the fatigue coefficients as recommended by Rauhut et al. (*9*), become the preferred technique. Of course, in using regression equations, accuracy, boundary conditions and limitations must be understood so that the equation is properly used.

2.1.2.1 Design/Evaluation Procedures

The common structural design procedure used by most state agencies is AASHTO. Therefore, the new AASHTO design procedures (*6*) should be closely tied to the outputs of AAMAS. Unfortunately, for flexible pavements, resilient modulus is the only material input that is used to select a layer coefficient for asphaltic concrete. Resilient modulus by itself is no more accurate than a Marshall stability value in predicting pavement performance. (Chapter 3 provides more detailed discussion on determining the structural coefficient from resilient moduli of asphaltic concrete materials.)

There are many mechanistic "response models" using elastic layer theory that predict the deflection of a pavement and stresses and strains in the layers due to wheel loadings. There are other models such as the VESYS series that combine response and "distress" models to predict fatigue cracking, rutting or serviceability loss with traffic. Table 6 lists those models that have been evaluated for use in designing pavements. Although some of these models are stochastic and consider variability of materials,

Table 6. Analytical models and procedures for designing or evaluating flexible pavements. Note that most of the analytical models use elastic layer theory or finite element analysis to compute deflection, stresses and strains in the pavement structure, and use empirical formulas for estimating pavement performance or life. This table lists some of the available models; numerous other models are also available.

Analytical Model	Type of Distress		
	Fatigue	Rutting	Thermal Cracking
VESYS IV (22)	X	X	X
ILLIPAVE (23)	X	X	X
Shell Method (8)	X	X	
PDMAP (10)	X	X	
POD (11)	X	X	
Corps of Engineers (24)	X	X	
OPAC (25)	X		X
WATMODE (26)	X		X
Rutting Subsystem (27)		X	
DEVPAV (28)		X	
Huschek Method (29)		X	
COLD (30)			X
Program TC (31)			X
ACOMDAS 2 (32)	X		
ACOMDAS 3 (33)		X	

the gross variations in material behavior and performance of pavements, where fracture is the failure mode (fatigue and thermal cracking) or where permanent deformations leading to pavement roughness are involved, make predictions for a specific case very unreliable.

2.1.2.2 Pavement Performance Measures

As "structural performance" is a rather general description, it is necessary to relate specific pavement performance measures to "functional failure" of flexible pavements. Functional failure implies an unsatisfactory ride quality, unsafe conditions, or levels of distress that warrant repair or rehabilitation. Most of the original structural design work that has been sponsored as part of FHWA and NCHRP project (*10, 11*) has recognized three basic types of distress. These are (1) thermal or low-temperature cracking, (2) fatigue cracking, and (3) rutting or permanent deformations. However, other distress types can be equally important, but historically have received much less study. These include reduced skid resistance, raveling, and bleeding. Recently, stripping (moisture damage) has been discussed in the literature as a distress, but it is not a distress manifestation in the traditional definition, as are the other distresses. Stripping is, however, an important distress mechanism that can significantly accelerate the occurrence of other distresses. Thus, it must be considered in AAMAS.

Pavement damage begins as soon as construction ends. Traffic is usually a much more severe factor than are environmental conditions, but for some distress mechanisms, e.g., moisture damage, a combination of the two factors act to cause the distress. The AAMAS, therefore, should address both anticipated traffic levels and environmental conditions.

Significant performance measures were established in other studies to define material properties needed for long pavement life (*15*) and for developing damage functions for cost allocation (*9*). Although others could be considered, it is believed that the following four types of distresses, resulting from load or environmental conditions, are the most important with respect to reduced serviceability and pavement performance: fatigue cracking, thermal cracking, permanent deformation, and moisture damage.

Asphalt hardening or aging is also very important to long-term pavement performance. However, this is not considered a distress, but a factor that has an extremely important impact on the distresses listed above. Thus, this phenomenon must also be evaluated. Secondary consideration should be given to surface deterioration in the form of raveling or disintegration and loss of skid resistance.

2.1.3 Testing Requirements

In order to design mixtures relating to pavement behavior and performance, it will be necessary to use a test method that will provide the necessary engineering properties and characteristics of the asphaltic concrete mixture. Some of the more conventional tests that have historically been used for evaluating mixture behavior, include the unconfined compressive strength, indirect tensile strength, and stability tests. Other less common tests that are required to evaluate pavement distress and performance by many mathematical models (Table 6) include resilient modulus, Poisson's ratio, creep compliance, fatigue, and permanent deformation.

To qualify as an acceptable test to measure the material and engineering properties of a mixture for use in AAMAS, a test must possess the following attributes: (1) reliability or accuracy, (2) repeatability, (3) sensitivity to mixture variables, (4) efficiency of testing, and (5) simplicity of testing.

In other words, testing procedures adopted for AAMAS must be able to document mixture variable sensitivity, be efficiently and reliably performed by laboratory personnel, and require a reasonable number of replicate specimens to produce statistically reliable results.

In general, there are three basic types of tests that have been used to evaluate bituminous mixtures. Flexural tests have been primarily used for fatigue and stiffness determinations; static and repeated load triaxial compression procedures (with and without confinement) have been used for stiffness, creep, and permanent deformation determinations; and static and repeated load diametral (indirect tension) procedures have been used for measuring all of the foregoing properties. Flexural procedures are the more complicated, specimens are more costly to prepare, and the results obtained are highly variable. Conversely, triaxial compression and indirect tension procedures are simple and specimens can be easily prepared to measure different properties. Triaxial compression is the more common, but testing cores from thin lifts are problematical because of end effects.

Indirect tensile testing procedures are becoming more popular and have been used to measure all properties commonly required for mechanistic analysis models. Baladi (*34*), Kennedy et al. (*35, 36, 37*), Regan (*1*), and Whitcomb et al. (*38*), among others, have found that results from the indirect tensile test are sensitive to mixture components, a key requirement of AAMAS. Previous studies have also found that material properties determined from indirect tensile testing procedures are comparable to those deter-

mined from testing flexural specimens. Thus, triaxial compression and indirect tension samples were selected for initial use in AAMAS.

2.1.4 Mixture Production/Construction Considerations

For a mixture analysis system to simulate and, hence, predict the behavior of a mixture in the field, it must take into consideration the production and construction process. Of course, the most obvious way to eliminate any differences between laboratory and plant production and between laboratory and field compaction is to use material produced through a plant and compacted in test strips for conducting the mixture design. However, this would be expensive and time consuming and was considered an impractical approach to performing mix designs on a routine basis. While it is readily recognized that AAMAS should simulate, as closely as practical, the compaction process obtained during construction, differences exist between laboratory and plant production of mixtures. These differences along with other critical factors of mixture design are discussed below.

2.1.4.1 Mixture Production

Considerable differences exist between the asphaltic concrete manufacturing processes used in the laboratory and those used in a batch or drum mix plant. It is important to look at those differences and understand how and why a mix design value, characteristic, or property determined in the laboratory might differ from that obtained from a plant prepared mix.

2.1.4.1.1 Aggregate. In the laboratory, the incoming aggregates are sometimes washed before they are used. In other cases, wet sieving instead of dry sieving is used to divide the aggregates into various fractions. In the field, the materials are incorporated into the mix as received from the aggregate supplier. If there is a considerable volume of fines clinging to the coarser material received, those fines are put into the "wrong" cold feed bin and delivered to the drier or drum mixer. This change in gradation does not normally occur in the laboratory, because the aggregates are shaken through the sieves until most of the fines have been broken loose and are retained on the proper screen. Thus, a difference in gradation, from laboratory to field, can exist.

The aggregates used to make laboratory samples are completely dry; i.e., there is essentially no moisture in the materials. For aggregates heated in a batch plant drier, it is possible to reduce the moisture content to about 0.1 percent by weight of the aggregates. In most cases, however, the moisture content in the aggregates can be up to 0.5 percent. This value will vary widely, depending on the amount of moisture in the incoming aggregates, the production rate of the drier, and the discharge temperature of the aggregates. In a few cases, the aggregates passed through a typical drier will be completely dry. Thus, there is a difference in moisture content during mixing between the laboratory and plant.

In the laboratory oven, the aggregates are uniformly heated. The coarse and fine portions of the aggregates will both be at approximately the same temperature. In the asphalt plant drier or drum mixer, the aggregates will generally flow through the drum in about 3 to 4 min, depending on the length and slope of the drum and on the amount of aggregate being heated. The coarse aggregates are usually heated to a somewhat lower temperature than are the fine aggregates. There is a distinct temperature differential between the two portions of the aggregates. In a batch plant, the temperature is equalized during pugmill mixing. In a drum mix plant, however, a heat balance is not obtained unless the material is held in the surge silo for a period of time.

If a wet scrubber is used in either a batch or drum mix plant, any fines captured in the exhaust gas air stream are carried out of the drier or drum and wasted. These fines are no longer part of the aggregate gradation. In some cases with particularly dirty aggregates, up to 2 percent of the fines can be carried out of the aggregates. If a baghouse is used as an air pollution control device on either type of plant, most or all of the gathered fines can be returned to the plant and thus to the mix. This availability or nonavailability of the fines can change the filler-bitumen ratio, and thus the stiffness of the resulting asphaltic concrete mix. The possible loss of fines is normally not taken into account in the laboratory mix design procedure. If the material enters the wet wash equipment, a significant change in the aggregate gradation can also occur.

If the plant is equipped with only a dry collector (knockout box), most of the fines returned will be larger than the number 200 sieve (75 micron sieve). With a fabric filter, particles as small as 5 micron size (smaller than the asphalt cement film thickness on the aggregate) can be reincorporated into the mix. These ultrafine particles, which do not exist as separate pieces in the laboratory, can act as extra asphalt cement, causing the mixture to look greasy and become tender. Thus, a stable mix in the laboratory can turn soft and tender in the field, if the baghouse is sending ultrafine aggregate back into the plant. For a plant equipped with a fabric filter, not only the quantity of the baghouse fines needs to be known, but also the size distribution (gradation) of those fines should be determined.

Both Marshall and Hveem mix design procedures are limited to 1-in. maximum size aggregate. For larger size aggregates that are typically used in dense-graded base layers, modifications to the aggregate gradation or sample size must be made.

2.1.4.1.2 Asphalt Cement. In an asphalt cement storage tank at the asphalt plant, the binder is held in bulk. It is usually circulated in some fashion through the pump and meter system. The amount of aging and hardening that occurs during storage is minimal. In the laboratory, the asphalt cement can be heated in an oven for various periods of time. It is usually handled in small quantities in containers that are open to air. The material is rarely, if ever, stirred. Some hardening has to occur during the process. The degree of hardening, however, is much less than that which occurs during mix production at the asphalt plant.

A drum mix plant may act like a horizontal refinery steam distillation tower. Temperatures are high—at times over 800°F at the point the asphalt cement is introduced into the mix. There is much steam inside the drum from the moisture in the aggregates. This steam and the high temperatures can strip the "light ends" from the asphalt cement, causing a decrease in penetration and an increase in viscosity in the binder material. This problem can be particularly acute when a recycled mix is being manufactured because the temperatures inside the drum are higher than for an all-new aggregate mixture. The change in the binder properties may be severe enough to change the mixture stiffness characteristics. Such a change does not occur, of course, when preparing asphaltic concrete mixtures in the laboratory.

2.1.4.1.3 Mixing Process. As the wet mix time increases in a batch plant pugmill, the degree of aging of the asphalt binder

also increases. For relatively short wet mix times (30 to 35 sec), the average asphalt cement will decrease in penetration from 30 to 45 percent. For longer wet mix periods (up to 45 sec), the decrease in penetration of the asphalt cement can be up to 60 percent. Mixing temperature is also very important in determining this drop.

The amount of hardening of the asphalt cement which typically occurs in a drum mix plant is less than that in the pugmill of a batch plant. The degree of hardening is quite variable and is a function of many factors. As the moisture content of the incoming cold aggregate increases, as the volume of aggregate in the drum increases, as the mix discharge temperature decreases, and as the production rate of the plant increases, less hardening of the asphalt cement occurs during the coating process. The change in penetration or viscosity of the asphalt cement in the drum mixing process is not well documented. It is usually less than that of the batch plant but is still much more than that occurring in the laboratory-heated asphalt cement. Thus, the mix stiffness of a material produced in the laboratory will probably be less than for a plant manufactured mixture.

2.1.4.2 Mixture Compaction

The idea of any compaction process is to simulate, as closely as possible, the actual compaction effort produced in the field by the rollers. This comparison includes such factors as particle orientation, total air void content, and void structure, such as number of interconnected voids. Voids are critically important because of their effect on the engineering properties, an effect which has been substantiated by other research and testing studies (*39, 40, 41, 42*).

In the laboratory, the compactive effort applied to the samples of asphaltic concrete is mostly vertical in direction, with the exception of the rolling wheel type compactors. Further, the mix being densified is confined in a mold and all of the compactive effort is directed to the specimen. On the asphaltic concrete mix placed on the roadway, however, the compactive effort applied by the rollers is really a shear type loading, directed to the mix at an angle as the roller moves forward and backward over the mat. While most of the compactive effort of the rollers is applied in a downward direction, some of the force is directed horizontally, causing the mix to want to move forward and shove.

This shear loading can cause the mix to creep under the compaction equipment. The amount of the creep or shoving is typically the greatest under the static steel wheel rollers, such as tandem and three wheel type equipment. The amount of creep that can occur is usually reduced when a single or double drum vibratory roller is used for breakdown compaction and normally does not occur, except along a free edge, when a pneumatic tire roller is employed to initially compact the asphaltic concrete mat. Thus, a mix which is relatively stiff and unworkable in the laboratory can exhibit an increase in workability under the action of the compaction equipment. The degree of increase is dependent of the type of roller used to compact the asphaltic concrete mixture.

Because of the infinite variety of roller combinations, roller passes, and roller patterns that can be used on a particular paving project, it is very difficult to predict in the laboratory the air void characteristics of a mix. The compaction process in the laboratory is very quick, usually completed within a few minutes. This is in direct contrast with the roller operation where final density levels might not be attained until 10 to 20 min or sometimes much longer after the mix is placed by the paver. During the laboratory compaction process, the mixture temperature is relatively constant. On the roadway, the temperature of the material is continually decreasing with time. The laboratory compaction effort is usually completely applied before the mix temperature declines to 240°F (Marshall) or 220°F (Hveem). In the field the mix will cool to 175°F or less before the compaction process is completed.

In the laboratory the asphaltic concrete mix is compacted against a solid foundation. In the field a wide variety of base types and stiffnesses are encountered. An asphaltic concrete mix can be placed as the first layer on top of a soft subgrade soil or as the final surface course on a thick full depth asphaltic concrete pavement structure. The material can be used as an overlay on an alligator cracked, pot-holed asphalt roadway or as resurfacing on a portland cement concrete pavement. The ability to obtain a particular level of density in an asphaltic concrete mixture may depend, in part, on the rigidity of the base. The differences between roadway support conditions and laboratory conditions can be significant.

Some studies have been conducted for comparing mix design values where different types of compaction devices were used to compact samples to approximately equal air voids or densities. One such study was conducted by Jiminez (*43*) for comparing specimens compacted by a vibratory kneading compactor and a Triaxial Institute compactor. Similarly, Finn et al. (*44*) compared various test results on samples compacted with the kneading compactor and Marshall hammer. However, any comparison is complicated because air voids were not kept constant on similar samples.

Unfortunately, there have been very few studies comparing the engineering properties of samples prepared in the laboratory (using different types of compaction equipment) to samples compacted in the field. Of the few studies documented, most indicate that the mixture properties will vary with compaction equipment (assuming identical sample size and air voids) (*45*). These differences may be a result of different particle or sample orientation, or of the fact that some of the impact type compactors fracture the material sooner than contact or roller type compactors.

2.1.4.3 Factors Affecting Compaction

There are a number of factors that affect the compatibility or workability of an asphaltic concrete mixture both in the laboratory and field. These factors can be divided into four primary areas: (1) properties of the aggregates, (2) properties of the asphalt cement, (3) properties of the asphaltic concrete mix, and (4) conditions during the compaction process. Differences between laboratory and field conditions were discussed above. The following subsection discusses the material-related properties that have an effect on mixture compaction or workability.

2.1.4.3.1 Properties of the Aggregates. The shape of the individual aggregate particles affects the degree of workability of the asphaltic concrete mix. Aggregates that are rounded are more easily moved or displaced by an applied load. Rounded materials tend to "slide by" each other when subjected to load. Aggregates that are angular will have a greater degree of interlock when a load is applied and will be more resistant to displacement by that load.

The smoother the surface texture of an aggregate particle, the greater will be its degree of workability. An aggregate that has a rough surface texture, similar to the particle with the angular shape, will be more difficult to compact. Thus, the particles with smooth surface textures will generally be more easily compacted than will the aggregates with the rough surface textures.

A blend of coarse and fine aggregates that is uniformly graded from the largest to the smallest particles will be more workable than will a combination of particles which is gap graded. When plotted on 0.45 power gradation graph paper, a blend of material that follows the maximum density line (plots as a straight line) will typically be the easiest gradation to compact because the individual aggregate particles all "fit together" properly and pack into the smallest space. In general, this combination of aggregates will therefore have the lowest voids in mineral aggregate (VMA) content.

Blends of aggregates that are finely graded are more workable and easier to compact than are blends of material that are coarsely graded. A blend of aggregates that is finely graded contains a greater percentage of fine aggregate in the combination of materials. When plotted on the 0.45 power gradation paper, this blend of material will fall above the maximum density line, to the fine side of the line, with greater percentages of material passing each particular sieve than for a coarsely graded combination of aggregates. The latter material will typically plot as a curved line located below the maximum density line. The more fine aggregate in the mix, generally the more workable is the blend of aggregates.

Aggregate blends that have a pronounced hump in the grading curve, particularly in the fine aggregate portion of the gradation, may be more workable than are mixes that are more uniformly graded in the fine aggregate portion of the total gradation. The hump occurs because a large amount of fine aggregate passes one particular sieve, such as the No. 40 sieve, and is retained on the next sieve in the series, such as the No. 80 sieve. The effect of the hump on the compactibility of the aggregates depends on the severity of the hump—the more pronounced the hump, the more tender the mix and the easier it will be to compact the blend of aggregates, in a confined laboratory mold. As discussed below, however, the hump in the fine aggregate portion of the total grading curve can make the same combination of aggregates very difficult to densify on the roadway under the contractor's compaction equipment.

2.1.4.3.2 Properties of the Asphalt Cement. For the Marshall mix design process, the selected mixing temperature and compaction temperature for the production of the asphaltic concrete mix are determined by the viscosity of the asphalt cement. The mixing temperature is selected as the temperature at which the asphalt cement has a viscosity of 170 ± 20 centistokes. The compaction temperature is chosen as the temperature at which the asphalt cement has a viscosity of 280 ± 30 centistokes. Using the viscosity to determine the mixing and compaction temperatures for each particular asphalt cement is intended to remove differences in workability among asphalt cements that have different degrees of temperature susceptibility.

An asphalt cement that is highly temperature susceptible will change viscosity more quickly with a change in temperature than will an asphalt cement that is less temperature susceptible. In the laboratory, however, because the mixing and compaction process takes place relatively quickly, the effect of temperature susceptibility on workability is probably small. The temperature susceptibility of the asphalt cement has a greater effect on the compaction of the asphaltic concrete mix on the roadway because the densification process occurs over a longer period of time.

2.1.4.3.3 Properties of the Asphaltic Concrete Mixture. To a point, the higher the asphalt content in the mix, the more easily compactible the mix should be. A low asphalt content in the mix provides a mix that does not have enough lubrication to allow the aggregate particles to be reoriented under the action of the laboratory compaction device. A high asphalt content in the mix, on the other hand, provides enough binder material to obtain a relatively greater film thickness on the individual aggregate particles and promotes the movement of the particles under the applied compactive effort.

Too much asphalt cement in the mix, however, can significantly increase the workability of the mix to the point that the desired compaction cannot be obtained. This is less of a problem with a laboratory prepared mix (because the sample is confined during the compaction process) than for a high asphalt content plant-produced mix placed and compacted on the roadway. If the asphalt content is too high in the laboratory mix, the aggregate particles are held apart by the excess binder material and the unit weight of the mix will be relatively low, even though the air void content of the mix will also be low.

In a laboratory-prepared asphaltic concrete mixture, the moisture content of the aggregates is typically zero. This is because these materials are held at elevated temperatures in an oven until the time for mixing with the asphalt cement. During the heating process, which can be as long as several hours or sometimes even overnight, any moisture in the coarse and fine aggregates is driven off. Both the surface moisture and any internal moisture in the aggregates are removed and the aggregates are dry at the time of mixing. If any moisture were left on the surface of the aggregate particles, this moisture would contribute to the increased workability of the asphaltic concrete mixture during the laboratory compaction process. Essentially, the moisture would act in a manner similar to additional asphalt cement in causing an increase in the lubrication for the aggregate particles.

Probably the single most important factor that affects the workability of an asphaltic concrete mixture under the compaction equipment is the temperature of the mix at the time of compaction. As an asphaltic concrete mixture cools, the viscosity of the asphalt cement increases. As the viscosity increases, the mix becomes stiffer and more difficult to compact. Essentially all workability is lost by the time the temperature of the mix drops to 175°F. Below this temperature, the viscosity of the asphalt cement binder has increased to the point that the mix is too stiff for the compaction equipment to be able to further densify the mix.

The temperature of the asphaltic concrete mix changes with time and is affected by a number of factors. The change in temperature with time is a function of the initial temperature of the mix at the time of placement, the thickness of the asphaltic concrete layer, the ambient air temperature, the temperature of the base being overlaid, the wind velocity, and the amount of cloud cover. Because workability is directly related to the temperature of the mix, factors that reduce the rate of cooling of the mix increase the workability of the mix and allow more time for the rollers to achieve the required level of density.

2.1.4.3.4 Conditions During the Compaction Process. The more confined an asphaltic concrete mix is on the roadway, the less workability of the mix will affect the ability of the compaction equipment to properly densify the material. Confinement

manifests itself in two ways—the degree of support from the underlying pavement layers and the amount of support along the longitudinal edge of the mat.

With the proper choice of compaction equipment, roller patterns, and roller passes, the stiffness of the underlying pavement layer does not affect the contractor's ability to achieve the required level of density in the newly placed asphaltic concrete layer. With an incorrect choice, however, the contractor may have difficulty achieving density when the underlying layers are soft and yielding. If the base layers are moving under the compaction equipment, the mix will become more workable and move more under the rollers. This increase in the workability of the mix can be so extreme as to preclude the contractor from obtaining the desired density level, with the type and weight of rollers, and roller patterns, being used.

The workability of the mix can also be a factor when the mix is unsupported along a free longitudinal edge. A mix which is relatively stable in the center of the mat where it is confined by the mix around it can become tender and shove under the rollers at or near the unsupported edge of the lift being placed. This increase in workability due to the lack of confinement results in the mix being displaced along that edge and an increase in the width of the layer being placed and compacted.

2.1.4.4 Time and Traffic Effects

The density obtained in the pavement layers during the rolling process is not the ultimate density level that will occur in the asphaltic concrete mix when subjected to traffic for a period of time. Most mixes are designed at an air void content of 3 to 5 percent. Most pavement layers are constructed with air void contents over 5 percent, and sometimes even over 10 percent. These pavements, particularly those with high initial air void levels, will become stiffer with time (due to asphalt hardening) and will densify further under traffic. This air void reduction process or one-dimensional vertical consolidation, often called rutting, is dependent on a number of mix design, construction, and environmental variables. In any case, in the laboratory, the density value obtained after compaction remains constant. Under traffic, the air void content of a pavement's asphaltic concrete mixture decreases with time. Some of these differences can be dramatic.

Moisture, which is not accounted for in the laboratory during the initial mixture design, is another variable that can have a significant effect on the asphaltic concrete mixture properties over a period of time. More important is the interaction between moisture, traffic, and age hardening on the performance of asphaltic concrete mixtures. Current test procedures, such as AASHTO T283, evaluate the effects of moisture on the mix, but do not take into account the effects of asphalt aging. Most are independent steps or conditioning methods, when in actuality, the moisture, asphalt aging, and traffic densification occur simultaneously in the field.

2.1.5 Summary

An asphaltic concrete laboratory mix design procedure should duplicate, as closely as possible, the properties and characteristics of the "same" mix manufactured in an asphalt plant and compacted in the field. Significant differences can occur, however, between materials produced in a batch plant and in a drum mix plant and between materials compacted over varying structures and in varying environmental conditions. Any mix design method selected for use should take into account as many of the actual plant production and construction variables as possible, and minimize the compromises which must be made between the laboratory procedures and "real life." Some of the critical factors that must be addressed in the final AAMAS include hardening, mixing temperature, gradation, maximum aggregate size, sample size, mixture workability, traffic densification, moisture conditioning, and compaction.

In short, the needs and demands of an AAMAS are large. However, the potential payoff of a rational mixture design procedure is even larger. Only after the first step toward AAMAS is taken can the second step, the evolutionary improvement of AAMAS, take place.

2.2 MIXTURES SELECTED FOR STUDY

Nine different mixtures were used in developing the AAMAS principles and mixture design methodology, and to establish procedural guidelines and design criteria for selected parameters. This section of the report discusses those materials and mixtures selected for study and presents the traditional mix design parameters for each. It should be understood, however, that nine mixtures alone cannot verify the mixture design and analysis methodology. Validation and support for its use can only come through time. It is expected that the SHRP Long Term Pavement Performance (LTPP) and Asphalt research programs will provide additional data that will support the procedures or may suggest slight modifications.

Five of the nine mixtures were produced and placed on roadways to ensure that AAMAS would reproduce mixtures in the laboratory with properties consistent with those placed on the roadway. These mixtures were supposed to have good performance characteristics for heavy traffic, if properly produced and placed. An additional four mixtures with inferior performance characteristics were studied in the laboratory using the AAMAS to provide supporting data that AAMAS would distinguish these mixtures as borderline for heavy traffic.

2.2.1 Material and Mixture Properties

Mix design data and material properties for the AAMAS mixtures were requested from each state highway agency. Information obtained on each of these mixes is presented in this section of the report. In a few cases, however, some data requested were unavailable. Where information was unavailable from project files, these data were measured.

2.2.1.1 Aggregate Blend

Grading analyses are discussed in detail in Appendix C. Gradations from a wet sieve analysis for each of the aggregate stockpiles used in the aggregate blend were measured from bulk samples and compared to construction records. Wet sieve analyses were also performed on extractions of the bulk mixture sampled from trucks at the plant. These gradations at various points in the production process are provided in Appendix C, and com-

pared to the FHWA "0.45 Power Curve." Tables 7 and 8 summarize the average aggregate gradations that were measured in the laboratory from each project and the target job mix formula (JMF).

As stated earlier in section 2.1, shape and surface texture of the aggregate particles influence workability and strength of the paving mixture. However, there is no ASTM or AASHTO test method for directly measuring surface texture and particle shape. There are procedures, such as ASTM D3398, "Index of Aggregate Particle Shape and Texture," which provide a quantitative measure of the aggregate shape and texture characteristics. McLeod and Davidson (*46*) have used this index value to evaluate how changes in aggregate shape and texture can affect stability and other properties. On the other hand, Baladi (*34*), among others, uses subjective ratings or an index scale to categorize different aggregate blends.

For the aggregate blends used in the AAMAS mixtures, Baladi's aggregate angularity value was used to initially rank the aggregate. The percentage of aggregate (based on dry unit weight) retained on the No. 8 sieve with two fractured faces was also estimated for each grading and mixture. These values are reported on Tables 7 and 8 for each of the nine mixtures.

Table 7. Summary of gradations and asphalt contents used in each of the mixtures placed on the roadway.

Aggregate Property	Colorado CO-0009		Michigan MI-0021		Texas TX-0021		Virginia VA-0621		Wyoming WY-0080	
	JMF	Extr.	JMF	Extr.	JMF	Extr.	JMF	Extr.	JMF	Extr.
Sieve Size										
2	-----	-----	-----	-----	-----	-----	-----	-----	-----	-----
1 1/2	-----	-----	-----	-----	-----	-----	100.0	-----	-----	-----
1	-----	-----	-----	-----	100.0	100.0	-----	98.8	-----	100.0
3/4	100.0	100.0	100.0	100.0	94.1	96.5	85.0	85.6	-----	95.6
1/2	93.4	90.0	92.2	88.8	77.1	81.6	-----	68.3	-----	72.0
3/8	68.3	75.0	79.9	75.8	67.6	70.0	-----	60.2	-----	63.3
No. 4	45.5	53.0	60.9	53.2	51.9	54.2	46.0	46.5	-----	40.0
No. 8	32.2	38.0	47.4	48.6	33.7	40.0	34.0	35.6	-----	29.0
No. 16	23.8	-----	-----	37.0	-----	34.3	-----	-----	-----	22.0
No. 30	17.5	-----	24.9	26.0	23.0	30.8	-----	19.4	-----	17.6
No. 50	11.2	14.0	-----	14.0	19.2	27.8	-----	12.1	-----	13.2
No. 100	7.7	-----	-----	7.0	-----	15.3	-----	-----	-----	9.0
No. 200	4.9	6.0	5.3	4.0	2.7	6.8	5.5	5.6	-----	5.5
Asphalt Concrete, Percent	5.5	5.0	4.95	5.36	5.5	5.57	4.5	4.56	2.75	4.74*
Particle Index	11.0		8.5		14.0		15.5		-----	
Aggregate Angularity Value(34)	3.2		2.8		3.8		3.8			3.0
Two Fractured Surfaces, %	90		65		95		95			75

JMF = Job Mix Formula Obtained from State Highway Agency

Extr. = Average Values from extractions of the bulk mixture samples at the plant during production of the mix.

* Value measured from extractions of a recycled mixture. Thus, the asphalt content may vary considerably along the project, depending upon the variability of the RAP material.

Table 8. Summary of gradations and asphalt contents used in each of the mixtures identified as inferior based on historical performance observations.

Aggregate Property	California CA-0001			Georgia GA-0001		New York-R NY-0001		Wisconsin WI-0001	
	JMF	Drum	Batch	JMF	Drum	JMF	Batch	JMF	Drum
Sieve Size									
2	---	---	---	---	---	---	---	---	---
1 1/2	---	---	---	---	---	---	---	---	---
1	---	---	---	100	100	---	---	---	---
3/4	100	100	100	92	89	---	---	100	100
1/2	97	99	92	77	70	100	100	98	97
3/8	85	85	88	68	62	86	89	90	90
No. 4	61	61	64	54	52	57	56	69	69
No. 8	47	53	52	38	39	39	32	53	55
No. 16	35	39	41	26	26	33	28	---	44
No. 30	25	27	31	19	19	26	20	---	37
No. 50	16	18	20	13	14	14	10	23	25
No. 100	10	11	13	9	10	6	4	---	15
No. 200	8	8	9	5	7	4	3	9.4	11
Asphalt Content, Percent	5.3	4.76	5.95	5.5	4.33	6.0	5.08	3.1	5.21*
Particle Index	11.7			14.8		9.2		15.5	
Aggregate Angularity Value(34)	3.0			4.0		2.5		3.8	
Two Fractured Surfaces, %	90			95		68		92	

JMF = Job Mix Formula Obtained from State Highway Agency.

Extr. = Average Values from Extractions of the Bulk Mixture Samples at the Plant during Production fo the Mix.

* Value measured from extraction of a recycled mixture. Thus, the asphalt content may vary considerably along the project, depending upon the variability of the RAP material.

2.2.1.2 Asphalt Cement

Asphalt supplier and grade information for the different types of binders used in these mixtures were initially obtained from construction records. Either AC-10 or AC-20 viscosity graded asphalt cements were used, with the exception of the Georgia and Wisconsin mixes. An AC-30 was used in the Georgia mix and an AC-5 in the Wisconsin mix. Penetration and viscosity values were measured on the "virgin" asphalt sampled at the plants. Table 9 summarizes these data, which have also been plotted on the viscosity-penetration chart shown in Figure 25. These asphalt characteristics were also compared to the requirements given in ASTM D3381, "Viscosity-Graded Asphalt Cement for Use in Pavement Construction." The asphalts used in the Texas and Wyoming projects are outside ASTM D3381-83 specification requirements.

Viscosity-temperature relationships were also determined for each asphalt cement used in the field test sections (i.e., the first five mixtures). These results are displayed in Figure 26. The viscosity-temperature profile is essential for defining the combined effects of temperature susceptibility and age hardening. For purposes of AAMAS, temperature susceptibility is defined as the rate of change of viscosity with temperature (Figure 26). The Virginia asphalt had the highest viscosity at 140°F (60°C), but the lower temperature susceptibility. The Michigan asphalt had the better asphalt characteristics for resistance to cracking, whereas, the Wyoming asphalt had the poorer characteristics.

2.2.1.3 Rice Specific Gravities

Rice specific gravities of the loose mix removed from the sealed containers were measured in accordance with AASHTO T209. Sufficient material was removed from each container to conduct three separate tests. Mixtures from a minimum of three containers were sampled from each field test section. These test results are summarized for each project in Appendix D.

For all projects, neither the mean nor standard deviation of Rice specific gravities measured for each of the sample containers was found to be statistically different. Therefore, the project mean Rice specific gravity was used to calculate air voids for all sections from each state. The mean values used are tabulated in

Table 9. Summary of asphalt information.

State/ Project	Asphalt Supplier and Type	Specific Gravity at 77F	Penetration at 77F	Viscosity at 104F Stokes
Colorado CO-0009	Sinclair Oil AC-10	1.017	85	1,071
Michigan MI-0021	Marathon 120-150	1.025	127	806
Texas TX-0021	Exxon AC-20	1.025	57	1,896
Virginia VA-0621	Chevron AC-20	1.035	91	2,250
Wyoming WY-0080	Sinclair Oil AC-20	1.026	65	2,306
California CA-0001	Shell Oil AR-4000	1.030	56 48	1,490 1,900
Georgia GA-0001	AMOCO AC-30	1.015	63	3,310
New York - R NY-0001	Elf Asphalt AC-20	1.036	87	2,032
Wisconsin WI-0001	Koch Asphalt 200-300 Pen	1.025	239	550

Table 10. Summary of Rice specific gravities measured for each mixture and used in air void calculations.

State/Project	Rice Specific Gravity		
	Mean Value	Standard Deviation	Coefficient of Variation, %
Colorado/0009	2.4759	0.01657	0.67
Michigan/0021	2.4748	0.01244	0.50
Texas/0021	2.4343	0.02498	1.03
Virginia/0621	2.7361	0.01871	0.68
Wyoming/0080	2.4516	0.01366	0.56
California CA-0001	2.459	0.01587	0.64
Georgia GA-0001	2.511	0.00778	0.31
New York - R NY-0001	2.499	0.00212	0.09
Wisconsin WI-0001	2.535	0.00721	0.28

Table 10. The Texas project (TX-0021) contained a much greater variation in Rice specific gravity than any of the other projects for some unknown reason. This project was also found to have the greater variation in materials from truck-to-truck sampling. This is the same project where a change in materials occurred during the production process and the JMF was revised during the day of construction for the AAMAS test sections.

2.2.1.4 Traditional Mixture Design Properties

Hveem (AASHTO T246-82) and/or Marshall (AASHTO T245-82) mixture design procedures were used to determine the

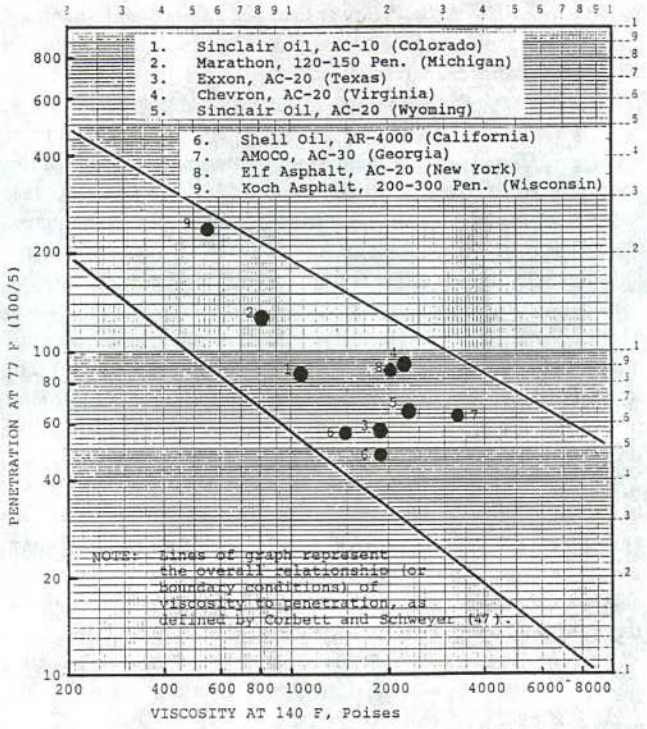

Figure 25. Relationship of penetration to viscosity for the asphalt cements used on the AAMAS projects.

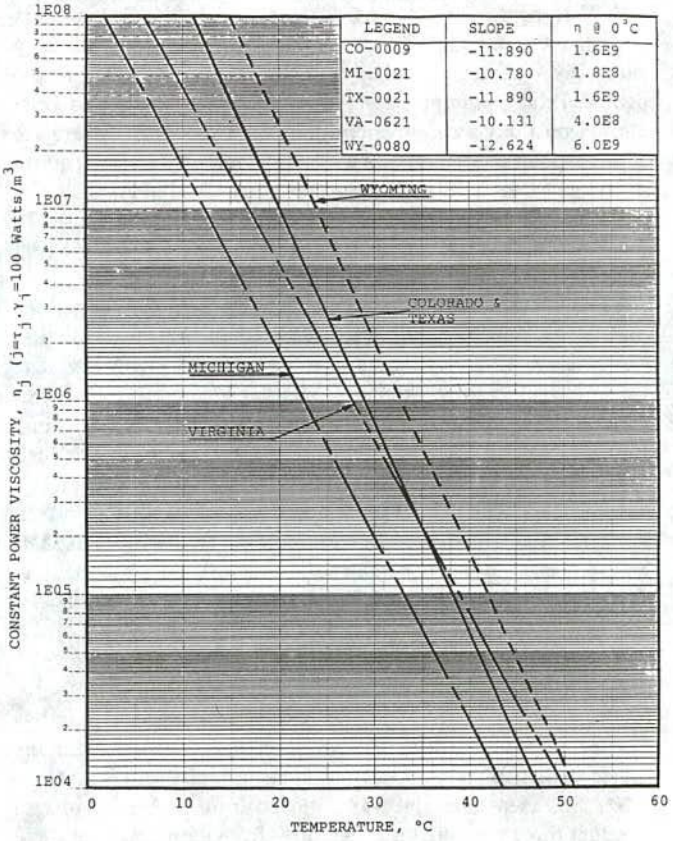

Figure 26. Viscosity-temperature relationship of the AAMAS asphalts measured on 365°F TFOT residue, viscosity (simulation of 18-month age hardening).

design asphalt content for the aggregate blends presented in Appendix C. All mixture design data and other information obtained from construction records have been presented in Appendix E. Figures 27 and 28 summarize and compare the different mixtures using Marshall mix design parameters. These include VFA, VMA, air voids, and stability. As shown, the mixtures represent a wide range of material combinations. In general, for aggregate blends with lower VMA contents, the difference in air voids between the kneading and Marshall compaction was small. Conversely, for aggregate blends with higher VMA contents there were large differences in air voids by the two methods.

Figure 29 displays a comparison of Hveem and Marshall air voids (Figure 29a) and stabilities (Figure 29b) for the same grading and asphalt contents. As anticipated, no general correlation was found between the two stabilities for the materials used in the AAMAS projects. For each specific mixture, however, the two stabilities are grossly related, with the exception of the Wyoming mix. The Wyoming mixture's VMA value was very low. Table 11 provides a comparison of the mixture design values, interpolated for the average asphalt content determined from extraction tests of bulk mixture (Table 7), and design criteria suggested in the Asphalt Institute's Manual Series No. 2 (*48*). As shown, none of the mixtures meet all criteria listed.

Mixture designs were also completed by each state highway agency on the four supplemental mixtures, but only using the individual agency's design procedure. A graphical summary of the results for each mix is provided in Appendix E. Table 12 summarizes the mix design values for the target asphalt content, and the asphalt content actually measured for all mixtures sampled during mix production. As shown, all mixtures, as designed, exceed or meet the specifications stated in the Asphalt Institute MS-2 manual (*48*). Unfortunately, many of these mixtures were not placed as originally designed.

Table 13 gives the asphalt content during plant production and the design asphalt contents based on Marshall and Hveem mixture design procedures. Note in the table that the Marshall procedure (50 blows) always resulted in a higher asphalt content requirement than Hveem for similar aggregate blends, because of the lower compactive effort (50 blows) applied to these specimens.

The optimum amount of asphalt was also calculated using a program entitled ASPHALT (*2*). The results from program ASPHALT for each aggregate blend used is presented and compared to the results from the standard mixture designs in Appendix E. All projects were found to correspond reasonably close to the calculations using this program. Figure 30 shows a comparison of the design asphalt contents using the above three proce-

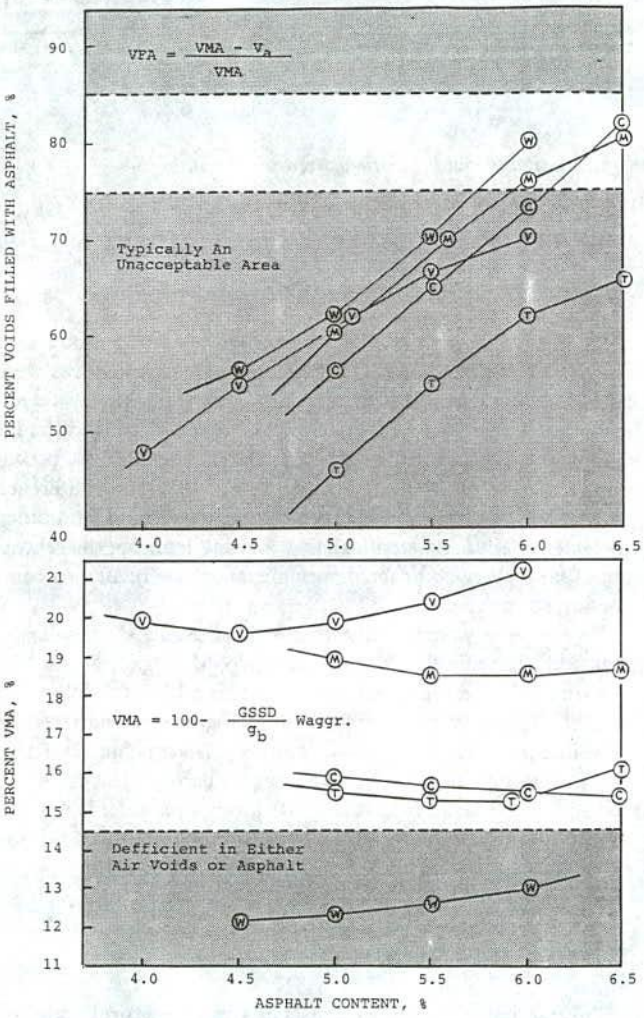

Figure 27. Percent VMA and VFA for the combined grading.

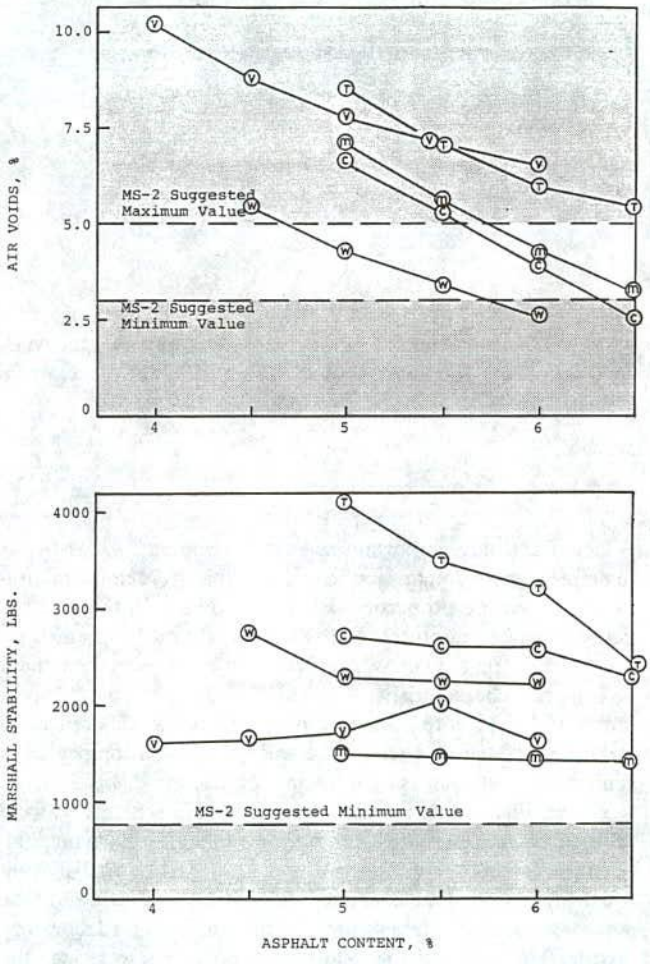

Figure 28. Comparison of stabilities and air voids measured for each of the aggregate blends during Marshall mix designs.

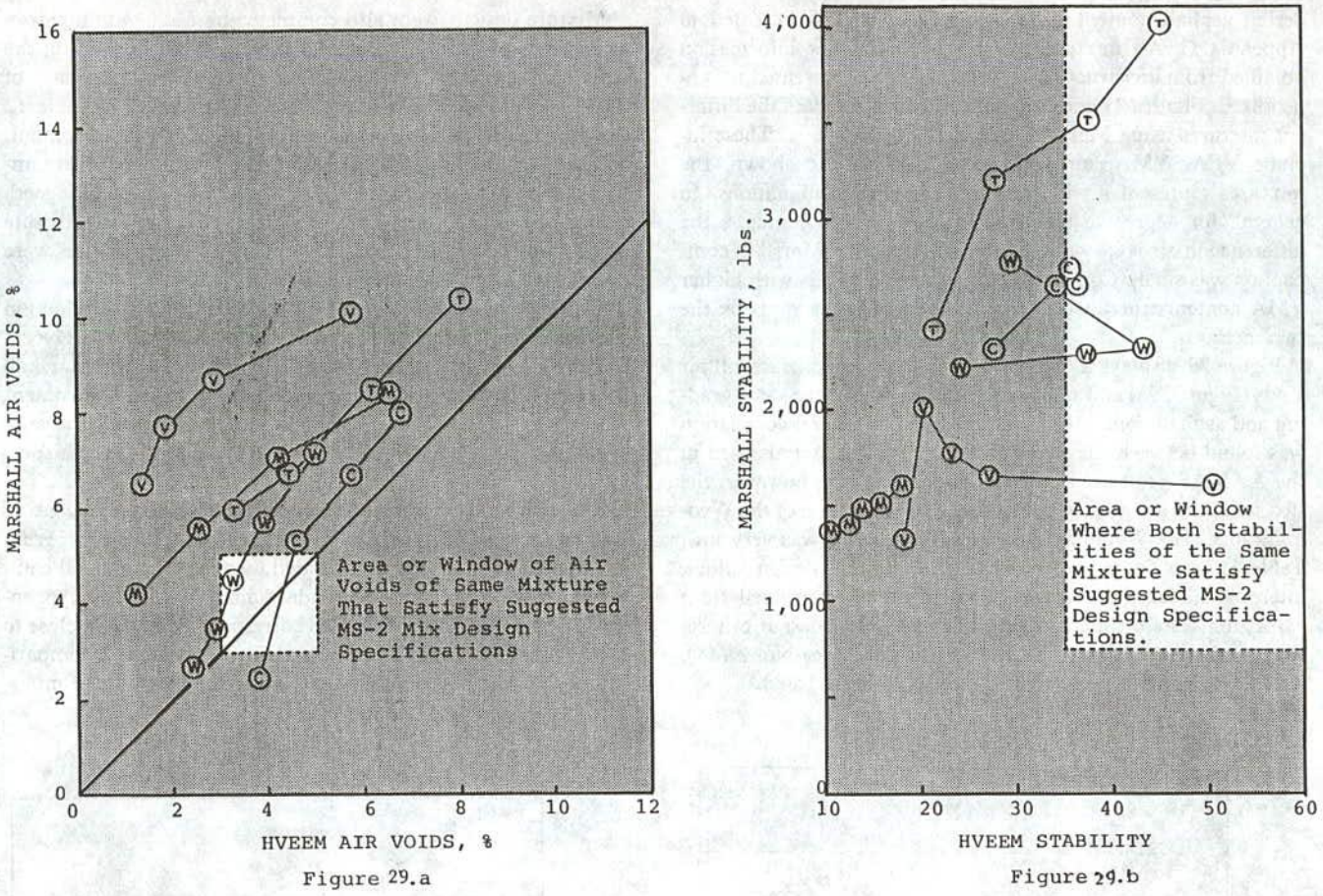

Figure 29. Comparison of typical Hveem and Marshall mix design variables as measured on the same aggregate blend from different projects.

dures. As shown, the optimum values calculated with program ASPHALT were generally below those determined by the Marshall procedure and above those determined by the Hveem procedure.

2.2.2 Field Test Sections

One of the more important tasks in developing an AAMAS is to define sample preparation techniques that yield in the laboratory, engineering properties that closely relate to those of the field-compacted mixtures. For example, Nunn (*45*) found substantial differences in density and some differences in permanent deformation characteristics between laboratory-compacted specimens and field cores. Jimenez (*43*) also found differences in stabilities and tensile strengths between specimens compacted to similar air voids but using different compaction devices.

To examine sample preparation techniques, test sections were selected in various states to obtain a range of environmental, aggregate, and compaction conditions for mixing and placing dense-graded asphaltic concrete mixtures (both surface and base materials), and to obtain samples of the materials for laboratory mixing. The intent of the field test sections was to reduce the independent variables within a section of pavement to as low a level as practical.

Samples of the bulk mixture were obtained during production and placement of the asphaltic concrete layers, and cores were recovered immediately after compaction on the roadway. Specimens were then compacted in the laboratory using different compaction devices and tested using the same laboratory procedures as were used for testing the field cores. Thus, any difference in strengths or stiffnesses between the field cores and laboratory specimens (assuming identical air voids and ignoring the reheating of laboratory-compacted specimens) can be related to compaction technique.

Five projects were initially selected for the field studies. These included one project each from Colorado, Michigan, Texas, Virginia, and Wyoming. Two projects were added for follow-up field studies to define the effects of aggregate size and to add a recycling project. These include one recycled asphaltic concrete mix in Virginia and one large aggregate base project in North Carolina. This section of the report provides a description and summary of each project. Table 14 summarizes information on the materials that were used to build the first five projects.

2.2.2.1 Colorado (CO-0009)

This section of roadway consists of a two-lane rural highway, designated as State Route 9, which runs north-south between

Table 11. Summary of mixture design criteria at the average asphalt content measured from extractions of bulk material. Note that shaded areas in the table represent those mix design variables that do not meet the specifications listed.

Mix Criteria	State/Project					Mix Specification* MS-2 Manual
	Colorado CO-0009	Michigan MI-0021	Texas TX-0021	Virginia VA-0621	Wyoming WY-0080	
Average Asphalt Content from Extractions	5.00	5.36	5.57	4.56	4.74	----
Avg. Air Voids from Cores/%	8.19	3.74	8.75	5.85	5.77	----
Marshall VFA, %	56	67	56	56	59	
Hveem VFA, %	63	80	68	81	62	75-85
Marshall VMA, %	15.9	18.6	15.2	19.6	12.3	
Hveem VMA, %	15.5	15.8	13.7	15.2	10.4	>14.5**
Marshall Air Voids,%	6.7	6.0	6.9	8.5	4.9	3-5
Hveem Air Voids,%	5.8	3.1	4.2	2.6	3.8	
Marshall Flow,(0.01")	11	9.6	11.4	14	20	8-18
Marshall Stability	2700	1490	3460	1650	2250	>750
Hveem Stability	33	13	38	26	20	>35

* Specifications represent those generally accepted for a medium traffic category.

** Minimum Value dependent on the maximum size aggregate used in mixture. For simplicity of comparison only one value listed which is for a 3/4 inch maximum aggregate size, and applicable for most of these mixtures.

Silverthorne and Kremmling. The actual test section locations are in the northbound driving lane, adjacent to a portion of the Green Mountain Reservoir, approximately 22 miles north of the junction with IH-70.

This project was a major strengthening of the existing pavement. The plans called for the placement of a leveling course, averaging 1.5 in. in thickness. On top of the leveling course, a nonwoven geotextile (Trevira) was laid. This was followed by the placement of two lifts, each 1.5 in. thick of a Type C surface course mix. The lower surface course layer was employed for the construction of the compaction test sections.

The aggregates incorporated into the Type C asphaltic concrete mix were supplied to Flatiron Paving from the L.G. Everest gravel pit. The mix consisted of 30 percent coarse aggregate and 70 percent fine aggregate. No mineral filler was used in the mix. The asphalt cement was an AC-10 viscosity graded material, and supplied by the Sinclair Oil Company. Pave Bond LP Liquid antistrip agent was added to the mix at the rate of 0.4 percent, by weight of asphalt cement.

The asphaltic concrete mix was produced in a new CMI drum mix plant. The material was discharged into the haul trucks from the surge silo at a temperature of approximately 280°F. A Blaw-Know PF 220 paver was used to place the mix at a minimum lift thickness of 1.5 in.

Each of the two test sections constructed was approximately 300 ft long. Test section 1-VB was compacted using two rollers. The breakdown roller was a Tampo RS-166A double drum vibratory roller. This equipment was operated at a frequency of 2,200 vibrations per minute in low amplitude. The breakdown roller made four coverages over each point on the pavement surface. The finish roller, which made two coverages over the mat, was a Hyster C 350 BT static tandem steel wheel machine.

Test section 2-PB was also compacted using two rollers. For this test section, however, the breakdown roller was a Hyster C 530, a pneumatic tire roller. The pneumatic tire equipment made four complete coverages of the roadway surface. Finish rolling was accomplished through the use of the Hyster static tandem steel wheel roller making two coverages over the mix.

Table 12. Summary of traditional test results at the design asphalt content selected by the state highway agency.

Mixture	Design Asphalt Content, %	Air Voids, %	Stability*
CO-0009	5.5	4.2	36-H
MI-0021	4.95	2.8	1,400-M
TX-0021	5.5	6.0	38-H
VA-0621	4.5	5.0	1,800-M
WY-0080	2.75	5.0	2,100-M
CA-0001	5.3	5.6	42-H
GA-0001	5.5	4.8	3,050-M
NY-0001	5.7	4.0	1,500-M
WI-0001	3.1	2.2	2,200-M

H - Hveem Stability Value
M - Marshall Stability Value

Table 13. Summary of selected asphalt contents using different procedures as compared to field extractions, percent. Note that the Marshall procedure (50 blows) always resulted in a higher asphalt content than Hveem for similar aggregate blends, simply because of the lower compactive effort (50 blows) applied to these specimens.

Method	State/Project								
	Colorado CO-0009	Michigan MI-0021	Texas TX-0021	Virginia VA-0621	Wyoming WY-0080*	California CA-0001	Georgia GA-0001	New York NY-0001	Wisconsin WI-0001
Hveem	5.4	4.9**	5.3	4.2	4.2	5.3	---	---	---
Marshall	5.9	5.7	6.0	5.4	4.6	---	5.5	5.7	5.1
Program "ASPHALT"	6.0	5.3	5.8	4.8	4.2	4.6	3.3	6.4	4.8
JMF, Plant	5.5	4.95	5.5	4.5	2.75*	5.3	5.5	5.7	3.1*
Extractions	5.00	5.36	5.57	4.56	4.74	4.76	4.33	5.08	5.21

* Recycled Mix, the asphalt content listed only include the Virgin Material added during production. For the extractions, the percent asphalt measured includes the RAP and virgin materials. The average a phalt content of the Wyoming RAP material was 4.34 percent and for the Wisconsin RAP was 5.4 percent.

** Hveem Stability values less than minimum value of 35, as recommended by the Asphalt Institute Criteria published in MS-2; 1984 Edition.

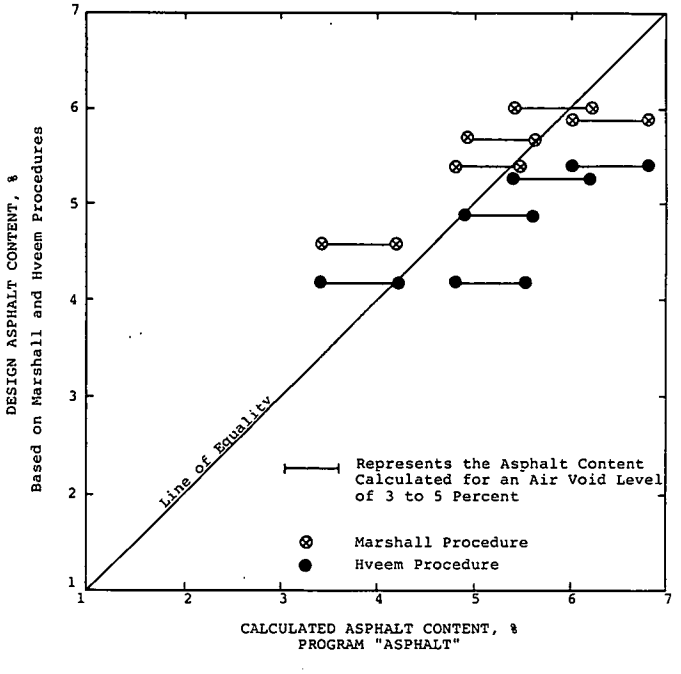

Figure 30. Selected or design asphalt contents determined by Marshall and Hveem mix design procedures compared to the optimum calculated with program ASPHALT.

2.2.2.2 Michigan (MI-0021)

Project MI-0021 was an overlay for a rural two-lane highway, designated as State Route M21, which runs east-wet between Flint and Owosso. The actual test section locations are in the eastbound lane, between Serr Road and Vernon Road, starting about 5 miles east of Owosso.

The coarse aggregate used in the asphaltic concrete mixture consisted of crushed aggregate (⅜-in. top size) from the Spartan Asphalt-Blakeley Pit. This coarse material made up 39 percent of the total aggregate combination. Three different fine aggregates, all natural sands, were blended together: 25 percent concrete sand from Blakeley Pit, 16 percent of a blend sand, and 20 percent 3CS sand from Fuoss Gravel Company. The asphalt cement was a 120-150 penetration graded material supplied by Marathon Oil Company. No additives (including liquid antistrip agents) or mineral fillers were added to the mix. The asphaltic concrete mix was designated Type 20 AAA.

The asphaltic concrete material was produced in a relatively old CMI drum mix plant. The plant had been modified by lengthening the drum and was equipped with a rotary center inlet to handle reclaimed asphaltic concrete material to produce recycled mixes. For this project, the contractor was feeding the coarse aggregate and two of the sands through the normal cold feed bins and into the mixing drum at the burner end. The third sand was introduced into the drum mixer from the reclaimed aggregate cold feed bin and through the rotary center inlet.

The asphaltic concrete mix was placed on M21 using a Blaw-Know PF 180H paver. The thickness of the mat was 1.5 in. thick throughout the project, except for the two AAMAS test sections. In order to assure that cores were at least 1.5 in. in height, the State and contractor agreed to increase the mat thickness in the area of the test sections to 1.75 in.

Each of the two test sections constructed was approximately 300 ft long. Test section 1-VB was compacted using two rollers. The breakdown roller was a Dynapac CC 42A double drum vibratory roller. This equipment was operated at a frequency of 2,400 vibrations per minute in low amplitude. The breakdown roller made four coverages over each point along the pavement's surface. The finish roller, which made two coverages over the mat, was a Bomag S 812A static tandem steel wheel machine.

Test section 2-PB was also compacted using two rollers. For this location, however, the breakdown roller was a Bros SP 3000 pneumatic tire roller. The pneumatic tire equipment made six complete coverages over the roadway surface. Finish rolling was

Table 14. Summary of plant job mix formulas and other information obtained during the production of mixtures for the AAMAS projects.

State / Project		Colorado CO-0009	Michigan MI-0021	Texas TX-0021	Virginia VA-0621	Wyoming WY-0080
Mixture Designation		Type C	Type 20AAA	Type B	Type B-3	---
Plant Type		CMI Drum	CMI Drum	Standard Havens Drum	CMI-Caterpiller Drum	CMI Drum
Aggregate Blend*	Coarse Aggregate	30% Pit Run Crushed Gravel, Granite	39% 5/8 Gravel Chip Glacial Deposits	35% 3/4" Crushed Limestone 33% 3/8" Crushed Limestone	60% Trap Rock (#56) 5% Trap Rock (#8)	40% RAP 40% Crushed Rock & Coarse Gravel, Alluvial (Granite, Quarzite, Basalt)
	Fine Aggregate	70% Pit Run Crushed Gravel, Granite	25% Crusher Sand 16% Blend Sand 20% 3CS Sand	15% Limestone Screening 17% Field Sand	20% Crushed Fines (#10) 15% Natural Sand	20% Fine Gravel, Alluvial (Granite Quarzite, Basalt)
Asphalt Type		Sinclair Oil (AC-10)	Marathon (120-150)	Exxon (AC-20)	Chevron (AC-20)	Sinclair (AC-20)
Asphalt Amount*		5.0	5.6	5.5	4.5	2.75***
Modifier/Additive Type		Pave Bond LP	---	---	ACRA 1000	Hydrated Lime
Amount		0.4**			0.6**	1.0***
Placement Temperature, (Average) °F		250 to 300 (280)	280	294 to 314 (310)	280	270 to 285 (275)

* Numbers are in Percent Based on Total Weight of Mixture
** Percentage Based on Weight of Asphalt
*** Percentage Based on Weight of Virgin Aggregate only.

again provided by the Bomag static tandem steel wheel roller, operated to make four coverages over the entire pavement surface.

The air temperature was over 90°F at the time of construction of the test sections, making it impossible to cut the cores the same day as the mix was placed. Because traffic could not be rerouted, vehicles were permitted to run over the newly placed asphaltic concrete mix within an hour or so of the time it was laid. There was some glazing or flushing of the hot mix under the suction action of the vehicle tires. This "extra" asphalt in the wheel paths of the roadway was evident the next day.

2.2.2.3 North Carolina (Vulcan's Plant)

The North Carolina project was not a fully completed AAMAS section. Bulk samples of the aggregate, RAP, and asphalt were not recovered, because this project was only used to verify the effects of aggregate size in relation to sample size. In summary, Vulcan materials were used for building an entrance/haul road for their plant's operation. The maximum size aggregate used in this mix was 2.5 in. Thus, only oversize cores (8 in. in diameter) were cut for testing. All coring was performed by Vulcan personnel.

2.2.2.4 Texas (TX-0021)

The Texas project was located in Burleson County on Highway 21 just west of the Bryan/College Station area. This was a major reconstruction project converting an existing two-lane roadway into a four-lane divided highway. The AAMAS test sections were in the westbound lanes; section 1-SB (standard compaction train) was along the outside lane and section 2-VB (alternate compaction train) along the inside lane. Paving was done in opposite directions on the same day.

The thickness of the asphaltic concrete lifts used for the AAMAS sections varies transversely across the roadway from 2 to 3 in. Therefore, cores along the Texas project were not taken at random, but along a specific line parallel to the roadway's centerline. The reason for taking the cores in a straight line was to decrease the variation of lift/core thickness and resulting air void distribution with lift thickness.

The aggregates used in the mixture consisted of crushed limestone and field sand. The crushed limestone was obtained from the Georgetown quarry and is considered to be an absorptive type aggregate. The grading used for the AAMAS study was a Type B grading, as per Texas State Department of Highways and Public Transportation criteria ($\frac{3}{4}$-in. nominal size aggregate). The asphalt cement was an AC-20 viscosity graded material obtained from Exxon Company located in Baytown, Texas. The aggregate blend used consisted of 35 percent of a Type D coarse aggregate ($\frac{3}{4}$-in. limestone) and 33 percent of a Type F coarse aggregate ($\frac{3}{8}$-in. limestone). The fine aggregate consisted of 15 percent limestone screenings and 17 percent field sand.

The type of plant that was used to produce the mix was a standard Havens drum mix plant. A No. 3 diesel fuel was being used as burner fuel during mix production. The temperature of the mix at the plant varied from 300 to 330°F.

Two sections were constructed along Highway 21. These sections were in adjacent lanes and placed on the same date (July 22, 1987). The temperature of the mix received on the roadway varied from 294 to 314°F. Test section 1-SB was compacted with the standard compaction train used by the contractor. This consisted of a static steel wheel roller for breakdown followed by a pneumatic rubber-tired roller followed by a static steel wheel for finish rolling. Test section 2-VB consisted of a vibratory roller for breakdown followed by a static steel wheel for intermediate and finish rolling.

The steel wheel rollers consisted of an Ingram three-wheel 10-ton roller. The rear rollers provided 354 lb per linear inch compression, while the front rollers provided 150 lb per linear inch compression. The pneumatic rubber-tired roller was an Ingram nine-wheel 10-ton roller. Air pressures in the tires varied from 75 to 90 psi. The vibratory roller consisted of a Rex Model SP-848 vibratory roller. For this project high frequency (approxi-

mately 1,800 vibrations per minute) and low amplitude were used to compact the asphaltic concrete mix.

2.2.2.5 (Virginia, VA-0621)

The Virginia VA-0621 was a reconstruction project of a two-lane highway located on State Highway 621 near Chantilly, Virginia, which runs east to west. Test section 1-VB was along the eastbound lane and test section 2-SB along the westbound lane. The contractor for this project was Tri-County Asphalt.

The project consisted of placing 4 in. of an asphaltic concrete base on top of an untreated aggregate base course. An asphaltic concrete binder and surface course were to be placed on top of the asphaltic concrete base mix. The base course lift was selected as the AAMAS mix to be sampled and cored because of the larger aggregate size.

The aggregates used in the mixture consisted of crushed trap rock and sand. The grading used on the bottom lift, which was sampled for AAMAS, consisted of 1-in. nominal size coarse aggregate. The asphalt cement used in the mix was an AC-20 viscosity graded material that was supplied by CHEVRON, located in Baltimore. The aggregate blend consisted of 60 percent of a No. 56 crushed coarse aggregate, 5 percent of a No. 8 crushed coarse aggregate, 20 percent screenings or a No. 10 dust material, and 15 percent concrete sand. An asphalt modifier, ACRA 1,000, was used in the mix and added at a rate of 0.6 percent, by weight of asphalt cement.

The type of plant that was used to produce this mix was a CMI-Caterpillar drum mix plant. Natural gas was being used as the burner fuel during mix production and the temperature of the mix was above 300°F.

Two test sections were constructed along State Highway 621. These sections were in opposite lanes and built on the same date. The temperature of the mix placed behind the paver was approximately 280°F. Test section 1-VB was compacted with the standard compaction train used by the contractor. This consisted of a vibratory roller for breakdown rolling followed by a static steel wheel for finish rolling. Test section 2-SB consisted of a static steel wheel for breakdown rolling followed by a pneumatic rubber-tired roller for intermediate rolling and a static steel for finish rolling.

The vibratory roller was a B-44 Caterpillar, tandem drum. Both drums were vibratory and used in the compaction process. The pneumatic rubber-tired roller was a Dynapac, CP-15, Model 87 roller. This roller consisted of four tires followed by five tires. The static steel wheel roller consisted of a Galion tandem 5-ton roller.

2.2.2.6 Virginia (VA-0279)

This section of roadway consisted of the construction of two new lanes of pavement in the eastbound direction to alter a portion of US Route 60 from a two-lane roadway to a four-lane divided highway. The majority of paving on this project was on SR 279, but the compaction test section was actually built on a portion of US 60 at the junction with SR 279. The inside, or passing lane of the new construction section was used for the test area.

The project consisted of placing 7 in. of an asphaltic concrete base course on top of an untreated aggregate base course. An asphaltic concrete binder and a surface course were to be placed on the asphaltic concrete base mix. The second base course layer, 3.5 in. thick, was used for the test section. The mix placed was a recycled asphaltic concrete containing 15 percent reclaimed material (RAP).

The new aggregates incorporated into the recycled asphaltic concrete mix were supplied by Lone Star Materials. The reclaimed asphaltic concrete had been obtained from cold planing jobs on various city streets in the Norfolk area. The mix design for the project called for the use of 50 percent No. 57 granite coarse aggregate, 10 percent No. 68 granite coarse aggregate, 25 percent concrete sand, and 15 percent reclaimed material. The asphalt cement used was furnished by Seaview Refinery and was an AC-20 viscosity graded material. An antistripping agent, Pave Bond Special, was added to the mix at a rate of 0.5 percent, by weight of asphalt cement. The asphaltic concrete was classified as a Type B-3 mixture.

The recycled asphaltic concrete mix was manufactured in a 1972 Cedar Rapids 5-ton pugmill capacity batch plant. In order to handle the reclaimed material, the dry mix time on the plant was extended to 6 sec while the wet mix time was 28 sec. There was a noticeable amount of dust carryout from the pugmill area when the heated new aggregates and the ambient temperature of the reclaimed material were emptied from the weigh hopper into the pugmill and dry mixing started. The mix was produced at a discharge temperature of approximately 280°F. The asphaltic concrete mix was placed on US 60 using a Cedar Rapids BSF 530 paver.

Only one test section (compaction train) was completed on this job. The primary reason for doing this project was to get one additional test section which used recycled asphaltic concrete mix, using a large aggregate size in the mix. Breakdown rolling was completed using a pneumatic rubber-tired roller. A double drum vibratory roller, operating in the vibratory mode, was used for intermediate rolling and in the static mode for finish rolling.

The pneumatic tire roller was a nine tire Dynapac CP-15 machine. The equipment made approximately 5 coverages over the surface of the asphaltic concrete base course mix. The number of coverages varied somewhat because of two major factors. First, the paver was moving very slowly due to the thickness of the mat it was placing and the lack of plant production. Second, because of the time of year and the weather conditions, it was desirable to start the compactive effort before the mix cooled too much to be properly densified. Thus, for this project, rolling was commenced before the paver had completely placed the whole 300-ft long test section. The roller was reversed within the length of the test section and the number of coverages made by the equipment was not consistent throughout the length of the test section.

Finish rolling took place in two parts. A Bomag BW 151 AD double drum vibratory roller made two coverages, in vibration, over the test section pavement. This was done to assure that adequate density was obtained along this section of pavement, because it was in the middle of what would be a very heavily traveled portion of highway. The same roller then made an additional three coverages, in the static mode, to remove any marks on the pavement's surface.

2.2.2.7 Wyoming (WY-0080)

Project WY-0080 consisted of the recycling/overlaying of a

four-lane divided interstate highway, designated as IH-80, which runs east-west between Rawlins and Rock Springs. The actual test section locations are in the westbound driving (outside) lane, about 2 miles west of the Town of Point of Rocks, which is approximately 28 miles east of Rock Springs.

On this project, 4 in. of the existing asphaltic concrete pavement in the driving lane in each direction was removed by cold planing. This material was recycled back into the asphaltic concrete mix on a basis of 40 percent reclaimed material and 60 percent new aggregate. The recycled mix was placed back on the interstate roadway in two 2-in. lifts, to bring the elevation of the driving lane back to the same level as the passing (inside) lane.

The new aggregates incorporated into the recycled asphaltic concrete mix were bank run gravel type materials that were available from a state-owned pit. The coarse and fine aggregates were used as a blend—only one new aggregate stockpile was employed by the contractor. The reclaimed asphaltic concrete material (40 percent of the total weight of the aggregate) was obtained from the driving lanes of IH-80 within the limits of the project. The asphalt cement used was an AC-20 viscosity graded material supplied by the Sinclair Oil Company and was added at a rate of 2.75 percent, by weight of recycled mix. One percent hydrated lime, weight of new aggregate only, was added as an antistrip agent. The asphaltic concrete mix was designated "Recycled Hot Plant Mix Bituminous Pavement."

The asphaltic concrete material was produced in a CMI drum mix plant. The plant was equipped with a rotary center inlet to handle reclaimed asphaltic concrete material to produce the recycled mix specified for the IH-80 paving. The new aggregates were fed into the drum mixes from the cold feed bins into the burner end of the drum. The hydrated lime additive was blended with the new aggregates in a small pugmill, located at the point of entry of the aggregates into the mixing drum.

The asphaltic concrete mix was placed using a Blaw-Know PF 180 H paver. The thickness of the mat was 2 in. and the AAMAS lift was placed as the first of two layers in the trench section created by the cold planing operation.

Each of the two test sections constructed was approximately 300 ft long. Test section 1-VB was compacted using two rollers. The breakdown roller was a Hyster C 727 A double drum vibratory roller. This equipment was operated at a frequency greater than 2,000 vibrations per minute in low amplitude. The breakdown roller made three coverages over each point in the pavement surface. The finish roller, which made two coverages over the mat, was a Raygo Rascal double drum vibratory roller which was operated in the static mode.

Test section 2-PB was also compacted using two rollers. For this test section, however, the breakdown roller was a small Ingram 9-2800 model pneumatic tire roller. Because of the size of tires on this machine, the air pressure in the tires was limited to only 60 psi. The pneumatic tire equipment made six complete coverages of the roadway surface. It was evident that this equipment was not heavy enough to get the desired level of density in the mix. Two coverages over the roadway surface were then made with the Raygo double drum vibratory roller operating in vibration. Finish rolling was accomplished by the same Raygo roller, operated in the static mode. The finish rolling was completed with three coverages over the whole pavement surface.

2.2.3 Materials Sampling Program

During the production and construction of each of the AAMAS projects, bulk materials were sampled and cores were cut from each test section. The sampling techniques used are presented and discussed in Appendix B.

2.2.3.1 Bulk Samples

Samples of each aggregate stockpile were taken and placed in separate bags or metal 10-gal containers. In most cases, front-end loaders were being used to transport the aggregate from the stockpiles to the cold feed bins. Therefore, bulk samples were taken from the stockpile as the front-end loader removed material from each of the stockpiles, with the exception of the Texas and Michigan projects. For the Texas project (TX-0021), bulk samples of each aggregate type were taken from the cold feed bins, as the front-end loader put aggregate into the hoppers. For the Michigan project (MI-0021), samples from each of these stockpiles were taken by hand without the use of front-end loaders.

Samples of the asphalt and other additives, when used, were taken by plant personnel from the storage tanks. The asphalt was placed in 1- or 2-gal containers, sealed and prepared for transport.

The asphaltic concrete mixture was also sampled from trucks and placed in specially sealed 10-gal. metal containers. The types of containers and sampling procedures are presented in Appendix B. Approximately 750 lb of bulk asphaltic concrete mixture were obtained for each section (approximately 1,500 lb from each project).

2.2.3.2 Coring Program (After Construction)

A minimum of 21 cores were cut from each section within a project. These cores were taken in most cases the following day after construction. The Colorado, Michigan, and Virginia projects received overnight traffic prior to core recovery. For the Colorado and Virginia projects, this was very minimal traffic.

2.2.3.2.1 Core Recovery. Four-inch diameter cores were taken on all projects. However, for the Virginia project (VA-0621), oversize cores were taken to investigate the effects of sample size as related to maximum aggregate diameter. Two additional projects were added to study the effects of large size aggregates on material properties. On these three projects, six to nine 8-in. diameter cores were taken per test section.

It was the original intent of the experimental program to dry-core all AAMAS test sections the same day after placement and compaction. However, many of the projects were built in very warm weather, so the mix cooled very slowly. During the Virginia project (VA-0621), dry ice was used in an attempt to cool the asphaltic concrete mix to an acceptable level that would allow cores to be recovered. Dry ice was applied to the pavement surface; however, recovery of the entire core was still not possible. In fact, during testing some of those cores that were taken the same day as mix placement and for which dry ice was used had significantly lower indirect tensile strengths than the cores that were taken one day after mixture placement. Apparently, dry-coring the asphaltic concrete caused disturbance to the sample and may have affected the adhesion of the asphalt to the aggregate. Therefore, on all remaining AAMAS test sections, cores were taken using wet-coring techniques after the mix had

Table 15. Summary of core thicknesses measured along each test section immediately after construction.

State/Project	Section	Mean Thickness, Inches	Standard Deviation Inches	Coefficient of Variation, %	Range, Inches
Colorado	1-VB	1.36	0.188	13.8	1.0-1.7
CO-0009	2-PB	1.34	0.134	9.97	1.1-1.7
Michigan	1-VB	1.89	0.113	6.00	1.7-1.7
MI-0021	2-PB	1.70	0.125	7.34	1.5-1.9
Texas	1-SB	2.53	0.205	8.12	2.2-2.9
TX-0021	2-VB	3.12	0.247	7.91	2.7-3.6
Virginia	1-VB	4.03	0.347	8.60	3.7-4.9
VA-0621	2-SB	3.55	0.279	6.70	3.2-3.9
Wyoming	1-VB	2.11	0.151	7.17	1.6-2.4
WY-0080	2-PB	2.25	0.114	5.06	2.0-2.4

been allowed to cool sufficiently so that core disturbance did not occur.

After recovery, all cores were allowed to dry prior to wrapping and sealing the cores for shipment. In some cases, cores were left unwrapped for an additional day to ensure that all moisture had evaporated.

2.2.3.2.2 Core Location. Locations for these cores were determined using random numbers for general sampling procedures in accordance with the Asphalt Institute's Manual Series No. 17. Core locations were varied both transversely and longitudinally down the paving width, with the exception for the Texas project (TX-0021). Random locations were not used on project TX-0021, because the lift used as the AAMAS section was along a transition lane and its thickness varied transversely from one paving edge to the other.

2.2.3.2.3 Core Thickness. After all cores were received in the laboratory, thickness measurements were made on each core in accordance with ASTM D3549, "Thickness or Height of Compacted Bituminous Paving Mixture Specimens." Measurements of thickness were also made on quarter points of each core and the average thickness determined. The average thickness for each core is summarized in Appendix A. Table 15 summarizes the average core thicknesses measured along each test site. As shown, only the Colorado project (CO-0009) had an insufficient thickness as compared to the required plan thickness previously referred to. Some of the CO-0009 cores were less than 1.25 in. in height and inadequate for indirect tensile testing.

2.2.3.3 Coring Program (After Traffic)

Cores were taken from each of the five initial projects approximately 2 years after construction. A minimum of 27 cores per section were recovered. These cores were taken using the same procedure initially used, as discussed above, with the exception of two areas. The difference between these two time periods was that at least six 6-in. diameter cores were recovered from every section and the locations were varied only in the longitudinal direction.

2.2.3.3.1 Core Location. Random numbers were used to locate the cores along three longitudinal lines parallel to the centerline. One line of cores was located in each wheelpath and the third between the wheelpaths. Nine cores were located between the wheelpaths and the remaining were located within the wheelpaths. Transverse variation was not used, so that the air voids of cores recovered within the wheelpath could be compared to those recovered between the wheelpaths.

2.2.3.3.2 Core Thickness. After all cores had been received in the laboratory, the same lift used for testing the original cores designated "after construction" was removed from the other lifts by sawing. The location of the AAMAS lift varied between the projects. After separation, thickness measurements were made on the AAMAS lift in accordance with ASTM D3549, and on quarter points of each sample. The thickness of each sample is given in Appendix A. The following is a summary of the mean thicknesses measured along each test site, as compared to the original measurements made after construction.

		Mean Thickness (inches)	
Project	Section	After Construction	After 2 Years
CO-0009	1-VB	1.36	1.36
	2-PB	1.34	1.35
MI-0021	1-VB	1.89	1.75
	2-PB	1.70	1.58
TX-0021	1-SB	2.53	2.58
	2-VB	3.12	2.83
VA-0621	1-VB	4.03	3.73
	2-SB	3.55	3.68
WY-0080	1-VB	2.11	1.99
	2-PB	2.25	2.02

Some of the CO-0009 samples were less than 1.25 in. in height and inadequate for indirect tensile testing.

2.2.4 Supplemental Mixtures

As stated in the opening discussion of section 2.2, four additional mixtures were selected for study to supplement the laboratory data used for developing the mixture design procedure based on performance-related criteria. These four mixtures were purposely selected with inferior performance characteristics to provide supporting data that AAMAS would distinguish those mixtures as borderline or inferior. Inferior was defined as a dense-graded mixture which was restricted from use on high volume roadways because of accelerated surface distress. These type mixtures were selected from California, Georgia, New York, and Wisconsin.

The same material sampling program discussed for the field test sections was used to sample both the mixtures and individual materials for the four inferior mixtures, with the exception that cores were not recovered. Tables 8 through 10 and 16 summarize information on the materials that were used to produce these mixtures.

2.2.4.1 California Mix

The California mix was produced from two different plants at the same time and for the same project along State Route 395. These plants were an Astec drum mix and batch plant. Bulk samples of the Type "A" mix were sampled from both of these plants. The average temperature of the mix was provided by

Table 16. Summary of plant job mix formulas and other information obtained during the production of the supplemental mixtures.

State		California	Georgia	New York - R	Wisconsin
Mixture Designation		Type A	Type B	Type 6F	Type A
Plant Type		Astec Drum/ Batch Plant	Astec Drum Mix Plant	3-Ton Stansfield Batch Plant	Astec Drum Mix Plant
Aggregate Blend	Coarse Aggregate	20% Coarse Crushed Gravel 12% Medium Crushed Gravel	41% Crushed Rock No. 57 10% Crushed Rock No.10 Granite	32% Crushed Dolomite (3/8" Stone) 26% Crushed Dolomite (1/4" Stone)	55% Crushed Gravel 45% RAP
	Fine Aggregate	35% Crushed Fines 33% Natural Fines	48% Crushed Fine (No.M10)	38% Natural Sand 4% Mineral Filler (Cement & Fly Ash)	Crushed Fines
Asphalt Type Asphalt Amount		Shell Oil (AR-4000) 4.76/5.95	Amoco Oil (AC-30) 4.33	Elf Asphalt (AC-20) 5.08	Koch Asphalt (Ac-5) 5.21
Modifier/Additive Type Amount, %		--- ---	Hydrated Lime 1.0	--- ---	--- ---
Production Temperature F		280	270	325	275

California DOT personnel and was approximately 280°F. The aggregates incorporated into this base mix were a local crushed gravel supplied to Baldwin Contracting from Hillside Deposits Inc. in Doyle, California. The crushed aggregates are highly absorptive. The blend included 20 percent coarse and 12 percent medium crushed fines, and 33 percent of natural fines. The asphalt cement was an AR-4000 graded material, and supplied by Shell Oil Company.

Department personnel expected that this mix would require rehabilitation or an overlay in less than 10 years. This aggregate blend is considered a "sensitive mix," because slightly lower asphalt contents result in a brittle mix and slightly higher asphalt contents result in a plastic mix that is susceptible to distortion. The design asphalt content for this blend was 5.3 percent. The asphalt content measured from bulk samples, however, was significantly different. The asphalt content of the mix produced through the drum mix plant was 4.76 percent and 5.95 percent for the batch plant.

2.2.4.2 Georgia Mix

The Georgia mix sampled for the project was a Type "B" mix that the Department has restricted from use on high volume roadways. This mixture is susceptible to moisture damage and permanent deformation, and degrades when subjected to heavy traffic. The aggregates used in this mix are 100 percent crushed material. The aggregate is a granite, high in micia content, and supplied by Colwell Rock Quarry in Blairsville, Georgia. The blend included 41 percent of a No. 57 and 10 percent of a No. 10 crushed granite and 48 percent of granite fines or a No. M10 material. Lime was added to the mixture at a rate of 1.0 percent of the aggregate dry weight because of its susceptibility to moisture damage. The asphalt cement was an AC-20 viscosity graded material, and supplied by AMOCO Oil. The asphaltic concrete base mix was used for an overlay project along Highway 129. It was produced in an Astec drum mix plant to a temperature of approximately 270°F for C.W. Matthews, Inc.

2.2.4.3 New York Mixes

Two different mixtures were sampled by the New York Department of Transportation personnel. One of these mixtures is placed on very high volume roadways with good results, and the other is restricted from use on high volume roadways because of its past performance characteristics. The mix with a good performance history is identified as the "Prima" mix (Holtsville, N.Y.), whereas the mix that is susceptible to rutting and surface distortions is identified as the "Rason" mix (Farmingdale, N.Y.).

Both mixtures include the same type of fine aggregate (natural sand) and asphalt. The difference between the mixes is the type of crushed coarse aggregate. The Rason mix uses a crushed Dolomite (trap rock) obtained from Hudson River Aggregates (Clinton Pit) in Farmingdale, New York. The Prima mix uses a crushed limestone supplied by Callanan in South Bethlehem, New York. Mineral filler (portland cement and fly ash) was added to both of the aggregate blends. The following listing summarizes and compares the aggregate blend of both materials for a Type 6F surface mix.

AGGREGATE	PRIMA	RASON
3/8 in. Stone	30%-Limestone	32%-Dolomite
1/4 in. Stone	27%-Limestone	26%-Dolomite
Natural sand (Brookhaven aggr.)	39%	38%
Mineral filler	4%	4%
Asphalt content	6.1%	6.0

The asphalt cement is an AC-20 viscosity graded material and supplied by Elf Asphalt.

2.2.4.4 Wisconsin Mix

The Wisconsin mix is a recycled mixture and was produced in an Astec drum mix plant. This mixture is restricted from use

on high volume roadways because of the amount of rutting that has occurred from past observations. The new aggregates incorporated into the recycled asphaltic concrete mix are a crushed gravel from the Thiesen pit in Madison, Wisconsin. The aggregates used for this mix were divided into two stockpiles, one for the crushed virgin materials and one for the RAP materials. The blend included 55 percent crushed gravel and 45 percent RAP. The new asphalt cement used in the mix was a 200-300 Pen asphalt (similar to an AC-5 viscosity graded material) and supplied by Koch Asphalt Company.

2.3 MIXTURE COMPACTION AND AIR VOIDS

The compaction of an asphaltic concrete paving mixture on the roadway is the single most important factor in providing a durable pavement structure. It is well known that an asphaltic concrete mixture that is compacted to a low air void content will have increased fatigue life, reduced permanent deformation, reduced distortion, reduced aging of the asphalt cement, and reduced moisture damage than will the same mixture that is compacted to a higher air void content. It is also well known that air voids decrease with the number of traffic applications. Thus, the air void level at which the engineering properties are measured is critically important, especially for "sensitive" mixtures. A sensitive mix is defined as one in which significant changes in engineering properties occur with small changes in asphalt content and density levels.

For some distress types, the critical air void is immediately after construction, whereas, for other distress types, the critical air void is after many thousands or millions of load applications. This section of the report discusses mixture compaction in the laboratory to simulate the initial and final air void levels. Specifically, it reviews the field compaction procedures used to compact the five mixes placed on the roadway, the laboratory devices used to compact specimens that match the field cores, and the expected change in air void level caused by traffic for each of the mixtures.

2.3.1 Field Compacted Mixtures

Five projects (see discussion in section 2.2.2) were selected for evaluating mixtures placed in the field. These five mixtures were used for comparing the engineering properties of mixtures placed in the field as compared to those compacted in the laboratory. This section of the report discusses the compaction procedures and resulting air voids of these mixtures placed in the field using different types of compaction trains.

2.3.1.1 Compaction Equipment and Procedure

Two compaction trains were used on the first five projects. Each compaction train represents a test section. The breakdown roller used by the contractor over the entire project was always used on the first section. This section was also always designated as the standard, but in some cases the intermediate roller used over the entire project was eliminated from the compaction train used on the AAMAS section. For the second or alternate section, a different breakdown roller and rolling pattern were used. The number of test sections for each type of breakdown roller used to compact the mixtures are as follows: double drum vibratory breakdown—5 sections; static steel wheel breakdown—2 sections; and rubber-tired, pneumatic breakdown—3 sections.

The compactive effort was not commenced for any section until the paver had placed asphaltic concrete over the whole length of the section. This was done to prevent the rollers from having to reverse direction within the test section length, thereby assuring the number of roller passes to be relatively constant over the area to be cored.

The compaction trains and rolling patterns used to compact each AAMAS test section are given in Table 17. These rolling patterns were selected to compact and densify the mix to an air void content in the range of 5 to 7 percent. The same target air

Table 17. Summary of rolling patterns used to compact the asphaltic concrete mixtures for each project.

State Project	Section	Type of Rolling		
		Breakdown	Intermediate	Finish
Colorado CO-0009	1-VB/SS	4 Coverages of a Tampo RS-166A Double Vibratory Drum Frequency = 2200 Vibration/min. Low Amplitude	---	2 Coverages of a Hyster C 350 BT Static Tandem Steel Wheel
	2-PB/SS	4 Coverages of a Hyster C 350 A Pneumatic Tire	---	2 Coverages of a Hyster C 350 BT Static Tandem Steel Wheel
Michigan MI-0021	1-VB/SS	4 Coverages of a Dynapac CC 42 A Double Vibratory Drum Frequency = 2400 Vibration/min. Low Amplitude	---	2 Coverages of a Bomag S 812S Static Tandem Steel Wheel
	2-PB/SS	6 Coverages of a Bros SP 300 Pneumatic Tire Roller	---	4 Coverages of a Bomag S 812 A Static Steel Wheel
Texas TX-0021	1-SB/PS	1 Coverage of an Ingram 10 Ton Static Three Steel Wheel	2 Coverages of an Ingram 10 Ton Pneumatic Rubber Tire Roller	1 Coverage of an Ingram 10 Ton Static Tandem Steel Wheel
	2-VB/SS	1 Coverage of a REX SP-848 Single Vibratory Drum Frequency = 1800 Vibrations/Min. Low Amplitude	2 Coverages of an Ingram 10 Ton Static Three Steel Wheel	1 Coverage of an Ingram 10 Ton Static Tandem Steel Wheel
Virginia VA-0621	1-VB/SS	4 Coverages with a B-44, Caterpillar Double Vibratory Drum High Frequency, Low Amplitude	---	6 Coverages with a Galion 5 Ton Static Tandem Steel Wheel
	2-SB/PS	4 Coverages with B-44 Caterpillar Double Vibratory Drum in the Static Mode	4 Coverages with a Dynapac CP-15 Model Pneumatic Tired Roller	4 Coverages with a Galion 5 Ton Static Tandem Steel Wheel
Wyoming WY-0080	1-VB/SS	3 Coverages of a Hyster C 727 A Double Vibratory Drum Frequency = 2000 Vibration/min. Low Amplitude	---	2 Coverages with a Raygo Rascal Double Vibratory Drum in the Static Drum
	2-PB/SS	6 Coverages with a Ingram 9-2800 Model Pneumatic Tire Roller	2 Coverages with a Raygo Rascal Double Vibratory Drum	3 Coverages with a Raygo Double Vibratory Drum in the Static Mode

void was used for both test sections within a project. The original plan called for "identical" voids between the test sections to evaluate any differences caused by different compaction trains. Unfortunately, some of the rollers used were not of sufficient size to achieve adequate density, which resulted in significantly different air void levels between the two sections of a project.

2.3.1.2 Establish Field Rolling Patterns

Both nuclear density gauge readings and cores were taken from each section. Nuclear density gauges were used to determine when the density magnitude leveled off and cores were cut to verify that air voids were adequate. It should be noted, however, that the Rice specific gravity was either assumed based on prior knowledge of state highway personnel, taken from project construction records, or measured in a field laboratory with minimum samples. On two projects (Colorado, CO-0009 and Texas, TX-0021), the maximum specific gravity measured in the field was found to be significantly different from those measured in the laboratory on bulk samples of the mixture. As a result, air voids were found in some cases to significantly exceed 8 percent.

2.3.1.3 Air Voids

All field cores recovered from each of the projects and test sections have been summarized in Appendix D. Air voids were calculated in conformance with AASHTO T268, "Percent Air Voids in Compacted Dense and Open Bituminous Paving Mixtures," using the Rice specific gravity as the maximum theoretical specific gravity (MTG) of the mix. The air voids calculated for each core are included in Appendix D. Table 18 summarizes the average air voids and statistical information for each AAMAS project and test section.

During the initial field work and coordination with each state highway agency, the rolling pattern was selected to result in a mean air void of 5 to 7 percent. The technique used to establish the rolling pattern was discussed previously under section 2.3.1.2. Unfortunately, half of the test sections did not meet this range (Table 18).

There are two primary reasons why some compacted mixes had high air voids. The first was that an inadequate breakdown rubber-tired roller was used in an attempt to compact the asphaltic concrete lift during placement of the second Wyoming test section. The other reason was that an erroneous Rice specific gravity value was used in the field for controlling air voids. For the Texas and Colorado sections, a significantly lower Rice specific gravity was used to establish rolling patterns than was measured on bulk samples of the asphaltic concrete mixture sampled during construction. On the CO-0009 project, it was also later determined that the nuclear density gauge was not operating properly.

The first section designated as the AAMAS test section was compacted using the same breakdown roller as used along the entire project. The second compaction train was the alternate or second test section. In all cases, the lowest average air void was measured in the first section where the standard breakdown roller was used. Table 19 summarizes the actual mean air voids measured on the field test sections as compared to the target or design air void provided by the state highway agency. As shown,

Table 18. Summary of air void information from the field cores taken immediately after construction.

State/Project	Variable	Compaction Train* VB/SS	SB/SS	PB/SS
Colorado CO-0009	Mean	8.19	---	8.98
	Std. Deviation (n-1)	0.936	---	1.0939
	Coefficient of Variation	11.42	---	12.18
	Range	6.3-10.5	---	7.4-11.9
Michigan MI-0021	Mean	3.74	---	4.2
	Std. Deviation (n-1)	0.942	---	0.630
	Coefficient of Variation	25.20	---	14.98
	Range	2.6-7.6	---	3.4-6.0
Texas TX-0021	Mean	10.17	8.75	---
	Std. Deviation (n-1)	1.160	0.966	---
	Coefficient of Variation	11.41	11.01	---
	Range	8.7-13.4	7.1-10.9	---
Virginia VA-0621	Mean	5.85	7.44	---
	Std. Deviation (n-1)	1.193	0.832	---
	Coefficient of Variation	20.40	11.18	---
	Range	4.1-7.7	6.1-9.1	---
Wyoming WY-0080	Mean	5.77	---	8.3
	Std. Deviation (n-1)	0.688	---	0.777
	Coefficient of Variation	11.92	---	9.28
	Range	4.8-7.4	---	6.5-9.9

* Definitions for Compaction Train are defined in Appendix C and Described in Table 17. The first two letters designate the type of breakdown roller and the last two designate the type of finish roller. Different intermediate rollers were used on the different projects, which have not been designated in the project identifier.

Table 19. Design air voids from asphaltic concrete mix design compared to mean air voids measured from the field cores.

State/Project	Target or Design Air Void,%	Initial Air Voids (Field Cores), % Section 1 Mean	Section 1 Range	Section 1 MSE	Section 2 Mean	Section 2 Range	Section 2 MSE
Colorado CO-0009	4.2	8.19	6.3-10.5	16.8	8.98	7.4-11.9	24.0
Michigan MI-0021	2.8	3.74	2.6- 7.6	1.0	4.21	3.4- 6.0	0.4
Texas TX-0021	6.0	8.75	7.1-10.9	8.5	10.17	8.7-13.4	18.7
Virginia VA-0621	5.0	5.85	4.1- 7.7	2.1	7.44	6.1- 9.1	6.6
Wyoming WY-0080	5.0	5.77	4.8- 7.4	1.1	8.37	6.5- 9.9	12.0

Section 1 was compacted using the same breakdown roller used by the Contractor along the entire project.

Section 2 represents an alternate compaction train using a different roller for breakdown.

MSE = Mean Squared Error (Using the Design Air Void as the Target Value

both the Colorado and Texas projects and the second section for the Wyoming projects have significantly greater air voids than the target value.

Mean squared errors (MSE) were also determined for each of the test sections as compared to the target air void content determined from the mixture design. These MSEs have been provided on Table 19. Based on a review of these data (Tables 18 and 19), the Texas, Virginia, and Wyoming test sections are different and must be treated as separate sections within the same project. This means that separate compactive efforts had to be used to compact the mix in the laboratory to the air void level measured on the field cores.

2.3.1.4 Air Void Gradients

Selected cores were also used to measure the air void gradient or change in air voids from the top to the bottom of the asphaltic

concrete lift. Depending on the thickness of the lift, field cores were sawed into three slices and the air voids calculated for each slice in conformance with AASHTO T268. All air void gradient data are provided in Appendix D. Tables D.4, D.5, and D.6 in Appendix D summarize the average air void difference (MAXDIF), the normalized values of this difference, ΔD, and air void ratio, V_{ar}, respectively, for each test section used in the air void gradient study. These values are defined below, and will be discussed in greater detail in Chapter 3.

MAXDIF = Maximum difference in air voids as measured through the sample (top to bottom).

$$\Delta D = (\text{MAXDIF}/V_a) \times 100 \quad (2\text{-}1)$$

$$V_{ar} = V_i/V_a \quad (2\text{-}2)$$

where V_i is air void of slice i for a particular sample, and V_a is mean air void value for the entire sample.

It is important to note that lower air voids or higher densities were consistently measured in the center portion of the cores. Hughes and Maupin (*49*) found a similar condition in comparing air void gradients in both thick (9 in.) and thin (2 in.) lifts that were compacted using different types of equipment. There seems to be little difference in air void gradients or density distribution caused by the use of different rollers.

2.3.2 Laboratory Compacted Specimens

Laboratory compaction should simulate, as closely as possible, the actual compaction effort and effects produced in the field by rollers. This simulation can be measured by such factors as particle orientation, total air void content, and air void structure. Voids are particularly important because of their effect on the engineering properties, as substantiated by Kennedy (*40*) and Powell (*41*), among others, through numerous research and testing studies.

Current methods of asphaltic concrete mixture design and materials evaluation are based on the use of mold-confined laboratory-compacted specimens. There are many different procedures and types of compaction that can be used to prepare specimens in the laboratory. In evaluating the engineering properties and response characteristics of asphaltic concrete mixtures, compaction of the laboratory samples becomes very critical. Although the Marshall hammer compactors are widely used for laboratory compaction across the United States, it is doubtful that they really simulate field compacted mixtures. An important aspect of this study was to determine the most practical laboratory method that best simulates field compaction and the behavior (fundamental engineering properties) of field compacted mixtures.

2.3.2.1 Laboratory Compaction Procedures

For the AAMAS projects five different types of laboratory compactors were used to prepare specimens so that a comparison of various properties between field and laboratory samples could be made. Those compactors selected and used in this study include: (1) the Marshall hammer, designated as MM/HC, to represent an impact type compaction; (2) the California-kneading compactor, CK/CC, to simulate a kneading type compaction; (3) the Texas gyratory shear compactor, MT/GS, to simulate gyratory/kneading action; (4) the Arizona vibratory/kneading compactor, AV/KC, to simulate the use of vibratory type compaction; and (5) the steel wheel simulator, MS/WC, to simulate a rolling type compaction. These five laboratory devices were used only to compact those mixtures placed on the roadways.

In order to keep the testing within reasonable limits, all five compaction techniques were used to compact bulk mixture sampled at the asphaltic concrete plant for three of the five AAMAS projects. These were the Michigan, Texas, and Virginia projects. For these projects, all laboratory specimens were prepared using 4-in. cylindrical molds. Limited testing was conducted on specimens compacted with all devices, with the exception of the AV/KC, for the Colorado and Wyoming projects. The AV/KC was not used to compact any specimens from these two projects.

2.3.2.1.1 Mechanical Marshall Hammer. The mechanical Marshall hammer was used to prepare laboratory samples to simulate an impact type compaction. All specimens were compacted in accordance with the procedure presented in AASHTO T245-82, "Resistance to Plastic Flow of Bituminous Mixtures Using the Marshall Apparatus," with the exception of mixing temperature and varying number of blows. As the materials were sampled from trucks and allowed to cool prior to compaction, the procedure presented in Appendix B was used to reheat the mixture to the compaction temperature recorded behind the paver.

To produce laboratory specimens with varying air voids, the number of blows was varied from 10 to 100 on both faces of the asphaltic concrete mix. The impact compaction was done with a 10-lb sliding hammer raised and dropped 18 in. on to a plate, as stated in the test standard. Figure 31 shows the reduction in air void with the number of blows for each of the mixtures. All specimens compacted with this device have been designated as MM/HC.

2.3.2.1.2 California Kneading Compaction. The Cox and Sons kneading compactor was used to simulate a kneading type compaction in this study. All specimens were compacted in accordance with AASHTO T247-80, "Preparation of Test Specimens of Bituminous Mixtures by Means of California Kneading Compactor," with the exception that the "leveling off" load was not used. Kneading compaction methods apply forces to a portion of a free face of an otherwise confined asphaltic concrete mix. Compaction forces are applied uniformly around the free face. The partial free face allows particles to move relative to each other, creating a kneading action that densifies the mix.

For each of the asphaltic concrete mixtures, the number of tamps was varied to select a compactive effort to compact laboratory specimens to the same air void level measured on the field cores.

The compaction temperature used was the same as discussed for the Marshall hammer above. Figure 32 shows the reduction in air voids of laboratory compacted mixtures with the number of tamps. All specimens compacted with the kneading device have been designated as CK/CC.

2.3.2.1.3 Arizona Vibratory/Kneading Compactor. The vibratory kneading compactor (VKC) was developed to densify laboratory asphaltic concrete specimens using low contact pressures. The diameters of these specimens have been varied from 2 in. to 17.5 in. Compaction is effected through the use of rapid impact loadings on a specimen that is rotating about an axis that is tilted

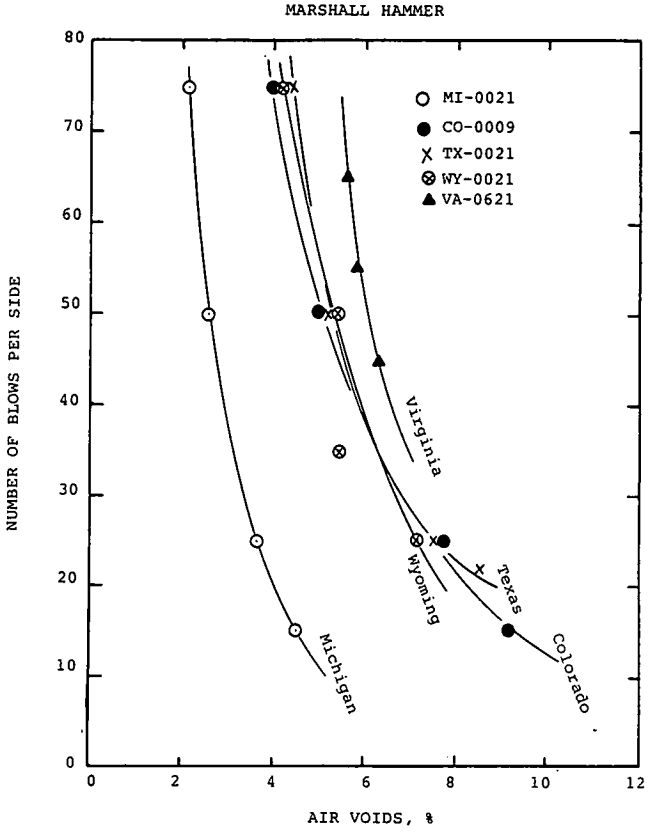

Figure 31. Compactive effort curves developed for each mix using the mechanical Marshall hammer.

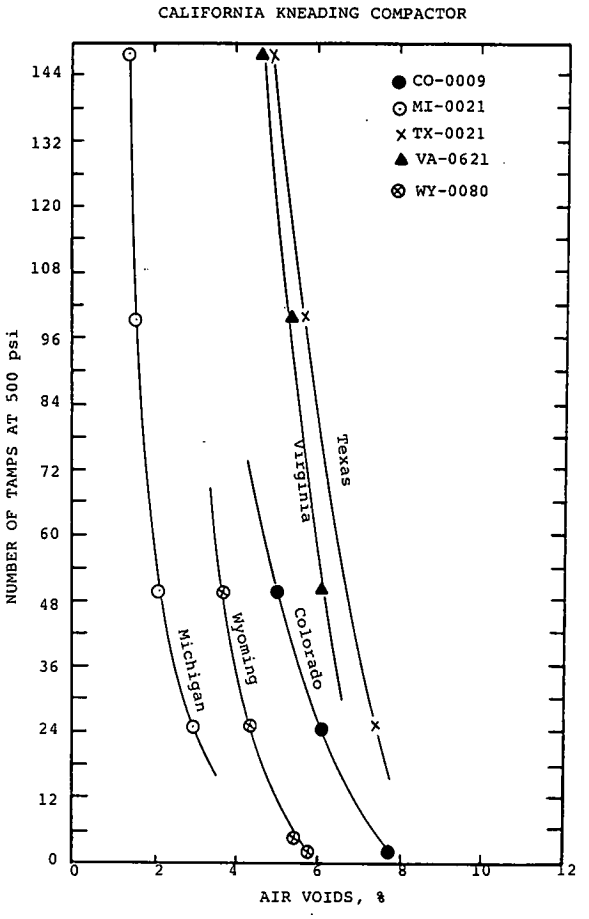

Figure 32. Compactive effort curves developed for each mix using the California kneading compactor.

to the direction of the load. The standard compactive effort was achieved with the following conditions: (1) load frequency = 1,200 cpm; (2) load due to eccentrics = 390 lb; (3) tilt to load = 1 deg; (4) duration of kneading load = 2.5 min; and (5) duration of leveling load = 0.5 min.

Variations in compactive effort have been obtained by changing the mass of the eccentrics and duration of kneading action. Because the exact force of compaction is not known, relative values of compactive effort are obtained as ratios of the products of force due to the rotation of the eccentrics times the duration of the kneading action. The compaction ratios used for different specimen heights to yield the same density is obtained by varying the duration of kneading compaction time in proportion to heights.

Bulk material was shipped to the University of Arizona for sample preparation using the VKS. Specimens were compacted to a height approximately equal to the lift thickness of each project. These specimens were labeled, properly wrapped and protected, and returned for testing. Figure 33 shows the reduction in air void level with compaction ratios for the first three mixtures tested. All specimens compacted with this device have been designated as AV/KC.

2.3.2.1.4 Gyratory Compaction. The Texas State Department of Highways and Public Transportation motorized gyratory shear type compactor was used to simulate gyratory compaction. Gyratory compaction methods apply normal forces to both top and bottom faces of the asphalt mix confined in a cylindrical mold. These normal forces are supplemented with a rocking or gyrating motion to work the mix into a denser configuration while totally confined. The angle of gyration for this device is 6 deg from a vertical plane.

All laboratory specimens were prepared in accordance with ASTM D4013-81, "Preparation of Test Specimens of Bituminous Mixtures by Means of Gyratory Shear Compactor." The ASTM D4013 procedure had to be modified to reproduce the air void level measured from field cores. To determine the amount of compactive effort required to match an equivalent air void level of the field cores, many of the laboratory compaction variables had to be varied for each of the mixes. These were number of gyrations, gyration pressure, or end pressure.

Initially, the number of gyrations were to be reduced to define the compactive effort to simulate the air voids of the field cores. Unfortunately, three gyrations (the minimum that can be easily used with the Texas device) resulted in significantly lower air voids than the field cores. Therefore, gyration and end pressure were varied for the minimum three gyrations to determine the compactive effort for matching the average air void measured from the cores. Figure 34 shows the reduction or change in air void as a function of end pressure. All specimens compacted with this device have been designated as MT/GS.

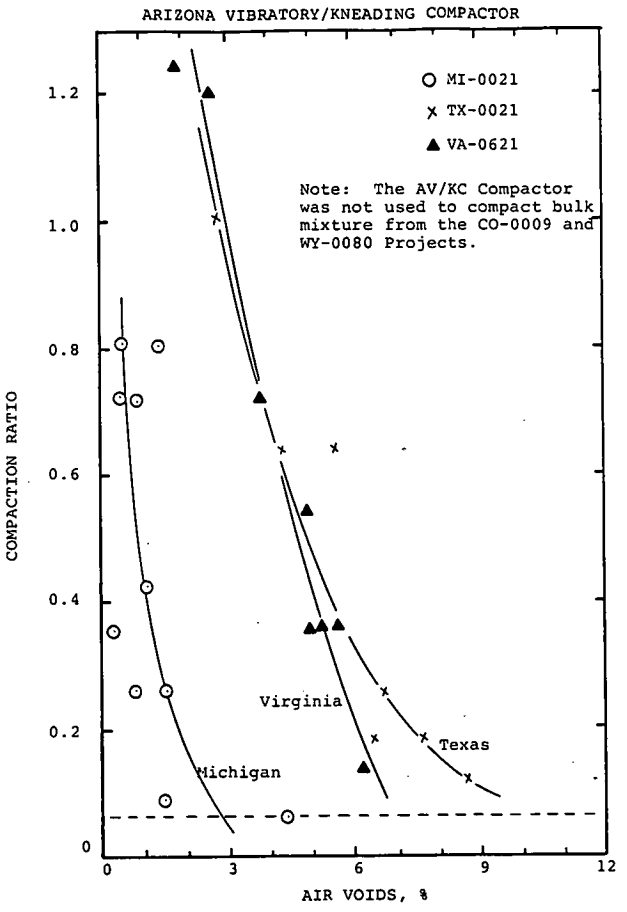

Figure 33. Compactive effort curves developed for each mix using the Arizona vibratory/kneading compactor.

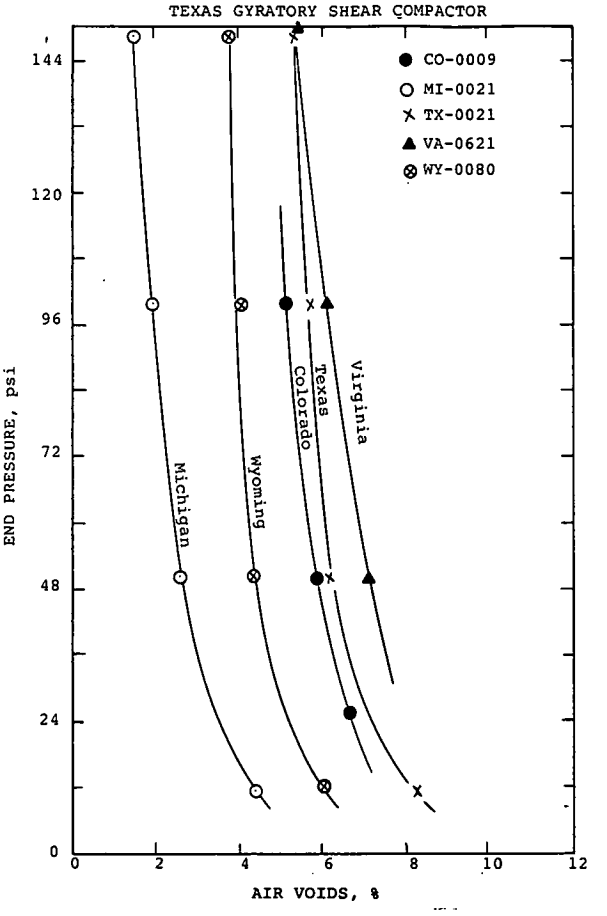

Figure 34. Compactive effort curves developed for each mix using the Texas gyratory shear compactor.

In addition to the Texas gyratory compactor, the Corps of Engineers gyratory shear compactor was used to compact laboratory specimens for the traffic densification study. The Corps of Engineers device, however, was not used in the initial compaction study. All specimens were prepared and compacted in accordance with ASTM D3387-83, "Compaction and Shear Properties of Bituminous Mixtures by Means of the U.S. Corps of Engineers Gyratory Testing Machine (GTM)." Figure 35 shows the reduction in air void as a function of number of gyrations. All specimens compacted with this device have been designated as CE/GS.

2.3.2.1.5 Rolling Type Compaction. The mobile steel wheel simulator was used to simulate a rolling type compaction of a static steel wheel. The rolling type compaction applies a force to a portion of the free face of an otherwise confined asphaltic concrete mix, similar to the kneading type compactors. Compaction forces are applied over the entire beam specimen using a curved foot to simulate the rolling pattern of a steel wheel roller. The partial free face allows the coarse aggregate to move relative to one another allowing the particles to orient themselves similar to that in the field. The specific steel wheel simulator used to compact laboratory specimens of each of the asphaltic concrete mixtures was obtained from the Federal Highway Administration at the Turner-Fairbanks office. The piece of equipment used is relatively unsophisticated in comparison to the typical European type compactors that simulate the rolling action of a steel wheel or rubber-tired roller.

Using the steel wheel simulator, all laboratory specimens were compacted in accordance with Appendix F. The number of revolutions of the steel foot was varied to determine the compactive effort required to match the average air void measured from the cores. Figure 36 shows the compactive effort curves for the steel wheel simulator for each of the mixes considered. All specimens compacted with this device have been designated as MS/WC.

2.3.2.2 Laboratory Compactive Efforts

As discussed previously, compactive effort curves were prepared for each of the compaction devices to determine a reduction in air voids as a function of increase in compactive effort. These compactive effort curves (Figures 31 through 36) were used to select the compactive effort required for each device to match the air void level measured from the field cores—thus reducing any effect of differences in air voids in comparing the engineering properties between the field cores and laboratory compacted specimens.

The compactive efforts used for each of the mixes and each compaction device are given in Table 20. As shown, there is a significant variation in compactive efforts required for each of

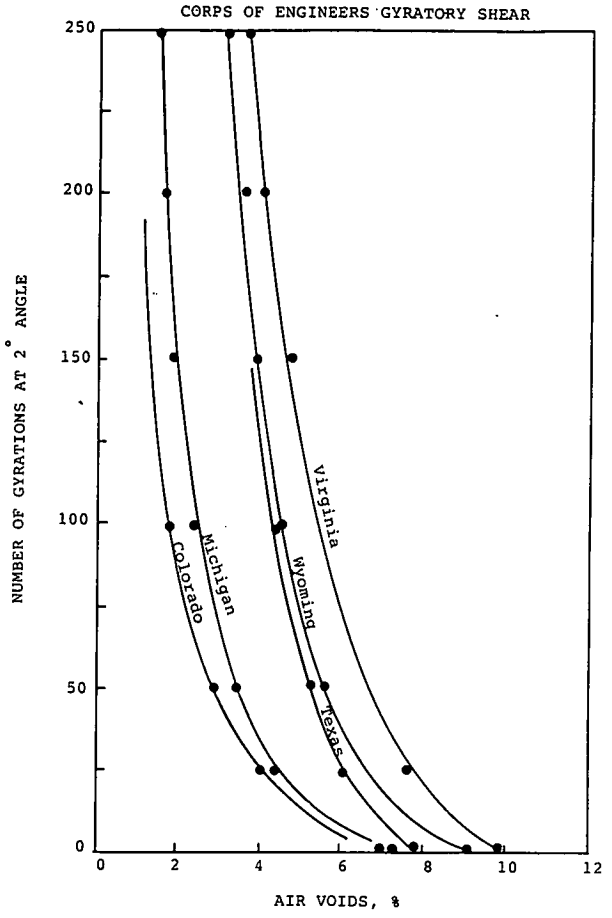

Figure 35. Compactive effort curves for the traffic densification study using the Corps of Engineers gyratory shear compactor.

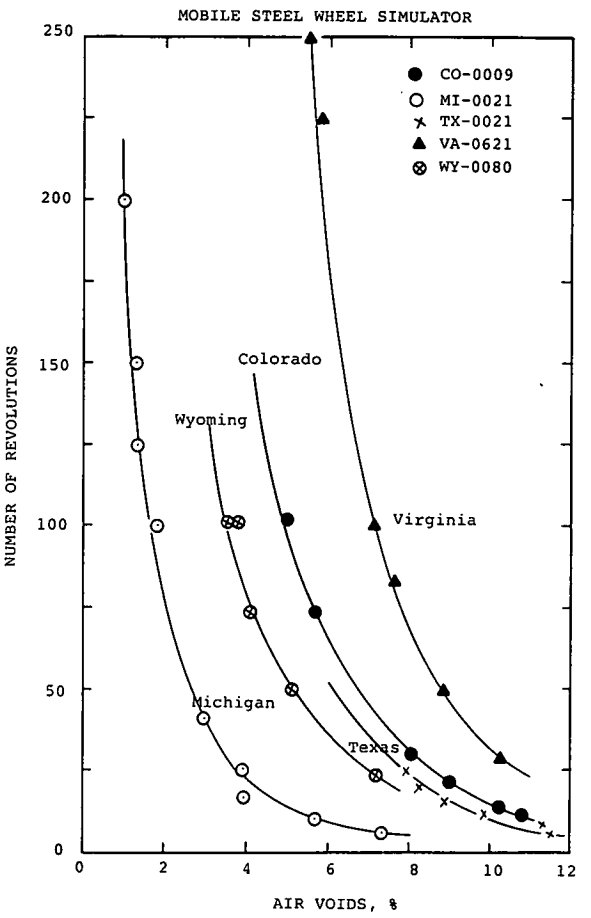

Figure 36. Example of compactive effort curves developed for each mix using the mobile steel wheel simulator that was obtained from FHWA.

the mixtures considered in AAMAS. More importantly, these values are much less than those required in AASHTO and ASTM test standards. However, air voids measured in the field were also greater than those required in design (Table 19), as expected.

2.3.2.3 Air Voids

The distribution of air voids of the laboratory specimens compacted using each of these devices has been graphically compared to the distribution of air voids measured on the field cores in Figures D.1 through D.5 in Appendix D. The mean values, standard deviation and coefficient of variation of air voids for the field cores and laboratory compacted specimens for each mixture are also summarized in Appendix D in Tables D.1, D.2 and D.3, respectively. As expected, the laboratory prepared specimens are much more uniform than the field cores.

2.3.2.4 Air Void Gradients

Selected specimens were used to measure the air void gradient or change in air voids from one end of the specimen to the other.

Table 20. Summary of compactive efforts required to compact laboratory specimens using different types of equipment to simulate air voids measured on field cores.

State/Project	Section	Compaction Equipment*				
		Arizona AV/KC	Marshall MM/HC	Cox CK/CC	Mobile MS/WC	Gyratory MT/GS
Colorado CO-0009	1	---	20	20(250)	---	25(3)250
	2	---	17	15(250)	---	25(3)250
	5%**	---	52	50(500)	---	50(3)500
Michigan MI-0021	1	0.06	26	32(500)	22	50(3)500
	2	0.06	18	25(500)	16	25(3)500
	5%**	0.06	13	6(500)	14	25(3)250
Texas TX-0021	1	0.14	18	20(250)	15	25(3)0
	2	0.06	14	14(250)	10	25(3)0
	5%**	0.48	55	24(500)	65	50(3)500
Virginia VA-0621	1	0.44	55	40(500)	175	100(3)2,500
	2	0.20	34	22(500)	90	50(3) 500
	5%**	0.54	100	50(500)	250	150(6)2,500
Wyoming WY-0080	1	---	39	20(250)	---	50(3)250
	2	---	18	14(250)	---	---
	5%**	---	54	26(250)	---	100(3)250

* The numbers listed under Compaction Equipment are defined as follows:

Arizona, AV/KC - Compaction Ratio Number

Marshall, MM/HC - Number of Blows on both faces from the Marshall Hammer

Cox, CK/CC - D(E): D = Number of Tamps
E = Tamping Pressure, psi

Mobile, MS/WC - Number of revolutions or cycles of the specimen under the steel roller.

Gyratory, MT/GS - A(B)C: A = Gyration Pressure, psi
B = Number of Gyrations
C = End Pressure, psi

** Laboratory compactive effort required to compact specimens with a 5 percent air void level.

All of the same air void gradient data measured for the field cores (listed and defined in section 2.3.1.4) were also measured on laboratory compacted specimens. These data are provided in Appendix D and include air void difference, normalized differences and air void ratio. Results of the testing indicate that the lower air voids of higher densities were consistently measured in the center portion of the laboratory specimens, with the exception of those compacted with the AV/KC device.

2.3.3 Mixture Compaction Properties

Asphaltic concrete mixtures that can be easily densified under the compaction equipment are said to be "workable." Asphaltic concrete mixtures that are difficult to compact are said to be "stable" or "harsh." Thus, the degree of workability of the mix is a factor in the ability of the contractor to achieve the proper density and air void content in the mix.

Table 20 summarized the compactive efforts required to compact each of the different mixes to a standard air void content of 5 percent. The Michigan mixture (MI-0021) has the greatest workability, requiring less compactive effort, whereas the Virginia mixture (VA-0621) has the least workability. In general, the coarser the mix, the greater the compactive effort required to achieve the same level of air voids.

There is, however, no quantitative definition for the degree of "workability" of an asphaltic concrete mixture. In fact, there are some differences of opinions regarding the meaning of workability. Thus, the term "compactibility" will be used in AAMAS.

Table 21. Summary of information and data related to the mixture's compactibility.

State/Project	Compaction Device	Compactibility *	C_1	C_2	V_o	V_u
CO-0009	AV/KC	----	----	-------	----	----
MI-0021		1.4	0.60	5.071	8.0	0.5
TX-0021		5.2	0.82	2.534	13.0	2.0
VA-0621		5.2	0.67	2.039	14.0	2.0
WY-0080		----	----	------	----	---
CO-0009	CK/CC	697	0.51	0.01670	13.0	2.7
MI-0021		338	0.69	0.03894	8.0	1.5
TX-0021		956	0.63	0.01987	13.0	5.0
VA-0621		811	0.46	0.02278	14.0	4.8
WY-0080		550	0.44	0.03386	11.0	3.0
CO-0009	MM/HC	537	0.83	0.02476	13.0	4.0
MI-0021		251	1.00	0.05412	8.0	2.2
TX-0021		555	0.89	0.03205	13.0	4.2
VA-0621		624	0.88	0.04973	14.0	5.5
WY-0080		490	1.00	0.03525	11.0	4.0
CO-0009	MS/WC	1294	1.00	0.04368	13.0	5.5
MI-0021		444	1.00	0.02560	8.0	1.0
TX-0021		1147	1.00	0.03014	13.0	3.0
VA-0621		1581	1.00	0.01816	14.0	5.6
WY-0080		1067	1.00	0.02297	11.0	2.7
CO-0009	MT/GS	1017	0.31	0.01992	13.0	5.0
MI-0021		457	0.29	0.00707	8.0	1.0
TX-0021		1192	0.14	0.00891	13.0	5.4
VA-0621		1344	0.32	0.01160	14.0	5.2
WY-0080		826	0.12	0.00811	11.0	3.6
CO-0009	CE/GS	500	0.50	0.02212	13.0	1.1
MI-0021		604	0.85	0.02257	8.0	1.4
TX-0021		890	0.50	0.01873	13.0	3.1
VA-0621		1358	0.62	0.01291	14.0	3.6
WY-0080		944	0.74	0.01916	11.0	3.2

* Compactibility is defined as the area under the Compactive Effort Curve (Air Voids versus Compactive Effort), within the following maximum limits:

AV/KC = 1.0 Ratio
CK/CC = 150 Tamps
MM/HC = 75 Blows
MS/WC = 200 Revolutions
MT/GS = 150 psi
CE/GS = 200 Gyrations

2.3.3.1 Compactibility

Compactibility will be defined as the ease of densification of the asphaltic concrete mix under some given compactive effort, either in the laboratory or on the roadway during the compaction of the mix by the rollers. Mathematically speaking, compactibility can be defined as the area under the compactive effort curve (compactive effort vs. air voids). These curves (Figures 31 through 36) can be mathematically expressed by the following equation:

$$V_a = C_1^{-cC_2}(V_o - V_u) + V_u \qquad (2\text{-}3)$$

where V_a = air voids of the compacted specimen using c compactive effort; V_o = air voids of the loose mixture, without any compactive effort; V_u = ultimate air voids of the mixture for a specific compaction device; and c = compactive effort applied by a single device defined as:

Marshall hammer—number of blows, both faces
kneading compactor—number of tamps
gyratory shear compactor—number of gyrations
steel wheel simulator—number of passes of roller

and C_1, C_2 = regression coefficients.

This equation simply represents the reduction in air voids with an increase in compactive effort for each of the compaction devices used in the compaction study. Coefficients for the compactive effort equation for each of the mixtures and compaction devices used were determined and are given in Table 21.

The air voids of the loose mix (V_o) are dependent primarily on the aggregate properties (as discussed in section 2.1.4.3) and independent of compaction device. The ultimate or refusal air void content is dependent on both the aggregate and compaction device. Refusal is defined as the air void level at which no significant reduction in air voids is obtained with additional compactive effort. The Arizona vibratory/kneading compactor (AV/KC) provides the lowest estimate of the refusal or ultimate air void content of each mixture. In other words, the vibratory/kneading compactor is able to densify the particles into a more dense arrangement than the other compaction devices.

The loose air void content for each of these mixtures has been compared with two aggregate properties (see Figure 37); particle index and Baladi's (*34*) aggregate angularity value (see Table 7). As illustrated, these aggregate properties were found to be at least related to the V_o coefficient. The other coefficients (V_u, C_1, C_2) are dependent on the compaction device, aggregate size and shape, gradation and asphalt content—all of which are interrelated.

The area beneath the compactive effort curves (represented in Figures 31 through 36) were calculated, using Eq. 2-3, for each of the compaction devices. To calculate the areas beneath the curve, the maximum compactive effort value was set as the practical limit for each compaction device. These areas are summarized in Table 21. Review of Table 21 shows that the largest area beneath the compactive effort curves occurred consistently for the Virginia mix, with the exception for the kneading compactor, CK/CC. Thus, all of the compaction devices provide a similar relative measure or ranking of compactibility for different mixtures.

The field or nuclear density growth curves (increase in density with roller pass) were not measured for each compaction train during construction. The number of roller passes were recorded for each section, but the decrease in air voids with roller pass

was not measured. Only the final air void level of the mixture was recorded. Figure 38 compares the air voids and number of total roller passes for all sections where vibratory rollers were used for breakdown. Although only the initial and final air voids of the compacted lift are available, these data can be used to provide a "gross" relative ranking of compatibility for each mixture. It should be understood, however, that the specific vibratory rollers used for breakdown and other rollers used for finish rolling did vary between projects. A ranking for mixture compactibility by compaction technique is shown as follows:

Project	Field Compaction	Laboratory Compaction Device CK/CC	MM/HC	MS/WC	MT/GS
VA-0621	1*	2	1	1	1
TX-0021	2	1	2	3	2
CO-0009	3	3	3	2	3
WY-0080	4	4	4	4	4
MI-0021	5	5	5	5	5

*Number 1 represents the most harsh mixture and 5 represents the most workable or compactible mixture. The gyratory and Marshall laboratory devices gave identical rankings to the field compaction ranking.

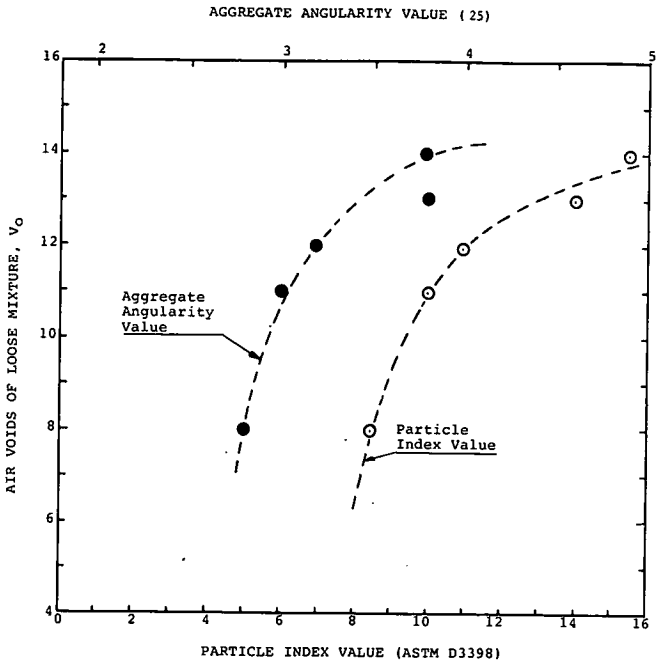

Figure 37. Comparison of the coefficient V_o, air voids of the loose mixture as measured using the MS/WC type specimen, and the aggregate angularity and particle index values.

2.3.3.2 *Density Index*

The compactive effort curves can also be used to determine the air void content to be specified after construction to reduce the occurrence of additional densification caused by traffic that results in rut depths. Measuring a compactive effort curve for a specific aggregate blend at different asphalt contents is time consuming and requires a significant amount of material. Historically, an air void content range or minimum percentage of a laboratory density has been used to control field compaction.

The air voids of any mixture, however, do not, in themselves, furnish a direct measure of their behavior under load. For example, of two mixtures at the same air void content, one mixture may be in a dense state, whereas the other may be loose. Thus, the relative density can be expressed numerically by a term called the density index, I_d, which is mathematically defined as:

$$I_d = \frac{e_{max} - e}{e_{max} - e_{min}} \qquad (2\text{-}4)$$

where e = actual void ratio of a compacted specimen,

$$e = V_v/V_s \qquad (2\text{-}5)$$

e_{max} = void ratio of a mixture in its loosest state, e_{min} = void ratio of a mixture in the densest state, V_v = volume of voids, and V_s = volume of aggregate or solids.

For dense-graded asphaltic concrete mixtures, the density index after compaction should approach a value of 1.0. Void ratio (Eq. 2-5) is a volume quantity, and can be used to calculate the air voids that a specific mix should be compacted to in the field. The maximum void ratio, e_{max}, is influenced by various properties of the aggregate (such as gradation, shape, texture, etc.), whereas the minimum void ratio, e_{min}, is strongly influenced by the compaction device and technique. Additionally, there is no standardized method that has been written for measuring or defining the void ratio of an asphaltic concrete mixture

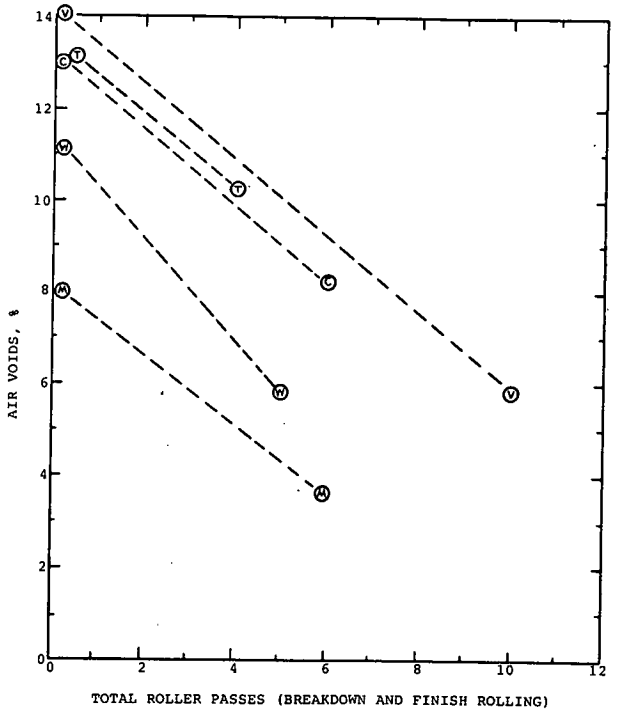

Figure 38. Comparison of air voids and total number of roller passes between the sections compacted using a vibratory roller for breakdown rolling to provide a relative ranking of mixture workability.

Table 22. Density indices calculated for each test section of the AAMAS project.

Project	Section	Mean Air Voids, %	Density Index
CO-0009	1-VB	8.19	.405
	2-PB	8.98	.338
MI-0021	2-VB	3.74	.645
	2-PB	4.21	.574
TX-0021	1-SB	8.75	.429
	2-VB	10.17	.286
VA-0621	1-VB	5.85	.784
	2-SB	7.44	.631
WY-0080	1-VB	5.77	.670
	2-PB	8.37	.337

in its loosest or densest state. Thus, the calculation of a density index for asphaltic concrete mixtures involves some uncertainty.

For illustration purposes, however, the compactive effort curves can be used to estimate the minimum and maximum void ratios. The air void of the loose mixture and refusal air voids given in Table 21 for the gyratory compaction device and defined in Eq. 2-3 were used to calculate the minimum and maximum void ratios of each mixture. Using the mean air voids and other mixture properties (Table 7) measured on the field cores, a density index was calculated for each test section. These calculated values are given in Table 22.

A density index greater than 0.65 will normally indicate that adequate compaction has been achieved, and those values less than 0.50 indicate that more compaction should have been applied in the field. Of course, any density index greater than about 0.90 after compaction may be susceptible to flushing or bleeding. Thus, maximum and minimum air void levels can be estimated for a particular aggregate blend, such that additional densification does not occur that will result in excessive rut depths but has sufficient air voids to reduce the probability for flushing or bleeding. Figure 39 shows the change in density index as a function of laboratory compaction for all mixtures using the gyratory shear compactor.

2.3.4 Summary

Although comparisons have been made between each compaction device used in the laboratory, the question that needs to be answered is, which compaction device best simulates the compactibility of the mix and the final air void content that will occur in the field after millions of traffic applications? This question, of course, cannot be answered for the specific AAMAS projects, simply because of the time constraints involved. Historically, kneading compaction or 75-blows per face with the Marshall hammer have been used for selecting the design asphalt content under heavy traffic for an air void level of 3 to 5 percent.

Cores were taken from the original five projects after 2 years of traffic to evaluate the change in mix density or air voids with time. These data are presented and discussed in section 2.4.5. Most of these 2-year values still exceed even the 5 percent level of air voids (see section 2.4.5). Another more important question that needs to be considered is how do the mixture properties change as the mix approaches the refusal air void content or density? Discussion on the effect of a reduction in air voids on the mixture's properties is covered in section 2.5.3.

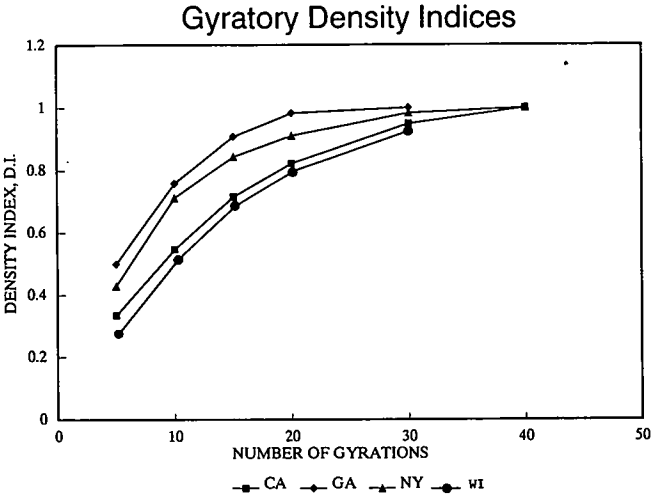

Figure 39. Density index as a function of the number of revolutions of the gyratory shear compactor for the four inferior mixtures studied in the laboratory.

2.4 MIXTURE TESTING AND EVALUATION

As stated earlier in section 2.1.3, the triaxial and indirect tension testing techniques were selected for use in AAMAS. These two types of tests are more commonly used and are the ones recommended for use from NCHRP Project 1-26 and Federal Highway Administration studies (*34*). This section of the report discusses the engineering properties measured on the field cores and laboratory compacted specimens using the two testing techniques.

2.4.1 Field Compacted Mixes

To determine the engineering properties of the mixtures as initially placed in the field, indirect tensile testing techniques were performed on cores selected from each test section. Those engineering properties measured on the field cores include indirect tensile strength, repeated load resilient modulus, creep compliance, and permanent deformation parameters. The engineering properties measured on the field cores recovered after 2 years of traffic are discussed in section 2.4.5.

2.4.1.1 Selection of Sample Sets

In evaluating the engineering properties of these mixtures, it is of paramount importance to compare the properties at comparable air voids. The compaction procedure used in the field was monitored very closely to reduce air void variation in each section. However, variation still exists with the coefficient of variations ranging from 10 to 20 percent. The air voids measured on these recovered cores are given in Appendix D. There is sufficient variation within a test section to cause differences in the test results; therefore, a specific procedure was used in selecting those cores for each sample set or cell to minimize air void differences between sample sets.

To begin with, all of the cores were arranged in order of increasing air voids. Three cores within each sample set were

then initially selected for testing. The selection procedure was to use one core with relatively high air voids (with respect to the average air void of all field cores), one core near the average air void content, and another core with an air void content below the overall average. Each set was selected for testing to obtain an average air void for the field cores within each cell as close to the overall mean of all the cores within the same test section. This arrangement of field cores was conducted to minimize the overall effect of air void differences between different sample sets or cells.

2.4.1.2 Indirect Tensile Strength

Indirect tensile strengths were measured in accordance with TEX-226-F (*50*) at three different temperatures (41, 77, and 104°F). A copy of test method TEX-226-F is included in Appendix G. Although only one test temperature is specified (77°F), two additional temperatures (41 and 104°F) were used to determine the effect of temperature on the mixture's indirect tensile strength. All indirect tensile strengths measured on the field cores are included in Appendix H.

Table 23 gives the mean indirect tensile strengths and coefficients of variation (COV) calculated for each mixture. Figure 40 shows the mean indirect tensile strength as a function of temperature. As shown, the Virginia mixture (VA-0621) is significantly stronger than the other mixtures, and is the coarser aggregate blend with the larger size aggregate. The CO-0009 and MI-0021 mixtures are weaker (in terms of tensile strength) than the other mixtures, and contain the smaller size aggregate and finer blend.

Table 23. Summary of indirect tensile test results for the field cores recovered immediately after construction.

State/ Project	Temperature °F	Test Section	Air Voids %	Indirect Tensile Strength, psi Mean	Cov	Resilient Modulus, ksi Mean	Cov	Strain at Failure, Mils/in. Mean	Cov
Colorado CO-0009	41	1-VB	7.56	361	1.8	1625	6.4	1.30	20.0
		2-PB	8.41	295	0.5	1991	66.8	1.80	23.4
	77	1-VB	8.30	90	10.2	583	11.2	15.40	15.7
		2-PB	8.67	88	4.7	460	14.9	13.17	2.2
	104	1-VB	7.92	30	23.6	329	31.3	16.38	47.2
		2-PB	9.63	27	37.5			15.40	13.9
Michigan MI-0021	41	1-VB	3.42	347	8.1	1473	29.0	6.40	12.8
		2-PB	4.17	382	5.5	2379	8.9	4.51	24.0
	77	1-VB	3.87	84	7.0	420	11.1	15.17	16.6
		2-PB	4.15	90	8.9	456	9.2	14.56	18.9
	104	1-VB	3.50	23	9.2	161	10.8	18.89	39.8
		2-PB	4.25	34	20.8	168	16.8	13.70	9.6
Texas TX-0021	41	1-SB	9.27	316	5.6	4480	43.7	1.21	24.8
		2-VB	9.58	291	14.9	1189	21.4	1.31	16.3
	77	1-SB	9.15	119	3.7	1287	11.0	9.01	12.0
		2-VB	10.88	106	29.6	709	29.1	11.23	30.5
	104	1-SB	9.16	33	3.5	242	1.5	11.01	5.5
		2-VB	10.50	32	17.3	267	19.8	16.12	19.0
Virginia VA-0621	41	1-VB	6.91	424	11.3	3449	17.4	2.38	82.1
		2-SB	7.25	407	11.9	1509	26.7	3.35	41.7
	77	1-VB	5.57	224	7.3	925	22.9	6.96	5.2
		2-SB	7.68	184	5.5	504	28.4	11.51	27.2
	104	1-VB	5.75	99	6.6	252	39.3	3.45	17.3
		2-SB	7.29	70	31.3	246	39.9	10.75	22.9
Wyoming WY-0080	41	1-VB	6.06	398	27.0	2062	74.2	0.95	15.7
		2-PB	8.07	446	11.6	1877	36.1	1.04	70.7
	77	1-VB	6.03	143	3.7	707	28.0	6.40	28.3
		2-PB	9.84	103	9.3	197	11.2	5.29	14.2
	104	1-VB	6.61	56	21.5	204	24.9	10.14	3.6
		2-PB	9.12	42	2.4	260	24.1	10.92	33.1

Figure 41 shows the effect of maximum aggregate size on indirect tensile strength. As displayed, aggregate size has a more distinguishable effect at the higher temperatures than at the lower test temperatures. At 41°F, air voids, gradation, and prop-

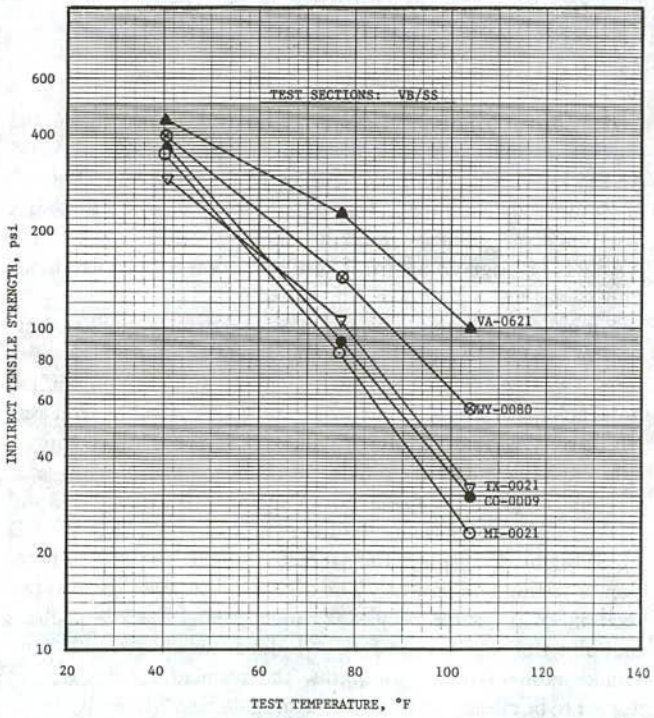

Figure 40. Indirect tensile strength as a function of test temperature for the VB/SS (vibratory breakdown rollers) test sections for the AAMAS field projects.

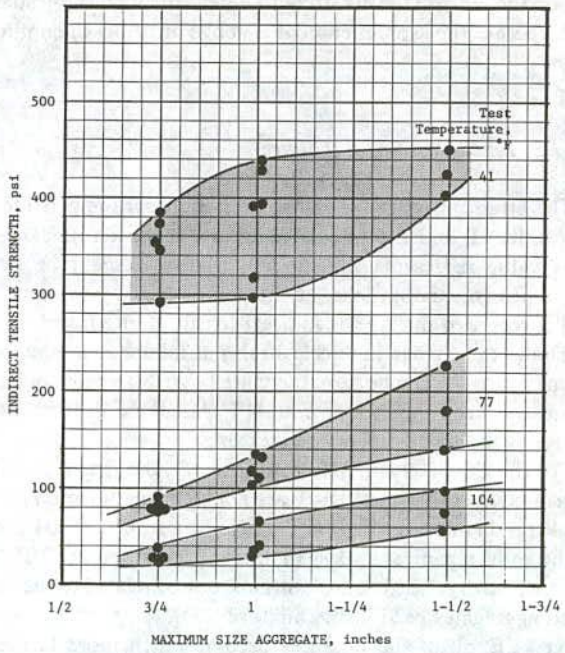

Figure 41. Effect of maximum size aggregate on indirect tensile strength of different mixtures for the AAMAS field projects.

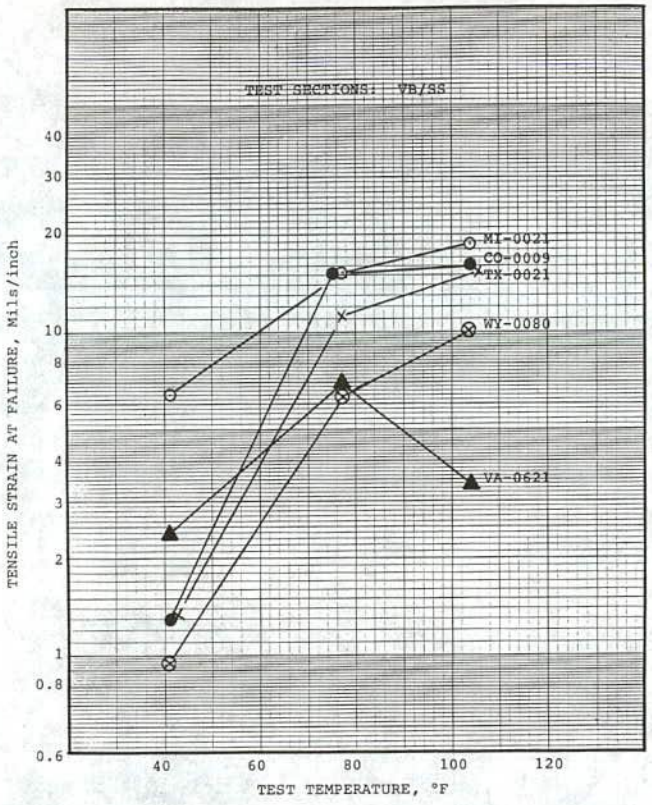

Figure 42. Tensile strain at failure as a function of test temperature for the VB/SS (vibratory breakdown rollers) test sections.

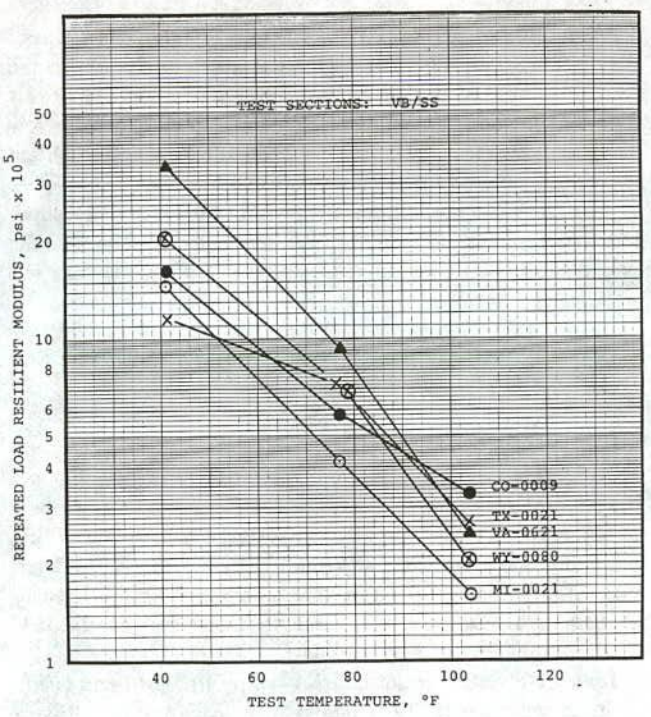

Figure 43. Repeated load resilient modulus as a function of test temperature for the VB/SS (vibratory breakdown rollers) test sections.

erties of the asphalt become more important relative to tensile strength. Additionally, the relative effect of maximum aggregate size on the indirect tensile strength is dependent on the gradation and whether the asphalt content is above or below the optimum value.

2.4.1.3 Tensile Strain at Failure

The strain at failure measured for each core is provided in Appendix H, and the calculated means are given in Table 23. This value represents the horizontal displacement or tensile strain near maximum load, at the point where cracking begins, and is recorded during the indirect tensile strength test. Figure 42 shows the change in tensile strains at failure as a function of temperature. As can be seen, there are large differences in failure strains between the mixtures at 41°F, but these differences decrease as the test temperature increases.

For the CO-0009 and MI-0021 mixtures, the strains at failure measured at both 77 and 104°F are not statistically different. For the Virginia mixture (VA-0621) the failure strains at 104°F were found to be significantly less than those measured at 77°F. This unexpected decrease in tensile strains may be related to the larger sized aggregates used in the mixture.

At 41°F, all of the mixtures become much more brittle, as expected. However, the failure strains measured at 41°F for the CO-0009, TX-0021, and WY-0080 mixtures are considered to be critically low for surface mixtures. In summary, the Wyoming recycled mixture was the more brittle, whereas the Michigan mix was the least brittle over the temperature regime used during testing.

2.4.1.4 Resilient Modulus

The instantaneous resilient modulus was measured on the same cores that were later tested for indirect tensile strength. ASTM D 4123-82, "Indirect Tension Test for Resilient Modulus of Bituminous Mixtures," was used to determine the total and instantaneous resilient modulus as recommended by the AASHTO Design Guide (*6*). These instantaneous resilient modulus values are reported in Appendix H.

For cylindrical samples tested in compression, a modified version of ASTM D 3497, "Dynamic Modulus of Asphalt Mixtures," was used to measure the resilient modulus. The modification included the use of a loading time of 0.1 sec with a rest period of 0.9 sec for a loading frequency of 1 cps. These compression modulus values are provided in Appendix I.

Table 23 gives the mean instantaneous resilient moduli and COVs measured for each mixture, in accordance with ASTM D 4123. Figure 43 displays the average resilient moduli as a function of testing temperature. The difference between the two test sections of the same project is much greater for the resilient modulus test results than for the indirect tensile strength data. Unlike indirect tensile strengths, the resilient moduli do not appear to be closely correlated to aggregate size. Air voids appear to be more predominant in relation to stiffness. The coefficient of variation of sample sets and test sections, however, did increase as aggregate size increased for the higher temperature.

As stated previously, the AASHTO Design Guide (*6*) recommends that the resilient modulus be measured at 68°F for use in structural design. Although this temperature was not used in the test program, values were interpolated for 68°F to determine the layer coefficients for each mixture. The instantaneous resilient modulus at 68°F and corresponding AASHTO layer coefficient for structural design (in accordance with AASHTO design recommendations) are as follows:

State	Instantaneous Resilient Modulus at 68°F, ksi	AASHTO Layer Coefficient (*6*)
Colorado, VB/SS	740*	0.44
Michigan, VB/SS	560*	0.44
Texas, SB/SS	1,800*	0.44
Virginia, VB/SS	1,300*	0.44
Wyoming, VB/SS	880*	0.44

*Moduli values that exceed limits of correlation.

The Guide (*6*) cautions against using mixtures with modulus values greater than 450 ksi at 68°F, because they are susceptible to thermal and fatigue cracks. All of these resilient moduli values are outside the range of the correlation between resilient modulus and layer coefficient, but are typical values obtained when using indirect tensile testing techniques. Experience with these mixtures and materials indicates that the TX-0021 mixture is susceptible to raveling and cracking, while the MI-0021 and VA-0621 mixtures are the least susceptible to cracking. A more detailed discussion of these results and the implications regarding structural design of flexible pavements is provided in Chapter 3, section 3.7.1.

2.4.1.5 Poisson's Ratio

Both vertical and horizontal movements were measured during the static and dynamic (repeated load) indirect tensile tests. Deformation ratios (DR) for each specimen tested are reported in Appendix J, and the mean values are provided in Table 24. Poisson's Ratio's, ν, were calculated from these measurements in accordance with ASTM D 4123. The calculated values are reported in Appendix J and summarized on Table 25.

As shown, values less than zero, or negative (−), and greater than 0.5 were calculated for all of the mixtures. These are unrealistic and impractical values for most pavement materials, as compared to those values reported in the literature. The reason for this is that it is a result of the mathematical formulation given in ASTM D 4123, which is provided below for easy reference, and is based on the theory of elasticity:

$$\nu = 3.59\,DR - 0.27 \qquad (2\text{-}6)$$

where DR is the deformation ratio measured during the indirect tensile test and is equal to

$$\Delta_H/\Delta_V \qquad (2\text{-}7)$$

in which Δ_H is the recoverable horizontal deformation measured during the indirect repeated load resilient modulus test, or the total horizontal deformation measured during the indirect tensile strength test; and Δ_V is the recoverable vertical deformation measured during the indirect repeated load resilient modulus test, or the total vertical deformation measured during the indirect tensile strength test.

Table 24. Summary of mean deformation ratios measured from the indirect tensile test.

State	Compaction Method	Static			Dynamic		
		41F	77F	104F	41F	77F	104F
CO-0009	VB/SS	0.050	0.229	0.291	0.134	0.096	0.125
	PB/SS	-----	0.227	-----	-----	0.120	-----
	AV/KC	-----	-----	-----	-----	-----	-----
	CK/CC	-----	-----	-----	-----	0.077	0.072
	MM/HC	-----	-----	-----	-----	-----	-----
	MS/WC	-----	-----	-----	-----	-----	-----
	MT/GS	-----	-----	-----	-----	0.046	-----
MI-0021	VB/SS	0.138	0.239	0.297	0.076	0.100	0.086
	PB/SS	0.113	0.292	0.267	0.037	0.158	0.099
	AV/KC	0.120	0.231	0.315	0.064	0.105	0.128
	CK/CC	0.050	0.261	0.307	0.045	0.100	0.073
	MM/HC	0.071	0.225	0.256	0.017	0.081	0.062
	MS/WC	-----	0.247	0.320	-----	0.092	0.079
	MT/GS	0.098	0.264	0.316	0.028	0.080	0.091
TX-0021	SB/SS	0.073	0.228	0.311	0.027	0.0239	0.073
	VB/SS	0.132	0.264	0.361	0.064	0.036	0.028
	AV/KC	0.063	0.093	0.206	0.019	0.040	0.009
	CK/CC	0.042	0.203	0.335	0.009	0.057	0.031
	MM/HC	0.016	0.138	0.217	0.016	0.017	0.024
	MS/WC	-----	0.214	0.253	-----	0.032	0.078
	MT/GS	0.036	0.210	0.320	0.042	0.023	0.061
VA-0621	VB/SS	0.116	0.284	0.152	0.015	0.025	0.024
	SB/PS	0.111	0.311	0.355	0.024	0.046	0.053
	AV/KC	0.061	0.155	0.262	0.028	0.042	0.020
	CK/CC	0.118	0.178	0.116	0.027	0.061	0.038
	MM/HC	0.098	0.209	0.250	0.016	0.035	0.055
	MS/WC	-----	0.217	0.297	-----	0.030	0.027
	MT/GS	0.084	0.198	0.247	0.078	0.052	0.035
WY-0080	VB/SS	0.030	0.139	0.171	0.013	0.064	0.036
	PB/SS	-----	0.135	0.205	-----	0.099	-----
	AV/KC	-----	-----	-----	-----	-----	-----
	CK/CC	-----	-----	-----	-----	0.038	0.039
	MM/HC	-----	-----	-----	-----	-----	-----
	MS/WC	-----	-----	-----	-----	-----	-----
	MT/GS	-----	-----	-----	-----	0.035	0.040

Table 25. Summary of Poisson's ratio calculated from data measured during the indirect tensile strength test at a loading rate of 2 in. per min.

State	Compaction Method	Test Temperature, °F		
		41	77	104
Colorado CO-0009	VB/SS	-0.090	0.557	0.777
	PB/SS	------	0.547	-----
	AV/KC	------	-----	-----
	CK/CC	------	-----	-----
	MM/HC	------	-----	-----
	MS/WC	------	-----	-----
	MT/GS	------	-----	-----
Michigan MI-0021	VB/SS	0.227	0.583	0.795
	PB/SS	0.140	0.780	0.685
	AV/KC	0.165	0.558	0.863
	CK/CC	0.190	0.667	0.830
	MM/HC	-0.017	0.537	0.650
	MS/WC	------	0.617	0.883
	MT/GS	0.090	0.677	0.863
	AV/KC	0.165	0.558	0.863
Texas TX-0021	SB/SS	-0.007	0.547	0.847
	VB/SS	0.205	0.585	1.025
	AV/KC	-0.185	0.063	0.470
	CK/CC	-0.120	0.460	0.933
	MM/HC	-0.210	0.223	0.510
	MS/NC	------	0.495	0.637
	MT/GS	-0.143	0.487	0.880
Virginia VA-0621	VB/SS	0.265	0.800	0.273
	SB/PS	0.380	0.786	1.005
	AV/KC	-0.052	0.288	0.670
	CK/CC	0.153	0.370	0.147
	MM/HC	0.083	0.480	0.627
	MS/WC	------	0.510	0.797
	MT/GS	0.003	0.443	0.583
Wyoming WY-0080	VB/SS	-0.160	0.083	0.350
	PB/SS	------	0.213	0.467
	AV/KC	------	-----	-----
	CK/CC	------	-----	-----
	MM/HC	------	-----	-----
	MS/HC	------	-----	-----
	MT/GS	------	-----	-----

Deformation ratios less than 0.075 will result in negative values for Poisson's ratio and deformation ratios greater than 0.215 will result in Poisson's ratio values greater than 0.5. Negative values have no physical meaning, and values greater than 0.5 mean that there is an increase in volume with the applied load.

Deformation ratios were found to be very low at 41°f, especially for the brittle mixtures, which means that the horizontal movements are small when compared to the vertical displacements (i.e., Δ_H is approximately 5 to 10 percent of Δ_V). As the temperature increased, the deformation ratios also increased. For example, at 104°F the horizontal movement is approximately 20 to 30 percent of the vertical movement. In other words, the relationship between Δ_H and Δ_V is not linear, but is temperature dependent. At short loading durations, however, the dynamic deformation ratios only increased slightly with an increase in temperature. Thus, elastic layer theory may be a gross assumption for some mixtures.

2.4.1.6 Creep Compliance and Recovery Curves

Indirect tensile creep compliance testing was conducted on selected field cores from each test section, in accordance with two test procedures. The first is an iterative procedure described by Kenis (*51*), and the second is provided in Appendix K. The iterative procedure includes the application of a static load over a series of loading and unloading times, while the procedure in Appendix K specifies only a one hour loading time and one hour recovery time. Similar creep compliance values were measured by both procedures at the same time intervals. Thus, the procedure described in Appendix K was used, because it requires less time to conduct the test.

Both creep and recovery or relaxation curves were measured for the cores at temperatures of 77 and 104°F. The results of this testing are reported in Appendix L. To describe the creep tests, and for comparison of the different mixtures, five variables were selected. These variables are the creep compliance at 120 and 750 sec, the slope and intercept of the creep curve, and the total creep measured at 3,600 sec or at failure if the sample began to crack prior to 3,600 sec. Table 26 gives the average values for each test section, and Figure 44 displays the average creep modulus curves (inverse of creep compliance).

At 77°F, the WY-0080 mixture has the smaller creep strains (least susceptible to rutting or surface distortions), and the MI-0021 mixture has the larger creep strains. However, at the higher test temperature (104°F), the MI-0021 mixture had the smaller creep strains in comparison to the other mixtures and failed at a much longer loading time. Most of the CO-0009 and TX-0021 cores failed during static creep testing at relatively small tensile strains, indicating less susceptibility to distortions but more susceptibility to fracture (i.e., low adhesion). The MI-0021 mixture is the more flexible or ductile and the CO-0009 mixture the more brittle one.

2.4.1.7 Repeated Load Permanent Deformation

Repeated load permanent deformation tests were conducted on selected cores at a test temperature of 77°F. The test results for each core are graphically illustrated in Appendix M. The average slope and intercept for each sample tested were calculated and are also provided in Appendix M. The slope and intercept are used in the calculation of alpha, α, and gnu, μ.

The alpha and gnu functions were originally developed by Brademeyer et al. (*52*) to describe the permanent deformation characteristics of asphaltic concrete mixtures. These two parameters are required for the VESYS (*22*) and modified ILLIPAVE (*23*) programs. Both values are given in Table 27, and mathematically defined as follows:

$$\alpha = 1 - m \tag{2-8}$$

$$\mu = \frac{Im}{\epsilon_r} \tag{2-9}$$

where m is the straight line slope of the logarithm of number of load repetitions versus logarithm of the accumulated permanent strain, ϵ_p; I is the intercept of the straight line slope (arithmetic strain value) with the accumulated permanent strain axis, i.e., value at which number of load repetitions scale equals 1; and ϵ_r is the resilient or recoverable strain.

These values are typically measured from testing cylindrical compression samples. Rauhut (*53*) suggests that reasonable values of alpha and gnu can only be calculated from compression samples after 100,000 load cycles. Kennedy (*36*), however, found that using the indirect tensile test to calculate alpha and gnu

Table 26. Summary of creep-compliance test data measured at 77°F for the field cores recovered after construction.

State/Project	Slope of Creep Curve*	Intercept of Creep Curve	Creep-Compliance D(t) x 10^{-9}		
			t=120	t=750	t=3,600
Colorado CO-0009,VB/SS	0.535	0.157	174.1	573.6	974.3**
Michigan MI-0021,PB/SS	0.363	0.490	307.0	736.9	1219.7**
Texas TX-0021,SB/PS	0.633	0.085	109.9	316.6	816.0**
Virginia VA-0621,VB/SS	0.391	0.550	221.3	478.8	860.0
Wyoming WY-0080,VB/SS.	0.412	0.123	93.3	232.6	613.3

* Slope of Creep Curve was calculated in the steady state range.

** Indicates that all of the cores failed during the Static Creep test.

Table 27. Summary of alpha and gnu values calculated from indirect tensile repeated load permanent deformation test data measured at 77°F.

State/Project	Instantaneous Resilient Modulus, ksi	Alpha	Gnu
Colorado CO-0009	287	.25	.13
Michigan MI-0021	215	.41	.16
Texas TX-0021	173	.27	.07
Virginia VA-0621	136	.34	.13
Wyoming WY-0080	167	.35	.03

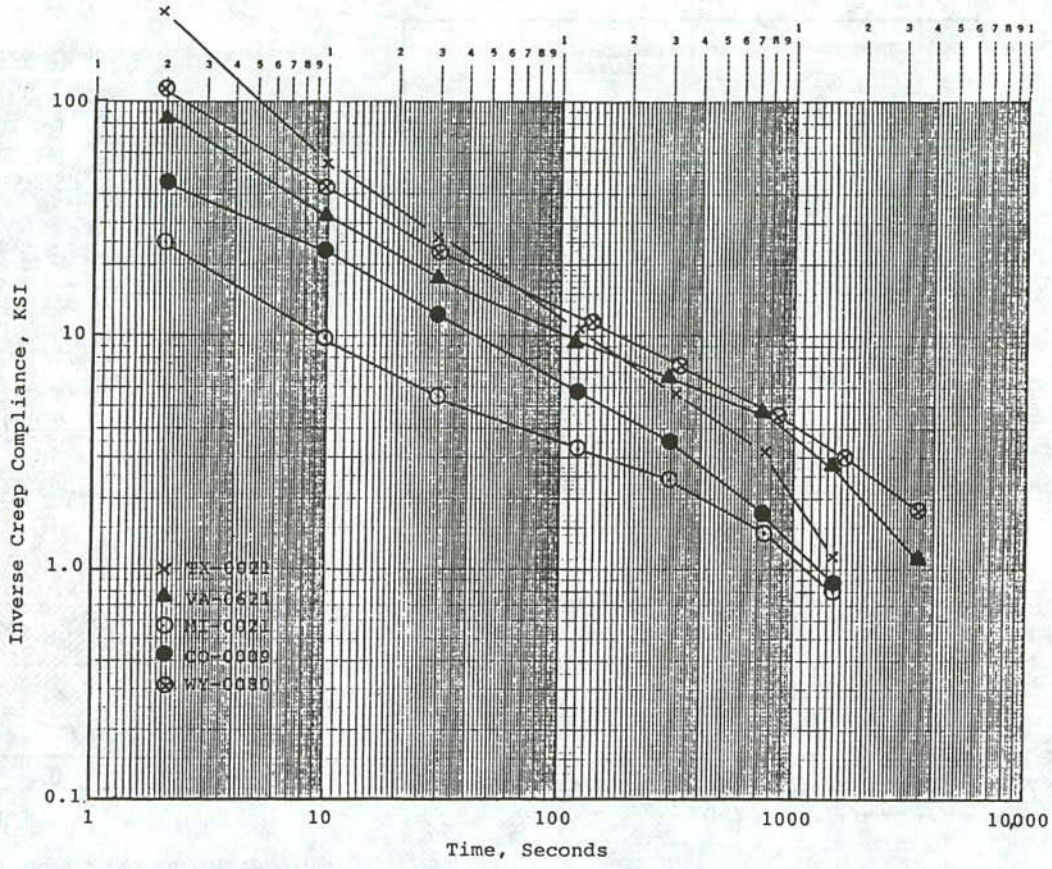

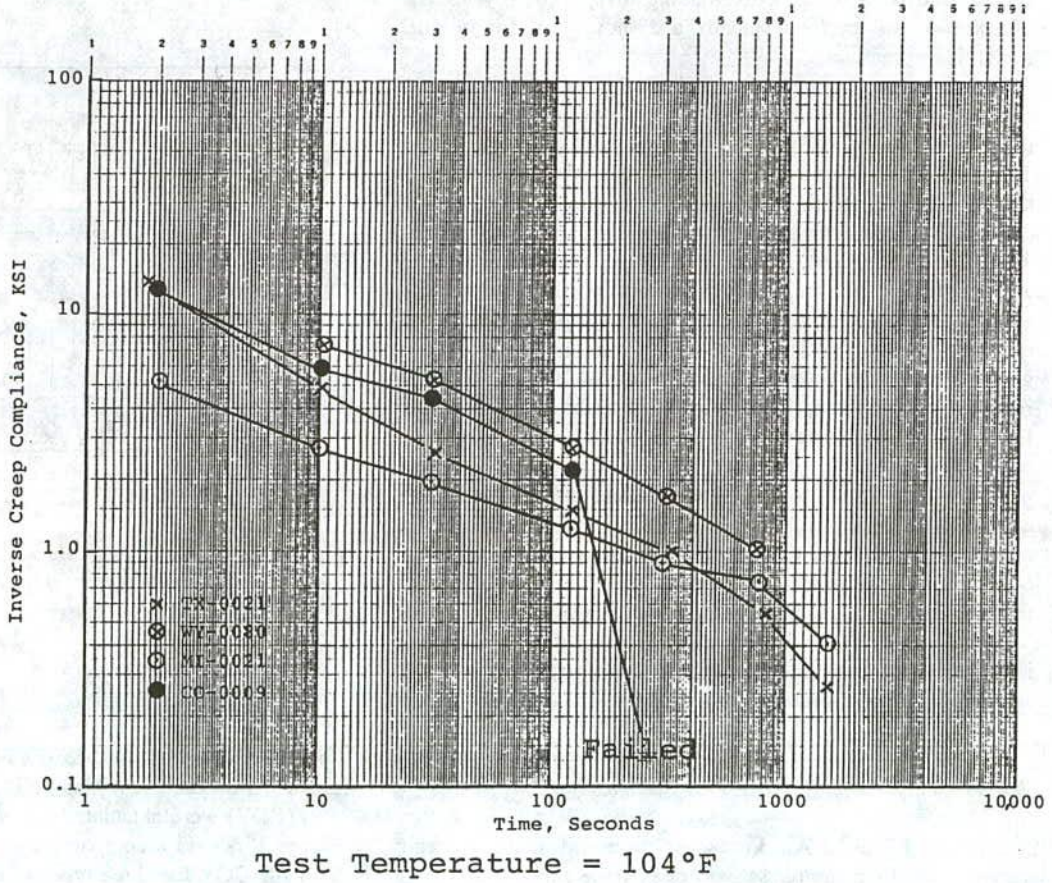

Figure 44. Inverse of creep compliance as a function of loading time for the VB/SS test sections.

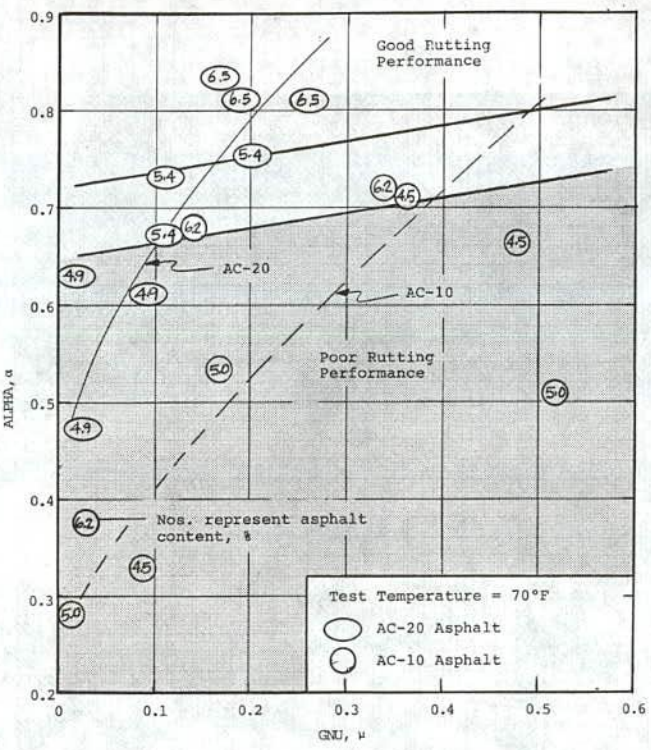

Figure 45. Alpha-gnu relationship as compared to pavement performance in terms of rutting (54).

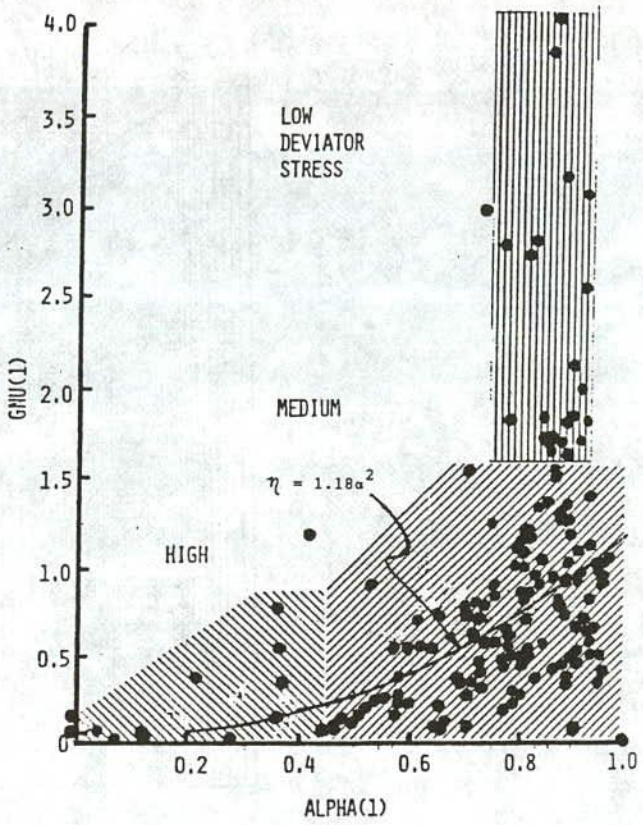

Figure 46. Relationship between alpha and gnu (84).

during the first 10,000 (10 percent) load cycles gave results comparable to the compression loading after 100,000 cycles. Use of 100,000 load cycles (typically a 28-hour test) for mixture design is impractical.

Von Quintus (*54*) has also used the indirect tensile test to measure permanent strains at 10,000 load cycles to compare the use of different asphalt grades over a range of asphalt contents. These results are shown on Figure 45. Baladi (*34*) also concludes that the indirect tensile test can be used to measure permanent deformation characteristics of mixtures for rutting analyses. Therefore, the indirect tensile test was used to calculate alpha and gnu for each of the mixtures (Appendix M).

All permanent deformation test results are presented graphically in Appendix M. Figures 46 and 47 compare the alpha and gnu values for the AAMAS mixtures to those that have been reported in the literature. As shown, the alpha values for all of the AAMAS mixtures are extremely low relative to the majority of those reported in the literature and are characteristic of those mixtures that have provided poor rutting performance. This assumes that the cyclic indirect tensile test is applicable for measuring permanent deformation characteristics of asphaltic concrete mixtures. Conversely, performance records of similar mixtures indicate that the VA-0621 mix is resistant to rutting. Thus, validity of the indirect tensile test for rutting predictions is of special concern and will be discussed in greater detail in section 2.6 and Chapter 3.

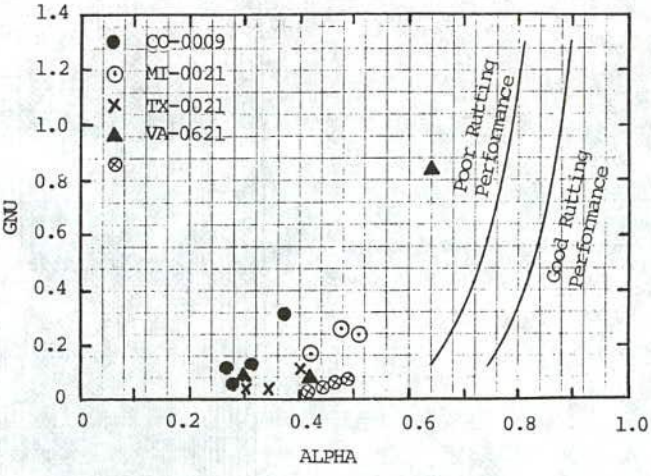

Figure 47. Alpha and gnu values calculated using the steady state portion of the permanent strain versus load application relationship for the AAMAS mixtures.

2.4.1.8 Comparison of Field Test Sections

2.4.1.8.1 Effect of Air Voids. As discussed above, air void variation within a sample set was of extreme concern in setting up the testing program because of the few number of samples tested within each cell. Mean air voids and coefficient of variation (COV) were calculated for each sample set or cell tested. Figure 48 shows a comparison of the COV based on air voids with the COV for three types of tests. As shown, there are no

clear trends. There was less variation within the indirect tensile strength test data than for the strain at failure or resilient modulus test results.

2.4.1.8.2 Effect on Breakdown Roller. From an air void analysis, the two test sections constructed in Colorado and Michigan are not significantly different, whereas the Texas, Virginia, and Wyoming test sections are different. Thus, each of the two test sections within the latter three projects must be considered as independent projects.

For the Colorado and Michigan projects, there does not appear to be a significant difference in engineering properties between the different test sections compacted using different breakdown rollers. Only slight differences in engineering properties were found between the Wyoming test sections, even though the air voids were significantly different. For the Texas and Virginia projects, there is a difference in the engineering properties between the different test sections. Evaluation of these differences is complicated by the extremely large differences in air voids between the two adjacent test sections and the larger aggregates used in these mixtures. Thus, no conclusions are warranted.

Figure 49 provides a comparison of indirect tensile strengths and repeated load instantaneous resilient moduli for the different materials and compaction trains used in the initial five AAMAS projects. For the mixtures with different amounts of crushed and uncrushed gravels (CO-0009, MI-0021, and WY-0080—as in Figure 49), the relationship between indirect tensile strength and instantaneous resilient moduli appears to be similar between all projects even though significantly different air voids were measured on the field cores from each test section. This suggests that the relationship may be independent of air voids. These data are more scattered for the crushed stone mixes (Figure 49b).

Figure 50 shows a comparison of strain at failure and repeated load resilient moduli for the same cores. As shown, strain at failure and resilient moduli are not well correlated, or are more material dependent than strength versus modulus. For the finer graded mixes (or smaller aggregates) with crushed and uncrushed gravels, the variation between test data is much smaller, when compared to the mixes with the larger crushed stone aggregates.

There does appear to be a slight difference between the materials compacted using different types of breakdown rollers, as shown in Figures 49 and 50. Evaluating these small differences is complicated by varying air voids and other mixture properties (i.e., gradation and asphalt characteristics) between samples. Thus, no valid statistical statement can be made regarding the effect of different breakdown rollers on material properties. Van Grevenynghe (*56*) summarized the results of studies conducted in France, Switzerland, and Germany and reported little to no effect on engineering properties of mixtures compacted using different types of breakdown rollers, assuming similar air voids in the final compacted mixture. The trend from the AAMAS data indicates similar findings, although the AAMAS data are minimal.

2.4.2 Laboratory Compacted Specimens

Both indirect tensile and uniaxial compression testing techniques were used to measure the mixture properties of laboratory compacted specimens. The indirect tensile testing technique was used to determine the engineering properties of laboratory specimens compacted with different devices in order to compare the results to field cores. The uniaxial compression testing technique

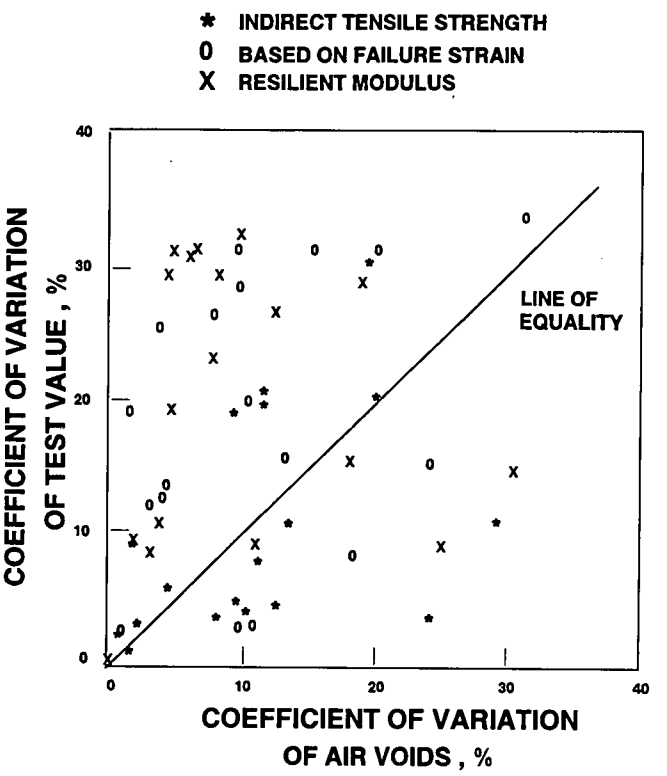

Figure 48. Comparison between coefficient of variation determined for air voids and the variation of test values measured in the laboratory.

was used to determine those engineering properties required to evaluate a mixture's resistance to distortion.

2.4.2.1 Indirect Tensile Properties

The indirect tensile properties measured on laboratory compacted specimens include those same properties measured on the field cores, discussed in section 2.4.1.

Tables 28 and 29 summarize the average tensile properties measured, which include indirect tensile strength, tensile strain at failure, resilient modulus, and creep compliance. The indirect tensile resilient modulus and strength test data are provided in Appendix H, and the static creep test data in Appendix L. These properties were measured using the same procedures and temperatures as used for the field cores.

2.4.2.1.1 Air Void Consideration. As discussed for the field cores, air void variations within the sample sets of each compaction device were also of extreme concern in setting up the testing program and comparisons. Therefore, the same type of procedure used to select samples to be tested within each sample set for field cores was also used for selecting laboratory compacted specimens. Basically, specimens within each sample set included the upper, lower, and mean range of air voids of all specimens compacted with each device.

2.4.2.1.2 Effects of Compaction Device. Without question, the mechanical Marshall hammer is the most common compaction device used by state highway agencies (3 to 1 over the kneading compactor). Therefore, the specimens compacted with the mechanical Marshall hammer were selected as the base value for

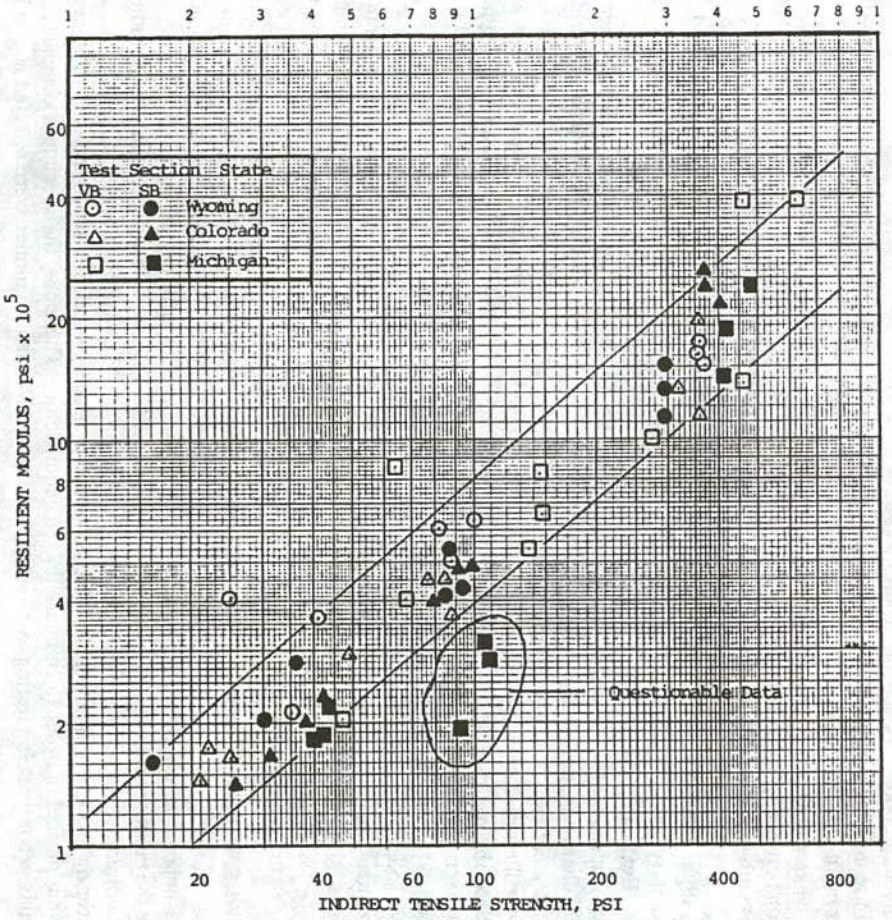

a. Mixes with Crushed and Uncrushed Gravels

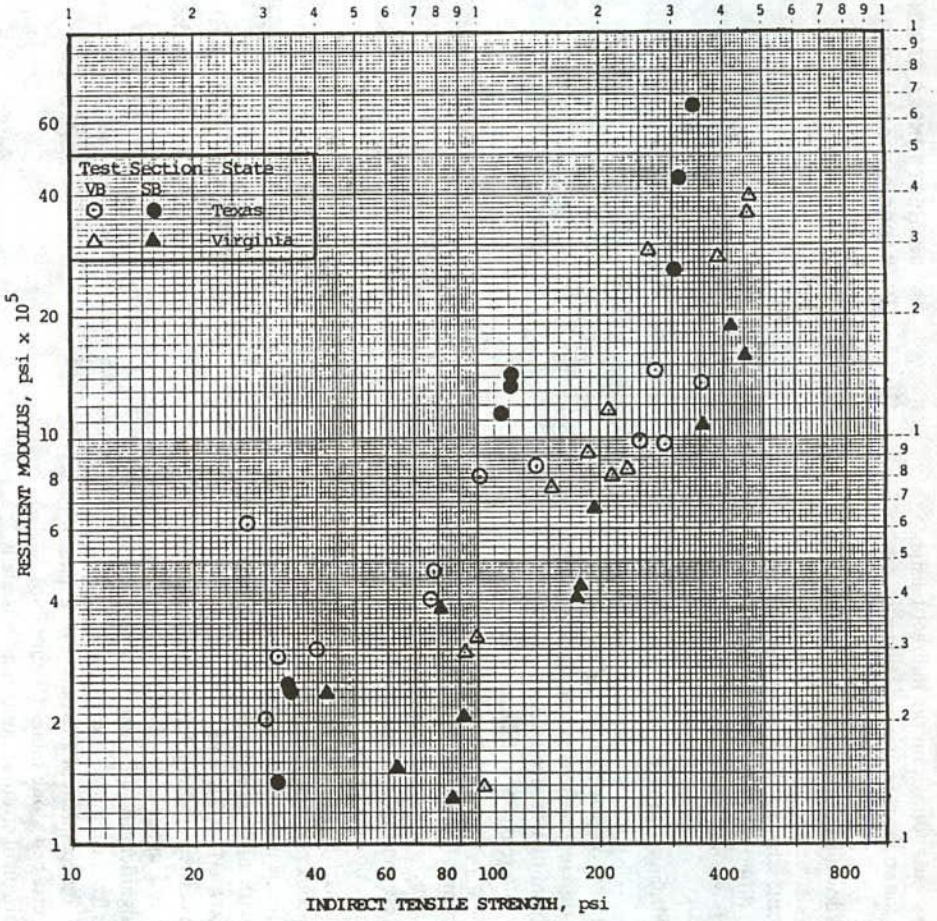

b. Mixes with Crushed Stones.

Figure 49. Relationship between indirect tensile strength and repeated load resilient modulus for mixes compacted with different breakdown rollers.

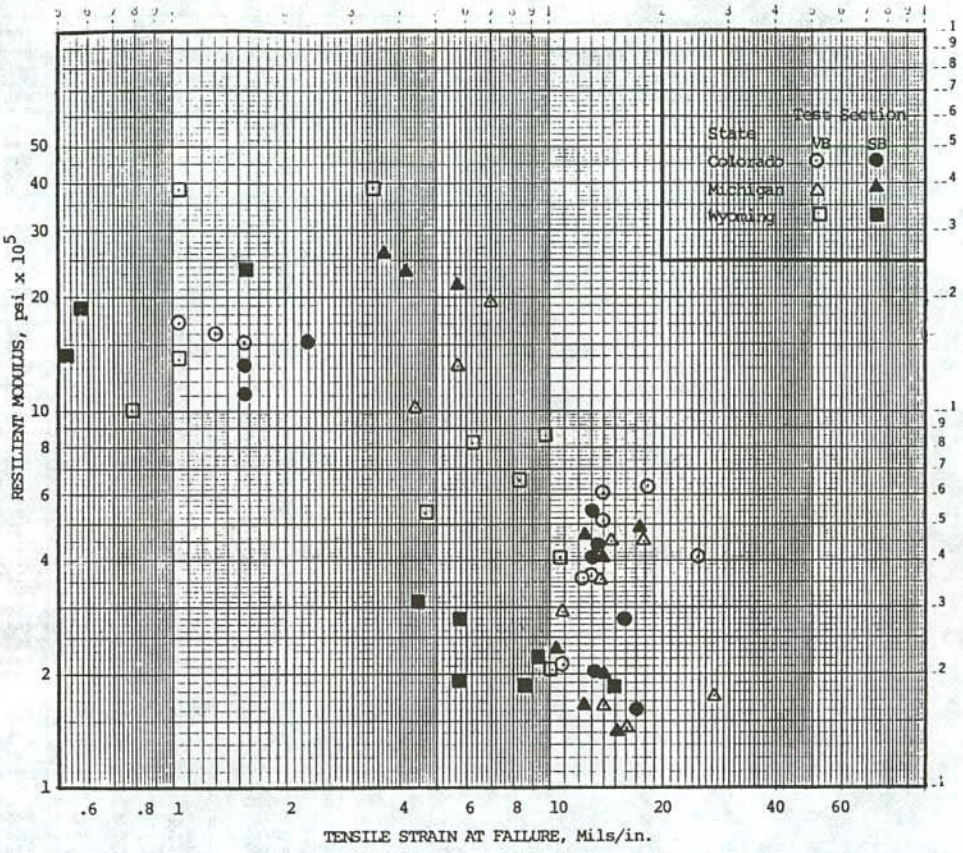

a. Mixes with Crushed and Uncrushed Gravels

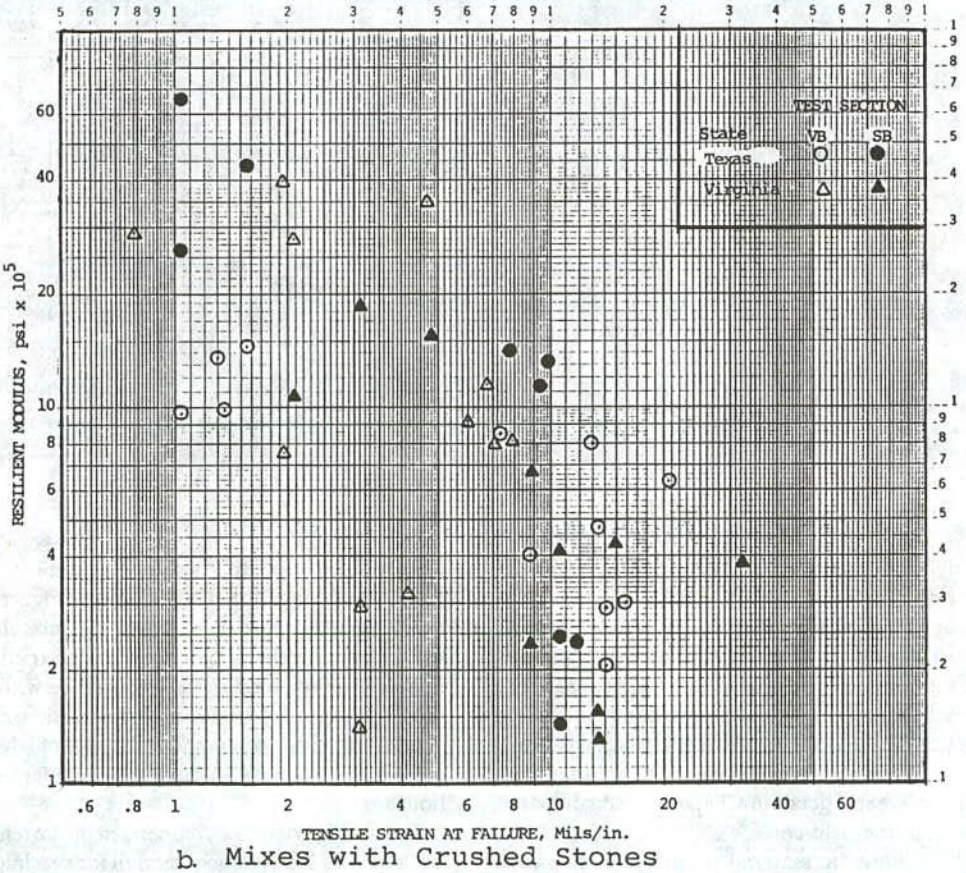

b. Mixes with Crushed Stones

Figure 50. Relationship between tensile strain at failure and repeated load resilient modulus as measured on field cores.

Table 28. Summary of indirect tensile testing data of specimens compacted with different laboratory equipment.

State, Project, Section	Temperature °F	Compaction Device	Mean Air Voids %	Indirect Tensile Strength, psi Mean	Cov	Instant. Resilient Modulus, ksi Mean	Cov	Strain at Failure, Mils/in. Mean	Cov
Colorado CO-0009 1-VB	77	MM/HC	8.39	103	2.1	1176	35.9	----	----
		AV/KC	----	---	----	----	----	----	----
		CK/CC	8.22	---	----	549	12.0	----	----
		MT/GS	8.66	100	3.2	510	27.1	----	----
		MS/WS	9.08	---	----	409	18.1	----	----
	104	MM/HC	----	---	----	----	----	----	----
		AV/KC	----	---	----	----	----	----	----
		CK/CC	8.22	---	----	233	10.4	----	----
		MT/GS	7.22	---	----	215	28.5	----	----
		MS/WC	----	---	----	----	----	----	----
Michigan MI-0021 2-PB	41	MM/HC	4.53	393	5.3	3776	39.1	3.73	4.0
		AV/KC	3.90	387	5.8	2386	67.0	3.90	40.0
		CK/CC	4.10	347	3.3	3154	25.3	4.16	21.7
		MT/GS	4.39	356	2.6	2217	34.2	4.68	0.0
		MS/WC	----	---	----	----	----	----	----
	77	MM/HC	4.20	103	6.7	683	19.9	9.19	6.5
		AV/KC	4.10	90	13.9	579	29.9	11.05	27.8
		CK/CC	3.93	94	1.6	633	21.6	9.01	21.9
		MT/GS	4.17	84	2.1	483	20.7	14.56	6.2
		MS/WC	4.61	89	7.4	424	5.0	15.67	6.2
	104	MM/HC	4.15	44	2.3	224	5.7	8.58	5.2
		AV/KC	4.06	41	4.9	211	59.9	13.46	18.0
		CK/CC	4.17	37	8.7	185	45.0	13.26	5.2
		MT/GS	4.14	30	3.9	178	35.4	16.30	1.8
		MS/WC	4.79	29	9.1	148	9.4	27.68	11.8
Texas TX-0021 1-SB	41	MM/HC	9.28	357	4.2	3502	17.4	0.43	34.9
		AV/KC	8.30	463	11.4	3070	13.4	0.69	37.7
		CK/CC	9.26	349	22.9	3616	17.7	0.88	15.7
		MT/GS	9.22	296	7.5	2856	14.6	1.13	35.1
		MS/WC	----	---	----	----	----	----	----
	77	MM/HC	9.13	172	5.8	1874	47.9	3.81	7.9
		AV/KC	8.64	170	1.4	771	61.4	3.84	37.2
		CK/CC	9.23	147	12.3	554	32.0	7.37	26.9
		MT/GS	8.32	129	5.7	601	2.7	9.01	8.8
		MS/WC	9.80	172	7.4	621	28.7	6.89	15.6
	104	MM/HC	9.32	66	7.0	285	25.8	6.24	0.0
		AV/KC	8.89	74	5.5	486	14.7	7.02	19.6
		CK/CC	9.56	45	19.9	255	15.1	11.27	7.0
		MT/GS	9.11	44	9.1	263	8.2	15.69	10.7
		MS/WC	9.58	62	10.7	324	22.7	12.17	11.8
Virginia VA-0621 1-VB	41	MM/HC	5.65	426	4.4	3945	19.8	2.25	35.3
		AV/KC	5.31	463	4.1	1769	57.1	2.44	30.7
		CK/CC	6.10	388	5.8	2609	27.9	3.21	16.9
		MT/GS	6.34	394	6.2	3048	20.4	2.77	47.2
		MS/WC	----	---	----	----	----	----	----
	77	MM/HC	6.00	153	9.7	1713	25.4	5.55	15.1
		AV/KC	5.15	213	9.9	477	28.5	3.62	30.7
		CK/CC	5.85	127	7.0	620	12.4	8.32	16.5
		MT/GS	6.17	114	9.3	759	20.5	7.97	3.8
		MS/WC	6.10	149	3.4	734	9.8	9.12	7.8
	104	MM/HC	5.93	77	8.2	310	24.2	6.24	14.4
		AV/KC	5.89	153	16.4	364	41.1	11.79	32.5
		CK/CC	5.97	51	4.9	193	8.1	4.51	26.6
		MT/GS	5.99	74	31.5	250	19.1	10.40	10.0
		MS/WC	5.32	85	12.5	279	26.0	10.83	9.2
Wyoming WY-0080 1-VB	77	MM/HC	5.19	161	6.5	933	5.9	-----	----
		AV/KC	----	---	----	----	----	-----	----
		CK/CC	6.19	---	----	661	14.9	-----	----
		MT/GS	6.88	82	8.1	656	12.7	-----	----
		MS/WC	6.41	---	----	729	17.8	-----	----
	104	MM/HC	---	---	----	----	----	-----	----
		AV/KC	---	---	----	----	----	-----	----
		CK/CC	6.84	---	----	178	27.1	-----	----
		MT/GS	6.06	---	----	237	10.4	-----	----
		MS/WC	----	---	----	----	----	-----	----

comparing the engineering properties of specimens prepared with the other devices.

Figures 51 through 55 show a comparison of those properties, noted above, for all laboratory compacted specimens. As may be seen from the figures, there are consistent differences when comparing these data measured on specimens compacted with the five different compaction devices. Indirect tensile strength is the least affected by the type of device used. These differences are evaluated in much greater detail in Chapter 3 and compared to the test results from the field cores.

Figures 56 and 57 show the material property relationships between the compaction devices for each project. Figure 56 provides a comparison of the indirect tensile strengths and repeated load resilient moduli. As shown, a similar type of relationship was also obtained for the field cores (Figure 48)—namely, that as the aggregate size increased in the mix, the variability of test values also increased. Since air voids varied between mixtures, these data also suggest (in concurrence with the test results on the field cores, Figure 49) that the relationship may be independent of air voids. In summary, the type of laboratory compaction device used appears to have no consistent effect on this relationship.

Figure 57 provides a comparison of the tensile strain at failure and repeated load resilient moduli for specimens compacted with each of the different devices. As for the indirect tensile strength data, the variation or dispersion of tensile strain at failure in-

Table 29. Summary of creep compliance, D(t), test data for laboratory compacted specimens using different compaction devices (test temperature = 77°F).

State Project Section	Compaction Device	Slope of Creep Curve*	Intercept of Creep Curve	Creep Compliance, 120 Sec	750 Sec	D(t), x10-6 36000 Sec
Colorado CO-0009	MM/HC	0.440	0.077	48.1	105.9	277.3
	AV/KC	-----	-----	-----	-----	------
	CK/CC	0.483	0.081	87.5	228.0	926.0**
	MT/GS	0.480	0.101	107.2	344.8	800.3
	MS/WC	0.482	0.153	117.2	280.5	710.8
Michigan MI-0021	MM/HC	0.282	.243	105.8	197.4	613.25
	AV/KC	-----	-----	109.3	232.8	770.1
	CK/CC	0.478	.163	134.6	327.3	1668.1
	MT/GS	0.454	.213	209.8	558.3	1417.2**
	MS/WC	0.470	.200	201.0	488.7	1302.7
Texas TX-0021	MM/HC	0.360	.076	32.3	61.4	128.0
	AV/KC	-----	-----	15.1	43.8	121.5
	CK/CC	0.445	0.091	50.4	110.2	273.7
	MT/GS	0.519	0.107	85.7	234.6	656.8
	MS/WC	0.530	0.076	56.0	137.9	377.3
Virginia VI-0621	MM/HC	0.305	0.147	42.3	76.6	177.4
	AV/KC	-----	-----	-----	-----	------
	CK/CC	0.376	0.163	72.6	142.6	399.4
	MT/GS	0.428	0.135	71.7	154.5	320.2
	MS/WC	0.401	0.080	38.4	77.1	141.3
Wyoming WY-0080	MM/HC	0.276	0.054	24.3	39.2	67.0
	AV/KC	-----	-----	-----	------	------
	CK/CC	0.393	0.080	59.8	129.2	332.0
	MT/GS	0.450	0.054	40.1	91.6	193.8
	MS/WC	0.457	0.113	70.3	159.6	360.0

* Slope of Creep Curve was calculated in the steady state range.

** Indicates that specimens failed during the Creep Compliance Test.

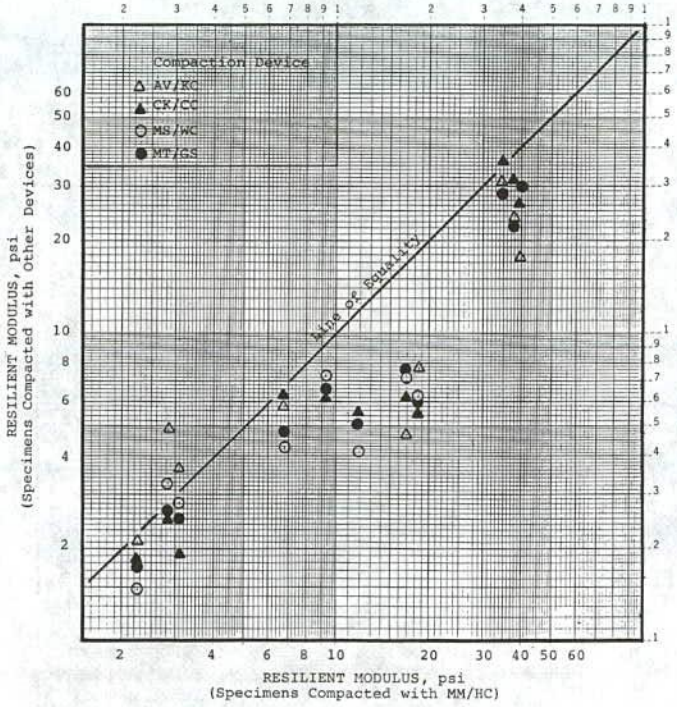

Figure 51. Comparison of resilient moduli values measured on specimens compacted with different laboratory devices.

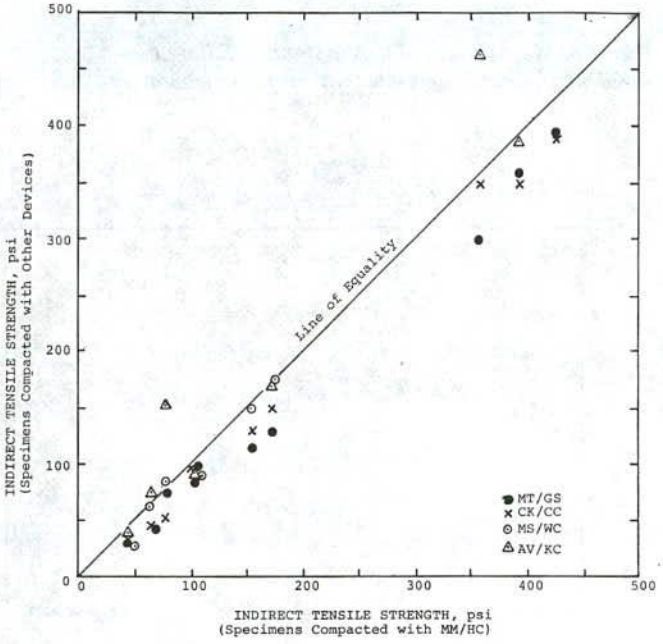

Figure 52. Comparison of indirect tensile strengths measured from specimens compacted with different laboratory devices.

creased as the aggregate size increased. In fact, as for the cores, the failure strains at 104°F were, in some cases, less than those measured at 77°F. Unlike indirect tensile strength, however, failure strain appears to be slightly affected by the type of laboratory compaction device, but the relationship, between failure strains and resilient modulus is mixture related (Figure 57).

2.4.2.1.3 Comparison of Mixtures. Table 30 summarizes the average indirect tensile properties for all mixtures, including those with inferior performance characteristics. As shown, the California, Colorado, Texas, and Wyoming mixtures are the more brittle at the lower test temperature (41°F). The California

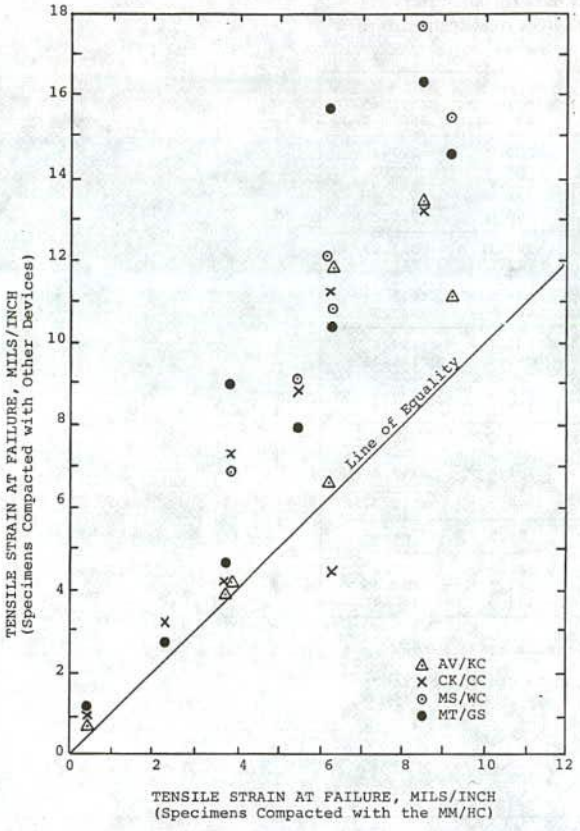

Figure 53. Comparison of tensile strain at failure measured on specimens compacted with different laboratory devices.

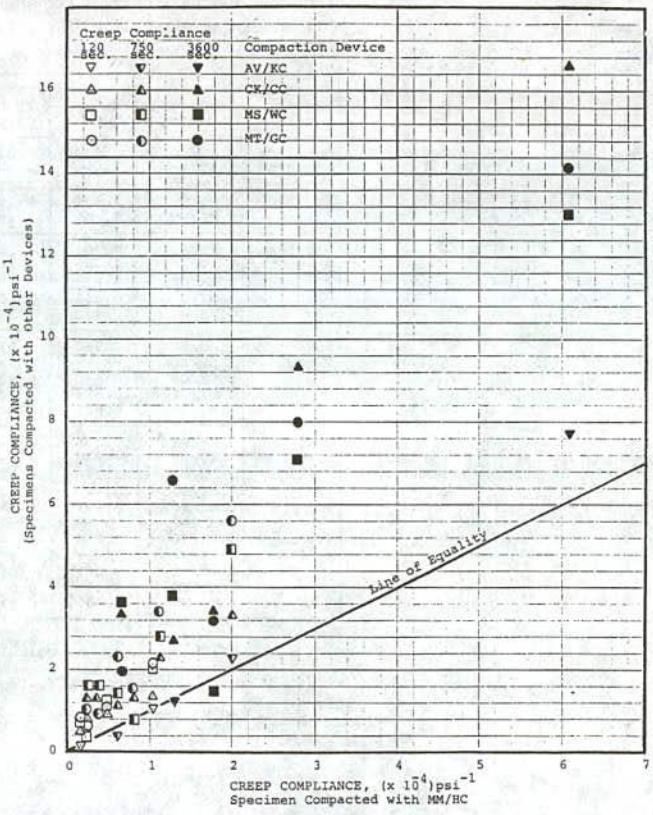

Figure 54. Comparison of creep compliance values measured at different times on specimens compacted with different laboratory devices.

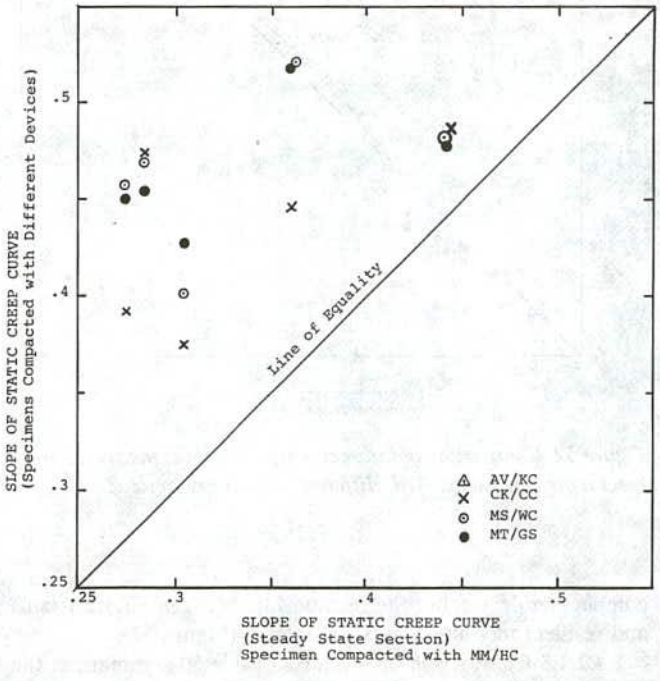

Figure 55. Comparison of the slopes of the creep curves measured under static load on specimens compacted with different laboratory devices.

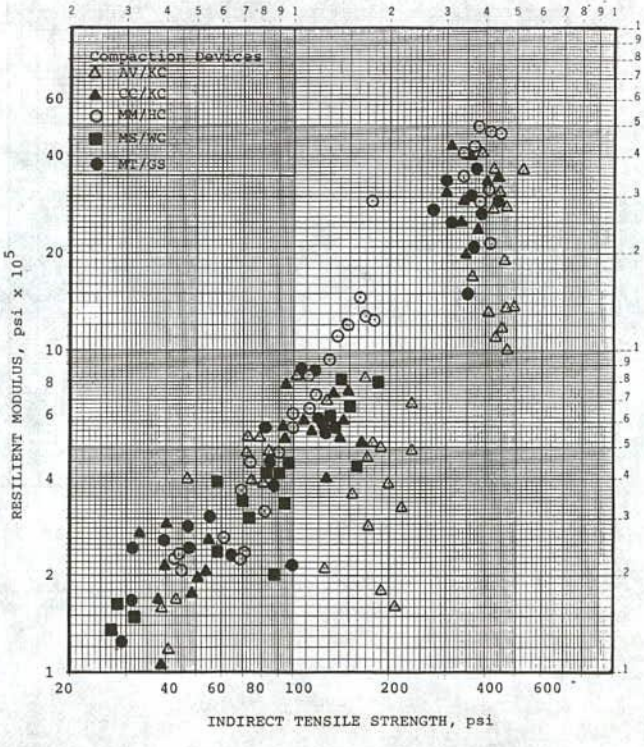

Figure 56. Relationship between indirect tensile strength and repeated load resilient modulus of laboratory compacted specimens.

Table 30. Summary of indirect tensile strength and resilient modulus test results for all mixtures.

Designation Mixture	Test Temp., F	Mean Air Voids, %	Indirect Tensile Strength, psi Mean	COV	Instantaneous Resilient Modulus, ksi Mean	COV	Strain at Failure Mils/In. Mean	COV
Colorado	41	7.6	361	1.8	1,625	6.4	1.30	20.0
Michigan	41	4.4	356	2.6	2,217	34.2	4.68	---
Texas	41	9.2	296	7.5	2,856	14.6	1.13	35.1
Virginia	41	6.3	394	6.2	3,048	20.4	2.77	47.2
Wyoming	41	6.1	398	27.0	2,062	74.2	0.95	15.7
California	41	6.3	480	8.8	3,867	6.3	1.89	24.4
Georgia	41	6.5	423	16.7	2,606	5.2	2.98	6.9
New York	41	6.3	307	24.1	2,449	10.5	4.62	12.9
Wisconsin	41	6.2	359	8.9	2,407	10.1	4.65	4.6
Colorado	77	8.7	100	3.2	510	27.1	15.40	15.7
Michigan	77	4.2	84	2.1	483	20.7	14.56	6.2
Texas	77	8.3	129	5.7	601	2.7	9.01	8.8
Virginia	77	6.2	114	9.3	759	20.5	7.97	3.8
Wyoming	77	6.0	143	3.7	656	12.7	6.40	28.3
California	77	6.3	243	6.8	1,693	4.0	5.58	6.0
Georgia	77	6.1	125	19.5	816	21.0	7.28	33.3
New York	77	6.3	79	5.3	385	15.3	14.05	12.6
Wisconsin	77	6.2	112	4.7	568	13.4	9.89	22.5
Colorado	104	7.2	30	23.6	215	28.5	16.38	47.2
Michigan	104	4.1	30	3.9	178	35.4	16.30	1.8
Texas	104	9.1	44	9.1	263	8.2	15.69	10.7
Virginia	104	6.0	74	31.5	250	26.0	10.40	10.0
Wyoming	104	6.6	56	21.5	237	10.4	10.14	3.6
California	104	7.1	83	4.7	702	7.9	16.52	15.1
Georgia	104	6.1	52	18.4	352	42.6	10.48	25.3
New York	104	6.5	23	13.6	118	20.0	24.73	15.4
Wisconsin	104	4.8	45	15.7	164	19.3	10.79	29.8

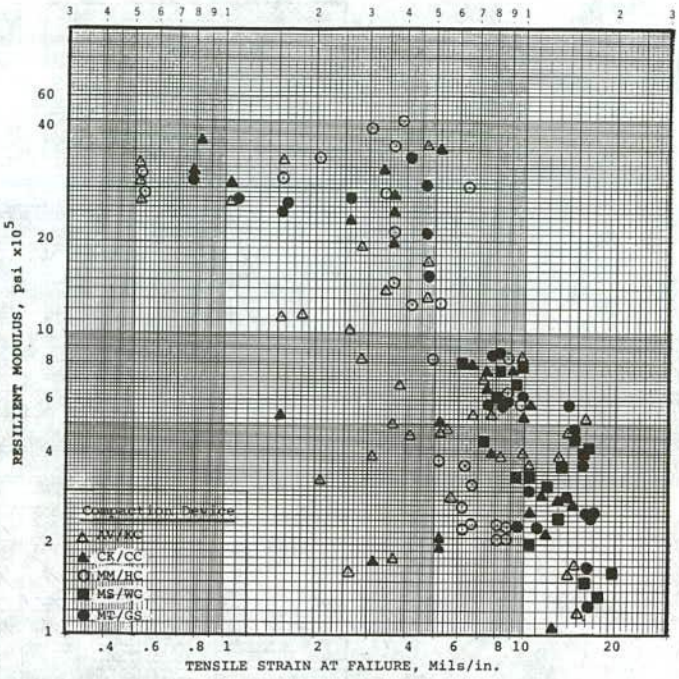

Figure 57. Relationship between tensile strain at failure and repeated load resilient modulus of laboratory compacted specimens.

Table 31. Summary of uniaxial compressive strength test results of all mixtures.

Mixture Designation	Test Temperature F	Mean Air Voids %	Unconfined Compressive Strength, psi Mean	COV	Instantaneous Resilient Modulus, ksi Mean	COV	Strain at Failure Mils/In. Mean	COV
Colorado	77	4.5	946	4.4	909	22.5	28.03	14.8
Michigan	77	1.3	939	2.9	566	19.8	35.18	8.4
Texas	77	4.5	1,744	5.9	741	25.6	25.42	3.7
Virginia	77	4.6	1,109	6.3	690	11.8	36.29	2.1
Wyoming	77	2.6	1,061	2.8	1,457	22.7	17.25	32.8
California	104	5.3	370	7.6	2,310	20.4	18.80	26.1
Georgia	104	3.7	155	29.3	719	84.2	22.28	11.4
New York	104	1.5	110	3.9	916	85.6	17.35	2.6
Wisconsin	104	1.6	165	14.6	459	54.5	23.76	7.6

Table 32. Summary of uniaxial compression creep test results of all mixtures.

Mixture Designation	Test Temp., F	Mean Air Voids %	Creep Curve Intercept Slope	(Mils./In)	Creep Modulus @ 3,600 sec., ksi	Percent Recoverable Creep, %
Colorado	77	4.4	0.240	1.13	12.5	18.8
Michigan	77	1.3	0.302	0.14	10.4	23.6
Texas	77	4.5	0.342	0.104	13.4	13.5
Virginia	77	4.6	0.224	0.328	18.4	37.4
Wyoming	77	2.6	0.295	0.498	15.6	25.5
California	104	5.3	0.333	1.97	20.3	15.4
Georgia	104	3.7	0.249	2.39	8.0	29.4
New York	104	1.5	0.279	2.32	3.3	14.8
Wisconsin	104	1.6	0.366	2.35	3.0	20.9

mix is the strongest and stiffest, whereas the Michigan and New York mixtures are the more flexible. None of the indirect tensile properties discussed earlier indicate that the California, Georgia, New York, and Wisconsin mixes would be inferior to the other mixtures tested. It should be noted, however, that the mixtures used in the field test sections (the first five mixes) may also be susceptible to premature distress under heavy traffic. Thus, it may be inappropriate to make a one-to-one comparison of properties between the field sections and those mixtures that are supposed to have inferior performance characteristics.

Figures 58 and 59 provide a comparison of the mean material property relationships between the different mixtures compacted with the same laboratory device (MT/GS). As shown, all mixtures have the same type of relationship.

2.4.2.2 Uniaxial Compression Properties

Unconfined compressive strengths and one-dimensional compressive creep tests were also performed on laboratory compacted specimens. Unconfined compressive strengths and uniaxial resilient moduli data are provided in Appendix I and the compressive creep data in Appendix N. These two properties were not measured on the cores because the lifts were too thin. Thus, they were not used in any of the comparisons between field cores and laboratory compacted specimens. Tables 31 and 32 give the average values measured for each of the mixtures tested. Uniaxial compression test results will be discussed in greater detail in section 2.5.3.

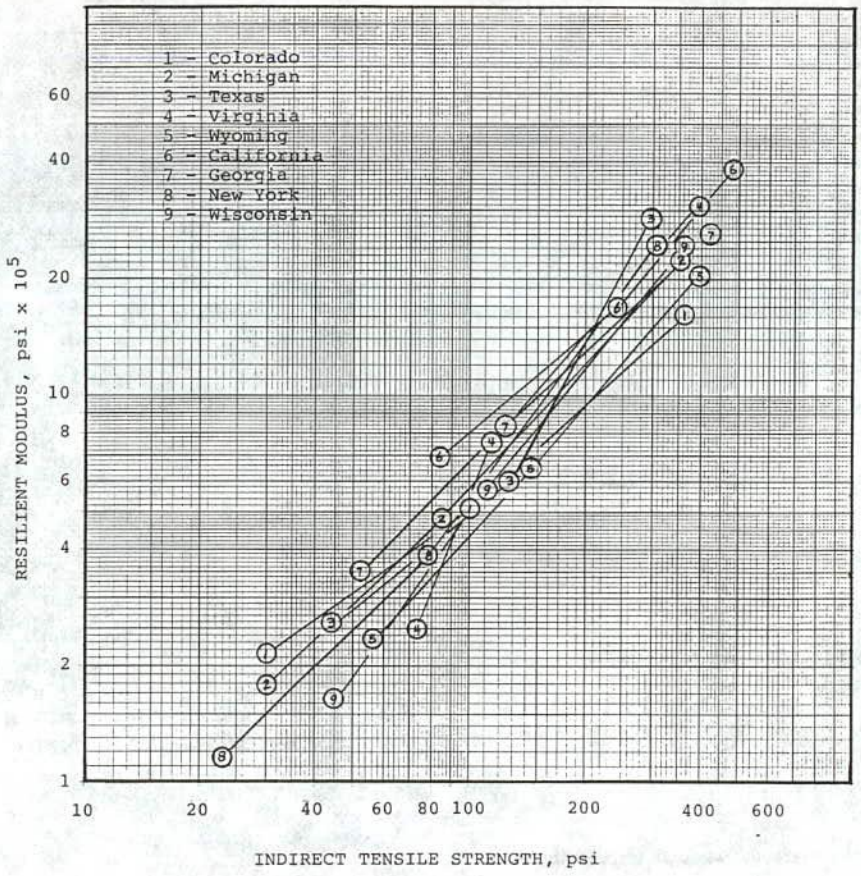

Figure 58. Comparison of indirect tensile strength versus resilient modulus for the nine different mixtures.

2.4.3 Effects of Storage Time

The time from sampling the material on site to preparing specimens in the laboratory, in some cases, exceeded one month. This brings up the question of whether properties of the mixture components changed significantly, and if so, could this change have an effect on the engineering properties of the field cores and laboratory compacted specimens? Therefore, both asphalt cement and gradation tests were performed at various points in the production and testing process.

2.4.3.1 Asphalt Aging Characteristics

One of the important factors in determining how properties of an asphaltic concrete mixture will vary with time is the hardening of the asphalt cement. Specifically, as the mixture is reheated in the laboratory during recompaction, the asphalt cement hardens, which has some effect on the strength and creep properties. These differences become extremely important when making comparisons between data sets that have been compacted at different points in time. To determine if the asphalt cement could be causing consistent differences of test results between cores and laboratory compacted specimens, asphalt was recovered from both cores and laboratory compacted specimens at various points in time.

Both viscosity and penetration tests were performed on the recovered asphalt. These data are summarized in Table 33. The data identified as "Before-Construction" were measured from samples of the "virgin" asphalt cement (see Table 9). After the bulk material was received in the laboratory, enough material was removed from three containers, selected at random, for extraction tests.

Both penetration and viscosity values of the recovered asphalt were measured for each sample to determine the amount of hardening caused by production and a short storage time. These data are given in Table 33 as "After Production." As may be seen, there was a decrease in penetration and an increase in viscosity as expected, with the exception for the Wyoming mixture, WY-0080. The reason for the lower viscosity is unknown at this time, but was also verified by the Wyoming Department of Transportation which reported similar test values for acceptance testing.

To evaluate any effects on reheating the bulk material for compacting laboratory specimens, additional replicate extraction tests were performed on both cores and laboratory compacted specimens after testing and after one-year of storage. As the reheating process and compaction temperature were the same for

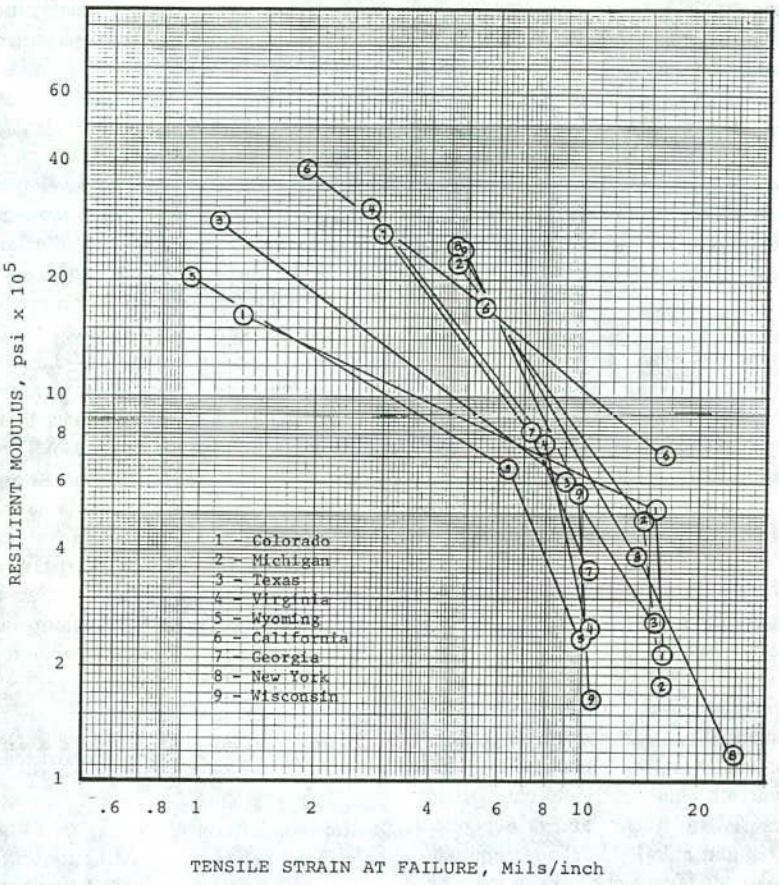

Figure 59. Comparison of tensile strain at failure versus resilient modulus for the nine different mixtures.

all compaction devices for a particular project, only specimens compacted with the Marshall hammer and Texas gyratory shear were used for extraction tests. The reason for using specimens prepared with these two compaction devices was that there was a greater difference in engineering properties (Figures 51 through 55) between these specimens. These data have been summarized in Table 33, and are identified as "After Testing" and "After 1-Year Storage."

From the penetration data, asphalt recovered from the TX-0021 laboratory specimens, after testing, were found to have a much lower penetration value than for the field cores after testing. However, only the Virginia material was found to have a significant difference in viscosity between the cores and laboratory compacted specimens after testing. In summary, there are differences, as expected, but there does not appear to be a consistent difference between the asphalt cement properties of laboratory compacted specimens as compared to field cores.

Even though differences in penetration and viscosity values between cores and laboratory specimens appeared to be minor, the reheating process definitely affected the compactibility or compactive effort required to achieve a certain air void level. For example, for the Virginia material a compactive effort curve was initially established using material that had been removed from one of the 10 gal containers. After the compactive effort curve was determined, unused material was allowed to cool to room temperature. This material was then reheated in the oven to the same compaction temperature used to develop the initial

Table 33. Summary of penetration and viscosity data of recovered asphalt.

Time of Test	State/Project				
	Colorado CO-0009	Michigan MI-0021	Texas TX-0021	Virginia VA-0621	Wyoming WY-0080
Type of Asphalt	AC-10	85-100	AC-20	AC-20	AC-20
PENETRATION DATA					
Before Const.	85	127	57	91	65*
After Production	44	107	47	68	-----
After Testing:					
Core	---	61	36	52	-----
Specimen - G	---	60	30	37	-----
Specimen - M	---	67	27	53	-----
After 1-Year Storage:					
Core	35	67	52	54	46
Specimen -G	44	53	38	84	65
Specimen - M	---	75	30	78	-----
After 2 Years on Roadway	30	85	21	41	55
VISCOSITY DATA					
Before Const.	1071	806	1896	2250	2306* 2649**
After Production	1195	1013	2568	3489	2089
After Testing:					
Core	---	2166	3698	4194	-----
Specimen - G	---	2144	4388	9255	-----
Specimen - M	---	1772	4470	6000	-----
After 1-Year Storage:					
Core	4918	2734	3131	6452	3341
Specimen -G	3567	3687	7848	4407	2789
Specimen - M	---	2092	6887	4106	-----
After 2 Years on Roadway	3490	1318	6453	6458	3713

M = Marshall Specimen
G = Gyratory Specimen
* = Virgin Asphalt
** = Extractions of RAP Material

compactive effort curve. Specimens were then recompacted using various number of blows of the Marshall hammer to determine the effect of reheating on the number of blows required to match the field air voids. As expected, additional compactive effort was required to obtain the same level of air voids from the initial compactive effort curve. Approximately 10 to 15 percent additional compactive effort was required after reheating. Thus, after material had been removed from the containers, reheated, and allowed to cool, it was not reused in any of the compaction studies.

2.4.3.2 Aggregate Degradation

Aggregate degradation is defined as the breakdown (grinding and/or fracture) of coarse aggregate particles into small particles through the physical process of laboratory and field compaction. Although aggregate degradation is not considered to be a distress, it can significantly increase raveling and water absorption (moisture damage). Goetz and Moavenzadeh (*57, 58*) among others have studied this factor both in the laboratory and the field to determine its impact on pavement performance and how changes in gradation, caused by plant production, affects mixture design properties.

Degradation can occur during various parts of the construction process. These include stockpiling, transporting the material from the stockpile to the mixing drum, movement of the aggregate through the asphalt concrete plant, and field compaction. Degradation can also be caused by traffic, and is dependent on the tire inflation pressures and axle loads. Thus, aggregate degradation is another property that must be considered when comparing and evaluating mixture properties.

Materials were sampled at various points during the construction process to determine if significant changes of the gradations were occurring at various points in the construction sequence. Using bulk material that was sampled from trucks after production, sieve analyses were performed on the aggregates from extraction tests. These test results have been discussed and summarized in Appendix C. Sieve analyses were not performed on extractions conducted on the field cores, because the coring operation cuts a significant portion of the coarse aggregate and block samples were not taken.

Sieve analyses were performed on the aggregate recovered from laboratory compacted specimens during the mix design process. These gradations have been summarized in Appendix E for each mixture. In summary, there is no detectable difference that can be attributable to aggregate degradation between compaction in the laboratory, as compared to production of the mix through the plant. It should be noted that the L.A. abrasion values for these aggregates were less than the maximum value specified (40 percent) by ASTM D-692, "Coarse Aggregate for Bituminous Paving Mixtures." L.A. abrasion values were obtained from state highway agency personnel, or construction records, in all cases.

2.4.4 Mixture Performance Predictions

Most of the mechanistic models given in Table 6 use similar engineering properties—such as Poisson's ratio, resilient moduli, tensile strength, and fatigue coefficients. The key requirement of AAMAS is that it use or produce material and engineering properties that are considered significant to the input parameters for the structural design of pavements.

One of the more common design procedures used by most state highway agencies is in the AASHTO Design Guide. The new AASHTO design guide uses resilient modulus which has been previously discussed in some detail. The objective of NCHRP Project 1-26 is to develop mechanistic models or equations that can be used to evaluate and design asphaltic concrete pavements. Thus, it is critically important that AAMAS and NCHRP Project 1-26 be tied closely together.

NCHRP Project 1-26 was in progress during the 9-6(1) study, so the mechanistic procedures were unavailable to be initially incorporated into AAMAS. Therefore, the VESYS IV program was initially used to compare pavement performance predictions (rutting, fatigue cracking, and thermal cracking) for the test results from each of the AAMAS projects. ACOMDAS 2 and 3 were used to predict the moisture damage for each mixture. Results from the moisture damage evaluation are included in Appendix O and discussed in section 2.5; therefore, they are not included in this section of the report. Additionally, as there are no known mechanistic models that can be used to predict disintegration (raveling, flushing, and loss of skid resistance), that is not discussed in this section of the report.

2.4.4.1 Rutting and Permanent Deformation

The VESYS IV program was used to predict rutting (one-dimensional consolidation) as a function of time or traffic for each of the mixtures. Although different values can be used to evaluate rutting, alpha and gnu are the properties required by VESYS IV. Thus, those values identified in Appendix M were used for this comparative study.

All mixtures were predicted to develop relatively high to severe levels of rutting under moderate traffic levels (3 million ESAL's within 20 years) because of the low alpha values (Figure 47) measured from permanent deformation tests. The following summarizes those predictions based on permanent deformation properties using indirect tensile testing techniques:

RUT DEPTHS PREDICTED AT 10 YEARS BASED ON CHANNELIZED TRAFFIC; I.E., NO LATERAL DISTRIBUTION, INCHES

	TYPE OF ENVIRONMENT	
PROJECT	COLD (MICHIGAN)	WARM (AUSTIN)
CO-0009	> 5	> 5
MI-0021	1.4	1.6
TX-0021	1.1	1.2
VA-0021	0.5	0.6
WY-0080	0.6	0.6

Gyratory shear values are another measure of shear strength and indirectly a measure of lateral flow. The gyratory shear stress values for each of the mixtures under the traffic densification process are discussed in section 2.5, and indicate significant shear reductions in the CO-0009 and TX-0021 mixtures; moderate reductions for the MI-0021 and WY-0080 mixtures; and no change in the VA-0621 mixture.

2.4.4.2 Fatigue Cracking

Fatigue tests were not performed in this study, simply because of the time requirement and typical variations associated with fatigue tests. Instead, the relationship between the fatigue coefficients (K_1 and K_2), temperature and resilient moduli, which Rauhut et al. (*9*) recommended for use, was used for predicting the amount of fatigue cracking for each mix. The K_1 and K_2 coefficients and the VESYS IV program were then used to compare each mixture in terms of fatigue cracking. The following summarizes the year at which the damage index (amount of fatigue cracking) exceeds 1.0:

YEARS PREDICTED TO FATIGUE CRACKING

	TYPE OF ENVIRONMENT		
PROJECT	COLD (MICHIGAN)	MODERATE (VIRGINIA)	WARM (AUSTIN)
CO-0009	12	7	5
MI-0021	10	5	3
TX-0021	8	7	6
VA-0621	20+	20	12
WY-0080	18	11	7

Using the Rauhut et al. (*9*) fatigue relationship or the relationship developed by Finn et al. (*10*), it was found that the lower the resilient modulus, the more fatigue damage per 18-kip equivalent single axle load. Thus, the mixes with higher resilient moduli (VA-0621) should have a longer fatigue life than those mixes with lower resilient moduli (MI-0021). As shown above, the VA-0621 mixture had the better fatigue characteristics and the MI-0021 mix the poorest, as predicted by VESYS IV. This statement is only valid, of course, if the fatigue coefficients are directly related to resilient modulus.

2.4.4.3 Thermal Cracking

A pavement analysis computer program developed at the University of Florida, entitled "CRACK3," was used to evaluate the combined effects of thermal and load stresses. The pavement section was purposely selected to produce high stresses at the lower temperatures, because the results are for comparative purposes only. They do not relate to the structural support provided by layers other than the asphaltic concrete on the five projects. Thermal stresses were assumed to be low primarily because the pavement cooling was stopped at 32°F in performing the CRACK3 analyses. However, the differences between asphalts in load stresses, stress ratio, and fracture energy ratio make it apparent that the crack resistant ranking of the different asphalts are:

Michigan—most resistant
Virginia
Colorado and Texas
Wyoming—least resistant

Although these analyses and comparisons are indicative of low temperature behavior of the mixtures, there are other key factors that must be included in any thermal/fatigue cracking analysis to realistically represent pavement cracking potential. Layer thicknesses and layer moduli for each project including variations in moduli (e.g., caused by subgrade moisture variations) and wheel loading characteristics (e.g., overloads, high tire pressures, etc.) are essential to define load-induced stresses. The rate of cooling or cooling curve is critical in evaluating thermal contraction stresses and may have a more substantial effect on applied energy than on load stress applications.

Prior analysis of the six Penn DOT test road sections by Ruth at the University of Florida illustrated that a rapid rate of cooling over a short time period at a sufficiently low temperature (high asphalt viscosity) would increase stresses and energy, rapidly resulting in fracture energy ratios increasing from the 0.35 range to 1.00 (failure) in 3 to 5°C. Therefore, thermal stressing conditions can not always be appraised by comparing asphalts of different temperature susceptibilities unless one consistently has a greater viscosity throughout the exposure temperature range.

2.4.5 Change in Mix Properties with Time

After 2 years of traffic, each of the original five field projects were recored to evaluate the change in properties with time. Indirect tensile strengths, resilient moduli, tensile strains at failure, and creep tests were performed on cores recovered from each of these test sections after 2 years in service. In addition to the engineering properties, air voids were measured on each of these cores and penetration and viscosity tests were measured on the recovered asphalt.

2.4.5.1 Air Voids

Air voids were measured on all of the cores recovered after two years under traffic. A summary of these results, both means and standard deviations, are presented in Table 34 and compared to the original as-constructed condition. The data are presented for both in the wheelpaths and between the wheelpaths for the 2-year cores. As shown, there is a significant difference between the as-compacted sections and after 2 years of traffic. On the other hand, there is little difference between those cores recovered at 2 years from the location between wheelpaths as compared to those taken in the wheelpaths.

Table 34. Summary of air void data measured on the field cores at different times.

Project Section	Mean Air Void Level, %			Percent Decrease %
	At Construction	2 Years of Traffic Between Wheel Path	2 Years of Traffic In Wheel Path	
CO-0009 VB/SS	8.19	5.76	6.61	19.3
PB/SS	8.98	5.87	6.65	25.9
MI-0021 VB/SS	3.74	2.46	2.20	41.1
PB/SS	4.21	2.76	2.99	29.0
TX-0021 SB/SS	8.75	7.01	7.12	18.6
VB/SS	10.17	9.45	9.30	8.6
VA-0621 VB/SS	5.85	5.25	5.25	10.3
SB/SS	7.44	5.68	6.14	17.5
WY-0080 VB/SS	5.77	4.89	4.42	23.4
PB/SS	8.37	6.59	6.42	23.3

2.4.5.2 Engineering Properties

As stated earlier, the indirect tensile strength, strain at failure, resilient moduli, and creep modulus values were measured for each of the projects after 2-years of traffic. These results are summarized on Tables 35 and 36. In most cases, the indirect tensile strength and resilient moduli increased with time, whereas the tensile strains at failure and creep compliance values decreased, as expected. Figures 60 and 61 provide a comparison between the indirect tensile properties measured on the cores recovered from the two different time periods.

There were a few cases, for example, mixtures CO-0009 and VA-0621, where the indirect tensile strengths actually decreased with time. The aggregates used in both of these mixtures are susceptible to moisture damage from past performance observations. In addition, during construction of the CO-0009 project, the mixture became wet because of rains prior to and during the compaction process.

The most significant change in properties was the decrease in tensile strains at failure of these mixtures at a test temperature of 77°F. A comparison of the test results between the two time periods is provided Figure 61. In summary, there was only a small change in failure strains at 41°F, but a dramatic decrease at 77°F. At a test temperature of 104°F, the failure strains decreased on the average of about 20 percent. Those mixtures that resulted in the greatest change with time were those with the higher air voids and aggregates with higher absorptions. It is expected that the magnitude of change of the indirect tensile strains at failure with time are related to asphalt aging and absorption.

Table 35. Comparison of indirect tensile strength test results for cores recovered at different times.

State/ Project	Section	Temp. (F)	Instantaneous Resilient Modulus, ksi Const. Cores	Instantaneous Resilient Modulus, ksi 2-Year Cores	Indirect Tensile Strength,psi Const. Cores	Indirect Tensile Strength,psi 2-Year Cores	Tensile Strain @ Failure Mils./in. Const. Cores	Tensile Strain @ Failure Mils./in. 2-Year Cores
Colorado CO-0009	1-VB	41	1,625	3,715	361	358	1.30	1.50
		77	583	577	90	70	15.40	1.17
		104	329	279	30	25	16.38	11.54
	2-PB	77	460	670	88	77	13.17	1.13
Michigan MI-0021	1-VB	77	420	804	84	89	15.17	5.94
	2-PB	41	2,379	1,796	382	283	4.51	5.64
		77	456	444	90	87	14.56	5.90
		104	168	157	34	32	13.70	8.79
Texas TX-0021	1-SB	41	4,480	4,156	316	486	1.21	0.88
		77	1,287	1,489	119	249	9.01	2.18
		104	242	434	33	75	11.01	9.56
	2-VB	77	709	1,116	106	196	11.23	1.66
Virginia VA-0621	1-VB	41	3,449	2,139	424	429	2.38	1.68
		77	925	1,245	224	183	6.96	1.48
		104	252	357	99	58	3.45	8.70
	2-SB	77	504	876	184	113	11.51	1.59
Wyoming WY-0080	1-VB	41	2,062	3,267	398	477	0.95	1.19
		77	707	1,086	143	184	6.40	1.39
		104	204	311	56	62	10.14	9.13
	2-PB	77	197	487	103	141	5.29	1.47

Table 36. Comparison of the indirect tensile creep test results from cores recovered at different times.

Project	Slope of Curve Const. Cores	Slope of Curve 2-Year Cores	Load Time, Sec.	Creep Modulus, ksi Const. Cores	Creep Modulus, ksi 2-Year Cores
CO-0009	0.535	0.553	10	20.2	25.0
			100	5.5	7.4
			1,000	---	---
MI-0021	0.363	0.395	10	9.6	11.2
			100	3.4	5.0
			1,000	1.0	1.7
TX-0021	0.633	0.550	10	59.8	128.6
			100	10.7	34.5
			1,000	1.9	9.1
VA-0621	0.391	0.490	10	20.1	110.0
			100	6.6	37.8
			1,000	2.2	11.5
WY-0080	0.412	.602	10	64.6	365.8
			100	15.5	97.5
			1,000	4.8	25.4

2.4.5.3 Material Properties

After each of these cores was tested, asphalt and aggregate were recovered from the test specimens. Penetrations and viscosity tests were performed on the recovered asphalt, and a sieve analysis was performed on the aggregate sample. The penetration and viscosity data are summarized in Table 33, as compared to the original values after production. As shown, there was a decrease in penetration and an increase in viscosity for all mixtures, as expected. The MI-0021 and WY-0080 mixtures had the least change in values with time, whereas the CO-0009 and TX-0021 mixes had the greatest change in values. The CO-0009 and TX-0021 sections have the higher air voids.

Results of the gradation tests are provided in Appendix C, as compared to the original values measured during construction. In summary, all mixtures were found to have a slight increase in percent passing each sieve. The TX-0021 mixture had the greatest change in gradation (increase in finer materials), whereas the VA-0621 mixture had the least change in gradation. The coarse aggregate used in the TX-0021 mix is a crushed limestone and susceptible to some degradation with time.

2.5 MIXTURE CONDITIONING

Another important question facing pavement and bituminous engineers today is, how does one simulate in the laboratory 10 to 20 years of traffic and time to determine their effects on the mixture's behavior and performance? Traffic and environmental conditioning can be subdivided into three areas: (1) moisture damage, (2) age-hardening (both plant and long-term environmental aging), and (3) traffic densification.

Each of these areas has received some study to establish guidelines and procedures to be used during mixture design. Historically, these three areas have been considered separately or as independent occurrences. Of course, under actual conditions, all three occur simultaneously in the field, and one may severely compound the effects of another. As an example, age hardening of the asphalt cement can significantly increase the moisture damage of a mixture under traffic loads. Each area is discussed below in more detail, as related to the test results for the AAMAS test sections.

2.5.1 Moisture Conditioning

Moisture damage testing on each mixture was done in accordance with AASHTO T283, "Resistance of Compacted Bituminous Mixture to Moisture Induced Damage." The procedure suggested for use by Lottman in NCHRP Report 246 (*59*) was

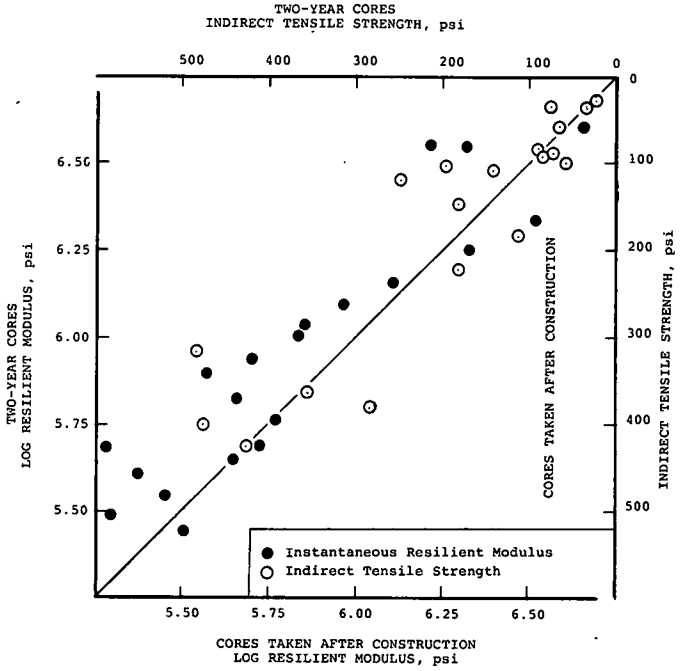

Figure 60. Comparison of instantaneous resilient modulus and indirect tensile strength measured on cores recovered from different time periods.

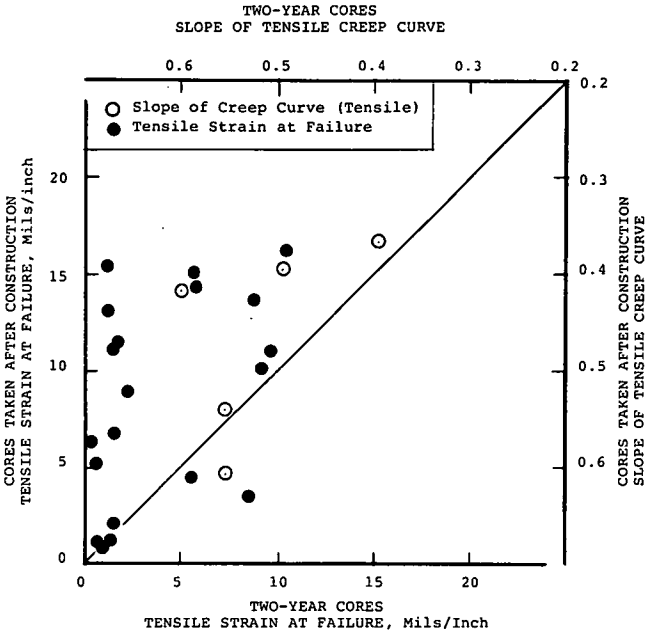

Figure 61. Comparison of tensile strain at failure and slope of the indirect tensile creep curve measured on cores recovered from two different time periods.

also used on the first five mixtures or those included in the field compaction study. The procedure suggested for use by Tunnicliff and Root (*39*) was considered, but not used for the initial moisture conditioning of these specimens. All moisture damage test results are provided in Appendix H.

Specimens conditioned and tested were prepared and compacted in the laboratory using bulk mixture sampled from the trucks (i.e., cores were not used). As for other tests, specimens were designated for testing in the moisture damage study to reduce the effects of air voids on the engineering properties of the mixtures. Only the Wyoming specimens had a sufficiently wide enough air void range to indicate some effect of air voids on the test results. Figure 62 illustrates this condition. However, the air void effect on indirect tensile strengths is still considered minimal.

Figure 63 shows the relationship between indirect tensile strength and resilient moduli for each of the mixes tested. As shown, this relationship is similar to the test results of unconditioned samples (Figure 56). It is also interesting to note that the same relationship was found for both the dry and wet conditions (unconditioned versus moisture-conditioned specimens). Moisture seemed to have little to no effect on the relationship between resilient modulus and indirect tensile strength. The only difference in data noted for this type of relationship (besides mixture differences) was found for the different loading rates used between the two procedures. This difference caused by different loading rates was expected. The effect of loading rate is discussed in a later section, 2.6.4, of this chapter.

Moisture damage potential can be evaluated by different factors, including percent stripping, moisture content susceptibility (full versus partial saturation), mechanical property ratios (tensile strength ratio and resilient moduli ratio), and predicted field wet life as compared to a theoretical all-dry life. Table 37 summa-

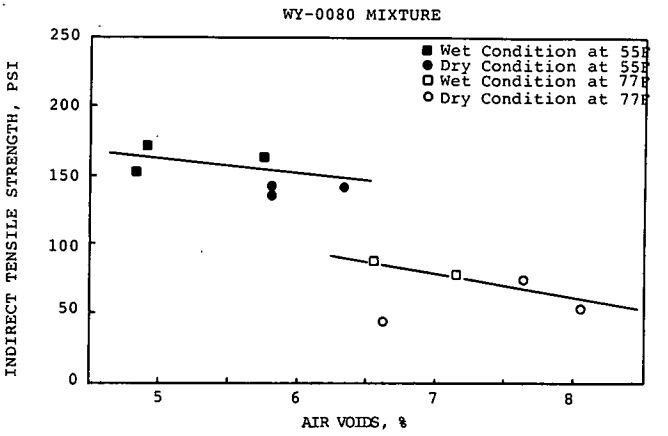

Figure 62. Effect of air voids on indirect tensile strength after moisture conditioning the WY-0080 mixture.

rizes the moisture damage susceptibility findings. Both the wet and dry life of these materials were predicted by the ACMODAS 2 and 3 programs (developed at the University of Idaho), and these results are provided in Appendix O. ACMODAS 2 is for cracking predictions and ACMODAS 3 is for rutting.

2.5.1.1 Comparison of Conditioning Procedures

Figures 64 and 65 show a comparison of percent stripping and indirect tensile strength ratio (TSR) and resilient modulus ratio (MRR) measured using both AASHTO T283 and the NCHRP

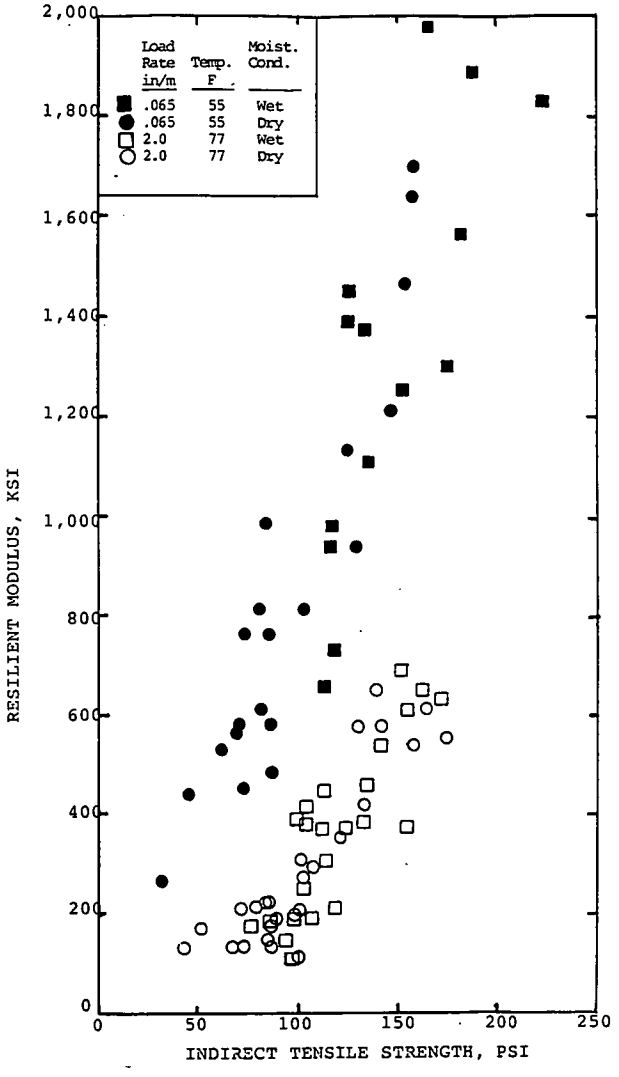

Figure 63. Relationship between indirect tensile strength and resilient modulus for different moisture conditioning tests.

Project 4-8(3) procedure (NCHRP Report 246). As shown, the Lottman moisture conditioning procedure is much more severe than the procedure specified in AASHTO T283. Poor correlation was found between percent stripping and the TSR or MRR value when using either conditioning procedure (Figure 66). However, the TSR ratio calculated from the NCHRP Report 246 conditioning procedure seemed to be more closely correlated to percent stripping.

Three of the initial five AAMAS projects (CO-0009, VA-0621, and WY-0080) contained some type of additive or modifier (see Table 38). MI-0021 and TX-0021 were the two mixtures without additives or modifiers, because severe stripping has not been observed with the use of these aggregates. Conversely, historical experience with the CO-0009, VA-0621, and WY-0080 mixtures suggests that moisture damage or stripping is the reason why additives were added to these mixes.

To evaluate any change in moisture damage susceptibility in these mixtures without additives, identical specimens (same gradation, asphalt content, and air voids) were prepared in the laboratory, with the exception that the additive was omitted.

Table 37. Summary of moisture damage evaluation.

STATE/ PROJECT	TEST DESIGNATION	%STRIP	%SWELL	TSR	MRR	WET LIFE
COLORADO	55 FS	12	.18	.65	.73	9.8
CO-0009	77 PS	9	.02	.82	.57	16.3
MICHIGAN	55 FS	38	.19	.70	.67	11.8
MI-0021	77 PS	25	.05	.89	1.03	12.7
TEXAS	55 FS	9	0	.80	.82	11.5
TX-0021	77 PS	1	.13	1.16	1.06	23.2
VIRGINIA	55 FS	2	.35	.88	.89	12.9
VA-0621	77 PS	0	.08	1.02	.92	27.0
WYOMING	55 FS	15	.03	.85	1.00	9.9
WY-0080	77 PS	12	.08	.86	.92	11.6
CALIFORNIA	77 PS	32	---	.61	.69	9.3
GEORIGA	77 PS	0	---	.98	1.16	11.8
NEW YORK, RASON MIX	77 PS	0	---	1.06	.94	14.2
WISCONSIN	77 PS	9	---	1.02	.64	11.4

Notes:
1. 55 FS means a test temperature of 55°F at full saturation; 77 PS means a test temperature of 77°F at partial saturation.
2. Wet life is the relative field performance life, and is to be compared to a 15 year, theoretical, all-dry field life.
3. TSR = Tensile Strength Ratio between wet and dry values.
4. MRR = Resilient Modulus Ratio between wet and dry values.

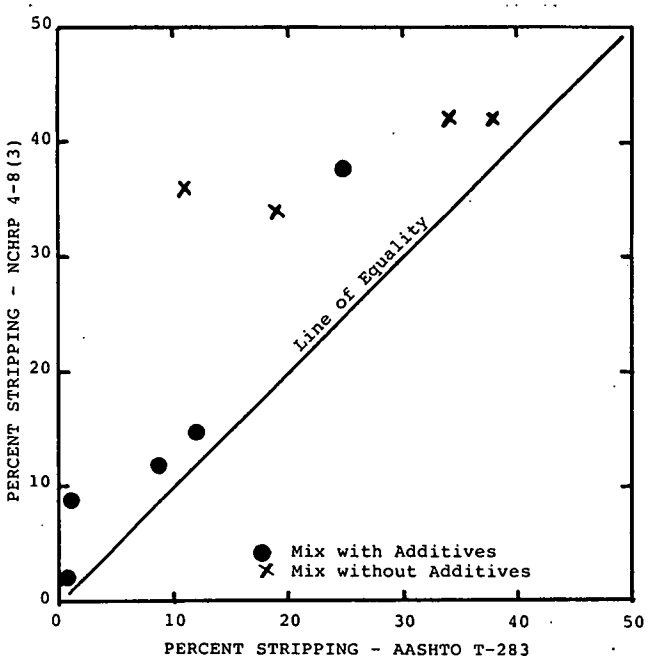

Figure 64. Comparison of percent stripping values from different moisture conditioning procedures.

These additional specimens were conditioned and tested using the same procedures as those specimens prepared with the additives. These test results are provided in Appendix H, and Table 38 summarizes the TSR and MRR values calculated for each condition. As summarized, AASHTO T283 is the least damaging conditioning procedure, both with and without the additives. A larger difference between the TSR and MRR values was found when using the NCHRP Report 246 conditioning procedure between the same mixes, but with and without the additives.

Similarly, there is a greater consistent difference between the wet and dry condition (smaller TSR and MRR values) when using the NCHRP Report 246 conditioning procedure (Table

Table 38. Comparison of TSR and MRR values using different conditioning procedures on mixtures with and without additives.

Moisture Damage Value	Moisture Conditioning Procedure	Additive Used	Mixture Designation		
			CO-0009	VA-0621	WY-0080
TSR	T283	Yes	.81	1.02	0.86
		No	.80	0.72	0.68
MRR		Yes	0.57	0.92	0.92
		No	0.58	0.69	0.95
TSR	Rpt. 246	Yes	0.65	0.88	0.85
		No	0.51	0.41	0.46
MRR		Yes	0.73	0.89	1.00
		No	0.36	0.29	0.45

Table 39. Summary of failure strains measured on the moisture conditioned specimens.

Mixture	Failure Strain, Mils./In.		Moisture Damage Ratios*		
	Unconditioned	Moisture Conditioned	FSR	TSR	MRR
California	7.43	5.65	.76	.61	.69
Georgia	7.60	4.60	.61	.98	1.16
New York	13.70	10.60	.77	1.06	.94
Wisconsin	8.40	8.77	1.04	1.02	.64

* FSR = Failure Strain Ratio
TSR = Tensile Strength Ratio
MRR = Resilient Modulus Ratio

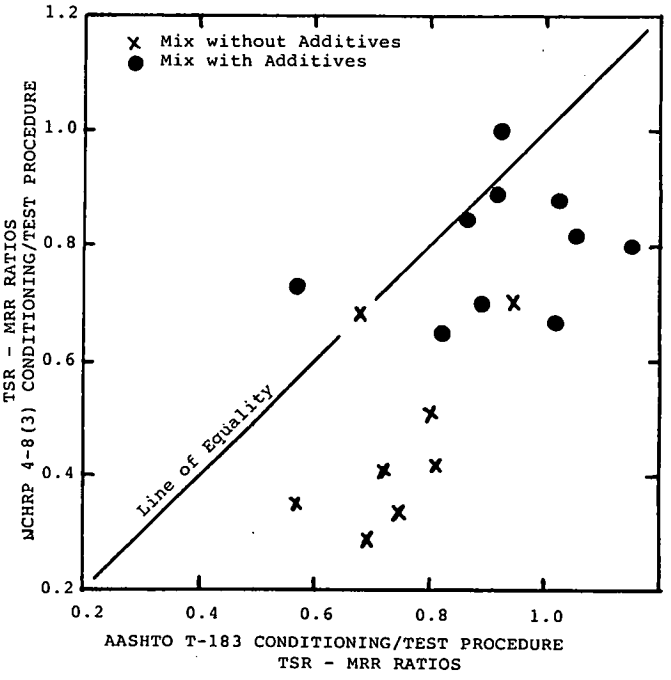

Figure 65. Comparison of test procedures for mixtures with and without additives.

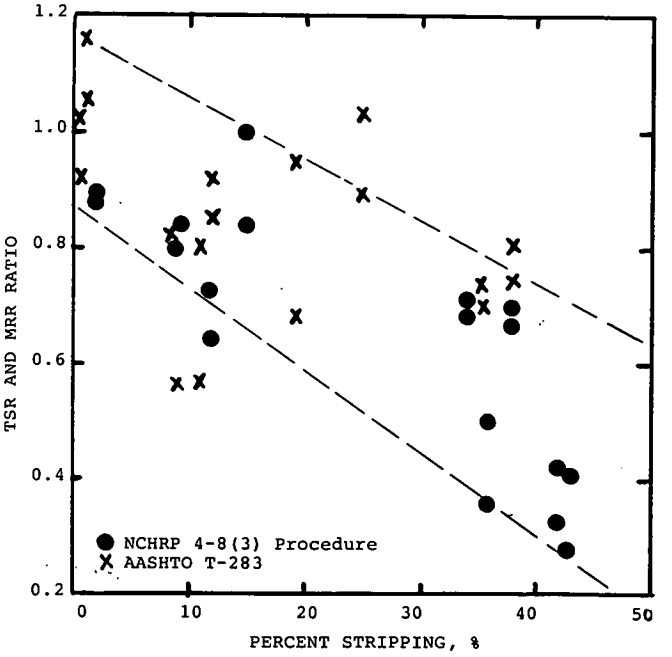

Figure 66. Relationship between percent stripping and the strength (TSR) and resilient moduli (MRR) ratios.

37). However, there are some differences of opinion in the industry regarding the severity of this conditioning procedure. It has been suggested that NCHRP Report 246 is an extreme procedure that may be unduly damaging the specimen prior to testing.

Review of the TSR and MRR values in Table 37 for the NCHRP Report 246 conditioning procedure (55 FS) indicates some moisture damage of all mixtures, but experience with the MI-0021, TX-0021, and VA-0621 (with antistripping additive in the Virginia mix) mixtures would indicate only minor moisture damage, especially for the Texas mixture. Use of the AASHTO T283 procedure for these same mixtures indicates only slight to minor stripping. Thus, the procedure documented and described in AASHTO T283 was used to identify those mixtures that are susceptible to changes caused by moisture.

2.5.1.2 Moisture Damage Potential of Mixtures

The procedure described in AASHTO T283 was used to evaluate the moisture damage potential of these mixtures. Analysis of the data in Appendix H and summarized on Table 37 indicates that the California mix shows the most dominate moisture damage of all the mixes tested. The California and Michigan mixtures have the greater percent stripping, but both the Colorado and Wyoming mixes also show signs of stripping and moisture damage. The Texas mix shows the least moisture damage of all mixtures tested.

The ACMODAS 2 and 3 programs were used to evaluate the relative moisture damage of all mixtures tested. These results are provided in Appendix O. In summary, the relative moisture damage of these mixtures using AASHTO T283, in decreasing order, is as follows.

Severe Moisture Damage	Moderate Moisture Damage	Low to No Moisture Damage
California	Wyoming	Virginia
Wisconsin	Michigan	New York
Colorado		Georgia
		Texas

The strains at failure were also recorded during the indirect tensile strength test, but only for the four mixtures that were added to the study. These failure strains measured on the unconditioned and moisture conditioned specimens are listed in Appendix H, and the average values in Table 39, along with the failure strain ratio (FSR). The FSR value is calculated in the same manner as the TSR and MRR values.

As shown, the failure strain decreased in all cases, with the exception of the Wisconsin mix. This means that after moisture conditioning most mixtures became more susceptible to fracture. Both the Georgia and New York mixtures also had a much greater change in failure strains than for strength and stiffness (i.e., the FSR value is significantly less than the TSR and MRR values). Thus, there was a significant change in at least one property of each mixture. The California mix is most susceptible to moisture damage (cracking, rutting, and raveling). The Wisconsin mix after moisture conditioning is more susceptible to fatigue cracking, and the Georgia and New York mixes more susceptible to fracture and raveling after moisture conditioning than before.

2.5.2 Age Hardening

Asphaltic concrete mixture properties are time-temperature dependent. The temperature-dependent characteristic is related to temperature susceptibility of the asphalt and can be measured directly in the laboratory. Viscosity as a function of temperature was measured for each asphalt, as previously shown in Figure 26. The engineering properties of the mixture can also be measured directly in the laboratory for different temperatures (for example; refer to Figures 40 through 44). The time-dependent characteristic, however, has to be predicted.

One critical factor that affects how properties of the mixture will vary with time is hardening of the asphalt cement. Thus, AAMAS has to be capable of predicting both short and long-term properties of the asphalt cement and mixture. This time effect can be estimated by placing the asphalt cement and compacted mixture in an accelerated weathering test to simulate plant aging, as well as long-term environmental aging. Long term for AAMAS is defined as 10 years.

2.5.2.1 Production Hardening Simulations

One of the questions to be resolved is at what temperature should the asphalt be heated to simulate the hardening that occurs during the production process, prior to compacting laboratory specimens. The two tests commonly used to estimate the approximate change in properties of asphalt during conventional hot-mixing are the thin film oven test (TFOT) and the rolling thin film oven test (RTFOT). The TFOT (AASHTO T179) was used to determine the change in penetration and viscosity values of the asphalts used in the first five AAMAS projects over a temperature range. The TFOT was selected because of similar work being conducted by Ruth (*60*).

Table 40 summarizes the percent penetration retained and absolute viscosity ratio as a function of oven temperature for different asphalts. These test results are graphically presented in Figures 67 through 69. The recovered penetration and viscosity values from extraction tests were used to determine the laboratory oven temperature needed to harden the asphalt so that the penetration and viscosity values of laboratory-aged materials would match those measured from plant-produced materials. As expected, the oven temperature is dependent not only on the type of asphalt, but also on the type of test (penetration versus viscosity measurements.)

Table 40. Summary of asphalt aging test results.

Asphalt Property		State/Project				
		Colorado CO-0009	Michigan MI-0021	Texas TX-0021	Virginia VA-0621	Wyoming WY-0080
Asphalt Supplier & Grade		Sinclair Oil AC-20	Marathon 85-100	Exxon AC-20	Chevron AC-20	Sinclair Oil
Specific Gravity		1.015	1.012	1.025	1.035	1.026
Penetration at 77°F	Original	85	127	57	91	65
	325F-TFOT	51	84	40	54	35[a]
	365F-TFOT	42	67	34	42	37[a]
Retained Penetration (325F)		60.0	66.1	70.2	59.3	54.8(a)
Viscosity at 140°F - Poises	Original	1071	806	1896	2250	2306
	325F-TFOT	2637	1741	3829	6580	5388
	365F-TFOT	4758	2701	5893	14288	10433
Viscosity Ratio	325F-TFOT	2.46	2.16	2.02	2.92	2.34
	365F-TFOT	4.44	3.35	3.11	6.35	4.52
	365F/325F	1.80	1.55	1.54	2.17	1.94

(a) Questionable Results

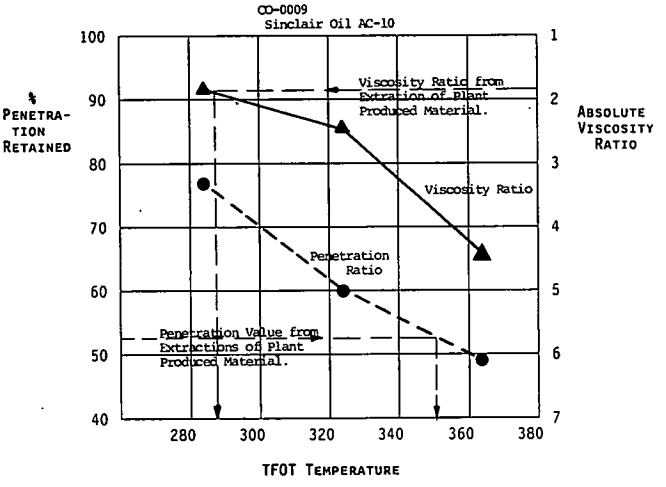

Figure 67. Relationship between oven temperature for the TFOT and percent penetration retained and absolute viscosity ratio for the CO-0009 mixture.

For all practical purposes, however, the TFOT temperature of 285°F appears to do a reasonable job of estimating the percent penetration retained and viscosity ratio of the recovered asphalts after mix production through drum mix plants on the AAMAS

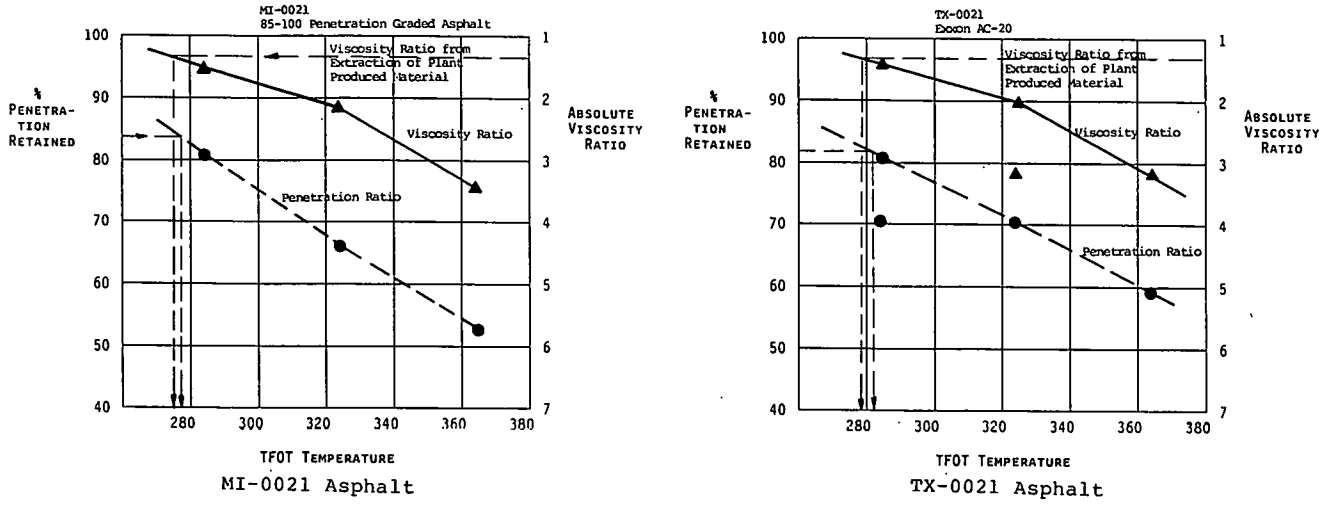

Figure 68. Relationship between oven temperature for the TFOT and percent penetration retained and absolute viscosity ratio for the MI-0021 and TX-0021 mixtures.

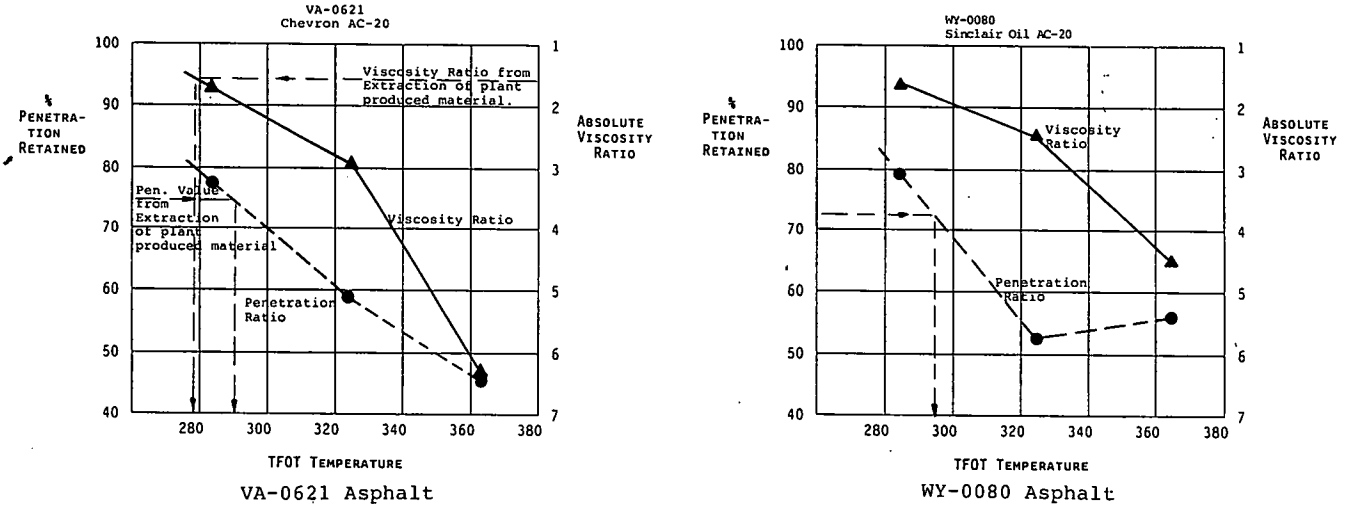

Figure 69. Relationship between oven temperature for the TFOT and percent penetration retained and absolute viscosity ratio for the VA-0621 and WY-0080 mixtures.

projects. It should be noted that plant discharge temperatures were similar for all projects, so only minor differences were expected. If discharge temperatures were different, a different TFOT temperature would likely be required to simulate plant hardening (i.e., below 270°F or above 310°F).

Although the TFOT can be used to simulate hardening of the asphalt during production, an excessive number of tests need to be conducted so that a sufficient amount of asphalt can be aged in the laboratory for mixture design purposes. This becomes somewhat impractical and time consuming. Additionally, hardening the asphalt prior to mixing can affect absorption, depending upon the aggregate characteristics. Therefore, materials were mixed and blended in the laboratory and then placed in an oven to simulate the production process. The temperature used for this production simulation was 275°F.

Samples were placed in a forced-draft oven and removed at various time intervals. These time intervals included 8, 16, and 24 or 36 hours. Figures 70 through 72 illustrate the change in penetration and viscosity values for different times of heating. As can be seen, large variations did occur, but a heating time interval of 3 to 14 hours did reproduce the penetration and viscosity values measured on the recovered asphalts after production. Table 41 summarizes the extended time of heating the loose mixture, in a forced draft oven, to match the penetration and viscosity values measured on asphalt recovered from bulk mix sampled immediately after production.

The CO-0009 and VA-0621 mixtures were found to have significantly greater extended heating times (6.2 to 13.5 hours). These two mixtures are the only ones that contained an antistripping additive. The simulated aging time for the remaining mixtures varied from 1.8 to 4.6 hours of heating.

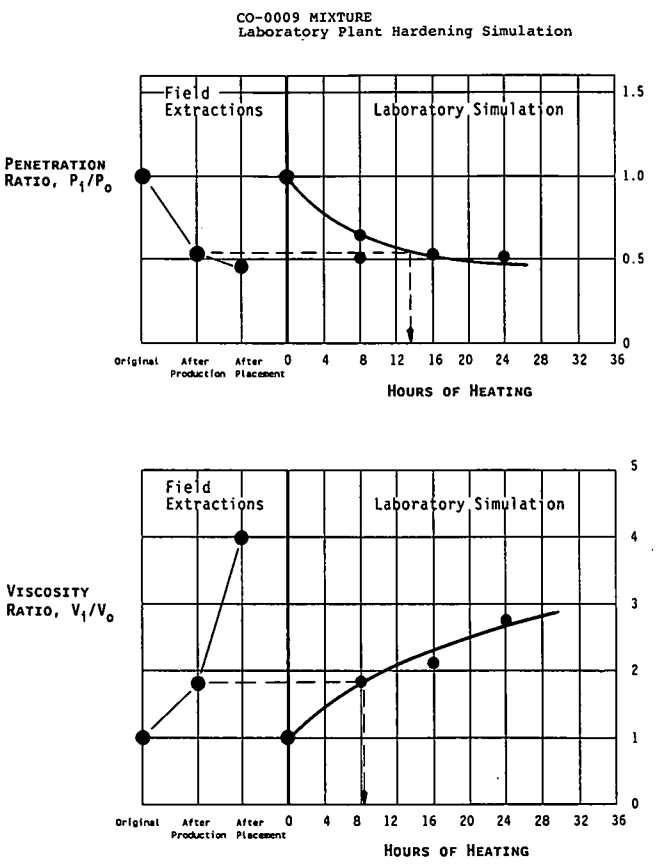

Figure 70. Change in asphalt properties during construction and with different laboratory heating time intervals for the CO-0009 mixture.

2.5.2.2 Long-Term Environmental Aging Simulation

Simulating the environmental aging over a period of time becomes much more difficult. Specifically, extrapolation is required for the AAMAS projects because test results over a period of 5 and 10 years simply do not exist. Therefore, historical data and 2-year cores from the initial five AAMAS projects were used to predict percent penetration and absolute viscosity values with time. These predicted values were then compared to values measured on the extracted asphalts from specimens subjected to different accelerated weathering procedures.

2.5.2.2.1 Laboratory Simulations. Accelerated procedures considered in the test program were initially studied by Chari (*61*) and Ruth (*60*) at the University of Florida. Based on these reports, use of the forced-draft oven appeared to consistently provide the more severe age hardening of various asphalt cements. It should be pointed out, however, that different techniques had varying effects on different asphalts. Regan (*1*) with the Corps of Engineers also recommended that the forced-draft oven be used to simulate 10 years of environmental aging on asphalt cements. Thus, use of the forced-draft oven was initially selected for use in AAMAS.

For the forced-draft oven, two different temperatures and time intervals were used to age laboratory compacted specimens. A set of six specimens was placed in a forced draft oven set at 140°F

Table 41. Comparison of plant simulated aging time in the laboratory using a forced draft oven.

Project	Plant Mix Temp., °F	Simulated Aging Time, Hrs.; Based on	
		Viscosity	Penetration
Colorado, Drum *	280	8.1	13.5
Michigan, Drum	280	3.0	3.5
Texas, Drum	310	4.0	10.5
Virginia, Drum*	280	6.2	11.0
Wyoming, Drum	275	**	**
California, Drum	---	4.6	3.2
California, Batch	280	2.1	1.8
Georgia, Drum	270	2.1	2.0
New York, Batch	285	2.1	2.3
Wisconsin, Drum	275	1.8	2.5

* Designates mixtures which contain anti-stripping additive.

** Penetration values increased and viscosity values decreased from virgin asphalt after plant production, indicating possible contamination.

for 2 days. After 48 hours, three specimens were removed and three were left in the oven for an additional 5 days with the temperature elevated to 225°F. All laboratory compacted specimens were rotated or repositioned in the oven from the fan at the midpoint of the aging process so that consistency of specimen hardening was obtained between the specimens. Ruth (*60*) found that asphalt aging (changes in penetration and viscosity values) varied according to where the specimens were placed in the oven. The specimens closer to the fan were aged more severely than those farthest from the fan.

An additional technique, Oregon's oxygen bomb or chamber (*62*), was considered to simulate environmental aging. A set of three specimens was placed in the oxygen chamber for a period of 5 or 10 days. Five days were used to simulate 5 years of environmental aging and ten days to simulate 10 years.

To evaluate these aging effects on the asphalt cement properties, penetrations and viscosities were measured on the recovered asphalt. These aged values are given in Table 42 for each set of specimens. Both aged and unaged values from Table 33 are included for a direct comparison. In summary, the forced-draft oven caused more hardening of the TX-0021 asphalt; whereas, for the MI-0021 asphalt, the oxygen chamber caused slightly more hardening. For some unknown reason, 5 days in the oxygen chamber hardened the VA-0621 asphalt more than 10 days did.

Figure 73 shows the approximate number of years simulated by each method using a regression equation developed by Shahin (*31*). This relationship was used to predict the penetration values of recovered asphalts with time. As shown, large differences do exist between the projects.

Indirect tensile strengths and repeated load resilient moduli values were measured at 77°F for each specimen used in the laboratory accelerated aging study. The test results are reported in Appendix F and are summarized in Table 41. Use of the forced draft oven resulted in greater indirect tensile strengths and much lower failure strains than use of Oregon's oxygen chamber.

2.5.2.2.2 Comparison to Field Cores. Both penetration and viscosity tests were measured on the recovered asphalts from 2-year cores. Table 33 shows these data as compared to the original values after production. These values are summarized

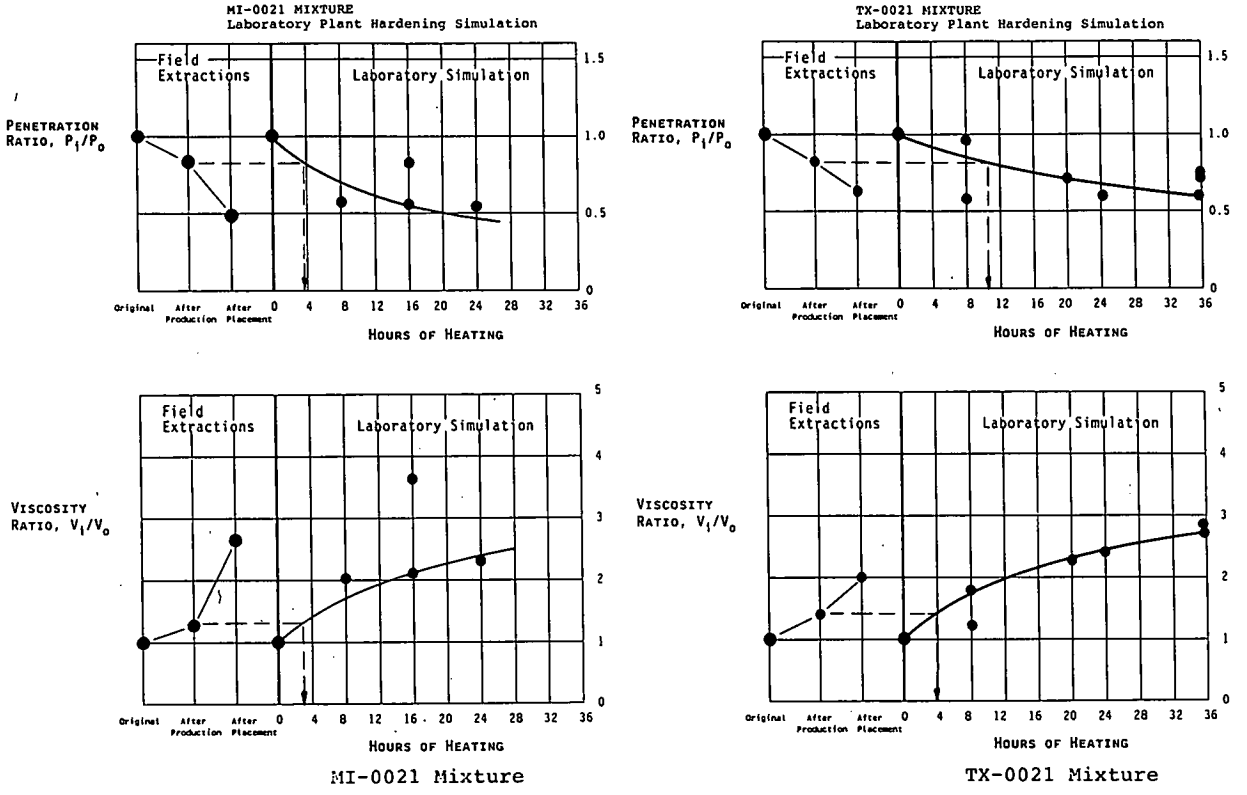

Figure 71. Change in asphalt properties during construction and with different laboratory heating time intervals for the MI-0021 and TX-0021 mixtures.

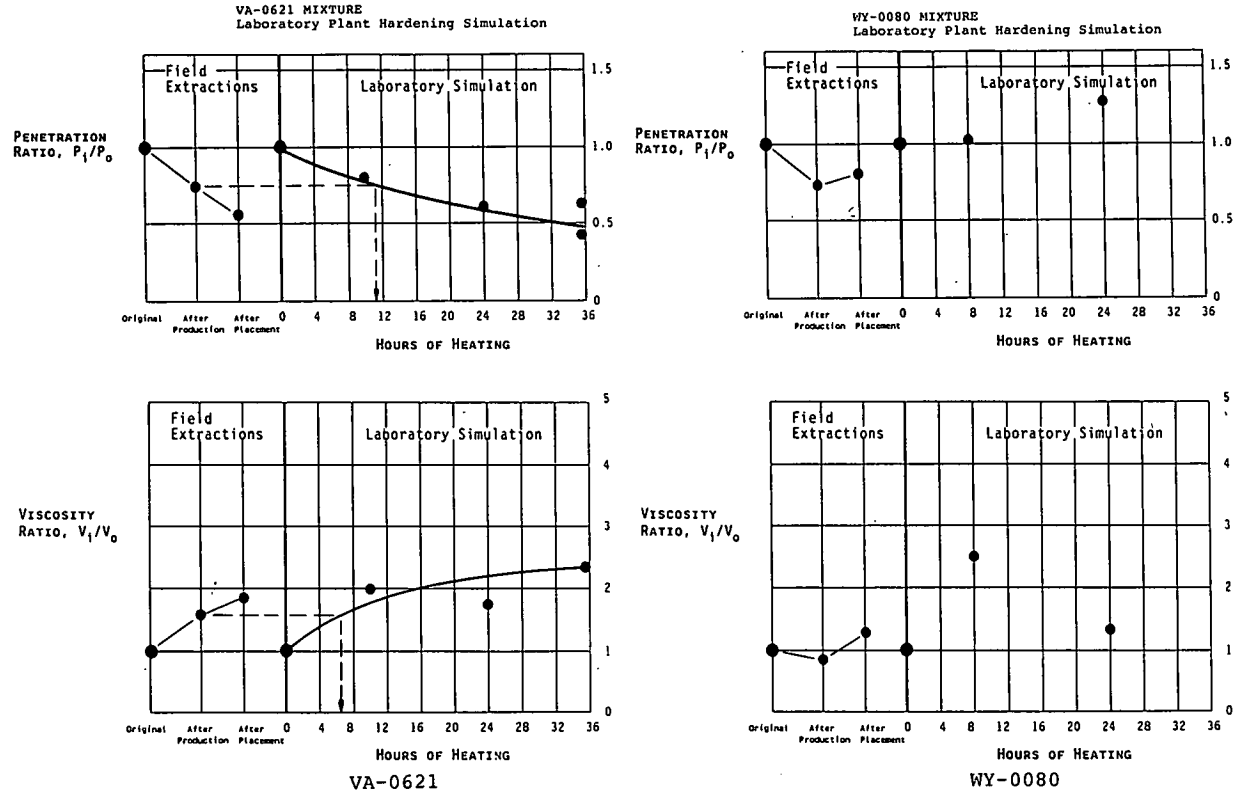

Figure 72. Change in asphalt properties during construction and with different laboratory heating time intervals for the VA-0621 and WY-0080 mixtures.

in Table 41 for a comparison to the long term aging simulations used in the laboratory for the initial five mixtures. Indirect tensile strength, strain at failure, and resilient moduli were also measured on each of these cores as compared to the laboratory-prepared specimen after aging simulations in the laboratory.

Table 42 also summarizes the comparison of the unaged, laboratory-conditioned, and 2-year cores for each of the test parameters. As shown, the indirect tensile strain at failure provided a more consistent comparison between the laboratory conditioned and field core test results. Figures 74 through 76 provide a comparison of indirect tensile strains at failure for each of the test conditions. Use of the 7-day forced-draft oven more closely matched the strain at failure at 2 years than any of the other methods used in the accelerated long term aging simulation.

2.5.2.2.3 Mixture Evaluation. The forced draft oven with 7 days of heating (2 days at 140°F followed by 5 days at 225°F) was also used to temperature condition the four additional mixtures. Both indirect tensile strength and static creep tests were performed on these mixtures at 41°F after accelerated conditioning. A loading rate of 0.05 in. per min was used for measuring the indirect tensile strength. These test results, summarized in Table 43, can be compared to the unaged properties given in Tables 31 and 32. In summary, the resilient modulus increased slightly, but there was a significant decrease in failure strains with the aging simulation, similar to the changes discussed above for the first five mixtures.

2.5.3 Traffic Densification

Traffic densification of asphaltic concrete mixtures is defined simply as an additional reduction in air voids after initial compaction. This additional reduction in air voids normally occurs during the summer months and increases at a decreasing rate with time. It is caused by one-dimensional consolidation and plastic flow.

In mixture design, consolidation is typically defined as an increase in unit weight through the removal of fluid caused by external pressures (or loads) applied to the mixture. For asphaltic concrete, however, consolidation refers to an increase in unit weight by the removal of fluid (reduction in total voids or VMA)

Table 42. Summary of indirect tensile test data for specimens conditioned using different accelerated age/hardening techniques.

State/ Project	Accelerated Aging Method	No of Days	Penetration (77F)	Viscosity (140F)	Indirect Tensile Strength psi	Strain at Failure Mils/in	Instant. Resilient Modulus ksi
Michigan MI-0021	Unaged After Production	0	60	2144	84	14.56	482
	Oxygen Bomb	5	63	3884	111	14.04	480
	Oxygen Bomb	10	43	7542	123	12.13	582
	Forced Draft Oven	2	76	2512	120	9.88	---
	Forced Draft Oven	7	49	5897	139	6.59	---
	2 Year Cores	---	85	1318	87	5.90	444
Texas TX-0021	Unaged After Production	0	30	4388	129	9.01	601
	Oxygen Bomb	5	55	3488	151	8.84	738
	Oxygen Bomb	10	64	2822	167	5.98	683
	Forced Draft Oven	2	37	5654	200	5.11	---
	Forced Draft Oven	7	30	9904	241	2.69	---
	2 Year Cores	---	21	6453	249	2.18	1,489
Virginia VA-0621	Unaged After Production	0	52	4194	114	7.97	758
	Oxygen Bomb	5	32	28021	128	10.23	569
	Oxygen Bomb	10	35	25021	121	10.66	431
	Forced Draft Oven	2	47	4401	146	5.37	---
	Forced Draft Oven	7	27	7910	177	2.69	---
	2 Year Cores	---	41	6458	183	1.48	1,245

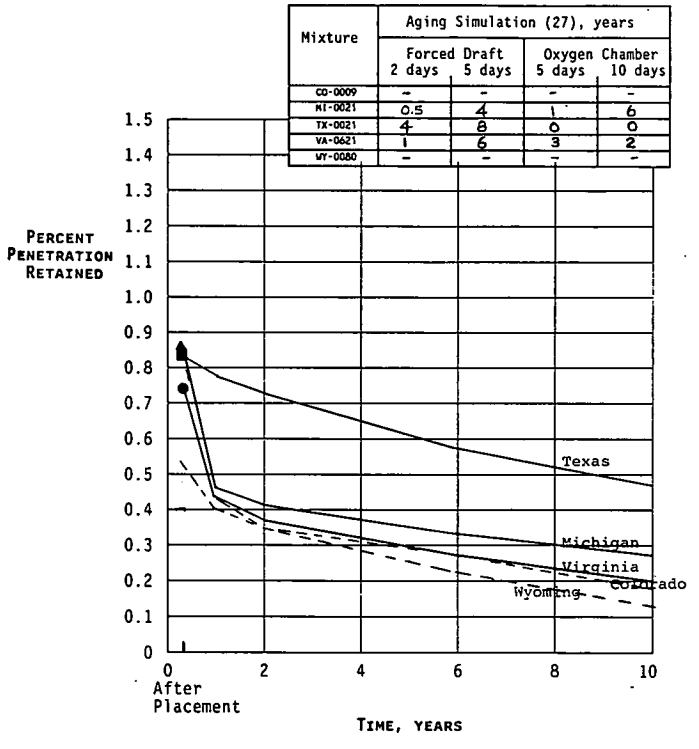

Figure 73. Expected decrease in penetration (77°F) for each of the mixtures based on historical data collected by Shahin (31).

Table 43. Summary of indirect tensile test results of environmentally aged specimens (test temperature = 41°F).

Type of Test	Mixture Designation			
	California	Georgia	New York Rason	Wisconsin
Instantaneous Resilient Modulus, ksi	4,260	3,140	2,731	3,065
Indirect Tensile Strength, psi	445.8	214.1	175.1	209.5
Tensile Strain at Failure, Mils/In.	1.15	1.19	4.08	2.47
Creep Modulus at 3,600 Sec., ksi	81.0	38.1	4.1	10.3
Slope of the Creep Curve	0.106	0.157	0.356	0.235
Percent Recoverable Creep, %	69.4	56.5	35.5	51.6

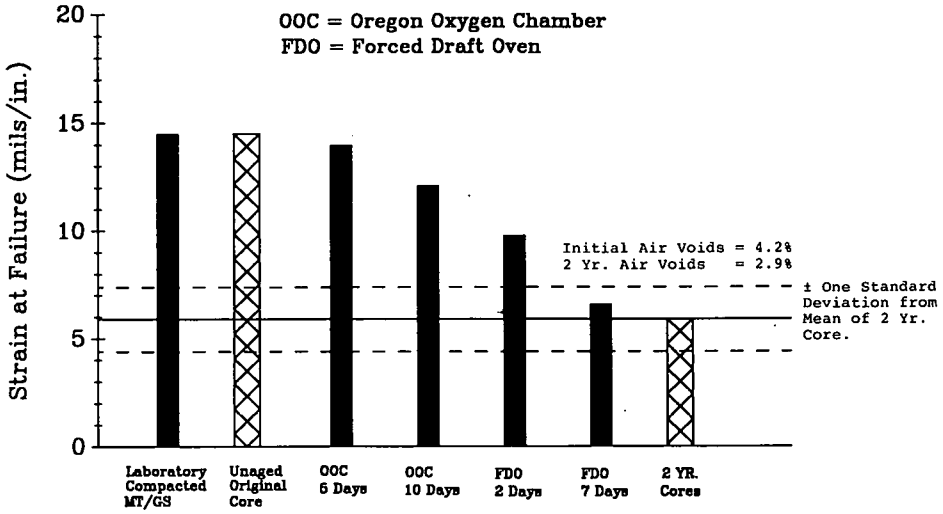

Figure 74. Accelerated age hardening or temperature conditioning compared to actual cores (AAMAS Project MI-0021).

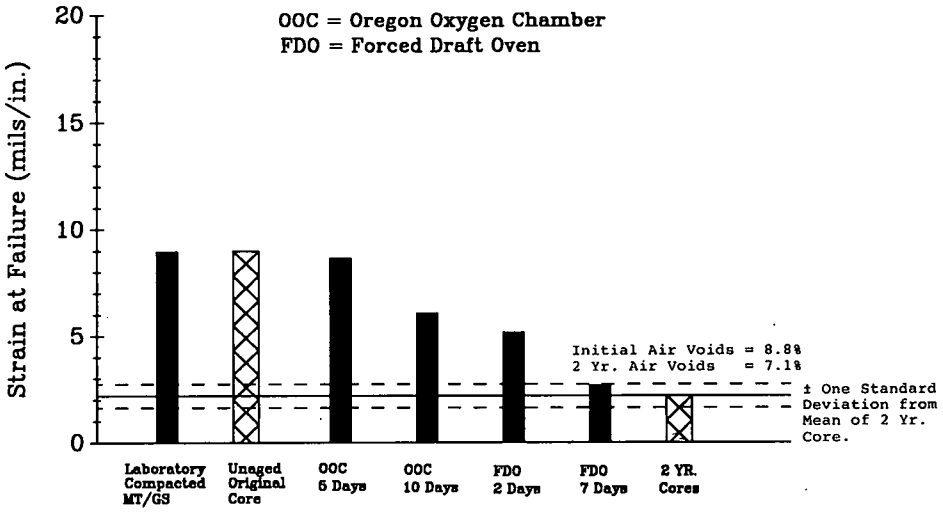

Figure 75. Accelerated age hardening or temperature conditioning compared to actual cores (AAMAS Project TX-0021).

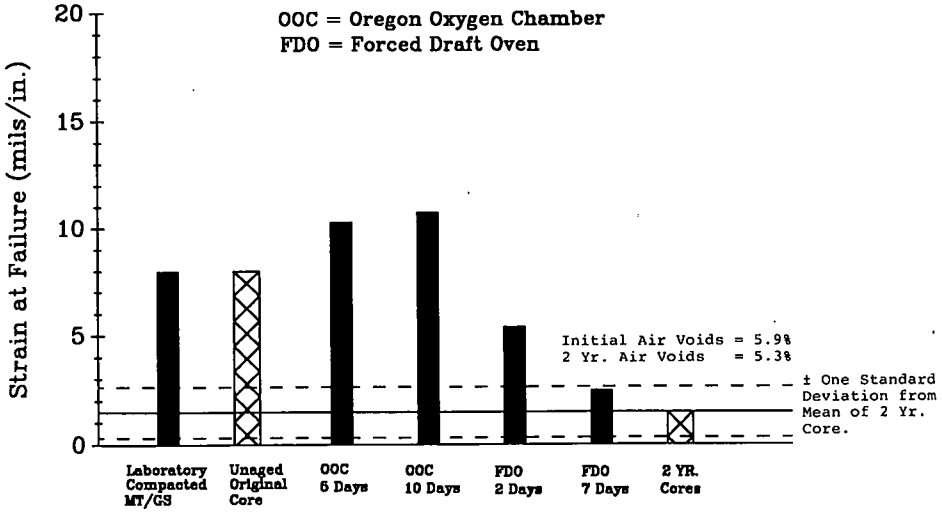

Figure 76. Accelerated age hardening or temperature conditioning compared to actual cores (AAMAS Project VA-0021).

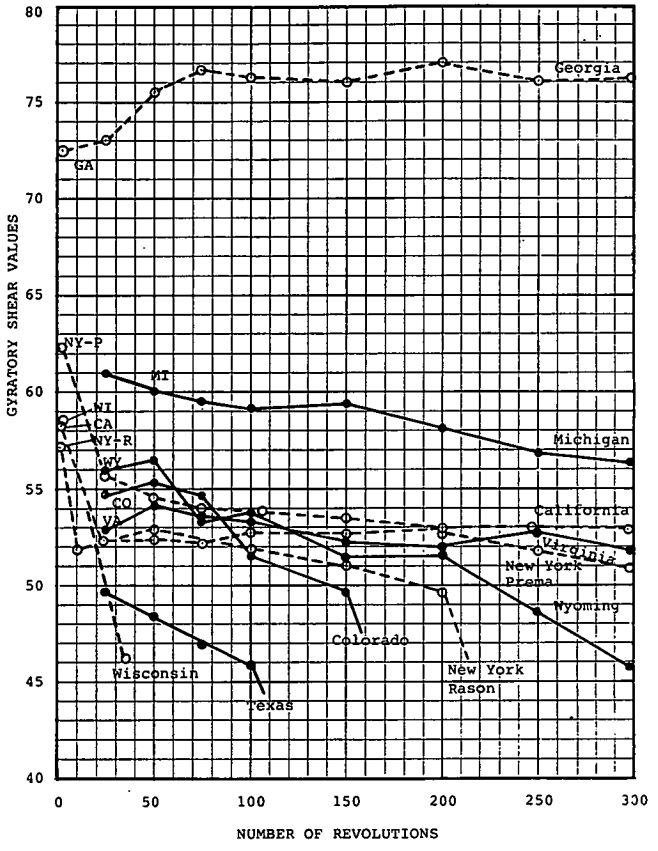

Figure 77. Change in the gyratory shear values with number of gyrations using the Corps of Engineers GTM.

or only a reduction in the air voids. For some mixtures, as the air void volume is reduced, pore pressures in the void space increase, forcing the binder to flow, depending on the temperature-viscosity relationship of the binder.

The amount and rate of traffic densification (consolidation) is dependent on many different factors. Some of these include the environment (long-term aging); traffic loads, rate of wheel load applications, and tire pressures; aggregate and asphalt characteristics; and initial air voids of the compacted mix. Aggregate degradation (reducing the size and altering the gradation of the aggregate), in combination with traffic, can also cause additional densification. Degradation caused by wheel loads, defined in section 2.4.3.2, is a result of concentrated pressures developed at the points of contact between particles.

Reorientation of particles after initial compaction produces a grinding effect that rounds off corners and edges (or even causes particle breakage), which permits the particles to fit more closely together (i.e., a reduction in air voids). This relocation of particles can only occur after friction between the particles is overcome. In fact, some mixes that have adequate internal friction and cohesion at the time of construction can become overlubricated (through a reduction in air voids) due to additional densification, or consolidation caused by traffic. From this densification, the strength and shear properties of the mix can be greatly reduced.

2.5.3.1 Gyratory Shear Mixture Evaluation

The Corps of Engineers gyratory testing machine (GTM) was used to study the effects of traffic densification. The GTM is the only device that can monitor the mixture's behavior during the densification process. Using the other compaction devices, test specimens must be initially compacted and then tested separately.

Aggregate samples from each project were mixed at selected asphalt contents (usually conforming to Marshall mix design) and compacted using the Model 6B-4C GTM with an air-roller. Initial compaction was achieved using either 12 or 18 revolutions. The GTM settings for compaction were a 3-deg angle, 100 psi ram pressure, and an air roller pressure of 10 psi.

The compacted specimens were allowed to cool prior to being placed in an oven set at 140°F. The GTM was set at a 2-deg angle, 100 psi ram pressure, and 13 psi air-roller pressure (approximately equivalent to 20 psi in the Model 4C GTM). The mold check heater was set at 140°F and traffic simulation tests were performed up to a maximum of 300 revolutions. Initial sample height readings were obtained prior to densification and concurrently with air roller pressure readings at 25, 50, 75, 100, 150, 200, 250, and 300 revolutions. Gyratory shear values were computed for each pressure reading. In some cases mixture resistance reduced excessively before reaching 300 revolutions. An excessive reduction in air roller pressure and increase in angle of gyration warranted stopping the test.

These results are presented in Figure 77 for all of the mixtures. The shear resistance of the CO-0009, New York-Rason, TX-0021, and Wisconsin mixtures was found to significantly decrease with an increase in number of gyrations, indicating mixtures sensitive to traffic loads. The gyratory shear value of the California, MI-0021, and WY-0080 mixes decreased, but at a more gradual rate with number of gyrations. The California, Georgia, MI-0021 and VA-0621 mixtures should have good resistance to densification under traffic, even though there was a consistent reduction in shear resistance with number of gyrations for the MI-0021 and California mixtures.

The Colorado and Texas mixes can be expected to densify appreciably under traffic, simply because of the high air voids in the mix after construction. In fact, the air voids were so high in the Texas mixture that those specimens tested did not provide sufficient shear resistance during densification; therefore, the test was terminated. The Colorado, New York-Rason, and Wisconsin mixtures became plastic during testing, indicating that these mixtures are susceptible to lateral flow.

Two similar mixtures were tested from New York. One is identified as Rason, which is restricted from use on high-volume roadways. The other one, identified as Prima, has performed adequately under heavy traffic. Results of the gyratory shear analysis indicate that the Rason mix became plastic (significant reduction in shear stress) around 170 revolutions. However, the Prima mix maintained adequate shear throughout the test, even though there was a slight reduction in shear stress at the beginning of the test.

The Michigan mix can be expected to experience flushing of the asphalt. In fact, additional densification with the gyratory shear compactor and rolling wheel compactor caused the MI-0021 mix to flush or bleed at air voids below 2 percent. Flushing also occurred in both of the New York mixes. The Wyoming mix will experience rutting with time under heavy traffic because of the gradual reduction in shear resistance with

number of gyrations. The following summarizes and compares the mixtures' rutting potential (note in the table that the mixtures are listed in order of increasing rutting potential (i.e., the Wisconsin mix is the one most susceptible to surface distortions):

Rutting Potential		
Low	Moderate	High
Georgia	New York (Prima)	Colorado
Virginia	Wyoming	Texas
Michigan		New York (Rason)
California		Wisconsin

2.5.3.2 Effect of Roller on Gyratory Shear Values

There are three different rollers that can be used with the Corps of Engineers GTM to compact the test specimens. These are a fixed roller, oil-filled roller, and air roller. When using a fixed roller, the GTM is just a compaction device and the gyratory shear strength can not be monitored and, therefore, will not be discussed in this section.

Both the oil-filled and air rollers were used to measure the gyratory shear strength of the four inferior mixtures. Results of the gyratory shear evaluation using the air roller were discussed previously and were also shown on Figure 77. Test specimens were also monitored and tested using the oil-filled roller identical to those prepared using the air roller. The compacted specimens were allowed to cool prior to being placed in an oven set at 140°F. The GTM was set at a 2-deg angle and a 120 psi ram pressure was used during the densification process. The mold check heater was set at 140°F and traffic simulation tests were performed to a maximum of 300 revolutions. Sample height readings were obtained prior to densification and concurrently with oil-filled roller pressure readings. Gyratory shear values were computed for each of the pressure readings. An excessive reduction in oil-filled roller pressure and an increase in angle of gyrations warranted stopping the test.

Figures 78 and 79 provide a comparison of the results for the air and oil-filled rollers. As shown, there are differences in the magnitude of the gyratory shear values. The oil-filled roller consistently measured higher gyratory shear values than the air roller after initial compaction. Thus, the two numbers are not interchangeable. Of those mixtures that became plastic during the traffic densification process (New York and Wisconsin mixes), the gyratory shear values measured using the oil-filled roller decreased substantially, once the shear values began to decrease. Although the magnitudes of the gyratory shear values are different, use of both rollers identified the same mixtures as being plastic during traffic densification and those that were not plastic. Thus, the end result of the traffic simulation test using both of the rollers gave the same result, but actual values measured are different.

2.5.3.3. Refusal Air Void Content

2.5.3.3.1 Effect of Roller. The air void contents at the end of the traffic simulation process were measured on the specimens densified using both the fixed roller and air roller for each of the mixtures. The oil-filled roller was used on only five of the mix-

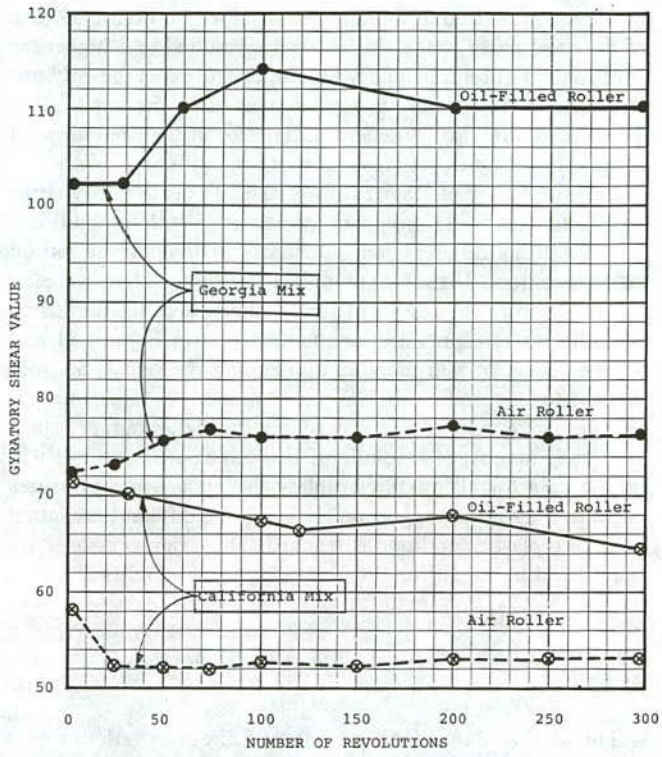

Figure 78. Comparison of gyratory shear values measured on the California and Georgia mixtures using different types of GTM roller modes.

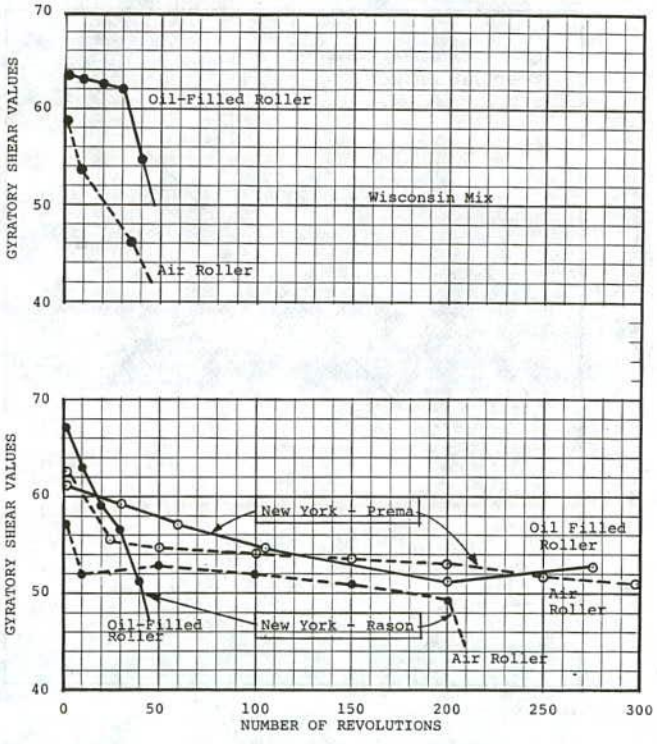

Figure 79. Comparison of gyratory shear values measured on the New York (Rason and Prima) and Wisconsin mixtures using different types of GTM roller modes.

tures. A comparison of these values is shown on Figure 80. Use of the fixed roller mode almost always resulted in a higher air void content at refusal. The Michigan mixture was the only one that resulted in a lower air void content using the fixed roller. Thus, there are also consistent differences in the final air void content in specimens compacted using the different rollers.

2.5.3.3.2 Effect of Ram Pressure. The Texas gyratory shear compactor was used to compact specimens of the four additional mixtures using different ram pressures for defining the refusal air void content. Three ram pressures were used. These were 25, 50, and 75 psi. The results of the specimen densification using the different ram pressures are summarized in Figures 81 and 82. The effect of ram pressure on defining the refusal air void content for a specific mix was very minimal. In effect, the air void content at refusal was achieved for the higher ram pressures at a lower number of revolutions. It is anticipated that this will be the case for all mixtures, unless the higher ram pressures begin to fracture the aggregate resulting in a different gradation or until a plastic condition is reached. Thus, ram pressures are not critical in measuring the air void content at refusal.

2.6 SUPPLEMENTAL ANALYSES AND STUDY AREAS

This section of the report presents and discusses various topics that relate to the development of AAMAS.

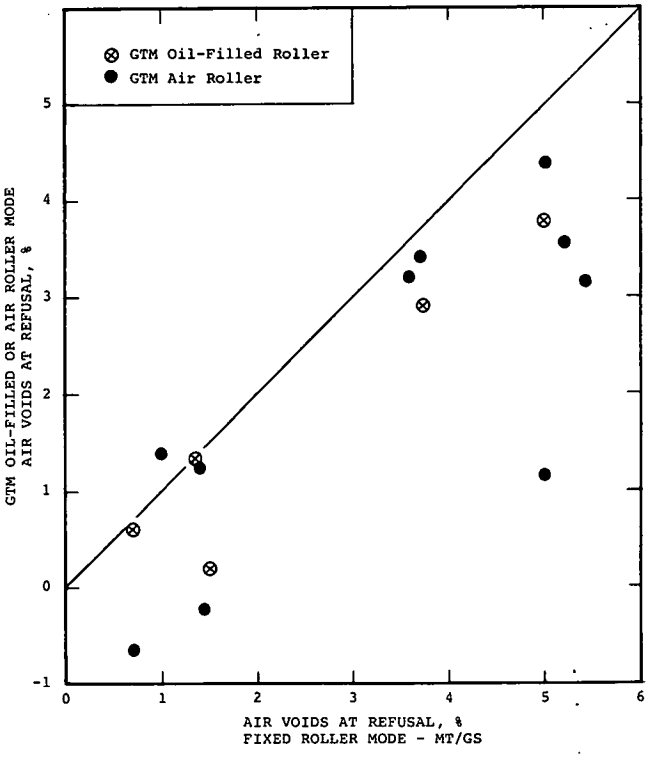

Figure 80. Comparison of air voids measured at refusal using different gyratory devices.

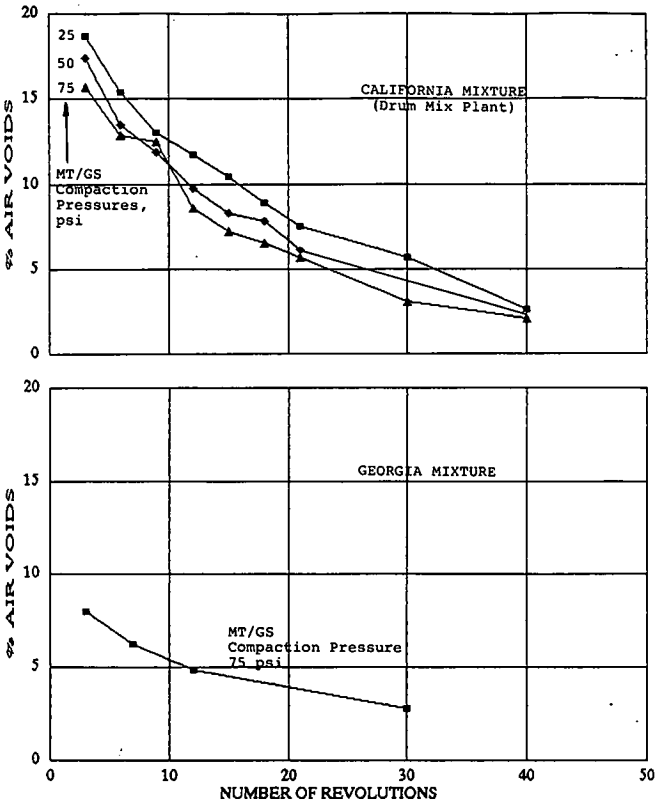

Figure 81. Compactive effort curves for the California and Georgia mixtures for different compaction or ram pressures of the MT/GS.

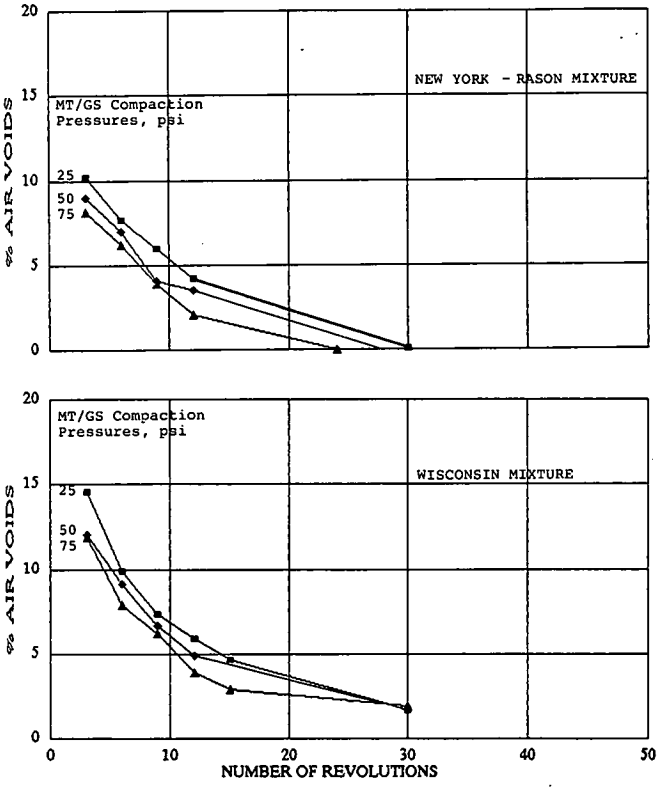

Figure 82. Compactive effort curves for the New York Rason and Wisconsin mixtures for different compaction or ram pressures of the MT/GS.

2.6.1 AASHTO Design Parameter—Resilient Modulus

As noted earlier, the resilient modulus at 68°F is used to estimate the AASHTO layer coefficient for pavement thickness design. Resilient moduli can be measured on cylindrical specimens tested in compression (ASTM D 3497) and in indirect tension (ASTM D 4123). It has been shown through previous studies that consistent differences do exist between resilient moduli measured from testing cylindrical compression specimens and diametral specimens at higher temperatures and at lower frequencies. For example, Figure 83 shows some of the differences that can occur between these two test procedures.

The AASHTO Guide (*6*) recommends that ASTM D 4123 be followed to measure the resilient modulus for pavement thickness designs. In addition to the type of test, however, there are other factors which can also have a significant effect on resilient modulus. These include the testing device, sample size, and recovery time or frequency. Each of these areas is discussed in more detail in the remainder of this section.

2.6.1.1 Testing Device Differences

Three different holding or testing devices were used to measure resilient moduli. These included; the Retsina device, Baladi's indirect tensile holder (*64*), and the holder used and referred to by Kennedy, et al. (*35*). This last device will be referred to as the standard in the remainder of this report. In order to reduce variability of the test results between different samples, the same specimen was tested along three different axes using each device. These data are presented and summarized in Appendix H by sample number and axis.

The use of Baladi's holder permits the measurement of specimen movement in three directions. Poisson's ratio and resilient modulus are then calculated using these three displacements. However, this requires at least 3 channels for monitoring the movement in each of the three directions. Because this would have required modifications to the monitoring equipment, displacements were monitored only along the vertical and horizontal diametral axis. The equations applicable for these two directions were then used to calculate resilient modulus and Poisson's ratio.

With the Retsina device, only horizontal deformations are measured for computing resilient moduli; whereas for Baladi's and the standard holder, both vertical and horizontal deformations were measured. Deformation ratios were, therefore, determined and Poisson's ratio calculated for the latter two holding devices. These values are recorded in Appendix L. Figure 84 shows a comparison of Poisson's ratio as computed from measurements using Baladi's and the standard holding devices. It can be seen from the Figure that negative values were generally obtained using Baladi's holder, whereas positive values were obtained using the standard device at 77°F.

The horizontal displacements measured using Baladi's device and the standard holder were very similar. The large differences in measured displacements were in the vertical direction. Only two reasons could have caused this substantial difference in test results. The first is specimen rotation during load application in the standard loading frame. All specimens were positioned very carefully so the effect of load eccentricity or specimen rotation, if any, would be minimal. The second reason is the difference in preload applied to the specimens. A larger preload was applied to the specimens in Baladi's device because of the loading head's weight. The larger preload used with Baladi's device could have caused more vertical movement in relation to the horizontal movements.

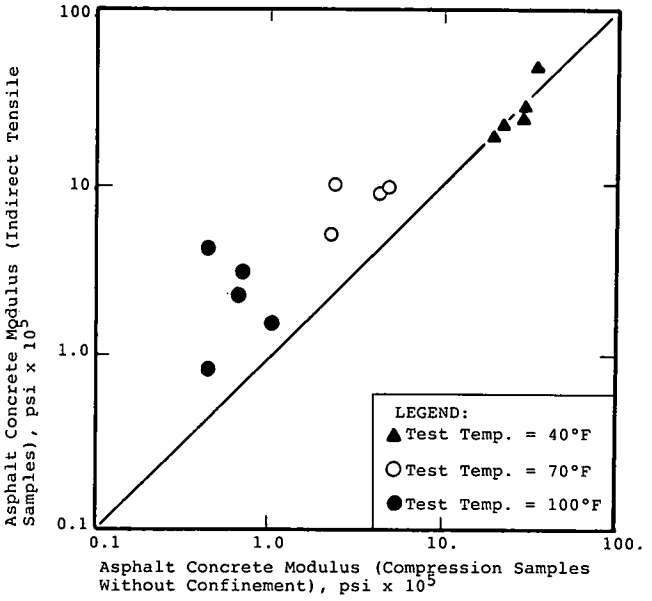

Figure 83. Comparison of test results between the unconfined compression and indirect tensile tests (63)

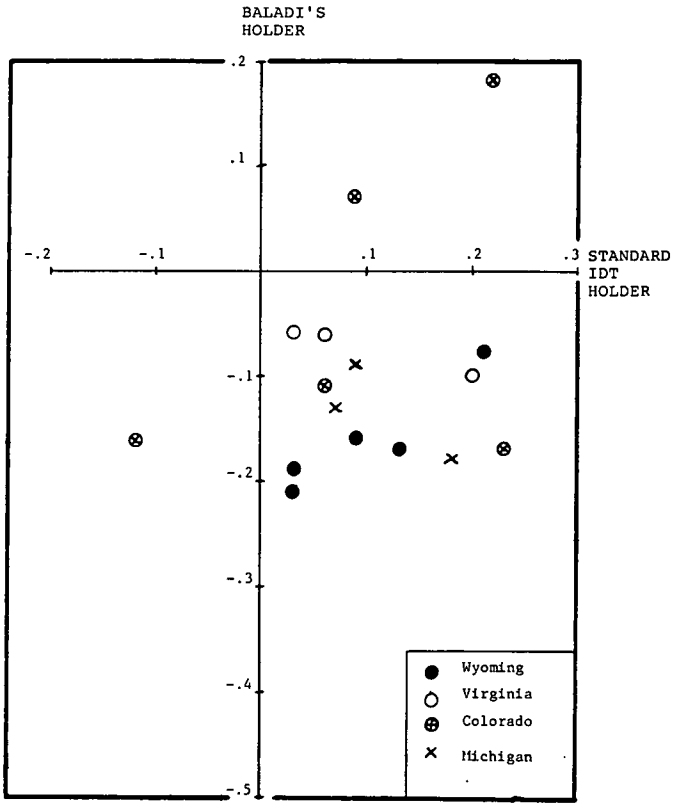

Figure 84. Comparison of Poisson's ratio as measured on identical samples with different holding devices.

Figure 85 provides a comparison between resilient modulus values measured from all three devices. Very large differences were obtained even though identical axes and load levels were used for each device. Standard deviations and COVs for the resilient moduli measured on the same specimen for each device are summarized in Table 44.

The COV is generally larger for the CO-0009 mixture. One reason for this larger dispersion of moduli is probably related to specimen thickness. The CO-0009 cores were thinner and below the minimum thickness requirement of 1.5 in., because the thicker cores were used for other testing.

Another particular item to note is the large variation of values measured along the different diametral axes on the same specimen (Appendix H). The test results for the MI-0021 mix had the least dispersion of moduli values and contains the smaller aggregates. In general, the COVs were larger for the mixes with the larger coarse aggregate, with the exception of the CO-0009 mix, which was explained in the previous paragraph.

For the standard holder, COVs were measured for each and compared to the COVs measured with the other devices on that same sample. Figure 86 shows a comparison of COVs on resilient moduli measured between each device. The Retsina device was found to produce the greater variation in test results, whereas Baladi's holder consistently resulted in more uniform measurements.

Table 44. Summary of resilient modulus variations measured using different testing/holding devices.

Mixture	Average Value	Testing Device		
		Standard	Baladi	Retsina
CO-0009	Std. Deviation	107	224	220
	Coefficient of Variation, %	40	37	48
MI-0021	Std. Deviation	1	14	73
	Coefficient of Variation, %	0.3	4.0	23
VA-0621	Std. Deviation	103	1	72
	Coefficient of Variation, %	33	0.6	37
WY-0080	Std. Deviation	39	25	114
	Coefficient of Variation, %	20	14	58

2.6.1.2 Nominal Aggregate Size

Of interest, also, to pavement and bituminous engineers is the effect of nominal aggregate size on resilient moduli and other engineering properties using a standard sample size for the indirect tensile test. In other words, as the nominal aggregate size of an aggregate blend increases, should the sample size increase accordingly? To evaluate this question on what effect, if any, nominal aggregate size has on resilient moduli using ASTM D 4123, oversize cores were taken on all projects where the nominal aggregate size exceeded a 1-in. diameter. This included the North Carolina and both Virginia projects.

The oversized cores were first tested along three different axes of the same sample. Each field core was then recored in the laboratory to a smaller diameter and the resilient moduli was measured along the same three axes. The results of this testing are summarized in Appendix F and graphically presented in

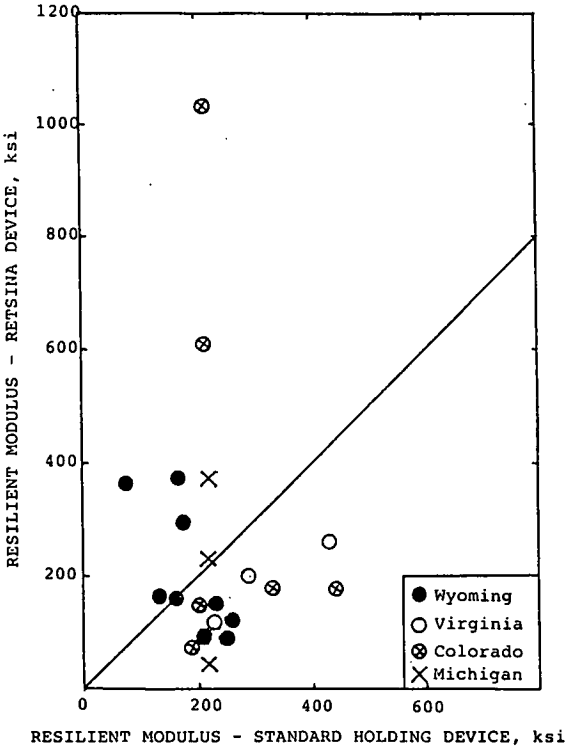

Figure 85.a Standard vs. Retsina

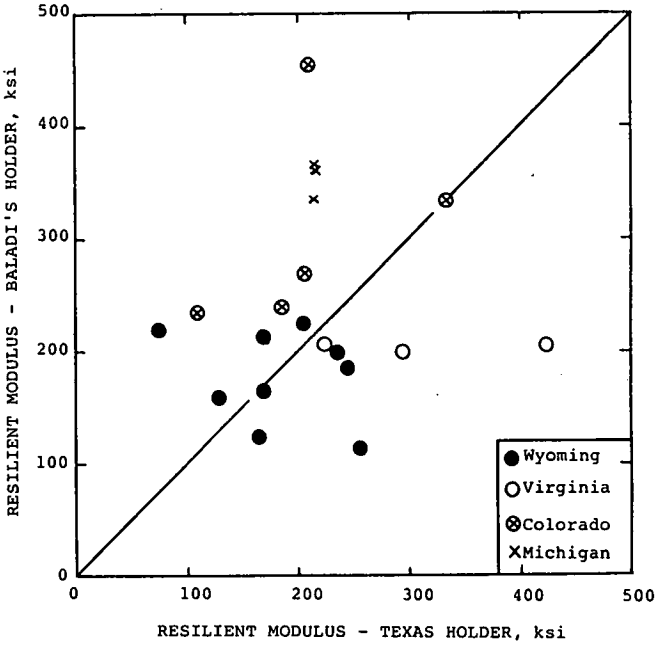

Figure 85.b Standard vs. Baladi

Figure 85. Comparison of resilient moduli measured on cores using different sample holding devices and test equipment.

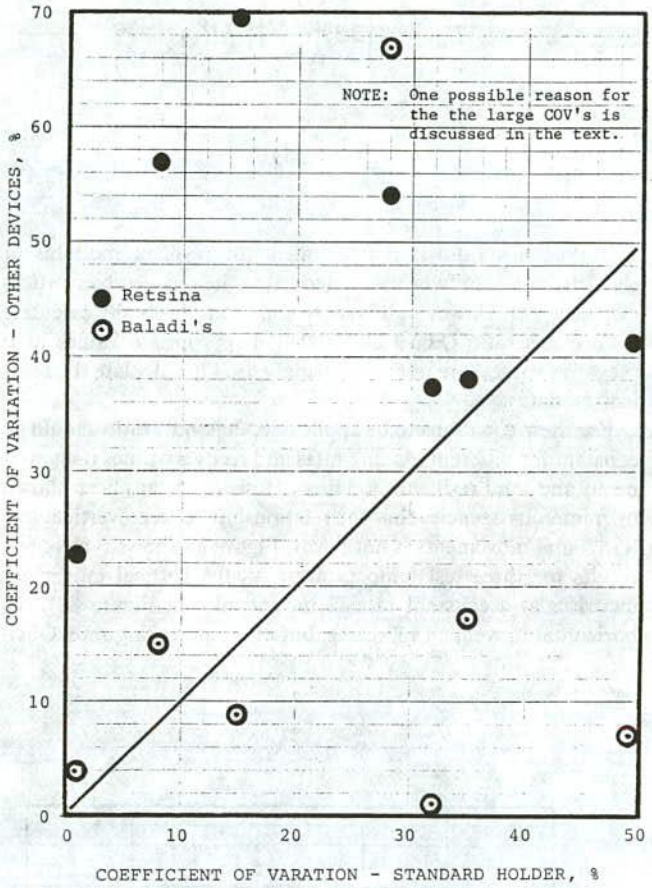

Figure 86. Comparison of COVs for resilient moduli measured on cores using different sample holding devices and test equipment.

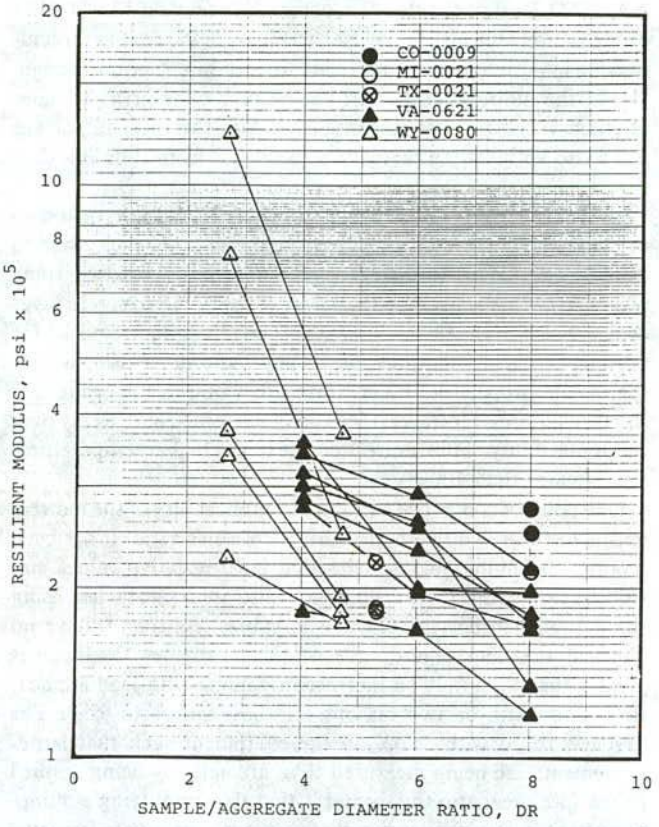

Figure 87. Effect of the specimen/aggregate diameter ratio on resilient modulus.

Figure 87. As can be seen, the resilient moduli increased with decreasing core diameter. Thus, the resilient moduli measured in the laboratory is affected by the nominal size aggregate in relation to sample diameter. Additionally, as the sample diameter decreased in relation to aggregate size, the variation in test results also increased.

2.6.1.3 Recovery Time—Instantaneous vs. Total

The ASTM D 4123 test procedure, recommended in the AASHTO Design Guide for measuring resilient moduli at 68°F, provides two equations for calculating the resilient modulus of elasticity; the Guide does not, however, state which one is to be used. One value relates to the instantaneous resilient modulus and the other to the total resilient modulus of elasticity. The question then becomes, is there a significant difference in resilient moduli at 68°F between the instantaneous and total resilient modulus, and if there is, which one should be used?

As complete load-deformation time traces were recorded during repeated load resilient modulus testing, both of these values were calculated for selected samples. Table 45 summarizes the differences between resilient moduli obtained from each equation. As shown and expected, larger differences occurred at 104°F; whereas smaller differences were found at 41°F because of the difference in creep and recovery properties between these two temperatures. These results are very similar, if not identical, to those findings by Von Quintus and Kennedy (*63*).

Table 45 also summarizes the resilient moduli measured prior to and after the repeated load permanent deformation tests. Significant differences were found because of the changing plastic strains with load repetitions.

2.6.2 Applicability of the Indirect Tensile Test

The indirect tensile test has been used by numerous agencies for evaluating dense-graded asphaltic concrete mixtures. The

Table 45. Summary of the difference between the instantaneous and total resilient modulus at different test temperatures.

Mixture	Modulus Ratio*, E_{Rt}/E_{RI}			E_{rp}**, ksi	Modulus Ration, E_{R_p}**/E_{RI}
	41F	77f	104F		
CO-0009	.88	.71	.67	255	.44
MI-0021	.82	.65	.58	216	.67
TX-0021	.90	.81	.60	173	.27
VA-0621	.88	.78	.58	137	.27
WY-0080	.92	.82	.65	234	.35

* Modulus Ratio = E_{Rt}/E_{RI}
E_{RI} = Instantaneous Resilient Modulus, as defined by ASTM D 4123
E_{Rt} = Total Resilient Modulus, as defined by ASTM D 4123

** E_{Rp} = Total Resilient Modulus at a Test Temperature of 77F, as Defined by ASTM D 4123, but Measured After the Permanent Deformation Testing

AASHTO Design Guide (*6*) recommends that ASTM D 4123 or the indirect tensile test be used to measure the resilient modulus of asphaltic concrete materials for use in structural design. Use of the indirect tensile test has become widespread because of some very practical reasons. Probably, the most important has to do with testing field cores recovered from thin lifts (less than 4 in. in thickness).

One of the major disadvantages of using a triaxial type test to measure the compressive resilient modulus of elasticity has to do with the length to diameter ratio that is required by some procedures. Typically, the thickness of asphaltic concrete layer or lift placed in the field will be much less than that required for adequate uniaxial compression testing. Another reason is that the tensile properties of a mixture are required for evaluating fracture failures. However, there has been some controversy over the applicability of the indirect tensile test at higher temperatures (i.e., greater than 100°F).

One point of concern regarding the applicability of the indirect tensile test has to do with measuring Poisson's ratio. It has been reported by numerous agencies that both negative values and values greater than 0.5 for Poisson's ratio are typical when using the indirect tensile test. Obviously, values less than 0 have no physical meaning regarding elastic layer theory, and values greater than 0.5 imply an increase in volume with load application. There can be two reasons for these values to exist. The first has to do with "slop" in the equipment such that larger movements are being measured than are actually being applied to the specimen, and the second is that the simplifying assumptions used in the indirect tensile test are inappropriate for some asphaltic concrete materials, (i.e., the equations may be inappropriate or the specimen is not responding as an elastic material, which is an assumed condition).

The purpose of this section is to review the indirect tensile testing procedures recommended and those that have been used for evaluating asphaltic concrete materials and provide some recommendations as to their applicability within the temperature regime used in most test programs. First considered is a review of the equations provided in ASTM D 4123 for calculating the indirect tensile properties of dense-graded asphaltic concrete materials. The instantaneous resilient modulus is calculated by:

$$E_{RI} = P(\nu_{RI} + 0.27)/hH_{RI} \qquad (2\text{-}10)$$

where E_{RI} is instantaneous resilient modulus of elasticity, psi; ν_{RI} is instantaneous resilient Poisson's ratio (Eq. 2-6); P is repeated load, lbf; h is thickness of the specimen, in.; and H_{RI} is instantaneous recoverable horizontal deformation, in.

The resilient modulus of elasticity can be calculated using an assumed Poisson's ratio or an actual measurement. If an assumed value is used it should be temperature-dependent, although the procedure (ASTM D 4123) does not require that different values be used at different test temperatures. Poisson's ratio values of 0.25, 0.35, and 0.40 were used to calculate the resilient modulus at test temperatures of 41, 77, and 104°F, respectively, for the AAMAS mixtures. By using Eq. 2-10, an increase in Poisson's ratio will increase the resilient modulus, and a decrease in Poisson's ratio will decrease the resilient modulus.

Substituting Eq. 2-6 into Eq. 2-10 yields the following formula:

$$E_{RI} = P\left[3.59\left(\frac{H_{RI}}{V_{RI}}\right) - 0.27 + 0.27\right]/hH_{RI}$$

$$E_{RI} = P\left[3.59\left(\frac{H_{RI}}{V_{RI}}\right)\right]/hH_{RI}$$

Thus,

$$E_{RI} = \frac{3.59P}{hV_{RI}} \qquad (2\text{-}11)$$

If Poisson's ratio is not assumed, the resilient modulus of elasticity can simply be calculated using the recoverable vertical displacement. However, it is more common to actually calculate a Poisson's ratio (Eq. 2-6), so that inappropriate values of ν (negative values) are not unknowingly used to calculate the resilient modulus.

For these equations to be applicable, Poisson's ratio should be constant for different loading rates and recovery times (instantaneous and total resilient modulus). However, it has been shown by numerous agencies that the relationship between vertical and horizontal movements is not linear. Figure 88 shows typical test results for three test temperatures. As the vertical movement increases at a constant rate (2 in. per min. in Figure 88), the horizontal movement increases, but at an increasing rate. Obvi-

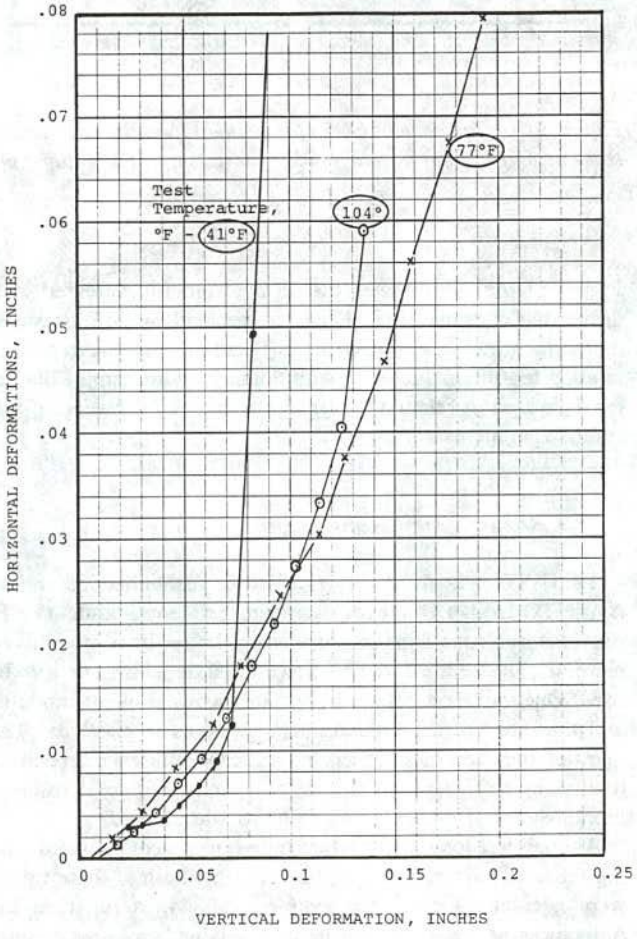

Figure 88. Typical indirect tensile strength test results for three test temperatures.

ously, none of the relationships are linear, so Poisson's ratio (or the horizontal to vertical deformation ratio) will vary with loading rate, loading time, and recovery time.

Figure 89 compares the horizontal deformations that have been normalized, using the horizontal deformation measured at peak load, to the deformation ratio, *DR*. The deformation ratio is used to calculate Poisson's ratio (Eq. 2-7). In Figure 89, it is seen that the deformation ratio varies with time (or vertical deformation) and exceeds the value of 0.215 that will result in a Poisson's ratio of 0.50 prior to peak load, especially for the higher test temperatures.

The problem is that most asphaltic concrete mixtures are viscoelastic or inelastic, and there can be a time delay before the horizontal movement is measureable after the vertical load is applied. This was illustrated by the horizontal versus vertical movement relationship in Figure 88. The following summarizes the mean time delays for the three test temperatures that have been measured from the vertical and horizontal deformation traces with time.

Test Temperature, °F	Mean Time Difference Between Initiation of Vertical and Horizontal Deformation Traces, Sec
41	0.376
77	0.290
104	0.126

At higher temperatures, the indirect tensile test is believed to overestimate the actual modulus of elasticity because of the time delay and other inelastic properties in the material response. For weaker or tender mixtures, compressive displacements are occurring between some of the aggregate, rather than horizontal displacement (i.e., more like a triaxial type test).

It should also be noted that when cracking begins to occur during an indirect tensile test, an increase in specimen volume occurs because of the internal separation of materials. Thus, Poisson's ratio values greater than 0.5 should be expected once these internal cracks start to develop (i.e., after initial yielding). This is illustrated in Figure 89. In either case, for use in routine mixture design, Poisson's ratio should be assumed and caution should be used in measuring the resilient modulus of elasticity and other properties at the higher test temperatures using indirect tensile testing techniques.

2.6.3 Specimen Height

One of the major disadvantages of using the uniaxial compression test for evaluating the compression properties of a mixture is the height to diameter requirement. Historically, a height-to-diameter ratio of 2 has been preferred for testing. Thus, 4-in. diameter cores are required to have heights of 8 in. This is impractical in testing field cores of the same material, because most lifts are less than 3-in. in thickness. There have been techniques used, such as "stacking" cores on one another, to achieve the required minimum height. In other cases, cores or Marshall specimens have been "glued" to meet the height requirement. The question becomes, is a height-to-diameter ratio of 2 required, and for practicality, will stacking or gluing specimens together result in the same compressive property of a continuous intact specimen.

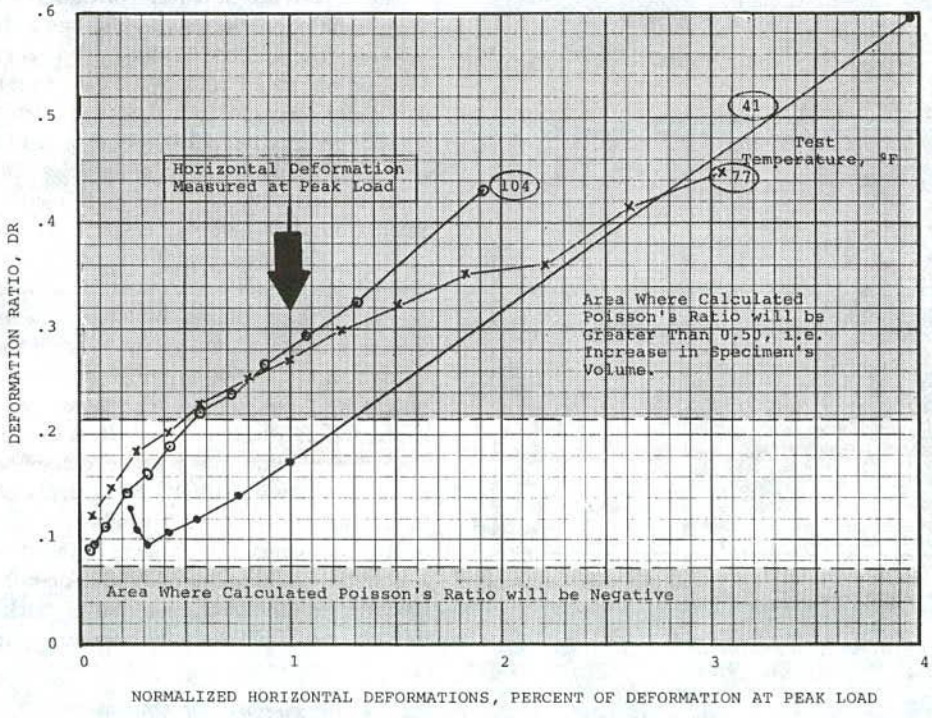

Figure 89. Typical indirect tensile test results comparing the deformation ratio to normalized horizontal deformations.

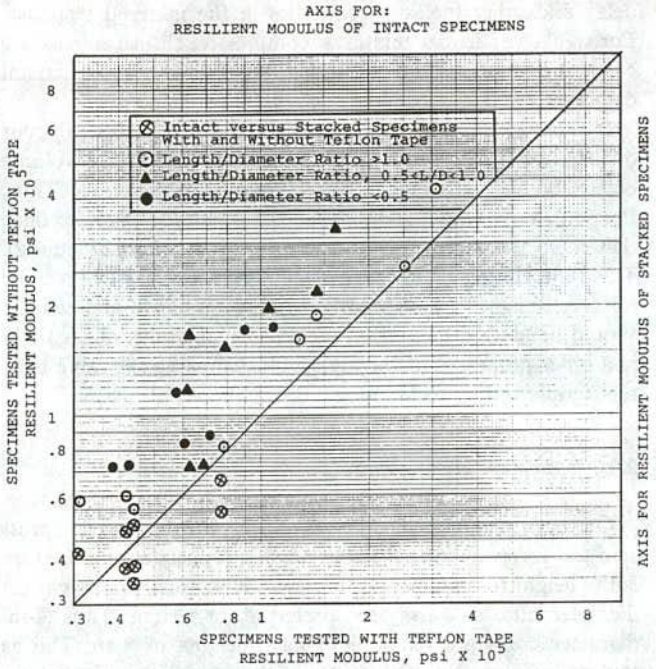

Figure 90. Comparisons of resilient modulus measured on specimens with and without Teflon tape, and between intact and stacked specimens.

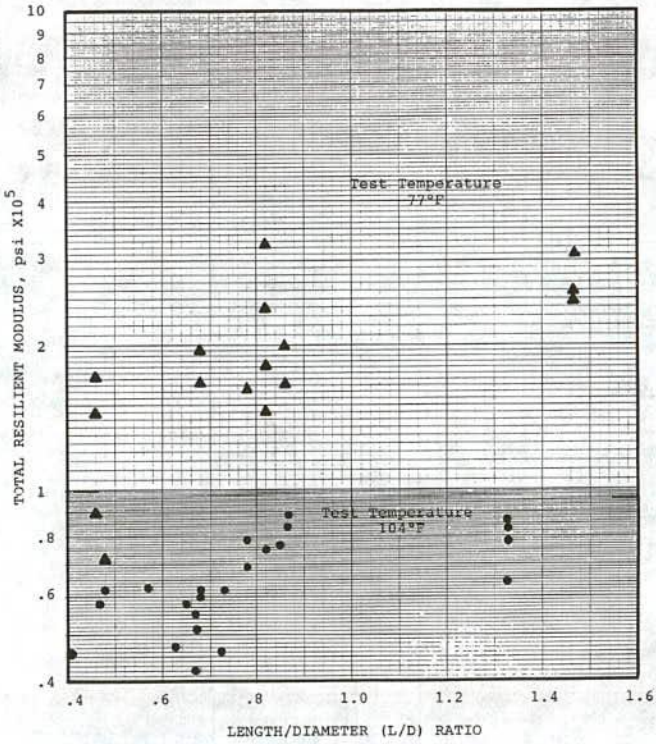

Figure 91. Comparison of resilient moduli measured on specimens with different heights.

To evaluate the sample height effects on the resilient moduli, 6-in. diameter by 8-in. high specimens were compacted in the laboratory. Each specimen was marked with two perpendicular lines on opposite sides, so that each could be repositioned, exactly as initially used in the test program, after sawing the specimens into two or more parts. The resilient modulus of the intact specimens was first measured both with and without Teflon tape. Teflon tape was used to determine if differences would be obtained with different end effects. Figure 90 shows the differences in resilient moduli results comparing values measured on specimens with and without Teflon tape for different height-to-diameter ratios. It is noted that there can be a significant difference between the two end conditions. In addition, as the height-to-diameter ratio decreased, the difference between the resilient modulus measured on specimens with and without Teflon tape increased.

After initial testing, each of the large specimens was sawed in half and each of the halves was retested using the same testing procedure. The results of this testing are shown on Figure 91. The resilient moduli decreased substantially as the height of the specimen decreased. The reason for this decrease in stiffness is believed to be a result that any "slop" in the testing apparatus becomes magnified as the specimen's height (or vertical deformation) decreases.

After testing, each of the sawed specimens was stacked along the same orientation line and the resilient moduli were measured on the stacked specimens. The results of this testing are included on Figure 90. A difference can be seen between the taller and shorter specimens. However, there is much less difference between the intact and stacked specimens than between the taller and shorter specimens.

2.6.4 Particle Orientation

The importance of particle orientation and its correlation to the material properties has been recognized and studied by previous researchers. Some of these previous studies have included Lee and Markwick (*65*), W.H. Goetz (*66*), Hennes and Wang (*67*), Puzinauskas (*68*), and Lees and Salehi (*69*). With the exception of the Lees and Salehi study, none of these studies defined numerically the orientation of particles and determined if differences existed between compaction methods. In the Lees and Salehi study, the angle of orientation of aggregate particles visible on a cut face was measured to determine if the particles were aligned at random or oriented in a preferred direction. Lees concluded that preferred orientations were measured and that the angle of orientation varied between compaction devices.

In order to describe a state of packing, it is necessary to know where every particle is—in terms of size, shape, location and space, and its orientation in space. If these factors can be defined in numerical terms, it is possible to describe the state of packing of an assembly of particles by an array of vectors in a matrix form. The size of a particle can be numerically described by the equivalent diameter of a sphere of the same volume. The shape of a particle is more complicated to describe numerically. Methods exist for expressing quantitatively such shape characteristics as roundness and sphericity, angularity, and surface texture.

2.6.4.1 Measurement of Orientation

Two methods were recognized by Lees (*69*) for the measurement of orientation. These are (1) the least projection method,

and (2) the center of area method. In the least projection method, elongation direction is the direction of the two parallel lines with the minimum amount of separation that can be drawn tangent to the particle projection. In the center of area method, elongation direction is the direction of the longest straight line that can be drawn through the center of area of the projection. The center of area is considered to be a two-dimensional equivalent of the center of mass that is the point about which the particle pivots when suspended in a fluid.

The method used in this study to evaluate particle orientation is based on examining the longest dimension of the particle visible on a given plane (i.e., two dimensional). It is simple in calculation and, as far as the investigation has been conducted, reveals the nature of orientation patterns. It is also the least time consuming method, without a significant loss of accuracy. However, the method can be extended to a three-dimensional analysis by measuring particle orientation projections on mutual perpendicular and parallel planes.

Step 1 of the method used is to define the projections of the particles on a given plane. For this purpose, the specimen whose orientation pattern is being investigated is cut into one or more sections. The orientation direction of the particles visible on the cut sections is then determined by finding the direction of the longest line that can be drawn along each particle.

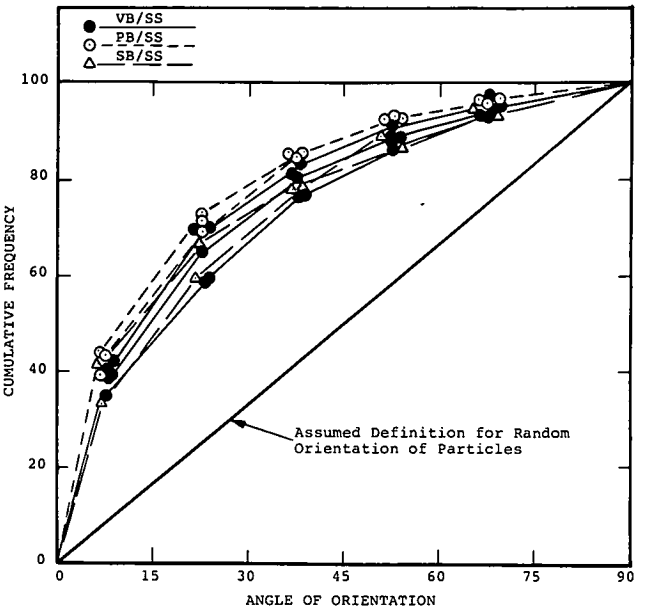

Figure 92. Summary of particle orientation data illustrating preferred orientation of particles measured from field cores.

2.6.4.2 Laboratory and Field Orientations

Selected cores and laboratory compacted specimens using the five different devices (AV/KC, CK/CC, MM/HC, MS/WC, and MT/GS) were cut perpendicular to the pavement's or specimen's surface to evaluate the angle of orientation of particles visible on the cut face. This evaluation process included the combination of video imaging and an AUTOCAD system. The video imaging consisted of a standard VCR camera, a Targa video imaging board, and a software driver to interface the Targa Board to the microcomputer operating system to generate an AUTOCAD overlay. The AUTOCAD system was used for mapping or tracing the aggregate particles visible on the cut face.

Almost 200 cores and specimens were sawed vertically to evaluate orientation of the particles. Basically, an angle for each particle was determined by finding the direction of the longest line that could be drawn for each particle. Figure 92 shows a cumulative frequency diagram for the angle of orientation by field compaction technique. All field compacted mixtures were found to have a preferred angle of orientation and no significant difference could be identified between projects. These data are summarized and presented in Appendix P. Examples of the graphics (AUTOCAD) printout of the larger particles are provided in Appendix P. Colored copies or prints of each specimen and core have been stored on floppy discs for future use.

2.6.5 Loading Rate

To evaluate the mixture indirect tensile strength for low temperature characterization, two loading rates were used. The standard rate of 2 in. per min (ASTM D 4123) was used to evaluate mixture strength at three temperatures (41, 77, and 104°F). For low temperature characterizations and predictions, however, thermal loads are applied at a much slower rate because of its effect on the mixture's tensile strength. Therefore, a loading rate of 0.05 in. per min was used at 41°F to measure mixture strength for low temperature cracking characterizations. On a few projects (Colorado, Michigan, and Texas), the loading rate of 0.05 in. per min was also used at 104°F to define the loading rate effect at higher temperatures.

Table 46. Effect of loading rate on the strength properties of each mixture.

State/ Project	Compaction Method	Test Temperature, °F	Loading Rate, (in./min.)	Indirect Tensile Strength, psi	Strain at Failure, (mils/in.)
Colorado CO-0009	PB/SS	41	2.00	360	1.04
			0.05	141	3.12
		104	2.00	30	18.07
			0.05	5	24.41
Michigan MI-0021	PB/SS	41	2.00	382	4.51
			0.05	207	4.94
		104	2.00	34	12.87
			0.05	10	10.49
Texas TX-0021	SB/PS	41	2.00	316	1.21
			0.05	225	2.60
		104	2.00	33	11.01
			0.05	9	11.27
Virginia VA-0621	SB/PS	41	2.00	407	3.35
			0.05	171	2.08
Wyoming WY-0080	VB/SS	41	2.00	274	0.78
			0.05	176	1.82

The indirect tensile strengths and failure strains at these different loading rates have been recorded in Appendix H and are summarized in Table 46. Review of the data indicates that the mixture strength is significantly less at the slower rate at both 104°F and 41°F, as expected. However, the tensile strains measured at yield, in most cases, are about the same between the two loading rates. This implies a strength dependency on loading rate, but not a yield strain dependency. Reasons for this effect

Table 47. Summary of work calculated for each of the different mixtures, ft-lb.

State/Project	Compaction	Mean Air Voids, %	Temperature F		
			41	77	104
Colorado CO-0009	VB/SS PB/SS	8.2 9.0	0.596 0.682	6.127 5.134	0.521 -----
Michigan MI-0021	VB/SS PB/SS	3.7 4.2	3.424 2.688	1.629 1.721	0.553 0.559
Texas TX-0021	SB/PS VB/SS	8.8 10.2	0.755 1.005	2.446 2.741	0.700 1.177
Virginia VA-0621	VB/SS SB/PS	5.9 7.4	5.019 5.125	4.442 4.632	1.072 1.705
Wyoming WY-0080	VB/SS PB/SS	5.8 8.3	1.240 1.578	1.588 0.971	1.142 1.243
California	MT/GS	6.6	3.62	4.88	1.80
Georgia	MT/GS	6.2	5.49	3.20	1.29
New York-Rason	MT/GS	6.4	2.21	2.51	0.73
Wisconsin	MT/GS	5.7	2.60	4.62	0.98

on strength are related to the creep and relaxation characteristics of asphaltic concrete mixtures. Thus, if strength and stiffness (resilient modulus) are used as field control variables, the loading rate must be closely controlled. On the other hand, if failure strains are used, loading rate becomes less important.

2.6.6 Mixture Toughness

Mixture toughness, or the strain energy density concept, is a parameter that has been used by some researchers to evaluate and compare asphaltic concrete mixtures. Toughness is defined as the amount of work per unit volume required to cause failure, or the area under the stress-strain curve to failure. Little and Richey (*70*) used this concept to evaluate the use of plasticized sulfur binders in asphaltic concrete, and they suggest that it gives a good indication of the optimum binder content.

2.6.6.1 Sensitivity to Temperature and Time

Using these same concepts, work (or area beneath the force-displacement curve) was computed for each mixture using the indirect tensile strength results. The computed values from each test are provided in Appendix Q, and summarized in Table 47. As can be seen, work values vary dramatically with temperature and mixture. However, work values were indifferent between test sections of the same project, even though the sections had statistically different air voids (TX-0021, VA-0621, and WY-0080).

Table 48 compares the work required to cause failure of cores recovered at different times (immediately after construction and 2 years after construction) from the initial five projects. The most significant change occurred for the Colorado mixture at a test temperature of 77°F. This project consisted of a mixture that was placed and compacted in a wet condition.

2.6.6.2 Sensitivity to Asphalt Content

Similar to the Little and Richey study (*70*), the work required to cause failure was computed at different asphalt contents for

Table 48. Comparison of work calculated from the indirect tensile strength testing of cores recovered at different times.

State/Project	Test Temp., °F	Section	Work, ft.-lbs.	
			Const. Cores	2-Year Cores
Colorado CO-0009	41	VB	0.60	0.68
	77	VB	6.13	0.91
	77	PB	5.31	1.03
	104	VB	0.52	0.31
Michigan MI-0021	41	PB	2.69	2.49
	77	PB	1.72	1.41
	77	VB	1.63	1.64
	104	PB	0.56	0.34
Texas TX-0021	41	SB	0.76	0.84
	77	SB	2.45	3.98
	77	VB	2.74	2.44
	104	SB	0.70	1.38
Virginia VA-0621	41	VB	5.02	3.58
	77	VB	4.44	5.08
	77	SB	4.63	3.35
	104	VB	1.07	1.58
Wyoming WY-0080	41	VB	1.24	1.86
	77	VB	1.59	2.56
	77	PB	0.97	1.73
	104	VB	1.14	1.14

four of the AAMAS mixtures using the indirect tensile strength test. These computed values have been graphically compared for different asphalt contents and temperatures in Figure 93 for the California mix. As shown, a binder content can be selected to maximize the work required to fracture each of the mixes. Using these concepts, a mixture could be designed such that the work continues to increase with a decrease in temperature at the asphalt content that maximizes the amount of work required to fail the specimen in fracture. Figures 93 through 96 show the change in work as a function of effective asphalt content (by volume) and temperature for the different mixtures.

2.6.7 Performance-Related Mixture Design Parameters

Those parameters considered for use in mixture design and evaluation must be sensitive to changes in binder content of the mix and, most importantly, must be related to pavement distress. Since it has been shown by numerous studies (*1*, *30* through *38*) that the resilient modulus, tensile strength, and other mixture properties are sensitive to changes in binder content and related to pavement distress, four of the mixtures were used to measure changes in these properties over a range of asphalt contents. Figures 97 through 100 show the change in mix properties as a function of effective asphalt content by volume.

For these four mixtures, the total resilient modulus and tensile strain at failure are the properties most sensitive to changes in binder content. The indirect tensile strength was the property least affected by changes in binder content. The California mix has the greatest indirect tensile strength, whereas the Georgia mix has the larger gyratory shear strength. When considering the individual parameters of indirect tensile strength and strain at failure (Figures 98 and 99), peak values were not always identified at one asphalt content. However, when combining these two parameters to calculate work or energy, peak values do exist in every case (refer to Figures 93 through 96). Those effective asphalt contents by volume that will maximize work, gyratory shear, and resilient modulus are as follows:

Mix	Work	Gyratory	Resilient Modulus
California	9.2	---*	---*
Georgia	7.4	7.1	7.8
New York-Rason	9.8	9.6	10.0
Wisconsin	9.0	8.2	8.4

*No Peak Value was Measured

As expected, maximizing each property results in a different asphalt content. Selecting one of the optimum values does not imply that the mixture's performance will be optimized nor does it imply that the mixture will meet the assumptions used in structural design. Selection of a design asphalt content or a range of allowable values for a specific mix will be discussed in greater detail in Chapter 3.

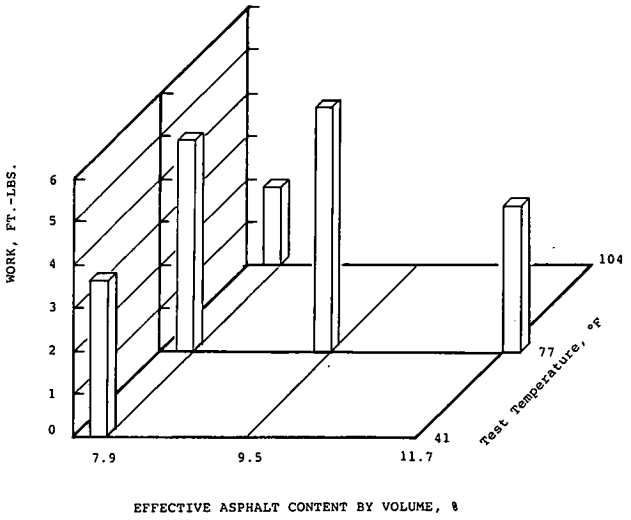

Figure 93. Work as a function of effective asphalt content by volume and temperature for the California mixture.

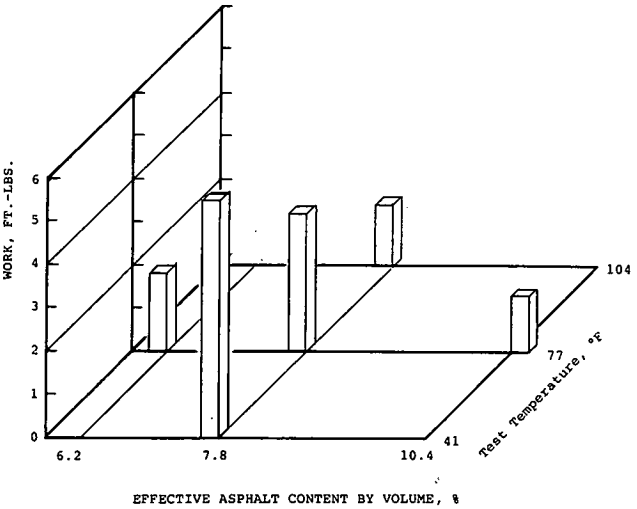

Figure 94. Work as a function of effective asphalt content by volume and temperature for the Georgia mixture.

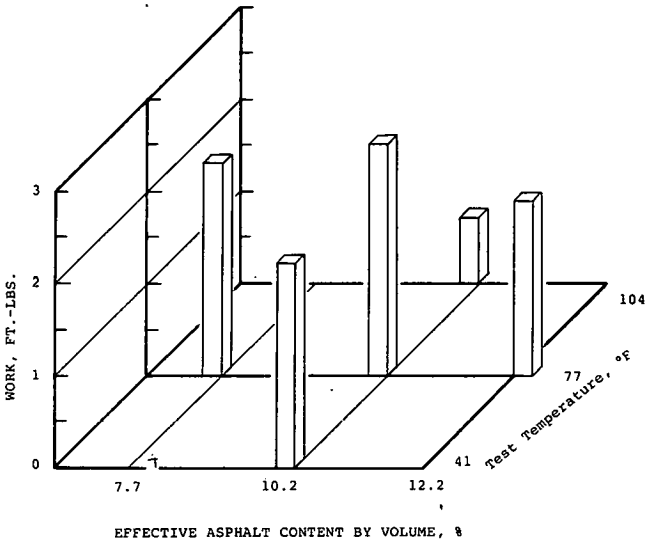

Figure 95. Work as a function of effective asphalt content by volume and temperature for the New York-Rason mixture.

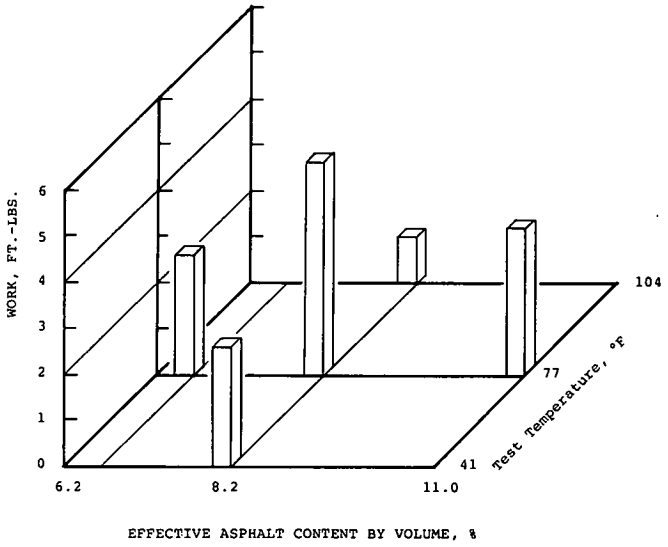

Figure 96. Work as a function of effective asphalt content by volume and temperature for the Wisconsin mixture.

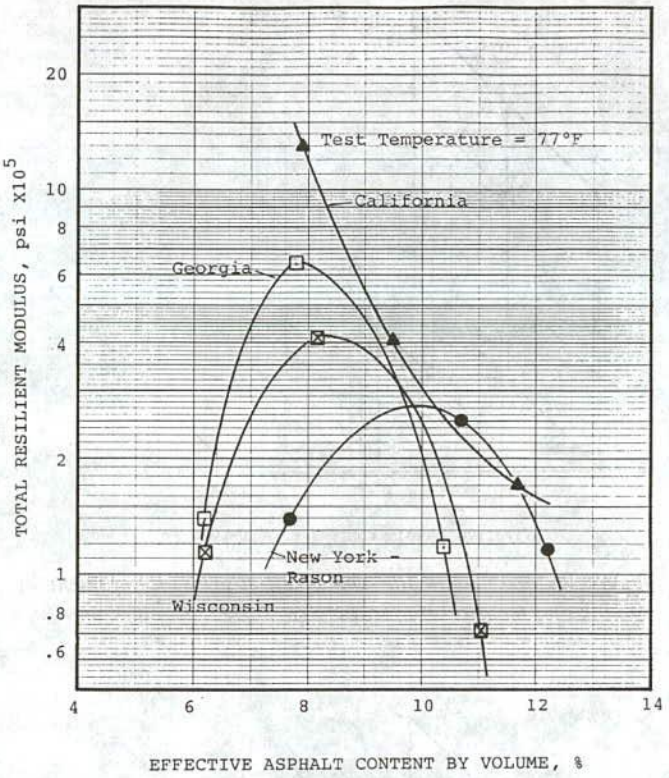

Figure 97. Total resilient modulus as a function of asphalt content by volume.

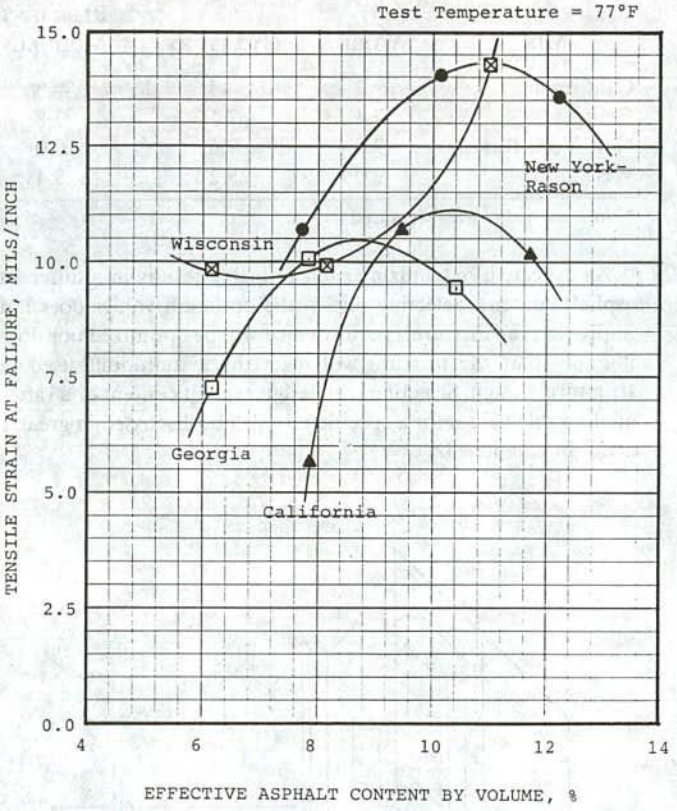

Figure 99. Tensile strain at failure as a function of asphalt content by volume.

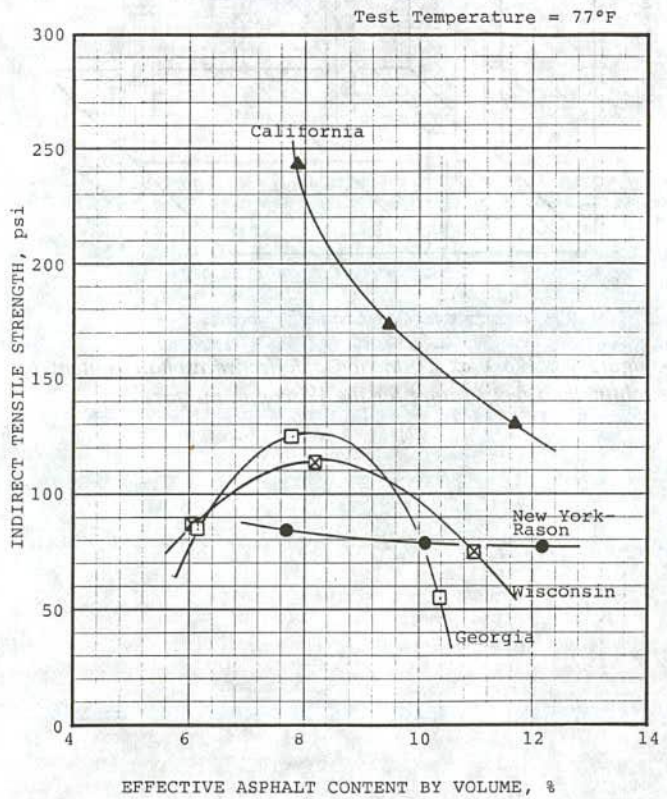

Figure 98. Indirect tensile strength as a function of asphalt content by volume.

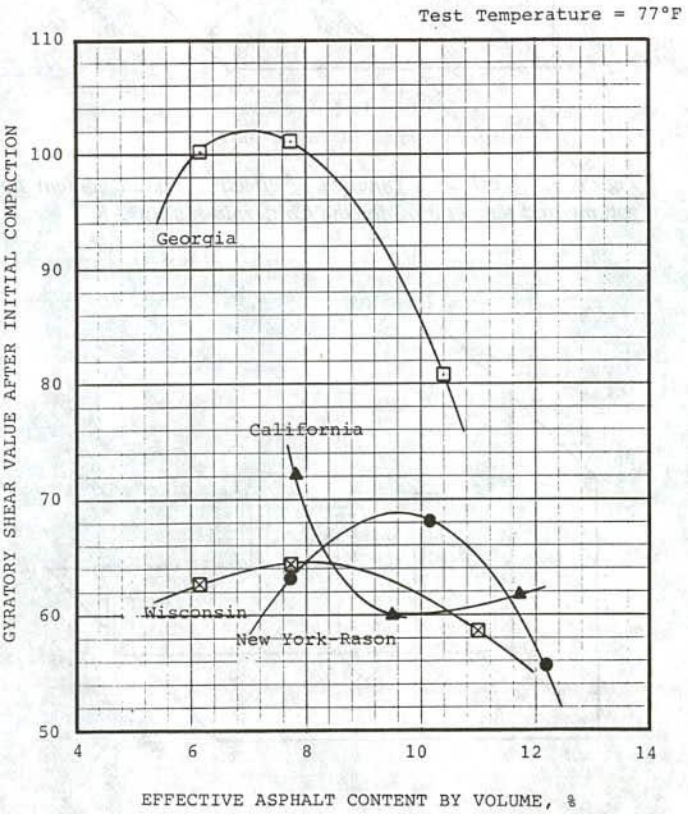

Figure 100. Gyratory shear stress as a function of asphalt content by volume.

CHAPTER 3
INTERPRETATION, APPRAISAL, APPLICATION

The focus of the NCHRP 9-6(1) work effort was to modify existing laboratory mixture design procedures and measure those properties used in structural design and pavement performance predictions. In other words, directly correlate mixture design with structural design (see Figure 1 in Chapter 1, section 1.4). This chapter of the report provides recommendations for the implementation of the results and findings presented in Chapter 2.

The initial approach taken in AAMAS was to build on presently accepted methods of mixture design which account for air voids and acceptable stabilities based on Hveem or Marshall procedures. Once an initial mixture design is developed, specimen preparation and conditioning procedures are used to measure those engineering properties used in structural design. Results of these mixture tests on conditioned specimens are then judged by applicable failure criteria for each distress mode specified to establish whether the "proposed" mixture design will satisfy the thickness design requirements. This initial process was taken one step further by using the AAMAS concept to develop a mixture design procedure based on performance-related criteria.

Unfortunately, what happens in the laboratory in some cases does not necessarily represent actual construction in the field. Take for example the Texas (TX-0021) and Colorado (CO-0009) projects, where an incorrect Rice specific gravity was used for calculating air voids and controlling compaction of the field mixtures. No mixture design or laboratory analysis procedure can be expected to predict how a mixture will perform when the materials change or when the mix is placed on the roadway and is not in conformance with the design requirements.

3.1 SELECTION OF MIXTURE COMPONENTS

The overall design process for asphaltic concrete mixtures is a compromise to optimize several mixture characteristics. Traditionally, mixture characteristics used for optimization have included stability, durability, unit weight, and air voids. All of these characteristics are dependent on the asphalt content (the mixture design curves are presented in Appendix E). Stability is commonly defined as resistance to deformation under load. This includes nonrecoverable deformations from both one-dimensional densification and plastic movement. Durability can be defined as the resistance to wear and weathering. Wear includes abrasive traffic effects on the aggregate and asphalt. Weathering includes changes to the asphalt cement from the environment (volatile losses and oxidation) and the effects of water on the mixture.

In selecting the optimum asphalt content for a dense-graded mixture, gradation, minus 200 material, air voids, VMA and VFA are factors that can be used as guidelines in determining the JMF (job mix formula). Figures 101 and 102 show the relationship between air voids and VFA and VMA, respectively, for the initial five AAMAS mixtures. Figure 103 displays the relationship between VMA and VFA (combining Figures 101 and 102 at identical air voids) for all of the mixtures considered in this study. As shown, most of the AAMAS mixtures are unable to satisfy all criteria simultaneously without changing the binder content or aggregate blend. Only the MI-0021, VA-0621 and New York (Prima) mixtures can satisfy both a VMA and VFA requirement. Thus, should the JMF have been changed or are some of these criteria inappropriate? This question will be addressed in the following sections.

3.1.1 Grading Considerations

In many cases, the types of aggregates used become a choice restricted by economical considerations (i.e., the use of locally available materials). It is not the intent of AAMAS to restrict the use of local materials that could be marginal, but to evaluate their use in terms of pavement performance. However, the use of a proper gradation for a dense-graded asphaltic concrete surface material can be critical to ensure a durable and stable mix.

The gradation of the aggregates sampled from the mix during plant production was compared to the grading specifications presented in ASTM D 3515 "Standard Specifications for Hot-Mixed, Hot-Laid Bituminous Paving Mixtures" for each mix. These graphical comparisons are provided in Appendix E. The Texas (TX-0021) and Wisconsin gradations are outside the D 3515 grading specifications. The Texas mixture has a relatively large amount of material retained between the No. 8 and 50 sieves (Figure E.1 in Appendix E). These two mixtures had the steepest creep curves (Table 32) and lowest gyratory shear values (Figure 77).

It is important to note that for three mixtures a significant difference was found between the combined grading curve used for mixture design and the sieve analyses of the individual stockpiles sampled during production. This difference occurred for the Colorado, Michigan, and Virginia projects. For the Texas and Wyoming projects, the combined grading curves used for mixture design were unavailable. There was also a significant difference between the gradations measured on the combined aggregate after production (shown on the mixture gradation charts in Appendix E) and the gradation curves of individual stockpiles sampled during construction. This difference implies some type of error or bias, either during stockpile sampling or sample separation in the laboratory.

The least difference occurred between the aggregate blend sampled during production and the aggregate blend obtained from mix design records (refer to mix gradation charts in Appendix E). Regardless, since the gradation of the combined aggregate from the mix and the aggregate blend obtained from mix design records are similar, the aggregate gradations measured from the mix sampled during production were used in all testing and mixture design studies.

In selecting a proper gradation, comparisons are made to the FHWA 0.45 power gradation chart using different combinations

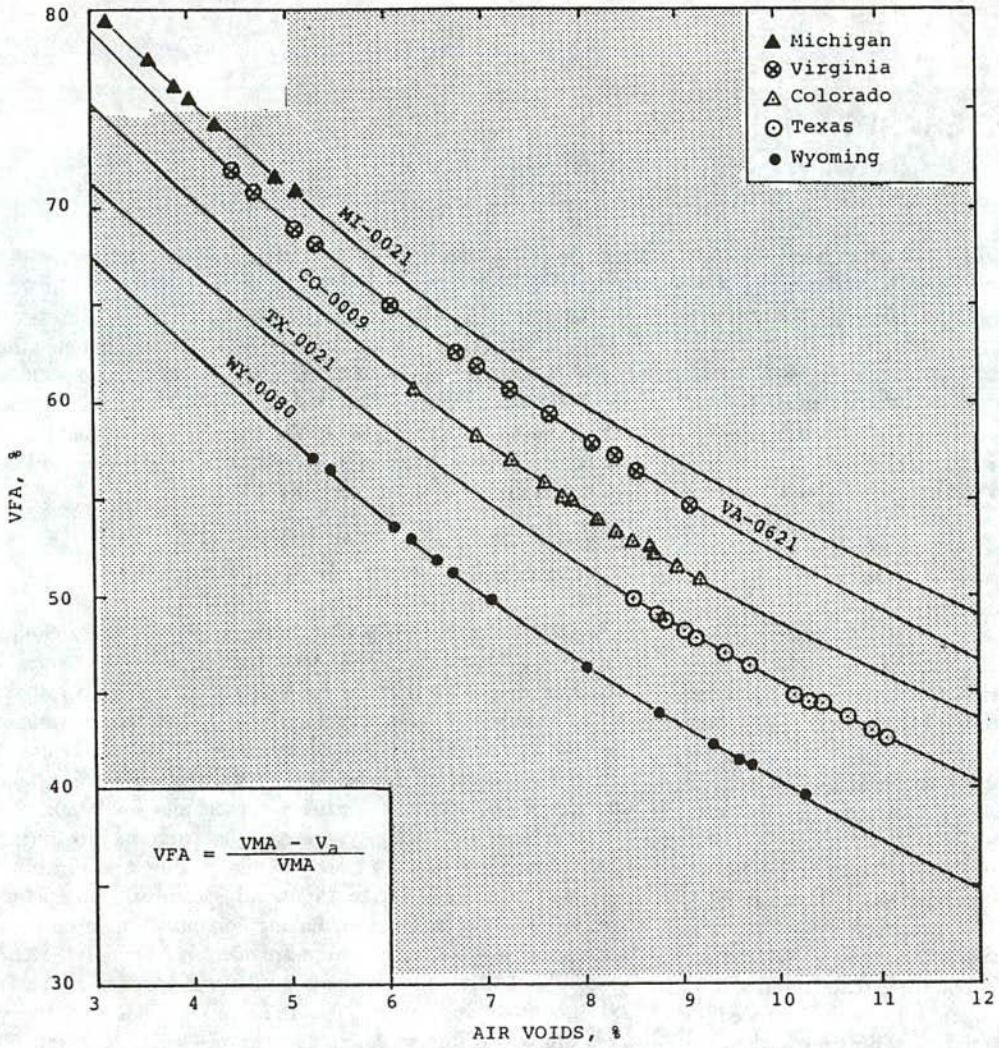

Figure 101. Relationship between air voids and VFA for each of the AAMAS mixtures.

of the coarse and fine aggregate. Both an absolute and arithmetic difference from the 0.45 power gradation curve or assumed maximum density curve (Appendix C) can be calculated for each aggregate blend (gradation curve) meeting the mixture gradation specifications. Gradations should be selected that are reasonably close to the 0.45 power gradation curve, but not so close that the VMA is so small requiring only a small amount of asphalt for adequate air voids.

The combined gradings for each of the AAMAS mixtures have been compared to the 0.45 power curve, which are graphically presented on mixture gradation charts in Appendix E. Values of "ABS DIFF" and "ARITH DIFF" were calculated for each grading, and are the absolute and arithmetic difference between the actual gradation and the 0.45 power curve, respectively. These values provide a measure of the similarity of the actual gradation curve to the assumed maximum density curve. The following lists these two values calculated from the average gradation measured from the bulk mixtures sampled at the plant during production:

STATE/PROJECT	ABS DIFF	ARITH DIFF
Colorado, CO-0009	12.7	1.7
Michigan, MI-0021	21.7	9.3
Texas, TX-0021	22.0	5.6
Virginia, VA-0621	9.0	−4.0
Wyoming, WY-0080	23.9	−9.5
California, CA	18.1	−4.1
Georgia, GA	14.5	7.7
New York-Rason	37.2	−37.2
Wisconsin	22.1	15.7

No correlations were found between these two values (ABS DIFF and ARITH DIFF) and the engineering or compaction properties. Thus, these values do not need to be calculated for mixture design.

Betenson et al. (*71*) have recommended that limits be placed on the "primary control sieves." Values suggested by the WASHTO Committee (*71*) are listed below:

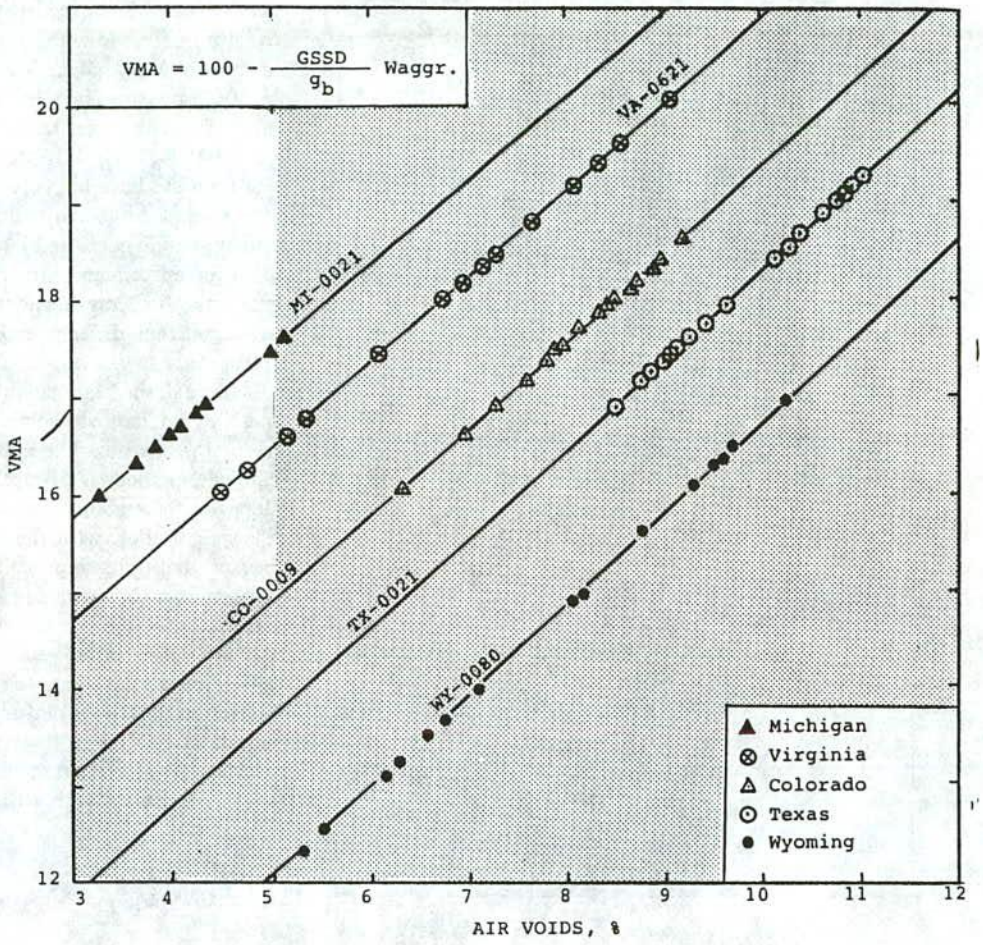

Figure 102. Relationship between air voids and VMA for each of the AAMAS mixtures.

Primary Control Sieve Size, No.	Maximum Percent Passing, %
4	55
10	37
40	16
200	3 to 7

Most of the gradations measured from bulk material sampled at the plant on the AAMAS projects meet these criteria, with the exception of the California, Texas, and Wisconsin blends. The Texas and Wisconsin mixtures were the only ones outside the grading specifications given in ASTM D 3515. For the Texas (TX-0021) and Wisconsin mixtures, the amount of material passing the No. 50 sieve was 28 and 24 percent, respectively, significantly greater than any of the other aggregate blends and the suggested limit on the No. 40 sieve listed above. The Texas mix also exhibited the "hump" in the gradation curve (refer to Figure E.1 of Appendix E). This condition significantly increased the creep measured on the mixture at the higher temperatures (Figure 44), and caused a significant reduction in shear strength (Figure 77).

At 77°F, the TX-0021 mixture had the steepest slope of all the creep curves, and the creep modulus values decreased significantly when the test temperature was increased from 77°F to 104°F (Figure 44). Removing the "hump" in the gradation curve (i.e., reducing the amount of material passing the No. 50 sieve) will increase the strength of the mixture and increase the creep modulus at the longer loading times and higher temperatures. Figures 104 and 105 illustrate this effect on the asphalt content-air void relationship for the different gradations. By eliminating the "hump" in the gradation curve for the TX-0021 mix (Figure 105), the asphalt content requirement at 5 percent air voids decreases from 5.4 to 4.8 percent, while the corresponding film thickness increases from 4.77 to 9.09 microns. For the CO-0009 mix (Figure 104), changing the fine-to-coarse aggregate blend only had a small effect on the asphalt content at 5 percent air voids, but a significant effect on film thickness.

For mixtures that support high tire pressures or heavy traffic loads, the magnitude of minus 200 material is important. Typically, the range of minus 200 material is limited to 3 to 6 percent by weight for high tire pressures (greater than 100 psi). The purpose of this limitation is to ensure that a stable, durable mixture is obtained. High amounts of minus 200 material result in the mixture having a higher asphalt content leading to lower stabilities but higher durability. All of the projects were within these limits (based on a wet sieve analysis), with the exception of the California and Wisconsin mixes (Table 8). The amount of minus 200 material in the Wisconsin mix was very high at 11 percent. This high percentage of fines increases the asphalt demand, and significantly reduces the creep modulus and shear

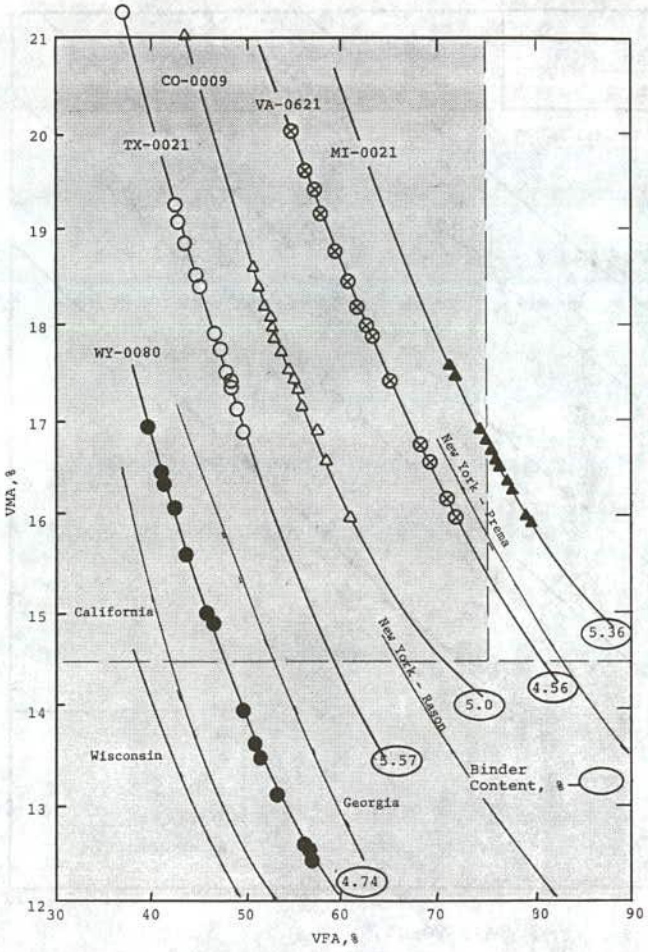

Figure 103. Relationship between VMA and VFA for each of the AAMAS mixtures.

strength of the mixture. Thus, maintaining a limit on the minus 200 and minus 40 or 50 material can be important in maintaining adequate shear strength and reducing creep.

3.1.2 Establish Range and Seed Value of Asphalt Content

Before specimens are prepared in the laboratory for mixture design, the range of asphalt contents is selected. This range is usually in 0.5 increments that include 4 or 5 values, typically selected from past experience. However, program ASPHALT can be used to calculate the asphalt content associated with a 4 percent air void level. This value would then represent the central or "seed" value used in mixture design. Two asphalt contents below and two above this "seed" value are used to prepare specimens for mixture design in increments of 0.5 percent.

Use of the Marshall (either 50 or 75 blow compactive effort) and Hveem mixture design procedures will result in different optimum asphalt contents, because of the differences in compactive effort (Figure 30 and Appendix E). Results from the Marshall procedure indicate that all mixtures should provide adequate performance, as designed, but not necessarily as constructed. On the other hand, the Hveem procedure indicates that only the Texas (TX-0021) mixture has adequate stability. Low Hveem stabilities have historically indicated mixtures susceptible to rutting (i.e., low shear strengths). The Texas mix had the lowest gyratory shear value. Conversely, the MI-0021 and VA-0621 mixtures had the greater gyratory shear values at 140°F of the first five mixes tested (Figure 77), and the greater toughness at 41°F (Table 47). On the other hand, the MI-0021 mixture was found to have high creep compliance values and low tensile strengths at 140°F. In addition, some of the Colorado, Texas, and Wyoming cores and laboratory specimens failed during the static creep test and were found to have very poor adhesion properties (i.e., low tensile strains at failure) at 41°F. Thus, there are significant differences between the results of the different tests.

Although the Marshall procedure is much simpler, the Hveem method did indicate some of those mixes with inferior engineering properties. These limited results, however, do not indicate one method significantly superior to the other. In fact, the slopes of the stability versus asphalt content curves (Appendix E) were similar, with the exception of the VA-0621 mixture. Because both are empirically based, experience plays the more important role. Thus, it is suggested that the method currently used by individual agencies be used to establish the initial design asphalt content when using empirical procedures. The AAMAS is then used to evaluate the mixture to ensure that the assumptions used in structural design will be satisfied. Section 3.5 provides a discussion on those parameters and engineering properties that are suggested for use in a performance-related mixture design procedure, rather than using an empirical method.

3.1.3 Air Voids

Any mixture design procedure must, as a minimum, provide for acceptable voids in the mixture and an acceptable level of stability. The asphalt content selected is based on a target air voids content following a laboratory compaction procedure which is designed to duplicate field compaction followed by densification caused by traffic. This is called final compaction, and the air void content associated with final compaction is called final voids content. These values are, of course, dependent on tire pressure, wheel load magnitudes and number of applications, and environmental conditions.

Pavement performance studies (*42, 72*) have shown that initial air voids less than 3 percent lead to excessive plastic flow. On the other side, final air void contents higher than 6 percent result in high air and water permeability which cause durability problems. For example, Kandhal (*73*) found mixtures with higher air voids to have greater extents of raveling. Thus, the range of an acceptable final air void content is a narrow one. Typically, a design air void range of 3 to 5 percent has been found to be acceptable in most environments.

Figure 106 compares the air voids calculated by program ASPHALT to those measured on specimens compacted with the Marshall (50-blow compactive effort) and Hveem procedures at the same asphalt content. Air voids versus asphalt content from all three procedures have been plotted on the mixture design curves provided in Appendix E. As shown, differences do exist, as expected, but the air voids calculated with program ASPHALT are more similar to the Hveem procedure than the Marshall 50-blow procedure. In either case, program ASPHALT can be used to estimate the relationship between asphalt content and air voids for different aggregate blends. This was illustrated

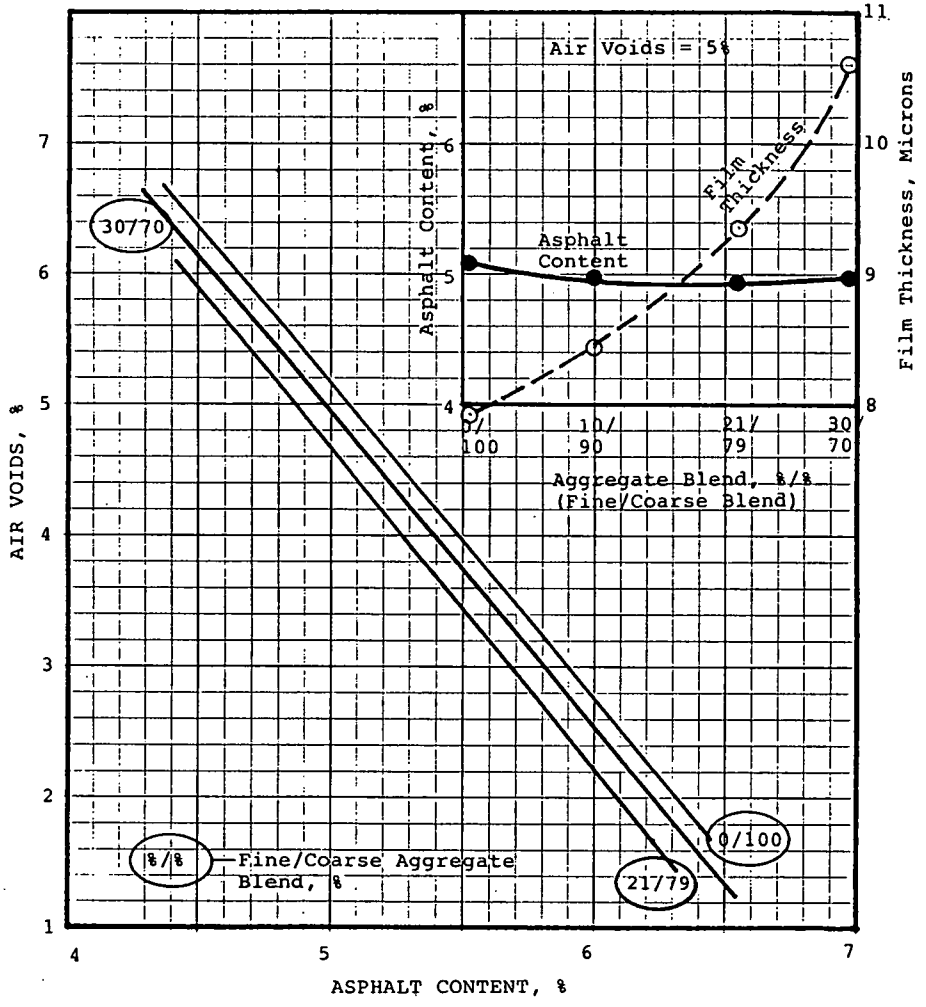

Figure 104. CO-0009 Aggregates

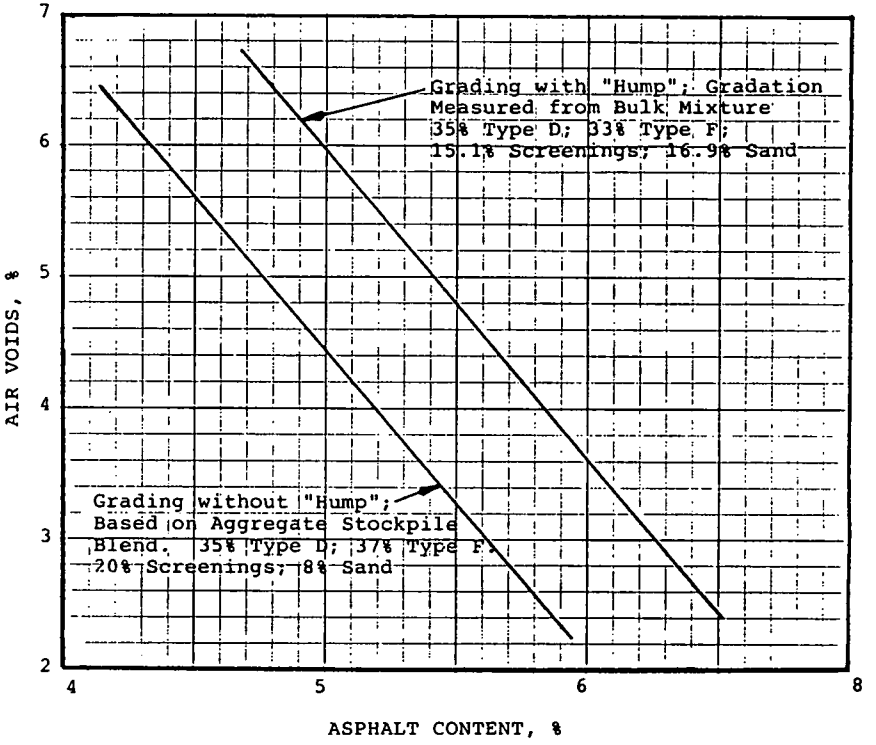

Figure 105. TX-0021 Aggregates

Figures 104 and 105. Asphalt content-air void relationships calculated with program ASPHALT using different aggregate blends for CO-0009 and TX-0021 mixtures.

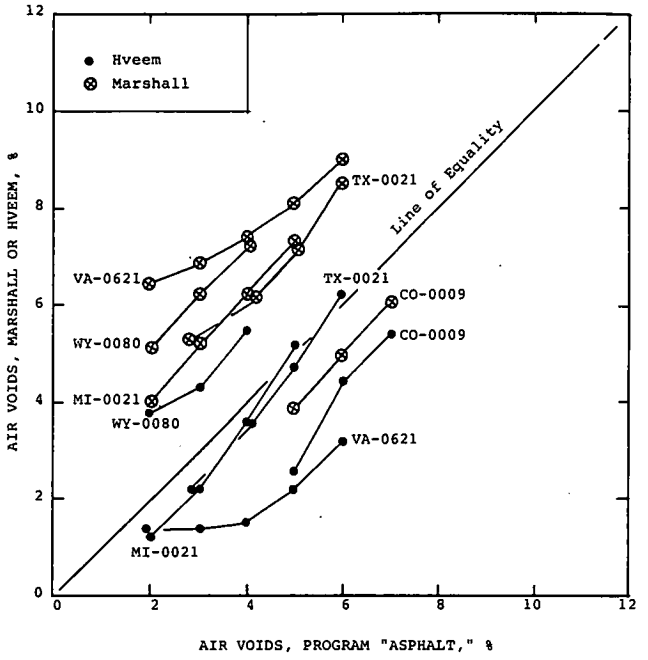

Figure 106. Comparison of air voids from samples prepared for the Marshall and Hveem mix design procedures and from program ASPHALT at the same asphalt content.

in Figures 104 and 105, which show the effect of changing the aggregate blend on the asphalt content and air void relationship for the TX-0021 and CO-0009 mixtures.

3.1.4 VMA and VFA Considerations

Both VMA and VFA have been considered for use in mixture design specifications. The Asphalt Institute (*48*) has adopted minimum VMA requirements for mixture design, and many state highway agencies have adopted these same requirements. The Corps of Engineers and Federal Aviation Administration (*74*) have adopted limits on air voids of 3 to 5 percent and a VFA requirement of 75 to 85 percent to ensure the mixture's durability. On the other hand, others such as NAPA (*75*) have argued that there are insufficient performance data to justify these minimum and maximum requirements.

If VMA or VFA are parameters related to pavement performance, the engineering properties that have a direct effect on pavement performance should be related to these values. Various correlations were made between VMA and VFA and different engineering properties to determine if either value was related to those properties required for pavement design/evaluation models. Figure 107 shows the effect of VMA on indirect tensile strength at a test temperature of 41°F. The data do show a trend, but no distinguishable relationship was found to exist.

On the other hand, indirect tensile strain at failure was found to be related to VFA at a test temperature of 41°F. These data are presented in Figure 108. The data measured at 41°F are much more related to VFA than the values measured at 77 and 104°F. Figure 109 shows the relationship between work and the product of VFA and maximum aggregate diameter for a test temperature of 41°F. These data indicate that mixture toughness increases with an increase in VFA and aggregate diameter. Regan (*1*) has also presented data showing that as VMA decreases, the cohesion of the mix increases.

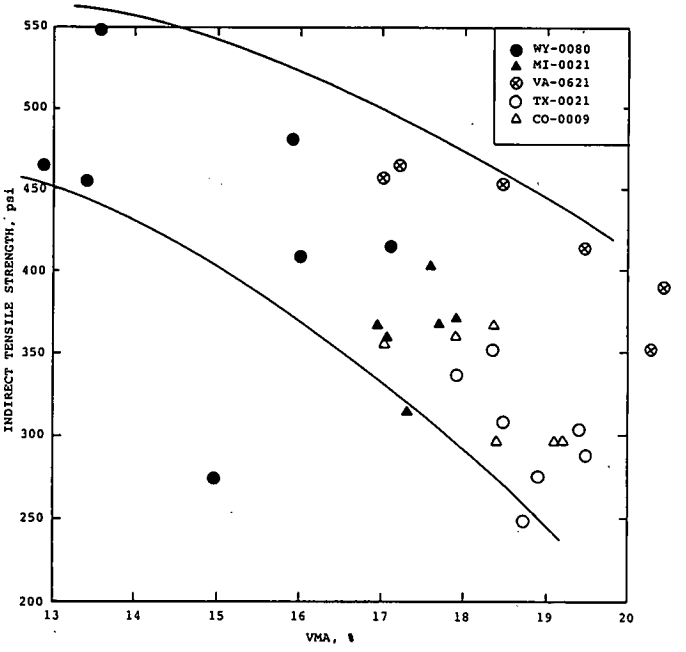

Figure 107. Indirect tensile strength as a function of VMA for a test temperature of 41°F.

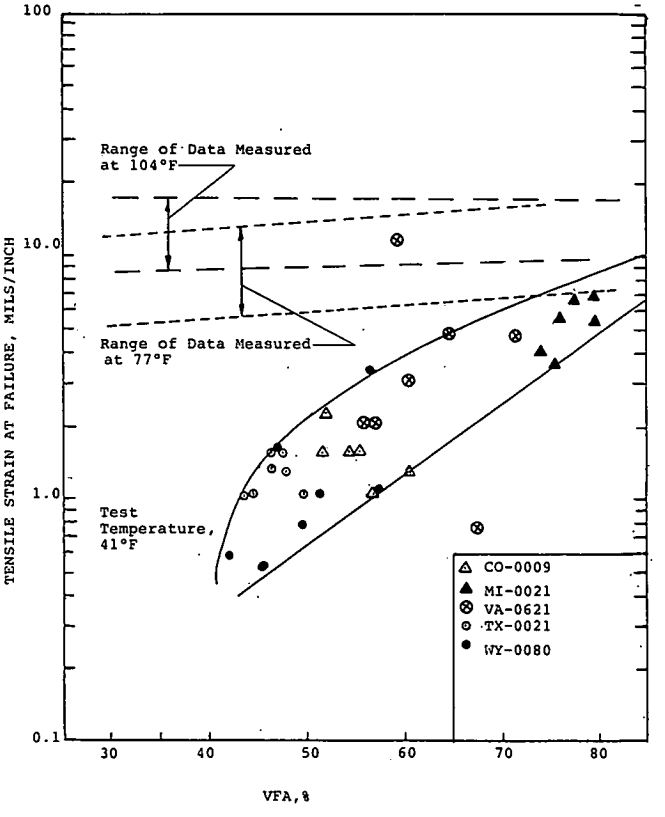

Figure 108. Indirect tensile strain at failure as a function of VFA.

Although performance data are limited, data are available from the literature that indicate a close tie between VMA and VFA and pavement performance measures. For example, Huber et al. (*42*) presented threshold values for air voids, VFA, and stability for mixtures placed in wet-freeze environments. Bjorklund (*76*) also presented data relating VMA and air voids to both permanent deformation and fatigue cracking. Bjorklund concluded that as VMA and air voids decreased, the resistance to deformation and fatigue cracking increased.

Figures 101 and 102 showed the relationship between air voids and VFA and VMA, respectively, for each of the AAMAS projects. These curves were determined by varying the compactive efforts used in the field and laboratory. It should be understood, however, that for each curve the asphalt contents and gradation within each mixture are assumed to be constant.

Figure 103 illustrated the relationship between VMA and VFA for each mixture, as previously explained. As shown, only the MI-0021, New York-Prima, and VA-0621 mixtures can satisfy both the VMA and VFA requirements suggested in the Asphalt Institute's MS-2 Manual, if adequately compacted. It is interesting to note that the MI-0021 and VA-0621 mixes were the only two mixtures where work continued to increase with a decrease in test temperature (Table 47), with the exception of the Georgia mix. The Georgia mix was the only one of the remaining seven that could not meet both criteria simultaneously, but maintained an increase in work with decreasing test temperature (Figure 94) and maintained adequate shear strength throughout the traffic densification procedure (Figure 77). For the other mixtures that do not meet the VMA and VFA requirements simultaneously, work decreased between test temperatures of 77 and 41°F.

Because of time constraint, there are no performance data available on the AAMAS mixtures—although the second section (VB/SS) of the TX-0021 project did crack and tear under vibratory compaction. Until extensive performance data become available, there will be controversy regarding VMA-VFA requirements for mixture design. The Long-Term Pavement Performance research of the Strategic Highway Research Program should provide this much needed data. In the interim, however, sufficient data have been presented in the literature to warrant limitations for VMA and VFA. For purposes of selecting a JMF and a design asphalt content, the following guidelines are suggested for VMA and VFA (unless local experience suggests a tighter control):

Property	Maximum Aggregate Size, Inch	Suggested Minimum Value	Suggested Maximum Value
VMA	1½	12*	---
	1	13*	---
	¾	14*	---
	½	15*	---
VFA	---	70	85

*Taken from the Asphalt Institute's MS-2 Manual (*48*).

3.2 LABORATORY SIMULATION OF FIELD COMPACTION

There are numerous procedures that can be used to prepare and compact laboratory specimens for testing and evaluation.

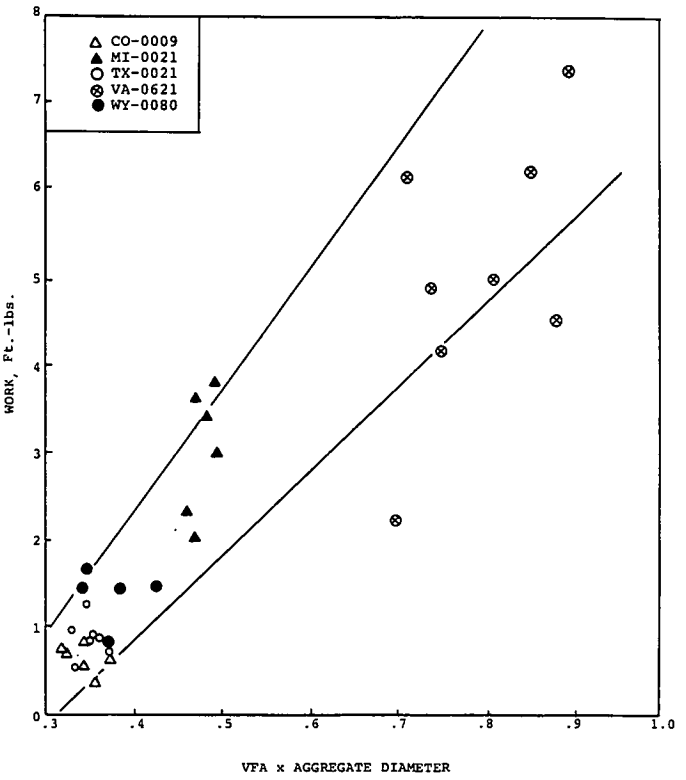

Figure 109. Effect of VFA and maximum aggregate diameter on work or toughness calculated for each specimen tested.

Some comparisons of different compaction techniques have been performed to determine if specimens compacted with different devices will have the same properties. One of the earlier comparative studies was performed by Fields (*77*) in 1958 who compared various versions of the Marshall hammers and the Hveem kneading compactor. Fields found differences in Marshall stabilities between specimens compacted with the different devices, and developed compaction equivalencies between the Marshall hammer and Hveem kneading compactor. Although the study was thorough, engineering properties were not measured nor were they included in the comparisons.

Epps et al. (*78*) conducted a compaction study in 1969 and also found differences in stabilities and strengths of mixtures compacted to the same air voids, but with different devices. The laboratory devices Epps used were the Texas gyratory, Corps of Engineers gyratory, Marshall hammer and California kneading compactor. However, the most critical item required for selecting a laboratory compaction procedure for AAMAS is ensuring that the engineering properties of laboratory prepared samples are equivalent to the properties of the in-place material.

It is the opinion of some researchers (*45*) that this can not be adequately achieved in the laboratory and, thus, requires the use of full-scale tests to evaluate asphaltic concrete mixtures. This is considered impractical unless all laboratory models are found to provide an unacceptable simulation of field-placed materials. Therefore, various mixture properties were used to compare different laboratory compaction techniques to field samples. These comparisons included an air void analysis, particle orientation, and mixture response (i.e., characterization of indirect tensile strengths, resilient moduli, and creep).

3.2.1 Statistical Analysis of Data

All data were analyzed using the PC version of the Statistical Analysis System (SAS). The statistical analyses that were conducted on the data included the use of two procedures. The first was to use t-tests and the Student-Newman-Keuls (SNK) mean separation procedure to identify statistically significant differences among the means of the different compaction methods or various sets of data. The second technique included the calculation of the mean squared error (MSE) between each of the laboratory compaction methods and the primary field compaction method for each project. The mean test value from the field cores was used as the target value. Table R.1 in Appendix R presents a summary of the field projects, the field compaction methods, the laboratory compaction methods, and the tests for which statistical analyses were conducted.

The laboratory compaction methods were evaluated by determining how well the test results for laboratory compacted specimens relate to the test results for the field compacted cores. The SNK results were used to identify which laboratory methods had results that were not significantly different from the field results. MSE values were used to rank the laboratory methods in order of how well they predicted the field results. The MSE value places equal weight on the variance of the laboratory data and the square of the bias (defined as the difference between the laboratory mean and the field mean). The best laboratory method is therefore the one with the smallest MSE value. Figures R.1 through R.10 in Appendix R provide a graphical comparison of the laboratory and field properties of the mixtures.

3.2.2 Air Voids

Although the original intent of the AAMAS test section was not to reproduce bad construction practices in the field (i.e., high air void contents of dense-graded asphaltic concrete mixtures), evaluation of the sections with high air voids can be used to ensure that the sample preparation techniques will simulate those properties of field cores both in an acceptable and high air void range.

Figures D.1 through D.5 (Appendix D) show the probability distribution of air voids for the field cores and laboratory compacted specimens. As expected, the variation of air voids in the field is much greater than that of the samples compacted in the laboratory. Thus, sample sets were selected such that the mean air void between the field cores and laboratory compacted specimens for an individual cell or sample set were approximately equal. In some cases, this was not always possible because significantly lower air voids were obtained in the compacted specimens. For example, use of the AV/KC consistently resulted in lower air voids (refer to Figures D.2 through D.4 in Appendix D).

During the preparation and compaction of beam specimens with the MS/WC device, it was much more difficult to compact the coarser mixes to the required air void content. The top surface and edges of the beam samples were very coarse, which resulted in high porosity in certain areas. Some beams were sawed into three equal sections, and the air voids near the ends where found to be significantly greater than the center section. Thus, the specimens used for air void determinations and other testing were only cored from the beam's center section. The ends and sides of the beams were discarded and not used in the testing program.

Samples were also sawed longitudinally from one end to the other to visually observe the distribution of the coarse aggregate particles. Segregation was noticeable in the coarser mixes. Thus, the mixture had to be remixed in the mold with a spatula to ensure that the coarse particles were not segregated or confined to the edges of the sample.

3.2.2.1 Mean Comparisons

Air void data were analyzed for all five laboratory compaction methods for all five projects, with the exception that there were no data for the AV/KC method for the CO-0009 or WY-0080 projects (Table R.2, Appendix R). There were no statistically significant differences between the means of the AV/KC, CK/CC, MM/HC, and MT/GS laboratory compaction methods. The MS/WC method was significantly different from the field method for three of the five projects.

3.2.2.2 MSE Results

The MSE rankings for the five laboratory compaction methods (Table R.3, Appendix R) indicate that the CK/CC method best matched the field air voids content, followed, in decreasing order, by the MM/HC, MT/GS, AV/KC, and MS/WC methods (Table R.4, Appendix R).

3.2.2.3 Air Void Gradients

Air void gradients measured through selected cores and specimens were also used to determine differences between compaction techniques. Two values were calculated as discussed in Chapter 2 (section 2.3.1.4). These were MAXDIF and air void ratio (Eqs. 2-1 and 2-2). Figure 110 provides a comparison of the MAXDIF values for the cores and laboratory specimens. it can be seen that the CK/CC consistently compacted specimens with a much greater air void difference, whereas the MT/GS consistently resulted in a slightly lower MAXDIF value.

The other value used was air void ratio, V_{ar}. Figure 111 summarizes these results by compaction device. As illustrated, the center slice of the cores and specimens, on the average, had the lower air void or higher density, with the exception of the Arizona vibratory/kneading compactor (AV/KC). The AV/KC consistently had the lower air voids or higher density on one end of the specimen.

These data indicate that all of the devices used can compact specimens in the laboratory to identical air voids measured on field cores by simply varying the compactive effort. The important question or consideration is, of course, what compactive effort is to be used in the laboratory during mixture design? This question is addressed and discussed in section 3.3.1.

3.2.3 Particle Orientation

Angles of orientation were measured for both cores and laboratory compacted specimens using the procedure discussed in Chapter 2. Appendix P provides a summary and listing of all data measured. These include the size of the sample, the number of particles analyzed, and the frequency distribution of the angle

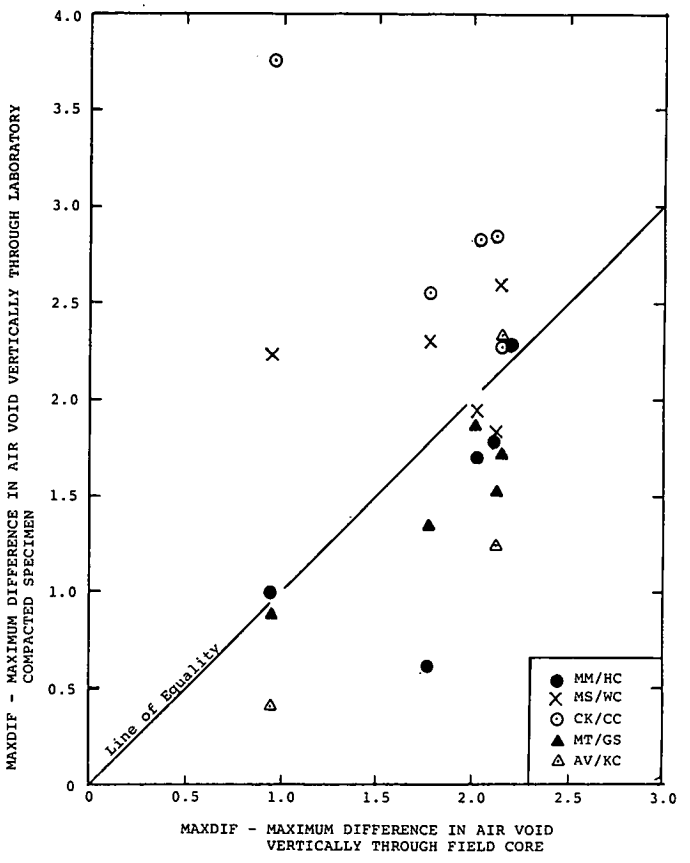

Figure 110. Comparison of air void difference (air void gradient) for the samples prepared by different techniques.

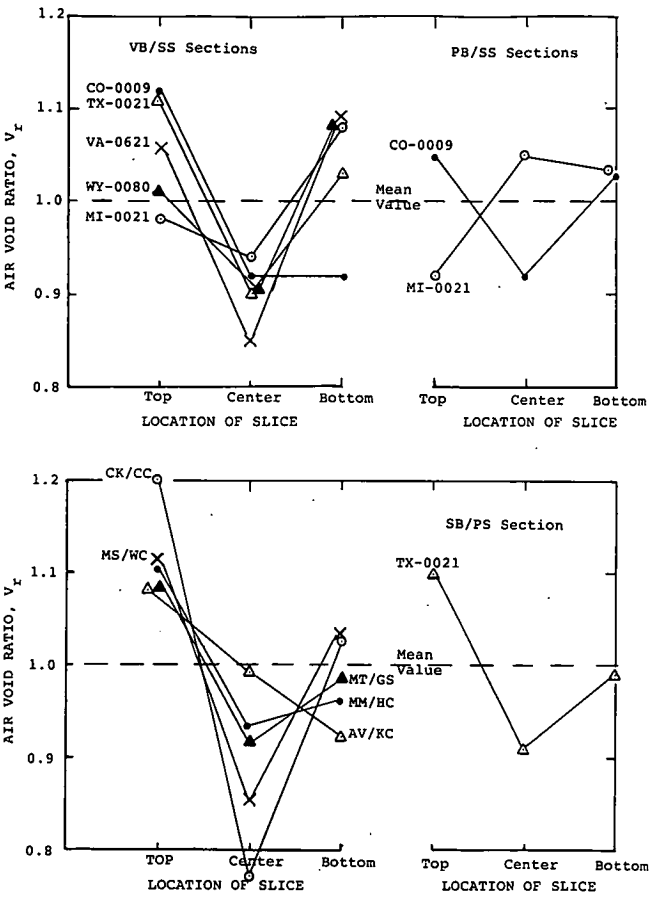

Figure 111. Comparison of air void ratios, V_r, for the field cores and laboratory compacted specimens.

of orientation. These values are used to determine if there is a preferred angle of orientation by compaction technique.

As used herein, the term preferred orientation refers to an arrangement of particles that can be statistically shown to exhibit a significant deviation from random orientation. The particles are said to be randomly orientated when the observed frequency distribution of the orientation is rectangular. The simplest way of testing this hypothesis is to use fundamental laws of statistics. For this purpose, the theory of sampling has been employed and the level of significance adopted for the test was 0.05 percent. In other words, if the calculated probability is less than 0.05 percent, the deviation from chance is considered significant or preferred orientation. On the other hand, if the probability is greater than 0.05 percent, the orientation is not regarded as significant, and may be accepted as to chance or random orientation.

Cumulative frequency or probability density diagrams were prepared for each type of laboratory compaction device used. These diagrams are shown on Figures 112 and 113, and compared to the range measured from the field cores. None of the laboratory compaction devices simulated the same range for all cases, and all devices had approximately the same preferred angle of orientation. The gyratory shear (MT/GS) and steel wheel simulator (MS/WC), in some cases, however, did more closely simulate particle orientations measured from field cores (Figure 113). In summary, all compaction methods produced a preferred orientation of the larger particles. For comparison, the following listing summarizes the average angle for each compaction technique and standard deviation of the means:

Compaction Method	Average Angle	Standard Deviation
Field Cores	25.0	3.7
Vibratory/kneading* (AV/KC)	34.0	5.6
Kneading (CK/CC)	33.6	4.3
Marshall (MM/HC)	32.9	3.8
Steel wheel (MS/WC)	29.2	5.6
Gyratory (MT/GS)	31.2	9.2

*Device used to compact only the MI-0021, TX-0021 and VA-0621 mixtures.

The results obtained from this study are consistent with the results from a similar study conducted by Lees and Salehi (*69*) in 1964. Their study indicated that field compaction caused preferred orientation. Specimens compacted with laboratory rolling wheels (similar to the rolling wheel compactor used in this study) also caused preferred orientation of the particles. Application of a static load resulted in preferred orientation, as well. However, the mean angle and variation from a static load were much greater than that for the field cores and specimens compacted with the laboratory rolling wheel.

3.2.4 Mixture Properties

All test results measured on the field cores and laboratory compacted specimens are presented in Appendixes H and L. Figures R.1 through R.10 in Appendix R show a comparison of the laboratory compacted specimens and field cores using each of the mixture properties. To evaluate the average difference in means between the laboratory compaction devices and the field cores, an average absolute difference, ΔMP, for each of these properties was calculated. The absolute difference simply represents the average percent difference between the field cores and laboratory compacted specimens. This is mathematically represented by the following equation.

$$\Delta MP = \sum_{i=1}^{N_p} \frac{\left[\dfrac{MP_c - MP_s}{MP_c}\right]_i}{N_p} \qquad (3\text{-}1)$$

where MP_c is the average material property measured on the field core, which becomes the target value; MP_s is the average material property measured from the laboratory compacted specimen; and N_p equals number of data points for each compaction device.

Table 49 summarizes the results of this simple comparison. As shown, the MT/GS laboratory compaction device was found to more closely match, on the average, the engineering properties of the field cores. Less variation was noted for the indirect tensile strength and tensile strain at failure data, whereas the largest differences were found for creep compliance.

Table 49. Summary of average differences between the field cores and laboratory compacted specimens, ΔMP.

Compaction Device	Creep Compliance at 77F	Indirect Tensile Strength	Tensile Strain at Failure	Instant. Resilient Modulus
Arizona V/K Compactor AV/KC	0.77	0.51	0.47	0.41
Marshall Hammer MM/HC	0.80	0.35	0.45	0.55
California Kneading CK/CC	0.59	0.21	0.27	0.42
Steel Wheel Simulator MS/WC	0.51	0.31	0.11	0.26
Gyratory Shear Compactor MT/GS	0.44	0.14	0.16	0.37

Note: A zero difference indicates that the laboratory specimens had identical properties of the cores (no difference).

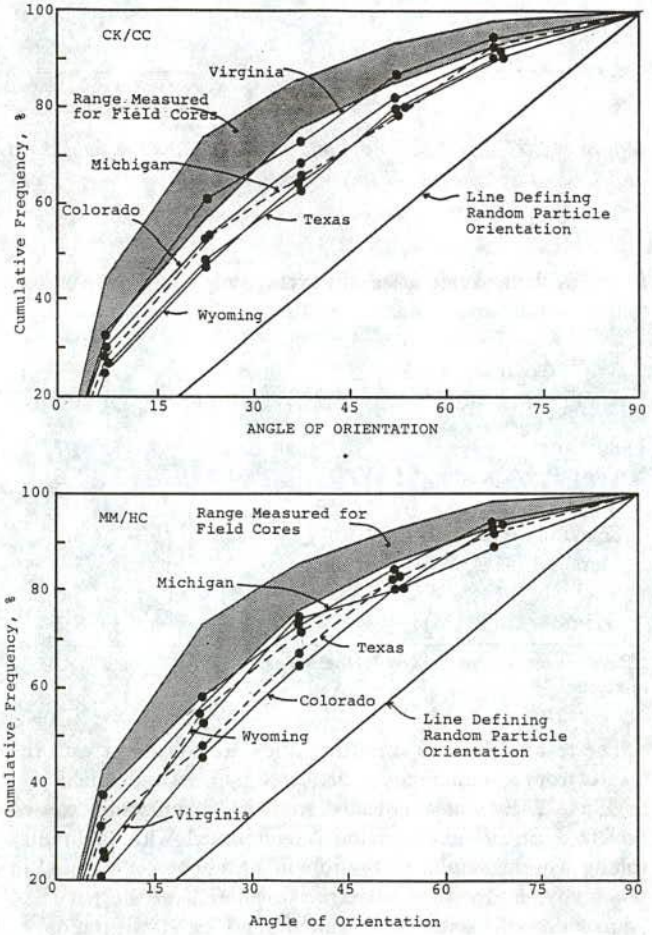

Figure 112. Graphical representation and summary of particle orientation data illustrating preferred orientation of particles measured from CK/CC and MM/HC specimens.

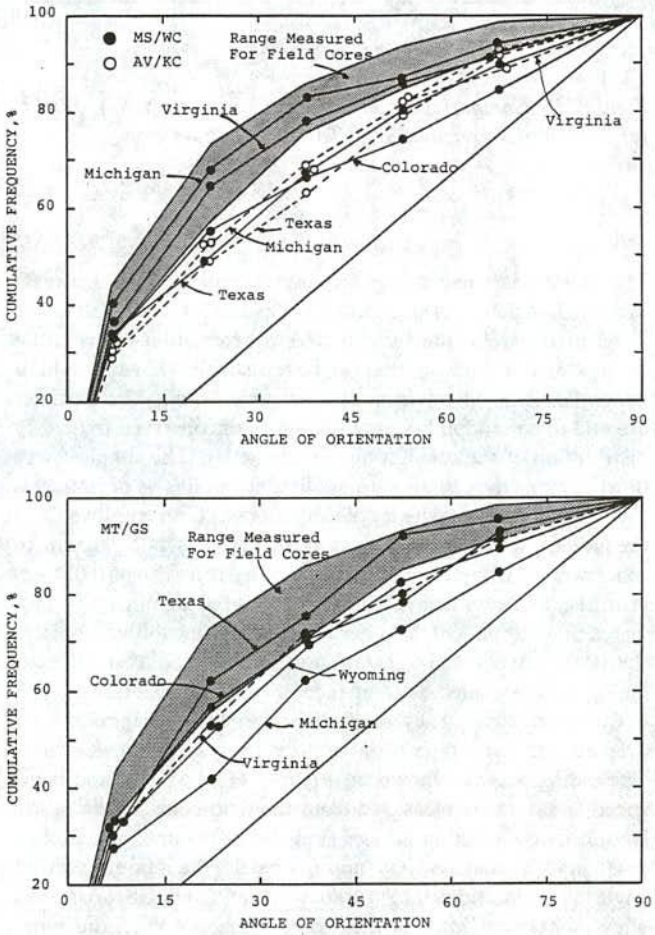

Figure 113. Graphical representation and summary of particle orientation data illustrating preferred orientation of particles measured from AV/KC, MS/WC and MT/GS specimens.

Two field compaction methods were used in each of the five projects. However, because of problems with the contractors' general unfamiliarity with the secondary compaction methods, only the field data from the primary (i.e., the method the contractor normally used in the state) compaction method were compared with the laboratory compaction methods. Data were analyzed for five laboratory compaction methods, although all five methods were not used for all tests for all projects.

The results of the statistical analyses can be summarized and presented in various ways. Appendix R discusses these data on a project basis, test basis, and temperature basis.

3.2.4.1 Results on a Project Basis

Since each project was constructed under different specifications, by different contractors, with different materials and with different field conditions, the data must be analyzed individually for each project. As noted previously, complete data for all three test temperatures were only received for the MI-0021, TX-0021, and VA-0621 projects.

Two analyses were conducted for each test for each project: a comparison of mean results (SNK procedure) and a determination of MSE values. In addition, an analysis of covariance was conducted on the creep curves at 77°F and 104°F. The results of the SNK analysis for each of the projects are summarized in Table R.2. The MSE results are summarized in Tables R.3 and R.4, while Table R.5 includes the analysis of covariance results.

There were insufficient data to analyze the results for DLOAD-104, because only three laboratory compaction devices were used on one project and only two laboratory compaction devices were used on two other projects. There were no data for the other two projects. The DLOAD-104 data were, therefore, not used in the analyses of the project data other than in the covariance analysis of the creep curves.

3.2.4.1.1 Michigan Project (MI-0021). The field compaction method for the MI-0021 project consisted of pneumatic breakdown and static steel secondary (PB/SS) rolling. Data were analyzed for all five laboratory compaction methods for most of the tests. There were no data for the MS/WC method for IDT-41 and MR-41.

The SNK mean separation technique was used to group the compaction methods that did not have significantly different means (at the 0.05 level of significance). The SNK results for the MI-0021 project are summarized in Table R.2. Data were available for eight different tests. None of the tests for any of the five laboratory compaction methods were significantly different from the field method.

A summary of the MSE results for the MI project is presented in Table R.3. This table lists the relative rankings for the five laboratory compaction methods on the basis of their MSE from the mean of the field compaction method. The rankings for each of the eight tests were averaged to determine an overall project ranking for each compaction method. The MT/GS and MS/WC methods tied for first overall, followed, in descending order, by the CK/CC, MM/HC and AV/KC methods (Table R.4).

3.2.4.1.2 Texas Project (TX-0021). The field compaction method for the TX-0021 project consisted of static steel breakdown and pneumatic intermediate (SB/PS) rolling. Data were analyzed for all five laboratory compaction methods for most of the tests. There were no data for the MS/WC method for IDT-41 and MR-41.

The SNK results for the TX-0021 project are summarized in Table R.2. Neither the MT/GS method nor the CK/CC method was significantly different from the field for any of the eight tests. The MM/HC method was significantly different for one of eight tests, the AV/KC method was significantly different for two of eight tests, and the MS/WC method was significantly different for two of six tests.

A summary of the relative rankings of the MSE results for the TX-0021 project is presented in Table R.3. The rankings for each of the eight tests were averaged to determine an overall project ranking for each compaction method. The MT/GS method was ranked first overall, followed, in descending order, by the CK/CC, MS/WC, MM/HC and AV/KC methods (Table R.4).

3.2.4.1.3 Virginia Project (VA-0621). The field compaction method for the VA-0621 project consisted of vibratory breakdown and static steel secondary (VB/SS) rolling. Data were analyzed for all five laboratory compaction methods for most of the tests. There were no data for the MS/WC method for IDT-41 and MR-41, or for the AV/KC method for DLOAD-77.

The SNK results for the VA-0621 project are presented in Table R.2. The CK/CC and MT/GS methods were significantly different from the field method for one of eight tests, while the MS/WC method was significantly different for one of six tests. The MM/HC method was significantly different for two of eight tests, and the AV/KC method was significantly different for two of seven tests.

A summary of the relative rankings of the MSE results for the VA-0621 project is presented in Table R.3. The rankings for each of the eight tests were averaged to determine an overall project ranking for each compaction method. The CK/CC, MS/WC and MT/GS methods tied for first overall, followed by the MM/HC and AV/KC methods (Table R.4).

3.2.4.1.4 Summary. For the three projects, both the CK/CC and MT/GS methods had means that were significantly different from the mean of the field method for only one of 24 tests. The MM/HC method was significantly different for three of 24 tests, the AV/KC method was significantly different for four of 23 tests, and the MS/WC method was significantly different for four of 18 tests. Based on the average MSE rankings for the three projects for each of the laboratory compaction methods, the MT/GS method ranked first in matching the test results of the field compaction method, followed, in decreasing order, by the MS/WC, CK/CC, MM/HC and AV/KC methods.

3.2.4.2 Results on a Test Basis

By sorting the results of the statistical analyses on the basis of the tests that were conducted, the laboratory compaction methods can be rated on their performance in matching the test results of the field compaction method for each of the tests that were conducted.

3.2.4.2.1 Indirect Tensile Strength (IDT). Indirect tensile strength test results at 41°F, 77°F and 104°F were analyzed for three projects, MI-0021, TX-0021, and VA-0621. There were no test results for the MS/WC method for the 41°F test, but results were received for all five laboratory compaction methods for the 77°F and 104°F temperatures. Both the CK/CC and MT/GS methods were significantly different from the field method for one of nine tests. The MM/HC method was significantly different for two of nine tests, the AV/KC method was significantly

different for three of nine tests, and the MS/WC method was significantly different for two of six tests.

The average MSE rankings of the five laboratory compaction methods for the three test temperatures for the three projects (Table R.3) indicate that the MT/GS method best matched the IDT results of the field method. The CK/CC and MS/WC methods tied for second, followed by the MM/HC and AV/KC methods (Table R.4).

3.2.4.2.2 Resilient Modulus (MR). Complete resilient modulus test results at 41°F, 77°F and 104°F were analyzed for the MI-0021, TX-0021, and VA-0621 projects with the exception of the MS/WC method at a test temperature of 41°F. Partial results were analyzed for the CO-0009 and WY-0080 projects for the 77°F and 104°F test temperatures, but these data are not considered in the discussion. Both the CK/CC and MT/GS methods were not significantly different from the field method for any of the nine tests, while the MS/WC method was not significantly different from the field method for any of the six available tests. Both the MM/HC and the AV/KC methods were significantly different from the field method for one of nine tests.

The average MSE rankings of the five laboratory compaction methods for the three test temperatures for the three projects (Table R.3) indicate that the MT/GS method best matched the resilient modulus results of the field method, followed, in decreasing order, by the MS/WC, CK/CC, MM/HC, and AV/KC methods (Table R.4).

3.2.4.2.3 Creep Test (DLOAD and Creep). With the exception of the AV/KC method for the VA-0621 project, creep test results at 77°F were analyzed for each of the five laboratory compaction methods for the MI-0021, TX-0021, and VA-0621 projects. Results were also analyzed for four laboratory compaction methods for the CO-0009 and WY-0080 projects. Very limited creep test results at 104°F were analyzed for three laboratory compaction methods for three of the projects. Because of incomplete results at 104°F and the generally limited results for the CO-0009 and WY-0080 projects, discussion is limited to a test temperature of 77°F for the MI-0021, TX-0021, and VA-0621 projects. The strain at a loading time of 300 sec (DLOAD-77) was selected as the basis for comparing the laboratory compaction methods with the results for the field method. There were no statistically significant differences between the laboratory and field results for the AV/KC, CK/CC, MS/WC, and MT/GS methods. The MM/HC method was significantly different from the field method for one of the three projects.

The average MSE rankings of the five laboratory compaction methods for the three projects (Table R.3) indicate that the MT/GS method best matched the DLOAD-77 results of the field method. The CK/CC and MS/WC methods tied for second, followed by the MM/HC and AV/KC methods (Table R.4).

An analysis of covariance was conducted on the creep test results to determine whether or not the creep curves of the laboratory compaction methods differed from the creep curves of the field compaction method. First, a regression analysis was conducted on the creep test data (log of load strain versus log of load time) for load times between 30 and 900 sec to fit a straight line to the data. An analysis of covariance was conducted to evaluate whether the slopes and intercepts of the regression lines for the laboratory methods differed significantly from the field method. The results are given in Table R.5.

Sufficient data to allow for comparisons were only received for the creep test at 77°F. For the five projects, in the majority of the cases (14 out of 23), there was a significant difference between the creep curve of the laboratory compaction method and that of the field compaction method. In 10 of the 14 cases, the intercepts were significantly different, while the slopes were different in the other four cases. Both the CK/CC and MS/WC methods were not significantly different from the field method for three of the five projects, while the MT/GS method was not significantly different for two of the five projects.

An analysis of the percent of total creep strain recovered after a one hour rest period was initially to be included in the statistical comparison. However, many of the field cores and some of the laboratory compacted specimens failed during creep testing, especially at a test temperature of 104°F. Too few data on creep recovery were available at the end of the test program to conduct a statistical analysis by mixture and temperature. The following lists the average percent of total creep strain recovered (or recovery efficiency) by the specimen after a one hour rest period.

Compaction of Specimens	Average Percent of Total Creep Recovered, %
Field Core	18.7
MT/GS	18.1
MS/WC	21.1
CK/CC	25.5
AV/KC	30.0
MM/HC	36.1

3.2.4.2.4 Summary. Based on the mean comparisons and MSE results, the CK/CC laboratory compaction method best matched the field air voids content (discussed previously), followed by the MM/HC, MT/GS, and AV/KC methods. For the indirect tensile strength results, the MT/GS method provided the best match to results from the field compaction method, followed by the CK/CC method. For resilient modulus, the MT/GS method best matched the field, followed by the MS/WC and CK/CC methods. For the creep load strain at 300 sec, the MT/GS method best matched the field results, followed by a tie between the CK/CC and MS/WC methods. For the covariance analysis of the creep curves, the CK/CC and MS/WC methods tied for the best match to the field results, followed by the MT/GS method.

3.2.4.3 Results on a Temperature Basis

The statistical analyses can be sorted and presented on a temperature basis to identify which of the laboratory compaction procedures best predict the effect of temperature on the test results for the field compaction method. Three testing temperatures, 41°F, 77°F, and 104°F, were used for the indirect tensile strength and resilient modulus testing. Only 77°F and 104°F were used for creep testing; however, sufficient data were not available to allow for analysis of the 104°F temperature for creep.

3.2.4.3.1 Low Temperature—41°F. Low temperature test results were available for indirect tensile strength (IDT-41) and resilient modulus (MR-41) for the MI-0021, TX-0021, and VA-0621 projects. No data were analyzed for the MS/WC method for either of these tests for any of the projects. It is, therefore, not possible to evaluate the performance of this method at 41°F.

There were six possible comparisons for the 41°F temperature (Table R.2). None of the six comparisons were significantly

different from the results for the field compaction method for the CK/CC, MM/HC, or MT/GS laboratory compaction methods. The AV/KC method was significantly different from the field method for two of six comparisons.

The MT/GS method had the best MSE ranking for both the IDT-41 and MR-41 tests. For the IDT-41 test, the MM/HC method was second, followed by the CK/CC and AV/KC methods. For the MR-41 test, the CK/CC method was second, followed by the MM/HC and AV/KC methods.

3.2.4.3.2 Room Temperature—77°F. Results were included for indirect tensile strength (IDT-77), resilient modulus (MR-77) and creep (DLOAD-77 and CREEP-77). Complete results were analyzed for the MI-0021, TX-0021 and VA-0621 projects, and partial data were analyzed for the CO-0009 and WY-0080 projects for MR-77, DLOAD-77 and CREEP-77. SNK results were obtained for the IDT-77, MR-77, and DLOAD-77 tests. Covariance analysis results were obtained for the creep curves at 77°F (CREEP-77). The discussion is limited to the three projects for which complete data sets were analyzed, although the data for all five projects are presented in Tables R.2, R.3 and R.5.

At the 77°F temperature, nine comparisons between the results for the field compaction method were possible for each of the five laboratory compaction methods (Table R.2). The AV/KC method was not significantly different from the field method for any of the eight comparisons (there were no data for this method for DLOAD-77), while the CK/CC, MS/WC, and MT/GS methods were significantly different from the field method for one of nine comparisons. The MM/HC method was significantly different for two of nine comparisons.

MSE results were available for the IDT-77, MR-77, and DLOAD-77 tests (Table R.3). The average MSE rankings for these three tests for the three projects indicated that the MS/WC method best matched the results for the field method at 77°F, followed by the CK/CC and MT/GS methods tied for second (Table R.4).

In the majority of the cases, 14 of 23, there was a significant difference between the creep curve of the laboratory compaction method and that of the field compaction method. In 10 of the 14 cases, the intercepts were significantly different, while the slopes were different in the other four cases. Both the CK/CC and MS/WC methods were not significantly different from the field method for three of the five projects, while the MT/GS method was not significantly different for two of the five projects.

3.2.4.3.3 High Temperature—104°F. Results were analyzed for all five compaction methods for indirect tensile strength (IDT-104) and resilient modulus (MR-104) at 104°F for the MI-0021, TX-0021, and VA-0621 projects. Partial results were analyzed for the creep test, but these were insufficient to allow comparisons to be made.

Six comparisons between each laboratory compaction method and field method were possible at 104°F. None of the five laboratory methods were significantly different from the field method for the MR-104 test results (Table R.2). In total, the CK/CC and MT/GS methods were not significantly different from the field method for any of the six comparisons, while the MM/HC and MS/WC methods were significantly different from the field method in one of six comparisons and the AV/KC method was significantly different in two of six comparisons.

MSE results were available for the IDT-104 and MR-104 tests (Table R.3). The average MSE rankings for these two tests for three projects indicated that the MT/GS method best matched the results for the field method at 104°F, followed by CK/CC, MS/WC, MM/HC, and AV/KC methods.

3.2.4.3.4 Summary. Based on the mean comparisons and MSE results, the MT/GS method best matched the results of the field compaction method at 41°F, followed by the CK/CC, MM/HC, and AV/KC methods. At 77°F, the MS/WC method provided the best match to the field cores, with CK/CC and MT/GS methods tied for second. At 104°F, the MT/GS method had the best match to the field results, followed by the CK/CC, MS/WC, MM/HC, and AV/KC methods.

3.2.4.4 Summary of Engineering Property Comparisons

All test results were sorted and analyzed on the basis of project, type of test, and temperature using the PC version of the Statistical Analysis System (SAS). Mixture properties evaluated using the SAS program included: indirect tensile strength at 41°F, 77°F, and 104°F; creep load strains at 77°F and 104°F for a loading time of 300 sec; and slopes of the creep curve at 77°F and 104°F. The data analysis is summarized below for the MSE comparisons.

Laboratory Compaction Method	Project	Average MSE Rankings by: Mixture Property	Temperature
AV/KC	5.0	4.8	4.7
CK/CC	2.0	2.0	2.0
MM/HC	4.0	3.5	3.3
MS/WC	1.7	2.8	2.0
MT/GS	1.0	1.5	1.3

While there is no single laboratory compaction method that always provided the best match to the results for the field compaction method, the MT/GS method was generally better than the other methods. The MT/GS method had the best average MSE ranking for the indirect tensile strength tests, for the resilient modulus tests, and for the creep load strain at 300 sec. The MT/GS method also had the best average MSE ranking for the tests at 41°F and 104°F, and was second to the MS/WC for tests at 77°F.

The CK/CC and MS/WC methods generally finished second and third in the MSE rankings, with both occasionally ranking above the MT/GS method. The results between the CK/CC and MS/WC methods are so close that it is difficult to select the "best" in a comparison of the two methods. They virtually tied for the second place ranking with respect to matching the test results for the field compaction method. The MM/HC and AV/KC methods generally finished fourth or fifth in the MSE rankings, with the MM/HC method generally ranking the higher of the two. This was expected, because the air voids measured on specimens compacted with the AV/KC were generally lower than the target or field cores. The following is an overall summary of the number of cells by compaction device, which were closer to the target value or field cores using all available data:

Compaction Device	Percentage of Cells with a No. 1 Rating, %	Percentage of Cells with a No. 1 or 2 Rating, %
Marshall hammer	7	30
Arizona vibratory/ kneading compactor	7	24
California kneading compactor	23	48
Steel wheel compactor	25	55
Gyratory shear compactor	45	72

The comparison of average percent of total creep recovered (paragraph 3.2.4.2.3, Creep Test) was identical to the foregoing listing.

In addition to calculating mean squared error, each data set was evaluated to determine if two adjacent cells were significantly different or indifferent based on the mean and variation using a confidence level of 95 percent. The following provides an overall summary of the percentage of cells for each compaction device that were indifferent when comparing field cores to laboratory compacted specimens:

Compaction Device	Percentage of Cells Indifferent from Target Value, %
Marshall hammer	35
Arizona vibratory/kneading compactor	41
California kneading compactor	52
Steel wheel compactor	49
Gyratory shear compactor	63

There was very good agreement among the results of the SNK mean comparison analyses and the MSE results. In fact, in all comparisons that were made, the laboratory compaction methods that had the largest values of MSE were those that were statistically significantly different from the results for the field compaction method in the SNK analyses. Thus, the internal structure and engineering or mechanical properties of the asphaltic concrete mixture can be dependent on the type of compaction device used. Huschek (*79*) and others have also concluded similar findings, namely, that the mechanical properties of a mix are dependent on the method of compaction.

3.2.5 Ranking Compaction Devices

For the compaction devices, three procedures were used to define which compaction device more closely simulates the engineering properties of field cores. Consistently, the MT/GS had the lower mean squared errors, more sample sets that were indifferent from the field cores, and a slightly lower absolute difference between the mean magnitudes for the five mixtures. Additionally, the air void gradient and particle orientation data indicated equivalent, if not slightly better, simulation of the field cores, as compared to the other devices used. Considering these different comparisons, the following lists, in order, those laboratory compaction devices that on the average more closely simulate or match the properties and characteristics of field compacted mixtures, immediately after construction:

1. Texas gyratory shear, MT/GS
2. California kneading compactor, CK/CC
3. Steel wheel simulator, MS/WC
4. Arizona vibratory/kneading compactor, AV/KC
5. Mechanical Marshall hammer, MM/HC

The Marshall hammer did the poorest job of simulating or matching the engineering properties of the field cores. It is also important to note that Aunan, et al. (*80*) found the same ranking of compaction devices in simulating the air void structure of field compacted sand, asphaltic concrete specimens, with the exception of the AV/KC which was not used. Use of the AV/KC generally compacted samples with much higher tensile strengths, but lower resilient moduli. It should be restated that the air voids of the AV/KC laboratory compacted specimens were consistently lower than that of the field cores.

3.2.6 Performance Differences Between Compaction Devices

Differences of engineering properties were detected on specimens compacted using the different compaction devices studied in this project. Although statistical differences were found, the question arises whether these differences are large enough to result in performance differences calculated with mechanistic/empirical models, or are they design differences using the AASHTO Design Guide. This section of the report will briefly discuss expected performance differences resulting from material property differences caused by different compaction devices.

Resilient moduli were interpolated at 68°F to determine the AASHTO layer coefficients for each mixture compacted with the different compaction devices. All laboratory design moduli exceeded the boundary conditions of the correlation. Thus, even though the resilient moduli are different, the structural layer coefficient for all mixtures and compaction devices would be 0.44, and no differences in structural design would result.

All pavement performance/design models in use today are at best gross simulations of actual pavement behavior and performance. Take, for example, fatigue cracking. Most asphaltic concrete fatigue curves relate initial tensile strains, resilient moduli, and number of load applications to failure. However, laboratory fatigue curves must be modified by some shift factor to relate laboratory and field conditions. These shift factors are generally based on a limited amount of data and are a gross representation of actual conditions. Thus, minor differences in resilient moduli, even those statistically different, may be insignificant regarding predictions of fatigue cracking.

Pavement performance predictions were made for the MI-0021, TX-0021, and VA-0621 mixtures using the measured engineering properties from the CK/CC, MM/HC, and MT/GS laboratory compacted specimens. These devices were selected because they represent the extremes of the comparisons and are the devices most commonly used in the U.S. Tables 28 and 29 summarize the average properties for the laboratory compacted specimens for each mixture. Using these values, pavement distresses were calculated using the same techniques described in section 2.4.4.

Table 50 summarizes and compares the predictions of fatigue cracking and rutting for specimens compacted using the three devices. As shown, the differences between the cores and CK/CC and MT/GS compacted specimens are small and insignificant considering the inaccuracies of the pavement performance models. However, large differences were calculated between the cores and MM/HC compacted specimens, because the resilient moduli and creep compliance values measured on these specimens were consistently higher and lower, respectively, than those measured on the cores. No differences of thermal cracking levels were calculated because of the small differences in indirect tensile strengths between compaction devices.

Although statistical differences do exist between resilient moduli, indirect tensile strength, tensile strain at failure, and creep compliance curves measured on the CK/CC and MT/GS specimens, these differences are relatively small and insignificant regarding the inaccuracies of the pavement performance models. Use of the MM/HC was the one device, which resulted in large differences of distress predictions.

Table 50. Fatigue cracking and rutting predictions using the material properties measured on specimens compacted with different devices to the same air voids as measured from field cores.

Mixture	Compaction Device			
	MM/HC	CK/CC	MT/GS	Field Core
* Fatigue Cracking - Years To A Damage Index = 1.0				
MI-0021	32.0	26.0	11.5	9.0
TX-0021	15.0	5.0	5.3	5.8
VA-0621	30.0	10.5	11.5	12.0
* Rutting - Rut Depths Calculated At 5 Years, Inches				
MI-0021	0.27	0.64	0.58	0.87
TX-0021	0.52	1.29	1.27	1.28
VA-0621	0.44	0.79	0.84	0.60

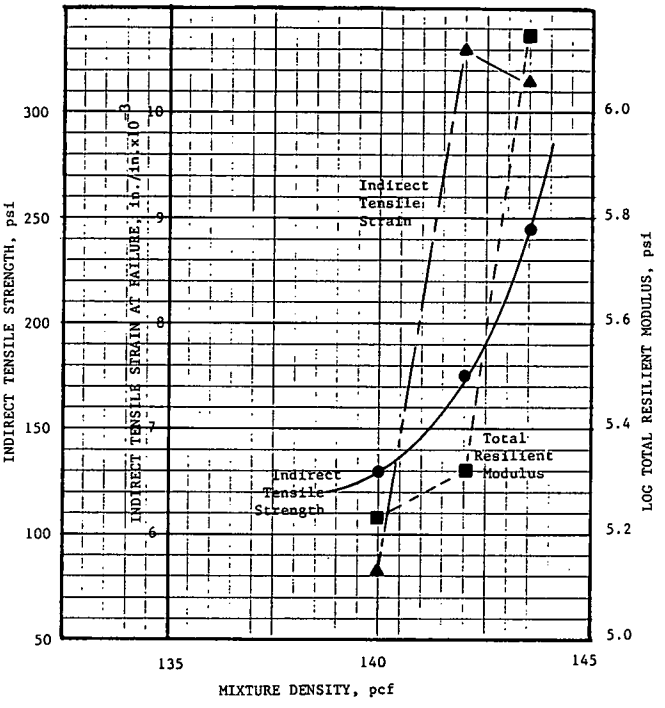

Figure 114. Effect of mixture density on selected properties.

3.3 SPECIMEN PREPARATION

Four areas of specimen preparation are considered important for evaluating or designing asphaltic concrete mixtures based on performance-related criteria. (A fifth area, type of compaction device, was discussed in the previous section.) The four areas are: (1) selecting a proper compaction effort, (2) using the correct sample size, (3) evaluating time effects on specimen behavior, and (4) determining the effect of moisture on the mix. Each of these is discussed in this section of the report, with the exception of moisture conditioning. Moisture damage is discussed in section 3.5.

3.3.1 Selection of Laboratory Compactive Efforts

Many studies have shown that the engineering properties of asphaltic concrete mixtures are related to mixture density. Epps et al. (*78*) presented data illustrating that high densities are required if the mixture is to be durable and have adequate strength, fatigue resistance, and stability. Figure 114 shows the effect of mixture density on selected properties measured on the AAMAS mixtures. As illustrated, the higher densities of a specific mix resulted in improved properties for mix performance. This would imply that the mix should be compacted to the greatest density possible. However, there are other distress factors that must be considered.

3.3.1.1 Maximum Aggregate Unit Weight Considerations

Regan (*1*) presented the effects of increased compactive effort on maximum aggregate density. One example of his data is illustrated in Figure 115, which indicates that as the comparative effort increases, the binder content to achieve maximum density decreases. Testing conducted by Regan on different dense-graded mixtures also showed that higher compactive efforts (greater than 75-blow Marshall hammer per side) produce stronger surface mixtures.

Unfortunately, decreasing the optimum asphalt content by increasing compactive effort for maximum aggregate unit weight (Figure 115) will result in reduced durability at some point, because film thicknesses decrease with a decrease in binder content (refer to Figure 104). Similarly, traffic loads and tire pressures must be considered because additional traffic densification will occur if the mixture does not have sufficient strength to resist shear distortions.

The 1969 Epps et al. study (*78*) also looked at traffic densification and found that air voids (in a range of 6 to 12 percent of bituminous mixtures with adequate stability) decreased by 2 to 8 percent of the additional 2-year densification caused by traffic during the first year or summer of traffic. Thus, comparative efforts (mixture unit weights and initial air voids) should be considered in the overall optimization of the JMF. In one case, for example, durability or lower compactive efforts may be more important, resulting in higher asphalt contents; whereas, in another case, mixture strength may dictate the use of much higher

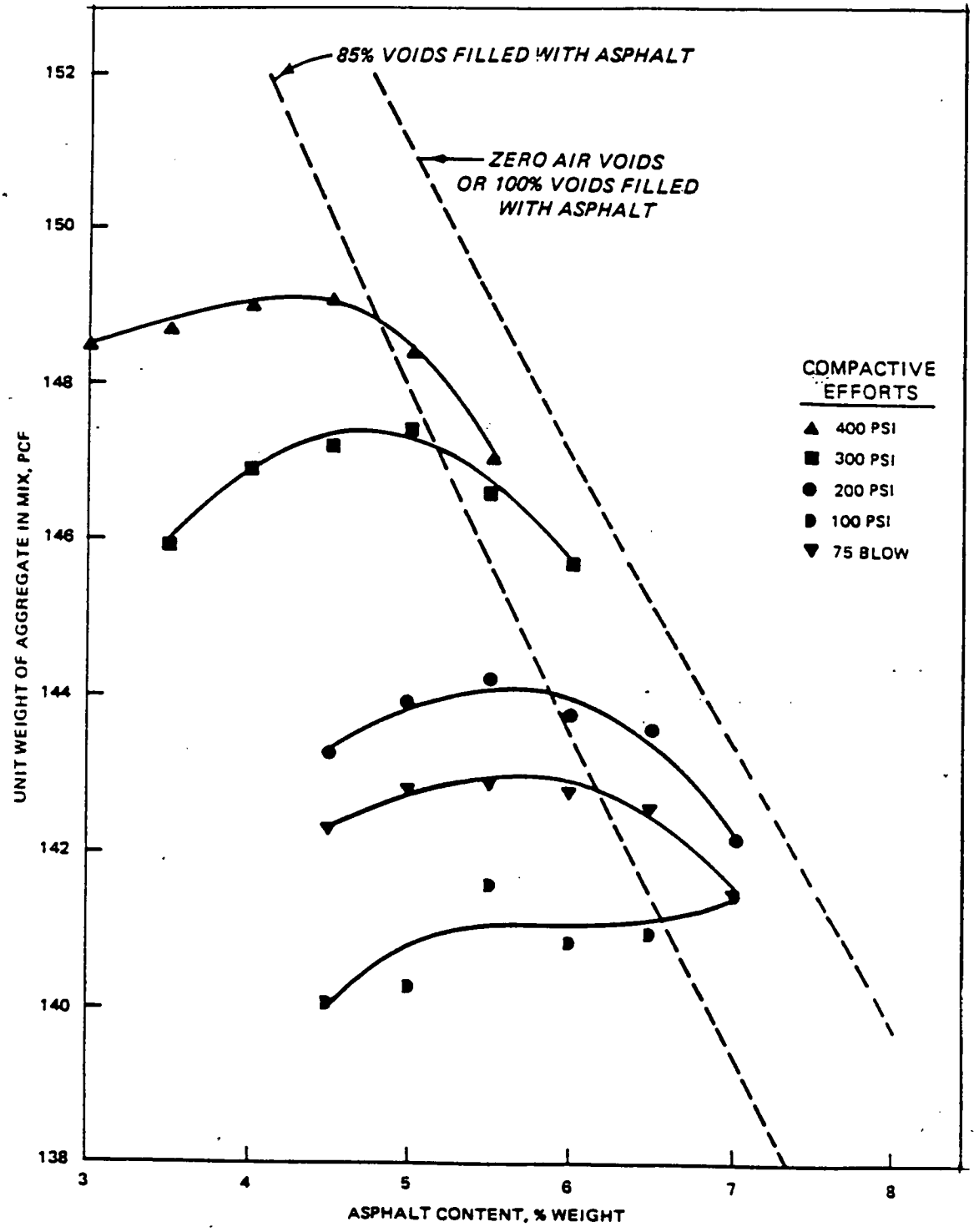

Figure 115. Compactive curves, ¾ in. and AC 40 mixtures (29).

compactive efforts resulting in lower asphalt contents. Nevertheless, the question remains; what compactive effort should be used during mixture design for selecting an optimum binder content?

3.3.1.2 Suggested Compactive Efforts for Mixture Design

There are insufficient data from the AAMAS projects to document the compactive effort required for different traffic loads and tire pressures. Historical data and experience must be used to establish guidelines, both for compacting the specimens during initial mixture design and for defining the loads (or stress levels) to be used during mixture testing in the AAMAS program. Suggested guidelines are presented in the AAMAS Procedural Manual, Part I of this report, and are given below for the compaction devices most commonly used in the U.S.:

Compactive Efforts for Initial Mixture Designs		
Traffic Level:	Low	Moderate to Heavy
18-kip ESALS/Yr.	< 20,000	> 20,000
Tire Pressures, psi	< 100	> 100
Compaction Device:		
Marshall	50 blows	75 blows
Kneading	150 tamps	150 tamps
Texas Gyratory	150 psi	150 psi
Corps of Engineers Gyratory	30 revolutions 100 psi 1-deg tilt	30 revolutions 120 psi 3-deg tilt

The foregoing values are equivalencies used by different agencies, and should only be considered as gross approximations. Equivalencies between the compaction devices will vary with materials and asphalt contents. For dense-graded asphaltic concrete materials placed over a rigid layer of portland cement concrete, the compactive efforts for the heavy traffic levels should always be used for mixture design.

Figures 116 through 118 illustrate the relationship between VFA and air voids for each of the mixtures. Relationships defined by both Marshall and Hveem mixture designs (constant compactive effort but varying asphalt contents) and the field and laboratory curves (varying compactive effort but constant asphalt content) are included. As displayed, the varying compactive effort curves intersect the mixture design curves at approximately the same asphalt content for both design methods. Similarly, Figures 119 through 121 illustrate the relationship between VMA and VFA for the mixture design curves at approximately the same asphalt content. This suggests that any compaction device can be used to establish the VMA-VFA and air voids-VFA relationships by simply varying the compactive effort.

These relationships (Figures 119, 120, and 121) define the matrix of asphalt contents and compactive efforts such that the VMA and VFA requirements can be met. Obviously, the compactive effort selected should minimize the VMA to as near the suggested lower limit as practical. Of course, the mixture may satisfy the VMA-VFA criteria, but still be inadequate for the traffic loads or environmental conditions. For these cases, a different aggregate blend, different types of aggregate or use of additives may be needed to require greater compactive efforts resulting in a stronger mix, while maintaining proper VMA-VFA levels.

3.3.1.3 Compaction Equivalency Curves

Based on the comparison of material factors and engineering properties discussed in section 3.2, there is a consistent difference between specimens compacted with different compaction techniques. Previous studies of using different compaction devices to evaluate asphaltic concrete materials have recognized the difference in compactive efforts between the use of different devices and have developed compaction equivalencies between different devices. Some agencies use one device for mixture design and another device for field control.

The Corps of Engineers developed an equivalency between the gyratory and mechanical Marshall hammer, whereas Field (*77*) developed an equivalency between different Marshall hammers and kneading compaction. The Corps of Engineers equivalency values between the Marshall hammer and GTM are: 100 psi,

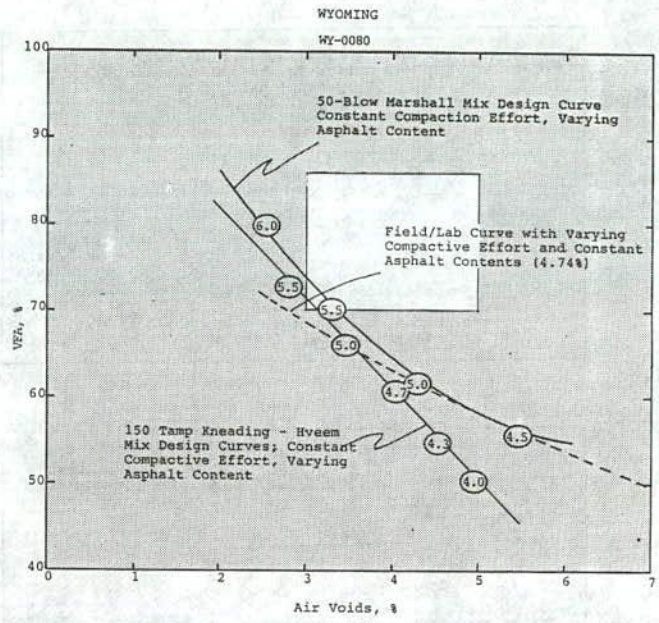

Figure 116. Comparison of VFA and air void relationships as defined by the Marshall and Hveem mixture design procedures for the WY-0080 mixture.

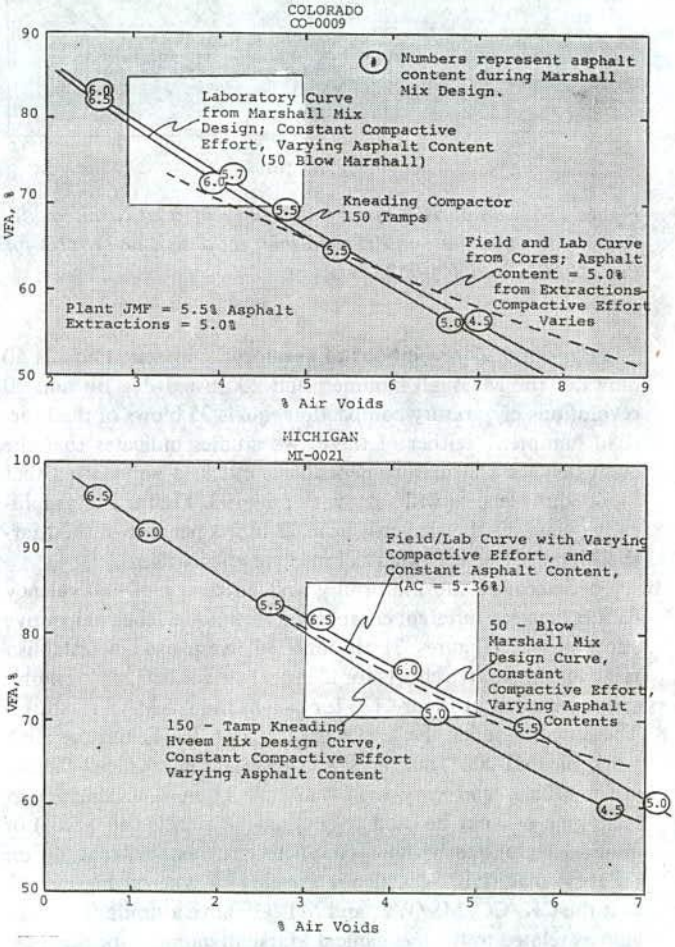

Figure 117. Comparison of VFA and air void relationship as defined by the Marshall and Hveem mixture design procedures for the CO-0009 and MI-0021 mixtures.

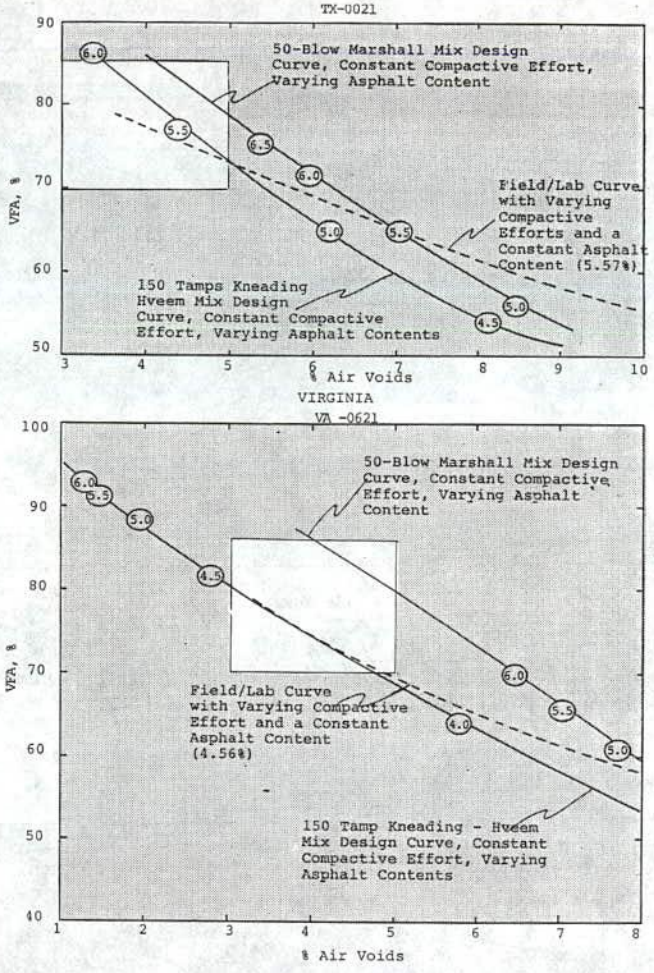

Figure 118. Comparison of VFA and air void relationship as defined by the Marshall and Hveem mixture design procedures for the TX-0021 and VA-0621 mixtures.

1-deg tilt and 30 revolutions of gyratory compaction equals 50 blows of the Marshall hammer; and 200 psi, 1-deg tilt and 30 revolutions of gyratory compaction equals 75 blows of the Marshall hammer. Neither of these two studies indicates that the equivalencies are mixture dependent, but it is anticipated that these equivalencies will vary with material. Figure 122 graphically compares the air voids from 75 blows per side of the Marshall hammer to the other compactive efforts used.

To determine the uniformity and adequacy of equivalency factors between different compaction techniques, the compactive effort curves (Figures 31 through 36) were used to establish relative compactive efforts for identical air voids. This is graphically presented in Figure 123 for two of the AAMAS mixtures. These two included the least workable (VA-0621) and the most workable (MI-0021) mixtures. As shown, the equivalency factors are nonlinear and vary with material. Thus, one compaction technique can not be used to predict the results (air voids) of another technique without conducting an extensive study on different materials. It is also interesting to note on Figure 123 that the CK/CC, MS/WC, and MT/GS have a similar relationship as related to the mechanical Marshall hammer for the most workable mixture (MI-0021). However, the difference between compaction techniques is much larger for the least workable or harsh mixture, VA-0621.

A compression index, C_c, was also calculated for the different compaction techniques for each mixture. The results of these calculations are provided in Table 51 and represent the slope of the upper portion of the compactive effort curve. The larger the number, the less change in air voids with additional compactive effort. It can be seen from the table that the values vary between mixture and device. The Marshall hammer was found to have the larger values for three of the cases. Thus, compactive effort equivalencies between compaction devices are not constant.

3.3.2 Minimum Sample Size

Oversized samples were tested on all projects to determine if differences in mixture response could be measured simply by changing the sample diameter or height. The effects of aggregate size and sample height on resilient modulus (Figure 87) and indirect tensile strength (Figure 41) are presented in Chapter 2.

3.3.2.1 Indirect Tensile Specimens

3.3.2.1.1 Specimen Diameter. The first procedure used to investigate the effects of sample size was to measure the resilient moduli of a particular sample along three different diametral axes. After initial measurements were made, the sample was recored and the resilient moduli were measured along the same three axes. Samples recovered from the field were cored two or three times. Figure 87 (in Chapter 2) summarizes the results of this testing effort. As previously discussed, the resilient moduli decreased as the specimen-to-aggregate diameter ratio increased.

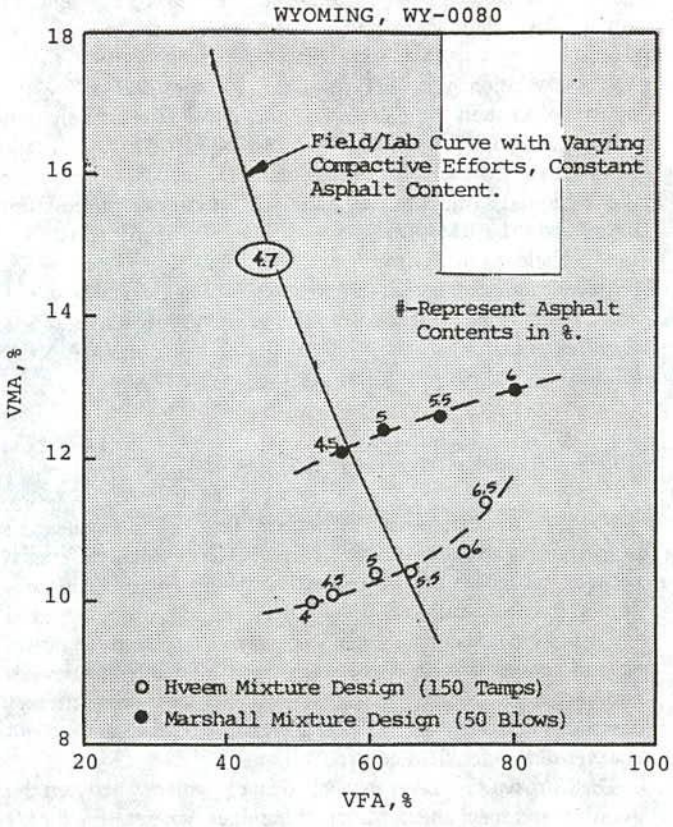

Figure 119. Comparison of VFA and VMA relationship as defined by the Marshall and Hveem mixture design procedures for the WY-0080 mixture.

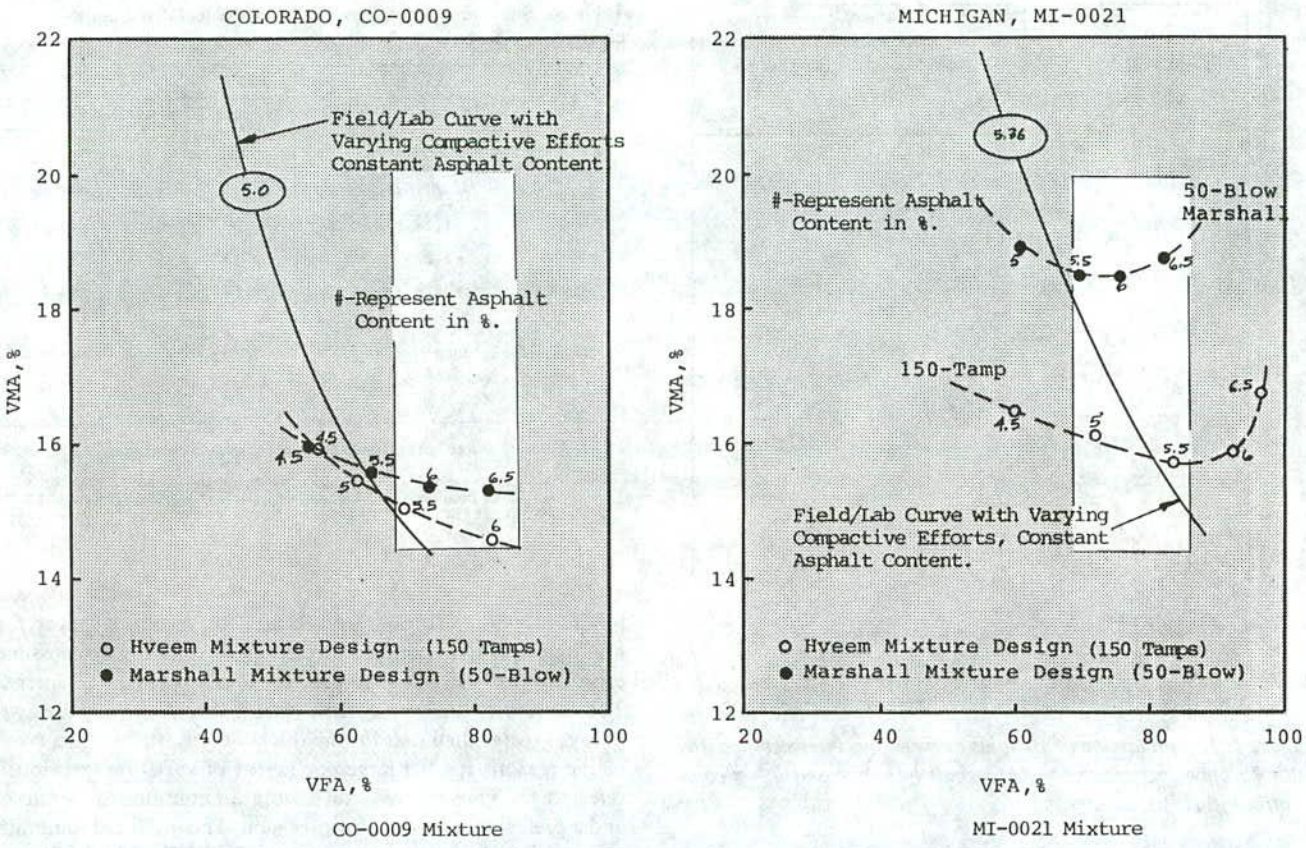

Figure 120. Comparison of VFA and VMA relationship as defined by the Marshall and Hveem mixture design procedures for the CO-0009 and MI-0021 mixtures.

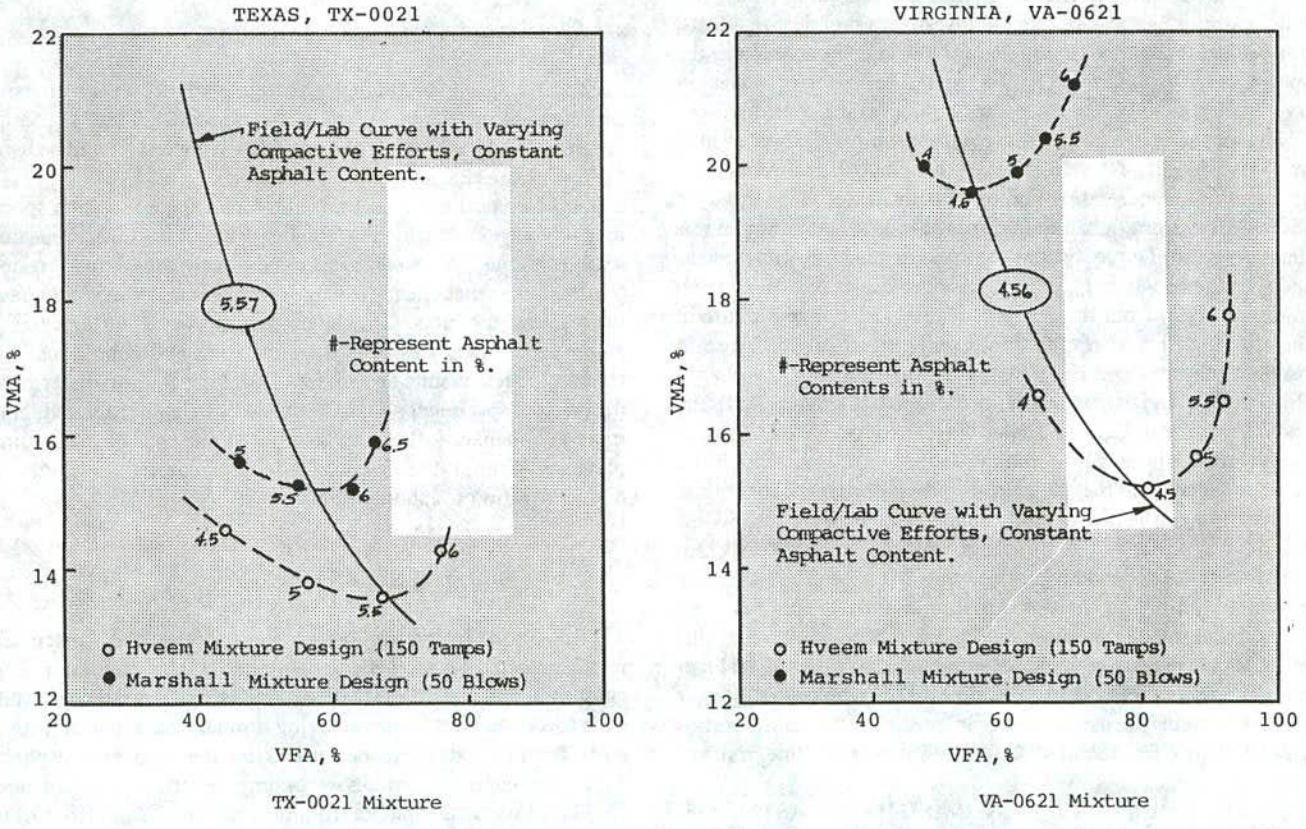

Figure 121. Comparison of VFA and VMA relationship as defined by Marshall and Hveem mixture design procedures for the TX-0021 and VA-0621 mixtures.

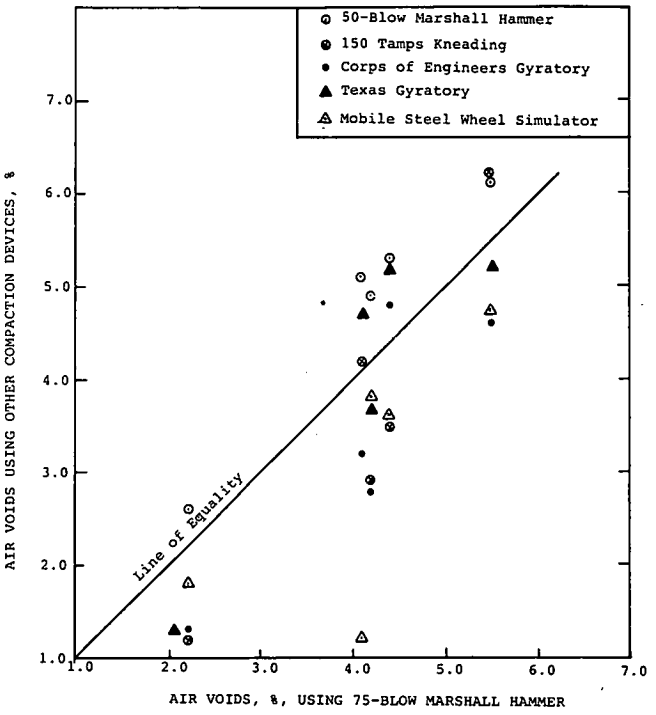

Figure 122. Comparison of air voids between specimens compacted with 75 blows per side of the Marshall hammer and other compactive efforts used.

Using this technique, the effect of variability between samples is eliminated. Indirect tensile strengths, creep compliance, and failure strains can also be used to investigate sample size effects, but require many more samples for testing, because once the specimen has failed, it can not be recored and retested. Variability between samples then becomes an important consideration.

The second technique used to evaluate sample size was to look at the variation of test results as related to the specimen-to-aggregate diameter ratio. Figure 124 illustrates an increase in the variation from the different types of tests as a function of this diameter ratio. The coefficient of variation generally increased as the specimen-to-aggregate diameter ratio decreased. Selecting a minimum ratio from these data is almost impossible because of the variation in test results. However, a significant increase in resilient modulus was measured when the ratio was less than 4 (Figure 87), and when the ratio exceeded 6 (Figure 124) the coefficient of variation decreased for each type of test.

Obviously, there is a minimum diameter ratio for which the test results become meaningless. In other words, the individual components of the mix are only being tested instead of the combined effect of the mix components. This minimum value is also expected to be dependent on the type of test or property being measured. Although there is only minimal data from one type of test to suggest a minimum value, it is recommended that this ratio be greater than 4, for accuracy, to reduce the resilient modulus differences between samples. Diameter ratios greater than 4 should be used whenever possible. Typically, ratios greater than 6 are required for testing most soil (fine-grained) mixtures.

3.3.2.1.2 Specimen Thickness. AASHTO and ASTM standards specify a minimum specimen height or thickness of 1.5 in. for measuring the repeated load resilient modulus and indirect

Table 51. Summary of compression indices calculated from the compactive effort curves for different laboratory compaction devices.

Compaction Device	Mixture				
	CO-0009	MI-0021	TX-0021	VA-0621	WY-0080
MM/HC	-6.08	-1.99	-4.77	-2.93	-5.28
CK/CC	-3.41	-0.85	-3.69	-3.41	-1.14
MS/WC	-4.26	-2.27	-4.26	-5.11	-3.41
MT/GS	-2.27	-3.12	-2.56	-5.11	-1.70
CE/GS	-2.84	-2.84	-2.84	-4.54	-3.41

Compression Index = $C_c = (V_1-V_2)/\log (c_1/c_2)$

where:

V_1 = Air Voids measured at compactive effort c_1

V_2 = Air voids measured at compactive effort c_2

Note: Larger negative values indicate less densification with the compaction device or more mixture resistance to consolidation from the applied load.

tensile strength. Cores were selected for testing to meet this minimum requirement. However, this was not always possible, especially for the CO-0009 project, as discussed in Chapter 2. The variability measured when testing these thinner cores was always greater than that for the thicker cores. In fact, this is one of the reasons for the large coefficient of variation, previously referred to. Thus, there is an absolute minimum for accuracy and a preferred minimum for precision. The preferred minimum specimen thickness-to-diameter ratio for all diametral testing is 0.5, whereas the absolute minimum ratio is 0.375.

3.3.2.2 Uniaxial Compression Specimens

3.3.2.2.1 Specimen Diameter. Specimen diameter for uniaxial compression or triaxial testing was not studied. Thus, the same requirement developed for the indirect tensile test should be used for testing specimens in the uniaxial direction.

3.3.2.2.2 Specimen Height. Large uniaxial compression specimens were compacted in the laboratory and tested using repeated load techniques. These large specimens were sawed and retested to determine what effect the length-to-diameter ratio would have on resilient modulus. This effect was presented in Chapter 2 along with differences caused by different end conditions. Although the test results are minimal, the length-to-diameter ratio for uniaxial specimens should be at least 1.0, if a friction reducing material (such as Teflon tape) is used on the ends of the loading platens. Without the friction reducing material a length-to-diameter ratio of 2 should be used.

3.3.3 Age Hardening Simulations

Two age hardening simulations were presented and discussed in Chapter 2. These were a plant hardening simulation and environmental aging simulation. Asphalt was extracted from each specimen used in the two aging simulations, and penetration and viscosity tests were performed on the recovered asphalt. These aged-simulated values were compared to those values measured on extracted asphalts from bulk mixtures sampled during construction, and from field cores taken immediately after construction and two years after construction.

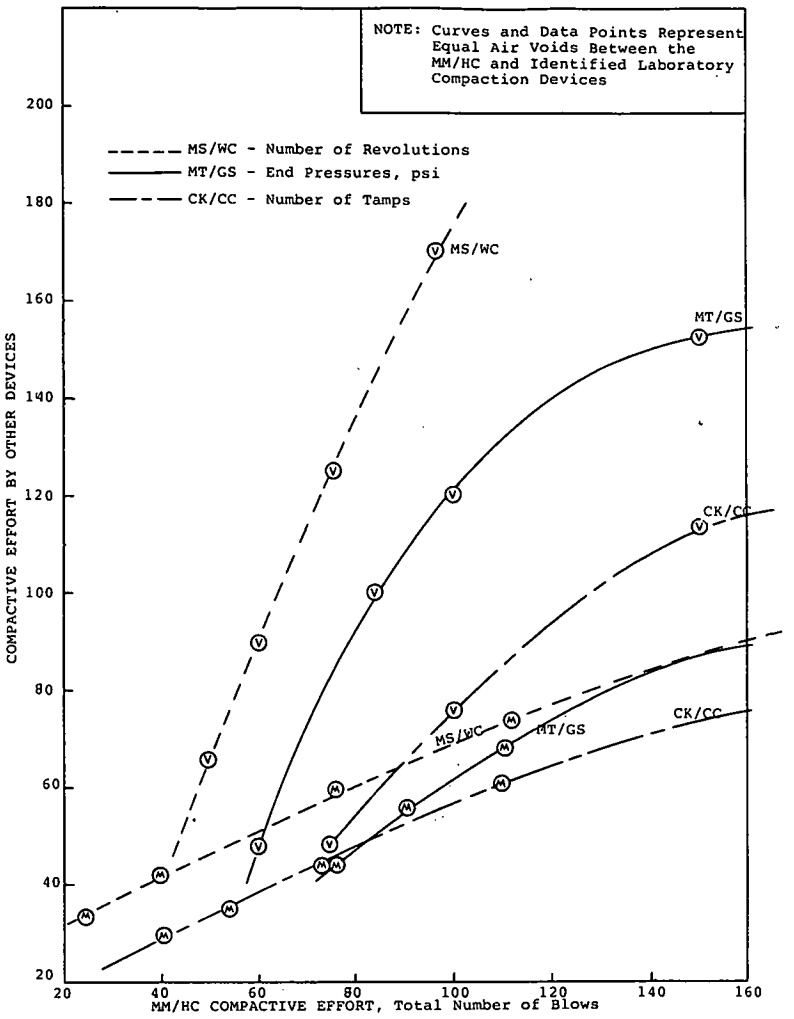

Figure 123. Comparison of compactive effort equivalencies (specimens compacted to the same air void level) for the different laboratory compaction devices for the MI-0021 and VA-0621 mixtures.

All penetration-viscosity data have been plotted on viscosity-penetration charts (see Figures 125, 126, and 127) and compared to the original asphalt properties. As shown, the slopes of the viscosity-penetration relationships for the asphalts used in the AAMAS mixes are within the boundary conditions defined by Corbett and Schweyer (*47*). The WY-0080 mixture (Figure 125) is the only one that did not result in a consistent penetration-viscosity relationship. This was a recycled mixture that may have been contaminated during production or milling operations. Both simulations are discussed below in terms of evaluating mixture properties for pavement distress.

3.3.3.1 Plant Hardening Effects

The first laboratory hardening simulation is to simulate the effects of mixture production and mixing through an asphalt concrete plant. Both AASHTO T-246 (Hveem) and T-245 (Marshall) include temperature recommendations for mixing and compacting bituminous mixtures that are dependent on the type of paving asphalt used. Hveem (AASHTO T-246) varies mixing temperatures with asphalt type, whereas Marshall (AASHTO T-245) varies mixing temperature to result in a constant viscosity of 170 ± 20 cst. For the initial mixture design, these same procedures should be used to compact specimens for stability testing. However, it is extremely difficult, if not impossible, to predict the effects of different plants, varying production temperatures and mixing times, moisture conditions, storage times, and numerous other variables on the asphalt characteristics with one specific procedure.

For example, penetration and viscosity values measured on extracted asphalt after production from the WY-0080 mixture indicate a softer asphalt than prior to production (Figure 125). These results suggest some type of contamination of the asphalt through the drum mix plant. Contamination, improper operation of the plant or paving equipment and other such factors can not be predicted in the laboratory during mixture design. These types of problems must be considered or handled in the material specifications. AAMAS, however, can be used to evaluate these types of problems (using recovered cores) by measuring their effects on mixture behavior and performance.

Compaction of the asphaltic concrete mixture, either in the

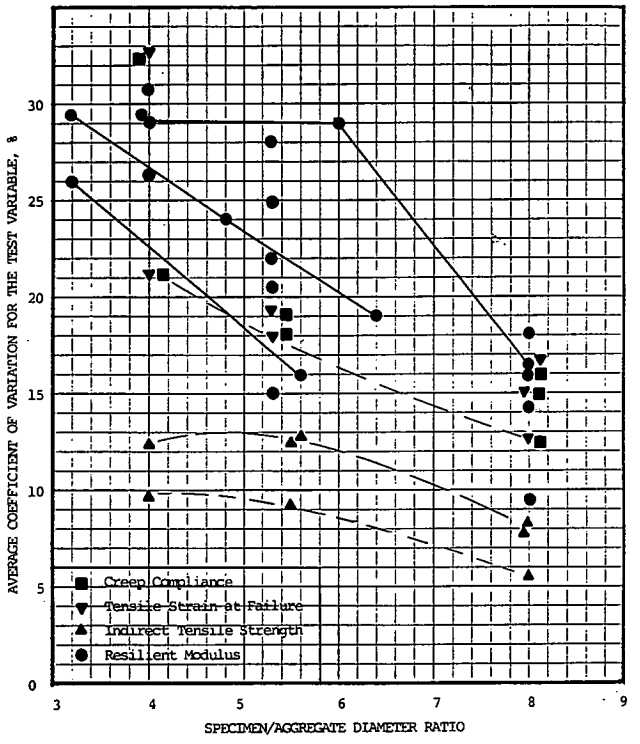

Figure 124. Relationship between variability of test results and the specimen-to-nominal-aggregate diameter ratio.

laboratory or field, is dependent on the viscosity of the asphalt. In preparing and compacting the specimens for testing in AAMAS, the asphalt properties were of particular concern. Thus, the laboratory heating time was varied so that the asphalt properties of laboratory compacted specimens were similar to those of field cores shortly after placement. The temperature used in these simulations was set at 275°F, which was the approximate production temperature of the AAMAS mixtures (Table 14). The production temperature was selected because there was very little heat loss between plant discharge and mixture placement on the roadway.

The heating time intervals which were found to simulate the asphalt characteristics measured on the recovered asphalts after production varied from 1.8 to 13.5 hours (Table 41). Four hours was the overall average for viscosity and six hours the overall average for penetration. From a practical standpoint, a heating time greater than 6 hours is impractical based on an 8-hour work day. In addition, viscosity has a greater effect on compaction than penetration.

Review of Table 41 in Chapter 2 indicates that the use of antistripping additives in the Colorado and Virginia mixtures significantly increased the required heating time to simulate the viscosity measured on asphalt extracted from the mix after production. Averaging the results for the other mixtures resulted in a 3-hour heating time. Therefore, a heating time interval of 3 hours was selected. This should provide sufficient time during an 8-hour work day for mixing and heating (to simulate plant production) and to compact specimens for testing. Certainly, there will be some cases where 3 or even 8 hours are insufficient to simulate the same asphalt characteristics measured on extracted asphalt after mix production. In these cases, it will be necessary to use elevated temperatures or longer heating times to simulate the additional hardening of the asphalt.

3.3.3.2 Environmental Aging

The other laboratory simulation was to consider 5 to 10 years of environmental aging for mixture evaluation. Use of an accelerated aging procedure is required for the thermal cracking evaluation part of AAMAS. Specimens were compacted and artificially aged using different procedures, as discussed in Chapter 2. Resilient moduli, indirect tensile strengths, and failure strengths were measured on specimens prepared with the MI-0021, TX-0021, and VA-0621 mixtures in order to measure changes of the engineering properties with different aging simulations. All test results of the aging simulation are provided in Appendix H and summarized in Chapter 2. Resilient moduli and indirect tensile strengths increased with different levels of aging, as expected. More importantly, however, was the significant decrease in tensile strains at failure (Figures 74, 75, and 76).

Tia et al. (*60*) and others have shown a similar increase in mix strength and stiffness with short time durations, both in the field and laboratory (Figure 128). An increase in strength and resilient modulus implies a more structurally sound material according to the Design Guide (*6*). However, most overlay design procedures suggest that a reduced layer or strength coefficient be used to represent in-service asphaltic concrete surface or base materials because of asphalt aging, even with low levels of traffic. In general, asphaltic concrete mixtures became more susceptible to cracking with a decrease in penetration and an increase in viscosity. Conversely, mixtures with higher strengths and, to some degree, higher elastic moduli are less susceptible to cracking. Both strength and stiffness increase with a relative increase in viscosity. Thus, strength and stiffness are the least desirable mix properties to evaluate aging effects.

On the other hand, tensile strain at failure decreased dramatically with different degrees of aging simulations, which implies a more brittle material (more susceptible to cracking); therefore, tensile strain at failure is a more desirable property for use in any cracking analysis. It is interesting to note that the tensile strains at failure for unaged samples were approximately equal for the cores and specimens used in the permanent deformation, creep compliance, and strength testing programs. After aging, however, the failure strains decreased significantly. This indicates a loss of the adhesion or bonding characteristics between the aggregate and asphalt after aging. Use of some accelerated aging procedure allows the mixture to be evaluated based on a thermal cracking and disintegration (raveling) analyses. As explained in Chapter 2 (section 2.5.2.2), use of the forced draft oven to simulate the environment consistently matched the engineering properties (in particular tensile strains at failure) measured on field cores taken at 2 years.

3.4 RELATIONSHIP BETWEEN MIXTURE AND STRUCTURAL DESIGN

The asphalt-aggregate mixture analysis system (AAMAS) concept is based on the recognized need to tie together asphaltic concrete mixture design and performance. An AAMAS should allow those who design pavement structures to develop specific assumptions for the engineering properties based on the locally

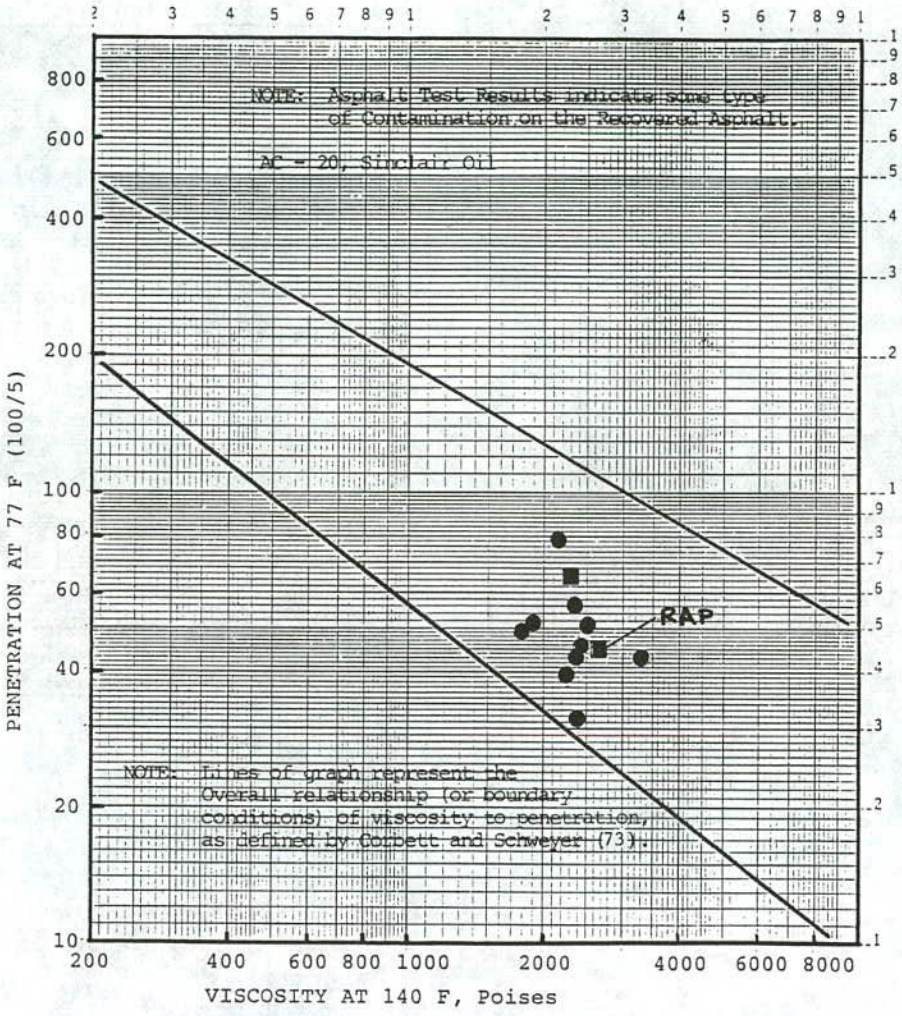

Figure 125. Relationship of penetration and viscosity for the recovered asphalts from the WY-0080 project.

available materials and job specifications. Those who design asphaltic concrete mixtures should be able to employ an AAMAS in the development of mixture designs and specifications which ensure that those assumptions made for pavement thickness designs are correct.

3.4.1 Asphaltic Concrete Characterization for AASHTO Design Procedure

The procedure recommended for defining the layer coefficient for HMAC surface courses requires an estimate of the elastic modulus of HMAC (E_{AC}) at 68°F. This value is used to determine the layer coefficient from a chart. For "bituminous-treated bases," a different chart is provided from which the layer coefficient can be estimated using the elastic modulus or the Marshall stability of the mixture. The AASHTO layer coefficients can also be calculated by the following equation (*6*):

$$a_1 = 0.40 \log (E_{AC}/450) + 0.44 \qquad (3\text{-}2)$$

where a_1 is the AASHTO layer coefficient for dense-graded asphaltic concrete, and E_{AC} is the elastic modulus measured in accordance with the AASHTO Design Guide, ksi.

The Guide (*6*) recommends that the elastic modulus for HMAC (E_{AC}) be estimated from the resilient modulus at 68°F as determined from ASTM D 4123. Two resilient moduli can be calculated in accordance with ASTM D 4123—an instantaneous and total resilient modulus. The Guide does not state which value is to be used. Therefore, layer coefficients have been calculated for both values for each AAMAS project. These values are given in Table 52.

The Guide cautions users against using resilient moduli greater than 450 ksi when estimating the layer coefficient. An E_{AC} value of 450 ksi corresponds to a layer coefficient of 0.44. As may be seen in Table 52, all mixtures exceed this value, with the exception of the Michigan and New York-Rason mixes when using total resilient modulus.

Although ASTM D 4123 is the test recommended for obtaining values to be used when entering the AASHTO charts to determine layer coefficients, the repeated load indirect tensile test was not used to characterize the stiffness of asphaltic concrete by Van Til, et al. (*81*). The HMAC stiffnesses were originally based on dynamic modulus data, as reported by Kallas and Riley (*82*). The dynamic modulus (as measured by compression

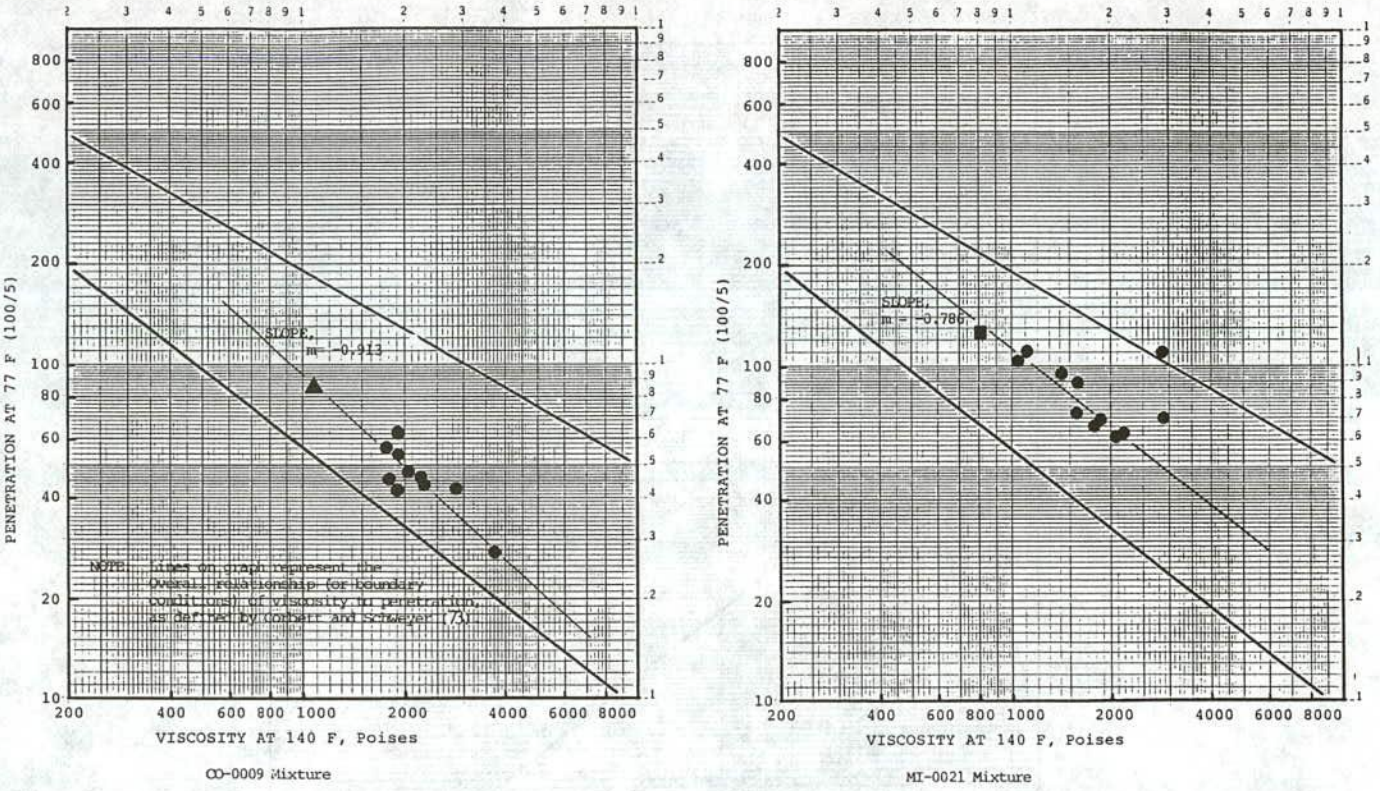

Figure 126. Relationship of penetration and viscosity values for the recovered asphalts from the CO-0009 and MI-0021 projects.

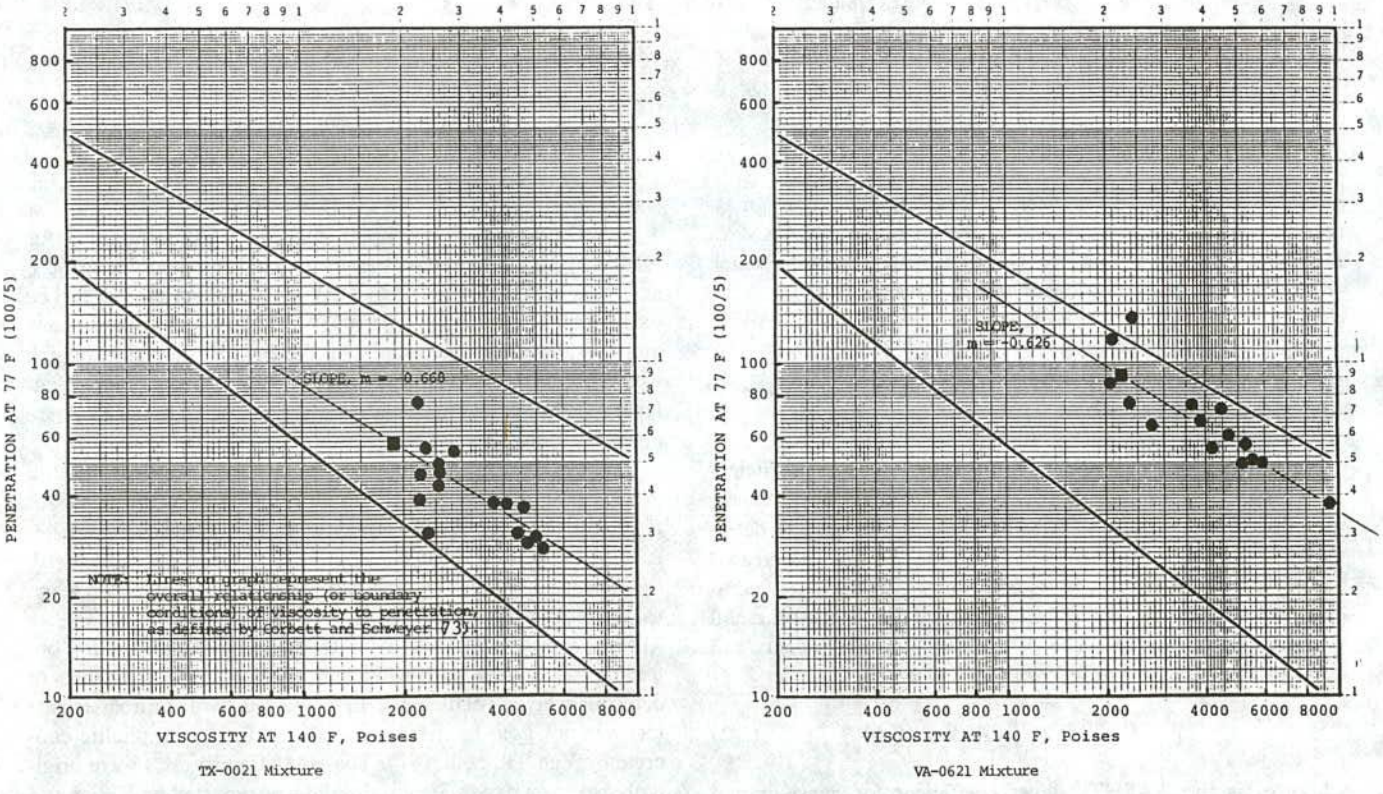

Figure 127. Relationship of penetration and viscosity for the recovered asphalts from the TX-0021 and VA-0621 projects.

tests) and resilient modulus (as measured by indirect tensile tests) are not the same values. The layer coefficient for a dense-graded HMAC surface layer was set at 0.44 (determined at the Road Test) for a modulus of 450 ksi, which was the average HMAC dynamic modulus measured at the average pavement temperature recorded during the Road Test (67.5°F).

To obtain the relationship between E_{AC} and layer coefficient, calculations of surface deflection, asphaltic concrete tensile strain, and vertical compressive strain on the subgrade were made for different levels of surface, base and subgrade stiffness and for varying surface and base thicknesses. The three limiting criteria mentioned above were chosen because of their observed or theoretical correlation with performance. Variation in asphalt concrete layer coefficients was also correlated with Marshall stability and Hveem cohesiometer values by several State Highway Agencies, which are included in the AASHTO Design Guide (*6*).

3.4.2 Relationship Between AAMAS and AASHTO Thickness Design Procedures

An AAMAS should permit the characterization of HMAC mixtures based on engineering properties which affect long-term pavement performance. The AASHTO procedure does not directly use or assume engineering properties of HMAC for the determination of pavement layer thicknesses. For the procedure given in the Guide for the structural design of flexible pavements, an AAMAS will not provide substantial improvement in the ability to account for the potential contribution of HMAC to the pavement structure, except for the definition of resilient modulus.

As previously mentioned, the Guide suggests the use of moduli at 68°F to estimate the layer coefficient of HMAC. Although the mean temperature of HMAC courses measured at the AASHTO Road Test may be relevant for the relationships developed from that data, this may not be the case of pavements exposed to different environmental conditions. Thus, the stiffness of HMAC at 68°F may not accurately characterize the same mix design used at the Road Test if it were used in Messina, New York, or Opelousas, Louisiana, because the environments are so different in those locales.

The suggested manner in which the elastic modulus of HMAC is to be estimated is also questionable. The Guide suggests using ASTM D 4123 (indirect tensile testing techniques) to obtain stiffness values in finding the layer coefficient, when moduli obtained from dynamic compressive tests were used during the development of the relationship between E_{AC} and layer coefficients, as previously noted. Differences in the results of these tests have been documented by Von Quintus (*63*), Bonaquist (*83*), and others (*34, 84*). These authors offer differing conclusions regarding the appropriateness of using moduli determined from repeated load indirect tensile tests in pavement modeling and design.

The design equation for flexible pavements calculates the number of 18 kip equivalent single axle loads which will reduce the serviceability index (PSI) by an assumed amount. PSI is primarily a function of ride quality (roughness), but is also affected by rutting, cracking, and patching. Rutting and types of cracking, such as thermal (low temperature) and fatigue cracking, will be more predictable as a result of an AAMAS. If roughness (particularly) and patching predictions could be related to specific asphaltic concrete properties, the predicted or assumed changes in PSI could be based on AAMAS.

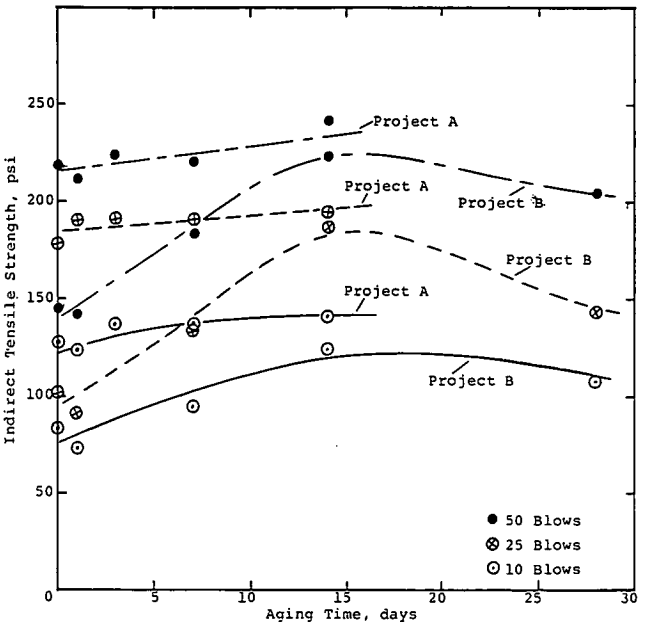

Figure 128. Variation of indirect tensile strength with length of oven aging at 140°F.

Table 52. Summary of AASHTO layer coefficients determined in accordance with the AASHTO Design Guide (6).

Mixture	Instant. MR at 68°F, ksi	AASHTO Layer Coefficient	Total MR at 68°F, ksi	AASHTO Layer Coefficient
CO-0009	740**	0.53	537**	0.47
MI-0021	560**	0.48	384	0.41
TX-0021	1,800**	0.68	1,476**	0.65
VA-0621	1,300**	0.62	1,040**	0.59
WY-0080	880**	0.56	739**	0.53
California	2,170**	0.71	1,800**	0.68
Georgia	1,100**	0.60	860**	0.55
New York - Rason	590**	0.49	370	0.41
Wisconsin	820**	0.54	620**	0.50

MR = Resilient Modulus, ASTM D 4123

** = Resilient modulus values that are outside the boundary conditions of the correlation presented in the Guide (9).

In the future, the National Pavement Data Base established by the Strategic Highway Research Program (SHRP) for the Long-Term Pavement Performance (LTPP) studies will enable the factors affecting the serviceability of pavements to be defined for a broader range of conditions. This should result in the merging of AAMAS with pavement structural design procedures. The other efforts to be undertaken by SHRP in the asphalt and maintenance technical research areas should further assist in these developments. One chapter in the Guide (*6*) discusses mechanistic-empirical thickness design procedures in general, and describes the framework for their development and application. When AASHTO adopts this type of procedure, the value of AAMAS will increase markedly.

In the interim, one technique that can be used to evaluate the environmental effects on the structural design is to consider seasonal fatigue damage. In other words, use seasonal resilient moduli to calculate seasonal fatigue damage and sum the sea-

sonal damage to determine an annual fatigue damage. This procedure was used by Von Quintus, et al. (*85*) in the development of a structural design method. An equivalent asphaltic concrete resilient modulus based on a fatigue cracking criterion can be calculated by the following equation:

$$E_{RE} = \sum \frac{E_{Rt}(i) \times FF(i)}{\sum FF} \qquad (3\text{-}3)$$

where E_{RE} is the equivalent total resilient modulus based on a fatigue damage approach, E_{Rt} is the total resilient modulus as measured by ASTM D4123 at the average pavement temperature for season *i*, and *FF* is the fatigue factor obtained from Figure 129.

Equation 3-3 includes only damage associated with fatigue cracking and ignores the damage caused by permanent deformation and disintegration. This is a necessary assumption because of the limited tie between resilient modulus and fatigue cracking and resilient modulus and layer coefficient. It does, however, allow for seasonal and environmental effects in estimating the AASHTO layer coefficient.

The AASHTO layer coefficients were recalculated using the foregoing procedure. For simplicity, seasonal pavement temperatures of 41, 70, and 104°F were assumed for the winter, fall and spring, and summer months, respectively. These revised AASHTO layer coefficients are given in Table 53. The layer coefficients for the Michigan, New York, and Wisconsin mixes are low and probably should not be placed in a hot environment.

This equivalent modulus concept should equal or exceed the modulus value used to estimate the AASHTO structural layer coefficient used for design. The GPS (General Pavement Sections) projects of the SHRP LTPP program should provide the necessary pavement performance data to determine if the resilient modulus-AASHTO layer coefficient relationship is adequate, with or without modifications, or inappropriate.

3.4.3 Summary

The only tie between an AAMAS and the current AASHTO thickness design procedure is the determination of a design resilient modulus which can be used to estimate the layer coefficient for HMAC. Until a thickness design procedure is adopted by AASHTO which separates the distress types from the all-encompassing present serviceability index, an AAMAS will not result in any substantial improvement to the characterization of HMAC layers. The adoption of such a procedure appears to be inevitable from the discussion included in the Guide, NCHRP Project 1-26, and the implementation of the SHRP LTPP studies. However, until NCHRP Project 1-26 and AAMAS can be tied together, resilient modulus is the only common parameter between mixture and structural design.

In summary, resilient modulus should be determined in accordance with ASTM D 3497. If ASTM D 4123 is used, as required by the AASHTO Design Guide (*6*), it is recommended that the total resilient modulus be used to determine the layer coefficient for use of structural design. This total indirect tensile

Table 53. Summary of AASHTO layer coefficients calculated using an equivalent annual modulus based on fatigue cracking.

Mixture	Equivalent Annual Modulus, *ksi	Layer Coefficient
CO-0009	449	0.44
MI-0021	206	0.30
TX-0021	326	0.38
VA-0621	311	0.38
WY-0080	263	0.35
California	953	0.57
Georgia	469	0.45
New York - Rason	143	0.24
Wisconsin	201	0.30

* Assumed Seasonal Pavement Temperatures:
Winter - 41°F, Spring and Fall - 70°F, Summer - 104°F

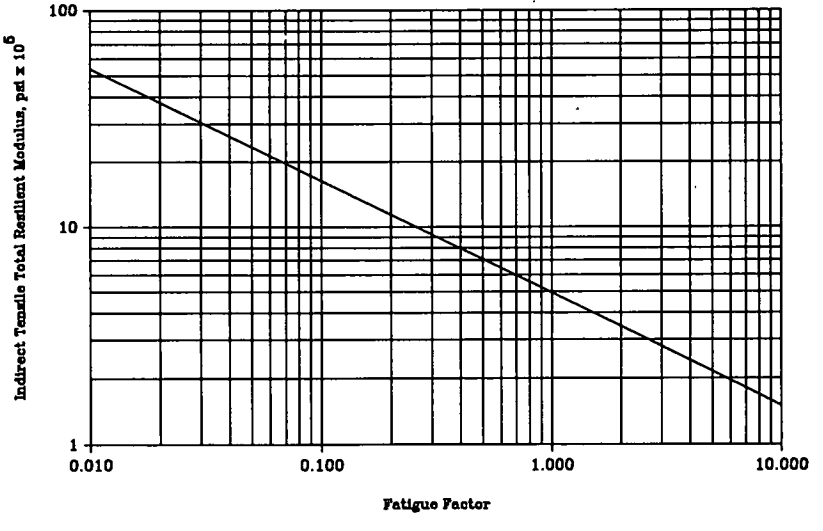

Figure 129. Estimation of the fatigue factor to determine an equivalent annual total resilient modulus for dense-graded asphaltic concrete mixtures (8).

resilient modulus will more closely simulate the direct compression moduli from which the stiffness-layer coefficient correlation was originally developed, but the values will still be greater at a test temperature of 68°F than the corresponding value measured using uniaxial compression testing techniques (Figure 83). Insufficient data exist to establish a reduction coefficient to equate indirect tensile and compressive resilient moduli. Using previous test results, the reduction varies from 1.00 to 1.75, but is material dependent. It is also suggested that the resilient modulus be measured along at least two diametral axes on a set of three specimens for each test temperature.

3.5 MIXTURE PERFORMANCE EVALUATION

The concept of basing a mixture design procedure directly on its effect on the performance of flexible pavements is clearly logical and appropriate. It is also logical and appropriate to base new initiatives for optimizing mixture designs on their effects on performance. Unfortunately, the mathematical models to support the methodology are simply too limited in their use.

There are many different mechanistic models currently available that can be used to calculate stresses, strains, and deflections within the pavement structure. However, the empirical or regression models relating the pavement response parameters to pavement distress, which are needed to support this methodology, simply do not exist or are very limited (especially for asphaltic concrete overlays). More specific, the performance models used in AAMAS must be tied closely to the results of NCHRP Project 1-26. As stated in Chapter 2, five distresses are considered in AAMAS. Each of these are discussed and reviewed in this part of the report for mixture evaluation.

3.5.1 Rutting

The earliest distress that must be designed against is rutting or shoving. It should not be expected, however, that a mix design procedure alone can overcome all cases of construction expediency. Resurfacing and rehabilitation have become major items in asphalt mixture usage. This usually means paving adjacent to traffic and opening the fresh mix to traffic, as soon as possible. Some restraint in this operation is necessary to prevent early rutting even with the most stable mixtures. Rutting within 24 hours of paving has been noted on high traffic roads as tractor trailers with heavy axle loads continue the compactive effort beyond the construction phase.

Ideally, pavements are constructed with an air void content in the range of 5 to 7 percent. However, ideal conditions often do not exist and an air void content range at completion of construction is often in the range of 8 to 12 percent. For example, this condition occurred for the Texas and Colorado projects. The effect of these different air void contents on rutting caused by traffic densifying high air void content mixtures is usually not considered during initial mixture design, because it is assumed that good engineering and construction practices will be followed and proper compaction will be achieved in the field. Current mixture design procedures do address rutting and instability caused by over-filling the air voids with asphalt.

3.5.1.1 Types of Rutting

Two types of rutting are considered in the AAMAS program. These are one-dimensional densification (reduction in air voids, only) and the lateral movement or plastic flow of asphalt from wheel loads (consolidation or a reduction in total voids). The more severe premature rutting failures and distortion problems of asphaltic concrete are related to the lateral flow of asphalt or shear distortion, rather than one-dimensional densification.

3.5.1.1.1 One-Dimensional Densification. This type of rutting can be estimated using the traffic densification procedure discussed in Chapter 2. Basically, it is a reduction in the air voids of the asphaltic concrete layers and is based on testing cylindrical compression samples. More directly, however, this reduction in air voids can be estimated using the Corps of Engineers gyratory shear compactor or any of the other compactors considered in the study by simply increasing the compactive effort to mix refusal (Figures 31 through 36). Densification using these devices is restricted to one direction, vertical.

The air void content at which no reduction in air voids occurs with additional compactive effort was defined as the ultimate air void content for the JMF. If the asphaltic concrete layers are compacted in the field to a proper air void range and the mix is designed such that the ultimate air void content is greater than 3 percent, one-dimensional densification of the mixture should not be a problem. The ultimate air void content was measured for each mixture using each compaction device. This was presented in Chapter 2 (section 2.3.3.1). The gyratory shear compactor and kneading compactors were found to provide similar estimates for this value.

3.5.1.1.2 Plastic Flow of Asphalt or Shear Distortion. The Corps of Engineers gyratory shear compactor is a very good tool for evaluating the reduction in shear resistance of the mixture after many thousands or millions of traffic applications. Kumar et al. (*86*) and Ruth at the University of Florida have both found it to be a good tool for measuring changes in compaction and shear strain properties due to traffic densification of asphaltic concrete materials. Both have suggested its use for mixture design and evaluation. Each of the AAMAS mixtures was tested in the traffic densification procedure using the Corps of Engineers GTM. These results were discussed and presented in Chapter 2.

The California, Georgia, MI-0021, VA-0621, and New York-Prima mixtures were found to retain their shear resistance properties after 300 revolutions. The other mixtures (CO-0009, TX-0021, New York-Rason, Wisconsin, and WY-0080) were found to have a significant reduction in the shear values with less than 200 revolutions of the gyratory shear compactor (Figure 77). Resistance to permanent deformation is strongly influenced by aggregate grading (*84*). Reducing the sand and asphalt content and obtaining proper compaction of the asphaltic concrete mixture in the field would have increased the shear resistance of the Colorado, New York-Rason, Texas, and Wisconsin mixtures. Contamination was measured in the Wyoming mix, which may have affected the long term or accelerated traffic densification procedure of this mixture.

Static unconfined uniaxial compression creep tests have been used by Regan (*1*), Brown (*84*), and others to rank mixes according to their deformation resistance to load. Indirect tensile tests are also being used, because the samples are easily prepared and the testing procedure is not complicated. Both types of tests were conducted on each AAMAS mixture, and differences were obtained, especially in the slopes of the creep curves. These are summarized as follows:

Mixture	Slopes of the Plastic or Creep Strain Curve: Repeated Load Permanent Deformation	Slopes of the Plastic or Creep Strain Curve: Static Creep
CO-0009	0.68	0.54
MI-0021	0.53	0.36
TX-0021	0.65	0.63
VA-0621	0.53	0.39
WY-0080	0.54	0.42

A comparison of compression to indirect tensile testing can not be made, because the air voids of the specimens were significantly different between the sample cells.

Unconfined compression tests were performed on all AAMAS mixtures. The results of this testing are, as follows, for each mixture:

Property at 77°F	Mixture: CO-0009	MI-0021	TX-0021	VA-0621	WY-0080
Indirect tensile strength, psi	100	84	129	114	82
Unconfined compressive strength, psi	946	939	1174	1109	1061
Cohesion, psi	155	135	280	195	150
Angle of internal friction, deg.	49	51	49	53	52

These results indicate that the TX-0021 mixture, if properly compacted, will have the higher shear resistance of the five mixtures. With the high air voids and traffic densification, however, the shear resistance of the TX-0021 decreases dramatically. It is interesting to note that the mixtures are ranked differently for different properties (strength, creep, stiffness). A combination of test values is required to optimize each mixture, with the exception of the Corps of Engineers GTM. The Corps of Engineers gyratory shear value provides a good parameter for mixture evaluation and design. If a GTM is unavailable for use, however, a combination of tests is required for mixture optimization. These are the unconfined compressive strength, indirect tensile strength, and static creep compliance using uniaxial compression testing techniques. Part I, the AAMAS Procedural Manual, provides the recommended testing procedure when a GTM is unavailable for use.

3.5.1.2 Rutting Relationships and Models

Most mechanistic and empirical models use mechanical properties (such as alpha and gnu, resilient modulus, or a creep stiffness) to predict the amount of permanent deformation with traffic applications. These properties are determined from compression testing of unconfined cylindrical specimens or indirect tensile testing of diametral specimens. NCHRP Project 1-26 originally recommended the use of the following type of rutting model:

$$RR = A\,(N)^m \qquad (3\text{-}4)$$

where RR is rutting rate per load application, N is number of repeated load applications, and A,m are constants developed from field calibrated laboratory testing data

The integral of the Eq. 3-4 over the total number of traffic applications is the expected rut depth. Another approach to modeling rutting (in terms of permanent strain) yields the following equation, which is more applicable to an asphaltic concrete mixture design procedure, but is still of the same form as equation 3-4.

$$\epsilon_p = A\,(N)^m \qquad (3\text{-}5)$$

or

$$\log \epsilon_p = \log A + m \log N$$

where ϵ_p is accumulated permanent strain in the asphaltic concrete layer, and A,m are constants measured from laboratory test data using repetitive loading techniques, and correlated to field performance data.

There is test equipment available to determine, more directly, the rutting characteristics of asphaltic concrete mixtures. For example, Lai (*87*) has developed a simplified laboratory test method to evaluate the rutting characteristics of asphaltic concrete mixtures, and use of the Corps of Engineers GTM has already been discussed. The Lai device is called a "loaded wheel tester" that requires beam or slab type specimens and measures rut depth with number of wheel load passes. Although this is a direct way to measure the rutting characteristics of mixtures, the specimens are difficult to prepare and are costly. Thus, a more standard approach was taken for AAMAS to be consistent with the NCHRP 1-26 project.

Both static creep and repeated load permanent deformation tests were performed on specimens using indirect tensile testing techniques. Static creep and resilient modulus tests were also performed on cylindrical compression samples for comparison with the indirect tensile test results. Figure 130 provides a comparison of the resilient modulus and inverse of creep compliance for the same mixtures. As expected, the two values are related.

Kennedy (*36*), Baladi (*34*), and others have suggested use of the indirect tensile test for measuring the permanent deformation characteristics of asphaltic concrete mixtures. Alpha and gnu (Eqs. 2-8 and 2-9) are calculated from plastic vertical deformations measured using indirect tensile testing techniques. Alpha and gnu can also be calculated from the plastic horizontal deformations, but these are generally associated with fatigue cracking criteria rather than permanent deformation. An important finding from this study is that different values will be calculated, similar to the differences between horizontal and vertical deformations. Others, such as Khosla (*88*) and Brown (*84*) have concluded that the direct uniaxial compression test provides a better simulation of actual performance, in terms of rut depths.

Without question, determining the permanent deformation characteristics of the alpha and gnu functions (required for the

VESYS and modified ILLIPAVE programs) is difficult, especially when using indirect tensile testing techniques. Additionally, at higher temperatures and loading times, applicability of the indirect tensile test is questionable because of the assumption of elastic layer theory as discussed in Chapter 2, section 2.6.2. Thus, uniaxial compression tests are recommended for permanent deformation characterizations. The remainder of this section discusses the two different types of rutting considered in AAMAS.

3.5.1.3 Creep Versus Repeated Load Tests for Mixture Characterization

One cycle of a repeated load permanent deformation test is identical to a creep-recovery test, with the exception that the times are very short. The following equation equates the different strains that occur during one loading cycle of a repeated load permanent deformation test.

$$\epsilon_{ct} = \epsilon_{rt} + \epsilon_p$$

The total applied strain, ϵ_{ct}, and total resilient or recovered strain, ϵ_{rt}, of a loading cycle are defined as:

$$\epsilon_{ct} = \epsilon_{i\ell} + \epsilon_{cr}$$

$$\epsilon_{rt} = \epsilon_{ir} + \epsilon_R$$

where $\epsilon_{i\ell}$ is the instantaneous strain (or deformation) measured after load application; ϵ_{cr} is the creep strain measured during one load application or cycle; ϵ_{ir} is the instantaneous resilient or recovered strain (or deformation) after load release; ϵ_R is the recovered strain (relaxation) during the rest period of one loading cycle; and ϵ_p is the permanent or plastic strain per loading cycle.

The permanent strain per load cycle can be defined by combining the above three equations and rearranging the terms to form Eq. 3-6:

$$\epsilon_p = \epsilon_{i\ell} + \epsilon_{cr} + \epsilon_{ir} - \epsilon_R \qquad (3\text{-}6)$$

A square wave was used in the test program to evaluate the different strain components of Eq. 3-6. A square wave was used rather than a haversine wave, to facilitate the difference between the creep strain, instantaneous applied strain, instantaneous resilient strain and relaxation strain for a particular loading cycle. A haversine wave form was not used, because the load is changing constantly with time, so it becomes impossible to distinguish between instantaneous deformation and creep over a short period of time.

Figure 131 illustrates the relationship between the instantaneous deformation or strain and instantaneous resilient strain. For a large number of test specimens, these two deformations or strains can be considered to be equal ($\epsilon_{i\ell} = \epsilon_{ir}$). Substituting this equivalency into Eq. 3-6 and simplifying results in the following equation for permanent strain per load application:

$$\epsilon_p = \epsilon_{cr} - \epsilon_R \qquad (3\text{-}7)$$

An equation that has been used to represent the total applied strain with time during a creep test is:

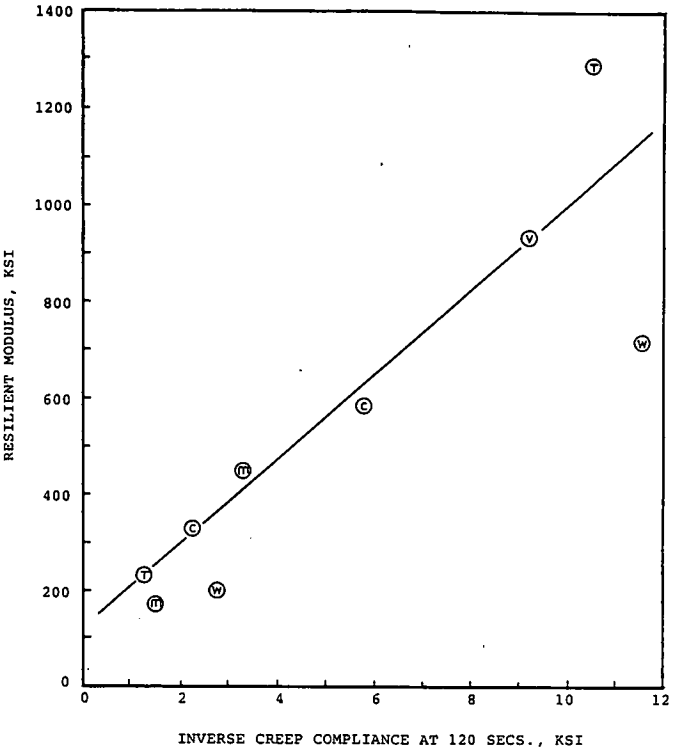

Figure 130. Relationship between inverse of creep compliance at a loading time of 120 sec and resilient modulus (instantaneous).

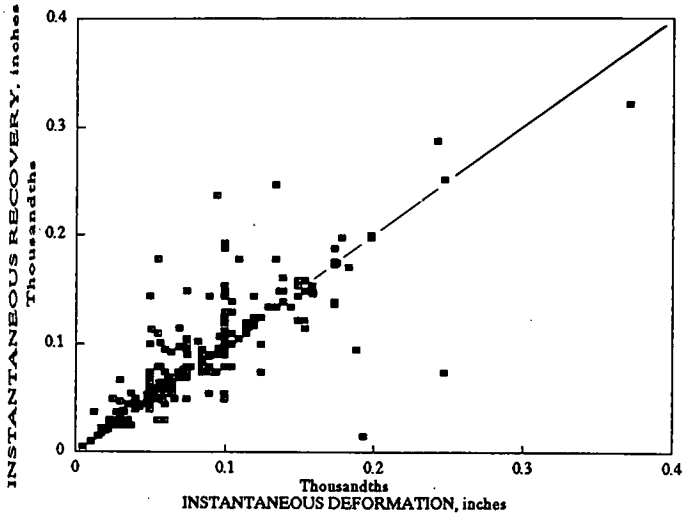

Figure 131. Comparison between the instantaneous deformation and instantaneous recovery for a repeated load test using a "square" loading wave.

$$\epsilon_{ct} = a\,(t_\ell)^{m_c} \qquad (3\text{-}8)$$

where t_ℓ is loading time, sec, and a,m_c are regression constants for the creep curve in the steady state region.

The creep strain, ϵ_{cr}, and relaxation strain, ϵ_R, can be rewritten as follows: $\epsilon_{cr} = \epsilon_{ct} - \epsilon_{i\ell}$; $\epsilon_R = \epsilon_{rt} - \epsilon_{ir}$.

Substituting Eq. 3-8 into the above equation for the creep strain (ϵ_{cr}) results in: $\epsilon_{cr} = a\,(t_\ell)^{m_c} - \epsilon_{i\ell}$.

Substituting the equation for creep strain (ϵ_{cr}) into Eq. 3-7 results in: $\epsilon_p = a\,(t_\ell)^{m_c} - \epsilon_{i\ell} - \epsilon_R$.

Substituting the equation for the relaxation strain (ϵ_R) and simplifying results in the following equation for the plastic strain: $\epsilon_p = a\,(t_\ell)^{m_c} - \epsilon_{i\ell} + \epsilon_{ir} - \epsilon_{rt}$

But, $\epsilon_{i\ell} = \epsilon_{ir}$, so the above equation can be further simplified to:

$$\epsilon_p = a\,(t_\ell)^{m_c} - \epsilon_{rt} \tag{3-9}$$

The total resilient strain, however, is time dependent, and can be represented by the same type of mathematical formulation for the total applied strain (Eq. 3-8).

$$\epsilon_{rt} = b\,(t_R)^{d} \tag{3-10}$$

where t_R is relaxation time, sec, and b, d are regression constants for the recovery or relaxation curve.

Equating Eqs. 3-5 and 3-9, results in the following expression: $A\,(N)^m = a\,(t_\ell)^{m_c} - \epsilon_{rt}$.

At the initial or first loading cycle, $N = 1$ and $t_\ell = t_{\ell 1}$; the two equations are identical. Thus, the coefficient for the permanent deformation can be expressed as a function of the initial creep-recovery test.

$$A = a\,(t_{\ell 1})^{m_c} - \epsilon_{rt} \tag{3-11}$$

where $t_{\ell 1}$ is loading time for one cycle of the repeated load permanent deformation test, sec.

Substituting Eq. 3-11 into Eq. 3-5 results in the following expression for the cumulative permanent strain measured during a repeated load permanent deformation test:

$$\epsilon_p = [a\,(t_{\ell 1})^{m_c} - \epsilon_{rt}]\,N^m \tag{3-12}$$

During all creep testing, the percent recoverable creep was calculated for each specimen at the end of the creep-recovery test. These values were previously summarized and discussed in Chapter 2 (Table 32). Thus, the total recovered strain can be calculated from a percentage of the total applied creep. The percent recoverable creep, X, is calculated using the following equation:

$$X = \epsilon_{rt}\epsilon_{ct} \tag{3-13}$$

where X is percent recoverable creep or the recovery efficiency from static loads.

Substituting Eq. 3-13 into Eq. 3-7 and simplifying results in the following equation:

$$\epsilon_p = \epsilon_{ct}\,(1 - X) \tag{3-14}$$

Substituting Eq. 3-8 into Eq. 3-14 results in a simplified expression for the plastic strain:

$$\epsilon_p = a\,(t_\ell)^{m_c}\,(1 - X) \tag{3-15}$$

In order to equate the permanent deformation test to the creep-recovery test, a specific loading time, t_ℓ, must be used for a specific number of load applications, N. To equate each relationship the following was assumed: $N = t/t_\ell$. This ensures that the loaded times for each test are at least equal. Equating Eqs. 3-15 and 3-12 and simplifying results in the following expression for the slope of the cumulative permanent strain curve based on the results of a creep-recovery test:

$$m = \frac{\log a + 3.5563 m_c + \log (1 - X) - \log [a(0.1)^{m_c} - \epsilon_{rt}]}{4.5563} \tag{3-16}$$

Using the results from the creep-recovery test, the slopes and intercepts of the permanent deformation test were calculated for each mixture. These calculated values from creep testing have been compared to those values actually measured on these same mixtures from the permanent deformation test. Figure 132 compares the measured to calculated values. A good comparison of the predicted to measured values was found. Thus, it is recommended that results from the creep testing be used to estimate the coefficients required with the NCHRP Project 1-26 recommendations.

3.5.1.4 Shearing Resistance Considerations

Shearing resistance of asphalt-aggregate mixtures directly influences the types and severity levels of distresses observed in hot-mixed asphaltic concrete (HMAC) pavement layers. Rutting and shoving of HMAC layers are two distress types that are functions of the shearing resistance of the material. Distress manifestations such as raveling and flushing, as well as fatigue cracking, reflection cracking, and potholes, are related to the shearing resistance of HMAC.

Neither the Marshall nor the Hveem mix design procedures defined the shearing resistance conventionally in the context of soil mechanics. Since the shearing resistance is a determining factor in a number of distress types, the question of whether or not it is acceptably accounted for indirectly in the other features of AAMAS is addressed.

The shearing resistance of HMAC is a function of the interparticle cohesion and friction as well as the amount of stress applied to the material. The cohesiveness of the mix depends on the amount of asphalt cement included in the mix, the degree to which the particles are coated by the asphalt cement, and by the properties of the asphalt cement itself. The properties of the asphalt cement affecting cohesion vary with temperature and age. The cohesiveness of the mixture may also be affected by its attraction (or lack thereof) to the aggregates used in the mix and by the surface area (texture) and porosity of the aggregates.

The internal friction which develops in an asphalt-aggregate mixture is a function of the applied stress, the shape and texture of the aggregate, the particle size distribution, the shearing resistance of the aggregate itself, and the properties and amount of asphalt cement used in the mix. Considering the number of factors involved which may affect the shearing resistance of asphaltic concrete, it is apparent that a single shear strength test or value can not adequately characterize an asphalt-aggregate mixture.

Both Hveem and Marshall mixture design procedures incorporate stability tests for the determination of a design asphalt

content. Although stability determinations account for resistance to deformation of an asphalt-aggregate mixture, the asphaltic concrete specimens being tested by either procedure are not in stress states which simulate those experienced from wheel loads. This may explain the poor correlation reported by many researchers between stability and rutting.

Creep testing is used in AAMAS to evaluate permanent deformation resulting from repeated loading and to determine the stiffness of the mixture during long duration stress application. Permanent deformation constants (alpha and gnu) are obtained from the relationship between accumulated strain and the number of load applications. These indices are used in viscoelastic models to predict rutting. Only axial (vertical) strains are considered in the VESYS model. The incremental static-dynamic direct compression test procedure is described in some detail by Kenis (*51*). Both incremental static-dynamic creep compression and static creep tests were performed on the CO-0009 and WY-0080 mixtures. Although only two of the five AAMAS mixtures were tested, similar creep compliance curves were obtained at comparable loading times.

Resistance to permanent deformation was also evaluated in research efforts undertaken in Great Britain by Brown and Cooper (*84*) to develop a mixture design procedure for structural asphaltic concrete layers. Shear strain was considered as the measure of permanent deformation, and was examined for various types of asphalt bound base materials used in Britain. A number of laboratory testing procedures were employed including repeated load triaxial creep, static triaxial creep, uniaxial creep, and Marshall stability. The authors concluded that the static unconfined creep test may be used to rank mixes according to their resistance to permanent deformation.

Brown and Cooper also discussed the interrelation on aggregate type and gradation, binder content, and level of compaction on deformation. They noted that mixes containing less fine aggregate and, possibly, less binder may result in mixes with greater resistance to permanent deformation. Davis (*89*) wrote that, historically, asphaltic concrete pavements with high volume concentration of aggregates resulting from the use of large top size aggregates with low air voids and low asphalt contents have exhibited outstanding performance. It was noted that some of these very old pavements had been subjected to vehicles, operating with narrow steel rimmed wheels, and to large trucks with solid rubber tires.

Davis' paper begins by addressing an increase in reports of stripping, which had been attributed to such factors as changes in asphalt cement properties, high tire pressures, and the use of very fine particles as mineral filler in HMAC. He postulated that much of the stripping which had been reported was actually a secondary mechanism, with the moisture damage being a result of shear displacement within the mixture. The increase in occurrence of "stripping," especially on pavements that had not previously exhibited any evidence of such, was thought to be a result

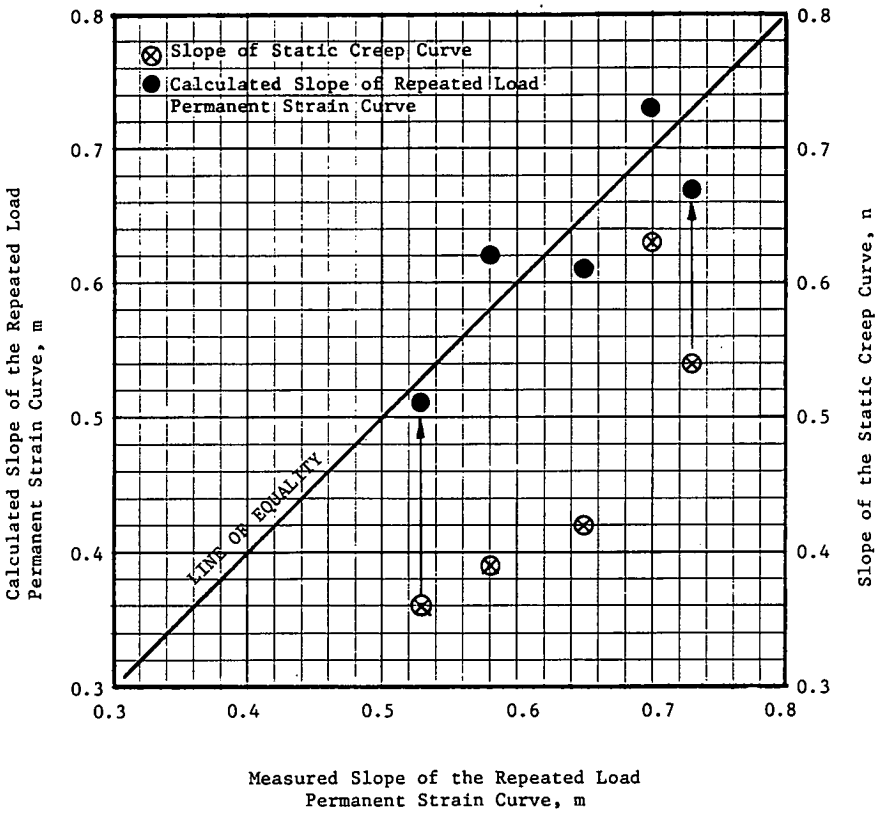

Figure 132. Comparison of the measured slopes and calculated slopes (from the static creep test results) of the repeated load permanent strain curve.

of increases in tire pressures. If shear displacement, i.e., lack of shearing resistance, is indeed the "culprit" behind the apparent increase in stripping described by Davis, the ability to rank mixes on the basis of shearing resistance or permanent shear strain would be extremely beneficial.

Often, the most evident cases of shear displacement are in locations where turning movements, braking, and acceleration from a dead stop are prevalent. Distress types such as slippage cracking and shoving were not considered in the development of AAMAS. Slippage cracking occurs at the interface between layers and is highly dependent on the texture and cleanliness of the surface on which the asphaltic concrete is placed. Construction and material specifications must address these type problems. Shoving, however, is dependent on the properties of the mix, particularly shearing resistance. Although deformation resulting from direct shear applied to the surface is not addressed directly, it is expected that the resistance to such deformation would result from the improvements in asphaltic concrete mixture design resulting from AAMAS. The Corps of Engineers GTM provides an indication of this shearing resistance of asphaltic concrete mixtures. Those mixtures included in this study that are known to be susceptible to shoving and lateral distortions were identified as such with the GTM. Thus, use of the GTM is recommended in the AAMAS procedure.

3.5.2 Fatigue Cracking

A longer term distress mode considered in most design/evaluation programs is fatigue. Fatigue failures are accelerated by high air voids which, in addition to creating a weaker mix, also increase the oxidation rate of the asphalt film. This was illustrated by the significant decrease in failure strains when artificially aging the mixtures. But, even with an initial air void content in the 4 to 6 percent range, asphalt film aging will still occur that has a detrimental effect on failure strains of the mixture (Table 30).

The development of fatigue cracks is related to the tensile strains at the bottom of the asphaltic concrete layer and stiffness of the material. In fact, most models use either two or three parameters for the fatigue curves that relate number of load applications to a tensile strain and stiffness of the material.

3.5.2.1 Fatigue Relationships

There are different relationships that can be used to estimate the fatigue constants K_1 and K_2. NCHRP Project 1-26 recommended use of Maupin's fatigue constants (*90*), which are estimated from the indirect tensile strength test. Obviously, it would be very advantageous that the same relationship be used between NCHRP Project 9-6(1) and Project 1-26. Measuring the indirect tensile strength is also much simpler than measuring the resilient modulus, and thus has some practical advantages over other relationships.

3.5.2.1.1 Maupin's Fatigue Constants. The fatigue relationship developed by Maupin is given below, and was developed from laboratory flexural fatigue tests using simply supported beams.

$$N = K_1 (\epsilon_t)^{-n} \tag{3-17}$$

where ϵ_t is tensile strain at the bottom of asphaltic concrete layer, in./in.

This relationship is similar to other fatigue curves that have been reported in the literature, but only represents flexural fatigue tests performed at 72°F. No other temperatures were used in the experiment. For a constant strain fatigue test, the fatigue constants were found to be related to the indirect tensile strength. The resulting relationships between the fatigue constants, K_1 and n, and indirect tensile strength are:

$$n = 0.0374\ \sigma_t - 0.744 \tag{3-18}$$

$$\log K_1 = 7.92 - 0.122\ \sigma_t$$

where σ_t is the indirect tensile strength measured at 72°F, psi.

Use of this relationship becomes advantageous because of the simplicity in measuring the indirect tensile strength at room temperature in the field laboratories for construction control. Most other relationships use a dynamic modulus of elasticity or an instantaneous or total resilient modulus of elasticity for estimating the fatigue constants. If the foregoing relationships (Eqs. 3-14 and 3-15) can be used over a range of temperatures, it would be practical for use in mixture design and for the field control of mixtures. Thus, Maupin's relationship was used to calculate the allowable number of load applications over a range of indirect tensile strengths and temperatures. The following tabulates the results using the indirect tensile strengths that can be expected at different temperatures.

Temperature °F	Indirect Tensile Strength psi	K_1	n	Allowable Number of Load Applications for $\epsilon_t = 1.2 \times 10^{-4}$ in./in.
104	40	1096	0.752	9.73×10^5
77	100	5.25×10^{-5}	2.996	2.93×10^7
41	350	1.660×10^{-35}	12.35	4.39×10^{13}

Based on the laboratory test results from actual mixtures, the allowable number of load applications calculated for the colder temperature (or for mixtures that have large indirect tensile strengths) are unreasonably high. The tensile strain of 1.2×10^{-4} in./in. was used because this strain is the approximate focal point of the Rauhut fatigue relationship (*9*). In other words, for this tensile strain the allowable number of load applications to failure is independent of stiffness, which is approximately 6.0×10^6 load applications. This value is close to Maupin's value at 77°F, as expected, but significantly different at the colder temperature.

3.5.2.1.2 Rauhut's Fatigue Constants. The Rauhut relationship has been found to provide reasonable results over a temperature range of 40°F to 100°F, and is similar to others found in the literature. In fact, the relationship is a modification of the fatigue curves developed by Finn et al. in the NCHRP 1-10B study (*10*). An example of the fatigue curves recommended by Rauhut (*9*) is presented in mathematical form, as follows:

$$N_i = K_1 (\epsilon_t)^{-k_2} \tag{3-20}$$

where ϵ_t is tensile or radial strain at the bottom of the asphaltic concrete layer for wheel load and axle configuration i; N_i is number of allowable applications of wheel load and axle configuration i;

$$K_1 = K_{1R}\left[\frac{E_R}{E_{Rr}}\right]^{-4} \quad (3\text{-}21)$$

$$K_2 = 1.35 - 0.252 \log (K_1) \quad (3\text{-}22)$$

E_{Rr} equals 500,000 psi (reference modulus from the AASHTO Road Test); K_{1R} equals 7.87×10^{-7} (reference coefficient at 500,000 psi based on AASHTO Road Test); and E_R is the modulus or stiffness of the asphaltic concrete at a selected temperature.

3.5.2.2 Equating the Fatigue Constants

Both of these fatigue relationships (Eqs. 3-17 and 3-20) are similar, in that each uses the initial tensile strain to calculate the allowable number of load repetitions to a predefined condition of failure, but there are differences. The difference between the two relationships is that the fatigue constants are estimated using different material properties. The Rauhut relationship relates the constants to the total resilient modulus of elasticity measured, and Maupin's relationship relates these same constants to the indirect tensile strength. Since the fatigue relationships are of the same type, the coefficients can be equated for evaluating any differences at room and other temperatures.

Equating the K_1 coefficients at room temperature:

$$\log K_1 \text{ (Maupin)} = \log K_1 \text{ (Rauhut)}$$
$$7.92 - 0.122\,\sigma_t = \log [7.87 \times 10^{-7} (E_R E_{Rr})^{-4}]$$
$$7.92 - 0.122\sigma_t = \log(E_R E_{Rr})^{-4} - 6.104$$
$$7.92 - 0.122\sigma_t = 4.692 + \log (E_R)^{-4}$$

Thus, in order for the two relationships to result in the same coefficient, the indirect tensile strength must be related to the total resilient modulus of elasticity by the following equation:

$$\sigma_t = 26.46 + 32.79 \log (E_R) \quad (3\text{-}23)$$

Equating the exponents at room temperature:

$$n \text{ (Maupin)} = K_2 \text{ (Rauhut)}$$
$$0.0374\sigma_t - 0.744 = 1.35 - 0.252 \log K_1$$
$$0.0374\sigma_t - 0.744 = 1.35 - 0.252 \log [7.87 \times 10^{-7} (E_R 500)^{-4}]$$
$$0.0374\sigma_t = 0.9116 - 0.252 \log (E_R)^{-4}$$

Thus, in order for the exponents to be the same, the indirect tensile strength must be related to the total resilient modulus of elasticity by the following relationship:

$$\sigma_t = 24.4 + 26.95 \log (E_R) \quad (3\text{-}24)$$

To illustrate the reasonableness of Eqs. 3-23 and 3-24, these two relationships were plotted against actual data measured on both field cores and laboratory compacted specimens. This comparison is shown in Figure 133. It can be seen from the Figure that a large difference can exist. At room temperature, however,

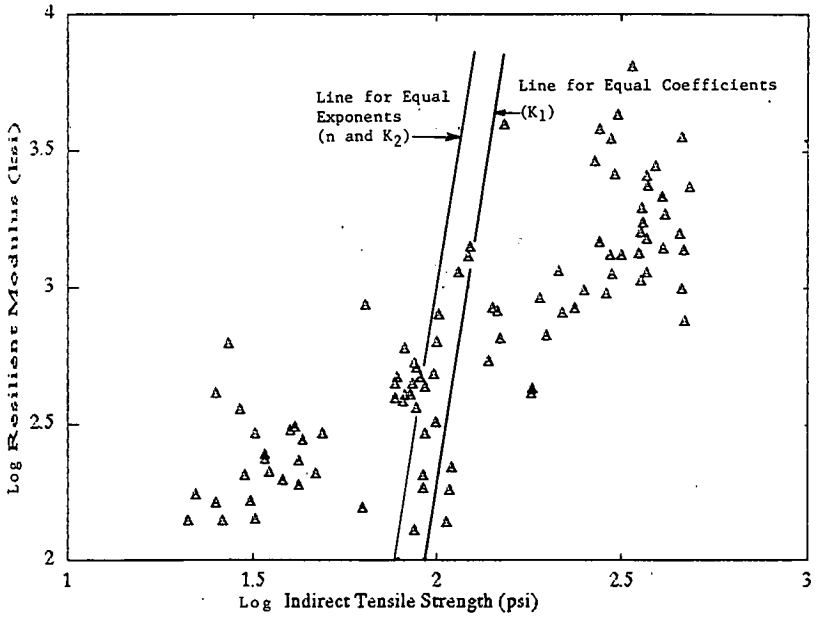

Figure 133. Relationship between indirect tensile strengths and resilient modulus for equating two fatigue curves, as compared to actual data.

the two are very close and result in comparable fatigue constants. As also illustrated in Figure 133, Eqs. 3-23 and 3-24 do not have the same relationship. However, the two fatigue relationships can be equated assuming that each has the same predefined failure condition, which may not be a true assumption.

$$K_1 (\epsilon_t)^{-k2} = K_1 (\epsilon_t)^{-n}$$
$$\log K_1 - K_2 \log (\epsilon_t) = \log K_1 - n \log (\epsilon_t)$$

Substituting for each of the coefficients and exponents and then simplifying results in the following relationship between indirect tensile strength and total resilient modulus of elasticity for a specific pavement structure or initial tensile strain, ϵ_t.

$$\sigma_t = \frac{3.228 + 0.912 \log \epsilon_t + 4 \log (E_R) [1 + 0.252 \log \epsilon_t]}{(0.122 + 0.0374 \log \epsilon_t)} \quad (3\text{-}25)$$

Equation 3-25 will always be bounded by Eqs. 3-23 and 3-24, which illustrates that the fatigue equations are not equivalent, at least at test temperatures different from room temperature and for mixtures with relatively high indirect tensile strengths. Thus, Maupin's relationship should not be extrapolated to other test temperatures that are significantly different from 72°F. For these reasons, the Rauhut (*9*) and NCHRP Project 1-10B (*10*) fatigue relationships were used in the AAMAS program for evaluating the fatigue properties of asphaltic concrete mixtures at more than one temperature.

3.5.2.3 Adjustment for Different Mixtures

Both the NCHRP Project 1-10B and Rauhut relationships were developed using AASHTO Road Test data. Rauhut's relationship was given in Eq. 3-20, and the NCHRP 1-10B relationship is shown as follows:

$$\log N = C_f - 3.291 \log \epsilon_t - 0.854 \log E_R \quad (3\text{-}26)$$

where C_f is the fatigue coefficient or transformation factor to field conditions and is dependent on the level or amount of fatigue cracks: $C_f = 14{,}820$ for crack initiation or laboratory conditions, $C_f = 15.947$ for 10 percent fatigue cracks, and $C_f = 16.086$ for 45 percent fatigue cracks.

3.5.2.3.1 Mixture Stiffness. Using both relationships, the fatigue curve for a specific mixture is dependent only on the mixture's stiffness, E_R. But is this reasonable? For example, take laboratory data from two actual mixtures, which are:

Mix	Stiffness or Resilient Modulus, psi	Indirect Tensile Strength, psi	Tensile Strain At Failure, $\times 10^{-3}$ in./in.
I	1,800,000	370	6.30
II	1,800,000	450	1.08

Both of the above mixes are assumed to have the same fatigue relationships or allowable number of load applications because the stiffnesses are the same, as defined by both the NCHRP Project 1-10B and Rauhut fatigue curves. It should be pointed out that the mixture stiffness used in each relationship is not the same value, especially at the higher temperatures. The modulus used in the development of each fatigue relationship was measured using different types of tests. These differences are recognized, but will be initially ignored for simplicity.

The failure strains for each mix, however, are extremely different. Mix I can sustain a much higher tensile strain prior to crack initiation than mix II. Thus, it seems only reasonable to expect that the fatigue characteristics of these two mixes should also be different. Mix I should have better fatigue properties than mix II because of the larger failure strains. Conversely, the use of Maupin's equation would indicate that mix II would be better than mix I. This would be somewhat similar to a stress/strength ratio used in some fatigue relationships for very stiff materials.

3.5.2.3.2 Maximum Strain Criterion. To examine the reasonableness of using a maximum strain criterion, in addition to a stiffness adjustment, the NCHRP Project 1-10B fatigue relationship (Eq. 3-26) was initially used. First, the tensile strain can be calculated as a function of mix stiffness to cause crack initiation (laboratory condition) for a specific number of load cycles by the following equation:

$$\log N = 14.820 - 3.291 \log \epsilon_t - 0.854 \log E_R \quad (3\text{-}27)$$

Figure 134 shows the relationship between ϵ_t and E_R for different number of loading cycles, including the first loading cycle ($N = 1$). One loading cycle simply represents a very fast indirect tensile strength test. Although the indirect tensile strength of an asphaltic concrete specimen is highly dependent on loading rate, the failure strain is much less dependent on the loading rate, especially at temperatures below 77°F. Kennedy, among others, has measured similar failure strains at the same test temperature using static loads (a creep test), a constant rate of loading (strength tests), or repeated loads (fatigue tests). Thus, it is assumed that at $N = 1$, the tensile strain calculated from Eq. 3-27 (for crack initiation) would be the same failure strain measured from an indirect tensile strength test at the same temperature. Using this assumption, the tensile strain at $N = 1$ can be calculated for different stiffnesses using the following equation.

$$\log \epsilon_t = 4.503 - 0.2595 \log E_R \quad (3\text{-}28)$$

This relationship is plotted on Figures 134 and 135 (identified as $N = 1$), and represents the AASHTO conditions and mixture. Actual indirect tensile strength data from five mixtures have also been plotted on Figure 135 as a comparison to the theoretical fatigue curve for failure at $N = 1$. These mixtures fall above and below the AASHTO relationship. Those above the relationship are assumed to have better fatigue characteristics (less susceptible to fatigue cracking), and those below the line are more susceptible to fatigue cracking, as compared to the AASHTO mixture.

The fatigue constants in Eq. 3-27 were developed from the AASHTO Road Test, and it is expected that these constants should be dependent on the maximum strain that a mixture can sustain. Thus, the AASHTO constants could be replaced by the following relationship to calculate the number of load applications to cause crack initiation at temperature T_1.

$$\log N(T_i) = 14.820 - K_r \log \epsilon_t (T_i) - C_r \log E_R(T_i) \quad (3\text{-}29)$$

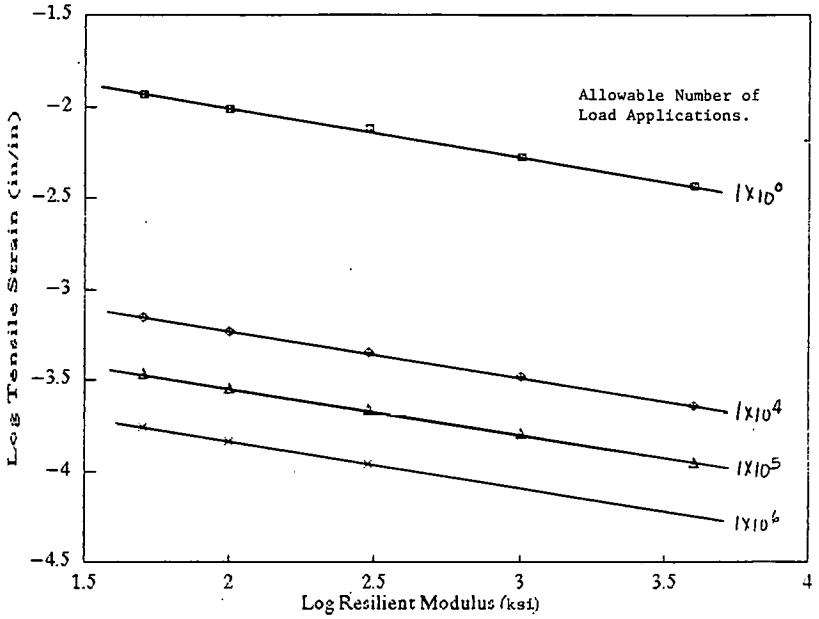

Figure 134. Relationship between maximum tensile strain and resilient modulus for different traffic loads (NCHRP Project 1-10B)

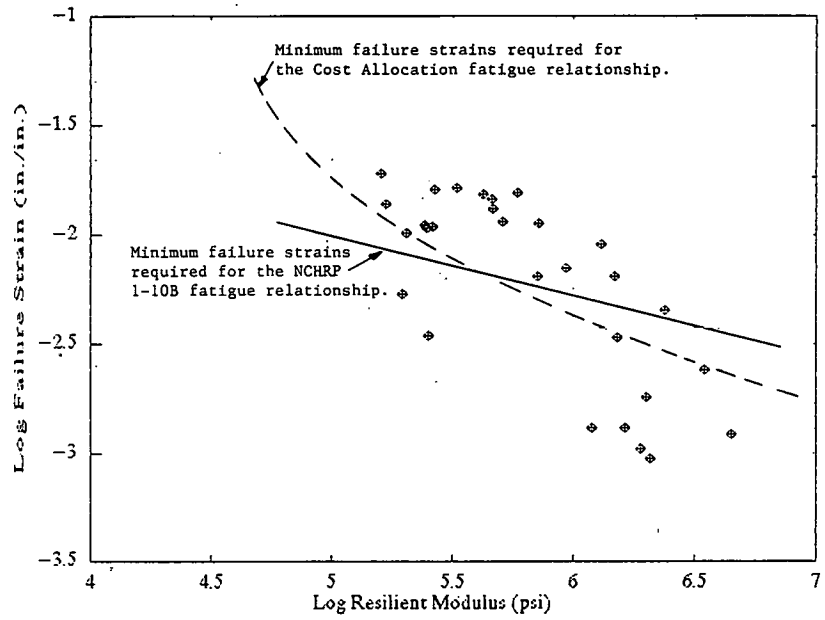

Figure 135. Relationship between minimum tensile failure strains and resilient modulus using the NCHRP 1-10B and cost allocation fatigue curves, as compared to actual test data.

At $N = 1$, Eq. 3-29 can be rewritten to establish a relationship between ϵ_t and E_R at different temperatures:

$$\log \epsilon_t (T_i) = \frac{14.820 - C_r \log E_R(T_i)}{K_r}$$

Solving these two equations simultaneously at different temperatures results in the following relationship between C_r and K_r for crack initiation, using the NCHRP Project 1-10B fatigue relationship.

$$C_r = K_r \frac{[\log \epsilon_t (T_1) - \log \epsilon_t (T_2)]}{\log E_R (T_2) - \log E_R (T_1)} \qquad (3\text{-}30)$$

Taking two totally different mixtures (for example, MI-0021 and WY-0080 as shown in Figure 135), the C_r and K_r constants can be calculated for crack initiation and are given in the following:

Mix	C_r/K_r Ratio	C_r	K_r
MI-0021	0.688	1.703	2.476
WY-0080	1.784	2.974	1.667

Thus, the fatigue relationships for these two mixes can be written as follows:

For MI-0021:

$$\log N = 14.820 - 2.476 \log \epsilon_t - 1.703 \log E_R$$

and for WY-0080:

$$\log N = 14.820 - 1.667 \text{ Log } \epsilon_t - 2.874 \log E_R$$

Using this approach, laboratory test results can be quickly compared to a standard fatigue curve (Figure 135) to estimate the fatigue cracking susceptibility of a mixture to a standard mixture, or the laboratory test results can be used to estimate a fatigue curve for that specific mix for use in structural design for fatigue cracking analyses.

3.5.2.3.3 Relationship Between Fatigue Constants. One of the primary improvements made by Rauhut from the NCHRP 1-10B fatigue curves was considering and using a relationship between K_1 and K_2 (Eq. 3-22). The NCHRP 1-10B curves assumed that the slope of all fatigue curves (log N versus log ϵ_t) are constant at 3.291. However, Rauhut recognized the fatigue work completed by Kennedy and others after the NCHRP 1-10B study was completed, and applied those results in modifying the NCHRP 1-10B fatigue equation (Eq. 3-20). Equations 3.21 and 3.22 were developed; however, AASHTO reference values had to be used because the NCHRP 1-10B curves were used as the "base" curves. Taking the same approach described previously, these AASHTO reference values can be replaced by the constants C_r and K_r, as shown below:

$$K_1 = C_r [E_R E_{Rr}]^{K_r} \quad (3\text{-}31)$$

The question becomes at what temperature should E_{Rr} be defined? In the development work for the cost allocation (*9*) and FHWA overlay design (*11*) studies, a reference temperature of 70°F was used. Currently, there is insufficient laboratory and field data to adequately determine if this is a correct value. Therefore, the stiffness measured at 68°F is suggested and will be used, for consistency between mix design and structural design using the AASHTO design procedures (*6*).

The AASHTO layer coefficient is estimated from the mixture stiffness measured at 68°F using indirect tensile testing techniques. It was originally expected that the SHRP LTPP research program could be used to define these values. However, as the strains at failure are not being measured on any field cores for which performance data will be collected, this will be impossible.

Replacing the AASHTO constants by C_r and K_r to calculate the number of load applications at test temperature T_1 results in the following equation.

$$\log N(T_i) = \log [C_r [E_R(T_i)/E_{Rr}(68)]^{-K_r}] - [1.35 - 0.252 \log [C_r [E_R(T_i)/E_{Rr}(68)]^{-K_r}]] \log \epsilon_t(T_i) \quad (3\text{-}32)$$

Using the same approach and assumptions discussed above, the failure strains can be calculated for different stiffnesses of the mix. Simplifying and rearranging the terms of Eq. 3-32 for $N = 1$ results in the following equation.

$$\log C_r = \frac{1.35 \log \epsilon_t(T_i)}{1 + 0.252 \log \epsilon_t(T_i)} + K_r \log[E_R(T_i)/E_{Rr}(68)] \quad (3\text{-}33)$$

Laboratory data at different test temperatures for a particular mix can be substituted into Eq. 3-33. For example, equations at 41°F and 104°F can be written and then solved simultaneously to define the C_r and K_r constants for each mix. Using this approach, Table 54 summarizes the results for five different mixes. Figure 136 compares the estimated fatigue curves for these mixtures at a constant stiffness of 500 ksi to the AASHTO fatigue curve for crack initiation. This can be mathematically defined by Eq. 3-34.

$$\log \epsilon_t = \frac{-6.635 - 4 \log [E_R E_{Rr}(68)]}{[3.022 + 1.008 \log [E_R E_{Rr}(68)]]} \quad (3\text{-}34)$$

As shown, the MI-0021 and VA-0621 mixtures have better fatigue characteristics when compared to the AASHTO fatigue curve, whereas the TX-0021 and WY-0080 mixtures are the more brittle and more susceptible to fatigue cracking. Thus, results from the indirect tensile strength test can be combined with the resilient modulus of elasticity test to estimate and compare the fatigue characteristics of a specified mixture to the fatigue curve of a standard mixture (for example AASHTO), or the test results can be used to estimate the fatigue curve of a mixture for use in structural design. Figure 135 compares the fatigue properties of different mixtures to a predefined standard. In this way, both failure strain and resilient modulus can be initially used in designing mixtures based on fatigue resistance parameters, without the requirement that actual fatigue tests be performed during mixture design.

The elastic stiffness can and has been measured using different test procedures to evaluate fatigue cracking potential. Kennedy

Table 54. Summary of material properties, the fatigue constants, and other parameters determined for the initial five AAMAS mixtures, as modified using maximum strain criteria.

Variable		Mixture				
		CO-0009	MI-0021	TX-0021	VA-0621	WY-0080
Total Resilient Modulus at 68°F, $E_{Rt}(68)$, ksi		640	490	1,570	630	770
Total Resilient Modulus at 77°F, ksi		510	400	1,120	440	610
Tensile Strain at Failure at 77°F, ϵ_h X10^{-3} in./in.		15.40	14.56	9.01	11.51	6.40
C_r		4.57×10^{-10}	9.96×10^{-6}	1.380×10^{-12}	3.673×10^{-8}	$1.531 \cdot 10^{-13}$
K_r		14.42	4.40	7.60	4.53	11.73
K_1	104°F	4.143×10^{-5}	1.82×10^{-3}	6.024×10^{-4}	5.326×10^{-6}	3.883×10^{-6}
	77°F	1.208×10^{-8}	2.433×10^{-5}	1.797×10^{-11}	1.867×10^{-7}	2.353×10^{-12}
	41°F	5.169×10^{-15}	1.795×10^{-8}	1.370×10^{-15}	1.333×10^{-9}	7.718×10^{-16}
K_2	104°F	2.85	2.44	2.56	3.08	3.11
	77°F	3.75	2.91	4.46	3.45	4.68
	41°F	5.35	3.70	5.50	3.99	6.06

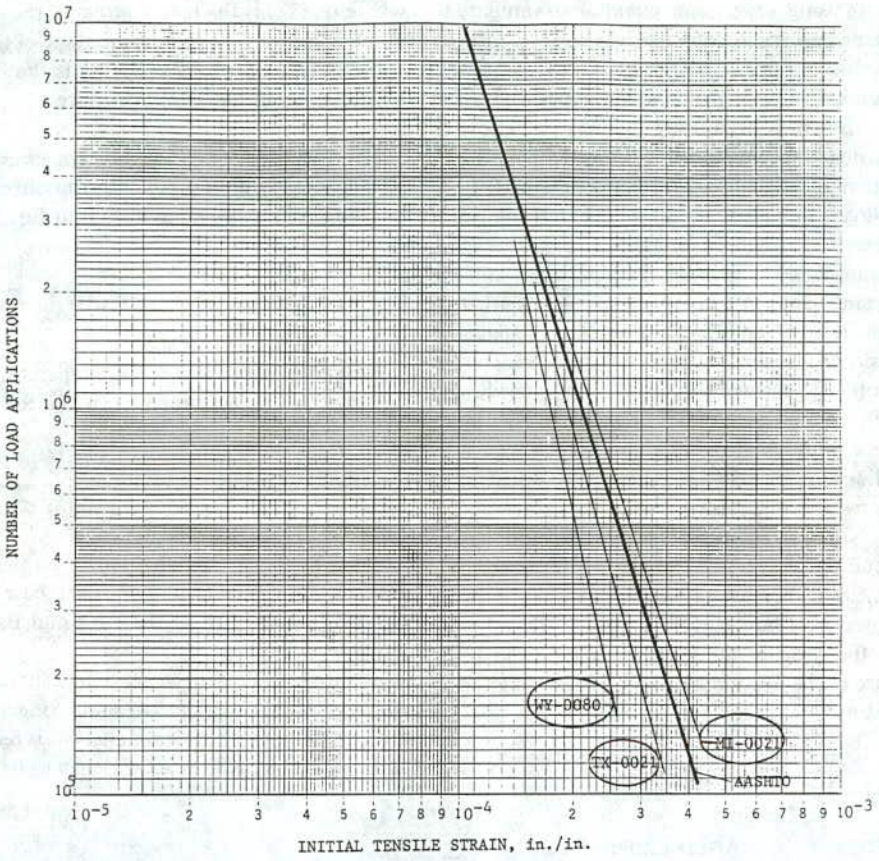

Figure 136. Fatigue curves using failure strains for a constant mix stiffness of 500 ksi compared to the AASHTO curve.

(*40*) and, more recently, Baladi (*34*), among others, have concluded that the indirect tensile test is a good tool for measuring the fatigue characteristics for asphaltic concrete materials. The reasoning used is that the indirect tensile test simulates the state of stress in the lower portion of the asphaltic concrete layer (or tension zone). Thus, the resilient modulus measured using indirect tensile testing techniques is used for mixture evaluation of specimens compacted in the laboratory both before and after the environmental aging simulation. This stiffness value is also compatible with the AASHTO Design Guide. For asphaltic concrete overlays over rigid or concrete pavements, a fatigue cracking analysis is not required because tensile stresses simply do not occur in the asphaltic concrete layer.

Using ASTM D 4123, as recommended by the Guide (*6*), either a total or instantaneous resilient modulus can be calculated. The one used for mixture evaluation depends on how the stiffness measurements were made during development of the fatigue curves. For example, the resilient modulus values considered in the above fatigue relationships were modified based on total recoverable deformations. Thus, the resilient modulus calculated from total recoverable deformations should be used for compatibility with the fatigue curves.

This same reasoning applies to the structural response model that is used to calculate tensile strains at the bottom of the asphaltic concrete layer. If tensile strains were calculated with elastic layer theory to develop the fatigue curves, elastic layer theory must also be used to calculate the same strains for a fatigue cracking analysis of a pavement structure to ensure compatibility. In other words, finite element analysis should not be used to calculate tensile strains for use with fatigue curves that were developed using elastic layer theory.

For AAMAS, the Rauhut fatigue curves (*9*) were used to evaluate each mixture for fatigue cracking potential. This inherently forces the use of elastic layer theory and total resilient moduli.

3.5.3 Thermal Cracking

This distress mode usually develops with time (depending on the environment and cooling rates), and is associated with relatively long loading times. As discussed in Chapter 2, a computer program entitled "CRACK 3" was used to predict the combined effects of thermal and load stresses. Program TC-1 (*31*) was also used to evaluate the mixtures, and both programs gave identical rankings for the mixtures (section 2.4.4.3).

The material properties required in Program TC-1 are penetration and viscosity of the "virgin" asphalt, the TFOT value at 325°F, Ring and Ball temperature, asphalt specific gravity, tensile strengths at different temperatures, asphalt content, asphalt concrete unit weight and coefficient of thermal expansion/contraction. Penetrations and viscosities are calculated with time

internally in the program using a regression equation to simulate mixture aging. This same regression equation was used to compare the penetration values measured on the extracted asphalts from the environmental aging study described in Chapter 2.

The mixture's strength is measured using the indirect tensile strength test on age-hardened specimens using the environmental aging simulation. A loading rate of 0.05 in. per min is used to represent the thermal loads imposed on the pavement. Table 46 (Chapter 2) summarizes the mixtures strength and strains at failure at different loading rates. The indirect tensile creep stiffness is another important value to consider. However, neither program uses the results from creep tests as input, but calculates the value from regression equations.

Program TC-1 and others, such as Program COLD, start with a very simple approach to calculate the tensile strain caused by a drop in temperature: $\epsilon_t = \alpha_A \Delta T$, in which α_A is the thermal coefficient of contraction, in./in./°F (the thermal coefficient of contraction does vary with temperature; however, an average value of 1.25×10^{-5} in. per in. per °F is typical, and has been used in other studies); ΔT is the change or decrease in temperature, °F; and ϵ_t is the increase in the tensile strain of the asphaltic concrete caused by a temperature drop of ΔT.

The following lists the drop in temperature that would be required to cause failure of the five initial mixtures, ignoring the relaxation stress with time:

	ΔT, °F	
ORIGINAL FIVE MIXES	UNAGED PROPERTIES	AGED PROPERTIES
Michigan	347	418 Most resistant to cracking
Virginia	205	124
Colorado	96	111
Wyoming	70	88
Texas	84	65 Least resistant to cracking

This is the same order that the "CRACK3" and TC-1 programs ranked each of these mixture's susceptibility to thermal cracks in Chapter 2, with the exception of Wyoming. The failure strains measured on the Texas mix were found to be much lower after aging than the Wyoming mixture because of the higher air voids (5.8 percent air voids for the WY-0080 mix, as compared to 8.8 percent for the TX-0021 mix).

In evaluating a mixture's susceptibility to thermal cracks, its tensile strength and tensile creep modulus must be considered. The tensile creep modulus is defined by: $E_{ct}(T) = \sigma_o / \epsilon_t(T)$.

The stiffness of the mixture can be related to the indirect tensile strength by the following mathematical relationship, similar to the results presented in Figure 58 in Chapter 2.

$$\log E_{ct}(T_i) = n_t \log(S_t) + \log E_o \qquad (3\text{-}35)$$

where S_t is the indirect tensile strength at temperature T_i, and E_o, n_t are regression coefficients of the relationship.

However, the stiffness and stress in the asphaltic concrete vary with both temperature and loading time, as the temperature decreases. In addition, the tensile strain is constant at a particular temperature change. But the tensile stress decreases because of stress relaxation during a constant strain test.

$$\sigma_t(T_i = \alpha_A \Delta T E_o(T_i)(t_r)^{-n_c} \qquad (3\text{-}36)$$

where $\sigma_t(T_i)$ is the tensile stress in the asphaltic concrete layer at temperature T_i, psi; n_c is the slope of the indirect tensile creep curve at temperature T_i; $E_o(T_i)$ is the intercept of the indirect tensile creep curve at temperature T_i, psi; and t_r is relaxation time, sec.

Given the above relationship, cracking occurs when the tensile stress exceeds the strength of the mixture. Thus, substituting Eq. 3-35 for the modified strength into Eq. 3-36 results in:

$$\left[\frac{E_{ct}(T_i)}{E_o}\right]^{1/n_t} = \alpha_A (\Delta T) E_o(T_i)(t_r)^{-n_c}$$

Rearranging the terms, the temperature drop at which cracking initiates can be estimated by the following relationship:

$$\Delta T = \left[\frac{E_{ct}(T_i)}{E_o}\right]^{1/n_t} \frac{t_r^{n_c}}{\alpha_A E_o(T_i)} \qquad (3\text{-}37)$$

where $\Delta T = T_i - T_f$, in which T_f is the temperature at which cracking initiates, °F; and T_i is the base temperature, which is typically assumed to be the Ring and Ball temperature in Program TC-1, °F.

Equation 3-37 can be used to estimate the temperature at which cracking begins for comparing or evaluating different mixtures. If a more in-depth analysis is required, a program such as TC-1, CRACK3, or COLD has to be used.

3.5.4 Moisture Damage

Moisture damage has become a very serious problem, particularly on high traffic roadways. This damage mode has been addressed by Lottman (Refs. 32 and 33) and more recently by Tunnicliff and Root (Ref. 39). AASHTO T-283 and NCHRP Report 274 were used to indirectly measure moisture damage effects on each of the mixtures. Using AASHTO T-283, specimens were conditioned to approximately 75 percent saturation and tested at 77°F using a loading rate of 2 in. per min. For NCHRP Report 274, specimens were conditioned to approximately 95 percent saturation and tested at 55°F using a loading rate of 0.065 in. per min.

ACOMDAS 2 and ACOMDAS 3 were used to predict both the wet and dry lives for each of the mixtures. The results and output of these programs have been included in Appendix Q and are summarized in Table 37 (Chapter 2). The following provides a brief summary of pavement performance predictions using the ACOMDAS 2 and 3 programs for moisture damage evaluation.

	YEARS TO FAILURE*	
MIXTURE	FATIGUE CRACKING	RUTTING
CO-0009	9.8	9.5
MI-0021	11.8	—
TX-0021	10.5	9.4
VA-0621	12.6	9.1
WY-0080	9.9	13.1
California	9.3	13.1
Georgia	11.8	17.0
New York-Rason	16.2	14.2
Wisconsin	19.2	14.4

* Dry reference life equals 15 years for each mixture for comparative studies

The moisture damage evaluation (tensile strength and resilient moduli ratios, TSR and MRR) of AAMAS is used as a means of accepting or rejecting a mixture. Using MRR and TSR threshold values of 0.70 and 0.80, respectively (suggested by Stuart, *91*), the California, CO-0009, MI-0021, and Wisconsin mixtures would be rejected or considered to be susceptible to moisture damage. Pave Bond LP was used in the CO-0009 mixture, whereas no additives were used in the California, MI-0021, and Wisconsin mixtures. All other mixtures (Georgia, TX-0021, VA-0621, New York-Rason and WY-0080) exceeded the threshold values. The VA-0621 mix contained ACRA 1000 and the Georgia and WY-0080 mixes contained hydrated lime (Tables 14 and 16, respectively). No additive was used in the New York and TX-0021 mixes.

To estimate the effect of additives, specimens of the original five mixes that contained additives were prepared without additives and tested using the same moisture conditioning procedures. These results were presented in Chapter 2 and Appendix H. In summary, all of the mixtures when tested without the additives (CO-0009, VA-0621, and WY-0080) were found to be susceptible to moisture damage. Thus, the additives used improved the VA-0621 and WY-0080 mixes, but had little to no effect on the CO-0009 mixture.

It is also interesting to note that some of the mixtures became stronger after moisture conditioning (ratios greater than 1.0). The MRR value was greater than 1.0 for the Georgia mix, and the TSR value was greater than 1.0 for the New York and Wisconsin mixes. Although ratios greater than 1.0 are not uncommon (especially for the resilient modulus), the mixture's performance will likely not improve under moist conditions. This suggests that indirect tensile strength and resilient modulus may not be the "best" properties for estimating moisture damage. Parker and Gharaybeh (*92*) have concluded that indirect tensile strength and resilient modulus do not distinctly differentiate reported stripping and nonstripping aggregate combinations.

Moisture damage is basically caused by a loss of adhesion or bond in the presence of moisture between the asphalt and aggregate, and the adhesion properties are more directly related to failure strains than strength or stiffness. Von Quintus suggests that the tensile strain ratio could provide more meaningful data than the resilient modulus ratio. For example, using ASTM D 4123, the resilient moduli is calculated using recoverable strains; no provision is provided for measuring the total or nonrecoverable strain. However, if the nonrecoverable or plastic strain after mixture conditioning increases more than the recoverable strain does and, if the total strain remains constant, then the resilient moduli will increase after moisture conditioning. A total strain analysis or ratio would be capable of evaluating these effects, whereas the MRR ratio can not.

Of those mixtures that had ratios greater than 1.0 (Georgia, New York, and Wisconsin) the indirect tensile strain at failure significantly decreased after moisture conditioning, with the exception of the Wisconsin mix. Considering a failure strain ratio in addition to the MRR and TSR values, the California, Georgia, and New York mixtures are more susceptible to fracture or raveling after moisture conditioning, whereas only the California, and to some degree the Wisconsin mix, are more susceptible to rutting. However, there are too few test data and performance observations to make any strong recommendations about using the indirect tensile strain as one of the criteria. For future test programs, it is suggested that the vertical and horizontal deformations be recorded and analyzed during moisture damage evaluation, and the mixture's performance monitored over time for field validation regarding stripping potential for different tensile strain ratios.

3.5.5 Disintegration

Disintegration is primarily related to environmental-material factors, but the severity of the distress is dependent on the magnitude and number of wheel load applications. Raveling and reduced skid resistance are the two disintegration distresses considered in AAMAS. These are important distresses but are considered secondary, because there are no mechanistic-empirical models that can be used to relate performance to mixture design values. Hopefully, the LTPP program of SHRP will collect sufficient performance and materials data to develop such models. In the interim, however, the following are offered as guidelines and criteria to be used for mixture design.

3.5.5.1 Raveling

This distress is related to a combination of asphalt consistency and film thickness, aggregate characteristics, air void content of the mix, and adhesion between the asphalt and aggregate. Asphalt contents should be selected to reduce air voids (but not to achieve compaction) and increase film thickness to prevent extensive raveling.

Reduced air voids will also reduce the aging rate of the asphalt binder. Although there are no known regression models relating these parameters to raveling, tensile strain at failure is a measure of the aggregate-asphalt bonding characteristics. Obviously, the greater the bond, the less probability for raveling. The following summarizes the bonding loss and other values for the three mixtures used in the environmental aging study.

Mixture	Unaged Tensile Strain at Failure (41°F) Mils/In.	Bonding. Loss, %	Thickness, Microns	Air Voids, %
MI-0021	6.40	45	9.1	3.7
TX-0021	1.21	30	5.0	8.8
VA-0621	2.38	34	11.2	5.9
California	1.89	39	4.3	6.4
Georgia	2.98	60	6.5	6.0
New York	4.62	12	10.7	5.6
Wisconsin	4.65	47	4.5	6.5

The bonding loss listed above was calculated by the following equation.

$$\text{Bonding loss} = [1 - \epsilon_{ht}\epsilon_{ho}] \times 100 \qquad (3\text{-}38)$$

where ϵ_{ht} is the tensile strain at failure after moisture conditioning or age-hardening, and ϵ_{ho} is the tensile strain at failure before any conditioning.

A negative number from Eq. 3-38 means that the bond increased or there was an improvement in the property. As shown, the TX-0021 had the greatest bonding loss, thinner film thick-

ness, and higher air voids. Experience with these type mixtures in Central Texas indicate they are susceptible to raveling when not properly compacted. Unfortunately, performance data are unavailable to document the threshold values to be used for mixture design. Until such data become available, tensile strain at failure should be measured before and after the environmental aging simulation, and used in the optimization of mixture design. As a general guide, tensile strains at failure should exceed 2 mils/in. at 41°F.

3.5.5.2 Reduced Skid Resistance

This distress is related to a combination of voids filled with asphalt, VMA, and aggregate properties. Regression models are available from the literature, but only for specific aggregates. Most models relate skid number to number of equivalent truck axles. An example of these equations is given as follows:

$$SN = C_4 (N_T/10^6)^{C_5} \quad (3\text{-}39)$$

where SN is skid number measured at 45 mph, N_T is number of truck axles applied to pavement surface, and C_4 and C_5 are regression coefficients.

Von Quintus et al. (*93*) conducted an analyses of these models and found that the coefficients of the relationships for different aggregates were related to L.A. abrasion and aggregate hardness. The relationships for the coefficients are:

$$C_4 = 0.52\ (LA) + 27.13 \quad (3\text{-}40)$$

$$C_5 = (-0.00034 + 0.00076H)\ C_4 - 0.38 + 0.014H \quad (3\text{-}41)$$

where LA is Los Angeles abrasion value, %; and H is Mohs hardness.

These correlations, however, were based on a very limited data base and asphalt mixture properties were unavailable. Thus, no comprehensive model exists that can be used to directly optimize mixture design values.

It is interesting to note that for the AAMAS mixtures, when the air voids were reduced below 2 percent to develop the compactive effort curves, flushing at the surface of the specimen was

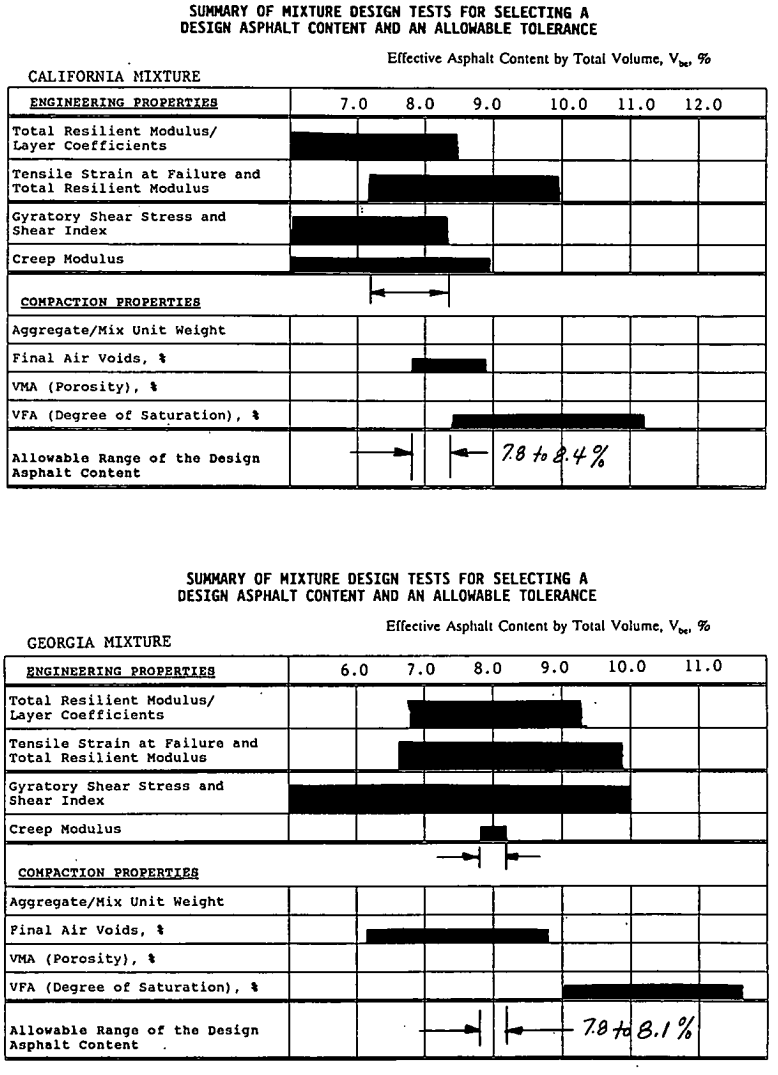

Figure 137. Worksheet for summarizing the test results and selecting allowable asphalt contents for the California and Georgia mixtures.

observed. Thus, aggregates with good skid resistance properties and low L.A. abrasion values should be used at the surface and the ultimate air void content of the mixture, as defined from the traffic densification study, should be greater than 2 percent.

3.5.6 Mixture Evaluation Summary

All mixtures were evaluated using the AAMAS methodology and criteria previously discussed. Table 55 presents an overall summary of this evaluation for high-volume roadways. As listed, some of the mixtures are expected to develop more than one type of pavement distress.

Four of the mixes (California, Georgia, New York, and Wisconsin) were used to evaluate the sensitivity of the engineering and material properties with changes in asphalt content. These data were provided in Chapter 2, sections 2.6.6 and 2.6.7. Using these results, two of the mixtures (California and Georgia) can be improved simply by changing the asphalt content. The design asphalt content and allowable range of values is shown in graphical form on Figure 137.

The other two mixtures (New York and Wisconsin) require major design changes in gradation and the addition of admixtures in order for these mixtures to provide satisfactory performance on high-volume roadways. The allowable asphalt contents for each property is shown on Figure 138. As can be seen, for some of the properties, none of the asphalt contents meet the established criteria.

Obviously, the accuracy and validation of these concepts and methodology can only be verified with time. However, based on the previous performance histories of these mixtures, the analyses and designs indicate that those mixtures, which are known to be the inferior mixtures (accelerated deterioration), are susceptible to selected distress types.

SUMMARY OF MIXTURE DESIGN TESTS FOR SELECTING A DESIGN ASPHALT CONTENT AND AN ALLOWABLE TOLERANCE

NEW YORK - RASON MIXTURE

Effective Asphalt Content by Total Volume, V_{be}, %

ENGINEERING PROPERTIES	7.0	8.0	9.0	10.0	11.0	12.0
Total Resilient Modulus/ Layer Coefficients	Insufficient Stiffness					
Tensile Strain at Failure and Total Resilient Modulus			■	■		
Gyratory Shear Stress and Shear Index	■	■				
Creep Modulus	Excessive Deformations					
COMPACTION PROPERTIES						
Aggregate/Mix Unit Weight						
Final Air Voids, %	Air Voids to Low					
VMA (Porosity), %	VMA too Low					
VFA (Degree of Saturation), %	■	■	■	■		
Allowable Range of the Design Asphalt Content						

SUMMARY OF MIXTURE DESIGN TESTS FOR SELECTING A DESIGN ASPHALT CONTENT AND AN ALLOWABLE TOLERANCE

WISCONSIN MIXTURE

Effective Asphalt Content by Total Volume, V_{be}, %

ENGINEERING PROPERTIES	6.0	7.0	8.0	9.0	10.0	11.0
Total Resilient Modulus/ Layer Coefficients			■	■		
Tensile Strain at Failure and Total Resilient Modulus				■	■	
Gyratory Shear Stress and Shear Index		■				
Creep Modulus		Excessive Deformations				
COMPACTION PROPERTIES						
Aggregate/Mix Unit Weight						
Final Air Voids, %	■					
VMA (Porosity), %		VMA too Low				
VFA (Degree of Saturation), %			■	■	■	
Allowable Range of the Design Asphalt Content						

Figure 138. Worksheet for summarizing the test results and selecting allowable asphalt contents for the New York and Wisconsin mixtures.

Table 55. Summary of mixture evaluations on the surface of high volume roadways for each distress using the AAMAS concept.

MIXTURE DESIGNATION	TYPE OF DISTRESS					
	FATIGUE CRACKING (1)	RUTTING	MOISTURE DAMAGE (2)	LOW TEMP. CRACKING	RAVELING	BLEEDING FLUSHING (3)
COLORADO	Reduced Fatigue Life	Highly Susceptible to Lateral Distortion	Highly Susceptible Even with Anti-Stripping Agent Used.	Borderline	Susceptible	√
MICHIGAN	√	Slightly Susceptible to Densification	Slightly Susceptible to Fracture	√	√	Highly Susceptible Accelerated Reduced Skid Resistance
TEXAS	Susceptible to Premature Cracking	Highly Susceptible to Densification	√	Inadequate for a Cold Environment	Highly Susceptible	√
VIRGINIA	√	√	√	√	Borderline	√
WYOMING	Highly Susceptible to Premature Cracking	Susceptible to Lateral Distortion	Slightly Susceptible to Fracture	Inadequate for a Cold Environment	Susceptible	√
CALIFORNIA	Reduced Fatigue Life	√	Highly Susceptible to Fracture and Distortion Additives	Inadequate in a Cold Environment	Highly Susceptible	√
GEORGIA	√	Susceptible to Permanent Deformations	√	Inadequate in a Cold Environment	Highly Susceptible	√
NEW YORK-RASON	√	Highly Susceptible to Lateral Flow and Distortion	√	√	√	Highly Susceptible - Accelerated Reduced Skid Resistance
WISCONSIN	Susceptible to Premature Cracking	Highly Susceptible to Lateral Flow and Distortion	Highly Susceptible to Lateral Distortion	√	Borderline	√

(1) The AASHTO Fatigue Curve (NCHRP 1-10B) is used as the Reference Value.
(2) Moisture Damage is based on the Modified Lottman Procedure.
(3) The susceptibility to Bleeding Flushing (i.e. Reduced Skid Resistance) is based only on the Refusal Air Void Content.

CHAPTER 4
CONCLUSIONS AND RECOMMENDATIONS

4.1 CONCLUSIONS

4.1.1 Mixture Evaluation Process

The laboratory evaluation portion of AAMAS has been divided into three phases. The first phase is simply the initial *mixture design phase,* which is conducted with current mixture design procedures, such as Marshall and Hveem. However, a mixture design procedure based on the AAMAS concept has also been presented. An agency can either use the AAMAS approach or its current procedure to determine the design asphalt content. The AAMAS approach also includes a method to estimate the allowable range of design asphalt contents based on the test results of the mixture's resistance to fatigue cracking, plastic deformations, and shear strains. This suggested mixture design procedure based on performance-related criteria is presented in Part I, the AAMAS Procedural Manual. Suggested guidelines for gradation, asphalt contents, and VMA-VFA values have also been provided to increase the mixture's strength and durability.

Once an initial mixture design has been completed, these materials are mixed, compacted, and conditioned in the second phase of the process. This phase provides an age-hardening simulation (both for production and the environment), moisture conditioning and evaluation, and specimen preparation for testing. This second phase is identified as the *mixture compaction/conditioning phase.*

Once the materials have been mixed, compacted, and conditioned, the specimens are tested in the third phase to measure mixture properties which can, in turn, be used to predict performance. This third phase provides the data that can be integrated into pavement design/analysis models to predict mixture performance, or can be simply compared to acceptance/rejection criteria. This third phase is identified as the *mixture evaluation phase.*

4.1.2 AAMAS Overview

Pavement Distress. A review was first made to identify the forms of pavement distress types that have a significant impact on asphaltic concrete pavements. Pavement distress and performance measures had been previously reviewed by numerous other researchers under studies for both NCHRP and FHWA projects. Those distresses selected for incorporation into AAMAS include rutting, fatigue cracking, low temperature cracking, and moisture damage. Secondary consideration is given to raveling or disintegration and loss of skid resistance.

Mixture Tests. Five tests are used as tools for mixture evaluation in AAMAS. These tests are the static cylindrical (unconfined compression) creep test, the gyratory shear strength test, the diametral resilient modulus test, the indirect tensile strength test, and the indirect tensile creep test. The AAMAS program, reported herein, requires a combination of these laboratory tests and conditioning procedures (summarized below) to evaluate the behavior and performance characteristics of asphaltic concrete mixtures.

All factors considered, tensile strain at failure, gyratory shear strength, and creep are the three properties most useful in evaluating and comparing different mixtures. Resilient modulus is required because of its incorporation into the AASHTO Design Guide and relationship to fatigue cracking. Thus, tensile strain at failure, resilient modulus, creep and gyratory shear strength are used to ensure that the mixture, as placed, will satisfy the structural design requirements. The following summarizes the specimen preparation, conditioning, and evaluation procedures used.

Initial Mixture Design Optimization Guidelines. Correlations were performed between the engineering properties and factors normally considered during mixture design. From these analyses, it was found that the product of VFA and aggregate diameter was related to work, VFA was related to tensile strain at failure, and VMA was related to indirect tensile strength. Program ASPHALT was found to be a good tool for selecting the "seed" asphalt content in mixture design, and for theoretically determining the asphalt content-air void relationship for mixture design.

Plant Hardening Simulation. The TFOT at 285°F appeared to do a reasonable job of matching the asphalt cement characteristics (penetration and viscosity value) after mix production. Thus, the TFOT is used to predict the physical characteristic of the asphalt after mix production. The virgin asphalt cement is then mixed with the aggregate blend and placed in a forced draft oven set at 275°F (or the expected mix discharge temperature from the plant) for 3 hours, mixing the material once after 1.5 hours.

The time the mixture is in the forced draft oven was determined from extraction tests on samples heated over different times (0, 2, 4, 8, 16, and 24 hours). The average time selected was that which hardened the asphalt binder to the penetration and viscosity values measured from the TFOT or from asphalt extracted from the mix after production. From the results reported herein, 3 hours was the practical time that simulated the asphalt properties after production.

Field Compaction Simulation. Compaction was one of the critical factors studied in preparing samples for laboratory evaluation. From an evaluation and comparison of field cores and laboratory compacted specimens, the gyratory shear compactor was found to more consistently match the engineering properties measured on field cores. The ranking of the compaction devices that were found to more consistently simulate the engineering properties of field cores are (1) gyratory shear compactor, (2) California kneading compactor and mobile steel wheel simulator, (3) Arizona vibratory/kneading compactor, and (4) Marshall hammer.

However, it was also found that any compaction device could be used to establish the relationships between VMA and VFA and air voids to ensure that the mix will meet the criteria discussed above.

Moisture Conditioning. Another critical item concerned moisture conditioning or moisture damage evaluation. Two procedures were used to evaluate the moisture susceptibility of asphaltic concrete mixtures. These were the modified Lottman procedure or AASHTO T-283 and the procedure documented in NCHRP Report 246. The procedure recommended in NCHRP Report 246 consistently showed a more severe conditioning and testing technique. However, the modified Lottman procedures were used in AAMAS because of the concern that the procedure in NCHRP Report 246 is too severe and is unduly damaging the specimens prior to testing. In addition, the test temperature of the modified Lottman procedure is 77°F, which is consistent with the other tests used in AAMAS. Thus, the modified Lottman has been recommended as the procedure to define the moisture susceptibility of each mixture under evaluation.

Environmental Aging Simulation. A long-term age-hardening simulation procedure was also suggested. However, the change in physical properties of the asphalt and mixture was only available for the AAMAS test sections over a short time period. The pavements were cored twice, immediately after placement and 2 years after placement. The recommended procedure is to place compacted specimens in a forced draft oven set at 140°F for 2 days. The specimens are then rotated, the oven's temperature is increased to 225°F, and the specimens are left in the oven for an additional 5 days. These heat-conditioned specimens are then used for measuring the resilient modulus, indirect tensile strength, strain at failure, and indirect tensile creep at 41°F.

Minimum Sample Size. Preliminary analysis of these test data indicate that nominal aggregate size will have an effect on certain properties of the mix. Resilient modulus, indirect tensile strength, and tensile strain at failure data indicate that an indirect tensile specimen diameter-to-nominal aggregate diameter ratio should be greater than 4, as a minimum. The preferred and absolute indirect tensile specimen diameter-to-thickness ratio should be greater than 0.50 and 0.375, respectively.

Resilient modulus testing of cylindrical specimens with different heights and end conditions suggest that the uniaxial compressive specimen height-to-diameter ratio should be greater than 1.0 when a friction reducing material is placed on both loading platens. A ratio of 2 is suggested if a friction reducing material is not used.

Performance Evaluations. Guidelines are also provided for selecting an aggregate blend and an initial asphalt content for optimizing the mixture's performance based on performance/distress predictions of fatigue cracking, rutting, and thermal cracking. Using the distress functions suggested for use in NCHRP Project 1-26, with the exception of fatigue cracking, criteria for mixture optimization and adequacy have been presented for a range of traffic and environmental conditions. For fatigue, resilient modulus and failure strains are used to estimate the constants of the fatigue equation, rather than indirect tensile strength as recommended in the NCHRP 1-26 report.

In conclusion, the development of AAMAS, as initiated through NCHRP Project 9-6(1), is a very important element of a multi-million dollar research effort involving SHRP, FHWA, and the asphalt pavement industry that will ultimately result in improved performance of asphaltic concrete pavements. Premature and costly pavement failures can be drastically reduced by (1) structural designs that more realistically consider traffic loading, climate, and material conditions; (2) selection of asphalt, aggregates, and additives or modifiers consistent with the structural design; (3) production of new or modified asphalt binders that provide the desired characteristics for minimizing distress; and (4) development and use of performance-related specifications for control of construction.

4.1.3 Summary of Test Results

The following summarizes the results and conclusions derived during the study:

- Inaccurate test results—No procedure can reasonably predict the performance of mixtures using incorrect values or values that have been determined for different materials under different conditions.
- Low VMA—Smaller differences in air voids by different compaction methods resulted between the Marshall and Hveem mix designs. However, large VMA differences in air voids occurred for the more harsh mixtures.
- Those mixtures with aggregate blends that did not meet the ASTM D 3515 grading specifications also had the lowest gyratory shear strength and poorer creep characteristics.
- Small differences in air void gradients were found through cores recovered from mixtures compacted by using different breakdown rollers in the field test sections. Similarly, small differences in air void gradients were found through specimens compacted in the laboratory using different compaction devices. The greatest density (lower air void content) was measured at the center of the sample for both field and laboratory compacted mixtures.
- Compaction in the laboratory is much more uniform than in the field, as expected.
- Equivalency factors between different laboratory devices are not constant; i.e., they are mixture dependent.
- The compaction device AV/KC was able to densify particles into a more dense arrangement than the other devices used in this study.
- All compaction devices, including the field rollers, provided a similar relative measure or ranking of mixture compactibility.
- Prior to performing the resilient modulus and indirect tensile strength test, the samples should be properly dried. Any moisture, from conditioning or from measuring the saturated surface dry specific gravity of the specimens, will have an effect on the resilient modulus and strength test results.
- The deformation ratios between the horizontal and vertical movements using indirect tensile tests are not linear. These do vary with time of loading, and thus Poisson's ratio will not be constant. Poisson's ratios greater than 0.50 can be expected after internal cracks in the specimens begin to develop because the volume of the specimen is increasing. The use of elastic layer theory in this area of testing is inappropriate.
- The variation in test results of the indirect tensile specimens and cores that were less than 1.5 in. in height was found to be much greater than that for specimens with thicknesses greater than 1.5 in. Thus, all indirect tensile test specimens should be at least 2.0 in. in height or greater.
- The use of different breakdown rollers did not result in a significant difference in the fundamental engineering properties of the mixture.
- Indirect tensile strain at failure decreased with a decrease in temperature and was found to be related to VFA at a test

temperature of 41°F. This relationship was not found at 77°F and 104°F.

- Aggregate size did have an effect on the tensile strength which was more predominant at the higher temperatures.
- Indirect tensile strain at failure was not dependent on type of loading.
- The relationship between indirect tensile strength and resilient modulus was not affected by air voids or by compaction technique. Most of the mixtures were found to have a similar relationship between indirect tensile resilient modulus and indirect tensile strength.
- The indirect tensile strain significantly decreased after aging, both in the field cores and laboratory heat-conditioned specimens.
- Reheating the mix did affect the compactive effort required to achieve a certain level of air voids. After the loose mix has been reheated, it is suggested that the mix not be reheated or reused in compactive effort studies.
- Loading rate has a large effect on the indirect tensile strength, but only a small effect on tensile strain at failure.
- Preferred orientation of aggregate particles was found in both field and laboratory compacted samples. Particle orientation of the mixes that were compacted using different field compaction trains did not vary between the use of different breakdown rollers. In addition, there were small differences in particle orientation as compacted by different laboratory devices, and on the average, the orientation of particles was slightly greater in the laboratory than in the field.

4.2 IMPLEMENTATION

It should be recognized and understood that implementing the AAMAS concepts and methodology will not be a quick process, because most of these tests and evaluation procedures will be unfamiliar to some state highway agency personnel. Therefore, it is important that each agency take a systematic approach in reviewing the AAMAS concept when considering its implementation. There should be at least four steps in the implementation process. These are: (1) familiarization with AAMAS, (2) training, (3) education, and (4) field pilot studies.

The familiarization with AAMAS is simply an understanding of the concepts and methodology employed by AAMAS. This is a relatively short term part of the implementation process.

The second step of the implementation process is training and is the more detailed in terms of how to run the tests and interpret the test results. Training is important to ensure that the tests are being performed in accordance with the procedure, and to ensure that the output of the tests are being properly interpreted.

The third part of the implementation is education. This is probably the most important step towards full-scale implementation of AAMAS. Basically, the education part is to evaluate, on a trial basis, mixes for high volume roadways. The objective is to allow the user to become confident in using AAMAS, understanding the properties measured and sensitivity of those properties to pavement performance, and establishing typical properties for their local materials. This part of the implementation process is also the more time intensive, because it involves most of the learning curve.

The final step of the implementation is conducting mix designs and analyzing those mixes for actual projects. This step is the one that leads to defining the time requirements that are required to perform the tests on a routine basis and to establish day-to-day operational procedures in a working laboratory.

4.3 RECOMMENDATIONS FOR CONTINUED RESEARCH

Project Compatibility. This section of the report briefly presents and discusses those areas which need additional study. The most important concerns the compatibility with other research projects. One of the requirements for the 9-6(1) study was that the final product be compatible with NCHRP Project 1-26.

AAMAS currently uses some simplistic distress functions and elastic layer theory to predict pavement performance with time and traffic. These predictions are based on properties measured in the laboratory during mixture design. It was mandatory that AAMAS use the same or similar distress functions and mathematical models from the NCHRP 1-26 study to maintain consistency between the two projects. Therefore, the initial results from the 1-26 project were incorporated in the AAMAS distress routines to ensure compatibility between these projects. A slightly different fatigue equation was used for mixture evaluation to be more adaptable to mixture design. Thus, any future work under the 1-26 project should be adaptable to AAMAS.

It should also be understood that the SHRP LTPP and SHRP asphalt research programs will provide additional data and may suggest modifications to the procedures presented herein regarding mixture evaluation. In particular, the SHRP A-006 project is to implement an AAMAS. It is anticipated that some of the results from A-006 will be different from the 9-6(1) study, because the A-006 project is not required to be correlated to the 1-26 study. However, it is strongly suggested and encouraged that the results from the SHRP A-006 project be compatible with the NCHRP 1-26 work or at least to a structural design procedure accepted by AASHTO. Compatibility between projects for full-scale implementation from design to construction (and laboratory to field) should be a top priority.

Time-Related Factors. Of all the areas studied in NCHRP Project 9-6(1), the two areas that may receive some controversy are the traffic densification and long-term age-hardening simulations. Cores were recovered from the five AAMAS test sections immediately after construction and 2 years after construction. The variation of the physical properties of these mixtures with time and traffic are based on this limited time frame. Historical data were used to select and define specific details of the simulations. Additionally, five projects are insufficient to establish detailed aging and traffic simulation procedures considering the range of materials used across the U.S. Thus, it is suggested that additional projects be added or a coordinated effort between the states be used to evaluate a more diverse range of mixtures.

Uncommon Tests. Gyratory shear strength or the use of the Corps of Engineers GTM was found to provide a reasonable evaluation of asphaltic concrete mixtures that were known to be "sensitive" mixtures or mixtures that are susceptible to a reduction in shear strength with traffic. However, this parameter is not used in any mechanistic model nor is it commonly used to evaluate mixtures. Thus, additional mixtures should be evaluated and designed with the GTM and then monitored to gain the critical performance data to validate its results.

Tensile strain at failure is another key parameter in evaluating asphaltic concrete mixtures. AASHTO T283 requires that only

the indirect tensile strength and resilient modulus be measured on moisture-conditioned samples. It is suggested that failure strains may provide more meaningful data, because these values can be an estimate of the mixture's adhesion (asphalt and aggregate). Thus, it is suggested that tensile strains at failure be used to calculate damage ratios for moisture damage studies and performance data be accumulated on mixtures with different levels of tensile strains at failure.

Initially, the GPS sites of the SHRP LTPP project potentially could have provided this critical performance and mixture test data on many sites across the U.S. (diverse materials and environments). However, tensile strains at failure are not being recorded, so these validation data will need to come from another source. It is suggested that mixtures placed on roadways where the as-constructed condition and mixture test data are available be monitored and evaluated over a period of time to provide the validation data.

APPENDIX A THROUGH APPENDIX R

UNPUBLISHED MATERIAL

Several appendices contained in the report as submitted by the research agency are not published herein. They are included under separate binding in the agency-prepared report entitled, "Asphalt-Aggregate Mixture Analysis System (AAMAS)—Appendices." A limited number of copies of that report are available on loan or for purchase ($25.00) from the NCHRP, Transportation Research Board, 2101 Constitution Avenue, N.W., Washington, D.C. 20418.

The titles of the available appendices are listed, as follows, for the convenience of those interested in the subject area:

Appendix A—Core Thickness and Sample Identification
Appendix B—AAMAS Procedural Manual/Guide for Field Studies
Appendix C—Aggregate Grading Analyses
Appendix D—Sample Identification, Specific Gravities and Air Voids
Appendix E—Asphalt Concrete Mix Designs
Appendix F—Preparation of Bituminous Mixture Beam Specimens by Means of the Mobile Steel Wheel Simulator
Appendix G—Test Method for Indirect Tensile Strength Testing of Bituminous Mixtures
Appendix H—Indirect Tensile Strength and Resilient Modulus Test Data
Appendix I—Unconfined Compressive Strength and Resilient Modulus Test Data
Appendix J—Deformation and Poisson's Ratio Test Data
Appendix K—Test Method for Creep Compliance Testing of Bituminous Mixtures
Appendix L—Static Indirect Tensile Creep Compliance/Recovery Test Data
Appendix M—Repeated Load Permanent Deformation Test Data
Appendix N—One-Dimensional Compressive Creep Compliance/Recovery Test Data
Appendix O—Results of Moisture Damage Evaluation Programs "ACMODAS2" and "ACMODAS3"
Appendix P—Particle Orientation Test Data
Appendix Q—Work Calculations for the Indirect Tensile Strength Test Data
Appendix R—Statistical Analysis of Data

REFERENCES

1. REGAN, G.L., "A Laboratory Study of Asphalt Concrete Mix Designs for High-Contact Pressure Aircraft Traffic." *Report No. ESL-TR-8566,* Air Force Engineering Service Center, Tyndall Air Force Base (July 1987).
2. JIMENEZ, R.A. and DADEPPO, D.A., "Asphalt Concrete Mix Design." *Report No. FHWA/AZ-86/189,* Arizona Department of Transportation (June 1986).
3. BALADI, G.Y., HARICHANDRAN, R., and DEFOE, J.H., "The Indirect Tensile Test—A New Apparatus." Interim Report prepared for the Federal Highway Administration, Michigan State University (Mar. 1987).
4. BALADI, G.Y., "Integrated Material and Structural Design Method for Flexible Pavements, Volume 3—Laboratory Design Guide." *Report No. FHWA/RD-88/118,* Federal Highway Administration (Dec. 1988).
5. GONZALEZ, G., KENNEDY, T.W., and ANAGNOS, J.N., "Evaluation of the Resilient Elastic Characteristics of Asphalt Mixtures Using the Indirect Tensile Test." *Research*

Report 183-6, Center for Highway Research, The University of Texas at Austin (Nov. 1975).

6. *AASHTO Guide for Design of Pavement Structures—1986.* American Association of State Highway and Transportation Officials, Washington, D.C. (1986).
7. *Thickness Design—Asphalt Pavements for Highways and Streets. Manual Series No. 1,* The Asphalt Institute (Sept. 1981).
8. CLAESSEN, A.I.M., EDWARDS, J.M., SIMMER, P., and UGE, P., "Asphalt Pavement Design—The Shell Method." *Proc.,* Fourth International Conference on Structural Design of Asphalt Pavements, Volume 1 (Aug. 1977).
9. RAUHUT, J.B., LYTTON, R.L., and DARTER, M.I., "Pavement Damage Functions for Cost Allocation Volume 1, Damage Functions and Load Equivalence Factors." *Report No. FHWA/RD-84/018,* Federal Highway Administration (June 1984).
10. FINN, F.N., SARAF, C., KULKARNI, R., NAIR, K., SMITH, W., and ABDULLAH, A., "Development of Pavement Structural Subsystems." Final Report NCHRP Project 1-10B, National Cooperative Highway Research Program (Feb. 1977).
11. AUSTIN RESEARCH ENGINEERS, INC., "Asphalt Concrete Overlays of Flexible Pavements—Volume I, Development of New Design Criteria." *Report No. FHWA-RD-75-75,* Federal Highway Administration (June 1975).
12. THOMPSON, M.R. and BARENBERG, E., "Calibrated Mechanistic Structural Analysis Procedures for Pavements." Project NCHRP 1-26, National Cooperative Highway Research Program (Mar. 1990).
13. KUMAR, A. and GOETZ, W.H., "The Gyratory Testing Machine as a Design Tool and as an Instrument for Bituminous Mixture Evaluation." *Proc.,* Association of Asphalt Paving Technologists, Volume 43 (1974).
14. MAHBOUB, K. and LITTLE, D., "Improved Asphalt Concrete Mixture Design Procedure." *Report No. FHWA/TX-87/474-1F,* Federal Highway Administration (July 1988).
15. RAUHUT, J.B., ROBERTS, F.L., and KENNEDY, T.W., "Models and Significant Material Properties for Predicting Distresses in Zero-Maintenance Pavements." *Report No. FHWA-RD-78-84,* Federal Highway Administration (June 1978).
16. WELBORN, Y., "State-of-the-Art in Asphalt Pavement Specifications." *Report No., FHWA/RD-84/075,* Federal Highway Administration (Jul. 1984).
17. HUGHES, C., "Performance Related Specifications for Bituminous Concrete." *Report No. VHTRC 85-R11,* Virginia Highway and Transportation Research Council (Nov. 1984).
18. ANDERSON, D., "Performance Related Specifications, NCHRP Project No. 10-26A, National Cooperative Highway Research Program." In-progress study, Pennsylvania State University.
19. "Development of Performance-Related Specifications for Asphaltic Concrete—Part II." Federal Highway Administration, in-progress study, Contract No. DTFH 61-89-C-00015, Austin Research Engineers, Inc.
20. VON QUINTUS, H.L., HUGHES, C.S., and KENNEDY, T.W., "Development of Asphalt-Aggregate Mixture Analysis System, Phase I—Feasibility of the AAMAS Concept." NCHRP Project 9-6(1), Preliminary Draft Final Report, National Cooperative Highway Research Program (Oct. 1986).
21. WOOD, L., "Correlation of Standard Drop Hammer Marshall Design with California Kneading Compactor." VHRC in-house report (Aug. 1971).
22. JORDAHL, P.R. and RAUHUT, J.B., "Flexible Pavement Model VESYS IV-B." Draft final report prepared by Brent Rauhut Engineering Inc. for the Federal Highway Administration (Aug. 1983).
23. UZAN, J. and LYTTON, R.L., "Structural Design of Flexible Pavements: A Simple Predictive System." *TRR No. 888,* Transportation Research Board, Washington, D.C. (1982).
24. BARKER, W.R. and BRABSTON, W.N., "Development of a Structural Design Procedure for Flexible Airport Pavements." *FAA Report No. FAA-RD-74-199,* U.S. Army Engineer Waterways Experiment Station, Federal Aviation Administration (Sept. 1975).
25. MEYER, F.R.P., CHEETHAM, A., and HAAS, R.C.G., "A Coordinated Method for Structural Distress Predictions in Asphalt Pavements." A paper presented at the Meeting of the Associates of Asphalt Paving Technologists, Lake Buene Vista, Florida (Aug. 1977).
26. MEYER, F.R.P. and HAAS, R.C.G., "A Coordinated Method for Structural Distress Predictions in Asphalt Pavements." *Proc.,* The Association of Asphalt Paving Technologists, Volume 47 (1978).
27. MONISMITH, C.L., INKABI, K., FREENA, C.R., and MCLEAN, D.E., "A Subsystem to Predict Rutting in Asphalt Concrete Pavement Structures." *Proc.,* Fourth International Conference on Structural Design of Asphalt Pavements, Volume I (Aug. 1977).
28. KIRWAN, R.W., SNITH, M.N., and GLYNN, T.E., "A Computer-Based Sub-System for the Prediction of Pavement Deformation." *Proc.,* Fourth International Conference on Structural Design of Asphalt Pavements, Vol. I (Aug. 1977).
29. HUSCHEK, S., "Evaluation of Rutting Due to Viscous Flow in Asphalt Pavements." *Proc.,* Fourth International Conference on Structural Design of Asphalt Pavements, Vol. I (Aug. 1977).
30. CHRISTISON, J.T., "Response of Asphalt Pavements to Low Temperatures." Ph.D. Dissertation, University of Alberta (1972).
31. SHAHIN, M.Y. and MCCULLOUGH, B.F., "Prediction of Low-Temperatures and Thermal Cracking in Flexible Pavements." *Report No. 123-14,* Center of Highway Research, The University of Texas at Austin (Aug. 1972).
32. WHITE, L.J., "A Pavement Performance Model for Fatigue Cracking Due to Moisture Damage in Asphalt Concrete." M.S. Thesis, University of Idaho (Sept. 1987).
33. FRITH, D.J., "An Asphalt Concrete Moisture Distress Pavement Performance Model Based on Wheelpath Permanent Deformation." M.S. Thesis, University of Idaho (Jul. 1988).
34. BALADI, G.Y., "Integrated Material and Structural Design Method for Flexible Pavements." *Report No. FHWA/RD-88/109,* Federal Highway Administration (Sept. 1987).
35. KENNEDY, T.W., GONZALEZ, G., and ANAGNOS, J.N., "Evaluation of the Resilient Elastic Characteristics of Asphalt Mixtures Using the Indirect Tensile Test." *Research*

Report 183-6, Center for Highway Research, The University of Texas at Austin (Nov. 1975).

36. KENNEDY, T.W., VALLEJO, J., and HAAS, R., "Permanent Deformation Characteristics of Asphalt Mixtures by Repeated-Load Indirect Tensile Test." *Research Report 183-7,* Center for Highway Research, The University of Texas at Austin (June 1976).
37. PORTER, B.W. and KENNEDY, T.W., "Comparison of Fatigue Test Methods for Asphalt Materials." *Research Report 183-4,* Center for Highway Research, The University of Texas at Austin (Apr. 1975).
38. WHITCOMB, W., HICKS, R.G., and ESCOBAR, S.J., "Evaluation of a United Design for Asphalt Recycling by Means of Dynamic and Fatigue Testing." *Proc.,* Association of Asphalt Paving Technologists, Vol. 50 (1981).
39. TUNNICLIFF, D.G. and ROOT, R.E., "Use of Antistripping Additives in Asphalt Concrete Mixtures, Laboratory Phase." *NCHRP Report 274,* National Cooperative Highway Research Program, Transportation Research Board (Dec. 1984).
40. KENNEDY, T.W. and NAVARRO, D., "Fatigue and Repeated-Load Elastic Characteristics of In-Service Asphalt—Treated Materials." *Research Report 183-2,* Center for Highway Research, The University of Texas at Austin (1975).
41. POWELL, W.D., LISTER, N.W., and LEECH, D., "Improved Compaction of Dense Graded Bituminous Macadams." *Proc.,* Association of Asphalt Paving Technologists, Vol. 50 (1981).
42. HUBER, G.A. and HEIMAN, G.H., "Effects of Asphalt Concrete Parameters on Rutting Performance: A Field Investigation." *Proc.,* Association of Asphalt Paving Technologists, Vol. 56 (1987).
43. JIMENEZ, R.A., "Structural Design of Asphalt Pavements." *Report No. ADOT-RS-13 (142),* Arizona Department of Transportation (Nov. 1975).
44. FINN, F.N., MONISMITH, C.L., and MARKEVICH, N.J., "Pavement Performance and Asphalt Concrete Mix Design." *Proc.,* Association of Asphalt Paving Technologists, Vol. 52 (1983).
45. NUNN, M.E., "Deformation Testing of Dense Coated Macadam—Effect of Method of Compaction." *Report No. TRRL 870,* Transportation Roads and Research Laboratory (1978).
46. MCLEOD, N.W. and DAVIDSON, J.K., "Particle Index Evaluation of Aggregates for Asphalt Paving Mixtures." *Proc.,* Association of Asphalt Paving Technologists, Vol. 50 (1981).
47. CORBETT, L.W. and SCHWEYER, H.E., "Viscosity Characterization of Asphalt Cement." *Viscosity Testing of Asphalt and Experience with Viscosity Graded Specifications ASTM STP 532,* American Society for Testing and Materials (1973) pp. 40–49.
48. "Mix Design for Methods for Asphalt Concrete and Other Hot-Mix Types." *Manual Series No. 2,* Asphalt Institute (1988).
49. HUGHES, C.S., and MAUPIN, G.W., JR., "Installation Report Thick Lift Bituminous Base: Construction and Materials Phase." *Report No. VHRC 72-R12,* Virginia Highway Research Council (Nov. 1972).
50. TEX-226-F, *Indirect Tensile Strength Test,* Volume 1-200-F Series, Manual of Testing Procedures, Texas State Department of Highways and Public Transportation (1987).
51. KENIS, W.J., "Predictive Design Procedures, VESYS Users Manual—An Interim Design Method for Flexible Pavements Using the VESYS Structural Subsystem." *Report No. FHWA-RD-77-154,* Federal Highway Administration (Jan. 1978).
52. MOAVENZADEH, F., SOUSSOU, J.E., FINDAKLY, H.K., and BRADEMEYER, B., "Synthesis for Rational Design of Flexible Pavements." Part III, Massachusetts Institute of Technology (Feb. 1974).
53. RAUHUT, J.B., O'QUINN, J.C., and HUDSON, W.R., "Sensitivity Analysis of FHWA Structural Model VESYS II." Vol. I, *Report No. FH 1/1,* Austin Research Engineers Inc. (Nov. 1975).
54. VON QUINTUS, H.L., "Evaluation and Comparison of Asphalt Concrete Mixtures." *Report No. BR86-33,* prepared for the city of Austin, Texas, Brent Rauhut Engineering Inc. (Feb. 1987).
55. RAUHUT, J.B., "Permanent Deformation Characteristics of Bituminous Mixtures for Pavement Rutting Predictions." *TRB Record No. 777,* Transportation Research Board, Washington, D.C. (1980).
56. VAN GREVENYNGHE, "Effect of Compaction Method on the Mechanical Properties of Asphalt-Aggregate Mixtures." *Proc.,* International Symposium, RILEM, Franch; French Laboratories des Ponts et Chaussees (Sept. 1986).
57. MOAVENZADEH, F. and GOETZ, W.H., "Aggregate Degradation in Bituminous Mixtures." *HRR Number 24,* Highway Research Board (1963) pp. 106–137.
58. MOAVENZADEH, F. and GOETZ, W.H., "Application of Statistical Mechanics to Analysis of Degradation of Aggregates." *HRR Number 51,* Highway Research Board (1964).
59. LOTTMAN, R.P., "Predicting Moisture-Induced Damage to Asphaltic Concrete, Field Evaluation." *NCHRP Report 246,* National Cooperative Highway Research Program, Transportation Research Board (May 1982).
60. TIA, M., RUTH, B.E., and CHARI, C.T., "Investigation of Original and In-Service Asphalt Properties for the Development of Improved Specifications." Project No. 99700-7361, Florida Department of Transportation (Aug. 1987).
61. CHARI, C. T., "Evaluation of Age Hardening on the Characteristics of Asphalts and Mixtures." Dissertation presented to the Graduate School, University of Florida (1988).
62. OK-KEE, K., BELL, C.A., WILSON, J.E., and BOYLE, G., "Development of Laboratory Oxidative Aging Procedures for Asphalt Cements and Asphalt Mixtures." *TRR No. 1115,* Transportation Research Board, Washington, D.C. (1987).
63. VON QUINTUS, H.L., RAUHUT, J.B., and KENNEDY, T.W., "Comparisons of Asphalt Concrete Stiffness as Measured by Various Testing Techniques." *Proc.,* Volume 51, Association of Asphalt Paving Technologists (1982).
64. BALADI, G.Y., HARICHANDRAN, R., and DE FOE, J.H., "The Indirect Tensile Test—A New Apparatus." Interim Report, prepared for Federal Highway Administration, Michigan State University (Mar. 1987).
65. LEE, A.R. and MARKWICK, H.D., "The Mechanical Properties of Bituminous Materials Under Constant Stress." *J. Soc. Chem. Industry,* Vol. 56 (1937).
66. GOETZ, W.H., "Comparison of Triaxial and Marshall Test

Results." *Proc.*, Associations of Asphalt Paving Technologists, Vol. 20 (1951).
67. HENNES, R.G. and WANG, C.C., "Physical Interpretation of Triaxial Test Date." *Proc.*, Association of Asphalt Paving Technologists, Vol. 20 (1951).
68. PUZINAUSKAS, V.P., "Influence of Mineral Aggregate Structure on Properties of Asphalt Paving Mixtures." *HRB Record 273,* Highway Research Board, Washington, D.C. (1969).
69. LEES, G. and SALEHI, M., "Orientation of Particles with Special Reference to Bituminous Paving Materials." *HRB Record 273,* Highway Research Board, Washington, D.C. (1969).
70. LITTLE, D.N. and RICHEY, B.L., "A Mixture Design Procedure Based on The Failure Envelope Concept." *Proc.*, Association of Asphalt Paving Technologists, Vol. 52 (1983).
71. BETENSON, H., JONES, MAYRUTH, ROSK, TEA, and WARBURTON, "Asphalt Pavement Rutting—Western States." *Report No. FHWA/TS-84/211,* Federal Highway Administration (May 1984).
72. "Investigation of the Design and Control of Asphalt Paving Mixtures." *TM 3-254,* U.S. Army Waterways Experiment Station, Vicksburg, Mississippi (May 1988).
73. KANDAHL, P.S., "Specifications for Compaction of Asphalt Pavements." *Proc.*, Association of Asphalt Paving Technologists, Vol. 52 (1983).
74. Standards for Specifying Construction of Airports, "Flexible Surface Courses, Item P-401 Bituminous Surface Course." *Advisory Circular 150/5370-10,* Department of Transportation, Federal Aviation Administration (Oct. 1974).
75. "The Effect of Voids in Mineral Aggregate on Pavement Performance." *Information Series 9/6/86,* National Asphalt Pavement Association (1986).
76. BJORKLUND, N.A., "Permanent Deformation and Resistance to Fatigue on Resurfaced Pavements. A Laboratory Investigation Performed on Beams Taken Across the Wheelpath and Resurfaced in the Laboratory." *Proc.*, Association of Asphalt Paving Technologists, Vol. 54 (1985).
77. FIELD, F., "Correlation of Laboratory Compaction with Field Compaction for Asphaltic Concrete Pavements." *Proc.*, Canadian Technical Asphalt Association, Vol. 4 (1959).
78. EPPS, J.A., GALLAWAY, R.M., HARPER, W.J., SCOTT, W.W., JR., and SEAY, J.W., "Compaction of Asphalt Concrete Pavements." *Research Report 90-2F,* Texas Transportation Institute, The Texas Highway Department (Jul. 1969).
79. HUSCHEK, S., "The Deformation Behavior of Asphaltic Concrete Under Triaxial Compression." *Proc.*, Association of Asphalt Paving Technologists, Vol. 54 (1985).
80. AUNAN, R.B., LUNA, R., ALTSCHAEFEL, A.G., and WOOD, L.E., "Reproduction of Thin Bituminous Surface Course Fabric by Laboratory Compaction Procedures." A paper prepared for presentation at the 1988 TRB Meeting, Washington, D.C. (1988).
81. VAN TIL, C.J., MCCULLOUGH, B.F., VALLERGA, B.A., and HICKS, R.J., "Evaluation of Interim Guides for Design of Pavement Structures." *NCHRP Report 128,* National Cooperative Highway Research Program, Transportation Research Board (1967).
82. KALLAS, B.F. and RILEY, J.C., "Mechanical Properties of Asphalt Pavement Materials." *Proc.*, Second International Conference on the Structural Design of Asphalt Pavements, University of Michigan (1967).
83. BONAQUIST, R., ANDERSON, D.A., and FERNANDO, E.G., "Relationship Between Moduli Measured in the Laboratory by Different Procedures and Field Deflection Measurements." *Proc.*, Association of Asphalt Paving Technologists, Vol. 55 (1986).
84. BROWN, S.F. and COOPER, K.E., "The Mechanical Properties of Bituminous Materials for Road Bases and Base Courses." *Proc.*, Association of Asphalt Paving Technologists, Vol. 53 (1984).
85. VON QUINTUS, H.L., FINN, F.N., HUDSON, W.R., and ROBERTS, F.L., "Fexible and Composite Structures for Premium Pavements: Volume 1—Development of Design Procedures." Unpublished report by Austin Research Engineers Inc., Federal Highway Administration (Nov. 1980).
86. KUMAR, A. and GOETZ, W.H., "The Gyratory Testing Machine as a Design Tool and as an Instrument for Bituminous Mixture Evaluation." *Proc.*, Association of Asphalt Paving Technologists, Vol. 43 (1974).
87. LAI, J.S., "Development of a Simplified Test Method to Predict Rutting Characteristics of Asphalt Mixes." *Report No. FHWA/GA/86-8503,* Federal Highway Administration (Jul. 1986).
88. KHOSLA, N.P. and OMER, M.S., "Characterization of Asphaltic Mixtures for Prediction of Pavement Performance." *TRB Record 1034,* Transportation Research Board, Washington, D.C. (1985).
89. DAVIS, R.L., "Resolution of Modern Hot Mix Asphalt Problems Through Historical Insights." (1987).
90. MAUPIN, G.W., JR., and FREEMAN, J.R., JR., "Sample Procedure for Fatigue Characterization of Bituminous Concrete." *Report No. FHWA-RD-76-102,* Federal Highway Administration (June 1976).
91. STUART, K.D., "Evaluation of Procedures Used to Predict Moisture Damage in Asphalt Mixtures." *Report No. FHWA/RD-86/090,* Federal Highway Administration (Sept. 1986).
92. PARKER, F., JR. and GHARAYBEH, F.A., "Evaluation of Indirect Tensile Test for Assessing Stripping of Alabama Asphalt Concrete Mixtures." *TRB Record 1115,* Transportation Research Board, Washington, D.C. (1987).
93. VON QUINTUS, H.L., RAUHUT, J.B., KENNEDY, T.W., and JORDAHL, P.R., "Cost Effectiveness of Sampling and Testing Programs." *Report No. FHWA/RD-85/030,* Federal Highway Administration (Jan. 1985).
94. KUMAR, A., "Effect of Film Thickness, Voids and Permeability on Asphalt Hardening in Asphalt Mixtures." *Report No. JHRP-76-19,* Purdue University, Indiana State Highway Commission (June 1976).

NOTATIONS AND SYMBOLS

A_0, A_1, A_2, A_3, A_4, A_5, A_6 — Constants used for calculating selected properties from the indirect tensile test.

A — Intercept of the straight line slope (arithmetic strain value) of the relationship between the logarithm of number of load applications versus logarithm of the accumulated permanent compressive strain.

A_f — Cross-sectional area of a specimen measured at the end of the uniaxial unconfined compression test.

A_s — Cross-sectional area of a uniaxial specimen prior to testing.

AV/KC — Arizona vibratory-kneading compactor.

a — Intercept of the straight line slope in the steady state region of the unconfined compressive creep curve (arithmetic strain value), i.e., time equals 1 second (log of loading time versus log of the compressive creep strain).

a_1 — AASHTO structural layer coefficient for a dense-graded asphaltic concrete.

B_1, B_2, B_3, B_4 — Constants used for calculating selected properties from the indirect tensile test.

b — Intercept of the straight line slope in the steady state region of the indirect tensile creep curve (arithmetic strain value), i.e., time equals 1 second (log of loading time versus log of the indirect tensile creep strain).

C_1, C_2 — Regression coefficients relating air voids to compactive effort.

C_c — Compression index.

C_r — Fatigue cracking or fracture coefficient defining the mixes sensitivity to cracking under repeated loadings, as related to the mixture's stiffness.

C_f — Fatigue coefficient or transformation factor to field conditions, and is dependent on the level or amount of fatigue cracks.

c — Compactive effort applied to a paving mixture.

CE/GS — Corps of Engineers gyratory shear compactor.

CK/CC — California kneading compactor.

COV — Coefficient of variation, %.

$D(t)$ — Creep compliance of a mixture measured at time t.

D_s — Diameter of the test specimen.

DR — Deformation ratio from the indirect tensile test.

E — Modulus of elasticity.

E_{AC} — AASHTO elastic modulus of asphaltic concrete.

E_c — Creep modulus, as determined from indirect tensile (E_{ct}) or uniaxial compression (E_{cq}) loading techniques.

E_{HT} — Horizontal tangent modulus from the indirect tensile test.

E_R — Resilient modulus

E_{RI} — Instantaneous resilient modulus, as determined from indirect tensile or uniaxial compression loading techniques.

E_{Rr} — Reference resilient modulus (for the asphaltic concrete mixture placed at the AASHTO Road Test E_{Rr} = 500,000 psi).

E_{Rt} — Total resilient modulus, as determined from indirect tensile or uniaxial compression loading techniques.

E_{RE} — The equivalent annual resilient modulus based on seasonal fatigue damage.

e — Actual void ratio of a compacted specimen.

e_{max} — Void ratio of a mixture in its loosest state.

e_{min} — Void ratio of a mixture in its densest state.

FF — Fatigue factors.

FSR — Failure strain ratio.

GTM — Gyratory testing machine.

G_a — The specific gravity of the asphalt cement.

G_{mb} — Bulk specific gravity of the compacted mixture, as measured in accordance with AASHTO T 166 or T 275, whichever applies.

G_{mg} — Maximum specific gravity of the paving mixture, as measured in accordance with AASHTO T 209.

G_{sb} — The bulk specific gravity of the combined aggregate blend.

G_{se} — The effective specific gravity of the aggregate blend and is the ratio of the weight in air of a unit volume of a permeable material (including only three voids impermeable to asphalt) at a stated temperature to the weight in air of equal density of an equal volume of gas-free distilled water at a stated temperature.

H_R — Resilient horizontal deformations measured after load release.

H_{RI} — Instantaneous resilient deformations measured along the horizontal axis using indirect tensile testing techniques.

H_{Rt} — Total resilient deformations measured along the horizontal axis using indirect tensile testing techniques.

h — Height of a specimen or thickness of an asphaltic concrete layer or lift.

I — Intercept of the straight line slope (arithmetic strain value) with the accumulated permanent strain axis, i.e., value at which the number of load applications scale equals 1.

I_d — Density index or relative density of a compacted paving mixture.

JMF — Job mix formula.

K_1, K_2 — Fatigue cracking regression constants developed from correlations between field and laboratory test data.

K_r — Fatigue cracking or fracture exponent defining the mixes sensitivity to cracking under repeated loadings, as related to the applied tensile strains.

LVDT — Linear variable differential transducer which is used for measuring deformations.

ℓ — Gauge length.

MAXDIF — Maximum difference in air voids as measured through the sample (top to bottom) by cutting the core or specimen into thin slices.

MM/HC — Mechanical Marshall hammer compactor.

MP — Material property of an asphaltic concrete mixture.

MRR — Resilient modulus ratio.

MSE — Mean squared errors.

MS/WC — Mobile steel wheel compactor.

MTG — Maximum theoretical specific gravity of a paving mixture.

MT/GS — Motorized Texas gyratory shear compactor.

m — Straight line slope of the relationship between the logarithm of the number of load applications versus logarithm of the accumulated permanent compressive strain.

m_c — Straight line slope in the steady state region of the unconfined compressive creep curve (logarithm of loading time versus logarithm of the compressive creep strain).

N — Number of repeated load applications.

N_n — Number of discrete lifts of an asphaltic concrete layer.

N_p — Number of data points or cells.

n — Straight line slope of the relationship between the logarithm of the initial tensile strain and the logarithm of the number of load applications to fatigue cracking.

n_c — Slope of the indirect tensile creep curve (log of loading time versus log of the indirect tensile creep strain).

n_t — Straight line slope of the relationship between the logarithm of the indirect tensile strength and the logarithm of the indirect tensile resilient or creep modulus.

P — Axial repeated or static load applied to a specimen.

P_a — The percentage of asphalt by total weight of the paving mixture, %.

P_{ba} — The asphalt that is absorbed by the aggregate as a percentage of the weight of aggregate or solids, %.

P_f — Maximum or total load sustained by a specimen to failure.

P_s — The aggregate or solids percentage by total weight of the paving mixture, %.

RR — Rutting rate in an asphaltic concrete layer or pavement, increase or change in rut depth per load application.

S_{qu} — Unconfined compressive strength.

S_t — Indirect tensile strength.

T — Temperature

TSR — Tensile strength ratio

t — Time

t_t — Time duration from initial specimen response of the load application to the peak of deformation using a haversine wave form.

t_ℓ — Time duration of the applied load.

$t_{\ell c}$ — Time duration of one loading cycle, including the rest period.

t_r — Relaxation time

VFA — Percentage of voids filled with asphalt, %.

VMA — Total voids in the mineral aggregate, %.

V_a — The percentage of total volume of the paving mixture that are air voids, %.

V_{ar} — Air void ratio.

V_b — The percentage of total bulk volume of the paving mixture that is asphalt, %.

V_{ba} — The asphalt that is absorbed by the aggregate and expressed as a percentage of the total volume of the paving mixture, %.

V_{be} — The effective asphalt content by total volume or the total asphalt content minus the asphalt content absorbed by the aggregates by total volume, %.

V_s — Volume of solids.

V_o — Air voids of a loose mixture (without any compactive effort).

V_u — The ultimate or refusal air void content of a paving mixture for a specific compaction device.

V_v — Volume of voids.

V_R — Resilient vertical deformations measured after load release.

V_{RI} — Instantaneous resilient deformation measured along the vertical axis of a uniaxial compression or indirect tensile specimen.

V_{Rt} — Total resilient deformation measured along the vertical axis of a uniaxial compression or indirect tensile specimen.

X — Recovery efficiency from an applied load.

α — Permanent deformation characteristic.

α_A — Thermal coefficient of contraction of an asphaltic concrete mixture.

Δ_c — Uniaxial vertical deformation measured during a static creep test.

Δ_h — Horizontal deformation at failure or where yielding is assumed to occur and is measured during the indirect tensile strength test.

Δ_H — Horizontal deformation.

Δ_v — Vertical deformation.

Δ_r — The resilient or recovered deformation measured after a static creep test. This deformation is the same as the repeated load total resilient deformation, V_{RT}, except it is measured over a much longer time period.

ΔE — Change in mixture stiffness.

Δh — Reduction in layer thickness from repeated wheel or axle loads.

ΔMP — Difference between the engineering properties measured on field cores and laboratory compacted specimens.

ΔT — Change in temperature.

ϵ_c — Compressive strain.

ϵ_{cr} — Creep strain under a tensile or compressive load.

ϵ_f — Accumulated permanent tensile (horizontal) strain from a repeated load indirect tensile test.

ϵ_h — Tensile (or horizontal) strain at failure or yielding from the indirect tensile strength test.

ϵ_{ir} — The instantaneous resilient (recovered) strain at load release.

ϵ_{il} — The instantaneous strain measured after load application.

ϵ_p — Accumulated permanent compressive strain from a repeated load compression test.

ϵ_{qu} — Compressive (or vertical) strain at failure from the unconfined compressive strength test.

ϵ_R — The relaxation or recovered strain after load release from a static creep test. This strain is the same as the repeated load total resilient strain, ϵ_{rt}, except that it is measured over a much longer time period.

ϵ_r — Resilient or recovered strain (total, ϵ_{rt}, or instantaneous, ϵ_{ir}, whichever applies) from the repeated load test.

ϵ_t — Tensile strain.

σ_1, σ_2, σ_3 — The first, second and third principal stresses, respectively.

σ_c — Compressive stress.

σ_t — Tensile stress.

τ_{oct} — Octahedral shear stress.

μ — Permanent deformation characteristic.

ν_R — Resilient Poisson's ratio.

THE TRANSPORTATION RESEARCH BOARD is a unit of the National Research Council, which serves the National Academy of Sciences and the National Academy of Engineering. It evolved in 1974 from the Highway Research Board which was established in 1920. The TRB incorporates all former HRB activities and also performs additional functions under a broader scope involving all modes of transportation and the interactions of transportation with society. The Board's purpose is to stimulate research concerning the nature and performance of transportation systems, to disseminate information that the research produces, and to encourage the application of appropriate research findings. The Board's program is carried out by more than 270 committees, task forces, and panels composed of more than 3,300 administrators, engineers, social scientists, attorneys, educators, and others concerned with transportation; they serve without compensation. The program is supported by state transportation and highway departments, the modal administrations of the U.S. Department of Transportation, the Association of American Railroads, the National Highway Traffic Safety Administration, and other organizations and individuals interested in the development of transportation.

The National Academy of Sciences is a private, nonprofit, self-perpetuating society of distinguished scholars engaged in scientific and engineering research, dedicated to the furtherance of science and technology and to their use for the general welfare. Upon the authority of the charter granted to it by the Congress in 1863, the Academy has a mandate that requires it to advise the federal government on scientific and technical matters. Dr. Frank Press is president of the National Academy of Sciences.

The National Academy of Engineering was established in 1964, under the charter of the National Academy of Sciences, as a parallel organization of outstanding engineers. It is autonomous in its administration and in the selection of its members, sharing with the National Academy of Sciences the responsibility for advising the federal government. The National Academy of Engineering also sponsors engineering programs aimed at meeting national needs, encourages education and research and recognizes the superior achievements of engineers. Dr. Robert M. White is president of the National Academy of Engineering.

The Institute of Medicine was established in 1970 by the National Academy of Sciences to secure the services of eminent members of appropriate professions in the examination of policy matters pertaining to the health of the public. The Institute acts under the responsibility given to the National Academy of Sciences by its congressional charter to be an adviser to the federal government and, upon its own initiative, to identify issues of medical care, research, and education. Dr. Samuel O. Thier is president of the Institute of Medicine.

The National Research Council was organized by the National Academy of Sciences in 1916 to associate the broad community of science and technology with the Academy's purpose of furthering knowledge and advising the federal government. Functioning in accordance with general policies determined by the Academy, the Council has become the principal operating agency of both the National Academy of Sciences and the National Academy of Engineering in providing services to the government, the public, and the scientific and engineering communities. The Council is administered jointly by both Academies and the Institute of Medicine. Dr. Frank Press and Dr. Robert M. White are chairman and vice chairman, respectively, of the National Research Council.

TRANSPORTATION RESEARCH BOARD
National Research Council
2101 Constitution Avenue, N.W.
Washington, D.C. 20418

ADDRESS CORRECTION REQUESTED

NON-PROFIT ORG.
U.S. POSTAGE
PAID
WASHINGTON, D. C.
PERMIT NO. 8970

000015M003-
MATERIALS ENGR

IDAHO TRANS DEPT DIV OF HWYS
P O BOX 7129
BOISE ID 83707